

**Faculty of Engineering and Computing
Department of Civil Engineering**

**Field Measurements and Back-Analysis of Marine Clay
Geotechnical Characteristics under Reclamation Fills**

Aputharajah Arulrajah

**This thesis is presented for the Degree of
Doctor of Philosophy
of
Curtin University of Technology**

February 2005

DECLARATION

This thesis contains no material which has been accepted for the award of any other degree or diploma in any university.

To the best of my knowledge and belief this thesis contains no material previously published by any other person except where due acknowledgment has been made.

The following publications have resulted from the work carried out for this degree. Copies of selected published or in print refereed journal papers are presented in Appendix 1. Copies of published refereed conference papers are presented in Appendix 2.

Refereed Journal Papers:

1. Arulrajah, A., Nikraz, H. and Bo, M.W. (2003a). "Factors Affecting Field Settlement Assessment and Back-Analysis by the Asaoka and Hyperbolic Methods", *Australian Geomechanics*, Journal of the Australian Geomechanics Society, Vol. 38, No. 2, June, pp. 29-37.
2. Arulrajah, A., Nikraz, H. and Bo, M.W. (2004a). "Factors Affecting Assessment and Back-Analysis by Piezometer Monitoring", *Australian Geomechanics*, Journal of the Australian Geomechanics Society, Vol. 39, No. 1, March, pp. 49-60.
3. Arulrajah, A., Bo, M.W. and Nikraz, H. (2004b). "Field Instrumentation Monitoring of Land Reclamation projects on Marine Clay Foundations", *Australian Geomechanics*, Journal of the Australian Geomechanics Society, Vol. 39, No. 1, March, pp. 69-78.
4. Arulrajah, A. and Nikraz, H. (2004c). "Field Instrumentation Assessment of Offshore Land Reclamation Works", *Journal of the International Society of Offshore and Polar Engineering*, Vol. 14, No. 4, December, pp. 315-320.
5. Arulrajah, A., Nikraz, H. and Bo, M.W. (2004d). "In-Situ Testing of Singapore Marine Clay at Changi", *Geotechnical and Geological Engineering*, An International Journal, Kluwer Academic Publishers, Vol. 23, No. 2, April 2005, pp. 111-130.

6. Arulrajah, A., Nikraz, H. and Bo, M.W. (2004e). "Factors Affecting Field Instrumentation Assessment of Marine Clay Treated with Prefabricated Vertical Drains", *Geotextiles and Geomembranes*, Journal of the International Geosynthetics Society, Vol. 22, No. 5, October, pp. 415-437.
7. Arulrajah, A., Bo, M.W., Nikraz, H. and Hashim, R. (2004f). "Piezocone Dissipation Testing of Singapore Marine Clay at Changi", *Geotechnical Engineering*, Journal of the Southeast Asian Geotechnical Society (accepted October 2003; in print).
8. Arulrajah, A., Nikraz, H. and Bo, M.W. (2004g). "Observational Method of Assessing Improvement of Marine Clay", *Ground Improvement*, Journal of the International Society of Soil Mechanics and Geotechnical Engineering, Vol. 8, No. 4, October, pp. 151-169.
9. Arulrajah, A., Nikraz, H. and Bo, M.W. (2004h). "Assessment of Marine Clay Improvement under Reclamation Fills by In-Situ Testing Methods", *Geotechnical and Geological Engineering*, An International Journal, Kluwer Academic Publishers (accepted October 2004; in print).
10. Arulrajah, A., Nikraz, H., Bo, M.W. and Hashim, R. (2004i). "In-Situ Pore Water Pressure Dissipation Testing of Marine Clay under Reclamation Fills", *Geotechnical and Geological Engineering*, An International Journal, Kluwer Academic Publishers (accepted August 2004; in print).
11. Arulrajah, A., Nikraz, H. and Bo, M.W. (2004j). "Finite Element Modeling of Marine Clay Deformation under Reclamation Fills", *Ground Improvement*, Journal of the International Society of Soil Mechanics and Geotechnical Engineering (accepted August 2004; in print).

Refereed Conference Papers:

1. Arulrajah, A. and Nikraz, H. (2003b). “Comparison of Degree of Improvement Assessed by Observational Methods Using Field Instrumentation”, *Field Measurements in Geomechanics: 6th International Symposium on Field Measurements in GeoMechanics*, Swets & Zeitlinger, The Netherlands, September, pp. 3-10.
2. Arulrajah, A., Nikraz, H. and Bo, M.W. (2004l). “Comparison Between the Performance Of Pneumatic and Electric Piezometers in a Land Reclamation Project”, *International Conference on Geotechnical Engineering*, Beirut, Lebanon, May, pp. 899-904.
3. Arulrajah, A., Nikraz, H. and Bo, M.W. (2004m). “Preloading and Prefabricated Vertical Drains Design for Offshore Land Reclamation Projects”, *International Conference on Geotechnical Engineering*, Beirut, Lebanon, May, pp. 351-356.
4. Arulrajah, A., Nikraz, H. and Bo, M.W. (2004n). “Assessment of Marine Clay Improvement by Observational Methods”, *International Symposium on Engineering Practice and Performance of Soft Deposits*, Osaka, Japan, June, pp. 269-274.
5. Arulrajah, A., Bo, M.W. and Nikraz, H. (2004o). “Characterization of Soft Marine Clay using the Flat Dilatometer”, *2nd International Conference on International Site Characterisation*, Porto, Portugal, September, pp. 287-292.
6. Arulrajah, A., Bo, M.W. and Nikraz, H. (2004p). “Pre-Reclamation Characteristics of Marine Clay using In-Situ Testing Methods”, *2nd International Conference on International Site Characterisation*, Porto, Portugal, September, pp. 1041-1046.

Signature:

Date:

Field Measurements and Back-Analysis of Marine Clay Geotechnical Characteristics under Reclamation Fills

ABSTRACT

Due to the scarcity of land at coastal regions around the world, land reclamation is commonly carried out for the future expansion of various infrastructure facilities. Marine clay is present at the coastal regions of Southeast Asia. Land reclamation on this highly compressible soil foundation often requires the use of soil improvement works to eliminate significant future settlements from occurring. The combination of prefabricated vertical drains with preloading is one of the most widely used ground improvement methods in land reclamation projects. The best means available for field measurement and back-analysis of the marine clay geotechnical characteristics under reclamation fills is by carrying out extensive field instrumentation and in-situ tests.

In-situ testing of marine clay was carried out at a test site. In-situ penetration testing was used to analyse the degree of consolidation, the improved shear strengths, overconsolidation ratio and the effective stress of marine clay prior to reclamation as well as after surcharge loading. In-situ dissipation testing was used to determine the coefficient of consolidation due to horizontal flow and horizontal hydraulic conductivity of the marine clay prior to reclamation as well as after surcharge loading. The in-situ penetration and dissipation tests were carried out by means of the field vane shear, piezocone, dilatometer, self-boring pressuremeter and BAT permeameter.

Field instrumentation methods, assessment and back-analysis of marine clay behaviour under reclamation fills forms the crux of this research. The factors that affect the field instrumentation assessment of marine clays treated with prefabricated vertical drains, forms an integral part of this research study. Settlement gauges and piezometers were used to monitor the performance of the vertical drains and to assess the degree of consolidation of the improved soil at two case study sites. The field settlement data were back-analysed by the Asaoka and Hyperbolic methods to predict the ultimate settlement of the reclaimed land under the surcharge fill. Back-analysis of the field settlement and piezometer monitoring data also enabled the coefficient of consolidation due to horizontal flow to be closely estimated. Finite element modeling of marine clay and prefabricated vertical drains was carried out and compared with the field surface settlement results at the two case study sites.

ACKNOWLEDGEMENT

I thank God for inspiring me and giving me the guidance, discipline, strength, patience, resolve, perseverance and endurance to complete these studies.

I wish to thank my supervisor Dr. Hamid Nikraz the Senior Lecturer at the Department of Civil Engineering, Curtin University of Technology (Bentley Campus, W. Australia) for his invaluable technical advice, guidance, assistance and encouragement throughout the period of my studies. I thank him for making this research study a reality and for the great interest and support he has shown in these studies and in my technical development. I thank him for constantly encouraging me to publish the findings of this research in the form of journal and conference papers. These studies would not have been possible without his immense support and faith in my technical abilities and interest in my works and publications. I am most proud to have him not only as my supervisor but also as a great friend.

I wish to acknowledge Dr. A. Vijiaratnam the Ex-Chairman of SPECS Consultants Pte. Ltd. (Singapore) for being a constant source of encouragement and inspiration throughout my career and these studies. His faith in my abilities over all these years has driven me to constantly put new goals for my career. I thank him for his interest and for his advise to me in my work, studies and personal life over all these years.

I am greatly indebted to my former senior colleague and very close friend, Dr. Bo Myint Win, Principal Geotechnical Engineer of Faber Maunsell, Bradford, United Kingdom (Formerly Bullen Consultants Ltd., United Kingdom) for his personal help with complementary data. I thank him for his invaluable input, technical advice and support throughout the duration of this research. These studies would not have been possible without his support, encouragement and brotherly advice since our working days together in Singapore (SPECS Consultants Pte. Ltd.; 1992-1997). I thank him for instilling in me the drive to pursue this PhD degree and to continually further my career since our working days together.

I am grateful to Prof. Dr. Victor Choa the Dean of Students at Nanyang Technological University (Singapore) for his invaluable technical advice, guidance and for imparting his research skills and knowledge to me. I wish to thank him for encouraging me to undertake these studies and for his support throughout this research. I am glad that after much persuasion from him since I was a young graduate engineer, I have now fulfilled his assessment of my then potential to complete this Ph.D study.

I wish to thank my wife, Lyn and children Ryan, Roy and Kristy for their love, support, encouragement, sacrifice and understanding throughout the course of these studies. I thank them for all the great times we have together every day, which provide an escape from these studies. I thank God for them and for the great joy that they bring to me. I am most thankful to God that He has still provided me time to spend with my family despite embarking on this time consuming research.

I wish to thank my parents Dr. V. Atputharajah and Dr. (Mrs) Y. Atputharajah for their considerable encouragement throughout these studies. In addition I also thank them for being supportive in my pursuit of further studies.

I would also like to thank Mrs A. Vijiaratnam for her support in these studies. I would also like to thank my friend, Mr. S. K. Rao, formerly of Ranhill Consulting, Malaysia for assisting in the preparation of the Auto-Cad drawings in this thesis.

TABLE OF CONTENTS

Contents	Page
Declaration	ii
Abstract	v
Acknowledgment	vi
Table of Content	viii
List of Figures	xv
List of Tables	xxix
List of Notations	xxxix
1.0 INTRODUCTION	1
1.1 Objectives of the Research	1
1.2 Background to the Research	3
1.3 Significance	4
1.4 Identification of the Research Needs	5
1.5 Research Method	5
1.6 Thesis Organisation	9
2.0 LITERATURE REVIEW	11
2.1 Distribution of Marine Clay Deposits in Southeast Asia	13
2.2 General Characteristics of Soft Marine Clay	14
2.3 Land Reclamation	15
2.4 Ground Improvement with Prefabricated Vertical Drains	15
2.5 Field Instrumentation of Marine Clays	17
2.5.1 Necessity and Shortcomings of Field Instrumentation	18
2.5.2 Settlement Gauges	18
2.5.3 Piezometers	19
2.5.4 Factors Affecting Field Instrumentation Assessment of Marine Clay	19
2.5.5 State of the Art: Field Instrumentation	19
2.6 In-Situ Testing of Marine Clays	20
2.6.1 Necessity and Shortcomings of In-Situ Testing	20
2.6.2 Field Vane	21
2.6.3 Piezocone	21
2.6.4 Flat Dilatometer	21
2.6.5 Self-Boring Pressuremeter	22

2.6.6	BAT Permeameter	22
2.6.7	State of the Art: In-situ Testing	22
2.7	Laboratory Testing of Marine Clays	23
2.7.1	Necessity and Shortcomings of Laboratory Testing	23
2.7.2	State of the Art: Laboratory Testing	23
2.8	Finite Element Modeling of Prefabricated Vertical Drains	24
2.9	Discussion on Literature Review	24
3.0	CHARACTERISTICS AND MINERALOGY OF SINGAPORE MARINE CLAY AT CHANGI	26
3.1	Description of Project Site	27
3.2	Site Investigation	29
3.2.1	Marine Sampling Boreholes	29
3.2.2	Bathymetric and Seismic Reflection Surveys	31
3.3	Laboratory Testing of Marine Clay	33
3.3.1	Consolidation and Physical Characteristics	33
3.3.2	Hydraulic Conductivity	39
3.3.2.1	Vertical Hydraulic Conductivity	39
3.3.2.2	Horizontal Hydraulic Conductivity	41
3.4	Field Vane Shear Testing of Marine Clay	43
3.5	Mineralogy of Marine Clay	45
3.5.1	X-Ray Diffraction	45
3.5.2	Scanning Electron Microscope	47
3.6	Geology and Formation History of Marine Clay	49
3.7	Photographic Identification of Marine Clay	51
4.0	OFFSHORE LAND RECLAMATION METHODOLOGY	54
4.1	History of Land Reclamation in the Republic of Singapore	54
4.2	Land Reclamation at the Changi East Reclamation Projects	55
4.3	Characteristics of Dredging Plant	57
4.3.1	Cutter Suction Dredger	57
4.3.2	Trailer Suction Hopper Dredger	59
4.3.3	Bottom-Opening Hopper Barge	59
4.4	Shore Protection Works	61

5.0	PRELOADING AND PREFABRICATED VERTICAL DRAINS	63
5.1	Preloading	63
5.2	History of Vertical Drains	64
5.3	Functions of Vertical Drains	64
5.4	Properties of Prefabricated Vertical Drains	65
	5.4.1 Discharge Capacity	66
	5.4.2 Properties of Filter	67
	5.4.3 Tensile Strengths	69
5.5	Quality Control Testing of Vertical Drains	69
5.6	Installation of Prefabricated Vertical Drains	70
	5.6.1 Installation Considerations and Details	70
	5.6.2 Installation Difficulties	73
	5.6.3 Installation Quality Control	74
5.7	Factors Affecting Design Predictions	75
5.8	Design and Theories of Prefabricated Vertical Drains	76
	5.8.1 Design of Surcharge Level	76
	5.8.2 Determination of c_h	77
	5.8.3 Consolidation Settlement	78
	5.8.4 Equivalent Thickness	79
	5.8.5 Vertical Consolidation	80
	5.8.6 Radial Consolidation	80
	5.8.7 Combined Vertical and Radial Consolidation	81
	5.8.8 Well Resistance	81
	5.8.9 Smear Effect	82
5.9	Prefabricated Vertical Drain Design Predictions	83
6.0	IN-SITU TESTING OF MARINE CLAY UNDER RECLAMATION FILLS	86
6.1	In-Situ Testing of Undrained Shear Strength, Overconsolidation Ratio and Degree of Consolidation of Marine Clay	87
6.2	In-Situ Dissipation Testing of Marine Clay	88
6.3	Location and Marine Clay Characteristics of the In-Situ Test Site	90
6.4	Laboratory Testing and Predictions	92
	6.4.1 Pre-Reclamation Laboratory Testing	92
	6.4.2 Laboratory Predictions	94
	6.4.3 Post-Improvement Laboratory Testing	94

6.5	Field Vane Test (FVT)	98
6.5.1	Field Vane Test Method	98
6.5.2	Comparison of Field Vane Shear Tests	100
6.6	Piezocone Test (CPT)	103
6.6.1	Piezocone Test Method	104
6.6.2	Comparison of Piezocone Tests	105
6.6.3	Piezocone Dissipation Test (CPTU)	108
6.6.4	Comparison of Piezocone Dissipation Tests	110
6.7	Flat Dilatometer Test (DMT)	117
6.7.1	Flat Dilatometer Test Method	117
6.7.2	Comparison of Flat Dilatometer Tests	119
6.7.3	Flat Dilatometer Dissipation Test	122
6.7.4	Comparison of Flat Dilatometer Dissipation Tests	126
6.8	Self-Boring Pressuremeter Test (SBPT)	131
6.8.1	Self-Boring Pressuremeter Test Method	131
6.8.2	Comparison of Self-Boring Pressuremeter Tests	133
6.8.3	Self-Boring Pressuremeter Dissipation Test	136
6.8.4	Comparison of Self-Boring Pressuremeter Dissipation Tests	137
6.9	BAT Permeameter Test (BAT)	139
6.9.1	BAT Permeameter Dissipation Test	140
6.9.2	Comparison of BAT Permeameter Dissipation Tests	142
6.10	Undrained Shear Strength, Overconsolidation Ratio and Degree of Consolidation of Marine Clay	143
6.10.1	Prior to Reclamation	143
6.10.2	Post-Improvement	146
6.11	Coefficient of Consolidation due to Horizontal Flow of Marine Clay	149
6.11.1	Prior to Reclamation	149
6.11.2	Post-Improvement	151
6.11.3	Discussions and Conclusions	154
6.12	Horizontal Hydraulic Conductivity of Marine Clay	155
6.12.1	Prior to Reclamation	155
6.12.2	Post-Improvement	156
6.12.3	Discussions and Conclusions	159

7.0	FIELD INSTRUMENTATION MONITORING OF LAND RECLAMATION PROJECTS ON MARINE CLAY FORMATIONS	160
7.1	Overview of Field Instrumentation Work	160
7.2	Field Instrumentation Monitoring	161
7.3	Off-shore Field Instrumentation	162
7.4	On-Land Field Instrumentation	167
7.5	Long-Term Field Instrumentation	168
7.6	Settlement Gauges	169
	7.6.1 Settlement Plate	169
	7.6.2 Deep Settlement Gauge	171
	7.6.3 Multi-Level Settlement Gauge	172
	7.6.4 Liquid Settlement Gauge	174
7.7	Assessment of Settlement Data	176
	7.7.1 Asaoka Method	176
	7.7.2 Hyperbolic Method	177
	7.7.3 Degree of Consolidation of Settlement Gauges	178
7.8	Piezometers	179
	7.8.1 Pneumatic Piezometer	179
	7.8.2 Electric Piezometer	180
	7.8.3 Open-Type Piezometer	181
	7.8.4 Water Stand-Pipe	183
7.9	Assessment of Piezometer Monitoring Data	183
	7.9.1 Degree of Consolidation	183
	7.9.2 Back-Analysis of Coefficient of Consolidation due to Horizontal Flow	184
7.10	Inclinometer	185
7.11	Deep Reference Point	187
7.12	Earth Pressure Cell	187
8.0	FIELD INSTRUMENTATION OF MARINE CLAY CASE STUDIES	189
8.1	Field Instrumentation of Marine Clay Case Study: Pilot Test Site	190
	8.1.1 Analyses of Settlement Gauges	194
	8.1.2 Analyses of Piezometers	207
	8.1.3 Comparison between Electric and Pneumatic Piezometers	215
	8.1.4 Comparison of Degree of Consolidation and c_h between Sub-Areas	219
	8.1.5 Findings for Field Instrumentation of Pilot Test Site	221

8.2	Field Instrumentation of Marine Clay Case Study: In-Situ Test Site	223
8.2.1	Analyses of Settlement Gauges	225
8.2.2	Analyses of Piezometers	231
8.2.3	Comparison of Degree of Consolidation	233
8.2.4	Back-Analyses of Field Consolidation Compression Parameters	234
8.2.5	Back-Analyses of Coefficient of Consolidation due to Horizontal Flow	236
8.2.6	Findings for Field Instrumentation of In-Situ Test Site	237
9.0	EVALUATION OF OBSERVATIONAL METHODS OF ASSESSING IMPROVEMENT OF MARINE CLAY UNDER RECLAMATION FILLS	238
9.1	Factors Affecting Assessment by the Asaoka method	239
9.1.1	Period of Assessment after Surcharge Placement and Selection of Time Interval	241
9.1.2	Back-Analysed Coefficient of Consolidation due to Horizontal Flow	243
9.2	Factors Affecting Assessment by the Hyperbolic Method	254
9.3	Factors Affecting Assessment by Piezometers	258
9.3.1	Period of Assessment After Surcharge placement	258
9.3.2	Back-Analysed Coefficient of Consolidation due to Horizontal Flow	258
9.3.3	Hydrogeologic Boundary Phenomenon	261
9.3.4	Correction for Settlement of Piezometer Tip	262
9.3.5	Reduction of Initial Imposed Load	264
9.4	Comparison between Asaoka, Hyperbolic and Piezometer methods	265
9.5	Findings and Recommendations	269
10.0	FINITE ELEMENT MODELING OF MARINE CLAY DEFORMATION UNDER RECLAMATION FILLS	271
10.1	Theory of Finite Element Modeling of Prefabricated Vertical Drains	271
10.2	Axi-symmetric Unit Cell Analysis of Prefabricated Vertical Drain	273
10.3	Full Scale Analysis of Prefabricated Vertical Drains	280
10.4	Full Scale Analysis of Untreated Control Embankments	284
10.5	Comparison of Finite Element Modeling Results	288
10.5.1	In-Situ Test Site	288
10.5.2	Pilot Test Site	291

11.0	PERFORMANCE VERIFICATION OF MARINE CLAY TREATED WITH PREFABRICATED VERTICAL DRAINS	295
11.1	Back-Analyses Using c_h from Asaoka Method	295
11.2	Proposed Modified Asaoka Equation	295
11.3	Conventional Design of PVD with Back-Calculated c_h	297
11.4	Finite Element Modeling of PVD	298
11.5	Findings and Discussion	300
12.0	CONCLUSIONS	302
12.1	Characteristics and Mineralogy of Singapore Marine Clay at Changi	302
12.2	In-Situ Testing of Marine Clay under Reclamation Fills	304
12.3	Field Instrumentation of Marine Clay Case Studies	308
12.4	Evaluation of Observational Methods of Assessing Improvement of Marine Clay under Reclamation Fills	309
12.5	Finite Element Modeling of Marine Clay and Vertical Drains	311
12.6	Performance Verification of Marine Clay Treated with Prefabricated Vertical Drains	313
	REFERENCES	315

APPENDIX 1: Published refereed journal papers resulting from this study

APPENDIX 2: Published refereed conference papers resulting from this study

LIST OF FIGURES

Figure No.	Title	Page
Figure 2.1	Distribution of marine clay deposits in Southeast Asia (After Broms, 1987)	13
Figure 3.1	Location and site plan of the Changi East Reclamation Project (modified from Choa et al., 2001).	28
Figure 3.2	Off-shore jack-up pontoon with boring rig.	30
Figure 3.3	Location of marine sampling boreholes.	30
Figure 3.4	Schematic view of survey vessel.	32
Figure 3.5	Isoline map of seismic survey contours.	32
Figure 3.6	Plasticity chart showing the classification of Singapore marine clay at Changi.	33
Figure 3.7	Variation of bulk density with depth.	36
Figure 3.8	Variation of specific gravity with depth.	36
Figure 3.9	Variation of water content and Atterberg limits with depth.	36
Figure 3.10	Variation of Atterberg limits with depth.	37
Figure 3.11	Variation of initial void ratio with depth.	37
Figure 3.12	Variation of maximum past pressure with depth.	37
Figure 3.13	Variation of compression index with depth.	38
Figure 3.14	Variation of recompression index with depth.	38
Figure 3.15	Variation of coefficient of vertical consolidation with depth.	38
Figure 3.16	Vertical hydraulic conductivity versus depth plot from laboratory testing.	40
Figure 3.17	Relationship comparison with c_{kv} to e_o of various clays (Bo, Arulrajah and Choa; 1998c).	41
Figure 3.18	Horizontal hydraulic conductivity versus depth plot from laboratory testing.	42
Figure 3.19	Variation of field vane undisturbed shear strength with depth	44
Figure 3.20	Variation of field vane sensitivity with depth.	44
Figure 3.21	X-ray diffraction results for marine clay at 10 meters depth.	46
Figure 3.22	X-ray diffraction results for marine clay at 18 meters depth.	46
Figure 3.23	Magnification of soil fabric under Scanning Electron Microscope (Plates 1-3 at 6 m depth; Plates 4-6 at 15 m depth).	48

Figure 3.24	Typical geological profile of the project site.	50
Figure 3.25	Photo identification of marine clay close to seabed level.	52
Figure 3.26	Photo identification of upper marine clay.	52
Figure 3.27	Photo identification of intermediate stiff marine clay.	53
Figure 3.28	Photo identification of lower marine clay.	53
Figure 4.1	Reclaimed land and their uses in the Republic of Singapore (Urban Housing Development of Singapore, 2000).	55
Figure 4.2	Land reclamation operations.	56
Figure 4.3	Land reclamation sand-pumping operations.	56
Figure 4.4	Schematic diagram of cutter suction dredger (After BS6349; 1991).	58
Figure 4.5	Cutter-suction dredger in operation.	58
Figure 4.6	Schematic diagram of a trailer suction hopper dredger (After BS6349; 1991).	60
Figure 4.7	Trailer suction hopper dredger in operation.	60
Figure 4.8	Bottom-opening hopper barge in operation.	61
Figure 4.9	Aerial view of shore protection works.	62
Figure 4.10	Close-up view of shore protection works.	62
Figure 5.1	Schematic diagram and photo of vertical drain stitcher.	71
Figure 5.2	Typical mandrels for prefabricated vertical drain (After Holtz et. al., 1991).	71
Figure 5.3	Typical detachable anchor shoes used with prefabricated drain mandrels (After Holtz et. al., 1991).	72
Figure 5.4	Vertical drains installation works at the project site (note existing airport in the background).	72
Figure 5.5	Close-up of vertical drain installation works (note roll of drain material which is threaded through mandrel).	73
Figure 5.6	Surcharge placement operations at the project site.	76
Figure 5.7	Aerial view of surcharge close to vertical drain installation works.	77
Figure 5.8	Smear effect and well resistance (After Hansbo, 1981).	83
Figure 5.9	Design Construction sequence for Vertical Drain Area (Arulrajah et al. 2004m).	84
Figure 5.10	Settlement curves for various c_h at Vertical Drain Area (Arulrajah et al. 2004m).	84
Figure 5.11	Design curves for Vertical Drain Area (Arulrajah et al. 2004m).	84
Figure 6.1	Location of In-Situ Test Site comprising Vertical Drain Area and Control Area (Arulrajah et al., 2004f).	91

Figure 6.2	Typical soil profile and engineering parameters at In-Situ Test Site (Arulrajah et al., 2004d).	91
Figure 6.3	Oedometer compression curves for the distinctive clays (PB39).	93
Figure 6.4	Comparison of preconsolidation pressure between Vertical Drain Area and Control Area.	96
Figure 6.5	Comparison of water content at Vertical Drain Area and Control Area.	96
Figure 6.6	Comparison of void ratio at Vertical Drain Area and Control Area.	97
Figure 6.7	Comparison of degree of consolidation from laboratory results at Vertical Drain Area.	97
Figure 6.8	Geometry and dimension of field vane (After Norwegian Geotechnical Society; 1979).	99
Figure 6.9	Field vane shear testing equipment.	99
Figure 6.10	Variation of FVT shear strength with elevation after 23 months of surcharge loading.	101
Figure 6.11	Variation of FVT OCR with elevation after 23 months of surcharge loading.	101
Figure 6.12	Variation of FVT effective stress with elevation after 23 months of surcharge loading.	102
Figure 6.13	Variation of FVT degree of consolidation with elevation after 23 months of surcharge loading.	102
Figure 6.14	Geometry and dimension of piezocone tip (After De Beer et. al.; 1988).	103
Figure 6.15	Piezocone tip.	103
Figure 6.16	Variation of CPT shear strength with elevation after 23 months of surcharge loading.	106
Figure 6.17	Variation of CPT OCR with elevation after 23 months of surcharge loading.	106
Figure 6.18	Variation of CPT effective stress with elevation after 23 months of surcharge loading.	107
Figure 6.19	Variation of CPT degree of consolidation with elevation after 23 months of surcharge loading.	107
Figure 6.20	CPTU dissipation test curves prior to reclamation (Arulrajah et al.,2004f).	109
Figure 6.21	CPTU dissipation test curves at Vertical Drain Area (Arulrajah et al., 2004f).	111

Figure 6.22	Comparison of piezometric heads at Vertical Drain Area (Arulrajah et al., 2004f).	111
Figure 6.23	CPTU dissipation test curves at Control Area (Arulrajah et al., 2004f).	112
Figure 6.24	Comparison of piezometric heads at Control Area (Arulrajah et al., 2004f).	112
Figure 6.25	Comparison of degree of consolidation from CPTU dissipation test between Vertical Drain Area and Control Area after 23 months of surcharge loading (Arulrajah et al., 2004f).	113
Figure 6.26	Comparison of coefficient of consolidation due to horizontal flow from CPTU dissipation test prior to reclamation and after 23 months of surcharge loading (Arulrajah et al., 2004f).	116
Figure 6.27	Comparison of horizontal hydraulic conductivity from CPTU dissipation test prior to reclamation and after 23 months of surcharge loading (Arulrajah et al., 2004f).	116
Figure 6.28	Geometry and dimension of Marchetti dilatometer blade (After Chang; 1991).	118
Figure 6.29	Dilatometer blade and accessories.	118
Figure 6.30	Variation of DMT shear strength with elevation after 23 months of surcharge loading.	120
Figure 6.31	Variation of DMT OCR with elevation after 23 months of surcharge loading.	120
Figure 6.32	Variation of DMT effective stress with elevation after 23 months of surcharge loading.	121
Figure 6.33	Variation of DMT degree of consolidation with elevation after 23 months of surcharge loading.	121
Figure 6.34	DMTA dissipation tests prior to reclamation (Arulrajah et al., 2004o).	123
Figure 6.35	DMTC dissipation test prior to reclamation (Arulrajah et al., 2004o).	123
Figure 6.36	Typical DMTA dissipation test and calculations prior to reclamation (elevation -20.39 mCD).	124
Figure 6.37	Typical DMTC dissipation test and calculations prior to reclamation (elevation -7.19 mCD).	125
Figure 6.38	Comparison of coefficient of consolidation due to horizontal flow from DMTA dissipation test prior to reclamation and after 23 months of surcharge loading (Arulrajah et al., 2004i).	127

Figure 6.39	Comparison of horizontal hydraulic conductivity from DMTA dissipation test between prior to reclamation and after 23 months of surcharge loading (Arulrajah et al., 2004i).	127
Figure 6.40	DMTA dissipation test at Vertical Drain Area (Arulrajah et al., 2004o).	128
Figure 6.41	DMTA dissipation test at Control Area (Arulrajah et al., 2004o).	128
Figure 6.42	Typical DMTA dissipation test and calculations at Vertical Drain Area (elevation – 12 mCD) (Arulrajah et al., 2004o).	129
Figure 6.43	Typical DMTA dissipation test and calculations at Control Area (elevation – 8.257 mCD) (Arulrajah et al., 2004f7).	130
Figure 6.44	Geometry and dimension of self-boring pressuremeter (Cambridge In-Situ,1993).	132
Figure 6.45	Self-boring pressuremeter and accessories.	132
Figure 6.46	Variation of SBPT shear strength with elevation after improvement	134
Figure 6.47	Variation of SBPT OCR with elevation after 23 months of surcharge loading.	134
Figure 6.48	Variation of SBPT effective stress with elevation after 23 months of surcharge loading.	135
Figure 6.49	Variation of SBPT degree of consolidation with elevation after 23 months of surcharge loading.	135
Figure 6.50	Comparison of coefficient of consolidation due to horizontal flow from SBPT (PPC) dissipation test prior to reclamation and after 23 months of surcharge loading (Arulrajah et al., 2004i).	138
Figure 6.51	Comparison of horizontal hydraulic conductivity from SBPT (PPC) dissipation test prior to reclamation and after 23 months of surcharge loading (Arulrajah et al., 2004i).	138
Figure 6.52	Geometry and dimension of BAT permeameter (Geonordic AB, 1991).	139
Figure 6.53	BAT permeameter filter tip.	140
Figure 6.54	Typical BAT permeameter test prior to reclamation (elevation –7.19 mCD).	141
Figure 6.55	Comparison of horizontal hydraulic conductivity from BAT permeameter test prior to reclamation and after 23 months of surcharge loading (Arulrajah et al., 2004i).	142
Figure 6.56	Comparison of horizontal hydraulic conductivity from BAT permeameter versus elapsed time between Vertical Drain Area and Control Area.	143

Figure 6.57	Variation of undrained shear strength with depth by various in-situ methods prior to reclamation (Arulrajah et al., 2004d).	145
Figure 6.58	Variation of OCR with depth by various in-situ methods prior to reclamation (Arulrajah et al., 2004d).	145
Figure 6.59	Variation of effective stress with elevation by various in-situ methods prior to reclamation.	146
Figure 6.60	Comparison of shear strengths from in-situ testing between Vertical Drain Area and Control Area after 23 months of surcharge loading (Arulrajah et al., 2004h).	147
Figure 6.61	Comparison of overconsolidation ratio from in-situ testing between Vertical Drain Area and Control Area after 23 months of surcharge loading (Arulrajah et al., 2004h).	148
Figure 6.62	Comparison of effective stress from in-situ testing between Vertical Drain Area and Control Area after 23 months of surcharge loading	148
Figure 6.63	Comparison of degree of consolidation from in-situ testing between Vertical Drain Area and Control Area after 23 months of surcharge loading (Arulrajah et al., 2004h).	149
Figure 6.64	Prior to reclamation coefficient of consolidation due to horizontal flow from various in-situ dissipation tests (Arulrajah et al., 2004d).	151
Figure 6.65	Comparison between coefficient of consolidation due to horizontal flow from in-situ dissipation tests between Vertical Drain Area and Control Area after 23 months of surcharge loading (Arulrajah et al., 2004i).	152
Figure 6.66	Comparison between coefficient of consolidation due to horizontal flow from in-situ dissipation tests between Vertical Drain Area and Control Area after 23 months of surcharge loading with prior to reclamation results.	152
Figure 6.67	Comparison between coefficient of consolidation due to horizontal flow from in-situ dissipation tests for Vertical Drain Area after 23 months of surcharge loading.	153
Figure 6.68	Comparison between coefficient of consolidation due to horizontal flow from in-situ dissipation tests for Control Area after 23 months of surcharge loading.	153
Figure 6.69	Prior to reclamation horizontal hydraulic conductivity from various in-situ dissipation tests (Arulrajah et al., 2004d).	156

Figure 6.70	Comparison between horizontal hydraulic conductivity from in-situ dissipation tests between Vertical Drain Area and Control Area after 23 months of surcharge loading (Arulrajah et al., 2004i).	157
Figure 6.71	Comparison between horizontal hydraulic conductivity from in-situ dissipation tests between Vertical Drain Area and Control Area after 23 months of surcharge loading with prior to reclamation results.	157
Figure 6.72	Comparison between horizontal hydraulic conductivity from in-situ dissipation tests for Vertical Drain Area after 23 months of surcharge loading.	158
Figure 6.73	Comparison between horizontal hydraulic conductivity from in-situ dissipation tests for Control Area after 23 months of surcharge loading.	158
Figure 7.1	Schematic diagram of an off-shore field instrumentation platform (Arulrajah et al., 2004b).	163
Figure 7.2	Picture of an off-shore field instrumentation platform after initial reclamation (Arulrajah et al., 2004b).	163
Figure 7.3	Construction steps 1,2,3 for off-shore field instrumentation works.	164
Figure 7.4	Construction steps 4,5,6 for off-shore field instrumentation works.	165
Figure 7.5	Construction steps 7,8,9 for off-shore field instrumentation works.	166
Figure 7.6	On-land field instrumentation clusters.	167
Figure 7.7	Typical details of long-term field instrumentation cluster (Arulrajah et al., 2004b).	168
Figure 7.8	Typical details of a seabed settlement plate.	170
Figure 7.9	Typical details of surface settlement plate.	170
Figure 7.10	Typical details of deep settlement gauge.	171
Figure 7.11	Typical details of a multi-level settlement gauge.	173
Figure 7.12	Accessories of a multi-level settlement gauge.	173
Figure 7.13	Comparison of settlement measured by deep settlement gauges and multi-level settlement gauges.	174
Figure 7.14	Schematic details of a liquid settlement gauge (Courtesy of Sinco).	175
Figure 7.15	Liquid settlement gauge (Courtesy of Sinco).	175
Figure 7.16	Relationship of slopes (α) of initial linear segments (between U_{60} and U_{90}) of theoretical hyperbolic plots (Tan, 1995).	178
Figure 7.17	Typical details and photo of pneumatic piezometer with protected guard cell (Courtesy of Dr M.W.Bo).	180
Figure 7.18	Typical details of an electric piezometer.	181
Figure 7.19	Electric piezometer.	181

Figure 7.20	Typical details of an open-type piezometer.	182
Figure 7.21	Typical details of a water level indicator.	182
Figure 7.22	Typical details of a water stand-pipe.	183
Figure 7.23	Typical details of an inclinometer.	186
Figure 7.24	Comparison of lateral displacement between inclinometers anchored at SPT 50 blows and SPT 100 blows (Arulrajah et al., 2004b; Bo, Arulrajah and Choa; 1998b).	187
Figure 7.25	Typical details of a total pressure cell.	188
Figure 7.26	Comparison between the results of earth pressure between cells placed with sensitive side up and down (Arulrajah et al., 2004b; Bo, Arulrajah and Choa; 1998b).	188
Figure 8.1	Location of field instrumentation case study sites (Arulrajah et al., 2004d).	189
Figure 8.2	Layout plan and vertical drain spacing of sub-areas at the Pilot Test Site (Arulrajah et al., 2003a).	190
Figure 8.3	Cross sectional profile showing instrument elevations at the Pilot Test Site (Arulrajah et al., 2004e).	191
Figure 8.4	Instrument elevations in A2S-71 (2.0m x 2.0m) .	192
Figure 8.5	Instrument elevations in A2S-72 (2.5m x 2.5m) .	192
Figure 8.6	Instrument elevations in A2S-73 (3.0m x 3.0m) .	193
Figure 8.7	Instrument elevations in A2S-74 (No Drain) .	193
Figure 8.8	Comparison of field settlement between sub-areas at the Pilot Test Site (Arulrajah et al., 2003a).	195
Figure 8.9	Comparison of field settlement isochrones between sub-areas at the Pilot Test Site (Arulrajah et al., 2004g).	196
Figure 8.10	Field settlement results of settlement plate and deep settlement gauges at A2S-71 (2.0m x 2.0m) (Arulrajah et al., 2004g).	197
Figure 8.11	Field settlement results of settlement plate and deep settlement gauges at A2S-72 (2.5m x 2.5m) (Arulrajah et al., 2004g).	198
Figure 8.12	Field settlement results of settlement plate and deep settlement gauges at A2S-73 (3.0m x 3.0m) (Arulrajah et al., 2004g).	199
Figure 8.13	Field settlement results of settlement plate and deep settlement gauges at A2S-74 (No Drain) (Arulrajah et al., 2004g).	200
Figure 8.14	Asaoka plot for A2S-71 (2.0m x 2.0m) at time interval of 28 and 56 days (Arulrajah et al., 2004g).	201
Figure 8.15	Asaoka plot for A2S-72 (2.5m x 2.5m) at time interval of 28 and 56 days (Arulrajah et al., 2004g).	202

Figure 8.16	Asaoka plot for A2S-73 (3.0m x 3.0m) at time interval of 28 and 56 days (Arulrajah et al., 2004g).	203
Figure 8.17	Combined Hyperbolic plot of settlement gauges at A2S-71 (2.0m x 2.0m) (Arulrajah et al., 2004g).	204
Figure 8.18	Hyperbolic plot at A2S-71(2.0m x 2.0m) after surcharge duration of 32 months (Arulrajah et al., 2004g).	204
Figure 8.19	Combined Hyperbolic plot of settlement gauges at A2S-72 (2.5m x 2.5m) (Arulrajah et al., 2004g).	205
Figure 8.20	Hyperbolic plot at A2S-72 (2.5m x 2.5m) after surcharge duration of 32 months (Arulrajah et al., 2004g).	205
Figure 8.21	Combined Hyperbolic plot of settlement gauges at A2S-73 (3.0m x 3.0m) (Arulrajah et al., 2004g).	206
Figure 8.22	Hyperbolic plot at A2S-73 (3.0m x 3.0m) after surcharge duration of 32 months (Arulrajah et al., 2004g).	206
Figure 8.23	Piezometric elevations at A2S-71 (2.0m x 2.0m) (Arulrajah et al., 2004g).	208
Figure 8.24	Excess pore water pressures at A2S-71 (2.0m x 2.0m) (Arulrajah et al., 2004g).	208
Figure 8.25	Piezometric elevations at A2S-72 (2.5m x 2.5m) (Arulrajah et al., 2004g).	209
Figure 8.26	Excess pore water pressures at A2S-72 (2.5m x 2.5m) (Arulrajah et al., 2004g).	209
Figure 8.27	Piezometric elevations at A2S-73 (3.0m x 3.0m) (Arulrajah et al., 2004g).	210
Figure 8.28	Excess pore water pressures at A2S-73 (3.0m x 3.0m) (Arulrajah et al., 2004g).	210
Figure 8.29	Piezometric elevations at A2S-74 (No Drain) (Arulrajah et al., 2004g).	211
Figure 8.30	Excess pore water pressures at A2S-74 (No Drain) (Arulrajah et al., 2004g).	211
Figure 8.31	Comparison of piezometer excess pore pressure isochrones between sub-areas 12 months after surcharge.	212
Figure 8.32	Comparison of piezometer excess pore pressure isochrones between sub-areas 24 months after surcharge.	212
Figure 8.33	Comparison of piezometer excess pore pressure isochrones between sub-areas 32 months after surcharge (Arulrajah et al., 2004g).	213

Figure 8.34	Comparison of piezometer excess pore pressure isochrones between sub-areas various periods after surcharge.	214
Figure 8.35	Comparison of degree of consolidation between sub-areas 32 months after surcharge (Arulrajah et al., 2004g).	214
Figure 8.36	Cross-sectional profile showing piezometer locations at the A2S-71 (2.0 m x 2.0 m) and A2S-74 (No Drain) sub-areas (Arulrajah et al., 2004l).	215
Figure 8.37	Comparison between electric (PZ) and pneumatic (PP) piezometer excess pore pressure isochrones at 12, 24 and 32 months after surcharge (Arulrajah et al., 2004l).	216
Figure 8.38	Comparison between electric (PZ) and pneumatic (PP) piezometer excess pore pressure isochrones at various periods after surcharge (Arulrajah et al., 2004l).	217
Figure 8.39	Comparison of degree of consolidation between electric (PZ) and pneumatic (PP) piezometer 32 months after surcharge (Arulrajah et al., 2004l).	217
Figure 8.40	Cross Sectional soil profile showing field instrumentation elevations at the In-Situ Test Site (Arulrajah et al., 2004b).	223
Figure 8.41	Instrument elevations in Vertical Drain Area.	224
Figure 8.42	Instrument elevations in Control Area.	224
Figure 8.43	Comparison of field settlement between Vertical Drain Area and Control Area (Arulrajah et al., 2004b).	225
Figure 8.44	Comparison of field settlement isochrones between Vertical Drain Area and Control Area (Arulrajah et al., 2004c).	226
Figure 8.45	Field settlement results of settlement gauges at Vertical Drain Area (Arulrajah et al., 2004b).	227
Figure 8.46	Field settlement results of settlement gauges at Control Area (Arulrajah et al., 2004b).	228
Figure 8.47	Asaoka plot of settlement plate at Vertical Drain Area (Arulrajah et al., 2004b).	229
Figure 8.48	Combined Hyperbolic plot of settlement gauges at Vertical Drain Area (Arulrajah et al., 2003b).	230
Figure 8.49	Hyperbolic plot of settlement plate at Vertical Drain Area (Arulrajah et al., 2004b).	230
Figure 8.50	Piezometric Elevations at Vertical Drain Area (1.5m x 1.5m).	231
Figure 8.51	Excess pore water pressures at Vertical Drain Area (1.5m x 1.5m) (Arulrajah et al., 2004c).	231

Figure 8.52	Piezometric elevations at Control Area (No Drain).	232
Figure 8.53	Excess pore water pressures at Control Area (No Drain) (Arulrajah et al., 2003b).	232
Figure 8.54	Comparison of piezometer excess pore pressure isochrones between Vertical Drain Area and Control Area 20 months after surcharge (Arulrajah et al., 2004b).	233
Figure 8.55	Comparison of degree of consolidation at Vertical Drain Area and Control Area 20 months after surcharge (Arulrajah et al., 2004b).	234
Figure 8.56	Field void ratio versus effective stress for sub-layers.	235
Figure 9.1	Comparison of variation in ultimate settlement for various time intervals by the Asaoka method.	242
Figure 9.2	Comparison of variation in degree of consolidation for various time intervals by the Asaoka method.	242
Figure 9.3	Comparison of variation in coefficient of consolidation due to horizontal flow for various time intervals by the Asaoka method.	244
Figure 9.4	Asaoka plots at A2S-71 sub-area (2.0m x 2.0m) 12 months after surcharge (Arulrajah et al., 2004e).	245
Figure 9.5	Asaoka plots at A2S-71 sub-area (2.0m x 2.0m) 24 months after surcharge.	246
Figure 9.6	Asaoka plots at A2S-71 sub-area (2.0m x 2.0m) 32 months after surcharge (Arulrajah et al., 2003a).	247
Figure 9.7	Asaoka plots at A2S-72 sub-area (2.5m x 2.5m) 12 months after surcharge.	248
Figure 9.8	Asaoka plots at A2S-72 sub-area (2.5m x 2.5m) 24 months after surcharge.	249
Figure 9.9	Asaoka plots at A2S-72 sub-area (2.5m x 2.5m) 32 months after surcharge.	250
Figure 9.10	Asaoka plots at A2S-73 sub-area (3.0m x 3.0m) 12 months after surcharge.	251
Figure 9.11	Asaoka plots at A2S-73 sub-area (3.0m x 3.0m) 24 months after surcharge.	252
Figure 9.12	Asaoka plots at A2S-73 sub-area (3.0m x 3.0m) 32 months after surcharge.	253
Figure 9.13	Hyperbolic plots at A2S-71 for various periods of assessments after surcharge (Arulrajah et al., 2003a).	255
Figure 9.14	Hyperbolic plots at A2S-72 for various periods of assessments after surcharge.	256

Figure 9.15	Hyperbolic plots at A2S-73 for various periods of assessments after surcharge.	257
Figure 9.16	Comparison of A2S-71 (2.0 x 2.0 m) piezometer excess pore pressure isochrones 12, 24 and 32 months after surcharge (Arulrajah et al., 2004e).	259
Figure 9.17	Comparison of A2S-72 (2.5 x 2.5 m) piezometer excess pore pressure isochrones 12, 24 and 32 months after surcharge .	260
Figure 9.18	Comparison of A2S-73 (3.0 x 3.0 m) piezometer excess pore pressure isochrones 12, 24 and 32 months after surcharge (Arulrajah et al., 2004a).	260
Figure 9.19	Comparison of A2S-74 (No Drain) piezometer excess pore pressure isochrones 12, 24 and 32 months after surcharge (Arulrajah et al., 2004e).	261
Figure 9.20	In-situ pore pressure which is lower than static pore pressure due to hydrogeologic boundary (after Schiffman et al., 1994).	262
Figure 9.21	Comparison of corrected and uncorrected piezometric elevation (A2S-72: PP-250) (Arulrajah et al., 2004e).	263
Figure 9.22	Comparison between corrected and uncorrected excess pore pressure (A2S-72: PP-250) (Arulrajah et al., 2004a).	263
Figure 9.23	Comparison between corrected and uncorrected piezometer excess pore pressure isochrones 24 months after surcharge at Pilot Test Site (Arulrajah et al., 2004e).	264
Figure 9.24	Comparison between variation in ultimate settlement at various surcharge periods by the Asaoka and Hyperbolic methods (Arulrajah et al., 2004e).	267
Figure 9.25	Comparison between variation in degree of consolidation at various surcharge periods by the Asaoka, Hyperbolic and piezometer methods (Arulrajah et al., 2004e).	267
Figure 9.26	Comparison between variation in c_h at various surcharge periods by the Asaoka and piezometer methods (Arulrajah et al., 2004e).	269
Figure 10.1	Axi-symmetric radial flow (Lin et al., 2000).	273
Figure 10.2	Conversion of the axi-symmetric unit cell from undisturbed marine clay with smear zone to that of equivalent horizontal permeability of surrounding soils (Arulrajah et al., 2004j).	274
Figure 10.3	Deformed mesh by axi-symmetric unit cell analysis of Vertical Drain Area (1.5m x 1.5m) at the In-Situ Test Site, 20 months after surcharge placement.	276

Figure 10.4	Vertical displacement by axi-symmetric unit cell analysis of Vertical Drain Area (1.5m x 1.5m) at the In-Situ Test Site , 20 months after surcharge placement.	276
Figure 10.5	Deformed mesh by axi-symmetric unit cell analysis of A2S-71 sub-area (2.0m x 2.0m) at the Pilot Test Site, 32 months after surcharge placement.	277
Figure 10.6	Vertical displacement by axi-symmetric unit cell analysis of A2S-71 sub-area (2.0m x 2.0m) at the Pilot Test Site, 32 months after surcharge placement.	277
Figure 10.7	Deformed mesh by axi-symmetric unit cell analysis of A2S-72 sub-area (2.5m x 2.5m) at the Pilot Test Site, 32 months after surcharge placement.	278
Figure 10.8	Vertical displacement by axi-symmetric unit cell analysis of A2S-72 sub-area (2.5m x 2.5m) at the Pilot Test Site, 32 months after surcharge placement.	278
Figure 10.9	Deformed mesh by axi-symmetric unit cell analysis of A2S-73 sub-area (3.0m x 3.0m) at the Pilot Test Site, 32 months after surcharge placement.	279
Figure 10.10	Vertical displacement by axi-symmetric unit cell analysis of A2S-73 sub-area (3.0m x 3.0m) at the Pilot Test Site, 32 months after surcharge placement.	279
Figure 10.11	PVD in 2-D plane strain flow (Lin et al., 2000).	280
Figure 10.12	Deformed mesh by full scale analysis of Vertical Drain Area (1.5m x 1.5m) at In-Situ Test Site, 20 months after surcharge placement (Arulrajah et al., 2004j).	283
Figure 10.13	Vertical displacement by full scale analysis of Vertical Drain Area (1.5m x 1.5m) at In-Situ Test Site, 20 months after surcharge placement (Arulrajah et al., 2004j).	283
Figure 10.14	Deformed mesh by full scale analysis of Control Area (No Drain) at In-Situ Test Site, 20 months after surcharge placement (Arulrajah et al., 2004j).	286
Figure 10.15	Vertical displacement by full scale analysis of Control Area (No Drain) at In-Situ Test Site, 20 months after surcharge placement (Arulrajah et al., 2004j).	286
Figure 10.16	Deformed mesh by full scale analysis of A2S-74 sub-area (No Drain) at Pilot Test Site, 32 months after surcharge placement.	287

Figure 10.17	Vertical displacement by full scale analysis of A2S-74 sub-area (No Drain) at Pilot Test Site, 32 months after surcharge placement.	287
Figure 10.18	Comparison between finite element modeling results with actual field settlement at In-Situ Test Site, 20 months after surcharge placement (Arulrajah et al., 2004j).	290
Figure 10.19	Comparison between ultimate settlement by finite element modeling with actual field settlement at In-Situ Test Site (Arulrajah et al., 2004j).	290
Figure 10.20	Comparison between finite element modeling results with actual field settlement at Pilot Test Site, 32 months after surcharge placement (Arulrajah et al., 2004j).	294
Figure 10.21	Comparison between ultimate settlement by finite element modeling with actual field settlement at Pilot Test Site (Arulrajah et al., 2004j).	294
Figure 11.1	Vertical drain performance verification comparison of degree of consolidation by various methods at, 20 months after surcharge (Arulrajah et al., 2004j).	299

LIST OF TABLES

Table No.	Title	Page
Table 3.1	Range of physical and consolidation characteristics of Singapore marine clay at Changi (Bo, Arulrajah and Choa; 1998a).	35
Table 3.2	Recommended design parameters of Singapore marine clay at Changi.	35
Table 5.1	Comparison between design ($c_h=2c_v$) with back-analysed field instrumentation results at In-Situ Test Site, 20 months after surcharge (Arulrajah et al., 2004m).	85
Table 6.1	Testing procedure for in-situ tests	88
Table 8.1.	Summary of Pilot Test Site sub-area vertical drain spacings (Arulrajah et al., 2003a).	190
Table 8.2	Comparison of average degree of consolidation using electric piezometers at various periods after surcharge placement (Arulrajah et al., 2004l).	219
Table 8.3	Comparison of Asaoka, Hyperbolic and piezometer methods at Pilot Test Site 32 months after surcharge - 41.9 months of monitoring (Arulrajah et al., 2004g).	220
Table 8.4	Comparison of Asaoka, Hyperbolic and piezometer methods at In-Situ Test Site 20 months after surcharge (Arulrajah et al., 2004b).	234
Table 8.5	Comparison of laboratory prediction and back-analysed field soil parameters.	235
Table 8.6	Back-analysed c_h results of settlement gauges (Asaoka method).	236
Table 9.1	Asaoka method with various time intervals 12 months after surcharge - 21.6 months of monitoring (Arulrajah et al., 2004e).	240
Table 9.2	Asaoka method with various time intervals 24 months after surcharge - 33.7 months of monitoring (Arulrajah et al., 2004e).	240
Table 9.3	Asaoka method with various time intervals 32 months after surcharge - 41.9 months of monitoring (Arulrajah et al., 2004e).	241
Table 9.4	Hyperbolic method at 12, 24 and 32 months after surcharge placement (Arulrajah et al., 2004e).	254
Table 9.5	Comparison of average degree of consolidation using piezometers for 12, 24 and 32 months after surcharge placement - 21.6, 33.7 and 41.9 months of monitoring (Arulrajah et al., 2004e).	259

Table 9.6	Comparison of Asaoka, Hyperbolic and piezometer methods 12 months after surcharge - 21.6 months of monitoring (Arulrajah et al., 2004e).	265
Table 9.7	Comparison between Asaoka, Hyperbolic and piezometer methods 24 months after surcharge - 33.7 months pf monitoring (Arulrajah et al., 2004e).	265
Table 9.8	Comparison of Asaoka, Hyperbolic and piezometer methods 32 months after surcharge - 41.9 months of monitoring (Arulrajah et al., 2004e).	266
Table 10.1	Soil parameters for axi-symmetric unit cell analysis of PVD (Arulrajah et al., 2004j).	275
Table 10.2	Soil parameters for full scale analysis of PVD (Arulrajah et al., 2003).	282
Table 10.3	Soil parameters for full scale analysis of untreated control embankment (Arulrajah et al., 2004j).	285
Table 10.4	Comparison between finite element modeling results with actual field settlement at In-Situ Test Site (Arulrajah et al., 2004j).	289
Table 10.5	Comparison of settlement assessed by Asaoka, Hyperbolic, piezometer and finite element modeling methods at In-Situ Test Site, 20 months after surcharge placement (Arulrajah et al., 2004j).	289
Table 10.6	Comparison of settlement between finite element modeling results with actual field settlement at Pilot Test Site, 32 months after surcharge placement (Arulrajah et al., 2004j).	293
Table 10.7	Comparison of settlement and degree of consolidation assessed by Asaoka, Hyperbolic, piezometer and finite element modeling methods at Pilot Test Site 32 months after surcharge (Arulrajah et al., 2004j).	293
Table 11.1	Comparison of vertical drain performance verification by settlement and degree of consolidation by various methods 20 months after surcharge (Arulrajah et al., 2004j).	299

LIST OF NOTATIONS

a	Vertical drain width
A_f	Pore pressure at failure (dilatometer test)
AOS	Apparent Opening Size
b	Vertical drain thickness
C_c	Primary compression index
c_h	Coefficient of consolidation due to horizontal flow
c_h'	Effective value of coefficient of consolidation due to horizontal flow
c_{kv}	Hydraulic conductivity change index,
C_r	Recompression index
c_u	Undrained shear strength
c_v	Coefficient of consolidation for vertical flow
c_{vr}	Coefficient of vertical reconsolidation
c_{vi}	Equivalent coefficient of consolidation for vertical consolidation
C_α	Secondary compression index
c_{ref}	Cohesion
D	Diameter of field vane
D/d	Drain spacing ratio
D_{85}	Size for 85% of passing of the soil particle.
D_{50}	Size for 50% of passing of the soil particle.
D_{15}	Size for 15% of passing of the soil particle.
D_{10}	Size for 10% of passing of the soil particle.
d_e	Diameter of equivalent soil cylinder
d_s	Diameter of smeared zone
d_w	Diameter of vertical drain
E_D	Dilatometer modulus
E_{oed}	Oedometer modulus
E_{ref}	Young's modulus
e_o	Initial void ratio
$F(n)$	Vertical drain factor
$F_s(n)$	Smear effect
F	Shape factor (BAT permeameter)
f_s	Sleeve friction (cone penetration test)
F_s	Reduction factor for permeability of vertical drains.
G	Shear modulus (self boring pressuremeter test)
G_{ref}	Shear modulus

G_s	Specific gravity
H	Thickness of clay layer
H_o	Thickness of clay layer
H_{dr}	Drainage path thickness
H_{dri}	Equivalent drainage path thickness
H_{Ti}'	Total equivalent thickness of all layers
I_D	Material index (dilatometer test)
K_D	Horizontal stress index (dilatometer test)
K_0	Coefficient of earth pressure at rest.
k	Permeability
k_e	Equivalent horizontal permeability of surrounding soils,
k_h	Horizontal hydraulic conductivity of soil
k_{hpl}	Horizontal permeability of undisturbed zone in plane strain unit cell
k_{hax}	Horizontal permeability of undisturbed zone in axi-symmetric unit cell
k_v	Vertical hydraulic conductivity of soil
k_r	Horizontal hydraulic conductivity of remoulded soil
k_f	Permeability of the vertical drain filter.
k_s	Permeability of the soil.
k_s	Horizontal permeability of soil within the smear zone
k_{sax}	Horizontal permeability of the smear zone in axi-symmetric unit cell
k_w	Coefficient of longitudinal permeability of the vertical drain
l_m	Length of vertical drain.
L	Vertical drain well resistance parameter
m	Slope of Hyperbolic plot
mCD	Admiralty chart datum in meters
m_v	Coefficient of volume compressibility
N_p	Pressuremeter constant (self boring pressuremeter test)
N_{KT}	Cone factor (cone penetration test)
n	Drain spacing ratio
n_i	Influence ratio
n	Porosity of the filter
OCR	Overconsolidation ratio
O_{95}	Apparent Opening Size of the filter.
O_{50}	Size which is larger than 50% of the fabric pores.
O_{15}	Size which is larger than 15% of the fabric pores.
PI	Plasticity index
P_0	Absolute initial system pressure (BAT permeameter)

P_t	Absolute pressure at time t (BAT permeameter)
q_c	Cone resistance (cone penetration test)
q_{req}	Required discharge capacity of vertical drain
q_w	Discharge capacity of vertical drain
q_T	Corrected cone resistance (cone penetration test)
R	Radius of cone shaft
R	Well resistance factor
r_e	Radius of influence zone
r_w	Equivalent radius of vertical drain
r_s	Radius of smear zone
s_i	Settlement at time i
S_t	Sensitivity of clay
S_t	Settlement at time t
S_{ult}	Ultimate settlement
s	Vertical drain spacing
s	Smear zone ratio
T	Time factor at 50% normalised excess pore pressure
T	Maximum measured torque (field vane shear test)
T_h	Time factor for consolidation by horizontal drainage
T_r	Time factor for consolidation by horizontal drainage
T_v	Time factor for consolidation by vertical drainage
t_{flex}	Time corresponding to point of reverse curvature on decay curve (dilatometer test)
U_i	Initial excess pore pressure
U_r	Average degree of consolidation with respect to radial flow
U_t	Excess pore pressure at time “ t ”
U_0	Static pore water pressure
U_v	Average degree of consolidation with respect to vertical flow
U_{vr}	Average degree of consolidation for combined vertical and radial flow,
$U\%$	Degree of consolidation
\bar{u}	Normalized excess pore pressure at time t (cone penetration dissipation test)
u	Pore pressure at time t (cone penetration dissipation test)
u_i	Initial pore pressure (cone penetration dissipation test)
u_0	Static pore pressure (cone penetration dissipation test)
u_{bt}	Pore pressure due to penetration (cone penetration test)
V_0	Initial gas volume (BAT permeameter)

z	Depth below seabed in meters
α	Theoretical slope factor for Hyperbolic plot
β	Slope of the constructed straight line of the Asaoka's plot
Δt	Selected time interval for Asaoka's plot
$\Delta\sigma$	Additional pressure due to fill placement
$\Delta\sigma'$	Additional preloading pressure
γ	Soil unit weight
γ_{bulk}	Bulk density
γ_w	Unit weight of water
γ_0	Radius of cavity
φ	Friction angle
κ^*	Modified swelling index
λ^*	Modified compression index
μ	Poisson ratio
ν	Poisson's ratio
σ_f	Final vertical effective stress
σ_c	Preconsolidation pressure
σ_o	Effective overburden pressure
σ_{ho}	Total lateral stress
σ_{ho}'	Effective lateral stress
σ_v'	Effective vertical stress of the soil
σ_{vo}	Total vertical stress
σ_{vo}'	Effective vertical stress
σ_y'	Effective yield stress
ψ	Dilatancy angle

1.0 INTRODUCTION

1.1 Objectives of the Research

This research study will provide a contribution to the field of Civil/Geotechnical Engineering particularly with regards to the field instrumentation, in-situ testing and finite element modeling of marine clays under reclamation fills at coastal regions. The objectives for this research study can be outlined as follows:

- (1) Characterisation of strength, consolidation, physical and mineralogical characteristics of Singapore marine clay at Changi. This includes a study into the geology and formation history of Singapore marine clay.
- (2) Description of offshore land reclamation methodology and associated dredging plants.
- (3) Description of the various theories and design processes involved in the design of a ground improvement project with vertical drains. The properties and installation methodology of the prefabricated vertical drains will also be described. Design predictions of a case study area was carried out and compared to field instrumentation results.
- (4) Description of testing procedures and comparison of the results of various in-situ testing methods carried out in Singapore marine clay. This includes in-situ penetration testing and long term dissipation tests.
- (5) Study of the increase in shear strength, stress history, degree of consolidation and effective stress of the Singapore marine clay under surcharge loading by means of in-situ testing and laboratory testing.
- (6) Determination of the coefficient of consolidation due to horizontal flow and horizontal hydraulic conductivity of the Singapore marine clay by means of in-situ dissipation tests.

- (7) Comparison of the in-situ testing results carried out after surcharge loading with the prior to reclamation results. Also a comparison of the in-situ testing of a sub-area area treated with vertical drains and surcharge with an adjacent untreated sub-area which was only surcharged.
- (8) Description of the type of field instrumentation suitable for the study of marine clay especially pertaining to those installed to monitor land reclamation projects.
- (9) Study of the assessment of field settlement gauges to predict ultimate settlement, degree of consolidation and coefficient of consolidation due to horizontal flow of marine clays.
- (10) Study of the assessment of piezometers to obtain the piezometric elevations, excess pore pressures, degree of consolidation and coefficient of consolidation due to horizontal flow of marine clays.
- (11) Comparison of the field instrumentation results of sub-areas treated with various spacings of vertical drains and surcharged with that of an adjacent untreated sub-area which was only surcharged.
- (12) An in-depth study into the factors that affect field instrumentation assessment of marine clay treated with prefabricated vertical drains. The factors that affect the assessment by the Asaoka, Hyperbolic and piezometer assessment methods were studied in detail, compared with each other and the findings reported.
- (13) Finite element modeling of prefabricated vertical drains and marine clay. Comparisons between the finite element modeling results and the actual field surface settlement to ascertain the accuracy of the soil model.
- (14) Performance verification of prefabricated vertical drains by various methods this being by back-analyses using c_h from Asaoka method, proposed modified Asaoka equation, conventional calculation and finite element modeling method.

1.2 Background to the Research

Land reclamation is carried out in large magnitudes in the Southeast Asian region. Marine clays is generally found in the near shore of the countries in this region and as such, land reclamation on this highly compressible soil foundation often requires the use of soil improvement works to eliminate significant future settlements from occurring due to the future imposed dead and live loads. The decision on which viable ground improvement technique to use depends generally on the future use, importance, and construction period of the project area. The simplest ground improvement technique is to put a surcharge preload of equal to or higher than the anticipated future load so as to preconsolidate the soil to the required effective stress. However, due to large vertical drainage paths of thick marine clay deposits, this technique often requires a long consolidation period, which is not ideal in many land reclamation or infrastructure projects.

The combination of prefabricated vertical drains and preloading with surcharge is a viable ground improvement option in such critical projects as they reduce the period for consolidation due to the introduction of shorter radial drainage paths. The combination of prefabricated vertical drains and surcharge is one of the most widely used and economical ground improvement methods in such land reclamation projects in the region and worldwide. The surcharge height to be placed will depend on the future-working load and allowances have to be made for the submergence effect and anticipated settlement during the design preloading period.

In such ground improvement projects, it is essential to have a good in-situ testing and field instrumentation programme so as to characterise and assess the deformation behaviour of the marine clay under the preload. These field measurement methods are used to assess the degree of consolidation of the marine clay under the surcharge load and to determine when the required degree of consolidation is achieved to enable the removal of the surcharge. As surcharge can only be removed after the clay has attained the required effective stress increase, it is vital to correctly assess the degree of consolidation of the improved clay prior to the commencement of surcharge removal works.

The data for this research study was obtained from a land reclamation and ground improvement project in the Republic of Singapore which the author was personally involved with for several years. Data was gathered before, during and after soil improvement works.

The research studied the various in-situ test results and the field instrumentation monitoring data, to determine the characteristics and behaviour of marine clay under reclamation fill. In-situ testing was carried out in one of the case study sites prior to reclamation and after the completion of surcharge loading. Field instrumentation results were monitored, assessed and back-analysed at two case study sites. Finite element modeling was carried out and the results of the modeling were compared to the field surface settlement.

1.3 Significance

This research is to serve as a reference guide for future land reclamation and ground improvement projects on soft clay. Actual field monitored case studies of the instrumentation works will serve as a future reference to the behaviour of marine clay under reclaimed fill and after ground improvement. The field instrumentation back-analysis methods used, will bring to light the various factors that affect the assessment of the marine clay treated with vertical drains as predicted by the Asaoka (1978), Hyperbolic (Tan, 1993) and piezometer (Arulrajah et al., 2003a) back-analysis methods. These methods are the best known back-analysis methods relevant for soft soils. Studies of the various factors that affect field instrumentation assessment of soft soil, have not been carried out in such depth previously. Finite element modeling of marine clay with vertical drains was carried out by means of the axi-symmetric unit cell and full scale analysis methods. Finite element modeling of marine clay without vertical drains was carried out by means of full scale analysis method.

Various in-situ testing methods as well as their interpretation will be highlighted in the study. The in-situ tests consist of penetration tests for the study of the shear strength increase, effective stress gain and degree of consolidation of the marine clay after surcharge loading. In-situ dissipation tests were carried out to determine the hydraulic conductivity and coefficient of consolidation due to horizontal flow of the marine clay before reclamation and after surcharge loading.

The study will highlight the various processes involved and methodology of carrying out land reclamation and installation of vertical drains. The design methodology of these works will also be highlighted so as to serve as a guide for future ground improvement and land reclamation projects.

1.4 Identification of the Research Needs

Field instrumentation methods, assessment and back-analysis based on case studies of marine clay behaviour forms the crux of this research. The factors that affect the field instrumentation assessment of marine clays treated with prefabricated vertical drains forms an integral part of this research study. Finite element modeling and in-situ testing of marine clay is also of importance in this research study.

Most ground improvement projects using prefabricated vertical drains specify the requirement for a certain degree of consolidation of the design surcharge load to be attained prior to the removal of surcharge. As such, the assessment of the degree of consolidation of the underlying soil is of critical importance for the determination of when the surcharge load can be removed. The assessment of the degree of consolidation of the marine clay as such has enormous technical, construction and financial implications for such ground improvement projects. The method of assessment of the degree of consolidation of the marine clay can be carried out by means of in-situ testing and field instrumentation methods.

Accurate prediction of the magnitude and time rate of settlement is dependent upon the selection of soil parameters and the engineer's judgment. In most cases, the prediction of ultimate settlement can be well predicted. However, field time rate of settlement is often slower than the predicted rate of settlement by use of conventional equations based on laboratory test results.

In most land reclamation projects, the coefficient of consolidation due to horizontal flow is assumed as twice that of vertical flow (Bo, Arulrajah and Choa, 1997b). In this study, the determination of coefficient of consolidation due to horizontal flow was carried out by various in-situ testing methods. Furthermore, the determination of coefficient of consolidation due to horizontal flow was also carried out from the back-analysis of the field instrumentation monitoring results. The predicted settlement curves for time rate of settlement of vertical drain improved area by the conventional design and finite element modeling methods was compared to the actual field settlement curves.

1.5 Research Method

In this study, various methods of analysis comprising in-situ testing, field instrument monitoring, laboratory testing and finite element modeling was used to ascertain the degree

of consolidation and back-analysed geotechnical parameters of the improved soil with vertical drains at field test sites. The research site in this study comprises of two field testing sites consisting of sub-areas of various vertical drain spacings. The type of ground treatment carried out at the treated sub-areas was with vertical drains and preloading while the untreated control sub-area was only preloaded. This enabled a comparison of in-situ testing, field instrumentation and laboratory results between the adjacent treated and untreated sub-areas. The entire planning, implementation, supervision and monitoring of the works in this research inclusive of land reclamation, ground improvement, in-situ testing, laboratory testing and field instrumentation works was carried out by the author during his involvement in the project.

The research was first carried out with an extensive literature review to ensure that the subject and problems were well understood. The literature review covered all aspects of the research and included land reclamation, preloading with vertical drains, marine clay characterisation, in-situ testing, laboratory testing, field instrumentation and finite element modeling of vertical drains.

Following this, the characterisation of the engineering properties of the marine clay at the research site was carried out prior to reclamation. The marine clay characterisation was carried out based on the findings of laboratory and in-situ tests carried out at the Project Site. Subsequently, an extensive site characterization was carried out to carefully and accurately predict the soil parameters of the Singapore Marine Clay. Clay mineralogy photos and close-up photographs of the marine clay were taken to assist in the characterisation of the marine clay.

The methods of offshore land reclamation technology and preloading with vertical drains was studied and elaborated on. The design theories and concepts of prefabricated vertical drains were reported in detail.

A series of in-situ tests was next carried out at the In-Situ Test Site prior to reclamation by means of various in-situ testing methods. to assess the degree of improvement of the marine clay in the Vertical Drain Area as well as in the adjacent untreated Control Area. A series of in-situ tests using the field vane shear, self-boring pressuremeter, dilatometer, cone penetration and BAT permeameter tests were carried out at the In-Situ Test Site prior to reclamation. The in-situ tests were analysed to obtain the in-situ shear strengths, over-consolidation ratios and effective stress of the marine clays. A series of in-situ tests were also carried out after surcharge loading and the results were compared with the results

obtained prior to reclamation. In-situ dissipation tests were also carried out in the In-Situ Test Site to obtain the coefficient of horizontal consolidation and horizontal hydraulic conductivity of the marine clay prior to reclamation and after surcharge loading.

Field instruments were installed in two Case Study Areas, this being the Pilot Test Site and In-Situ Test Site prior to the installation of prefabricated vertical drains. The case study sites consist of vertical drains installed at various spacings as well as an untreated control sub-area. Surcharge of the same height was placed over each of the sub-areas at each of these Case Study Areas. The surcharge load was left at the Pilot Test Site for 32 months and at the In-Situ Test Site for 20 months. Soil instruments comprising surface settlement plates, deep settlement gauges and piezometers installed just prior to the installation of the vertical drains were analysed. Instrument readings were also taken at close frequencies. Instrumented data collected from the case study areas were analysed at various durations after the completion of surcharge placement. Comparison were carried out between the instruments in the various vertical drain sub-areas for which different spacings of vertical drains were installed as well as the untreated control sub-area. The degree of consolidation of the marine clay was determined after the preloading period at the various sub-areas by assessment of the settlement gauges and piezometers.

An in depth and exhaustive study was carried out for the three vertical drain sub-areas of the Pilot Test Site to determine the various factors that affect the field instrumentation assessment of marine clay treated with prefabricated vertical drains. Factors affecting the assessment by the Asaoka, Hyperbolic and piezometer methods were investigated and compared. This study has not been carried out to such depths and details in the past and the author has made significant findings on this aspect of the research.

The settlement plates at the three vertical drain sub-areas of the Pilot Test Site were back-analysed by the Asaoka and hyperbolic methods to determine the estimated ultimate settlement and coefficient of consolidation due to horizontal flow of the marine clay under the surcharge load. The settlement gauge readings between the various sub-areas were compared to ascertain the difference in magnitude and degree of consolidation due to the installation of the various drain spacings. Back-analysis of the settlement behaviour of the marine clays with vertical drains was compared with the design predictions. A study was carried out to determine the influence of time interval on the prediction of ultimate settlement by the Asaoka and hyperbolic methods. This was carried out by varying the time intervals and time of assessment of the settlement plate readings. The degree of

consolidation of the marine clay was determined after the preloading period at the various sub-areas by assessment of the settlement gauges.

Piezometers were analysed at the Case Study Areas to obtain the piezometric elevations, excess pore water pressures and degree of consolidation of the marine clay at various periods of preloading time. The piezometer readings for the various sub-areas were compared to ascertain the difference in piezometric elevations, excess pore water pressure and degree of consolidation due to the installation of the various drain spacings. The piezometer readings were corrected for the effect of large strain settlement of the piezometer tip by using the deep settlement gauge readings from deep settlement gauges which are installed at or close to the same elevation of the piezometer. Water stand-pipes were installed in each of the sub-areas to enable interpretation of the piezometer readings. The water stand-pipe readings were used to determine the static water pressure and this enabled the excess pore water pressure of the piezometers to be calculated. Factors affecting the assessment of piezometers such as correction for large strain settlement of the piezometer tip due to the reclamation load were also studied in detail and its findings reported. The degree of consolidation of the marine clay was determined after the preloading period at the various sub-areas by assessment of the piezometers and this was compared with the settlement gauge results.

Finite element modeling of marine clay and prefabricated vertical drains under reclamation fill was studied by means of the Plaxis Version 8 (2002) numerical modeling software. The finite element modeling was carried out for the In-Situ Test Site and the Pilot Test Site consisting of vertical drain treated areas and an untreated control area. Prefabricated vertical drains were modelled by both the axi-symmetric unit cell and full scale analysis methods. The untreated marine clay was modelled by the full scale analysis method. The finite element modeling results were compared with the actual field settlement.

Performance verification of prefabricated vertical drains was studied at the In-Situ Test Site by various methods this being by back-analyses using c_h from Asaoka method, proposed modified Asaoka equation, conventional calculation and finite element modeling method. The results were also compared to that of using the back-analysed coefficient of horizontal flow for the conventional and finite element modeling methods.

1.6 Thesis Organisation

The thesis has been divided into various chapters to highlight the various aspects of the study:

Chapter 1 consists of an introduction into the entire research study in general and highlights the needs, scope, objectives, methodology and organisation of the study.

Chapter 2 consists of literature review of the following: ground improvement of soft clay, land reclamation, prefabricated vertical drains, field instrumentation of marine clays, in-situ testing of marine clays, laboratory testing of marine clays and finite element modeling of prefabricated vertical drains.

Chapter 3 describes the characteristics and mineralogy of Singapore marine clay. The chapter describes the site investigation methods in land reclamation projects. The consolidation characteristics, physical characteristics and undrained shear strength of the Singapore marine clay at Changi are described in this chapter. The mineralogy, geology, formation history and photographic identification of Singapore marine clay is also described in this chapter.

Chapter 4 describe the methodology and the affiliated dredging plant used in land reclamation works.

Chapter 5 describes the vertical drain history, functions, properties, quality control testing and installation methods. The design methodology and associated theories involved in the design process of prefabricated vertical drains is also described in this chapter.

Chapter 6 describes the location and the characterisation of the In-Situ Testing Site comprising the Vertical Drain Area and the untreated Control Area prior to reclamation and after surcharge loading by means of in-situ testing. The various in-situ tests used in the characterisation study of Singapore marine clay in the testing site is described. Also covered in this chapter is the interpretation of stress history, shear strength, effective stress and degree of consolidation by the various in-situ testing methods. The interpretation of in-situ dissipation tests prior to land reclamation and after surcharge loading by the various testing methods is also described in this chapter.

Chapter 7 discusses the various types of field instrumentation involved in offshore, on-land and long term field instrumentation works for land reclamation projects on soft clay. The various types of settlement gauges and piezometers and the methods of assessment and back-analyses of their field measurements are discussed in the chapter. Furthermore, the use of inclinometer, deep reference point and total pressure cell is also discussed in the chapter.

Chapter 8 describes the field instrumentation case study at two locations within the project site. The settlement gauges and piezometers are assessed and back-analysed in this chapter. The degree of consolidation and coefficient of consolidation due to horizontal flow is also determined at these two test locations.

Chapter 9 studies the various factors that affect the field instrumentation assessment of marine clay treated with prefabricated vertical drains. The various factors that affect assessment by the Asaoka, Hyperbolic and piezometer assessment methods are described in depth and compared in this chapter.

Chapter 10 studies the finite element modeling of marine clay and vertical drains. The vertical drains are modelled in this chapter by both the axi-symmetric unit cell and full scale analysis methods while the untreated adjacent embankment is modelled by the full scale analysis method. The modeling results are also compared with the actual field settlements.

Chapter 11 studies the performance verification of prefabricated by various methods this being by back-analyses using c_h from Asaoka method, proposed modified Asaoka equation, conventional calculation and finite element modeling method. The results were also compared to that of using the back-analysed coefficient of horizontal flow for the conventional and finite element modeling methods.

Chapter 12 concludes the findings of this research study.

2.0 LITERATURE REVIEW

Land reclamation on soft compressible clays for vital facilities requires some form of ground improvement. The prefabricated vertical drain with preloading method is a popular and well documented method of soil improvement of compressible soils. Prefabricated vertical drains are used to accelerate the consolidation of the marine clays. This method of ground improvement was used in the ongoing Changi East Reclamation Project in the Republic of Singapore. Prior to the removal of the surcharge load, the degree of improvement attained by the foundation soil must be ascertained to confirm whether the design criteria has been achieved. The determination of the degree of improvement of the soft soil can be determined by means of field instrumentation, in-situ testing and finite element modeling.

Field instrumentation monitoring is the only means available of providing continuous records of the ground behaviour from the point of instruments installation. Without a proper soil instrumentation method or program, it would be impossible to monitor the current degree of improvement of the soil at any point of time. By analyzing the field instrument monitoring results, it is possible to verify the degree of consolidation of the foundation soil before allowing the removal of the surcharge load. During the process of consolidation, the settlement gauges monitoring data was analyzed by means of the Asaoka and Hyperbolic methods to determine the ultimate settlement and degree of consolidation of the underlying soft marine clay due to the fill and surcharge load. Piezometer monitoring data was used to determine the dissipation of excess pore water pressures and degree of consolidation of the marine clay.

The main objective of this research is the field measurements and back-analysis of marine clay geotechnical characteristics under reclamation fills by means of field instrumentation and in-situ testing. The various factors that affect predictions of degree of consolidation and back-analysed coefficient of consolidation due to horizontal flow of the soft soil by means of field instrumentation, were analysed and reported. The various factors such as time interval and time of assessment of the settlement plate and piezometer data was studied in this research to ascertain their influence on the assessment of the ultimate settlement and degree of consolidation of the marine clay. There has been very little previous study on this aspect of field instrumentation assessment of marine clay behaviour under reclamation fills prior to this research study. The author has carried out extensive analysis and reported on this particular aspect of field instrumentation and as such, this forms an important aspect of this research.

In the last two decades, there has been an emergence of in-situ testing methods as an alternative to laboratory testing methods. The geotechnical strength and overconsolidation parameters of the soft soil as well as the permeability and consolidation properties of the soil particularly in the horizontal direction are important design parameters in vertical drain projects. In-situ testing and in-situ dissipation tests have emerged as a useful method to obtain the required geotechnical parameters for the design of vertical drain projects. The in-situ penetration and dissipation tests were carried out with the field vane, piezocone, flat dilatometer, self-boring pressuremeter and BAT permeameter.

In-situ penetration tests were conducted to determine the undrained shear strength and overconsolidation ratio of the marine clay prior to and after surcharge loading. In-situ dissipation tests provide a means of evaluating the in-situ coefficient of horizontal consolidation and horizontal hydraulic conductivity of marine clays, prior to and after surcharge loading. In-situ dissipation testing is an alternative to traditional laboratory testing methods to determine the horizontal consolidation and permeability parameters of soft soil. These tests can be conducted at various levels in the marine clay and hence variations of the horizontal coefficient of consolidation and horizontal hydraulic conductivity with depth can be obtained. The determination of these geotechnical parameters is traditionally based on laboratory tests. However laboratory testing does not yield appropriate properties of soil due to different loading, drainage conditions and sample disturbance as compared to the actual in-situ soil condition.

The performance of the prefabricated vertical drains were also predicted by the finite element modeling method and the results compared to that of the field instrumentation at two case study areas. The analyses included the modeling of the consolidation behaviour of marine clay under reclamation fills with and without prefabricated vertical drains. Modeling of the sub-areas treated with vertical drains was carried out by both the axi-symmetric unit cell and full-scale analysis methods. Modeling of untreated control sub-areas was carried out by the full-scale analysis method.

2.1 Distribution of Marine Clay Deposits in Southeast Asia

Soft clays are fairly widespread and the majority of these are of marine origin. Several extensive deltaic deposits exist in Southeast Asia as indicated in Figure 2.1, some of which are of considerable importance because of their occurrence at the sites of major cities. Soft clays present severe but interesting geotechnical engineering problems (Brand et al., 1989). By their nature, soft clays are of low strength and high compressibility, often with water contents at or close to their liquid limits (Skempton, 1969). Although they are commonly normally consolidated, they nearly always exhibit light over-consolidation caused by self-weight consolidation, dessication and the rise and fall of sea levels in the geological past.

The very nature of soft clay deposits of marine origin, is that they are arguably the most interesting soil to work with from the viewpoint of geotechnical engineering. At the same time, marine clays lend themselves wonderfully to field measurements by either field instrumentation or in-situ testing which is not always possible for most other soil types.

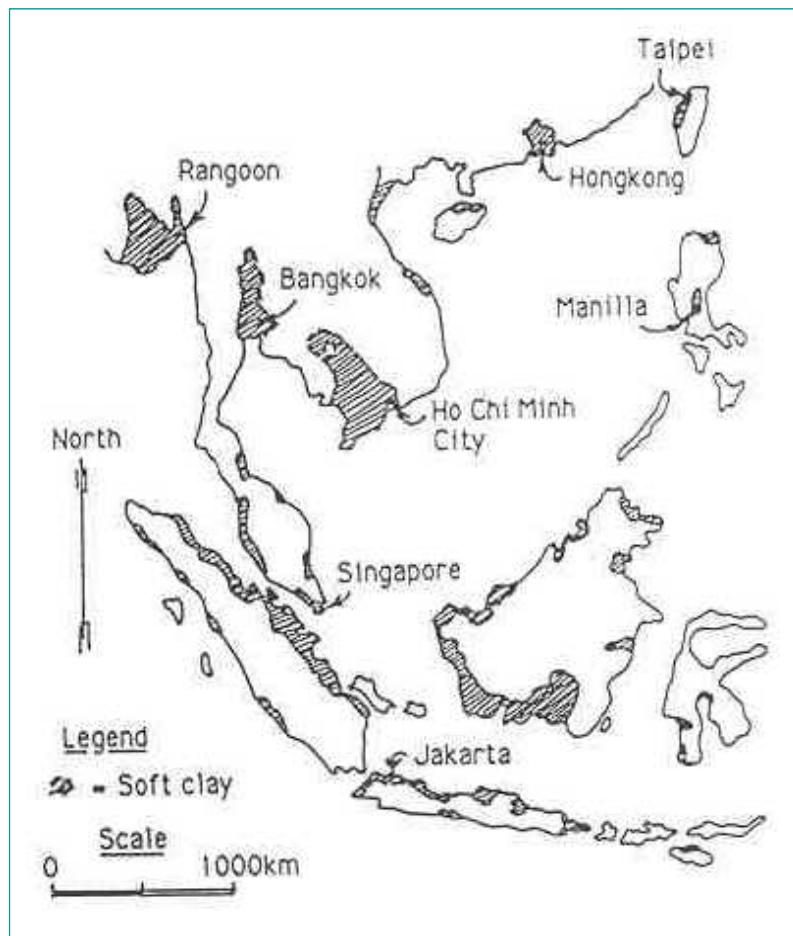


Figure 2.1 Distribution of marine clay deposits in Southeast Asia (After Broms, 1987)

2.2 General Characteristics of Soft Marine Clay

Studies on the general characteristics of marine clays found in the coastal regions of various countries have been carried out to date by various authors.

Tanaka and Tanake (1999) have reported on the characteristics of Ariake clay in Japan. Torrance (1999) has reported on the mineralogy of Ariake clay in Japan. Yashima et al. (1999) and Mimura et al. (2003) have reported on the microstructure and characteristics of Osaka Bay marine clay in Japan. Tsuchida has reported on the natural water content of marine deposits found in Japan. The general characteristics of marine clay in the Taipei Basin of Taiwan have been reported by Lee et al. (1993) and Feng (1993). Kim et al. (1999) have reported on the general characteristics and distribution of marine clay in South Korea.

The characteristics and distribution of Bangkok clay of the Chao Phraya Plain in Thailand has been reported by Bergado et al. (1992) and Shibuya et al. (1999). Balasubramaniam et al. (1993) have also discussed on the general characteristics of Bangkok Clay.

The study of the general geotechnical characteristics of Malaysian marine clay at Muar has been reported by Poulos et al. (1989), Brand et al. (1989) and the Malaysian Highway Authority (1987). The geotechnical characteristics of coastal marine clay at Kuala Perlis has been studied by Hussein et al. (1996). Bo et al. (1998g) and Rahardjo (1998) have reported on the characteristics of marine clay found in the Jakarta Bay in Indonesia.

Leroueil (1999) has reported on the characteristics, geology and mineralogy of Quebec marine clay in Canada. The study of the general geotechnical characteristics of Norwegian marine clay has been reported by Bjerrum (1967). Lunne and Lacasse (1999) have reported on the characteristics of Drammen clay in Norway.

The general characteristics, mineralogy and geology of Singapore marine clay has been described briefly in the past by Bo, Arulrajah and Choa (1998a), Choa et al. (1996) and Yong et al. (1990).

2.3 Land Reclamation

The methods of land reclamation and the types of machinery involved have been discussed in detail in the British Standard (BS 6349: Part 5: 1991). The standard describes the methods of investigation, dredging processes, site control and environmental considerations. Land reclamation experiences in coastal areas in the Republic of Singapore have been elaborated by Bo, Arulrajah, Choa and Chang (1998a), Bo, Arulrajah, Choa and Na (1998d), Na, Choa, Bo and Arulrajah (1998) and Bo et al. (2004).

The land reclamation methodology and characteristics of dredging plant used in the Changi East Reclamation Project in Singapore described in this chapter has been discussed by the author (Arulrajah et al., 2004c) during the course of this research study.

2.4 Ground Improvement with Prefabricated Vertical Drains

There are various ground improvement methods at present that provide soil strength improvement, mitigation of total and differential settlement, shorten construction time, economical construction costs and other characteristics which may impact on their utilisation to specific projects. Factors such as the significance of the structure, applied loading, site conditions, period of construction have to be considered in the selection of the ground treatment method (Bergado et al., 1992).

The various ground improvement methods currently available for soft ground projects include ground improvement by vertical drains, vibro-replacement with stone columns, lime/cement columns and sand compaction piles. With special regard for the ground treatment of marine clays in land reclamation projects, the vertical drain with preloading technique remains the most widely used and economical method employed in this region.

The methods of assessing the performance of vertical drains and preloading techniques by various analytical means inclusive of design predictions, field instrumentation monitoring and in-situ testing was investigated in this research study. The one-dimensional consolidation settlement behaviour of clays is described by Terzaghi (1925). This method when used in conjunction with Barron (1948) and Carrillo (1942) methods can be used for the design of vertical drains. Imai (1995) has also written on the time rate of settlement effect of clays. Bo, Arulrajah and Choa (1997a, 1997b, 1998b), Indraratna and Bamunawita (2002),

Hansbo (1979) and Choa (1981, 1984) have also described the consolidation behaviour of clays by using prefabricated vertical drains.

Holtz et al. (1991) offers an in-depth coverage of the study of vertical drains. Holtz et al. (1991) and Bo et al. (2003a) have also provided in-depth coverage on the method of installation of vertical drains be it static penetration or vibratory driving, types of mandrels and type of shoes.

Bo et al. (2003a), Indraratna and Bamunawita (2002) and Bergado et al. (1992) have also described the use of vertical drains for ground improvement. These publications too have coverage on the theories and mechanisms of vertical drains. The various types of vertical drains and their characteristics are also covered in these publications as well as design methodology and consolidation processes. Case histories of installation of sand drains on soft Bangkok clay, which have been fully instrumented, are covered in the report. In addition, Van Impe (1989), Hausmann (1990) and Schaefer (1997) have also described the theories and mechanisms of vertical drains. Onoue (1988) have suggested a simplified formula for the average degree of consolidation with respect to radial flow. Yoshikuni and Nakado (1974), has described the effects of well resistance on the vertical drain permeability and provided coefficients to be used.

Choa (1981, 1985) has discussed on the combination of vertical drains with preloading. Choa (1981, 1985) has also discussed on the design of the preloading and the dissipation of excess pore water pressure with time as well as encompassing the design theories and concepts of vertical drains. Special attention is also paid to the back analysis of field observation data to obtain the ultimate settlement and coefficient of consolidation due to horizontal flow by means of the Asaoka method. Case study of instrumented embankments with various vertical drain spacing at the Changi Airport second runway reclamation which were carried out in the 1970's has also been described. Choa et al. (1984, 1985) has also discussed the methods of installation of vertical drains as well as the field instrumentation and assessment of performance of vertical drains in Singapore marine clays.

Bo et al. (1998f, 2000b) and Indraratna and Redana (1998) have discussed the study of the smear effect of vertical drains due to mandrel penetration. Field results have also been verified with laboratory results. Permeability results before and after mandrel penetration in Singapore marine clays have also been compared in the studies. Bo et al. (2000d) has also studied the comparison of various vertical drains at different drain spacing for Singapore marine clays. Bo et al. (2000d) have made special reference to the laboratory testing of the

discharge capacity of vertical drains under straight and buckled conditions and also the reduction of discharge capacity with hydraulic gradient.

With particular reference to land reclamation projects in Singapore, Choa et al. (1995) and Bo, Arulrajah and Choa. (1998a) have in-depth descriptions of the investigation, design and construction processes involved. Holtz et al. (1991) has provided in-depth coverage on the method of installation of vertical drains be it static penetration or vibratory driving, types of mandrels and type of shoes.

The various theories, considerations, design methodologies and design predictions for the ground treatment of marine clay with prefabricated vertical drains in such off-shore projects has been discussed by the author (Arulrajah et al., 2004m) during the course of this research study.

2.5 Field Instrumentation of Marine Clays

Field instrumentation of the case study areas in this research study comprises of settlement plates, deep settlement gauges, pneumatic piezometers, electric piezometers and water stand-pipes. The instruments were monitored for a long duration enabling the behaviour of the marine clay to be assessed under the reclaimed fill and surcharge load. The settlement gauge readings were analysed to ascertain the ultimate settlement of the marine clay and the corresponding degree of consolidation under the reclaimed fill. Piezometers were analyzed to obtain the piezometric elevations, excess pore water pressures and degree of consolidation at various stages of the preloading period. Comparisons were carried out between the instrumented readings for various vertical drain sub-areas as well as an adjacent untreated control sub-area.

The field instrumentation case studies and assessment of marine clay in offshore land reclamation works described in this thesis have been discussed in detail by the author (Arulrajah et al., 2003a, 2003b, 2004b, 2004c, 2004e, 2004g, 2004l) during the course of this research study.

2.5.1 Necessity and Shortcomings of Field Instrumentation

Prior to the removal of surcharge in ground improvement projects with vertical drains, the degree of consolidation attained by the foundation soil must be ascertained to confirm whether the design criteria has been achieved. Field instrumentation is the only means available of providing continuous day to day records of the ground behaviour from the time of instrument installation. Without a proper soil instrumentation method or program, it would be difficult to monitor the current degree of improvement of the soil. By analysing the field instrumentation monitoring results, it is possible to assess the degree of consolidation of the foundation soil before allowing the removal of the surcharge load. It will also be possible to ascertain the achievement of required effective stress and to indicate the necessity for remedial action.

Care must be taken in interpretation of monitoring data, as some correction may be required. For instance, correction for settlement of piezometer tip is required to obtain actual piezometric elevation of the pore water. Instruments are also subject to damage at site due to malfunctioning instruments and movement of machinery. Instruments must be installed correctly at site following required guidelines and to the correct levels. Manpower is required to monitor the instruments regularly. Monitoring records have to be correctly recorded. Monitoring reports have to be carefully studied and interpreted.

2.5.2 Settlement Gauges

Bo, Arulrajah and Choa (1997a, 1998b) and Choa (1984, 1985) have previously published on the use and case studies by the Asaoka and Hyperbolic method for the estimation of ultimate settlement in land reclamation projects. These publications describe how the degree of consolidation of marine clays under reclamation fills can be ascertained from the settlement plate readings. Tan (1993, 1995, 1996) and Bujang (1996, 2002) have published on the estimation of ultimate settlement from field settlement by means of the Hyperbolic method. Tan (1996) and Bo et al. (1999) have also previously compared between the estimation of ultimate settlement by the Hyperbolic and Asaoka methods.

The assessment of field settlement plates by the Asaoka and Hyperbolic methods described in this thesis have been discussed in detail by the author (Arulrajah et al., 2003a, 2003b, 2004b, 2004c, 2004e, 2004g) during the course of this research study.

2.5.3 Piezometers

Bo, Arulrajah and Choa (1998b) and Choa (1984, 1985) have previously published on the use and case studies of pneumatic and vibrating wire piezometers installed in land reclamation projects. These publications describe the methods used to obtain the degree of consolidation of the marine clays under the surcharge loads. These publications describe the methods used to obtain the degree of consolidation of the marine clays under the surcharge loads. These publications also elaborate on suitable protection methods for piezometers and the need for correction of the piezometer tip settlement. Hanna (1985) and Dunnycliff (1988) have also published comprehensive books on field instrumentation describing the types of instruments, planning of instrumentation, method of instalment and method of measurement of various instruments. The assessment of piezometers described in this thesis have been discussed in detail by the author (Arulrajah et al., 2003b, 2004b, 2004c, 2004e, 2004g, 2004i) during the course of this research study.

2.5.4 Factors Affecting Field Instrumentation Assessment of Marine Clay

The influence of factors such as time interval and time of assessment of the settlement plate and piezometer data was studied in this research to ascertain their influence on the assessment of the ultimate settlement and degree of consolidation of the marine clay. There has been very little study on this aspect of field instrumentation with respect to marine clays subject to reclaimed fill prior to this research study. Factors that affect prediction by the Asaoka method are the period of assessment after surcharge placement as well as the time interval used for the analysis. Factors that affect prediction by the Hyperbolic method are the period of assessment after surcharge placement. Factors that affect the analysis of piezometers include period of assessment, hydrogeologic boundary condition, settlement of piezometer tip and reduction of initial imposed load due to submergence effect (Arulrajah et al., 2003a, 2004a, 2004e).

Factors affecting field instrumentation assessment of marine clay treated with prefabricated vertical drains described in this thesis have been discussed in detail by the author (Arulrajah et al., 2003a, 2004a, 2004e) during the course of this research study.

2.5.5 State of the Art: Field Instrumentation

Other field instruments used in ground improvement projects include, multilevel settlement gauges, inclinometers, liquid settlement gauges and earth pressure cells. Of late, long-term remote monitoring instrument clusters in which instruments are connected to an automatic data acquisition system powered by battery and solar panels have been used in large ground improvement projects. This multi-tasking operating system allows for continuous logging,

control and storage of all measurements taken from the site under all weather conditions. Due to the auto-logging capabilities of the acquisition system, no manual monitoring of the instrument readings is necessary. In the long-term instrument clusters, the liquid settlement gauges and electric piezometers are the common instruments. Currently, the hydrostatic profile gauge is also commonly used in embankment projects.

2.6 In-Situ Testing of Marine Clays

In-situ testing works in this research study comprises the use of field vane shear, piezocone, flat dilatometer, self-boring pressuremeter and the BAT permeameter by means of penetration testing and dissipation tests. All these in-situ testing methods used have been well proven for use in soft clays. Studies of various in-situ testing in Singapore marine clays at reclamation projects have been out particularly by Bo, Arulrajah, Choa and Chang (1998a), Bo, Chang, Arulrajah and Choa (2000a), Choa (1984, 1985) and Chang et al. (1986, 1997).

The in-situ testing of marine clay described in this thesis has been discussed in detail by the author (Arulrajah et al., 2004d, 2004f, 2004i, 2004h, 2004o, 2004p) during the course of this research study.

2.6.1 Necessity and Shortcomings of In-Situ Testing

In-situ testing can be used to assess the degree of improvement of soils. In every ground improvement project with vertical drains, the duration of the preloading period is set in advance based on the predetermined time rate of consolidation of the compressible layer. If prediction is accurately done, the required degree of consolidation is met at the predetermined preloading time. As such, there is a requirement for in-situ tests to be carried out just prior to the removal of surcharge to assess the degree of consolidation of the improved ground. In-situ tests may also determine the shear strength, overconsolidation ratio and effective stress gain of the foundation soil.

The cost for mobilisation and testing can be relatively high depending on the type of test to be carried out. The operator's experience is important to the quality of the test. Various checks and calibrations have to be meticulously carried out prior to the testing. The test equipment will require regular maintenance and servicing. Different in-situ tests could provide different test results when compared to each other. As such, engineering experience is required to decipher the actual soil properties. Various empirical equations are used in the

evaluation of soil properties by these in-situ tests and as such site-specific refinements of the empirical equations may have to be carried out.

2.6.2 *Field Vane*

The use of the field vane shear tests as well as the determination of the undrained shear strength has been described by the Norwegian Geotechnical Society (1979), Flaate (1966) and Aas (1967). Most geotechnical textbooks similarly cover the field vane shear test, as it is arguably the most common equipment used for the determination of the undrained shear strength of soft clays. Mayne and Mitchell (1988) have provided an interpretation method of the overconsolidation ratio of clays by using the field vane shear test results.

The in-situ testing of marine clay with the field vane described in this thesis has been discussed in detail by the author (Arulrajah et al., 2004d, 2004h, 2004p) during the course of this research study.

2.6.3 *Piezocone*

The piezocone has seen a surge in its use in soft clays in this region as a better alternative to other crude field testing equipments notably the Mackintosh probe and the standard penetration test. Campanella and Robertson (1988) have described the standard guidelines for the use of the piezocone test equipment. The authors have also provided various interpretation charts to be used in conjunction with the cone penetration test results. Sugawara (1988) has provided a method of estimating insitu overconsolidation ratio of clays by using the piezocone test. Baligh and Levadoux (1980), De Beer et al. (1988) and Gupta et al. (1983, 1986) have written on the piezocone dissipation test methods and the determination of the excess pore water pressure in clays. By this determination of the excess pore pressures in the clay, the degree of consolidation of the clay can be easily calculated.

The in-situ testing of marine clay with the piezocone described in this thesis has been discussed in detail by the author (Arulrajah et al., 2004d, 2004f, 2004i, 2004h, 2004p) during the course of this research study.

2.6.4 *Flat Dilatometer*

Marchetti (1980, 1981, 1989) has provided a detailed description of the flat dilatometer and its interpretation methods. The determination of undrained shear strength and overconsolidation ratio from dilatometer tests has been extensively covered by Marchetti (1980) and Chang (1986, 1997). Chang (1986) has described the methods and interpretation of flat dilatometer dissipation tests. The method of interpretation of coefficient of

consolidation due to horizontal flow values from dilatometer holding tests have been described by Marchetti and Totani (1989).

The in-situ testing of marine clay with the flat dilatometer described in this thesis has been discussed in detail by the author (Arulrajah et al., 2004d, 2004f, 2004i, 2004h, 2004o, 2004p) during the course of this research study.

2.6.5 *Self-Boring Pressuremeter*

Mair and Wood (1987) have described the methods of testing of various pressuremeters including the self-boring pressuremeter. Windle and Wroth (1997) has described the determination of the undrained properties of clay by means of the self-boring pressuremeter. Whittle et al. (1993) has described the lift-off stress and analysis of the initial stress distribution of the six arm self-boring pressuremeter. Chang (1994) has described the methods and interpretation of self-boring pressuremeter dissipation tests.

The in-situ testing of marine clay with the self-boring pressuremeter described in this thesis has been discussed in detail by the author (Arulrajah et al., 2004d, 2004f, 2004i, 2004h, 2004p) during the course of this research study.

2.6.6 *BAT Permeameter*

The BAT permeameter device has been used for the determination of in-situ permeability of clays. Torstensson (1983, 1986) has described the equipment, its functions, methods of conducting the tests and the method of interpretation of the data. Bo, Arulrajah and Choa (1998c) have successfully used the device for determining the in-situ permeability of clays.

The in-situ testing of marine clay with the BAT permeameter described in this thesis has been discussed in detail by the author (Arulrajah et al., 2004d, 2004i) during the course of this research study.

2.6.7 *State of the Art: In-situ Testing*

Current state of the art in insitu testing includes the use of the cone pressuremeter test in soft clays. The cone pressuremeter is suitable for carrying out tests in soft clay where pushing condition is favourable. It is also suitable for use in sand where preboring is difficult. The testing method is similar to that of the self-boring pressuremeter. Cao (1998) has published on the testing method, theory and interpretation of the results of this test in marine clay. The cone penetrometer and hand-held field vane are also tools often used in soft clays.

2.7 Laboratory Testing of Marine Clays

Geotechnical books cover extensively the various laboratory testing equipments and describe the testing methods for the testing of soft clay. Sridharan and Sreepada (1981) have particularly written on the method of using the Hyperbolic fitting method for one-dimensional consolidation.

To date, studies of various laboratory tests in Singapore marine clays at the Changi reclamation projects have been extensively carried out particularly by Bo, Arulrajah, Choa and Chang (1998a) and Choa (1985).

2.7.1 Necessity and Shortcomings of Laboratory Testing

Laboratory testing enables the physical and consolidation properties of the foundation soil to be ascertained. The expected post improvement effective stress can also be determined. Post-investigation boreholes can be carried out at a designated time close to the surcharge removal period and from the laboratory results the degree of improvement can be assessed. Void ratio after improvement can be compared with prior to reclamation and expected values. Laboratory testing however takes time to conduct and can also be expensive. In addition there are a lot of complexities involved such as borehole quality, sample quality, testing quality, testing methods and interpretation methods.

2.7.2 State of the Art: Laboratory Testing

Currently the GDS stress path equipments has been used for laboratory testing of clays in Singapore and Southeast Asia. The tests though relatively expensive compared to other laboratory tests, is able to provide stress path history of the clays by drained or undrained tests. Direct simple shear tests and Mikasa shear tests have successfully been carried out on marine clays in Singapore. Large diameter Rowe cells and hydrocon is also being used for the consolidation testing of soft clays. The laboratory vane is also commonly in use to determine shear strengths of clays while the cone penetrometer is increasingly used for the determination of liquid limit.

Electro-osmosis consolidation laboratory tests have also been carried out by means of modified triaxial apparatus in which soil sample has an electric current applied and its volumetric change is accurately measured. Bo et al. (2000c) has described the test apparatus, procedures and result analysis of Singapore marine clays.

2.8 Finite Element Modeling of Prefabricated Vertical Drains

Lin et al. (2000) has previously verified the performance of using the interface element to simulate vertical drains in soft Bangkok clay by the finite element method. Lin et al. (2000) stated that the interface element can be used to act as a drainage channel to dissipate excess pore water pressure during the consolidation process which is the basic function of vertical drains. In the modeling of the vertical drains in Bangkok clay by Lin et al. (2000), the interface element was used with the same soil property as the adjacent soil except for its permeability. Furthermore, the conversion scheme for well resistance was achieved by using interface elements. Bo, Arulrajah and Choa (1997b) has previously carried out a performance verification study of prefabricated vertical drains installed in Singapore marine clay by means of the Sage Crisp numerical modeling software.

The finite element modeling of marine clay deformation under reclamation fills described in this thesis have been discussed in detail by the author (Arulrajah et al., 2004j) during the course of this research study. The analyses carried out by the author included the modeling of the consolidation behaviour of marine clay under reclamation fills with and without prefabricated vertical drains. Modeling of the sub-areas treated with vertical drains was carried out by both the axi-symmetric unit cell and full-scale analysis methods. Modeling of untreated control sub-areas was carried out by the full-scale analysis method.

2.9 Discussion on Literature Review

Ground improvement of soft clay, land reclamation and prefabricated vertical drains has been discussed in this chapter with references to various publications. The theories and mechanisms for the design of the vertical drains will be discussed further in a later chapter.

In-situ testing of marine clays by various penetration and dissipation testing methods has been highlighted. These include references to publications on field vane shear, piezocone, self-boring pressuremeter, flat dilatometer and BAT permeameter. The latest state-of-the-art in in-situ testing has been discussed.

Field instrumentation of soft clays has been referenced to various books and papers with respect to the method of instrumentation and analysis namely settlement gauges and piezometers. In addition, the latest state-of-the-art methods of field instrumentation and

laboratory testing have been discussed. Previous finite element modeling methods used for the modeling of prefabricated vertical drains installed in soft clays have also been discussed.

In conclusion it can be said that there is no dearth of existing literature on the aspects of ground improvement with prefabricated vertical drains and the associated in-situ testing and instrumentation works. The state of the modern day society is such that there are always countless new innovations and theories on methods of analysis, testing and interpretation of works. As such the need arises for a Geotechnical Engineer to keep abreast of the latest publications and findings in Geotechnical Engineering so as not to be left behind in this modern age.

3.0 CHARACTERISTICS AND MINERALOGY OF SINGAPORE MARINE CLAY AT CHANGI

Singapore marine clay at Changi is a quaternary deposit that lies within valleys cut in the Old Alluvium. It is locally known as Kallang formation. Prior to the commencement of land reclamation works on this marine clay formation, it is essential to carry out a proper site characterization of the marine clay consolidation and physical characteristics to obtain the required design parameters.

The pre-reclamation general site characterization was carried out by means of marine sampling boreholes, field vane testing and laboratory testing. It was carried out for the purposes of determining the consolidation characteristics, stratigraphy, geology, strength characteristics and stress history of the marine clay at Changi.

A preliminary survey inclusive of a desk study of existing data and geophysical seismic reflection surveys was carried out prior to the detailed soil investigation which was planned based on the marine geophysical seismic reflection survey and marine bathymetric results.

Physical and compressibility parameters of the marine clay at Changi were characterized from the laboratory tests while the shear strengths were evaluated from the field vane shear tests data obtained. The consolidation properties of marine clay are needed prior to land reclamation activities in order to predict the magnitude and rates of settlement with the expected fill load and future service load. These properties are also needed for the design of soil improvement works.

The shear strength values are required for foundation stability analyses of general fills and surcharge during reclamation and for the short and long term stability analyses of shore protection works.

Clay mineralogy tests were carried out by X-ray diffraction and scanning electron microscope to determine the mineralogical properties of the marine clay. Photographic identification of the marine clay was carried out to visually record the marine clay colour and texture.

The objective of this chapter is to report on the characteristics of the consolidation, strength mineralogy and formation history of Singapore marine clay at Changi, as determined from

laboratory and field vane shear tests. The following aspects of the characteristics and mineralogy of marine clay are discussed and presented in this chapter:

- Description of Project Site
- Site investigation
- Marine geophysical seismic reflection surveys
- Marine bathymetric surveys
- Laboratory testing
- Physical and consolidation characteristics
- Vertical hydraulic conductivity
- Horizontal hydraulic conductivity
- Field vane shear testing
- Determination of clay mineralogy by means of X-ray diffraction
- Determination of clay mineralogy by scanning electron microscope
- Geology of Singapore marine clay at Changi
- Formation history of Singapore marine clay at Changi
- Photographic identification of marine clay

3.1 Description of Project Site

The site for the research is located in the Changi East Reclamation Project in the Republic of Singapore. The project comprises the on-going land reclamation and ground improvement works to allow for the future expansion of Changi International Airport comprising the runway, taxiways, turn-offs and associated airport facilities.

The area is submerged underwater with seabed elevation varying from – 2 mCD to – 8 mCD (Admiralty Chart Datum, where mean sea level is +1.6 mCD). The Northern Area of the project area is underlain by marine clay up to 40 meters in thickness in certain areas and it is this portion of the project area that was investigated in this research study.

Figure 3.1 indicates the location and site plan of the Changi East Reclamation Project in the Republic of Singapore.

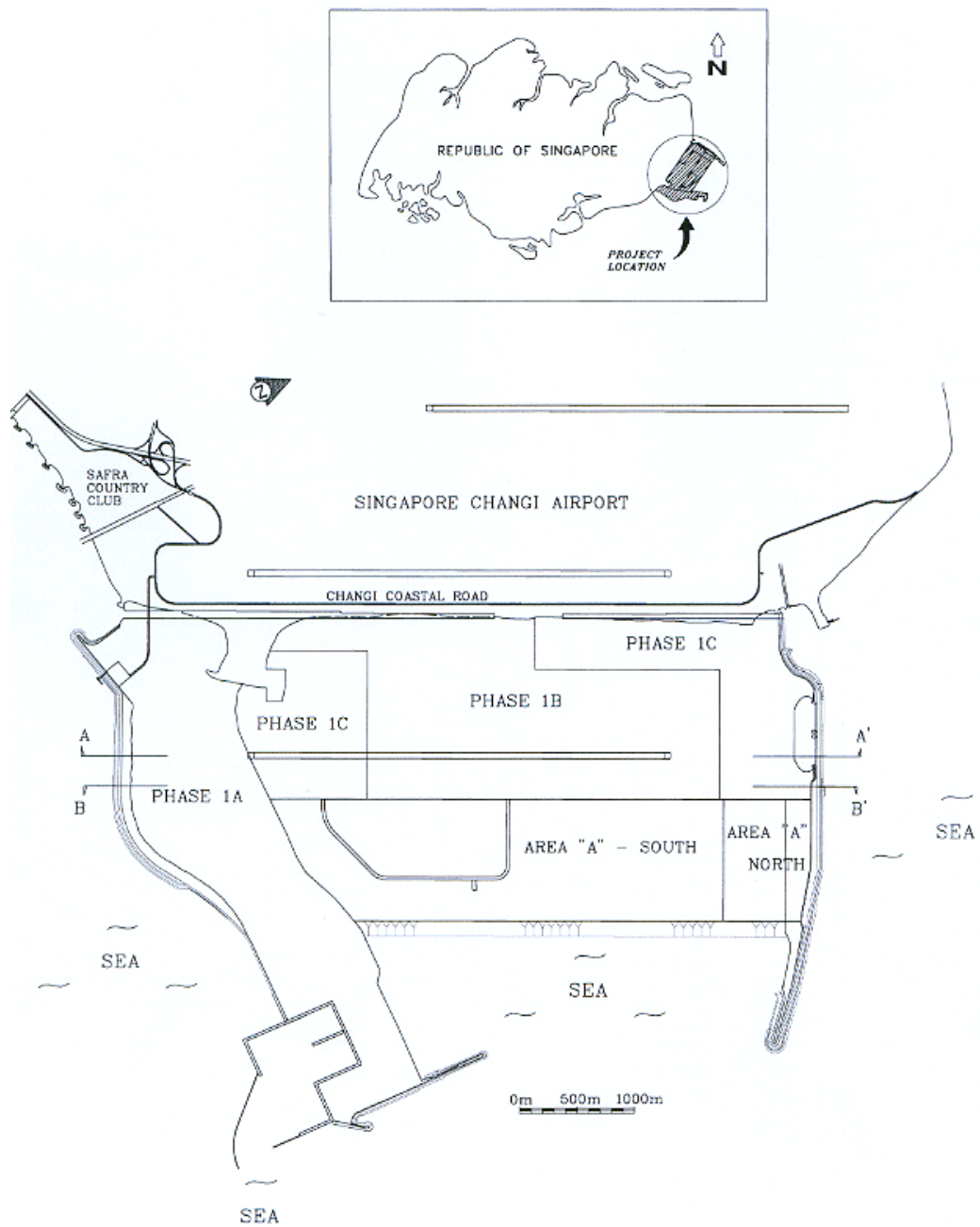


Figure 3.1 Location and site plan of the Changi East Reclamation Project (modified from Choa et al., 2001).

3.2 Site Investigation

Extensive soil investigation works consisting of marine boreholes, in-situ tests and laboratory tests were carried out for the preliminary site investigation to obtain the general characteristics and trends of the marine clay. Undisturbed samples taken from boreholes were tested in the laboratory to determine the physical, mineralogical, strength and consolidation characteristics of the marine clay. A desk study was first conducted on existing marine boreholes which had been carried out earlier by other parties and site profiles and geology of the underlying soil were then derived. Additional investigations clarifying the stratigraphy, geology and the soil characteristics and stress history of the marine clay was found to be necessary. The characterization study involved the execution of about 50 marine soil investigation boreholes.

Marine bathymetric surveys together with marine geophysical seismic reflection surveys of the project area were carried out with the use of a water surface-towed boomer profiling system. The elevations of the bases of the compressible layers and the distribution of soft marine clay pockets deposited in submarine valley cuts were determined from the marine bathymetric and seismic reflection surveys. The marine bathymetric and seismic reflection survey was used to complement the determination of the marine sampling borehole locations at the site.

3.2.1 Marine Sampling Boreholes

Marine soil investigation works were planned with the aid of a geophysical seismic reflection survey. Boreholes were drilled at locations with thick marine clay and other locations for determination of the marine clay profile. Due to the large extent of the project area and the variations in the underlying soil profile, a large number of marine boreholes were carried out with the use of offshore jack-up pontoons. Continuous undisturbed sampling was carried out throughout the marine clay layer for all boreholes. Following the completion of each sampling borehole, the rig on the offshore jack-up pontoon was shifted about one meter and a field vane shear test (FVT) was next carried out using a Geonor vane at one meter depth intervals. Laboratory tests to determine the physical characteristics of the marine clay such as Atterberg limits, moisture content and bulk density were carried out on the retrieved samples. Conventional oedometer and consolidation tests were also conducted on undisturbed soil samples retrieved from the site. The objective of these tests was to establish the characteristics of the foundation soil and to obtain the soil parameters needed for the design. Figure 3.2 shows an off-shore jack-up pontoon with boring rig. Figure 3.3 shows the location of the marine sampling boreholes.



Figure 3.2 Off-shore jack-up pontoon with boring rig.

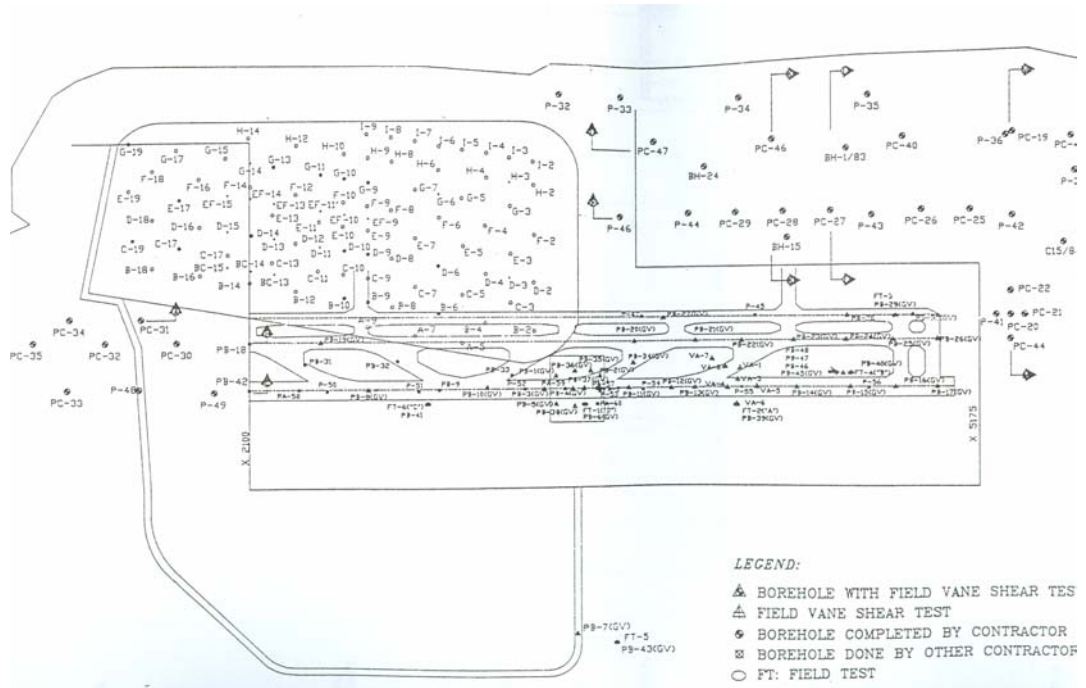


Figure 3.3 Location of marine sampling boreholes.

3.2.2 Bathymetric and Seismic Reflection Surveys

Marine bathymetric surveys together with marine geophysical seismic reflection surveys of the project area were carried out with the help of a water surface-towed boomer profiling system. The elevations of the bases of the compressible layers and the distribution of soft marine clay pockets deposited in submarine valley cuts were determined from the marine bathymetric and seismic reflection surveys.

The seismic survey vessel was fitted with a Del Norte DDMU 540 trisponder, Atlas Deso 20 echo sounder and a boomer profiling system. The survey operation was run at lines of 50 meter spacing in alternate directions. Cross lines were run at 50 meter spacing in alternate directions, as specified by a geophysical specialist for accurate interpretation of the seismic survey results. Figure 3.4 indicates a schematic view of the survey vessel.

For horizontal control of the survey, a trisponder positioning system was used to control the location of the survey vessel along pre-computed lines. A total of 4 shore stations were used at any one time. For vertical control of the survey, the tidal reduction of the survey area was carried out using tide levels observed at a tide gauge.

Tidal data was obtained from the Port of Singapore, Hydrographical Department. The echo sounder enabled the contouring of the seabed elevation profile while the boomer enabled the isoline of the base elevation of the marine clay to be plotted. Hence the geological sequence description could be obtained based on the interpretation of the boomer data and this could be correlated with the existing marine boreholes data provided over the survey area.

Based on the seismic survey and bathymetric survey results, additional boreholes were planned to accurately profile the marine clay at the project site. This was done by filling in gaps of uncertain data or deep pockets of marine clay by providing additional boreholes. Figure 3.5 shows an isopach map result of the seismic survey of the Project Site.

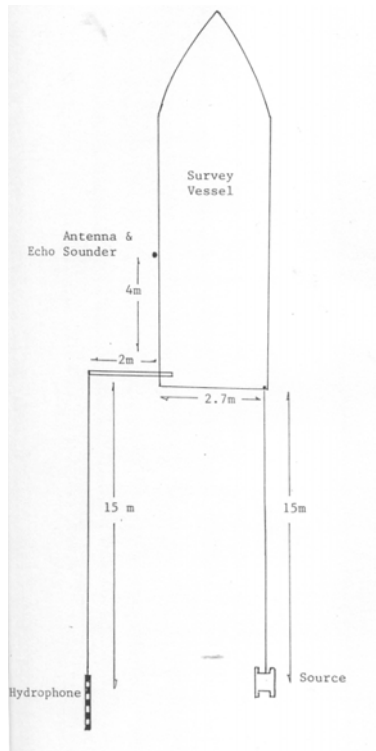


Figure 3.4 Schematic view of survey vessel.

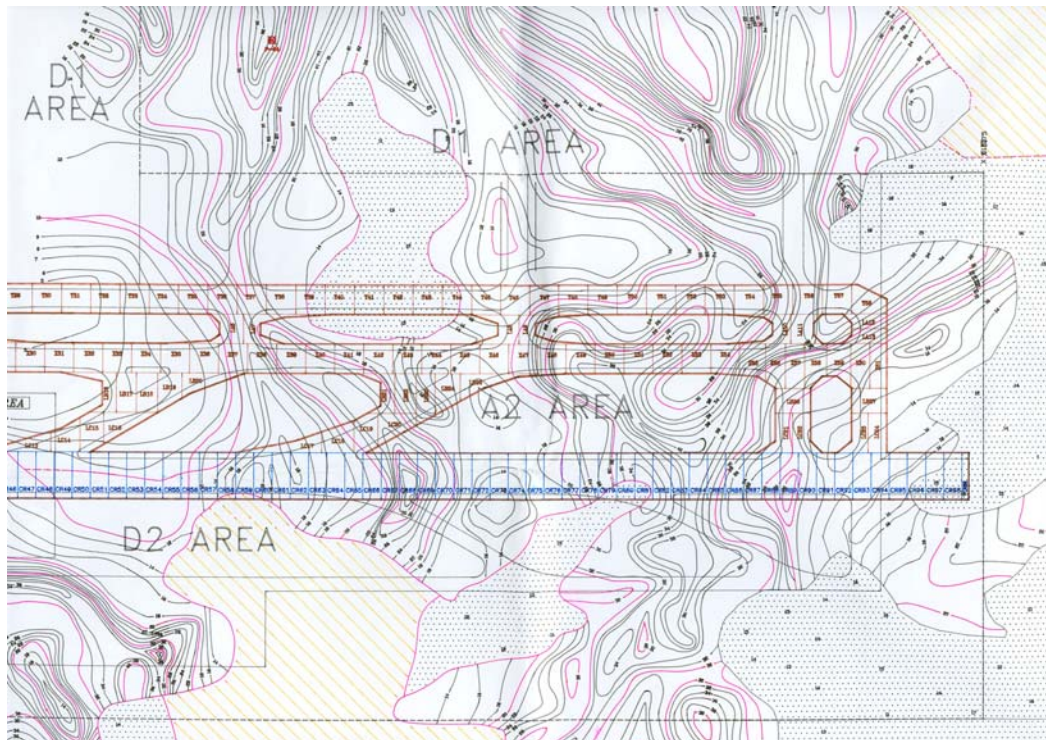


Figure 3.5 Isoline map of seismic survey contours.

3.3 Laboratory Testing of Marine Clay

The characterization study indicated the presence of two distinct layers of marine clay which are the “Upper Marine Clay layer” and the “Lower Marine Clay layer” (Arulrajah et al., 1995). The “Intermediate Stiff Clay layer” which is also present is in reality the desiccated layer of the lower marine clay, which separates these two distinct marine clay layers (Bo, Arulrajah and Choa 1998a). The primary compression and secondary compression characteristics of the marine clay were determined from oedometer tests. The upper marine clay with an average compression index (C_c) of 1.0 is found to be more compressible than the lower marine clay.

3.3.1 Consolidation and Physical Characteristics

Based on the results obtained, the marine clay in the Northern Area can be described as high to very highly plastic silty clay, except for the intermediate stiff clay as shown in the plasticity chart in Figure 3.6.

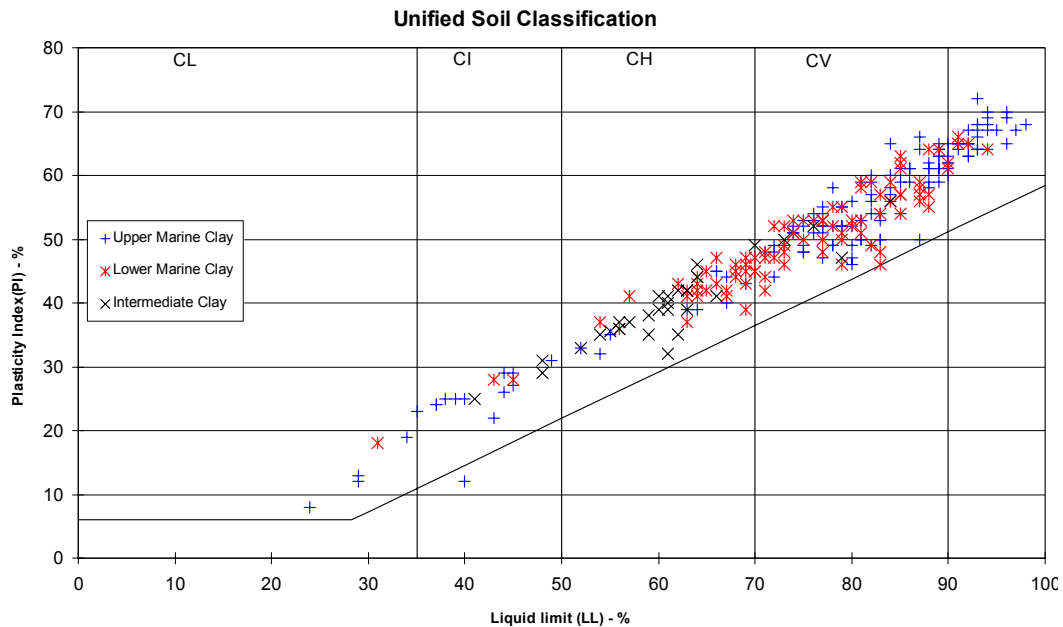


Figure 3.6 Plasticity chart showing the classification of Singapore marine clay at Changi.

The range of physical and consolidation characteristics of the upper, lower and intermediate marine clay is tabulated in Table 3.1. The recommended design parameters of the various marine clay layers based on the results of the marine boreholes and laboratory tests (Bo, Arulrajah and Choa 1998a) is tabulated in Table 3.2 and were design parameters used in the design of the reclamation and ground improvement works.

Typically the upper marine clay ranges between 0-5.5 meters to about 10-25 meters below the seabed. The upper marine clay has a liquid limit of between 80-95%, plastic limit of between 20-28% and water content of 70-88%. The upper marine clay is generally overconsolidated with overconsolidation ratio (OCR) of about 1.5-2.5. The upper marine clay has a compression index (C_c) of 0.6-1.5 and secondary compression index (C_α) of 0.012-0.025. The coefficient of consolidation for vertical flow (c_v) of the upper marine clay is between 0.47-0.6 m²/year while the coefficient of consolidation due to horizontal flow (c_h) is between 2-3 m²/year.

The lower marine clay ranges to a depth of 30-50 meters below the seabed. The lower marine clay has a liquid limit of 65-90%, plastic limit of 20-30% and water content of 40-60%. The lower marine clay is lightly overconsolidated with OCR of 2. The lower marine clay has a compression index (C_c) of 0.6-1.0 and secondary compression index (C_α) of 0.012-0.023. The compression index is used for the calculation of field settlement caused by settlement. The coefficient of consolidation for vertical flow (c_v) of the lower marine clay is between 0.8-1.5 m²/year while the coefficient of consolidation due to horizontal flow (c_h) is between 3-5 m²/year.

The intermediate stiff clay is sandwiched between the upper marine clay and lower marine clay. This 3-5 meter thick layer comprises of predominantly stiff sandy silt or sandy clay. The intermediate stiff clay has a liquid limit of about 50%, plastic limit of 18-20% and water content of 10-35%. The intermediate stiff clay is moderately overconsolidated due to desiccation, with OCR of 3-4. The intermediate stiff clay has a compression index (C_c) of 0.2-0.3 and secondary compression index (C_α) of 0.0043-0.023. The coefficient of consolidation for vertical flow (c_v) of the intermediate marine clay is between 1-4.5 m²/year while the coefficient of consolidation due to horizontal flow (c_h) is between 5-10 m²/year.

The variations of soil properties with depth are presented in Figures 3.7 to 3.15. These plots are based on combined information of all boreholes in the Northern area of the project. Trends may not be present due to differences in location and variability in the soil stiffnesses and characteristics from borehole to borehole.

Table 3.1 Range of physical and consolidation characteristics of Singapore marine clay at Changi. (Bo, Arulrajah and Choa 1998a).

Parameters	Upper Marine Clay	Intermediate Stiff Clay	Lower Marine Clay
γ_{bulk} (kN/m ³)	14.23-15.7	18.64-19.6	15.7-16.67
WC (%)	70-88	10-35	40-60
LL (%)	80-95	50	65-90
PL (%)	20-28	18-20	20-30
e_0	1.8-2.2	0.7-0.9	1.1-1.5
G_s	2.6-2.72	2.68-2.76	2.7-2.75
C_c	0.6-1.5	0.2-0.3	0.6-1.0
C_α	0.012-0.025	0.0043-0.023	0.012-0.023
C_r	0.09-0.16	0.08-0.15	0.14-0.2
c_v (m ² /yr)	0.47-0.6	1-4.5	0.8-1.5
c_{vr} (m ² /yr)	3-7	10-30	4-10
c_h (m ² /yr)	2-3	5-10	3-5
OCR	1.5-2.5	3-4	2

Table 3.2 Recommended Design parameters of Singapore marine clay at Changi (Bo, Arulrajah and Choa 1998a).

Parameters	Upper Marine Clay	Intermediate Stiff Clay	Lower Marine Clay
γ_{bulk} (kN/m ³)	14.91	19.13	16.2
WC (%)	80	30	50
LL (%)	90	50	75
PL (%)	25	19	25
e_0	2.0	0.8	1.3
G_s	2.67	2.72	2.73
C_c	1.0	0.25	0.8
C_r	0.13	0.1	0.17
c_v (m ² /yr)	0.5	2	1
c_{vr} (m ² /yr)	5	20	10
OCR	2	3.5	2

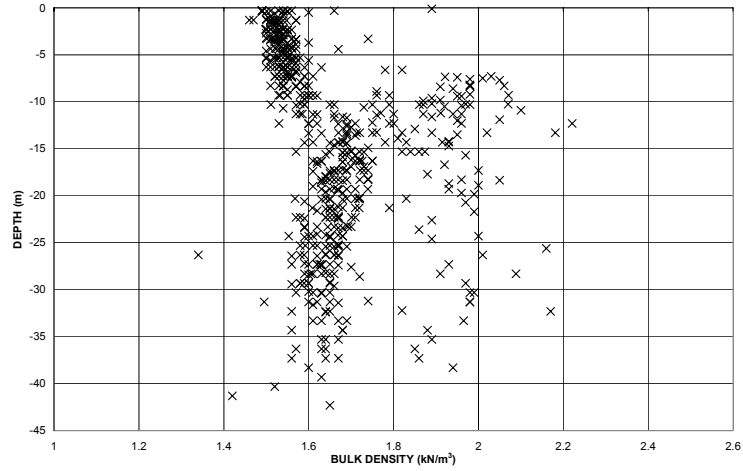


Figure 3.7 Variation of bulk density with depth.

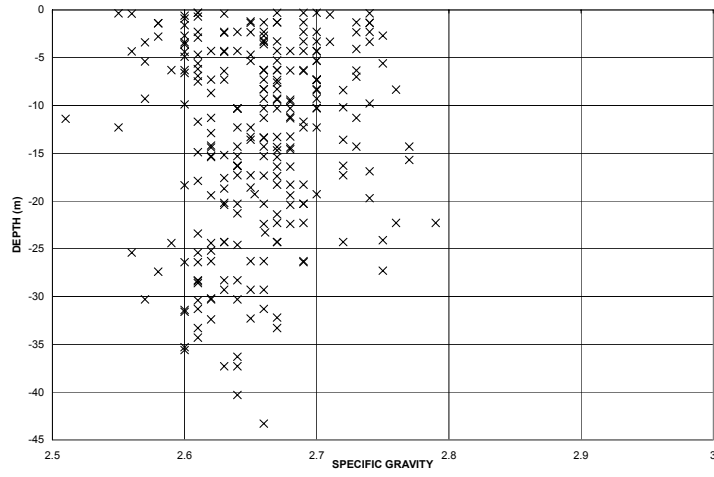


Figure 3.8 Variation of specific gravity with depth.

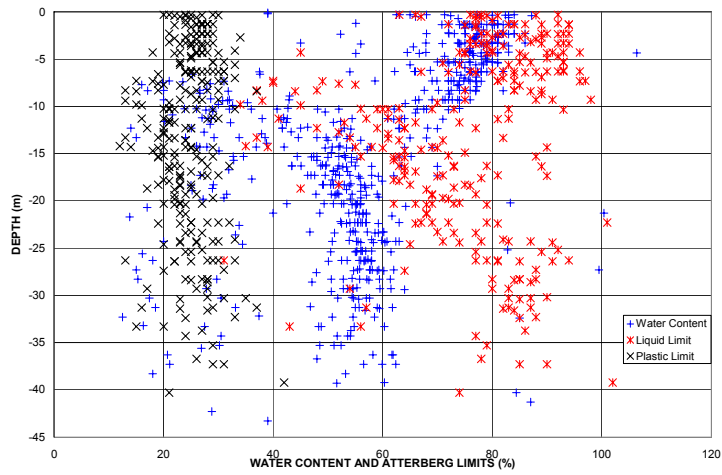


Figure 3.9 Variation of water content and Atterberg limits with depth.

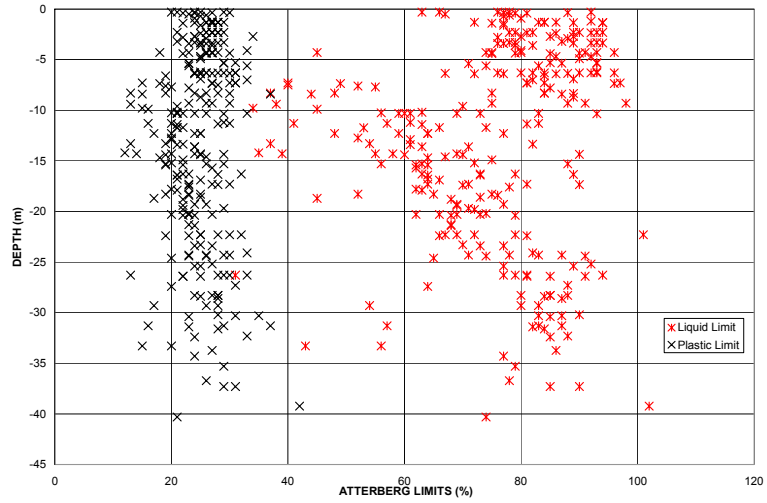


Figure 3.10 Variation of Atterberg limits with depth.

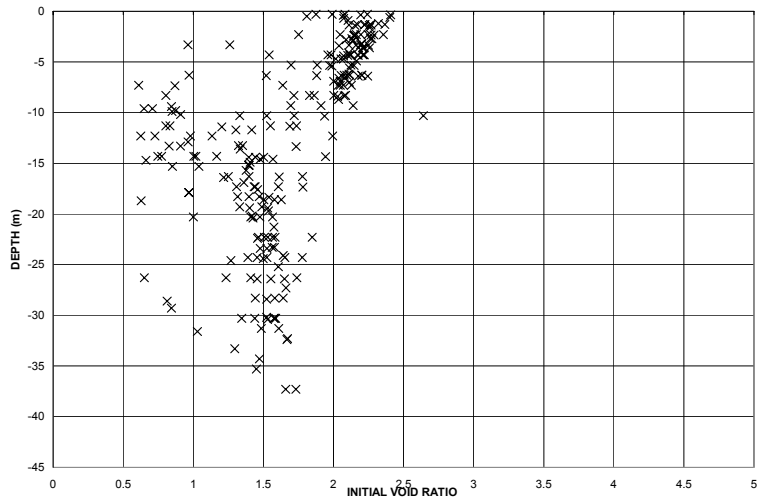


Figure 3.11 Variation of initial void ratio with depth.

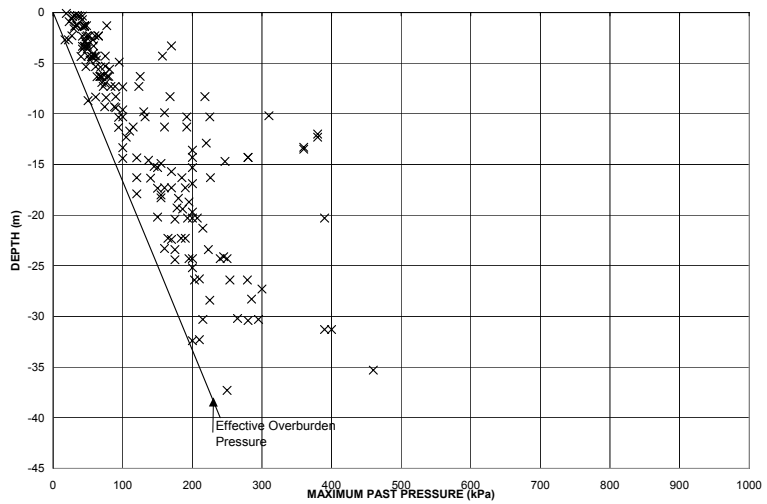


Figure 3.12 Variation of maximum past pressure with depth.

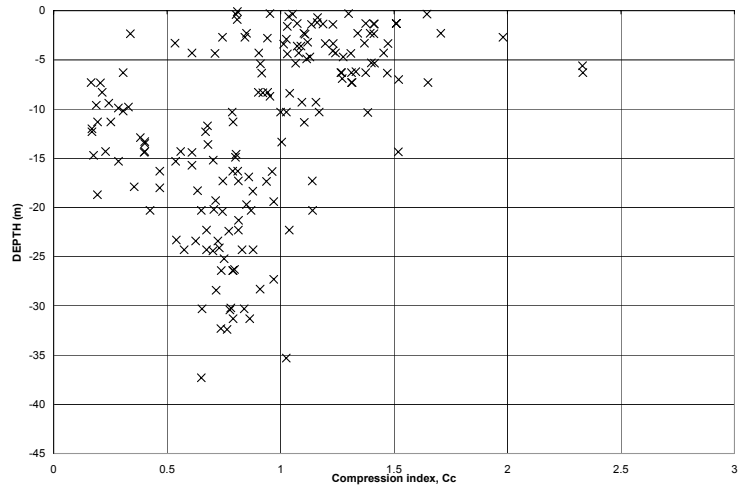


Figure 3.13 Variation of compression index with depth.

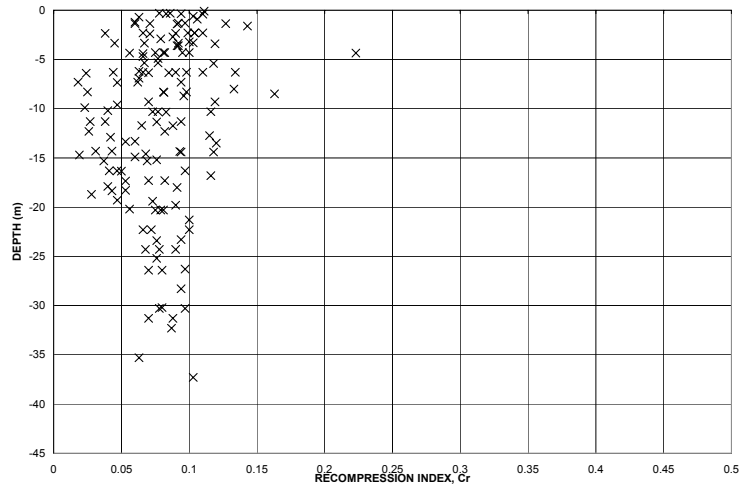


Figure 3.14 Variation of recompression index with depth.

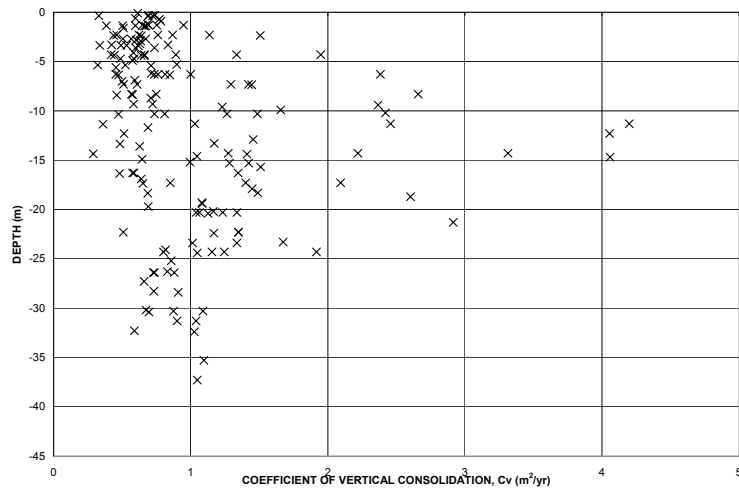


Figure 3.15 Variation of c_v with depth (oedometer).

3.3.2 Hydraulic Conductivity

For the vertical hydraulic conductivity measurement, conventional one-dimensional oedometer tests were carried out. Rowe cell tests were carried out for the horizontal hydraulic conductivity measurements. The collected samples were sealed immediately with a wax and Vaseline mixture at site and sent by boat to the on-site laboratory.

3.3.2.1 Vertical Hydraulic Conductivity

The oedometer specimens were 63.5 mm in diameter and 19 mm in height. The samples were conventionally trimmed horizontally (i.e., the loading surface is perpendicular to the axis of the sampling tube) so that the compressibility and coefficient of consolidation due to vertical flow could be measured. The consolidation load was applied in 24 hour loading stages with a load increment ratio of unity. Vertical hydraulic conductivity (k_v) was obtained from $e - \log k$ relation and taken at the natural void ratio. k_v values were generally calculated from coefficient of consolidation results (Bo, Arulrajah and Choa; 1998c):

$$k_v = c_v m_v \gamma_w \quad (\text{Eq. 3.1})$$

where:

c_v is the coefficient of consolidation for vertical flow in m^2/yr

m_v is the coefficient of volume compressibility in m^2/kN

γ_w is the unit weight of water in kN/m^3

Figure 3.16 shows the vertical hydraulic conductivity versus depth plots for the marine clay. Vertical hydraulic conductivity values were found to range between 2×10^{-10} to 1.5×10^{-8} m/s for the Singapore marine clay at Changi. Vertical hydraulic conductivity values from laboratory tests do not show a systematic decrease with increasing depth.

Tavenas et al. (1983) has highlighted the weakness of evaluating hydraulic conductivity values from step-loaded oedometer tests. Tavenas et al. (1983) has explained that in the oedometer test there is a non-homogeneous condition and c_v is much faster near the drainage boundary than in the middle of the specimen. However c_v values are taken as an intermediate value and it would be difficult to transform into hydraulic conductivity values using the suggested equation. This is because proper quantification of corresponding m_v , void ratio and effective stress is difficult. This could thus be the reason for the non-systematic variation of the hydraulic conductivity values. However, vertical hydraulic conductivities were evaluated from c_v values derived from Taylor's method (Taylor 1948) which is likely to give a closer estimation to the actual in-situ hydraulic conductivity.

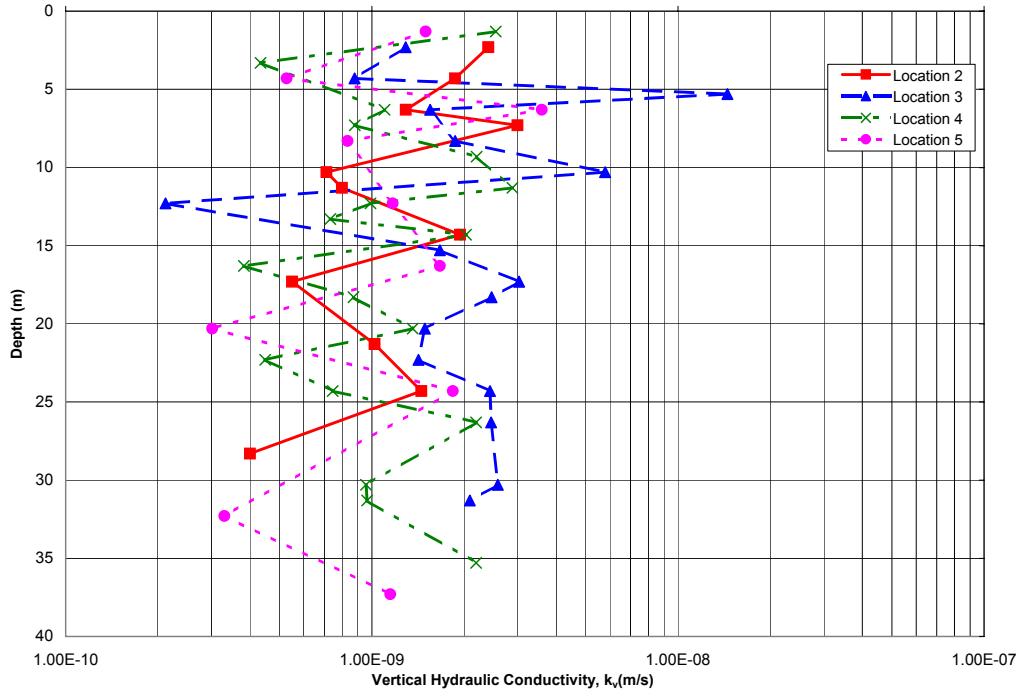


Figure 3.16 Vertical hydraulic conductivity versus depth plot from laboratory testing.

The change of hydraulic conductivity with void ratio is defined as the hydraulic conductivity change index, c_{kv} which was found to range between 0.3 to 0.87 for the marine clay (Bo, Arulrajah and Choa; 1998c). Leroueil et al. (1992) stated that c_{kv} deduced from oedometer tests under-estimates the real values. Tavenas et al. (1983) explained that the underestimation of void ratio versus log hydraulic conductivity relationship at small void ratios could be associated with the use of mean values instead of void ratio at the upper boundary where hydraulic conductivity is measured.

The relationship between in-situ initial void ratio (e_0) and c_{kv} as shown in Figure 3.17, is found to be $c_{kv} = 0.3 e_0$ for Singapore marine clay at Changi (Bo, Arulrajah and Choa; 1998c).

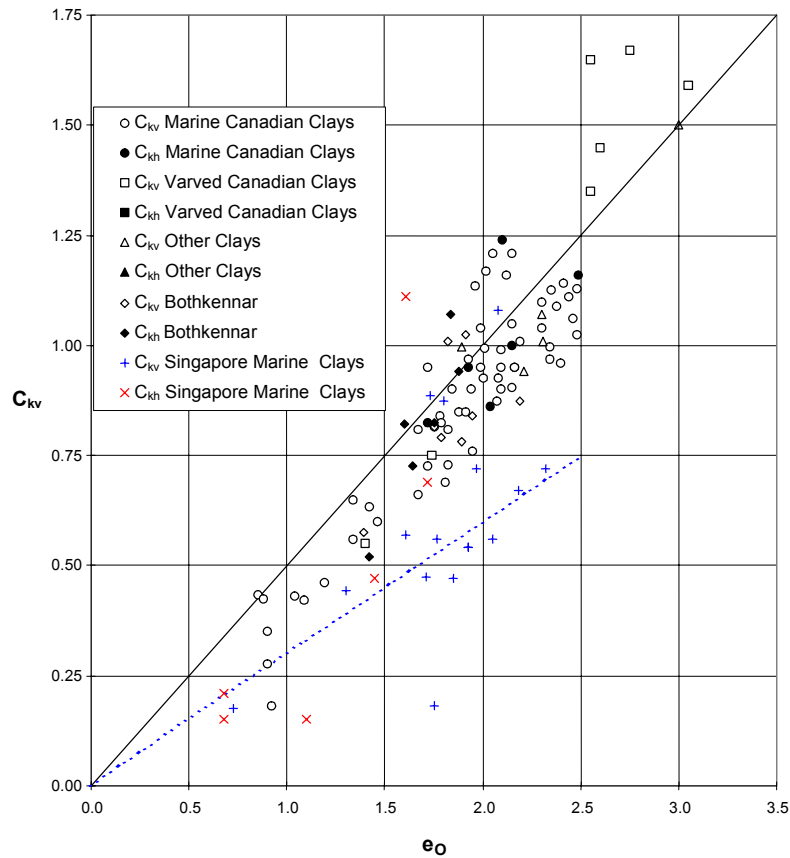


Figure 3.17 Relationship comparison with c_{kv} to e_o of various clays (Bo, Arulrajah and Choa; 1998c).

3.3.2.2 Horizontal Hydraulic Conductivity

As the oedometer test does not permit horizontal drainage, Rowe cell tests (Rowe, 1966) which have provisions for horizontal drainage were used to determine coefficient of consolidation due to horizontal flow (c_h) and horizontal hydraulic conductivity (k_h) of the marine clay. The Rowe cell used was 75 mm in diameter and 30 mm in thickness. The prepared samples were 72.5 mm in diameter and as such the thickness of the side drain was 2.5 mm. The consolidation load was applied in 24 hour stages with a load increment ratio of unity. Horizontal hydraulic conductivity, k_h was taken from values at the natural void ratio and calculated from coefficient of consolidation due to horizontal flow.

Consolidation tests were carried out with Rowe cell and the horizontal hydraulic conductivity values were calculated from coefficient of consolidation due to horizontal flow, c_h . k_h from laboratory tests versus depth plots are shown in Figure 3.18.

Horizontal hydraulic conductivity values were found to range between 3×10^{-9} to 8×10^{-8} m/s, which is much higher than the laboratory vertical hydraulic conductivity. Hydraulic conductivity anisotropy is not significant for the marine clay. The k_h/k_v ratio for the Singapore marine clay at Changi is about 1.5. It can therefore be concluded that the hydraulic conductivity anisotropy is negligible for the Singapore marine clay at Changi.

Tavenas et al. (1983) stated that permeability anisotropy is not a significant parameter in most massive marine clays. Larsson (1981) stated that isotropy of Swedish clay with the difference between k_h and k_v is in the range of measurement error. Rowe (1972) stated that oedometer consolidation tests carried out on a small diameter Rowe cell should give lower value of c_h and k_h if the fabric effect is significant. This may not be the case for Singapore marine clay at Changi, which is of recent Quaternary age, where the type of clay is homogeneous with less frequent silt-sand lamination.

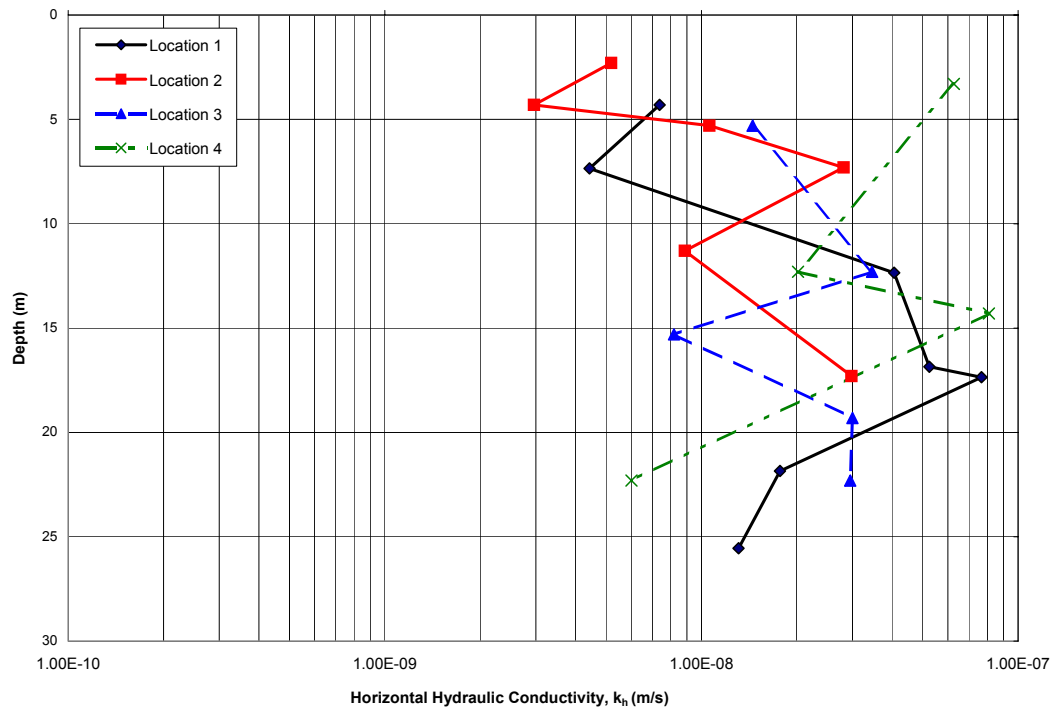


Figure 3.18 Horizontal hydraulic conductivity versus depth plot from laboratory testing.

3.4 Field Vane Shear Testing of Marine Clay

The undrained shear strength obtained from the field vane tests was analysed to obtain empirical correlations of the shear strengths and the normalized shear strength ratios of the marine clay. A Geonor field vane was used in the testing and both undisturbed and remoulded shear strengths were obtained from the tests. The in-situ field vane shear testing of Singapore marine clay at Changi have been discussed in detail by the author (Arulrajah et al., 2004d) during the course of this research study.

The undrained shear strength of the upper marine clay is between 10 to 30 kPa while that of the lower marine clay is between 30 to 60 kPa. The graphical plots of the field vane test results are found in Figure 3.19. The empirical correlations suggested for the field vane tests in Changi marine clay by Bo et al. (2003b) were used in the characterisation. The empirical correlations obtained indicate that the marine clay is soft and slightly overconsolidated.

$$\begin{aligned}c_u &= 10 + 1.6 z && (\text{kN/m}^2) && (\text{for upper marine clay}) && \text{Eq. (3.2)} \\c_u &= 10 + 2 z && (\text{kN/m}^2) && (\text{for lower marine clay})\end{aligned}$$

The normalised shear strength ratio is defined as follows:

$$c_u / \sigma_{vo}' = 0.37 \quad \text{Eq. (3.3)}$$

where:

$$\begin{aligned}c_u &= \text{undrained shear strength in kN/m}^2 \\z &= \text{depth below seabed in meters} \\\sigma_{vo}' &= \text{effective stress in kPa}\end{aligned}$$

For many naturally deposited clay soils, the undrained shear strength is much less when the soils are tested after remoulding without any change in the moisture content. This property of clay is called the sensitivity. The degree of sensitivity is the ratio of the undrained shear strength in an undisturbed state to that in a remoulded state:

$$S_r = c_u (\text{undisturbed}) / c_u (\text{remoulded}) \quad \text{Eq. (3.4)}$$

The sensitivity of the marine clay at Changi varies from 3 to 8 which can be described as highly sensitive marine clay. Figure 3.20 indicates the sensitivity of the marine clay at the Northern Area of the Project Site.

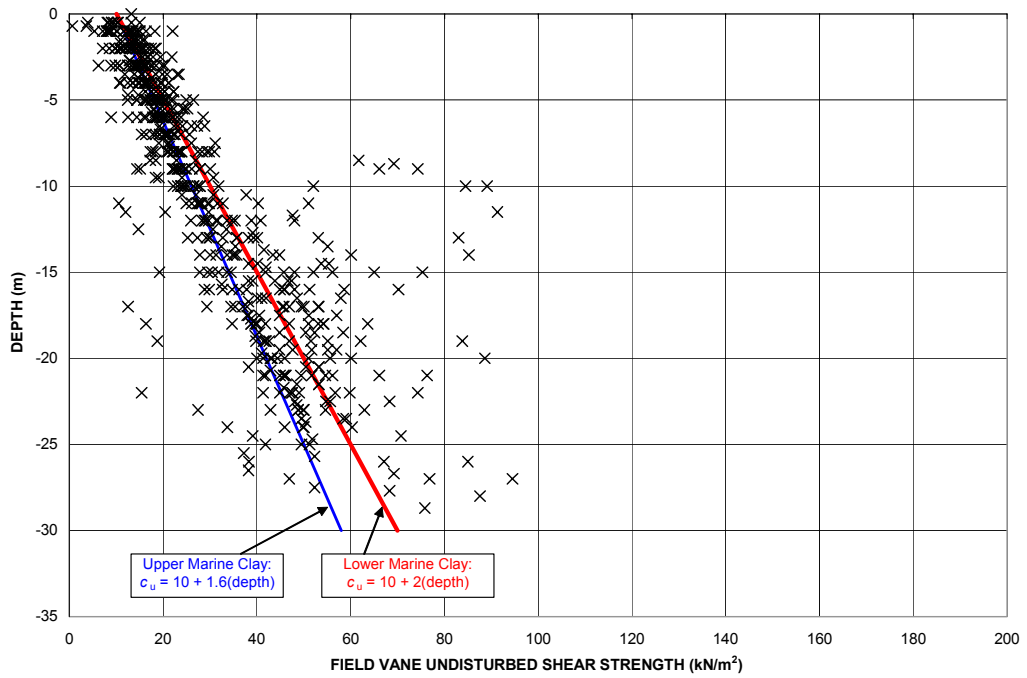


Figure 3.19 Variation of field vane undisturbed shear strength with depth

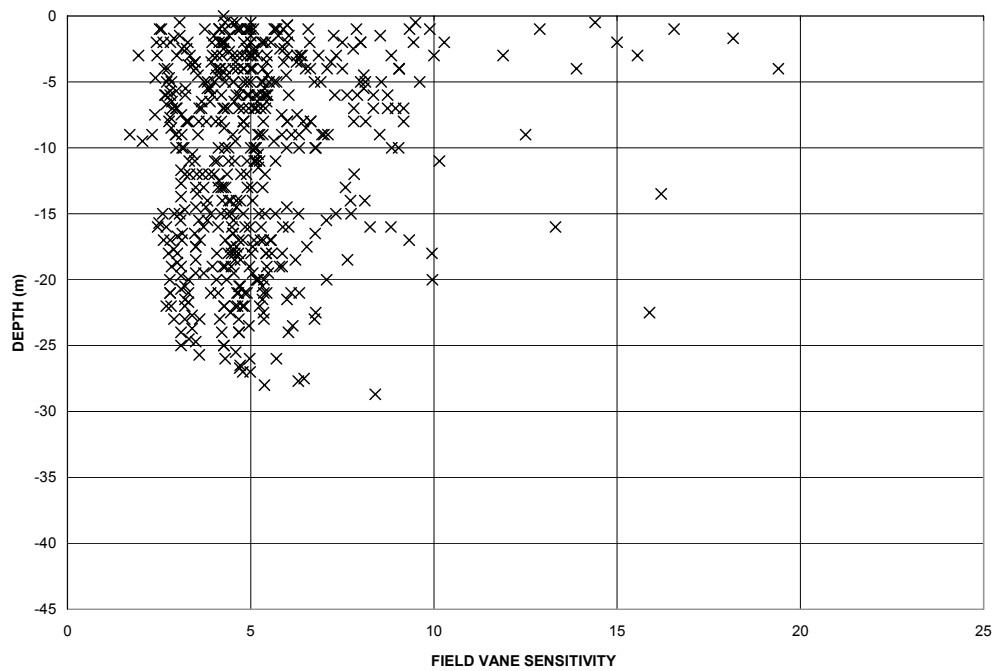


Figure 3.20 Variation of field vane sensitivity with depth.

3.5 Mineralogy of Marine Clay

The mineralogy of the marine clay was determined by the extraction of piston samples which were stored and sent to the British Geological Survey for X-ray diffraction (XRD) and scanning electron microscope (SEM) analysis. The tests were carried out according to the British Standards.

3.5.1 X-Ray Diffraction

A representative portion of each sample was removed and dispersed in distilled water using a reciprocal shaker by treatment with ultrasound. The suspension was then sieved on 63 μm and the <63 μm material placed in a measuring cylinder and allowed to stand. In order to prevent flocculation of the clay crystals, 2 ml of 0.1M 'Calgon' (sodium hexametaphosphate) was added to each suspension. After a period dictated by Stoke's Law, a nominal < 2 μm was then re-suspended in a minimum of distilled water and pipette onto a ceramic tile in a vacuum apparatus to produce an oriented mount.

The XRD analysis was carried out using a Philips PW1700 series diffractometer equipped with a cobalt-target tube and operating at 45kV and 40mA. Clay mineralogy was determined after scanning the air-dry, glycol-solvated and heated to 550° C/2 oriented mounts from 1.5-32 °2 θ at 0.48 °2 θ /minute. Diffraction data was analysed using Philips APD1700 software coupled to a JCPDS database running on a DEC MicroVax 2000 micro-computer system.

The XRD analysis indicates the major content of minerals to be kaolinite and smectite with 'mica' and chlorite being the minor minerals.

The XRD result for a sample at 10 meters depth is shown in Figures 3.21. The XRD result for a sample at 18 meters depth is shown in Figures 3.22.

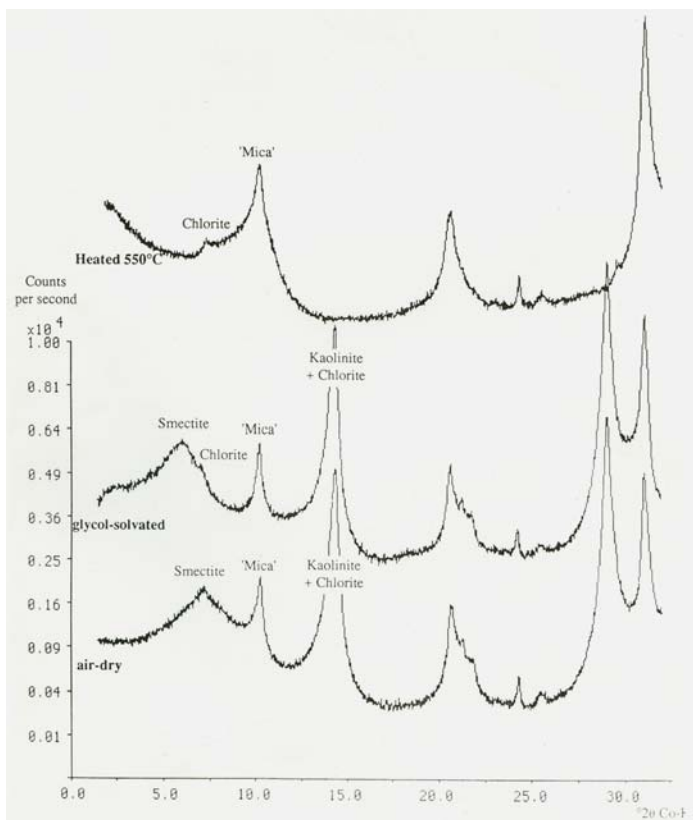


Figure 3.21 X-ray diffraction results for marine clay at 10 meters depth .

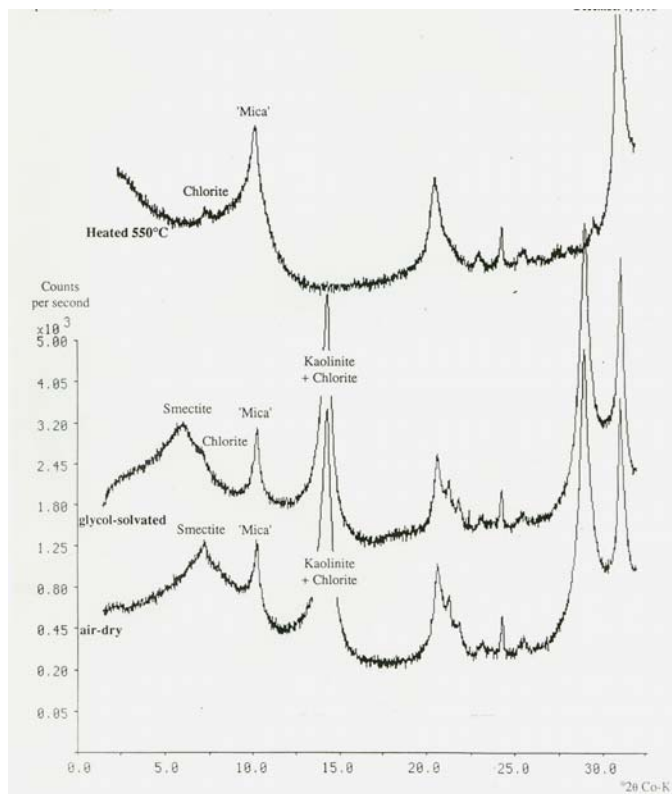


Figure 3.22 X-ray diffraction results for marine clay at 18 meters depth.

3.5.2 *Scanning Electron Microscope*

A sub sample approximately 2 cm x 1cm² was freeze dried prior to specimen preparation. This involved rapidly freezing the sub sample in liquid nitrogen followed by drying in an Edwards Modulyo Freeze Drier for approximately 24 hours. Once dry the samples were carefully fractured to produce a freshly exposed surface for SEM examination. These specimens were then mounted on aluminium stubs and coated in a layer of carbon approximately 25 nm thick in an Edwards 306A carbon evaporation coater.

The SEM specimens were examined in a Cambridge Instruments SEM S250 Mk 1 fitted with a Link 860A energy dispersive X-ray analysis (EDXA) system which provided qualitative chemical information from areas of interest. An accelerating voltage of 20 kV was used throughout this study. The qualitative chemistry of each clay mineral is identified as a list of elements detected. The elements listed in brackets are listed in approximate order of decreasing concentration estimated from peak heights in the qualitative EDXA spectra.

Under the SEM, the clays appear poorly consolidated. The fabric of the clays appears generally open with porosities optically estimated at up to 30% based on SEM interpretation. The clay samples are generally composed of ragged clay mineral flakes typically less than 10 µm in diameter. The flakes have a chemistry with K, Fe aluminium silicate dominating in most samples as obtained from the EXDA. Such a chemical composition probably corresponds with the micaceous clay mineral identified by XRD. Rarer flakes with a Mg, K, Fe (tr Ca) aluminium silicate to a K, Fe (tr Ca, Ti) aluminium silicate composition may relate to the smectite-group mineral identified by XRD. Kaolinite generally forms discrete subrounded particles intimately associated iron oxides, too fine grained to be resolved by SEM. Rare detrital muscovite flakes, quartz and K-feldspar silt grains and shell fragments are distributed throughout the clay matrix. Authigenic pyrite occurs as isolated subspherical particles and rare framboids suggesting an anoxic diagenetic environment. Poorly developed clay flakes, apparently associated with the pyrite have a Fe, K, Mg, Al, Si chemistry and may be composed of chlorite. These interpretations were provided in the test report of the British Geological Survey.

The SEM photomicrographs are shown in Figure 3.23 (Plates 1-6). Plates 1 and 4 shows the typical clay morphology. Plate 2 shows the typical clay morphology and open, poorly compacted texture. Plate 3 indicates the presence of rare framboical pyrite. Plate 5 indicates the presence of kaolinite particles within the clay matrix. Plate 6 shows the typical open, porous clay fabric.

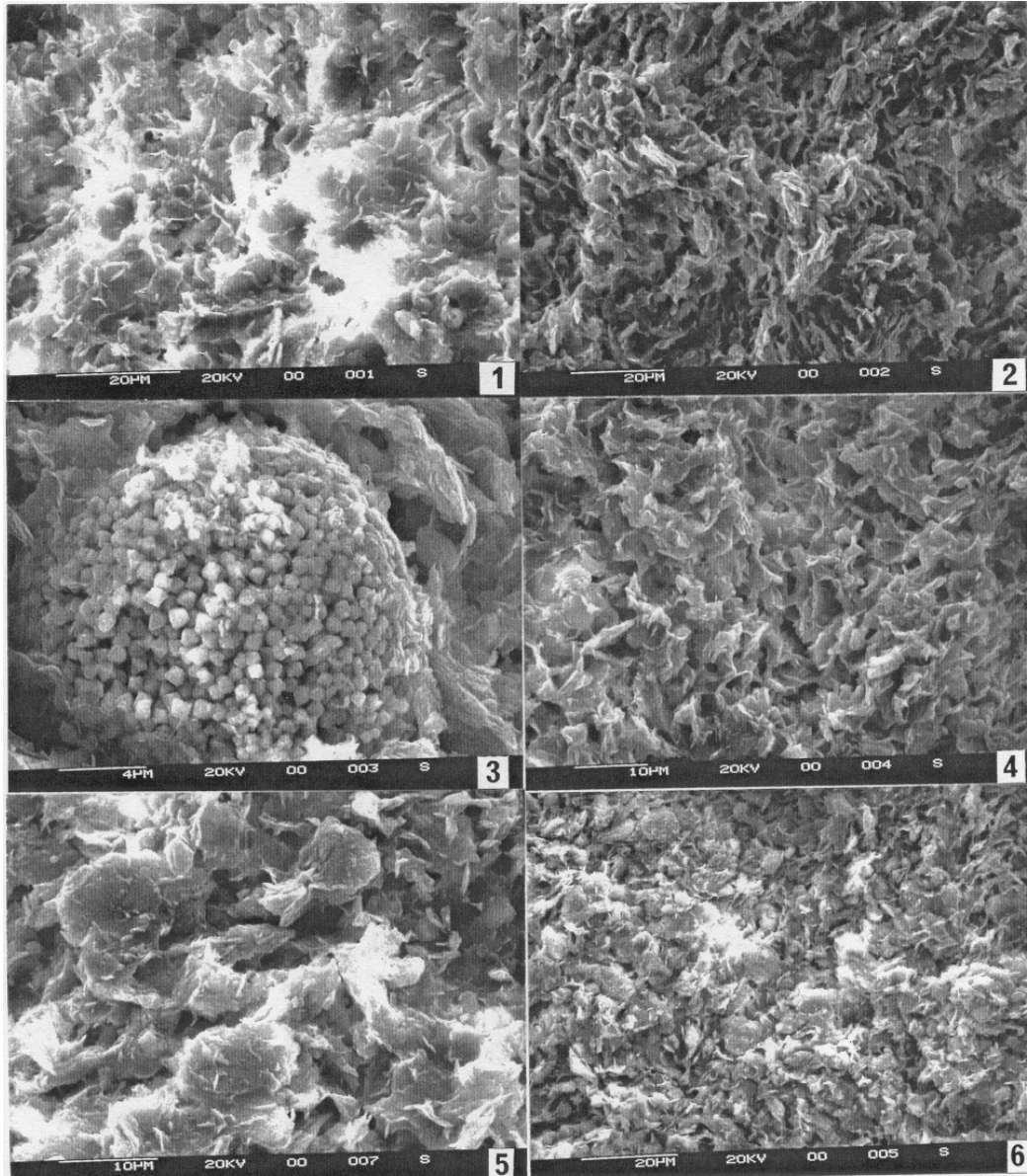


Figure 3.23 Magnification of soil fabric under Scanning Electron Microscope (Plates 1-3: at 6 m depth; Plates 4-6 at 15 m depth) .

3.6 Geology and Formation History of Marine Clay

The marine clay found in the project site belongs to the marine member of the Kallang Formation. This formation is underlain by Old Alluvium. The most important influence on the sedimentation history of recent sediments in the coastal areas of Southeast Asia has been the sea level fluctuations which have occurred in the late Pleistocene and Holocene periods (Yong et al., 1990). These sea level fluctuations during glacial advance and retreat led to the erosion of deep valleys in all earlier formations and the subsequent sea level rises were accompanied by the filling of these valleys with the alluvial and marine members of the Kallang formation. The infilled valleys of marine clays were found to be up to 40 to 50 meters in depth. At some localities, sand layers which are alluvial deposits laid at river mouth during the pause in marine deposition, were found instead of the dessicated clay. The lower marine clay in turn is underlain by the old alluvium comprising of cemented silty clayey sand. The preliminary site investigation and geophysical survey of the project site revealed that the Singapore marine clay at Changi consists of two marine members locally known as the upper and the lower marine clays. These soft to medium stiff clay members, as determined by in-situ or laboratory tests, are recent deposits of estuarine origin. The upper and lower marine clays are separated by a layer of medium stiff to stiff clay 2 to 5 meters in thickness. This layer locally termed as intermediate clay is reddish in colour and is believed to be the dessicated crust of the lower marine clay resulting from the exposure of the seabed to the atmosphere during the rise and fall of the sea levels in the geological past.

It is the onset of the Wurm/Wisconsin glacial period approximately 75,000 years ago which brought on an extremely rapid drop of sea level to about 140 meters below the present sea level about 18,000 years ago. There has been a tremendous transgression of the sea over the land in the last 10,000 to 20,000 years. With further uplift of land and regression of the seas, more erosion and deposition took place. These cycles of aggregation and erosion had occurred many times throughout the geological ages before giving rise to the present marine clay formation in Eastern Singapore. This is evident in the geological profile of the project site, in which three successive layers of marine clay are observed, suggesting that at least three cycles must have taken place. Most recent estuarine and littoral deposits of the Kallang Formation have been deposited since sea level has been established at or close to its current level. For Singapore marine clay, with reported thickness of 40 meters, the age of these deposits must be younger than 12,000 years (Yong et al., 1990). The typical geological profile of the project site shown in Figure 3.24.

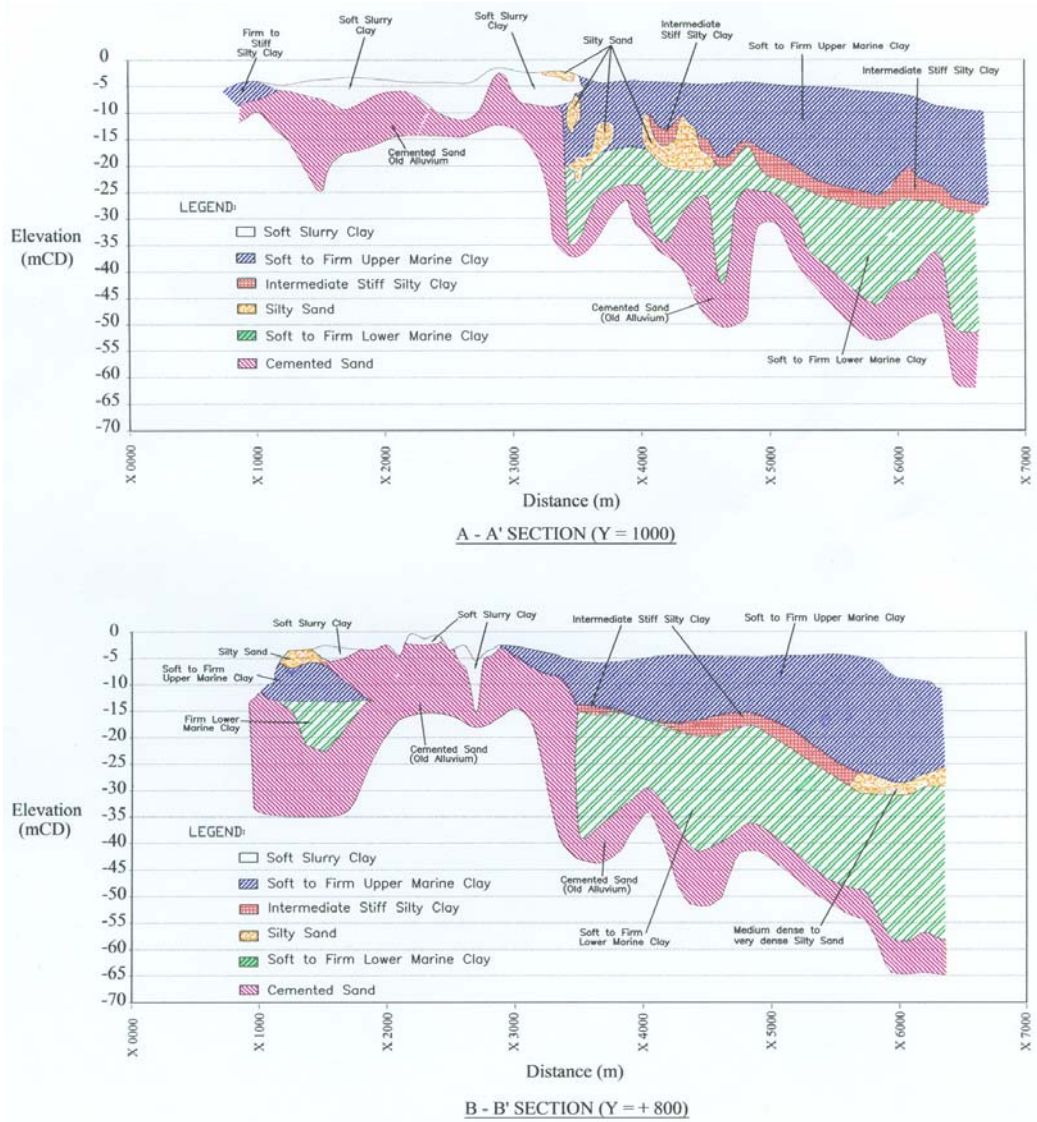


Figure 3.24 Typical geological profile of the project site.

3.7 Photographic Identification of Marine Clay

Photographic identification of the marine clay was carried out in the site laboratory. The marine clay samples were obtained from a marine sampling borehole and the samples were sent by boat to the site laboratory for photographic purposes.

The marine clay samples were extruded and the entire length of the sample was carefully cut and subsequently broken open. Opening the sample as such exposed the inner core of the sample to identify the lamination of the marine clay. The colour of the marine clay was compared with colour charts to positively describe the colour of the various layers of marine clay.

Photographic identification of the marine clay in this manner allow to feature the degree of the lamination of the marine clay. The identification depths of sand seams, organic material, layers of past exposure to oxidation etc. could thus be determined. The same soil sample has been cut in half and split apart as shown in the left hand and right hand side of Figure 3.25 to Figure 3.28.

Figure 3.25 shows that the marine clay found close to the seabed consists of interbedded sand seams due to the geological deposition of seabed sand into this layer.

Figure 3.26 shows the brownish-blue upper marine clay layer consisting of organic deposits.

Figure 3.27 shows the intermediate stiff clay layer which is reddish due to oxidation of the layer as a result of exposure of the seabed to the atmosphere during the rise and fall of the sea levels in the geological past.

Figure 3.28 shows brownish-blue lower marine clay layer consisting of organic deposits. Fine sand particles are observed in both the upper and lower marine clay layers.

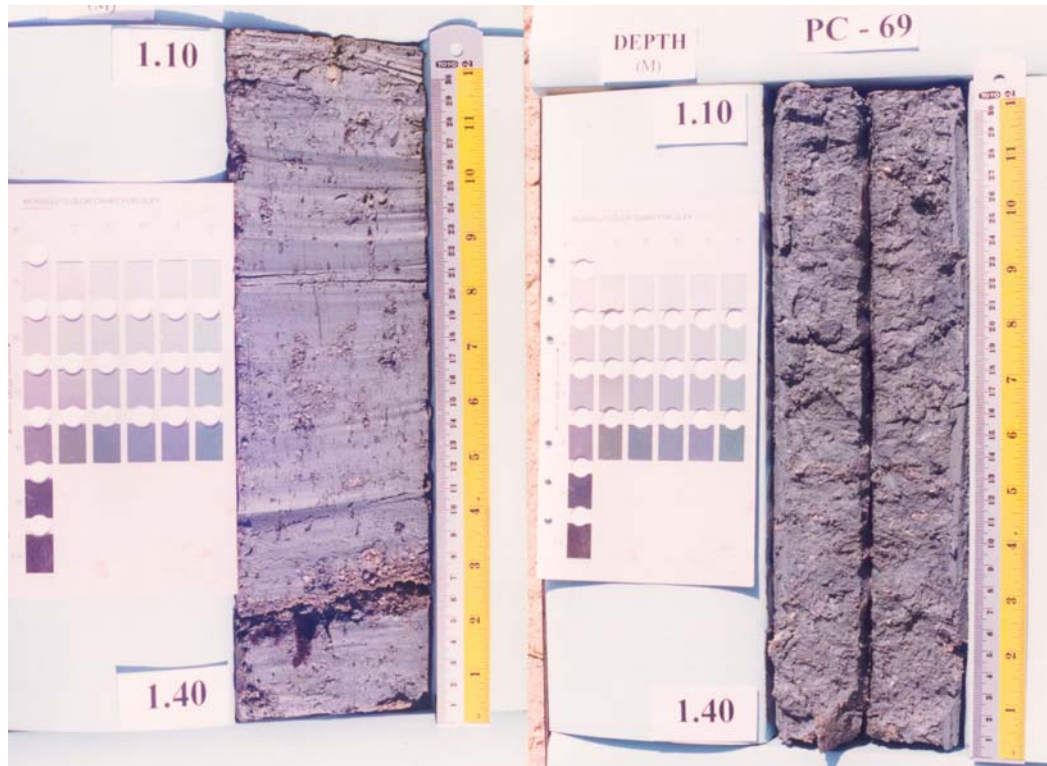


Figure 3.25 Photo identification of marine clay close to seabed level.

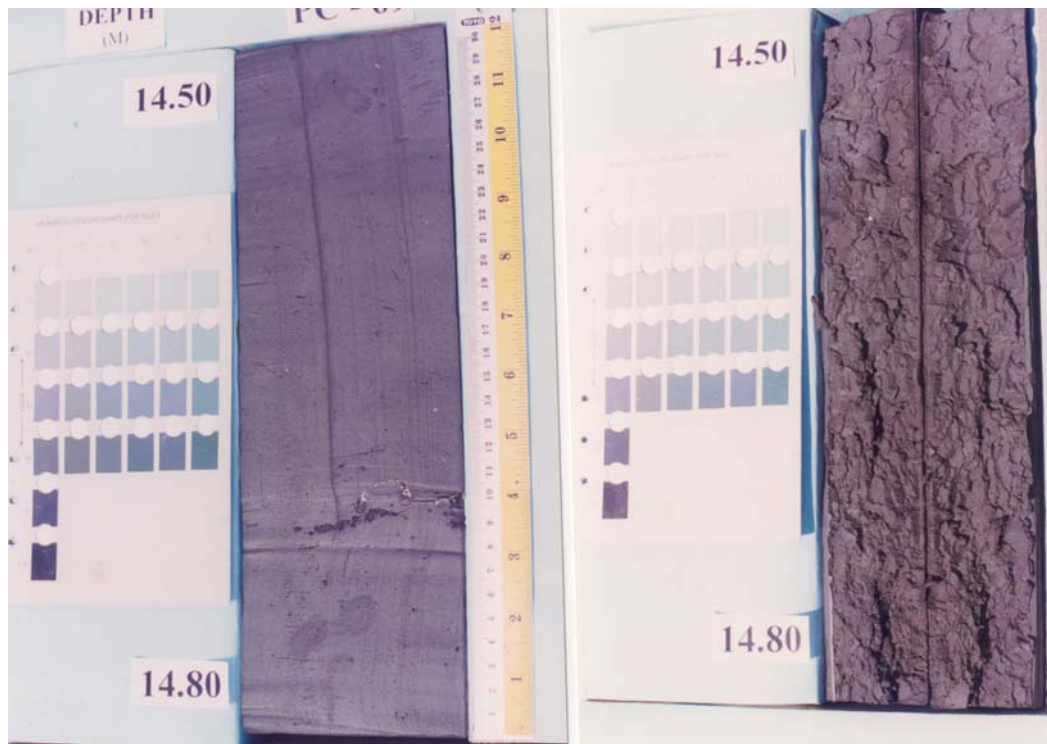


Figure 3.26 Photo identification of upper marine clay.

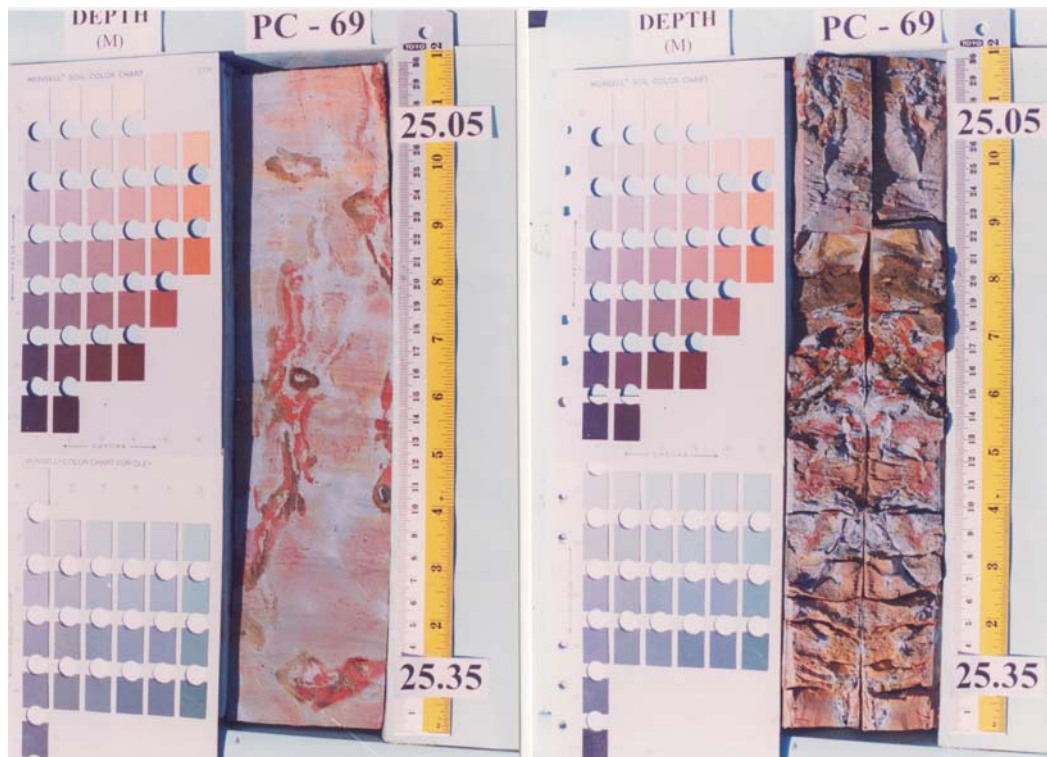


Figure 3.27 Photo identification of intermediate stiff marine clay.

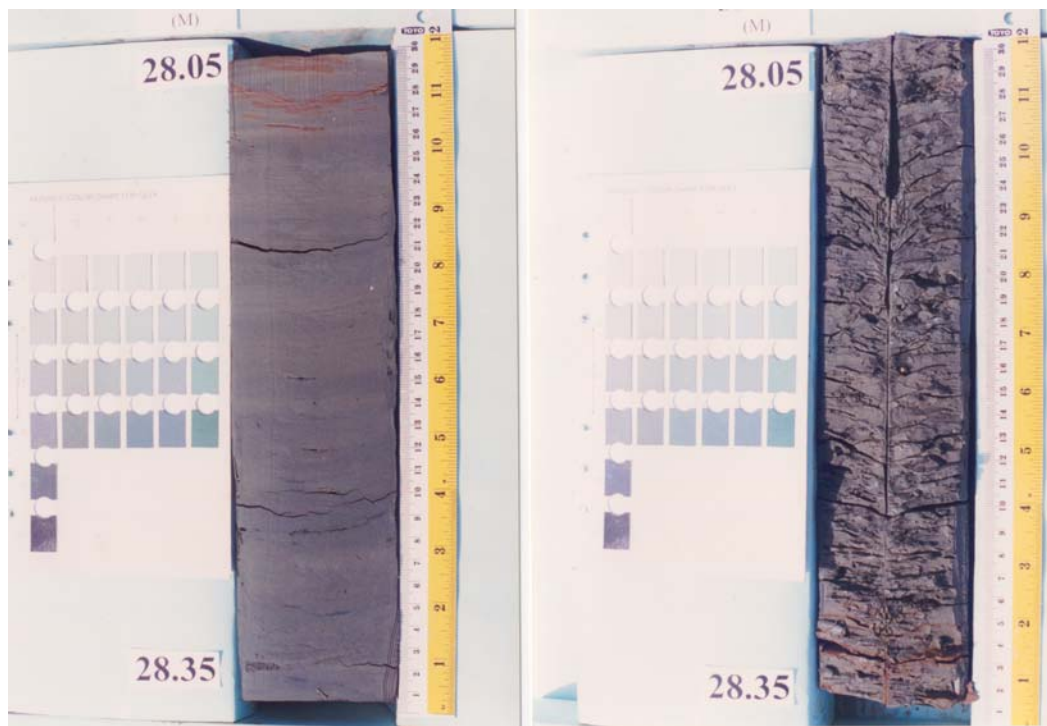


Figure 3.28 Photo identification of lower marine clay.

4.0 OFFSHORE LAND RECLAMATION METHODOLOGY

The land reclamation methodology and characteristics of dredging plant used in the Changi East Reclamation Project in Singapore described in this chapter has been discussed by the author (Arulrajah et al., 2004c) during the course of this research study.

4.1 History of Land Reclamation in the Republic of Singapore

Land reclamation in Singapore dates back to the 19th Century where one of the earliest being the Telok Ayer reclamation project between 1879 and 1887 in which hill cut soil was used (Yong et al., 1990).

Large scale land reclamation has been undertaken in various parts of the Republic of Singapore since the 1960's. This is necessary because of the small size of the country (total area being about 581.5 square kilometres prior to 1960) and the rising demand for more land as the population increases. Land has been reclaimed for building homes for the growing population, expanding commercial and industrial activities and also to meet transport needs such as port and airport facilities. By 1990, the total land area of Singapore was 633 square kilometres. This was an increase of 51.5 square kilometres and makes up 8.9% increase of the total land area from the 1960's. With continuing land reclamation, it is estimated that land area in Singapore will increase by another 100 square kilometres by the year 2030 (Urban Housing Development of Singapore, 2000). Figure 4.1 shows the locations of reclaimed land in Singapore and their uses.

The limiting constraints as to how much more land the country can reclaim is the significantly higher cost of land reclamation works in deeper waters as well as the constrictions of the sea lanes when pushing the reclamation further offshore. Land reclamation has modified the coastline of Singapore, extending it seawards especially on the eastern, north-eastern and western parts of the island and changing it quite beyond recognition. Large coastal areas have also been straightened by the building of dykes across estuaries. Many offshore islands have also become larger. (Urban Housing Development of Singapore, 2000). In the early years of land reclamation in Singapore, fill materials were evacuated from the hills in various parts of Singapore and used for filling the reclamation areas. However, these days, reclamation filling sand is mostly imported into Singapore from neighbouring countries.

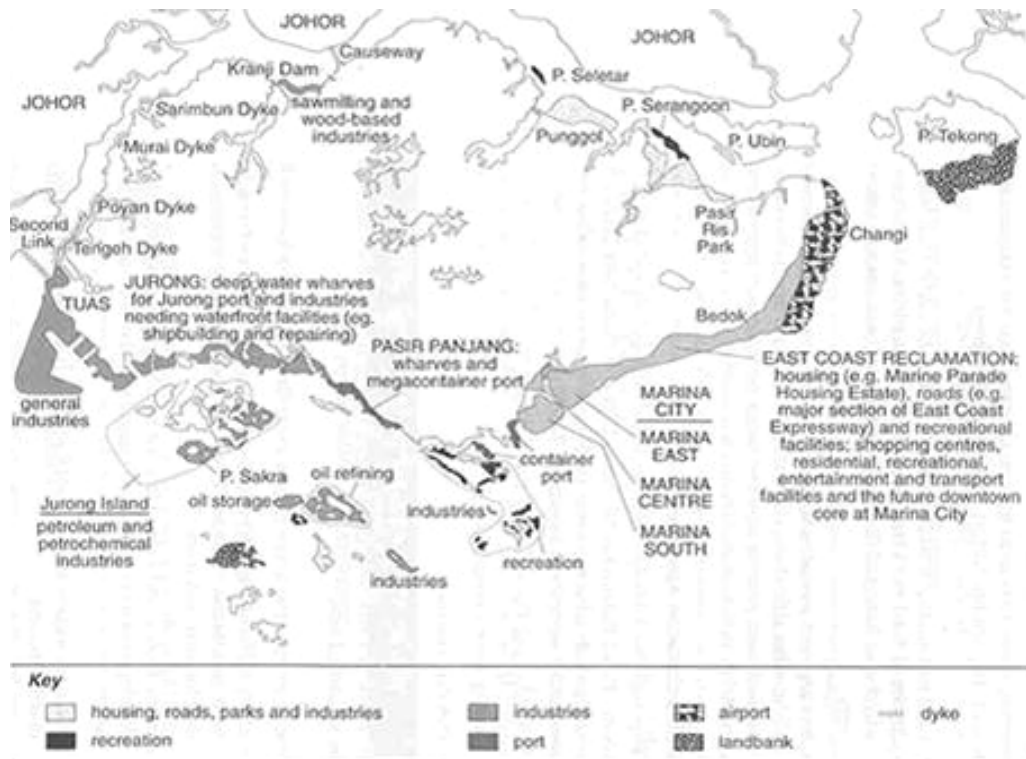


Figure 4.1 Reclaimed land and their uses in the Republic of Singapore (Urban Housing Development of Singapore, 2000).

4.2 Land Reclamation at the Changi East Reclamation Projects

Since the early 1990's, the still ongoing Changi East Reclamation Projects in the East of Singapore has involved the filling of 200 million cubic meters of sand for the reclamation of a total land area of 2500 hectares. Land reclamation works is carried out primarily with cutter suction dredgers, trailer suction hopper dredges and bottom-opening hopper barges. Land reclamation is carried out using fill materials derived from dredging granular material from the seabed at the borrow source in neighbouring countries. Sea sand obtained from the seabed is the source of fill materials for land reclamation and is imported from neighbouring countries. Land reclamation at Changi East requires areas that are permanently submerged to be raised to levels that are permanently above the sea level. The sea sand is well-graded, free draining sand with fines and shell contents of less than 10%. When the fill is placed by pumping, fines may also be released with the draining water when flow velocities within the area of reclamation are sufficiently high to maintain fine particles in suspension. When fill is placed hydraulically without containment bunds, the free escape of draining water normally removes most of the fine particles. Figure 4.2 and 4.3 shows land reclamation operations at the Changi East Reclamation Project.



Figure 4.2 Land reclamation operations. (note cutter-suction dredgers in background).



Figure 4.3 Land reclamation sand-pumping operations.

4.3 Characteristics of Dredging Plant

The principal type of dredging plant used in the land reclamation works are the cutter-suction dredger, trailer suction hopper dredger and the bottom-opening hopper barge. The characteristics of these dredging plants have been discussed in British Standard 6349 (1991). Other equipment commonly used in offshore land reclamation activities include dredging plough, bucket dredgers, grab dredgers, crane pontoons, backhoe dredgers and stone dumping pontoons.

4.3.1 Cutter Suction Dredger

In the Changi East Reclamation Projects, cutter-suction dredgers were positioned at both the borrow area in neighbouring countries as well as at the rehandling pit in the project site. Cutter-suction dredgers stationed at the borrow areas were utilised to load bottom-opening hopper barges which were then towed to deep water rehandling pits in the reclamation site. The cutter-suction dredgers stationed at the rehandling pit would be used to redredge sand from the rehandling pit and pump it via a floating pipeline to the area of reclamation. Cutter suction dredgers currently available can have total installed diesel power varying up to 27,150 kW (Jan De Nul, 2003).

The cutter-suction dredgers used in the project were dumb (non-self propelled). Dredging only takes place with the dredger moored in some way and it involves an initial powerful cutting action with suction and pumped discharge to barges or via pipeline to an onshore area for land reclamation.

The positioning and control of the cutter-suction dredger is usually by means of a combination of spuds and winches. The discharge from the dredge pumps passes over the stern of the pontoon to a heavy hose or flexible coupling, to which is connected a floating pipeline which in turn is connected to an onshore pipeline. An intermediate seabed pipeline is often used.

Figure 4.4 and 4.5 shows the schematic diagram and picture of a cutter suction dredger.

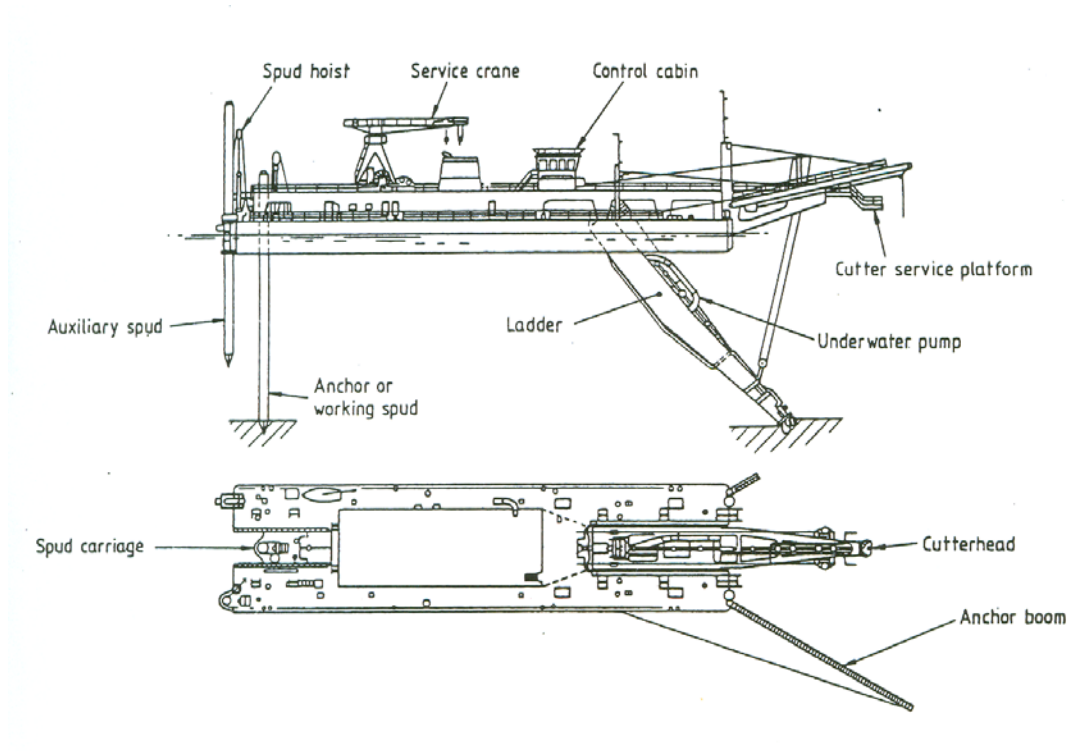


Figure 4.4 Schematic diagram of cutter suction dredger (After BS6349; 1991).



Figure 4.5 Cutter-suction dredger in operation.

4.3.2 Trailer Suction Hopper Dredger

A trailer suction hopper dredger is a ship that has the ability to hold its own, normally called a hopper, by means of centrifugal pumps. Loading takes place when the ship is under way. Discharge is normally by means of a bottom dumping arrangement or by pump discharge to the shore. The trailer suction thus has the independent ability to dredge sand from the borrow area, transport the sand to the project site and discharge the sand directly from the hopper into the reclamation area. The trailer suction hopper dredger is rated according to the maximum hopper capacity, which can vary up to 44000m³ (Jan De Nul, 2003).

The intake end of the suction pipe is fitted with a 'draghead' designed to maximise the concentration of solids entrained from the sea bed. Since the dredge pumps of the trailer suction hopper dredger are usually low head pumps, the trailer suction hopper dredger can not normally pump discharge through long pipelines unless intermediate booster pumps are employed. Figure 4.6 and 4.7 shows the schematic diagram and picture of a trailer suction hopper dredger.

Depending on draft and local conditions, the trailer suction dredger may pump directly ashore or they may discharge into a rehandling pit just offshore. At this point, a cutter suction dredger pumps the dredged sand ashore through a floating pipeline.

4.3.3 Bottom-Opening Hopper Barge

The bottom-opening hopper barges were utilised in combination with the use of tug boats to transport the fill material which is loaded into the hoppers from the borrow source to the discharge point at the rehandling pits. The borrow area itself is in neighbouring countries and as such the dredging cycle (i.e. the time to sail to and from the borrow source and the time to unload) is an important factor in project economics.

In deep waters, the bottom-opening hopper barges can discharge fill material from the hopper directly into the reclamation area due to its shallow draft. Barge capacities are as much as 3000 m³ and the loaded draught is generally less than 4 meters dredger (BS6349; 1991).

Figure 4.8 shows a bottom-opening hopper barge with tug boat.

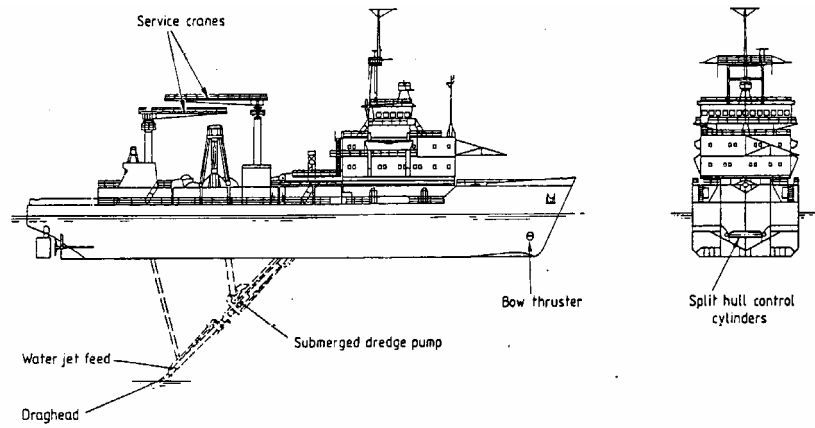


Figure 4.6 Schematic diagram of a trailer suction hopper dredger (After BS6349; 1991).



Figure 4.7 Trailer suction hopper dredger in operation.



Figure 4.8 Bottom-opening hopper barge in operation.

4.4 Shore Protection Works

Shore protection works in land reclamation can be in the form of revetments, rip-raps, groynes and headlands. The purpose of the slope protection work is to protect the reclaimed land from the erosive effects of waves and currents. Armour rocks and smaller rocks are used in the construction of the shore protection works. Geofabric is used to prevent the underlying sand layer penetrating into the upper rock layer and from there being flushed out (Centre for Civil Engineering Research and Codes, 1995). In general, the hydraulic loads exerted on shore protection works are in the form of wind waves, ship waves, tidal levels, wind waves and swell and currents.

Construction of shore protection works involves the underwater placement of geofabric and rocks from marine barges with the aid of global positioning systems and specialist deep sea divers. Of prime geotechnical importance in the design of the shore protection works is the stability and settlement of the structures. Therefore it is important to correctly assess the shear strength and consolidation parameters of the marine clay underlying these protection works. Figure 4.9 and 4.10 shows shore protection works at the project site.



Figure 4.9 Aerial view of shore protection works.



Figure 4.10 Close-up view of shore protection works.

5.0 PRELOADING AND PREFABRICATED VERTICAL DRAINS

The prefabricated vertical drain (PVD) with preloading method was considered the most feasible treatment option for the project based on the depth of treatment, cost, time available for preloading and other considerations. The objective of using the vertical drains with preloading technique is to accelerate the rate of consolidation and to minimize future settlement of the treated area under the future dead and live loads. Preloading increases the bearing capacity and reduces the compressibility of weak ground by forcing soft soils to consolidate (Van Impe, 1989). Soil improvement works is carried out in such a way that a specified degree of primary consolidation is designed to be attained within the desired time frame by improving the soil drainage system. The characteristics of the marine clay and the description of the Project Site has been presented earlier in Chapter 3.

The various theories, considerations, design methodologies and design predictions for the ground treatment of marine clay with prefabricated vertical drains in such off-shore projects has been discussed by the author (Arulrajah et al., 2004m) during the course of this research study.

5.1 Preloading

The idea of preloading consists of first loading the foundation layer in such a manner and over a well-chosen area so that the settlements related to this preloading already, either completely or to a large extent, constitute the initial expected deformation for the final construction (Van Impe, 1989). Preloading, with or without vertical drains is only effective in causing substantial pre-emptive settlement if the total applied load significantly exceeds the preconsolidation pressure of the foundation material (Hausmann, 1990).

Soil stresses and pore water pressures are increased by the extra weight, the pore water pressure temporarily. If the excess pore water is then expelled, only the increased effective stresses remain. The initial effective stresses after preloading may thus increase considerably, leading to soil improvement during construction.

5.2 History of Vertical Drains

The American engineer D.J. Moran, first proposed the use of sand drains as a means for deep stabilisation in 1925. The first practical sand drain installation were constructed in California a few years later (Holtz et al., 1991).

In Sweden in the mid to late 1930's, Kjellman began experiments and obtained patents on the first prototype of a prefabricated drain made entirely of cardboard. It was soon discovered that the prefabricated drains were subject to undesirable rapid deterioration, particularly near the top of the drained clay layers. Even with these difficulties, Kjellman wick drains have been used occasionally in both Europe and Japan during the past 50 years. However, until the early 1970s, the vast majority of vertical drains installed in the world were sand drains. In 1971, Wager improved on the Kjellman wick by using a grooved plastic (polyethylene) core in place of the cardboard one. This drain was called Geodrain and the first models utilised Kraft paper filters. Later models were provided with non-woven textile filters (Holtz et al., 1991).

In the last 20 years, a new frontier seems to have opened for vertical drains. A large number of prefabricated drains have appeared on the market. This competition has decreased the cost of the drains appreciably. Installation procedures too have improved and rapid installation to depths up to 60 meters can now be achieved at rates of 1 m/s. Currently vertical drains are the most common form of deep ground treatment in this region and their applications are vast in projects such as roads, railways, ports, airports and various other infrastructure projects.

5.3 Functions of Vertical Drains

In order to reduce, in cohesive layers, the time required to reach a high degree of consolidation under preloading, improved drainage should be used in the form of prefabricated vertical drains (Van Impe, 1989).

The primary use of prefabricated vertical drains is to accelerate consolidation to greatly decrease the settlement time of embankments over soft soils such that the final construction can be completed in a reasonable time with minimal post construction settlement. By doing so the vertical drains also accelerate the rate of strength gain of the in-situ soft soils. Furthermore, vertical drains decrease the amount of surcharge or preload material required to

achieve a settlement in a given time. Without installing vertical drains, bearing failures may occur during placement of the fill and settlement of soft soils may extend over many years. Due to the highly efficient drain installation methods, preloading combined with vertical drains has become an economic alternative to the installation of other ground improvement methods (Hausmann, 1990).

Vertical drains accelerate primary consolidation only, because significant water movement is associated with it. Secondary consolidation causes only very small amounts of water to drain from the soil and as such secondary settlement is not speeded up by vertical drains. Only relatively impermeable soil potentially benefit from vertical drains. Vertical drains are particularly effective where a clay deposit contains many thin horizontal sand or silt lenses (so-called microlayers).

Prefabricated vertical drains are band shaped (rectangular cross-section) products consisting of a geotextile filter material surrounding a plastic core. The size of the prefabricated vertical drain is typically 10 cm wide by 3 to 4 mm in thickness (Bo et al., 2003a). The material consists of a plastic core formed to create channels which are wrapped in a geotextile filter (Schaefer, 1997). The main function of the filter of the vertical drain is to ensure that fine particles cannot pass through and clog the drainage channels in the core (Hansbo, 1981).

5.4 Properties of Prefabricated Vertical Drains

Prefabricated vertical drains consist of a core and filter sleeve which are made of polymers. The dimension of the drain is normally 100 mm wide and 3-4 mm thick. The performance of the vertical drain is affected not only by the drain itself but also by the type of soil and the installation method (Bo et al., 2003). The filter interacts with the soil and the properties of it control the entry of water into the drains. The method of installation used requires for the vertical drain to possess a certain tensile strength to sustain the tensile stresses subjected to it during the installation process.

The main properties of vertical drains that need to be specified in a ground improvement project are discussed as follows (Bo et al., 2003; Indraratna and Bamunawita, 2002; Holtz et al., 1991):

5.4.1 Discharge Capacity

The purpose of using the prefabricated vertical drains is to release the excess pore water pressure in soil and discharge water. Therefore, the higher the discharge capacity of the vertical drains the better the performance of the vertical drain.

Factors affecting the performance of vertical drains are as follows:

- Consolidation stress.

The discharge capacity of vertical drains decreases with increasing consolidation stress. This is predominantly due to the reduction in the cross-sectional surface area of the vertical drain as the drain is compressed under pressure and the penetration of the filter into the drain groove. (Broms et al., 1994).

- Deformation of drain

With the consolidation of soil, the drain will buckle or deform inside the soil. The discharge capacity of the buckled drain will normally be smaller than that of a straight drain (Chu and Choa, 1995).

- Time

The discharge capacity of the vertical drain may change with time. This is attributable to the creep deformation of the drain material particularly the filter which will cause the effective cross-section area of the drain to reduce (Chu and Choa, 1995).

- Clogging of drain

When the pores of the filter are too large, the fines may ingress into the drain thereby clogging the drain.

- Hydraulic gradient

The discharge capacity measured varies with different hydraulic gradients and is smaller when a higher hydraulic gradient is used.

- Temperature

The higher the temperature, the faster the flow and the larger the discharge capacity.

When the discharge capacity of the vertical drain is smaller than the amount of water that needs to be discharged, well resistance will occur. Ideally the discharge capacity of the drain, q_w should be sufficiently large in order for well resistance to be ignored in the design.

According to Xie (1987) and Wang and Chen (1996), the following condition must be met in order to hold the well resistance to an insignificant level:

$$\frac{\pi}{4} \frac{k_h}{q_w} l_m^2 < 0.1 \quad \text{Eq.(5.1)}$$

where:

k_h is the horizontal hydraulic conductivity of soil (m/s).

l_m is the length of the vertical drain (m)

For this condition to hold, the discharge factor must hold by the following equation:

$$D = \frac{q_w}{k_h l_m^2} \geq 7.85 \quad \text{Eq.(5.2)}$$

The required discharge capacity after applying a reduction factor to consider all the influencing factors on discharge capacity reduces to:

$$q_{\text{req}} \geq 7.85 F_s k_h l_m^2 \quad \text{Eq.(5.3)}$$

where:

q_{req} is the required discharge capacity (m³/s).

F_s is the reduction factor which is a value of between 4 to 6.

Mesri and Lo (1991) has compared discharge capacity mobilised in field situations to that required for negligible well resistance. From their findings, the minimum discharge capacity should be no less than 100 m³/yr or 3 x 10⁻⁶ m³/s. Bo et al. (2003a) states that it is unnecessary to use an excessively high reduction factor for discharge capacity. This is because, although the discharge capacity reduces with the deformation of vertical drain and time, the permeability of soil reduces with consolidation (Arulrajah et al., 2004f, 2004i), so the amount of water discharged also reduces with time.

5.4.2 Properties of Filter

There are two basic filter design criteria that have to be met. The first is that the Apparent Opening Size (AOS) has to be sufficiently small so that it can prevent the ingress of clay particles into the drain. The second is that the permeability of the filter has to be sufficiently

large. The criteria adopted for prefabricated vertical drains is listed below (Bo et al., 2003; Holtz et al., 1991):

- Soil retention ability

Carroll (1983) stated that the following condition has to be met for the soil retention ability:

$$O_{95} \leq (2 \text{ to } 3) D_{85} \quad \text{Eq.(5.4)}$$

$$O_{50} \leq (10 \text{ to } 12) D_{50} \quad \text{Eq.(5.5)}$$

where:

O_{95} is the AOS of the filter. $O_{95} = 75$ mm is often specified for vertical drains.

O_{50} is the size which is larger than 50% of the fabric pores.

D_{85} is the size for 85% of passing of the soil particle.

D_{50} is the size for 50% of passing of the soil particle.

Bergado et al. (1993) has adopted the following criteria for Bangkok clay:

$$O_{95} \leq (2 \text{ to } 3) D_{85} \quad \text{Eq.(5.6)}$$

$$O_{50} \leq (18 \text{ to } 24) D_{50} \quad \text{Eq.(5.7)}$$

- Permeability

The permeability of the filter should be at least one order of magnitude higher than that of the soil. As the soil to be treated by prefabricated vertical drains usually has very low permeability, this requirement should be easily met in most cases (Bo et al., 2003):

$$k_f \geq 10 k_s \quad \text{Eq.(5.8)}$$

where:

k_f is the permeability of the filter and k_s is the permeability of the soil.

- Clogging resistance

Clogging occurs when the soil particle is trapped in the filter due to the particle grading sizes. To prevent clogging, Wang and Chen (1996) has recommended that the following conditions be met to meet the requirement of clogging resistance:

$$n \geq 30\% \quad \text{Eq.(5.9)}$$

$$O_{95} \geq 3 D_{15} \quad \text{Eq.(5.10)}$$

$$O_{15} \geq (2 \text{ to } 3) D_{10} \quad \text{Eq.(5.11)}$$

$$100 k_s < k_f < 100 \text{ m/s} \quad \text{Eq.(5.12)}$$

where:

n is the porosity of the filter

O_{15} is the size which is larger than 15% of the fabric pores.

D_{15} is the size for 15% of passing of the soil particle.

D_{10} is the size for 10% of passing of the soil particle.

5.4.3 Tensile Strengths

Prefabricated vertical drains should have adequate strength to sustain the tensile stresses subjected to it during the installation process. Therefore, the core, strength of filter, strength of the entire drain and strength of the spliced drain should be specified in both the wet and dry conditions (Bo et al., 2003). Kremer et al. (1983) stated that a drain should be able to withstand at least 0.5 kN of tensile force without exceeding 10% in elongation. It is common nowadays to specify the tensile strength of the entire drain at wet and dry condition as larger than 1 kN at a tensile strain of 10% (Bo et al., 2003). A spliced vertical drain should also be required to have a tensile strength comparable to that of an unspliced drain.

5.5 Quality Control Testing of Vertical Drains

Quality control testing of vertical drains is used to assess the various drain properties such as discharge capacity, tensile strength, permeability, Apparent Opening Size (AOS) etc. The required set of vertical drain testing equipment and testing methods have been established and discussed by Bo et al. (2003a) as well as Chu and Choa (1995). The in-depth testing methodology has been described by Bo et al. (2003a). Some of the essential facilities required for the quality control implementation of prefabricated vertical drain projects are listed below:

- Discharge capacity testing with straight drain tester.
- Discharge capacity testing with buckled drain tester.
- Discharge capacity testing with kinked drain tester.
- Tensile strength testing.
- Cross-plane permeability testing of filter.
- Apparent Opening Size (AOS) of filter.

5.6 Installation of Prefabricated Vertical Drains

Vertical drain installation is commonly by static, vibratory, combined static and vibratory methods. The vertical drains are installed with the use of a vertical drain stitcher which comprises a crawler crane or a crawler excavator. The installation of deep depths of vertical drains requires an installation mast mounted to a crane in order to provide stability. In some situations, the installation mast has to be secured with guy wires (Schaefer, 1997). Figure 5.1 shows a schematic diagram and photo of vertical drain stitcher.

5.6.1 Installation Considerations and Details

The suitability of the vertical drain rigs is as follows (Bo et al., 2003a):

- Static rig – Normal ground conditions
- Static rig with water balancing system – Very soft soil
- Vibratory rig – Firm to stiff soil

Selection of the type of vertical drain rig to use depends on the following factors:

- Bearing capacity of the platform
- Depth of installation
- Type of soil
- Production capacity of rig

The vertical drain rigs are driven by the following mechanisms:

- Chain system
- Pulley and roller system
- Additional hydraulic cylinders to penetrate hard ground
- Additional clamps to push down mandrel

A steel covering mandrel protects the drain material as it is installed and is used for the installation of the vertical drains. The mandrel must be rigid enough to penetrate the formation vertically and at the same time not too big such as to disturb the soil in which it is installed. The four main shape types of mandrels are rhombic, rectangular, square and circular. The rhombic and rectangular mandrels are the most commonly used mandrel types while the circular mandrel is the least commonly used. The drain material comes in rolls and is threaded through the mandrel. Figure 5.2 shows a typical mandrel for installation of prefabricated vertical drains. Bo et al. (2004) has described in detail the typical mandrels used in the Changi Reclamation Projects in Singapore.

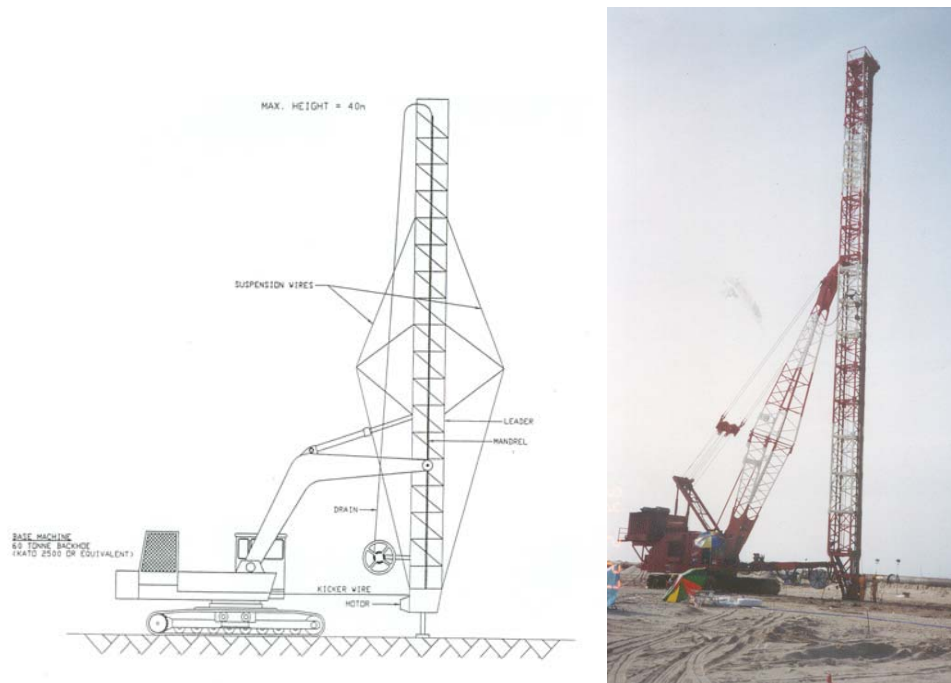


Figure 5.1 Schematic diagram and photo of vertical drain stitcher.

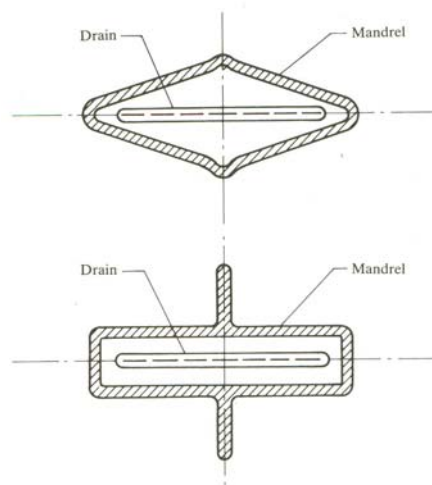


Figure 5.2 Typical mandrels for prefabricated vertical drain (After Holtz et. al., 1991).

An anchoring system is employed to hold the drain material in place while the mandrel is withdrawn. The anchor has to be strong enough to anchor the vertical drain into the dense/stiff formation. The anchor also functions to prevent soil ingress into the mandrel. The anchors in common use are steel bars and flexible metal plate. Steel bars is the preferred type of anchor due to the minimum disturbance in the soil caused by its usage. In rare cases the vertical drain material itself is used as an anchor though this is not a suggested method. Figure 5.3 shows a typical detachable anchor shoes used with prefabricated drain mandrels.

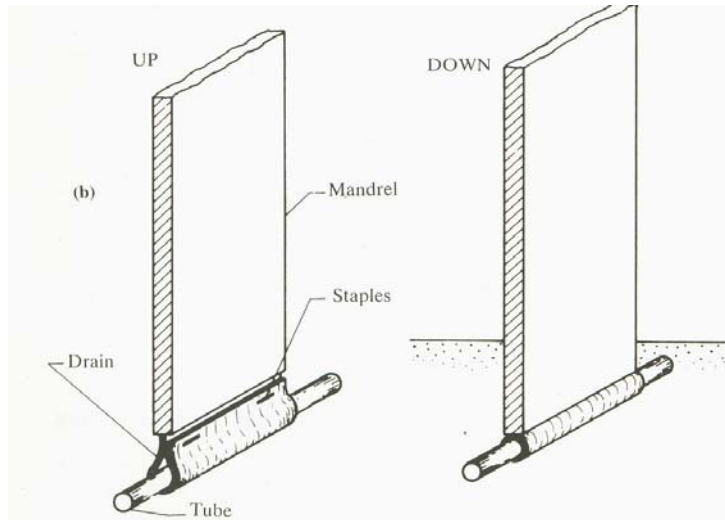


Figure 5.3 Typical detachable anchor shoes used with prefabricated drain mandrels (After Holtz et. al., 1991).

Vertical drains were installed in the Project Site at the platform level of +4 mCD, the level of which was predetermined and fixed to ensure that the drains are installed in dry working conditions above the astronomical spring tide level (about +3.3 mCD). Additional allowance is provided to cater for the immediate settlements due to the drain installation. As sand is used for the reclamation filling works, the required sand blanker drainage layer for the vertical drains to function is automatically provided to enable a clear drainage path for the dissipation of the excess pore water pressures. Figure 5.4 shows vertical drains installation works at the project site while Figure 5.5 shows a close-up of the vertical drain installation works.



Figure 5.4 Vertical drains installation works at project site



Figure 5.5 Close-up of vertical drain installation works (note roll of drain material which is threaded through mandrel).

Selection of the type of vertical drain rig to use depends on the following factors (Bo et al., 2003):

- Bearing capacity of the platform
- Depth of installation
- Type of soil
- Production capacity of rig

The vertical drain rigs are driven by the following mechanisms:

- Chain system
- Pulley and roller system
- Additional hydraulic cylinders to penetrate hard ground
- Additional clamps to push down mandrel

5.6.2 *Installation Difficulties*

The various installation difficulties encountered during installation in marine clay is as follows (Bo et al., 2003):

- Dessicated hard crust encountered at the original seabed level
- Intermediate stiff soil encountered at intermediate depth in the soft marine clay
- Hard or dense formation encountered at intermediate deep depths overlying soft marine clay
- Installation difficulties in soft or ultra-soft clays

The dessicated hard crust and intermediate stiff soil encountered can be overcome by the use of prepunching or augering equipment. Alternatively, a vertical drain rig with a vibratory system can be used.

The hard or dense formation at deep depths on the other hand will require a high powered, low speed vertical drain installation rig which can punch through the layer and enable vertical drain installation in the marine clay underlying this layer. Leaving the underlying thick soft marine clay beneath this layer untreated can result in detrimental settlements arising in the future.

Installation of prefabricated vertical drains in soft or ultra-soft clays can result in the extrusion of mud along the annulus of the penetration hole resulting in contamination of the drainage layer. The intrusion of the material into the mandrel can lead to unsuccessful anchoring of the vertical drain. This installation difficulty can be minimised by introducing a water balancing system to counterbalance the water encountered in the formation. A smaller dimension mandrel with a smaller anchor is also suitable for such situations.

5.6.3 Installation Quality Control

Prefabricated vertical drains are installed at the project site to refusal. The refusal depth is often taken in the design as 1-3 meters below the base of the marine clay. The estimation of vertical drain depths is made by the Design Engineer based on the pre-reclamation site investigation and the seismic reflection survey results. Following reclamation to the vertical drain platform level, another series of site investigation can be directed to reconfirm the estimated depths of the vertical drains. This series of site investigation is often carried out with the use of the relatively quick cone penetration test.

The installation length of vertical drains is recorded by the following means (Bo et al., 2003):

- Visual readings of scale markings on mast – distinct painted markings
- Visual readings of dial gauge – drain depth determined by rotations of driving chain sprocket
- Automatic digital counter – computerised recording of reference points and penetration length

The automatic digital counter is currently a requirement in the implementation of many large ground improvement projects. This recording method enables the penetration length of each and every installation point to be recorded and the subsequent production of the as-built

records of an entire panel of vertical drain works. Furthermore, any points which have to be offset or omitted due to any obstructions can also be identified and shortlisted for remedial works which would likely be the installation of additional points.

The predetermined vertical drain design predicted lengths can hence be used as a gauge of the expected site installation lengths and differences between the lengths can be studied with the use of further post-installation site investigations.

5.7 Factors Affecting Design Predictions

The main variables of the design predictions area:

- the surcharge level;
- the vertical drain spacing;
- the preloading period;
- the degree of consolidation; and
- the coefficient of consolidation due to horizontal flow (c_h)

Prediction of the magnitude and time rate of settlement with vertical drains plays a major role in the design of soil improvement projects with prefabricated vertical drains and surcharge. Accurate prediction of the magnitude and time rate of settlement is dependent upon the selection of soil parameters and the engineer's judgement. In most cases, field time rate of settlement is slower than the predicted rate of settlement even though the soil parameters are obtained from controlled laboratory tests or in-situ tests. Magnitude and time rate of settlement could also differ from field settlement due to smear effect, variation of soil in nature and many other factors.

Prediction of the magnitude of primary consolidation settlement is largely dependent upon geotechnical parameters such as initial void ratio(e_0), compression index(C_c), recompression index(C_r) and preconsolidation pressure(P_c). In order to get accurate void ratios for each sub-layer, moisture content tests were carried out and the dry density and void ratio were calculated. Compression index and recompression index were obtained from 24 hours loading oedometer tests with load increment ratio of one. For the accurate prediction of time rate of settlement, the correct selection of design parameters for the coefficient of consolidation for vertical flow (c_v) and horizontal flow (C_h) is essential. Conventional methods (Terzaghi 1925, Barron 1948) were used for the settlement predictions.

5.8 Design and Theories of Prefabricated Vertical Drains

5.8.1 Design of Surcharge Level

The aim of the surcharge placement works is to preload the foundation soil to attain an effective stress which exceeds the pressure due to the design load. The design load comprises the future anticipated dead and live loads, which in the case of the proposed runway area would include the future runway pavement and the live airplane loads.

The time required to achieve the required degree of consolidation depends largely on the spacing of the vertical drains, which in turn will depend on the available time for completion of the project.

In the case of the airport runway, a drain spacing of 1.5 meters was considered viable due to several reasons. Firstly, the tight construction programme necessitated a closer drain spacing to be used and the surcharge period as specified. Secondly, c_h was considered to fall between 2 to 3 times c_v based on previous reclamation experiences in the area. Figures 5.6 and 5.7 shows surcharge placement operations at the project site.



Figure 5.6 Surcharge placement operations at the project site.



Figure 5.7 Aerial view of surcharge close to vertical drain installation works.

5.8.2 Determination of c_h

Since quaternary marine formation has been deposited under quiet marine conditions, there is no significant stratification. As such, the hydraulic properties are considered to be nearly isotropic. Due to this, the coefficient of consolidation due to horizontal flow and vertical flow may not be much different. The common practice for vertical drain installation in marine clays is to assume a c_h value of twice c_v ($c_h=2c_v$) since there is some lamination and foliation in the marine clay formation. However, based on experiences the c_h value obtained from laboratory and in-situ results, c_h values of as high as $6c_v$ could sometimes be obtained. Therefore, even with smear effect c_h values of at least $3c_v$ could be expected. Even though c_h was assumed as twice c_v ($c_h = 1$ and $2 \text{ m}^2/\text{year}$ for upper and lower marine clay respectively), the design prediction analysis has been carried out for various c_h to c_v ratios.

The design equations adopted in the study for the vertical drain areas incorporated the use of various equations namely Terzaghi's one-dimensional (1943), Barron's theory (1948) and Carillo's (1942) theory. Most consolidation with vertical drain software in the market today enables the consolidation and time rate of settlement of only a single layer to be calculated. As the marine clay in the Vertical Drain Area comprises of several distinct layers, the method of utilizing "equivalent c_v " was used in the design calculations for the multiple layers similar to that used by Arulrajah and Bo (1995) and Choa et al. (1992) in land reclamation projects in Singapore.

5.8.3 Consolidation Settlement

The consolidation settlement equations used are as defined by Terzaghi for one-dimensional consolidation. The equations were used to calculate the ultimate settlement for the filling works at the vertical drain platform level, as well as for the surcharge placement works at the surcharge level. Consolidation settlements were calculated separately for each of the various layers and this was then summed up to obtain the ultimate settlement.

Ultimate settlement, S_{ult} :

$$S_{ult} = Cc \frac{H_o}{1 + e_o} \log \frac{\sigma_f}{\sigma_c} + Cr \frac{H_o}{1 + e_o} \log \frac{\sigma_c}{\sigma_o} \quad \text{if } \sigma_f > \sigma_c \quad \text{Eq.(5.13)}$$

$$S_{ult} = Cr \frac{H_o}{1 + e_o} \log \frac{\sigma_f}{\sigma_o} \quad \text{if } \sigma_c > \sigma_f \quad \text{Eq.(5.14)}$$

where:

Cc = compression index

Cr = recompression index

e_o = initial void ratio

H_o = thickness of layers

σ_c = preconsolidation pressure

σ_f = final vertical effective stress,

Overburden Pressure at Centre of Layer:

$$\sigma_o = (\gamma_{bulk} - \gamma_w) H_o / 2 \quad (\text{kPa}) \quad \text{Eq.(5.15)}$$

where:

H_o is the thickness of layer (m)

Additional Pressure (due to Fill Placement):

$$\Delta\sigma = (\gamma_{bulk} - \gamma_w) H_{f1} + (\gamma_{bulk} H_{f2}) \quad \text{Eq.(5.16)}$$

where:

H_{f1} is height of fill below ground water level

H_{f2} is height of fill above ground water level

Final vertical effective stress, σ_f :

$$\sigma_f = \sigma_o + \Delta\sigma \quad \text{Eq.(5.17)}$$

5.8.4 *Equivalent Thickness*

As the marine clay consists of several layers, the equivalent thickness of the marine clay had to be calculated to enable the equivalent thickness, equivalent drainage and coefficient of vertical consolidation to be used as input values. The equations used for computation of equivalent thickness is as follows:

Equivalent Thickness of layer 1, $H_{1'}$:

$$H_{1'} = H_1(c_{vi} / c_{v1})^{0.5} \quad \text{Eq.(5.18)}$$

where:

c_{vi} is an initial assumed value

Total Equivalent thickness of all layers, $H_{Ti'}$:

$$H_{Ti'} = H_{1'} + H_{2'} + H_{3'} \dots H_{n'} \quad \text{Eq.(5.19)}$$

Equivalent drainage thickness, H_{dri} :

$$H_{dri} = H_{Ti'} / 2 \quad \text{Eq.(5.20)}$$

Equivalent coefficient of vertical consolidation, c_{vi} :

$$c_{vi} = H_{Ti'}^2 / (c_{v1} H_{Ti'}) \quad \text{Eq.(5.21)}$$

5.8.5 Vertical Consolidation

The equations applicable for the calculations of the time rate of settlement are as follows:

Time factor for consolidation by vertical drainage, T_v :

$$T_v = c_{vi} t / H_{dri}^2 \quad \text{Eq.(5.22)}$$

Average degree of consolidation with respect to vertical flow, U_v :

$$U_v = (4T_v / \pi)^{0.5} / [1+(4T_v / \pi)^{2.8}]^{0.179} \quad (\%) \quad \text{Eq.(5.23)}$$

5.8.6 Radial Consolidation

A square pattern of drain installation was designed for the project site. Hansbo (1979) suggested that the equivalent diameter, d_w should be that of a cylinder having the same circumference.

Diameter of equivalent soil cylinder, d_e :

$$d_e = 1.13s \text{ for square pattern} \quad \text{Eq.(5.24)}$$

$$d_e = 1.05s \text{ for triangular pattern} \quad \text{Eq.(5.25)}$$

Diameter of vertical drain, d_w :

$$d_w = 2(a + b) / \pi = 0.0675 \text{ for the type of drain used in study} \quad \text{Eq.(5.26)}$$

Drain spacing ratio, n :

$$n = d_e / d_w \quad \text{Eq.(5.27)}$$

where:

s is the drain spacing (m)

a is the drain width (m)

b is the drain thickness (m)

The time factor and average degree of consolidation with respect to radial flow computations are relevant for the simulation of settlement after installation of vertical drains at the drain installation level as well as analysis throughout the surcharge duration. The solution for

radial water flow toward the central drain goes back to Rendulic (1936). The result is generally expressed in terms of the average consolidation ratio for radial drainage U_r .

Time factor for consolidation by horizontal drainage, T_r :

$$T_r = c_h t / d_c^2 \quad \text{Eq.(5.28)}$$

Onoue (1988) suggested a simplified formula given below for the average degree of consolidation with respect to radial flow, U_r . The equation uses Yoshikuni and Nakanodo (1974) well resistance coefficient, L defined later in Section 5.8.8.

$$U_r = 1 - \exp \frac{-8 T_r}{F(n) + 0.8L} \quad \text{Eq.(5.29)}$$

$$F(n) = \frac{n^2}{(n^2 - 1)} \log_e(n) - \frac{3n^2 - 1}{4n^2} \quad \text{Eq.(5.30)}$$

where:

n is the drain spacing ratio

5.8.7 Combined Vertical and Radial Consolidation

Carrillo (1942) derived how the average degree of consolidation for combined vertical and radial water flow, U_{vr} can be calculated:

$$(1 - U_{vr}) = (1 - U_v)(1 - U_r) \quad \text{or} \\ U_{vr} = 1 - [(1 - U_v)(1 - U_r)] \quad \text{Eq.(5.31)}$$

Time rate of total settlement, S_t with vertical drains can be calculated at any particular time for the various surcharge heights by the following equation:

$$S_t = S_{ult} (U_{vr}) \quad \text{Eq.(5.32)}$$

5.8.8 Well resistance

The relevant features for the design and performance of vertical drains are their hydraulic properties: the discharge capacity of the cross-section and their filter permeability. If during the consolidation period the discharge capacity of the drain is reached, the overall consolidation process is retarded. In such cases, the drains present resistance to the water

flowing in them. The longer the drainage path within the drain, the slower will be the consolidation and gain in strength in the zone furthest from a permeable layer adjoining the soil being treated.

Well resistance can develop and increase as the deterioration of the drain filter may lead to reduction of the cross-section. Furthermore fine soil particles may pass through the filter and decrease the area available for flow. Finally, folding of the drain because of large settlements may result in a reduced discharge capacity. (Holtz et al., 1991). For the calculations in this study, the well resistance parameter, L as developed by Yoshikuni and Nakanodo (1974) has been used.

Well resistance parameter, L:

$$L = [32 / (\pi)^2] (k_h/k_w) (H_{dri}/d_w)^2 \quad \text{Eq.(5.33)}$$

where:

k_h is the horizontal hydraulic conductivity of the soil = 0.0315 m/yr,

k_w is the coefficient of longitudinal permeability of the drain = 34689.6 m/yr

5.8.9 *Smear Effect,*

It is often assumed that the installation of the drain does not change the properties of the surrounding soil. In actuality however, drain installation disturbs the soil to a degree, depending on its sensitivity and macro-fabric (Rowe, 1968). Disturbance of the soil adjacent to the drain is likely to decrease its permeability and thus slow down the consolidation process. This effect is described as “smear”. The smear effect is believed to increase with increasing drain diameter and is also dependent on other factors such as method of installation, size of mandrel and size of anchor plate. Barron (1948) and Hansbo (1979, 1981) analysed the effect of this soil disturbance by assuming an annulus of smeared clay around the drain. Within this annulus of diameter, d_s the remoulded soil has a lower coefficient of permeability, k_r than the k_h of the undisturbed clay as illustrated in Figure 5.8. This leads to a new boundary condition between the undisturbed zone and the smeared annulus, and this affects the solution by changing the drain factor F(n) defined earlier to as follows:

Smear effect, Fs(n):

$$Fs(n) = \log_e[n / s] - 0.75 + [(k_h / k_r) \log_e(s)] \quad \text{Eq.(5.34)}$$

where:

k_h / k_r assumed to be 2

$s = \text{smear zone ratio} = d_s / d_w$

d_s is the diameter of smeared zone

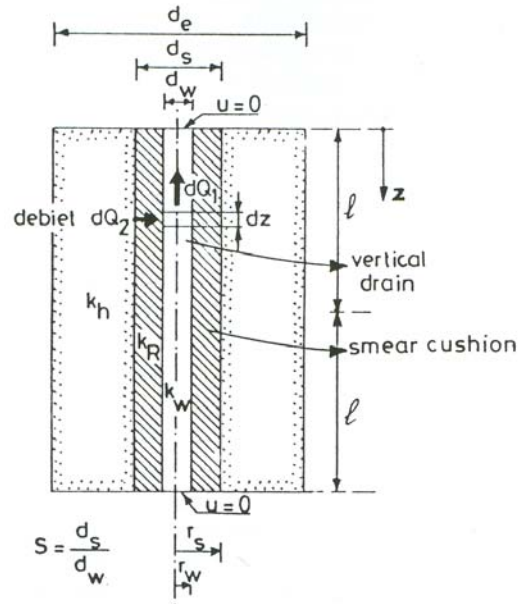


Figure 5.8 Smear effect and well resistance (After Hansbo, 1981).

5.9 Predictions of Magnitude and Time Rate of Settlement with PVD

Figure 5.9 shows the design construction sequence at the case study area (Vertical Drain Area at the In-Situ Test Site). Figure 5.10 and Figure 5.11 shows prediction of settlement and degree of consolidation curves generated from the design of vertical drains with preloading for the Vertical Drain Area. Vertical drains were designed to be installed in the Vertical Drain Area at the platform level of +4 mCD at 1.5 meters square spacing. Surcharge placement of 6 meters in height (+10 mCD) was designed to be carried out. The characteristics of the marine clay has been described by the author in Chapter 3. Curves were plotted for various c_h to c_v ratios. For the design predictions, the coefficient due to horizontal flow (c_h) was assumed to be 2 times that of c_v that is, $c_h = 1$ and $2 \text{ m}^2/\text{year}$ for upper and lower marine clay.

Design predictions for the ground treatment of marine clay with prefabricated vertical drains has been discussed by the author (Arulrajah et al., 2004m) during the course of this research.

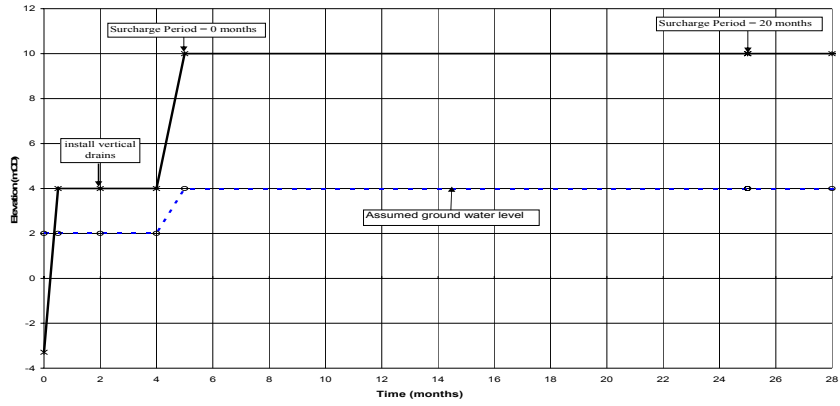


Figure 5.9 Design Construction sequence for Vertical Drain Area (Arulrajah et al., 2004m).

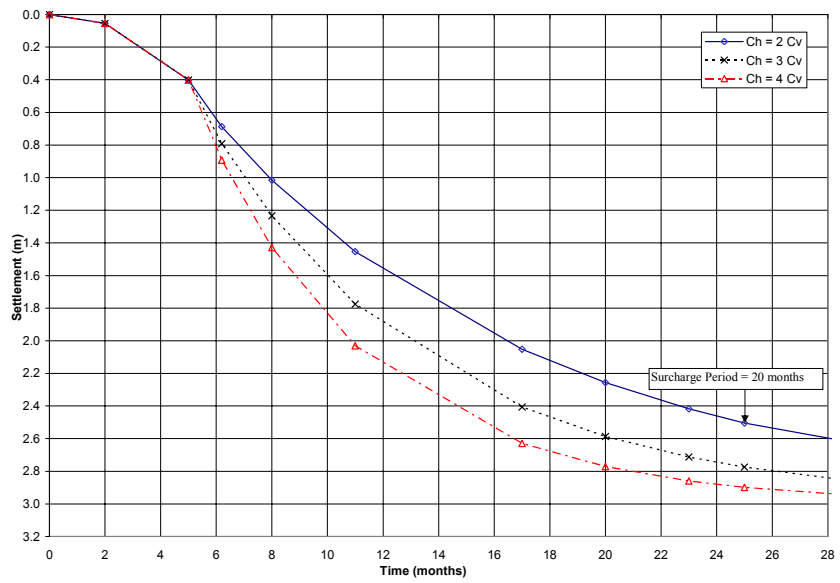


Figure 5.10 Settlement curves for various c_h at Vertical Drain Area (Arulrajah et al., 2004m)

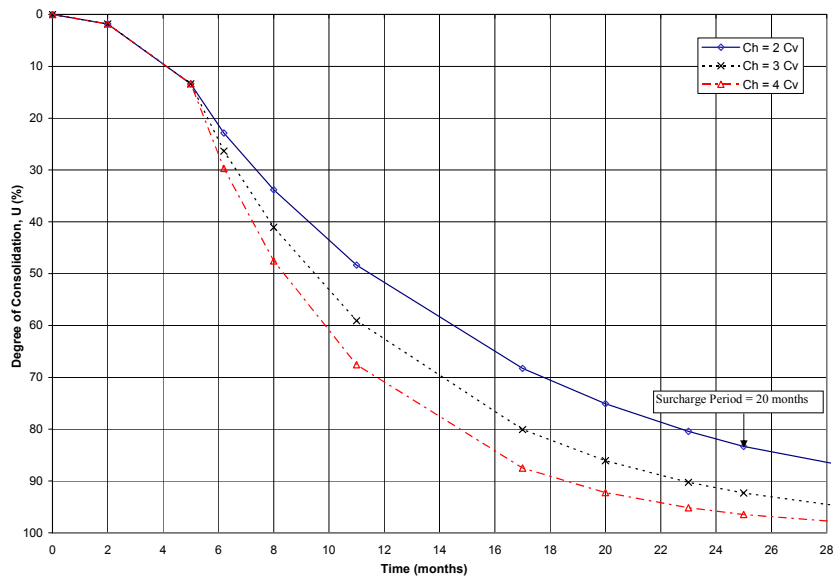


Figure 5.11 Design curves for Vertical Drain Area (Arulrajah et al., 2004m).

Table 5.1 presents a comparison of the design prediction results with that of the back-analysed field instrumentation results at the case study area (Vertical Drain Area at the In-Situ Test Site), 20 months after surcharge. The field instrumentation results and assessment of the Vertical Drain Area (In-Situ Test Site) is discussed fully in Section 8.2.

The results of the design predictions are found to be in excellent agreement with that of the back-analysed field instrumentation results. The degree of consolidation obtained by the design predictions is found to be only slightly higher than that of the field instrumentation results. For the Vertical Drain Area (In-Situ Test Site), a degree of consolidation of 83.3% was obtained from the design predictions as compared to 80.1% from the Asaoka method, 80.0% from the Hyperbolic method and 80.0% from the piezometer method.

Table 5.1 Comparison between design ($c_h=2c_v$) with back-analysed field instrumentation results at Vertical Drain Area, 20 months after surcharge (Arulrajah et al., 2004m).

Sub-Area	Comparison	Design	Asaoka	Hyperbolic	Piezometer
Vertical	Ultimate Settlement(m)	3.005	3.000	3.005	-
Drain	Settlement to date (m)	2.504	2.404	2.404	-
1.5 x 1.5 m	Degree of Consolidation,U%	83.3	80.1	80.0	80.0

6.0 IN-SITU TESTING OF MARINE CLAY UNDER RECLAMATION FILLS

In every embankment project the duration of preloading period is set in advance based on the predicted time rate of consolidation of the compressible layer. If prediction is accurately done the required degree of consolidation is met at the pre-determined preloading time. Therefore close to the surcharge removal time, in-situ tests should be carried out to assess the degree of consolidation. In the last two decades, there has been an emergence of in-situ testing methods as an alternative to laboratory testing methods. The shear strength, overconsolidation ratio and degree of consolidation are important parameters which can be determined from in-situ testing. In-situ dissipation tests on the other hand provide a means of evaluating the in-situ coefficient of horizontal consolidation and horizontal hydraulic conductivity of marine clays.

Prior to the commencement of land reclamation works, a series of in-situ tests were conducted in marine conditions with the use of various in-situ testing equipment at the In-Situ Test Site. The In-Situ Test Site was located in the Northern area of the project where the thickest compressible marine clay layers existed. The in-situ tests carried out prior to reclamation were with the field vane, piezocone, flat dilatometer, self-boring pressuremeter and BAT permeameter. In-situ tests were conducted to determine the undrained shear strength and overconsolidation ratio of the marine clay. In-situ dissipation tests by means of piezocone, dilatometer, self-boring pressuremeter and BAT permeameter were utilised to determine the coefficient of horizontal consolidation and horizontal hydraulic conductivity of marine clay. The in-situ tests methodology and results are discussed in this chapter.

Following the completion of ground improvement works with prefabricated vertical drains and preloading, another series of in-situ penetration tests and in-situ dissipation tests were carried out in the In-Situ Test Site for comparison purposes. These post-improvement in-situ tests were carried out after a surcharge period of about 23 months in the Vertical Drain Area where vertical drains were installed at 1.5 meter square spacing as well as an adjacent Control Area where no drains were installed for comparison purposes. The locations of these in-situ tests were done close to each other so as to enable a good comparison of the degree of consolidation of the areas treated with and without vertical drains when subjected to the same magnitude of preloading. In-situ tests were conducted to determine the undrained shear strength, overconsolidation ratio and degree of consolidation of the marine clay. In-Situ dissipation tests were similarly carried out after surcharge loading in the Vertical Drain Area as well as in the adjacent untreated Control Area to determine the coefficient of horizontal consolidation and horizontal hydraulic conductivity of Singapore marine clay after ground

treatment with and without vertical drains. All in-situ tests and dissipation tests carried out in the Vertical Drain Area after surcharge loading, were carried out at the centroid of the vertical drain grid.

Accordingly, the objectives of this paper are: 1) to describe the testing and analysis procedure for the various in-situ tests; 2) to determine the undrained shear strength and overconsolidation ratio of Singapore marine clay at Changi prior to reclamation and after surcharge loading; 3) to determine the coefficient of consolidation due to horizontal flow (c_h) of Singapore marine clay prior to reclamation and after surcharge loading; 4) to determine the horizontal hydraulic conductivity (k_h) of Singapore marine clay prior to reclamation and after surcharge loading; 5) To compare and discuss the results of the various in-situ test prior to reclamation and after 23 months of surcharge loading with and without vertical drains.

The in-situ testing of marine clay described in this chapter has been discussed in detail by the author (Arulrajah et al., 2004d, 2004f, 2004h, 2004i, 2004j, 2004o, 2004p) during the course of this research study.

6.1 In-Situ Testing of Undrained Shear Strength, Overconsolidation Ratio and Degree of Consolidation of Marine Clay

In-situ tests were carried out at the In-Situ Testing Site to determine the undrained shear strength, overconsolidation ratio (OCR), effective stress and the degree of consolidation of marine clay.

In-situ tests were carried out prior to reclamation as well as after surcharge loading. In-situ tests were carried out in a Vertical Drain Area as well as in an adjacent untreated Control Area 23 months after 23 months of surcharge loading for comparison purposes. The purpose of this research is to determine and compare the differences in undrained shear strength, overconsolidation ratio (OCR), effective stress and the degree of consolidation of marine clay prior to reclamation as well as after ground treatment with and without vertical drains by means of in-situ tests. The degree of consolidation by the various in-situ testing methods after surcharge loading was calculated by the method of Bo et al. (2003).

Tests carried out were the field vane shear test (FVT), cone penetration test (CPT), dilatometer test (DMT), self-boring pressuremeter test (SBPT) and BAT permeameter test (BAT). Table 6.1 summarises the various in-situ tests and their related testing procedures.

The in-situ testing of undrained shear strength, overconsolidation ration and degree of consolidation of marine clay described in this chapter has been discussed in detail by the author (Arulrajah et al., 2004d, 2004f, 2004h, 2004i, 2004o, 2004p) during the course of this research study.

Table 6.1 Testing Procedure for In-Situ Tests (Bo, Chang, Arulrajah and Choa, 2000a).

Testing Method	Equipment Type	Installation Method	Penetration Depth Pattern	Waiting Time	Rotation Rate
FVT	Geonor Vane	Preboring followed by short penetration	Five times borehole diameter beneath the bottom of borehole.	5 min	12 deg/min
CPT	Gouda G.D. C.F.I.P (50,500, 20)	Static pushing using hydraulic force.	Continuous	Negligible	20 mm/s
DMT	Marchetti Flat Dilatometer	Static pushing using hydraulic force.	Stop at every 20 mm	Negligible	20 mm/s
SBPT	Cambridge In-Situ	Preboring and than self-boring during installation.	Full embedment	5 min	Strain controlled (17%/ min)

6.2 In-Situ Dissipation Testing of Marine Clay

As vertical drains are used to accelerate the consolidation of the marine clays, the permeability and consolidation properties of the soil particularly in the horizontal flow are important design parameters. The determination of these design parameters are traditionally based on the multiplier of coefficient of vertical consolidation, c_v value obtained from the laboratory consolidation tests. Results of these laboratory tests however are usually subject to uncertainties primarily due to inevitable sample disturbances and uncertain multiplier values.

In-situ dissipation tests have emerged as a useful method to obtain the required horizontal consolidation and permeability parameters for the design of vertical drain projects. The coefficient of consolidation due to horizontal flow and horizontal hydraulic conductivity of marine clays are important parameters for the design of vertical drain projects. The determination of these design parameters are traditionally based on the multiplier of coefficient of vertical consolidation, c_v value obtained from the laboratory consolidation tests. Results of these laboratory tests however are usually subject to uncertainties primarily due to inevitable sample disturbances and uncertain multiplier values. Laboratory testing

also does not yield appropriate properties of soil due to different loading and drainage conditions as compared to the actual in-situ soil condition. In-situ dissipation tests are an alternative to these traditional laboratory testing methods and furthermore the effect of disturbance to marine clays is minimal. These dissipation tests can be conducted at various levels in the marine clay and hence variations of the coefficient of consolidation due to horizontal flow and horizontal hydraulic conductivity with depth can be obtained. In-situ dissipation testing has emerged as a useful method to obtain the required horizontal consolidation and permeability parameters for the design of vertical drain projects. The in-situ dissipation testing of marine clay described in this chapter has been discussed by the author (Arulrajah et al., 2004d, 2004f, 2004i, 2004o) during the course of this research study.

In-situ dissipation tests by means of piezocone (CPTU), dilatometer (DMT), self-boring pressuremeter (SBPT) and BAT permeameter (BAT) were utilised in the characterisation of the coefficient of horizontal consolidation and horizontal hydraulic conductivity of Singapore marine clay in this research study. In-situ dissipation tests were used to determine the coefficient of consolidation due to horizontal flow and horizontal hydraulic conductivity prior to reclamation and after surcharge loading with and without vertical drains. Coefficients of consolidation due to horizontal flow, c_h can be determined from the CPTU, DMT and SBPT dissipation tests as well as laboratory tests. Horizontal hydraulic conductivity, k_h can be obtained directly from the BAT permeameter tests and indirectly from the c_h results of the other in-situ tests. This will be discussed later in this chapter.

In-situ dissipation tests were carried out prior to reclamation as well as after ground improvement with prefabricated vertical drains, and preloading to compare the changes in the coefficient of horizontal consolidation and horizontal hydraulic conductivity prior to and after surcharge loading.

In-situ dissipation tests were carried out in a Vertical Drain Area as well as in an adjacent untreated Control Area, after 23 months of surcharge loading, to compare the improved parameter under the different degree of consolidation stages. The purpose of this research is to determine the horizontal consolidation and hydraulic conductivity parameters of Singapore marine clay prior to reclamation as well as after ground treatment with and without vertical drains by means of in-situ dissipation tests.

The objective of this research is to investigate the comparison of in-situ dissipation tests prior to and after surcharge loading in a vertical drain area and adjacent untreated area, as well as between the various test methods. Studies have been carried out previously by Bo,

Arulrajah and Choa (1998c) and Chu et al. (2002) in the same reclamation site for dissipation tests carried out prior to land reclamation. However, comparisons of the dissipation test results prior to and after surcharge loading have only been carried out briefly. The in-depth evaluation of this particular research of dissipation tests should make these test methods valuable for application to ground improvement projects on soft soil or marine clay.

6.3 Location and Marine Clay Characteristics of the In-Situ Test Site

The In-Situ Test Site was located in the Northern area of the project where the thickest compressible layers existed and a portion of where the future airport runway would be located. The In-Situ Test Site consists of two adjacent sub-areas namely the Vertical Drain Area where vertical drains were installed at 1.5 meter square spacing and the Control Area where vertical drains were not installed. The two sub-areas are located adjacent to each other and are subject to the same construction sequence and surcharge heights and as such this enabled a comparison to be made between the two areas.

Figure 6.1 shows the location of the In-Situ Test Site. Field tests carried out prior to reclamation were denoted as FT-2. Field tests carried out in the Vertical Drain Area after improvement and 23 months of surcharge loading, were denoted as FT-8. Tests carried out in the untreated Control Area after 23 months of surcharge loading were denoted as FT-9. A pre-reclamation borehole and various in-situ tests were carried out prior to the commencement of land reclamation works to characterize the marine clay properties. The test results are discussed later in this chapter. Figure 6.2 indicates the soil profile of the In-Situ Test Site prior to reclamation.

As evident in Figure 6.2, the In-Situ Test Site comprises of two distinct layers of marine clay, which are the “Upper Marine Clay layer” and the “Lower Marine Clay layer”. The “Intermediate Stiff Clay layer” separates these two distinct marine clay layers. The upper marine clay is soft with undrained shear strength values ranging from 10 to 30 kPa. The intermediate layer is a silty clay layer and its formation is believed to have occurred during the lowering of sea level, which was then followed by a rise in sea level and further deposition of the upper marine clay layer. The lower marine clay is lightly overconsolidated with an undrained shear strength varying from 30 to 50 kPa. It is not homogeneous but occasionally interbedded with sandy clay, peaty clay and sand layers. Below the lower marine clay is a stiff sandy clay layer locally known as Old Alluvium. The original seabed level in the In-Situ Test Site was 3.29 meters below Admiralty Chart Datum (–3.29 mCD).

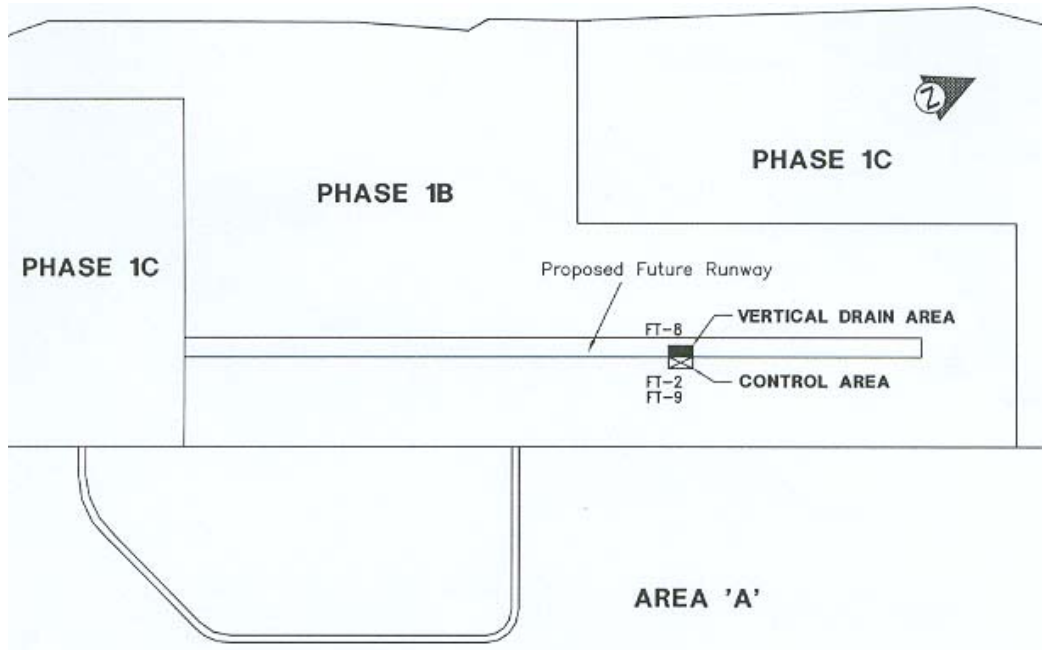


Figure 6.1 Location of In-Situ Test Site comprising Vertical Drain Area and Control Area (Arulrajah et al., 2004f).

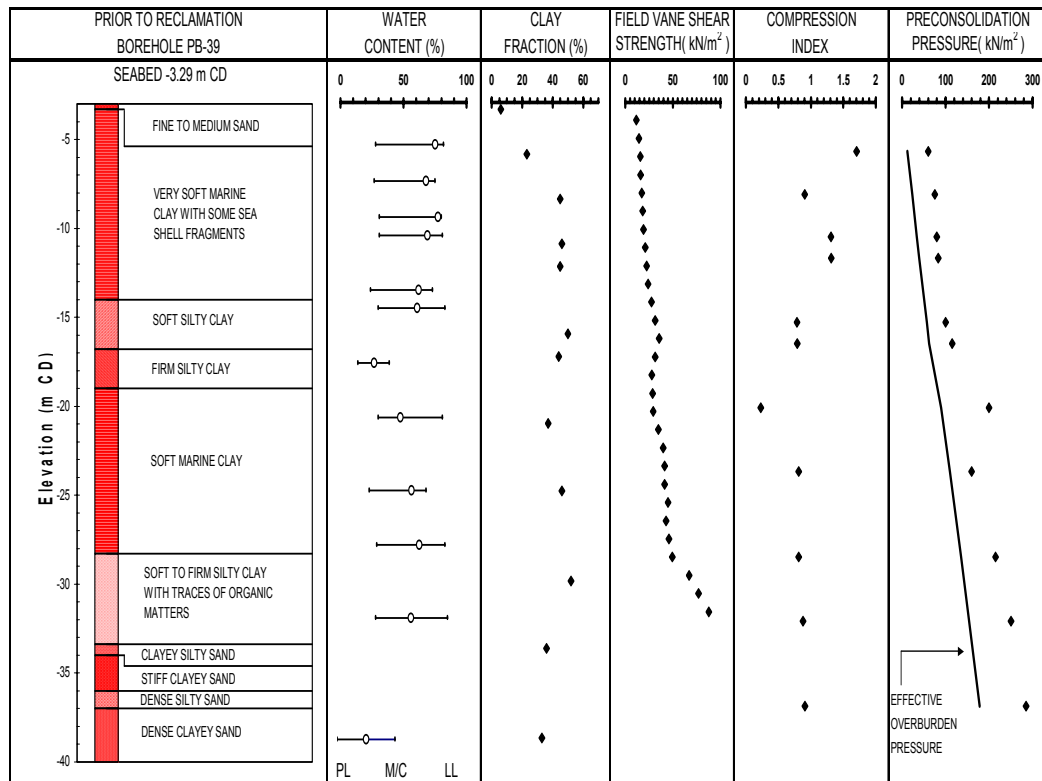


Figure 6.2 Typical soil profile and engineering parameters at In-Situ Test Site (Arulrajah et al., 2004d).

Following the completion of the pre-reclamation in-situ tests, land reclamation was carried out by hydraulic placement of sand until the vertical drain platform level of 4 meters above Admiralty Chart Datum (+4 mCD). Vertical drains were next installed at this elevation at the 1.5 meter square spacing according to the design, to depths of up to 35 meters in the Vertical Drain Area. Soil instruments were placed in both the Vertical Drain Area and Control Area either just before or immediately after the installation of the vertical drains at this vertical drain platform level. Surcharge, with reclamation sandfill, was next placed until the design elevation of 10 meters above Admiralty Chart Datum (+10 mCD) for both areas. Another series of in-situ tests were carried out after a surcharge loading period of about 23 months in the Vertical Drain Area and adjacent untreated Control Area for comparison purposes.

Close to the end of the surcharge period, post-improvement boreholes and various in-situ tests were carried out in both the Vertical Drain Area as well as the adjacent untreated Control Area. These boreholes and in-situ tests enabled for comparison of the results of the post-improvement boreholes and in-situ tests with that of the pre-reclamation boreholes and in-situ tests. In addition, the presence of the similarly instrumented adjacent untreated Control Area enabled comparison to be made between areas treated with vertical drain and surcharge with that of an untreated area with surcharge only.

A detailed site characterisation of the soil consolidation and physical characteristics was essential for the In-Situ Test Site comprising the Vertical Drain Area and the Control Area. The pre-reclamation site characterisation of the In-Situ Test Site was carried out by means of laboratory testing of the recovered samples from a marine sampling borehole and by in-situ field testing by various methods, as described later in this chapter. These testing results are applicable to both the future Vertical Drain Area as well as the Control Area.

6.4 Laboratory Testing and Predictions

6.4.1 Pre-Reclamation Laboratory Testing

Laboratory tests were carried out on the recovered undisturbed samples from the pre-reclamation borehole. Tests carried out include oedometer tests, water content, Atterberg limit and various other classification tests. The primary function of these tests was to determine the various soil parameters for the In-Situ Test Site. The tests were also carried out as a comparison with the in-situ testing results.

Based on the results obtained, the marine clay can be described as high to very high plasticity silty clay based on the British Standards, except for the intermediate stiff clay layer. The characterization study of the In-Situ Test Site, indicated the presence of the two distinct layers of marine clay which are the “Upper Marine Clay layer” and the “Lower Marine Clay layer” similar to that found in the general site characterization study discussed in Chapter 3. The engineering parameters of the In-Situ Test Site are within the ranges obtained from the general site characterization study and as such the suggested design parameters and empirical field vane test correlation can be applied to the In-Situ Test Site.

Compression index and recompression index were obtained from 24 hours loading oedometer tests with a load increment ratio of one. Although 24 hours loading duration includes secondary compression, it has been largely accepted that 24 hours strain in oedometer is equivalent to end of primary in the field (Imai, 1995). The coefficient of vertical consolidation (c_v) of the marine clay for the reclamation area was determined by one-dimensional oedometer tests. However the accurate determination of preconsolidation pressure is still under question as preconsolidation pressure can differ due to method of testing, load increment ratio, duration of loading, method of interpretation and some other complexities such as the salt content, strain rate and temperature (Bo et al., 2003a). There are quite a large number of methods to determine the preconsolidation pressure from the oedometer tests such as Casagrande (1936) method, Janbu (1969) method, Butterfield (1979) method and Sridharan (1991) method. Among the tests the resulting values can differ by 10-15 % (Bo, Arulrajah, Choa and Chang, 1998a). Figure 6.3 indicates the typical void ratio versus effective stress load-unload curves of the marine clays in the In-Situ Test Site.

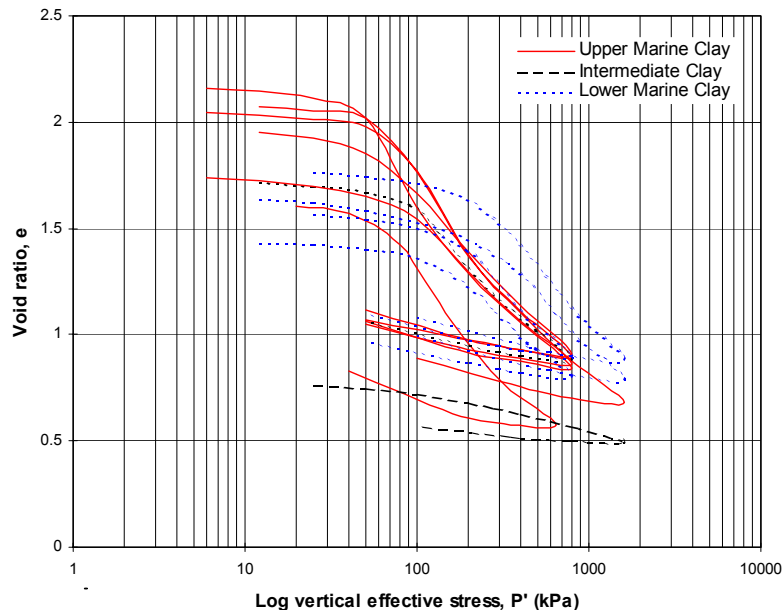


Figure 6.3 Oedometer compression curves for the distinctive clays (PB39).

6.4.2 *Laboratory Predictions*

From the borehole carried out prior to reclamation, the consolidation and shear strength of marine clay can be characterised. From the void ratio versus log effective stress curve, the expected void ratio after soil improvement can be predicted. Expected post improvement effective stress for 90% degree of consolidation can be worked out from the following equation:

$$\sigma_{vf}' = \sigma_{vo}' + (\Delta\sigma' 0.9) \quad \text{Eq. (6.1)}$$

where:

$\Delta\sigma'$ is additional preloading pressure taking into account surcharge effect and settlement.

σ_{vo}' is effective vertical stress (kPa)

Undrained shear strength related to final load for Singapore marine clay can be estimated by using Skempton's (1969) equation for normally consolidated clays:

$$c_u / \sigma_{vo}' = 0.11 + 0.0037 \text{ PI}$$

$$c_u = (0.11 + 0.0037 \text{ PI}) \sigma_{vo}' = 0.25 \sigma_{vo}' \quad \text{Eq. (6.2)}$$

6.4.3 *Post-Improvement Laboratory Testing*

Post investigation boreholes with continuous sampling were carried out after a surcharge period of about 23 months. From the laboratory results of collected sample, improvement can be assessed. However care should be taken in comparing this data, as some adjustment of elevation after soil improvement is required due to settlement of ground and sub-layers. Void ratio determination will also not be realistic if sample is disturbed. Undrained shear strength may also be underestimated if some disturbance and stress release in samples has occurred.

Degree of consolidation can be worked out from measured void ratio and undrained shear strength. A conventional way to assess the degree of consolidation is to determine the preconsolidation effective stress from oedometer tests. Degree of consolidation can be worked out from the preconsolidation effective stress as follows (Bo, Arulrajah and Choa; 1997a):

$$U\% = [\sigma_y' / (\sigma_{vo} + \Delta\sigma')] 100 \quad \text{Eq. (6.3)}$$

where:

σ_v' is effective yield stress (kPa).

There are several methods to determine the preconsolidation pressure from the oedometer tests. In this study, the Sridharan (1991) method was used. It is to be noted that the accurate determination of preconsolidation pressure can differ due to method of interpretation and other complexities such as salt content, strain rate and temperature.

Figure 6.4 to 6.6 shows the comparative laboratory results from pre-reclamation and post improvement investigation boreholes. Figure 6.7 shows the comparative plot of degree of consolidation assessed from void ratio, yield stress and undrained shear at the Vertical Drain Area. The post improvement laboratory testing results are found to be slightly lower degree of consolidation than the expected improvement results. In the comparisons, the laboratory tests in the Vertical Drain Area improved with vertical drains indicate the expected improvements as compared to the Control Area. The water content and void ratio of the Vertical Drain Area as expected are found to be lower than that of the Control Area. The intermediate clay layer is again clearly identified in the laboratory results based on its lower void ratio and higher degree of consolidation. The preconsolidation pressures of the Vertical Drain Area are higher than that of the Control Area.

The degree of consolidation of the In-Situ Test Site is found to be inconclusive due to the wide scatter in the values by the different methods. It is to be noted that laboratory testing is subject to many complexities such as sample disturbance, borehole quality, testing quality, testing method and interpretation method. Samples recovered at the field are subject to disturbance at the field, during transportation to the laboratory, during sample extrusion and during testing preparations. In addition, laboratory testing takes time to test and can also be expensive depending on the type of laboratory tests specified.

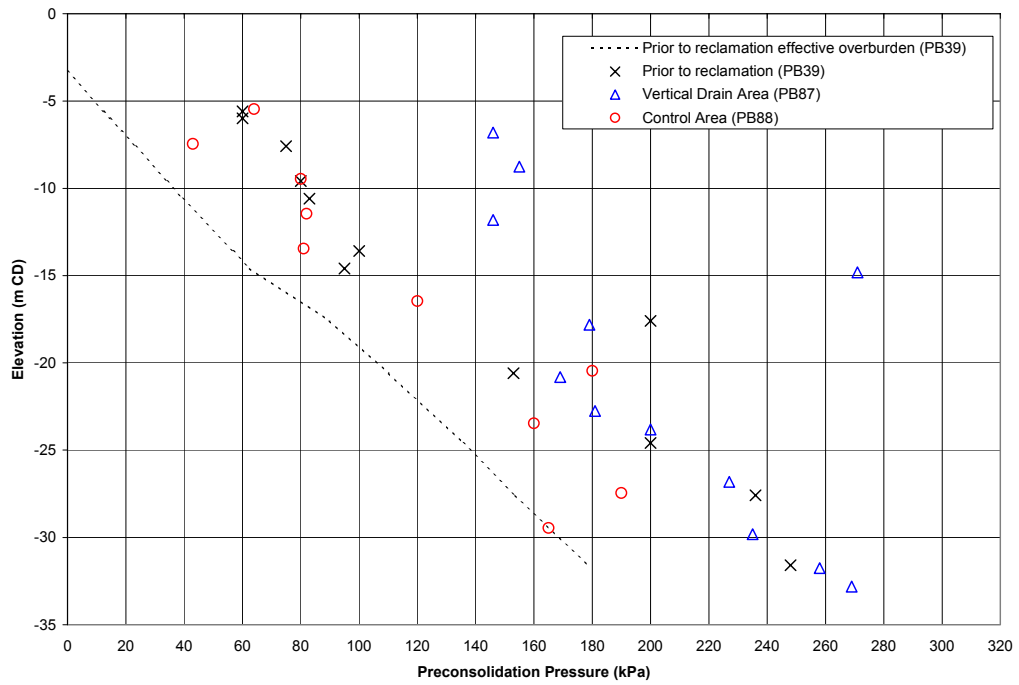


Figure 6.4 Comparison of preconsolidation pressure between Vertical Drain Area and Control Area.

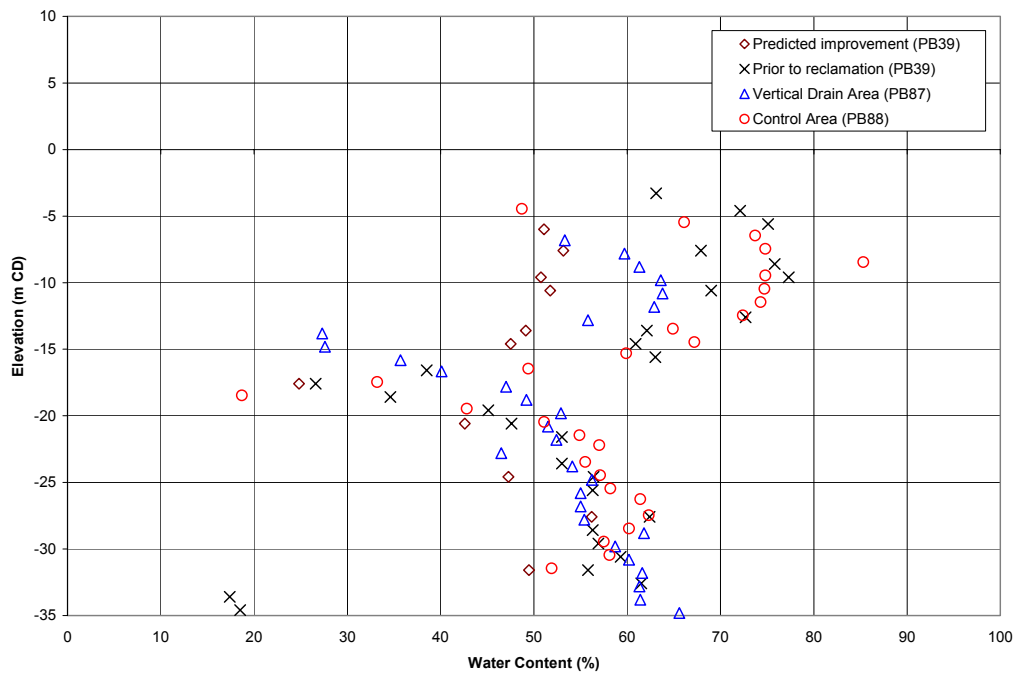


Figure 6.5 Comparison of water content at Vertical Drain Area and Control Area.

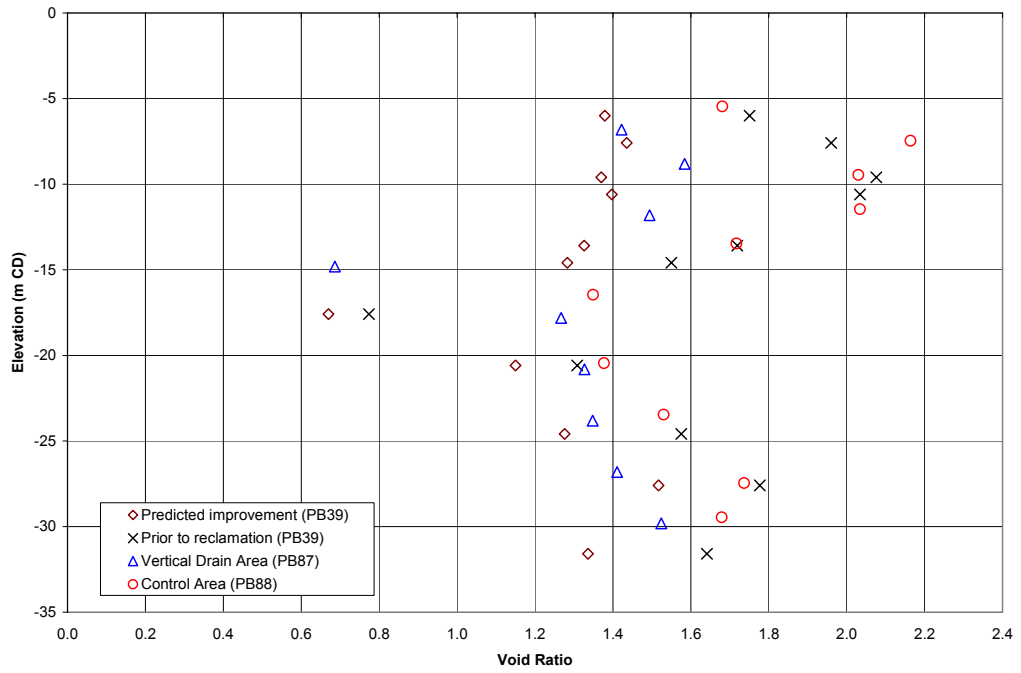


Figure 6.6 Comparison of void ratio at Vertical Drain Area and Control Area.

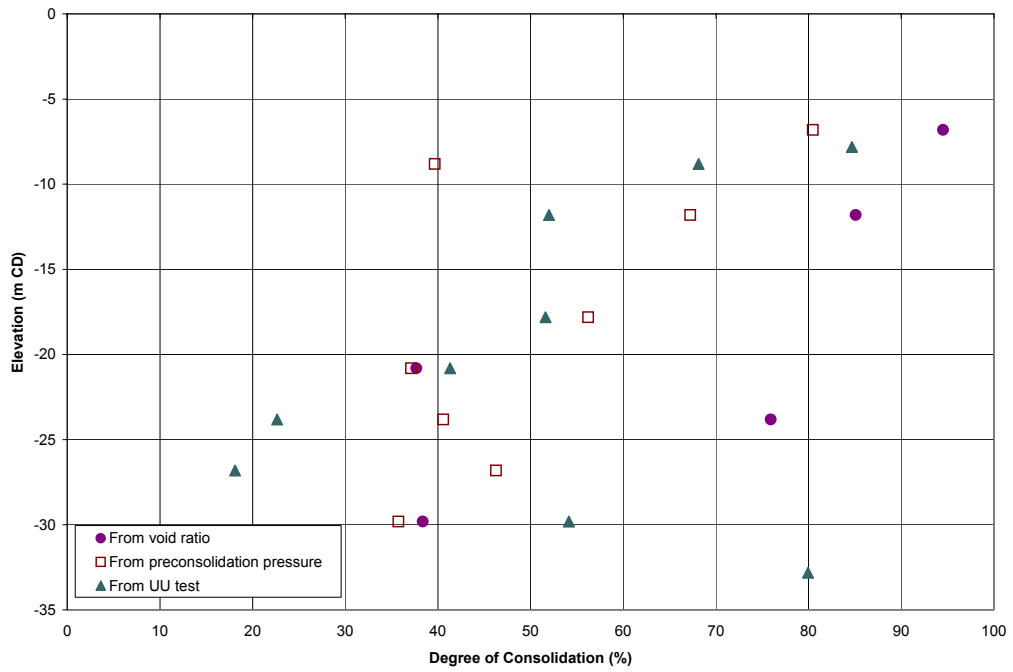


Figure 6.7 Comparison of degree of consolidation from laboratory results at Vertical Drain Area.

6.5 Field Vane Test (FVT)

The type of field vane instrument used in the In-Situ Test Site was a Geonor vane (Norwegian Geotechnical Society, 1979). The vane blade dimensions were 65 mm by 130 mm and with a blade thickness of 2 mm. Vane testing consists of pushing a vane into clay and measuring the maximum torque required to rotate the vane at a given rate of rotation. It follows that the failure surface is cylindrical around the vane (Cadling and Odenstad, 1950). Figure 6.8 shows the geometry and dimensions of the field vane used in the research. Figure 6.9 shows the field vane shear testing equipment. The in-situ testing of marine clay with the field vane described in this chapter has been discussed in detail by the author (Arulrajah et al., 2004d, 2004h, 2004p) during the course of this research.

The testing procedure was carried out by the method described by the Norwegian Geotechnical Society (1979) for which a waiting time of five minutes after penetration was imposed to allow for the equalization of pore water pressure generated during penetration of the vane blade. Following the advancement of the borehole, the vane was pushed steadily for a distance of about five times the diameter of the borehole to the proposed test level. Following this, a torque was applied at the surface to the vane blade with a rod rotation rate of 12 degrees per minute. This would ensure that the rotation would not introduce significant viscous effect and drainage effects on the soil. The maximum torque required for mobilization of the vane was recorded. The way in which the test is carried out, including any delay between penetration and vane rotation and time to failure also influence the results (Flaate, 1966 and Aas, 1967).

6.5.1 Field Vane Test Method

Field vane shear tests were carried out to determine the field vane shear strength of the marine clay at the In-Situ Test Site. The vane shear strength is found to be increasing with depth as is normally the trend for marine clays in this region. The interpretation of undrained shear strength, assumes full and uniform mobilization of shear stress over the entire failure surface and is determined from the following relationship (Flaate, 1966):

$$c_u = 6/7 (T / \pi D^3) \quad \text{Eq. (6.4)}$$

where:

c_u is in units of kN/m²

T is the maximum measured torque (kN.m)

D is diameter of field vane (m)

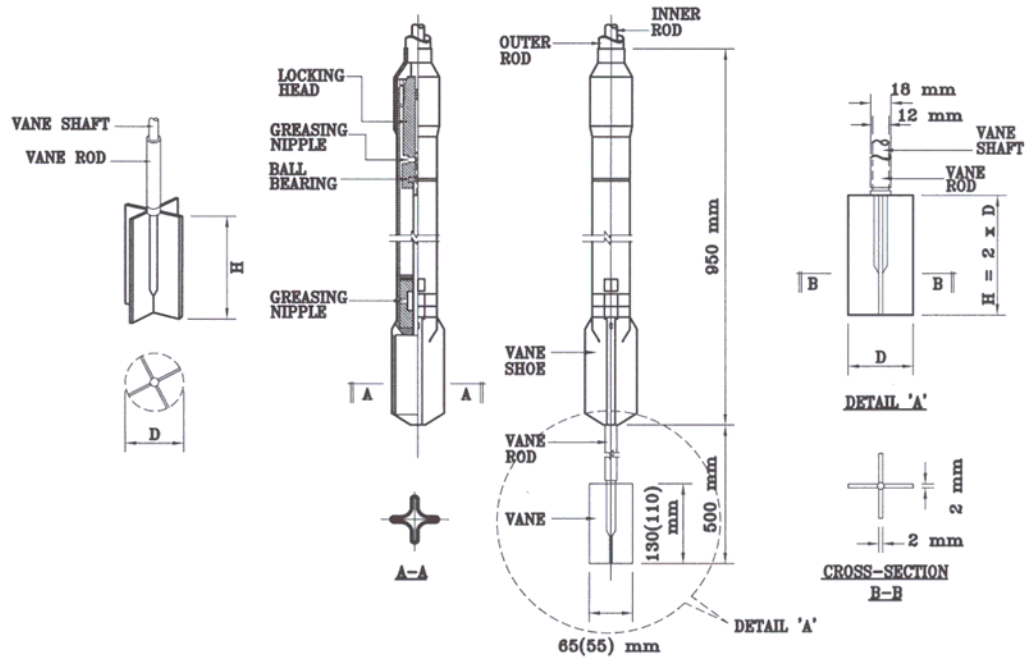


Figure 6.8 Geometry and dimension of field vane (After Norwegian Geotechnical Society, 1979).



Figure 6.9 Field vane shear testing equipment.

Mayne and Mitchell (1988) suggested that OCR can be estimated from undrained shear strength. As such, it can therefore be assessed whether the improved soil has attained an OCR close to unity with the surcharge load:

$$\text{OCR} = 22 \text{PI}^{-0.48} [c_u / \sigma_{vo}] \quad \text{Eq. (6.5)}$$

where:

c_u is in units of kN/m^2

PI is the plasticity index

σ_{vo}' is the effective vertical stress.

6.5.2 Comparison of Field Vane Shear Tests

The comparison of the FVT results after 23 months of surcharge loading is shown in Figures 6.10 to 6.13.

Notably, the FVT in Control Area indicates less effective stress than the prior to reclamation results. This could be attributable to variations in soil stratigraphy or submerged weight of soil at the FVT testing locations.

The FVT test indicates that the degree of consolidation of the vertical drain treated Vertical Drain Area had attained a degree of consolidation of about 60-80% while the Control Area had attained a degree of consolidation of about 20-30%. The degree of consolidation was obtained by the method of Bo, Arulrajah and Choa (1997a).

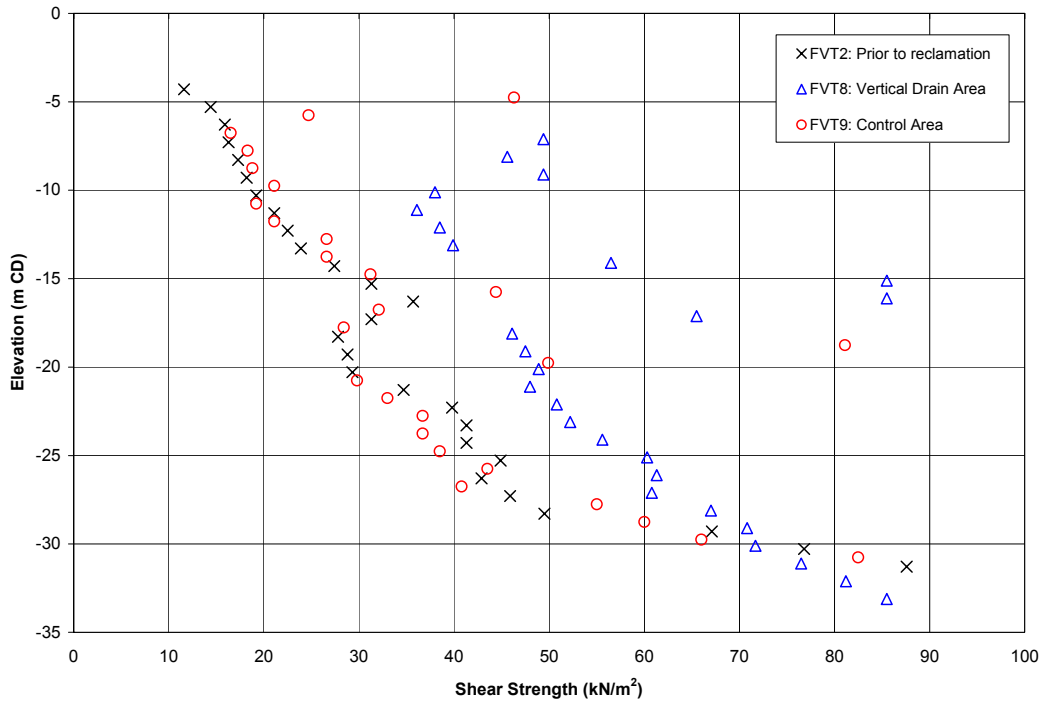


Figure 6.10 Variation of FVT shear strength with elevation after 23 months of surcharge loading.

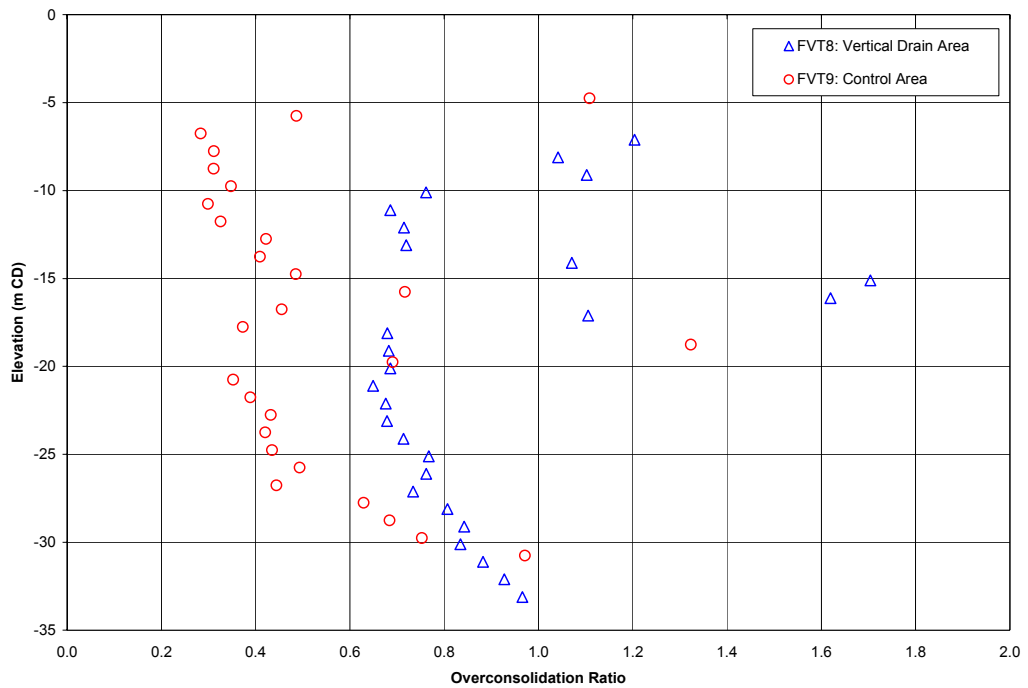


Figure 6.11 Variation of FVT OCR with elevation after 23 months of surcharge loading .

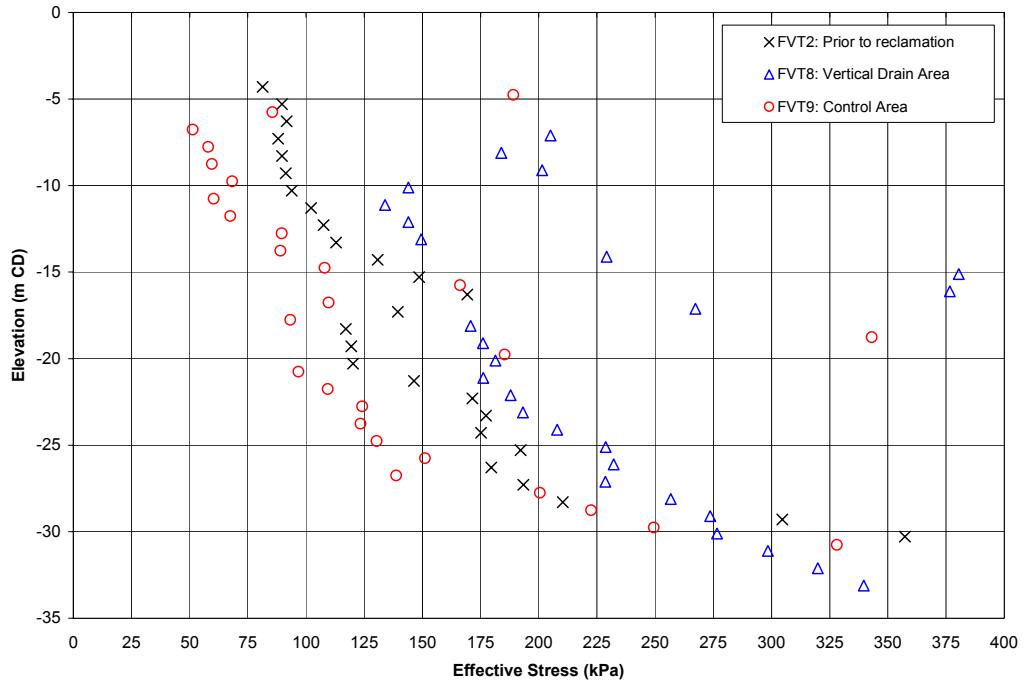


Figure 6.12 Variation of FVT effective stress with elevation after 23 months of surcharge loading.

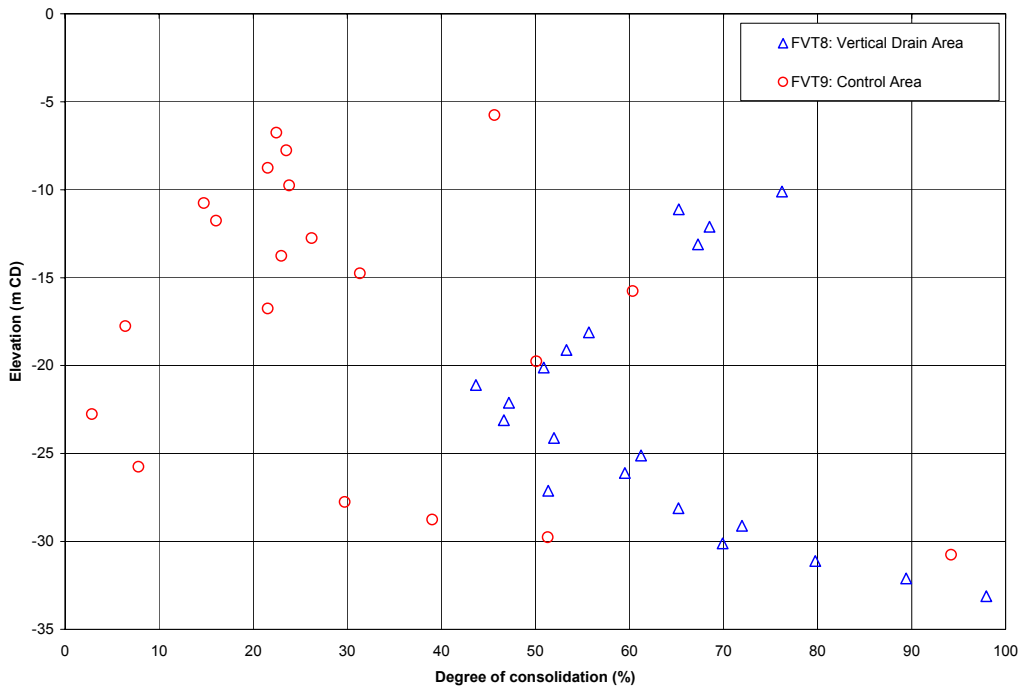


Figure 6.13 Variation of FVT degree of consolidation with elevation after 23 months of surcharge loading.

6.6 Piezocone Test (CPT)

The type of cone used in the piezocone tests was a Gouda cone, capable of registering a cone resistance of up to 50 MN/m², sleeve friction of up to 500 kN/m² and a maximum pore pressure of 2000 kN/m². The cone had a 60 degree cone tip, projected cross-section area of 10 cm², friction sleeve area of 150 mm² and an unequal area ratio “a” of 0.8035. The pore pressure filter was located at the base immediately behind the cone tip. The cone was advanced into the soil with a 20 ton dutch cone rig. Figure 6.14 shows the geometry and dimensions of the piezocone tip used in the research study. Figure 6.15 shows the piezocone tip. The in-situ testing of marine clay with the piezocone described in this chapter has been discussed in detail by the author (Arulrajah et al., 2004d, 2004f, 2004h, 2004i, 2004p) during the course of this research study.

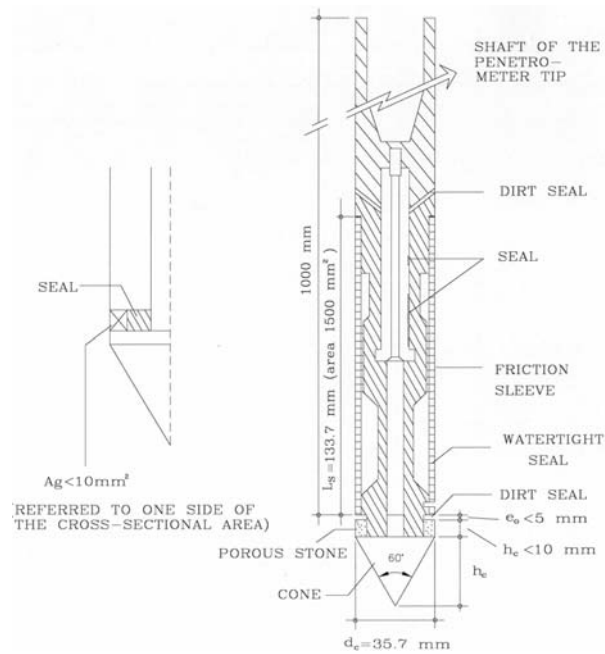


Figure 6.14 Geometry and dimension of piezocone tip (After De Beer et. al., 1988).



Figure 6.15 Piezocone tip.

6.6.1 Piezocone Test Method

The piezocone has seen a surge in its use in soft clays in this region. Campanella and Robertson (1988) have described the standard guidelines for the use of the piezocone test equipment. Campanella and Robertson (1988) have also provided various interpretation charts to be used in conjunction with the cone penetration test results. Sugawara (1988) has provided a method of estimating in-situ overconsolidation ratio of clays by using the piezocone test. The piezocone is economical, easy to carry out and is widely available in the region. The test can be done relatively quickly over the whole soil profile.

The testing procedure was carried out by the recommended international practice (De Beer et al., 1988) with a continuous penetration at a prescribed rate of 20 mm per second. The recorded parameters of the penetration test were cone resistance (q_c), sleeve friction (f_s), penetration pore pressure (u_{bt}) and inclination.

From the measured cone resistance reading, the corrected cone resistance readings were calculated using the following equation to account for the unequal bearing area effect (Campanella et al., 1988):

$$q_t = q_c + (1 - a) u_{bt} \quad \text{Eq. (6.6)}$$

where:

q_c is the cone resistance (MN/m^2)

u_{bt} is the penetration pore pressure (MN/m^2)

a is the unequal bearing area effect which is 0.8035 for the type of cone used.

Campanella and Robertson (1988) has described that the undrained shear strength c_u can be estimated from the corrected cone resistance q_t , total over-burden pressure σ_{vo} and cone factor N_{KT} :

$$c_u = (q_t - \sigma_{vo}) / N_{KT} \quad \text{Eq. (6.7)}$$

where:

c_u is in units of kN/m^2

N_{KT} for Singapore Marine Clay at Changi was taken as follows (Bo, Arulrajah and Choa, 1997a):

$$N_{KT} = 23.8 - (1 / 3.8) PI \quad \text{Eq. (6.8)}$$

Sugawara (1988), proposed that OCR can be estimated from the corrected cone resistance and total and effective overburden pressure as follows:

$$(q_T - \sigma_{vo}) / \sigma_{vo}' = K \cdot OCR \quad \text{Eq. (6.9)}$$

where:

K is constant and varies between 2.5 and 5.0. A K value of 3.136 was used for the marine clay, and the following equation was used for the marine clay:

$$(q_T - \sigma_{vo}) / \sigma_{vo}' = 3.136 OCR \quad \text{Eq. (6.10)}$$

6.6.2 Comparison of Piezocone Tests

If compressible soil is fully consolidated with present surcharge load, overconsolidation ratio of soil will become unity with current surcharge load. Therefore the improvement of soil can be assessed whether it is close to unity with current load or not. If compressible foundation is fully consolidated under additional surcharge load, it becomes normally consolidated with current overburden pressure. Therefore normalized shear strength ratio c_u / σ_{vo}' can be expressed as mentioned by Skempton (1957):

$$c_u / \sigma_{vo}' = 0.11 + 0.0037 PI \quad \text{Eq. (6.11)}$$

The comparison of the CPT results after 23 months of surcharge loading is shown in Figures 6.16 to 6.19.

The CPT penetration test indicates that the degree of consolidation of the Vertical Drain Area had attained a degree of consolidation of about 70-80% while the Control Area had attained a degree of consolidation of about 30-40%.

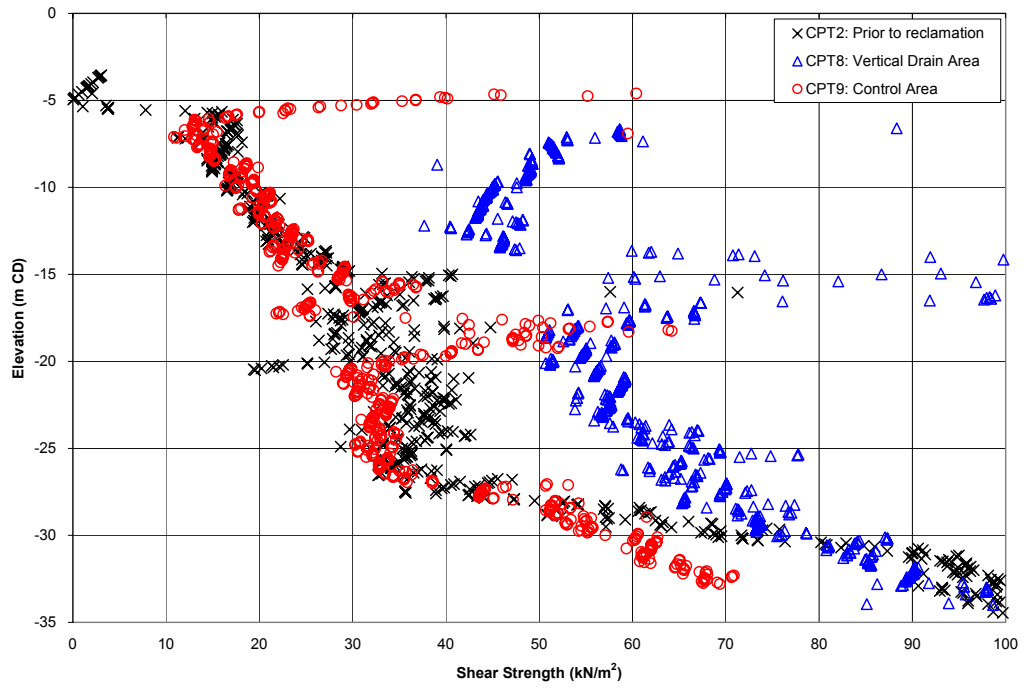


Figure 6.16 Variation of CPT shear strength with elevation after 23 months of surcharge loading.

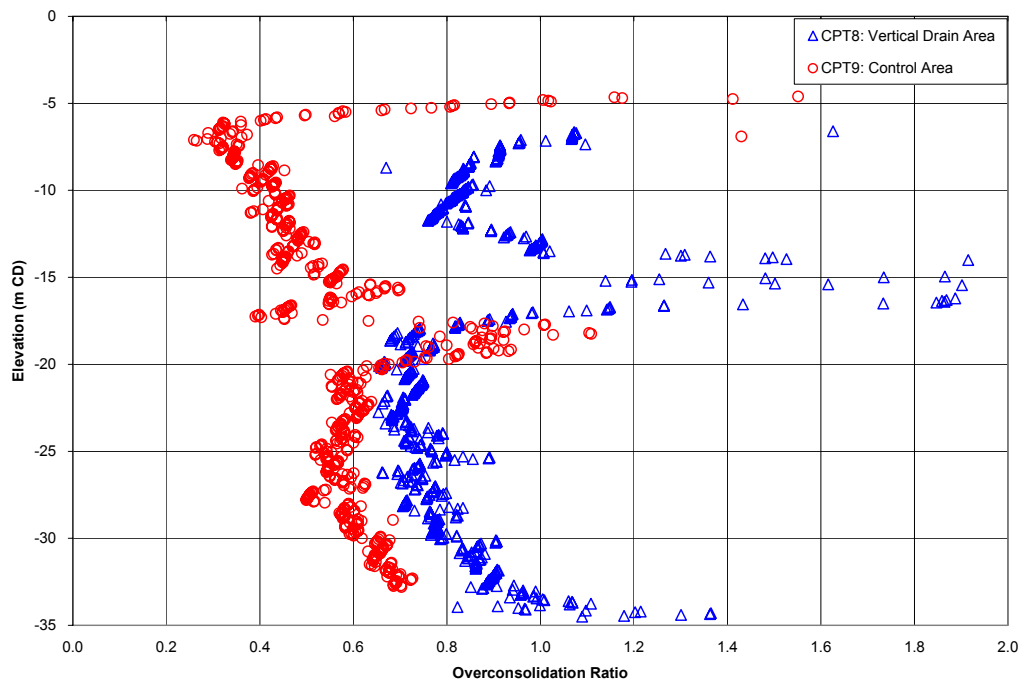


Figure 6.17 Variation of CPT OCR with elevation after 23 months of surcharge loading.

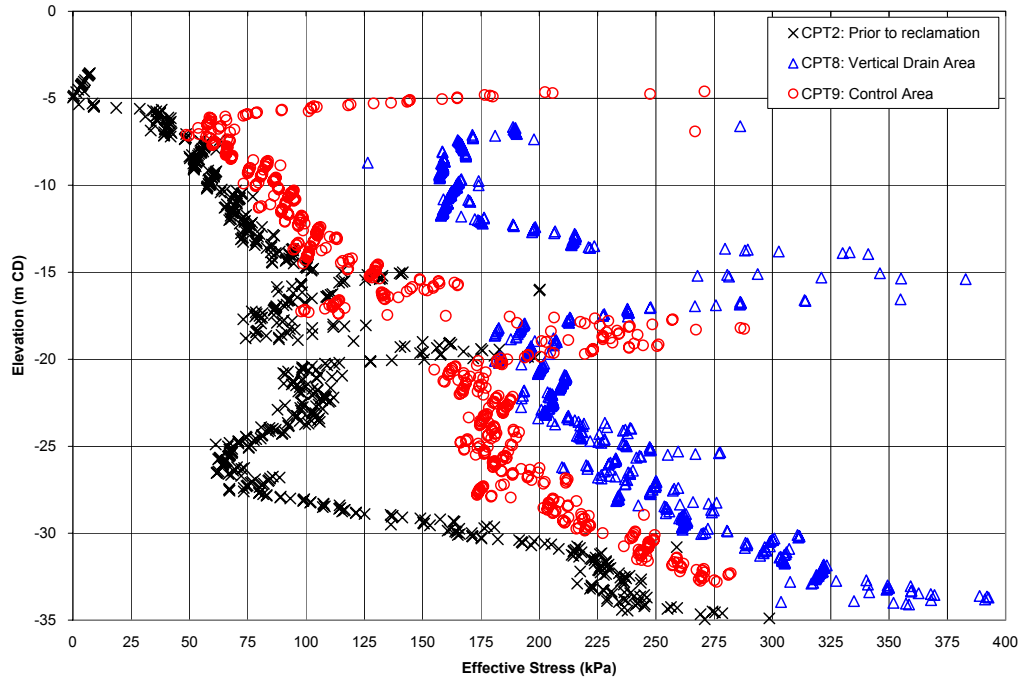


Figure 6.18 Variation of CPT effective stress with elevation after 23 months of surcharge loading.

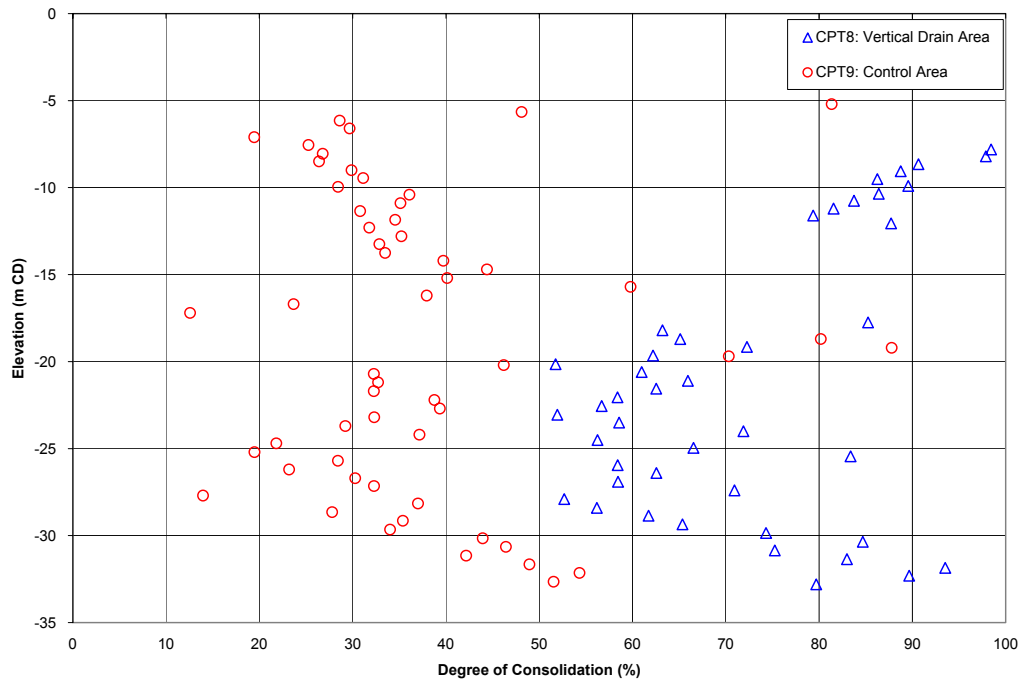


Figure 6.19 Variation of CPT degree of consolidation with elevation after 23 months of surcharge loading.

6.6.3 Piezocone Dissipation Test (CPTU)

The cone penetrometer used in this study had the pore pressure filter located just behind the cone tip. The piezocone dissipation tests (CPTU) were carried out at various elevations. Coefficient of consolidation due to horizontal flow was estimated by the method suggested by Baligh and Levadoux (1986).

When piezocone is penetrated into soft soil, some excess pore pressure will generate due to penetration. However if the cone is held in the same elevation, pore pressures will dissipate until it reaches the equilibrium pore pressure at the quasi-static state. This equilibrium pore pressure will be the same as pore pressure in the soil at the time of testing.

The first step in the prediction method consists of normalizing dissipation records and plotting the normalized excess pore pressure versus log time. In general, the normalized excess pore pressure decreases monotonically from 1.0 (at $t = 0$) to 0 (at t approaching infinity):

$$\bar{u} = (u - u_0) / (u_i - u_0) \quad \text{Eq. (6.12)}$$

where:

- \bar{u} is the normalized excess pore pressure at time t
- u_0 is the static pore pressure
- u_i is the initial or penetration pore pressure (at $t=0$)
- u is the pore pressure recorded at time t

At a given degree of consolidation, the predicted coefficient of consolidation due to horizontal flow can be obtained from the following expression given by Baligh and Levadoux (1986):

$$c_h (\text{probe}) = (R^2 T_{50}) / t_{50} \quad \text{Eq. (6.13)}$$

where:

- $c_h (\text{probe})$ is in units of m^2/yr
- R is radius of cone shaft in meters which is 0.01785 m for the cone used
- T_{50} is time factor, which is 3.65 for a 60 degree tip at 50% normalised excess pore pressure
- t_{50} is time elapsed for 50% degree of consolidation to take place

For clays consolidated in the normally consolidated range, estimates of the coefficient of consolidation due to horizontal flow can be estimated from c_h (probe) by means of the following expression published by Baligh and Levadoux (1986):

$$c_h (\text{NC}) = (C_r / C_c) [c_h (\text{probe})] \quad \text{Eq. (6.14)}$$

where:

c_h (NC) is in units of m^2/yr

C_r = recompression index

C_c = compression index

Figure 6.20 shows the piezocone dissipation test curves prior to reclamation.

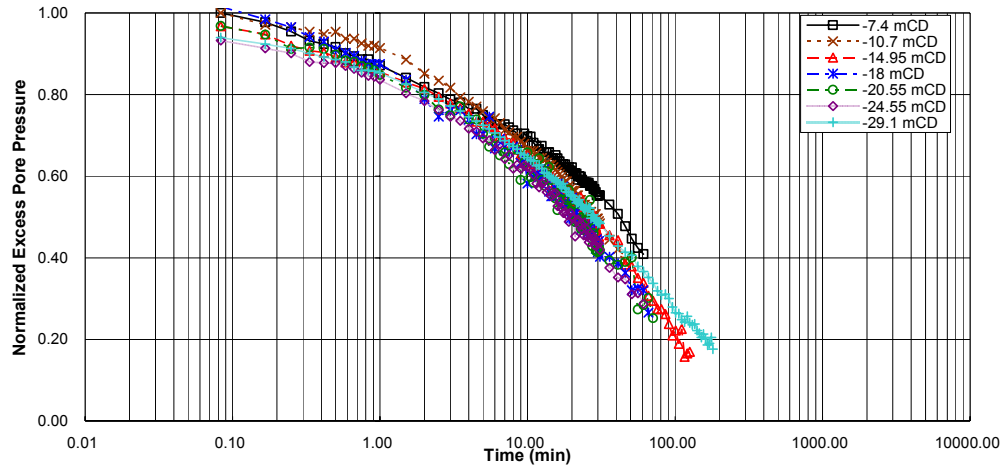


Figure 6.20 CPTU dissipation test curves prior to reclamation (Arulrajah et al., 2004f).

In order to obtain the hydraulic conductivity in the normally consolidated condition, a correction taking the recompression ratio into account needs to be applied. The horizontal hydraulic conductivity can be estimated from:

$$k_h = (\gamma_w / 2.3\sigma'_v) (RR) c_h \quad \text{Eq. (6.15)}$$

where:

k_h is horizontal hydraulic conductivity in m/yr

γ_w is unit weight of water in kN/m^3

RR is recompression ratio, C_r/C_c

σ'_v is mean effective vertical stress of the soil in kPa .

6.6.4 Comparison of Piezocone Dissipation Tests

When the CPTU cone is held in the same elevation for a long time period, pore pressures will dissipate until it reaches the equilibrium pore pressure at the quasi-static state. This equilibrium pore pressure will be the same as pore pressure in the soil at the time of testing. With this measured equilibrium pore pressure from CPTU tests, a counter check can be done with piezometric pressures from piezometer instruments and the average degree of consolidation can be computed:

$$U(\%) = 1 - (U_t / U_i) \quad \text{Eq. (6.16)}$$

where:

U_t = excess pore pressure at time “t”

U_i = initial excess pore pressure which is equal to additional load ($\Delta\sigma'$).

Figure 6.21 indicate the CPTU dissipation test curves in the Vertical Drain Area after ground improvement with vertical drains and surcharge loading for 23 months. Figure 6.22 presents the comparison of piezometric heads between CPTU dissipation tests and piezometers in the Vertical Drain Area. The dissipation tests in the Vertical Drain Area were carried out for up to 50 hours. It can be seen that the normalized excess pore pressures at all elevations have stabilised close to this time period. It is evident that the ground improvement with vertical drains has significantly dissipated the excess pore water pressures built up due to the surcharging load.

Figure 6.23 indicate the CPTU dissipation test curves in the Control Area after surcharge loading for 23 months. Figure 6.24 presents the comparison of piezometric heads between CPTU dissipation tests and piezometers in the Control Area. The dissipation tests in the Control Area were carried out for up to 42 hours. The normalized excess pore pressures at all elevations have stabilised after 1000 minutes. Without ground improvement, a slight dissipation of the excess pore water pressures built up due to the consolidation was observed. The CPTU dissipation test and piezometer readings indicate good agreement in piezometric pressures.

Figure 6.25 shows the degree of consolidation from the CPTU dissipation tests for the Vertical Drain Area and Control Area as compared to the instrumentation results. The field instrumentation results of the In-Situ Test Site will be described in detail in Chapter 8.2. The CPTU dissipation test and piezometer readings are in good agreement for both the Vertical Drain Area and Control Area. The deep settlement gauges in the Vertical Drain Area were

also analysed by both the Asaoka and hyperbolic methods to attain the ultimate settlement and subsequently the degree of consolidation from the settlement gauges were computed. The method of analysis of the deep settlement gauges was carried out by the method proposed by Bo, Arulrajah and Choa (1997a). These too were in good agreement with the CPTU dissipation test results in the Vertical Drain Area. Based on the CPTU results, the Vertical Drain Area has attained a degree of consolidation of 80-85%. The Control Area without vertical drains on the other hand has attained a degree of consolidation of 10-22%.

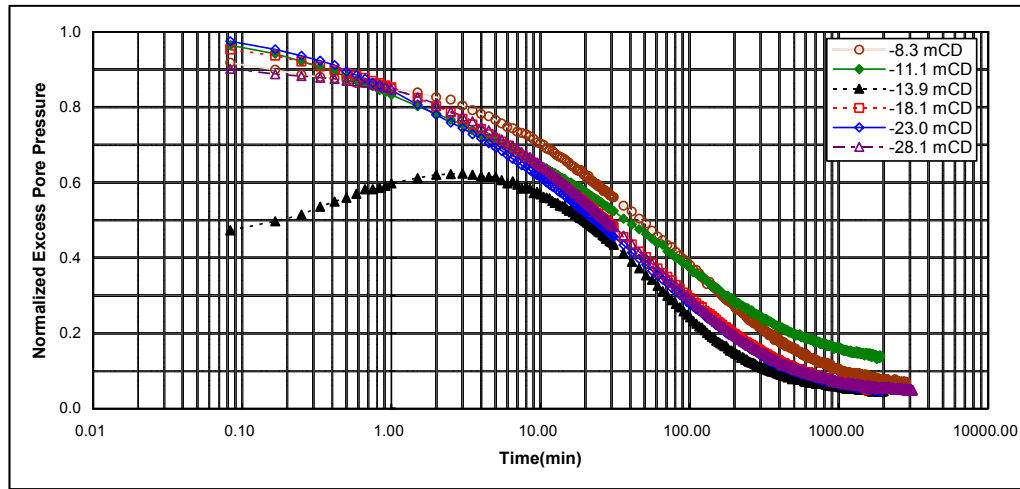


Figure 6.21 CPTU dissipation test curves at Vertical Drain Area (Arulrajah et al., 2004f).

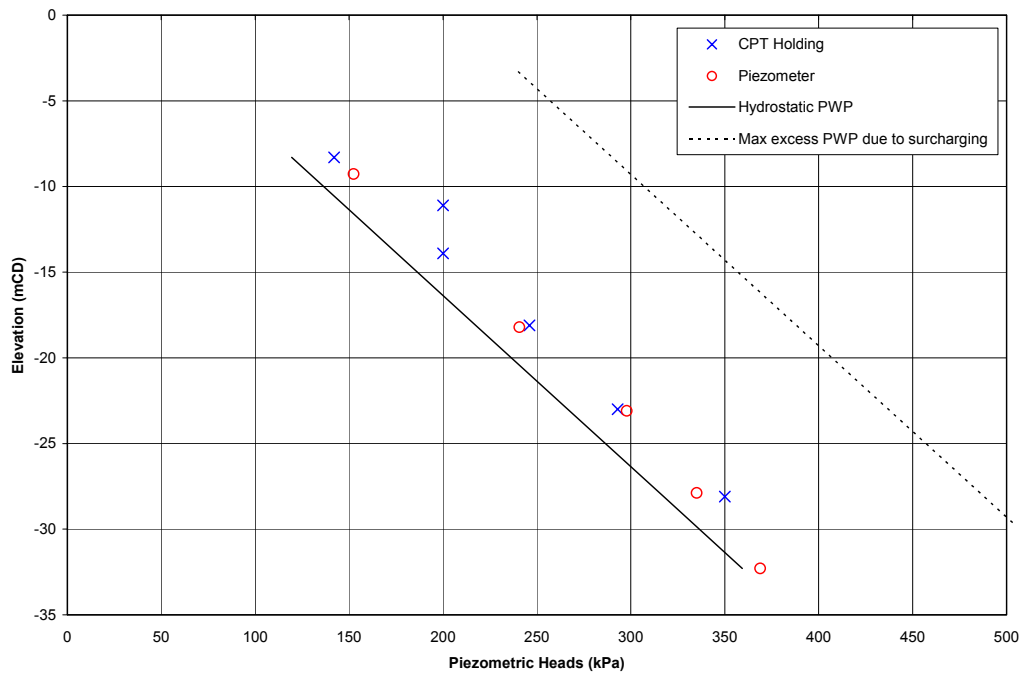


Figure 6.22 Comparison of piezometric heads at Vertical Drain Area (Arulrajah et al., 2004f).

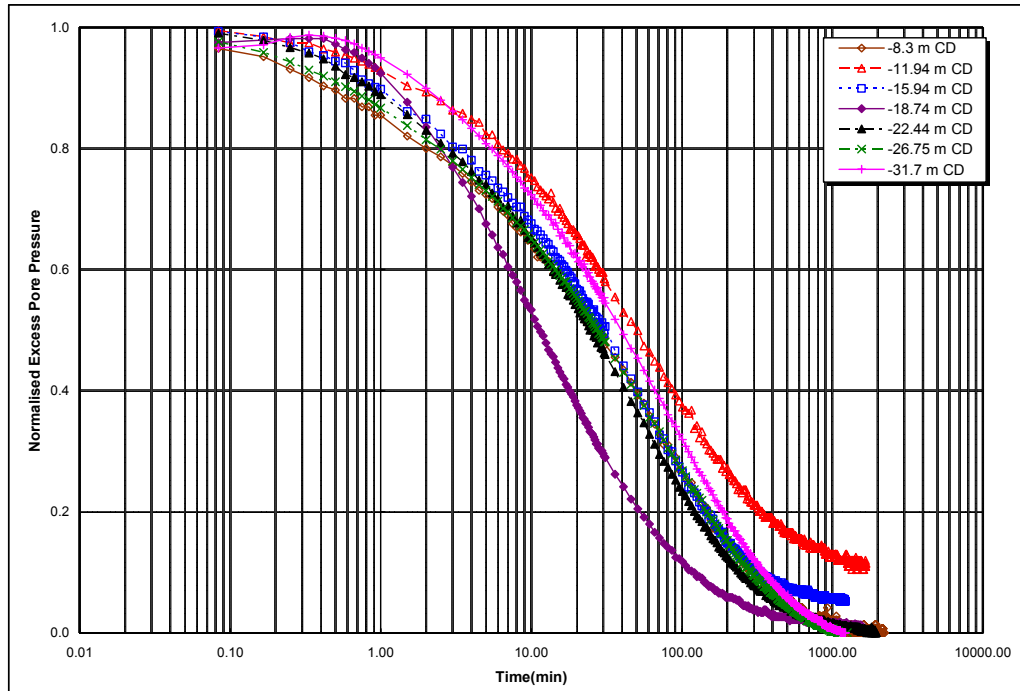


Figure 6.23 CPTU dissipation test curves at Control Area (Arulrajah et al., 2004f).

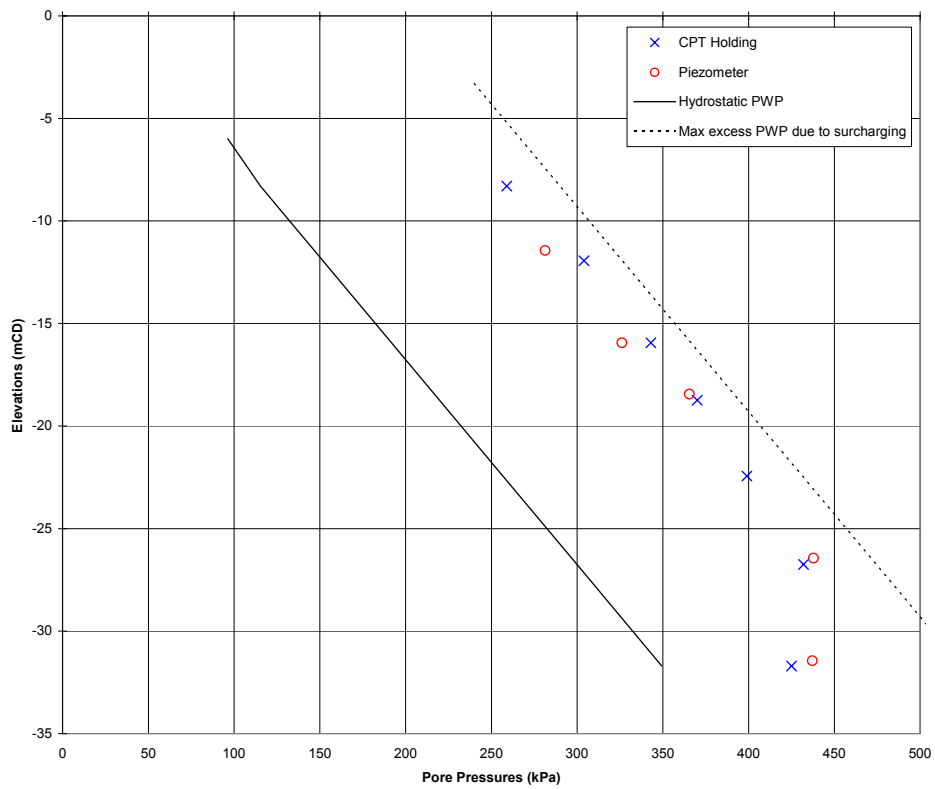


Figure 6.24 Comparison of piezometric heads at Control Area (Arulrajah et al., 2004f).

Piezocone dissipation tests have been utilised as a tool to obtain the piezometric heads of marine clays after surcharge loading as well as to assess the degree of consolidation of the improved marine clay. The results indicated that pore pressure measured from the CPTU holding tests are in agreement with the piezometric pressures from piezometer instruments in both the Vertical Drain Area and the Control Area.

The CPTU test results were also successfully used for the determination of the equilibrium pore pressure and degree of consolidation of the improved areas as confirmed by instrumentation results. This confirms that long term piezocone holding tests can be used as an alternative to piezometer instruments in marine clays.

Based on the CPTU results, the Vertical Drain Area was found to have attained a degree of consolidation of 80-85%. The Control Area without vertical drains on the other hand has attained a degree of consolidation of 10-22%. Figure 25 compares the degree of consolidation from CPTU dissipation test between the Vertical Drain Area and Control Area after 23 months of surcharge loading.

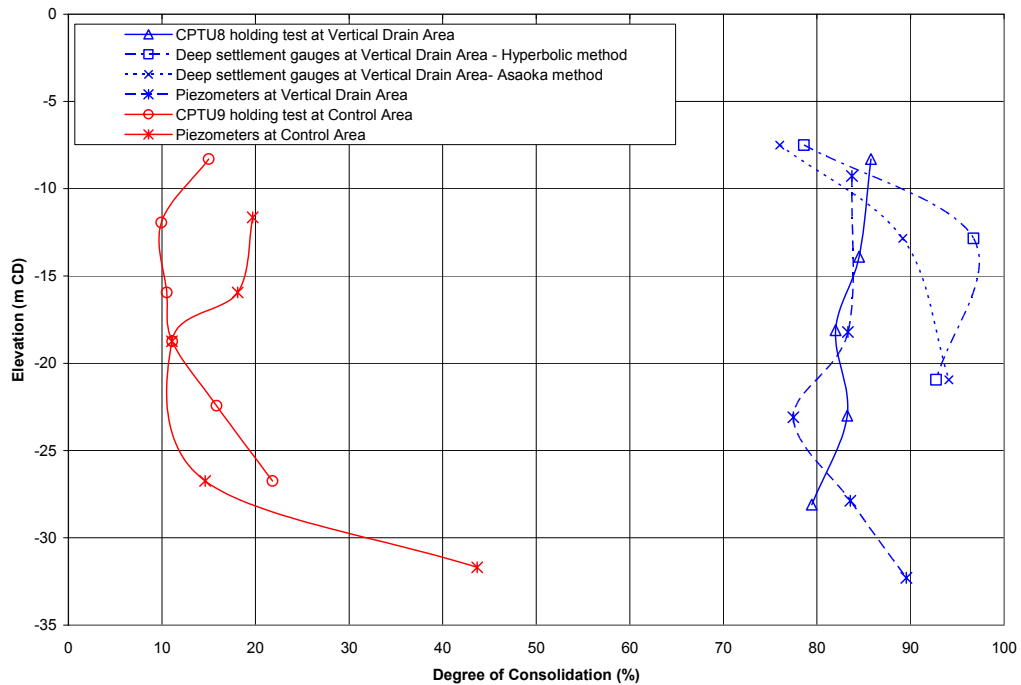


Figure 6.25 Comparison of degree of consolidation from CPTU dissipation test between Vertical Drain Area and Control Area after 23 months of surcharge loading (Arulrajah et al., 2004f).

Figure 6.26 presents the c_h results from the CPTU dissipation tests for the Vertical Drain Area and Control Area after 23 months of surcharge loading as compared to the pre-reclamation dissipation test.

The pre-reclamation dissipation tests indicate large c_h values in the intermediate stiff clay layer. The c_h values for the laboratory tests were obtained from radial flow Rowe cell of 75 mm diameter and 30 mm thickness and also from horizontally cut 63.5 mm oedometer test samples and were found to be in the same range as that of the CPTU.

The c_h value seems to be higher in the Vertical Drain Area at some elevations as compared to the Control Area. This is either due to the greater reduction in the coefficient of volume change after consolidation, local geology or it was simply affected by the correction factors used. A clear increase in the c_h values is obtained in the intermediate marine clay layer.

Figure 6.27 shows the k_h results from the CPTU dissipation tests for the Vertical Drain Area and Control Area after 23 months of surcharge loading as compared to the pre-reclamation dissipation test.

It can be observed that the pre-reclamation k_h values are decreasing with depth. The piezocone test results also show high k_h values in the intermediate desiccated zone. It is apparent that the prior to reclamation k_h is higher than that of the Vertical Drain Area and Control Area after 23 months of surcharge loading. This is expected due to reduction in the void ratio after surcharge loading. It is also apparent that the k_h in the Vertical Drain Area is lower than that in the Control Area which is expected due to higher void ratio changes and smear effect. Smear effect also affects the k_h in the vertical drain treated area due to insertion of the mandrel into the ground.

The pre-reclamation CPTU dissipation test indicate that the c_h values of the upper and lower marine clay varies between 2 to 6 m^2/yr . c_h values of 4 to 7 m^2/yr were obtained in the intermediate stiff clay, separating the upper and lower marine clay layers. The pre-reclamation dissipation tests indicate large c_h values in the intermediate stiff clay layer. The pre-reclamation CPTU indicates that k_h varies between 10^{-8} and 10^{-9} m/s.

c_h varies between 3 and 6 m^2/yr in the Vertical Drain Area and between 3 and 5 m^2/yr in the Control Area, after 23 months of surcharge loading. k_h varies between 10^{-9} and 10^{-10} m/s in the Vertical Drain Area and Control Area, after 23 months of surcharge loading.

The major factor that accounts for the lower c_h values back calculated from field settlement measurements is the smear effect incurred from the insertion of the mandrel during the installation of vertical drains. For soft marine clay, the smear effect can be quite significant as the spacing of the drains is normally 1.5 meters (Chu et al., 2002).

Bo et al. (1998b) has reported that the permeability of soil in the smear zone could be reduced by 1 order of magnitude or to the k_h of the remoulded clay as a result of the smear zone. The smear zone was reported by Bo et al. (1998b) to be 4-5 times the equivalent diameter of the vertical drain. When drains are installed at close spacing, the back-calculated c_h values will generally be greatly influenced by this smear zone (Chu et al., 2002).

The smear effect also affects the CPTU measurements for k_h and c_h . In the CPTU dissipation test, a penetrometer has to be pushed into the clay and a smear effect similar to the insertion of a mandrel could have been introduced prior to the measurements. This finding also indicates that when vertical drains are used in soft clay, the smear effect on the consolidation properties of soil has to be taken into consideration in the design (Chu et al., 2002).

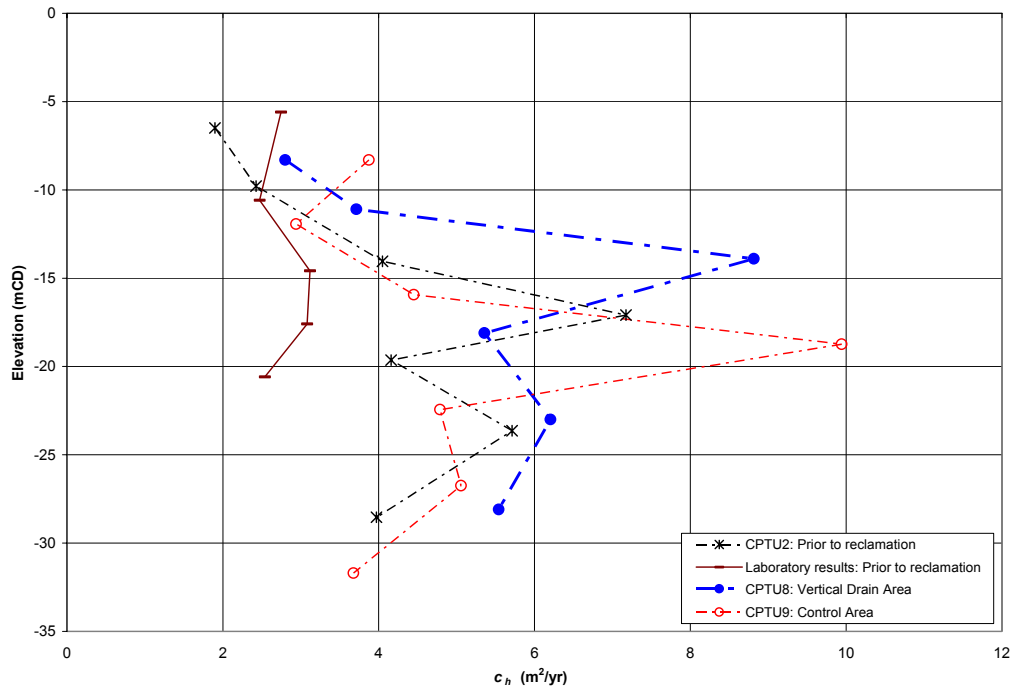


Figure 6.26 Comparison of coefficient of consolidation due to horizontal flow from CPTU dissipation test prior to reclamation and after 23 months of surcharge loading (Arulrajah et al., 2004f).

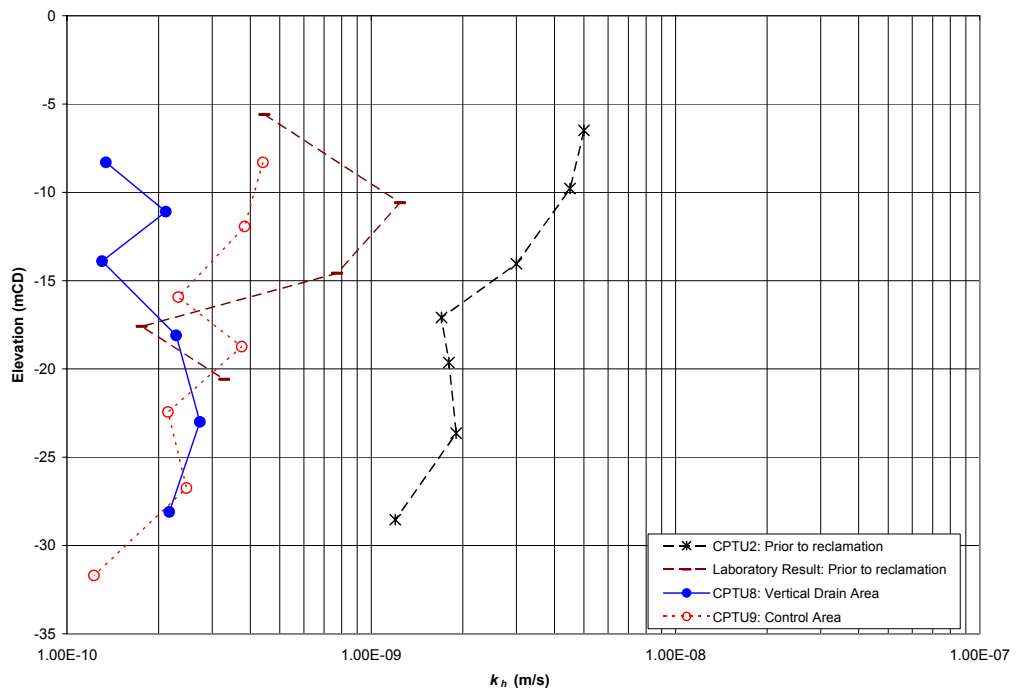


Figure 6.27 Comparison of horizontal hydraulic conductivity from CPTU dissipation test prior to reclamation after 23 months of surcharge loading (Arulrajah et al., 2004f).

6.7 Flat Dilatometer Test (DMT)

A Marchetti flat dilatometer (Marchetti and Crapps, 1981) was used for the tests, which consists of a steel membrane on one side of the blade. The dilatometer blade is 96 mm in width and 230 mm in length. The diameter of the membrane is 60 mm. Marchetti (1980) has provided a detailed description of the flat dilatometer and its interpretation methods. The determination of undrained shear strength and overconsolidation ratio from dilatometer tests has been extensively covered by Marchetti (1980), Chang (1986) and Chang et al. (1997). Chang (1986) has described the methods and interpretation of flat dilatometer dissipation tests. The method of interpretation of coefficient of consolidation due to horizontal flow values from dilatometer holding tests have been described by Marchetti and Totani (1989). The dilatometer requires certain specialised skill and technical knowledge to operate. Figure 6.28 shows the geometry and dimensions of the Marchetti dilatometer blade used in the research study. Figure 6.29 shows the dilatometer blade.

The in-situ testing of marine clay with the flat dilatometer described in this thesis has been discussed in detail by the author (Arulrajah et al., 2004d, 2004h, 2004i, 2004o 2004p) during the course of this research study.

6.7.1 Flat Dilatometer Test Method

The testing procedure followed that described by Marchetti and Crapps (1981). The testing consisted of pushing the flat dilatometer blade gradually into the soil at a prescribed rate of 20 mm per second with the use of a 20 ton dutch cone rig. The pushing was temporarily stopped at each of the proposed testing levels at which the two pressure readings A and B corresponding to two prefixed states of expansion of the membrane was recorded. The first pressure reading that is A-reading (p_0) corresponds to the membrane lift-off pressure in units of bar, while the second pressure reading that is B-reading (p_1) corresponds to the pressure required for the centre of the membrane to deflect by a preset distance of 1 mm into the soil in units of bar.

From the two pressure readings, three dilatometer indices are obtained being the material index (I_D), horizontal stress index (K_D) and dilatometer modulus (E_D):

$$I_D = (p_0 - p_1) / (p_0 - u_0) \quad \text{Eq. (6.17)}$$

$$K_D = (p_0 - u_0) / (\sigma_{v0} - u_0) \quad \text{Eq. (6.18)}$$

$$E_D = 34.7 (p_1 - p_0) \quad \text{Eq. (6.19)}$$

Marchetti (1980) proposed the following correlation between the undrained shear strength, c_u in units of kN/m^2 , with the horizontal stress index K_D :

$$c_u = 0.22 \sigma_{vo}' (0.5 K_D)^\eta \quad \text{Eq. (6.20)}$$

$$K_D = (P_0 - U_0) / \sigma_{vo}' \quad \text{Eq. (6.21)}$$

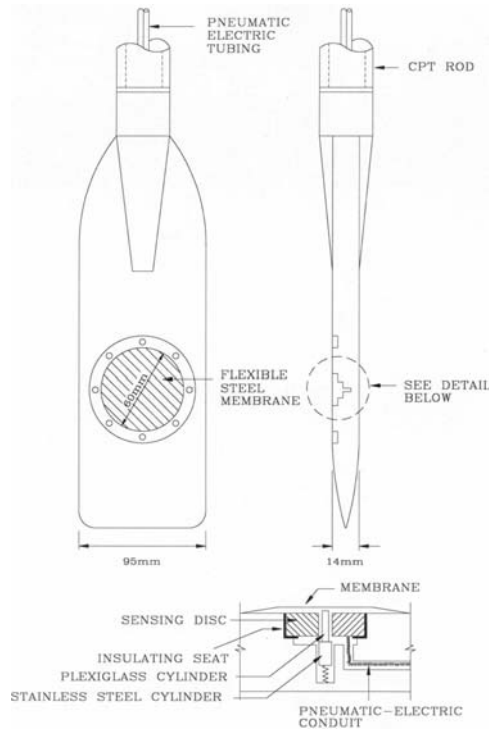


Figure 6.28 Geometry and dimension of Marchetti dilatometer blade (Chang, 1986).



Figure 6.29 Dilatometer blade and accessories.

where:

σ_{vo}' is vertical effective stress (kPa)

K_D is the horizontal stress index

η is a constant depending on the clay type

P_0 is the A reading from dilatometer (kPa)

U_0 is pre-inserting water pressure (kPa)

For Singapore Marine Clay at Changi, η can be taken as 1 for upper marine clay and intermediate clay while η can be taken as 0.7 for lower marine clays (Bo, Arulrajah, Chang and Choa; 2000a).

Marchetti (1980) proposed the following correlation for the estimation of OCR for clays:

$$\text{OCR} = (0.5 K_D)^n \quad \text{Eq. (6.22)}$$

For Singapore Marine Clay at Changi, n can be taken as 1 for upper and lower marine clays and 0.8 for intermediate clays (Bo, Arulrajah and Choa; 1997).

6.7.2 Comparison of Flat Dilatometer Tests

Care should be taken in determining the horizontal stress index, K_D , when soil is still undergoing consolidation with current surcharge load. In this case, current pore pressure values from the piezometer instruments should be used for equilibrium pore pressure. With OCR values worked out from the dilatometer tests the degree of improvement of compressible soil can be evaluated.

The comparison of the DMT results after 23 months of surcharge loading is shown in Figures 6.30 to 6.33. The DMT test indicates that the degree of consolidation of the Vertical Drain Area had attained a degree of consolidation of about 70-80% while the Control Area had attained a degree of consolidation of about 40%.

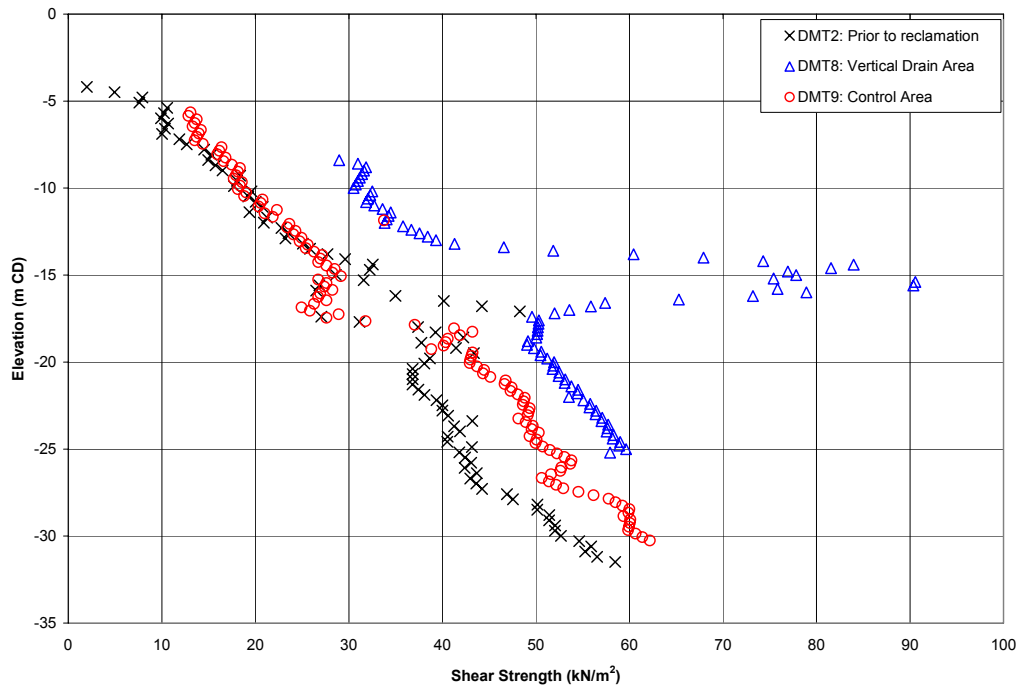


Figure 6.30 Variation of DMT shear strength with elevation after 23 months of surcharge loading.

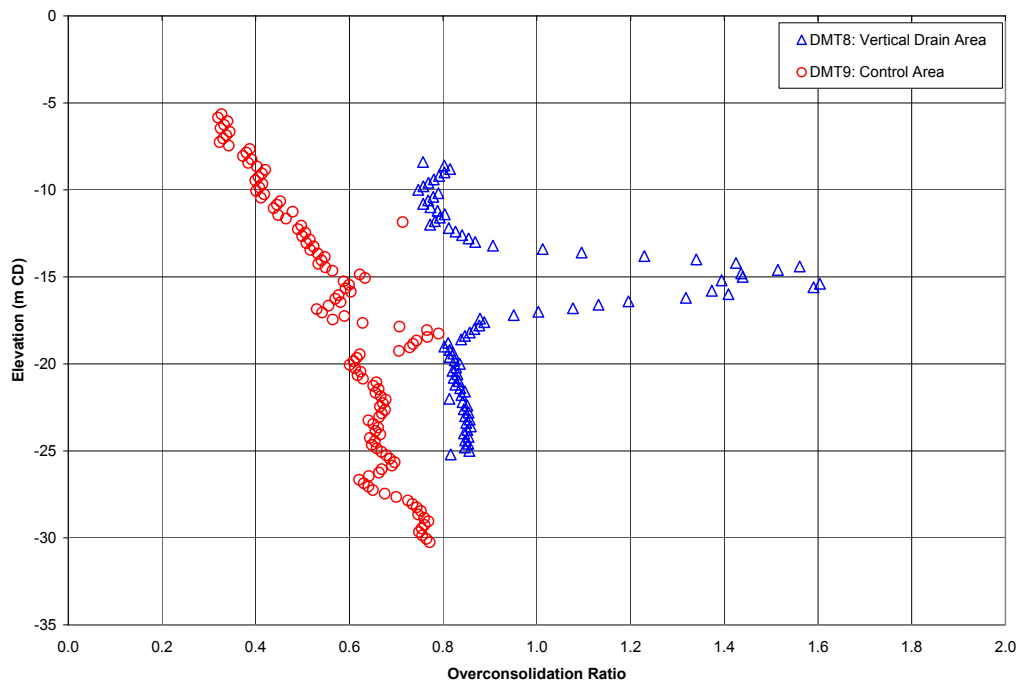


Figure 6.31 Variation of DMT OCR with elevation after 23 months of surcharge loading.

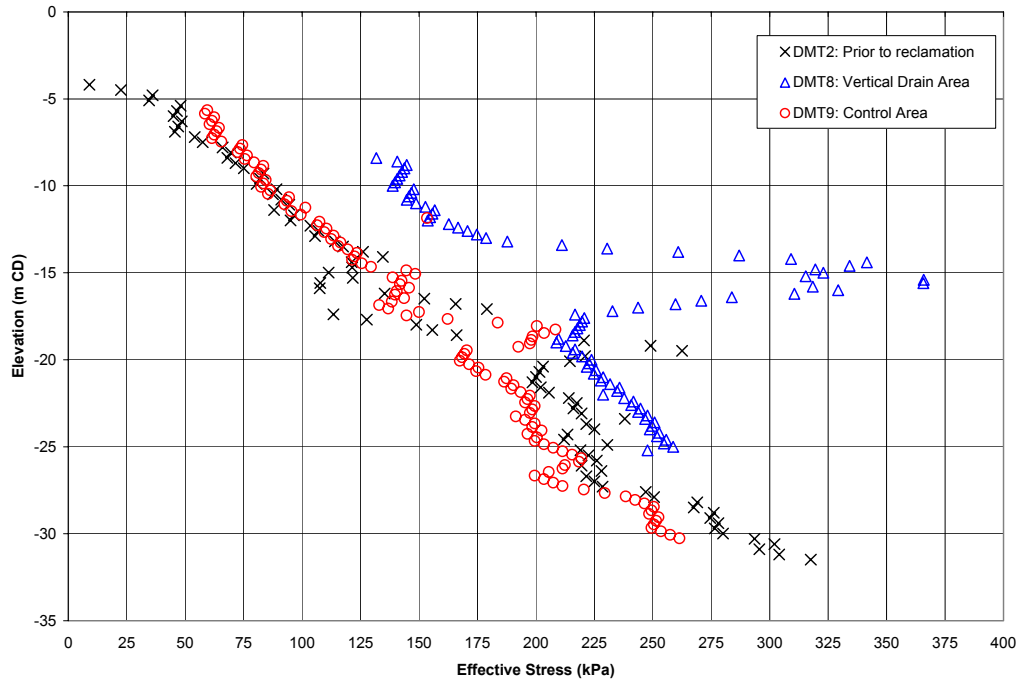


Figure 6.32 Variation of DMT effective stress with elevation after 23 months of surcharge loading.

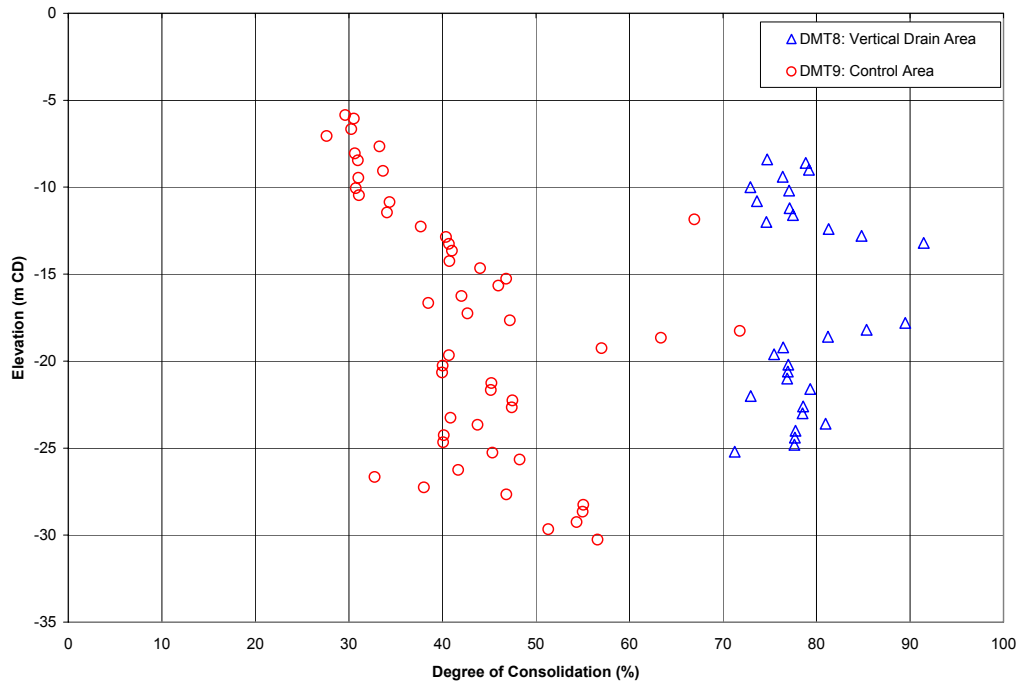


Figure 6.33 Variation of DMT degree of consolidation with elevation after 23 months of surcharge loading.

6.7.3 Flat Dilatometer Dissipation Test

The dilatometer test has the potential of providing estimates of the in-situ coefficient of consolidation due to horizontal flow from dissipation tests. The common dilatometer dissipation test involves two different procedure, one by recording the change of A-reading with time and the other the change of C-reading with time. The C-reading is the pressure reading, which corresponds to the resumption of the lift-off position of the membrane during deflation subsequent to taking the B-reading. The dissipation test which makes use of the A reading is called the DMTA dissipation test and can be performed at any depth by the procedure described by Marchetti and Tottani (1989). In this method, the A-reading is taken at different time intervals and plotted against log time. The time corresponding to the point of reverse curvature on the A-decay curve, T_{flex} is used as a basis for the interpretation of the c_h . For the DMTA dissipation test, the following expression was proposed by Marchetti and Tottani (1989) :-

$$c_h \text{ (DMTA)} \times T_{flex} = 5 - 10 \text{ cm}^2 \quad \text{Eq. (6.23)}$$

where:

$$c_h \text{ is in units of cm}^2/\text{min}; \text{ for Singapore marine clay } c_h \text{ (DMTA)} \times T_{flex} = 5 \text{ cm}^2$$

In the dissipation test procedure which makes use of the C-reading, the C-reading is plotted against square root time and the time corresponding to 50% consolidation, t_{50} is determined and used in the interpretation of c_h (Schmertmann, 1988). Gupta et al. (1983) procedure, developed for piezocone dissipation analysis was modified and used in the interpretation of c_h . The dissipation test which makes use of the C-reading is called the DMTC dissipation test and can be performed at any depth. The procedure involves estimating rigidity index, E_u / c_u , and pore pressure at failure, A_f , for the clay and determining the time factor corresponding to 50% pore pressure dissipation, T_{50} , from the dissipation curves for $A_f = 0.9$ (Schmertmann, 1988). An adjustment of the time factor may be required if A_f is different from 0.9. The T_{50} can then be used in the following equation which assumes $R^2 = 600 \text{ mm}^2$ for a test involving the standard Marchetti dilatometer (Chu et al., 2002):

$$c_h \text{ (DMTC)} = 600 (T_{50} / t_{50}) \quad \text{Eq. (6.24)}$$

where:

c_h is in units of mm^2/min

T_{50} is the theoretical time factor;

t_{50} is time elapsed for 50% degree of consolidation to take place.

Similar to CPTU tests, the c_h values determined from either DMTA or DMTC corresponds to the unloading/reloading range. Corrections have to be made to obtain the in situ c_h value. When converting the c_h (DMT) values into the c_h value at the normally consolidated state, the conversion using Eq. (6.14) has been found to provide consistent results. Eq. (6.15) can be used to determine the horizontal hydraulic conductivity of the marine clay. Figures 6.34 to 6.37 show the DMTA and DMTC testing results and interpretation.

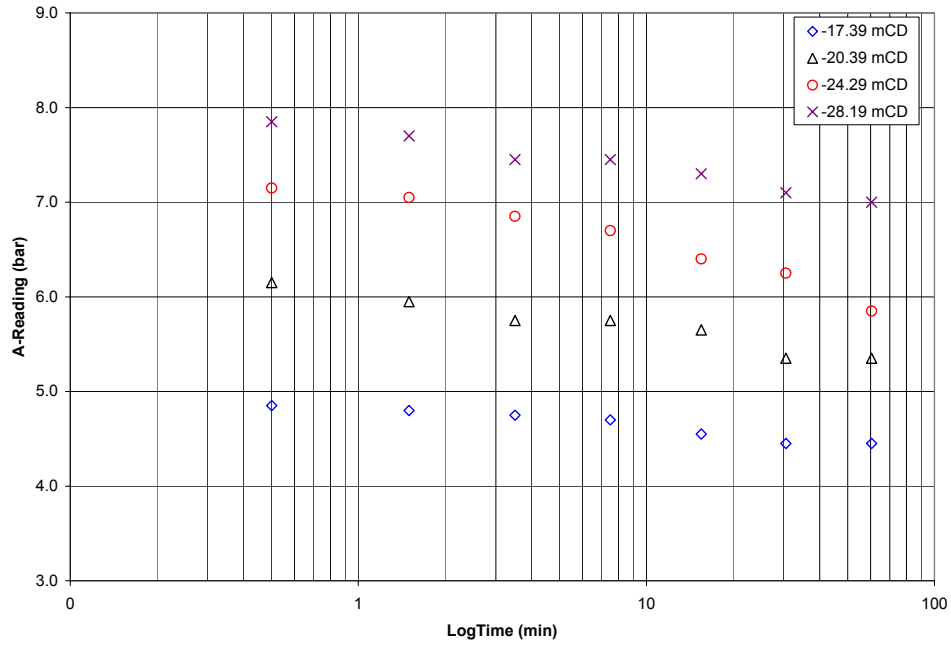


Figure 6.34 DMTA dissipation tests prior to reclamation (Arulrajah et al., 2004o).

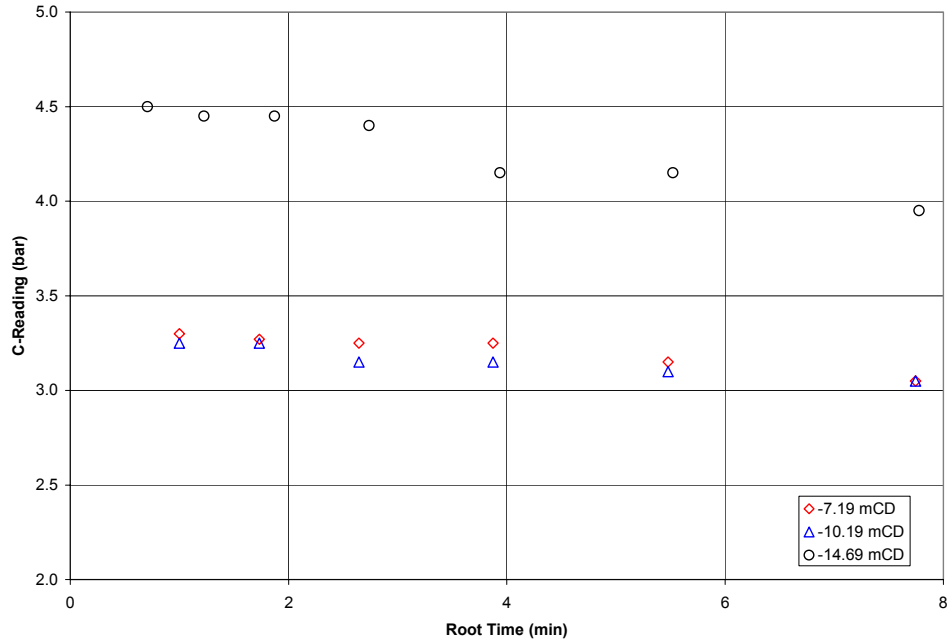
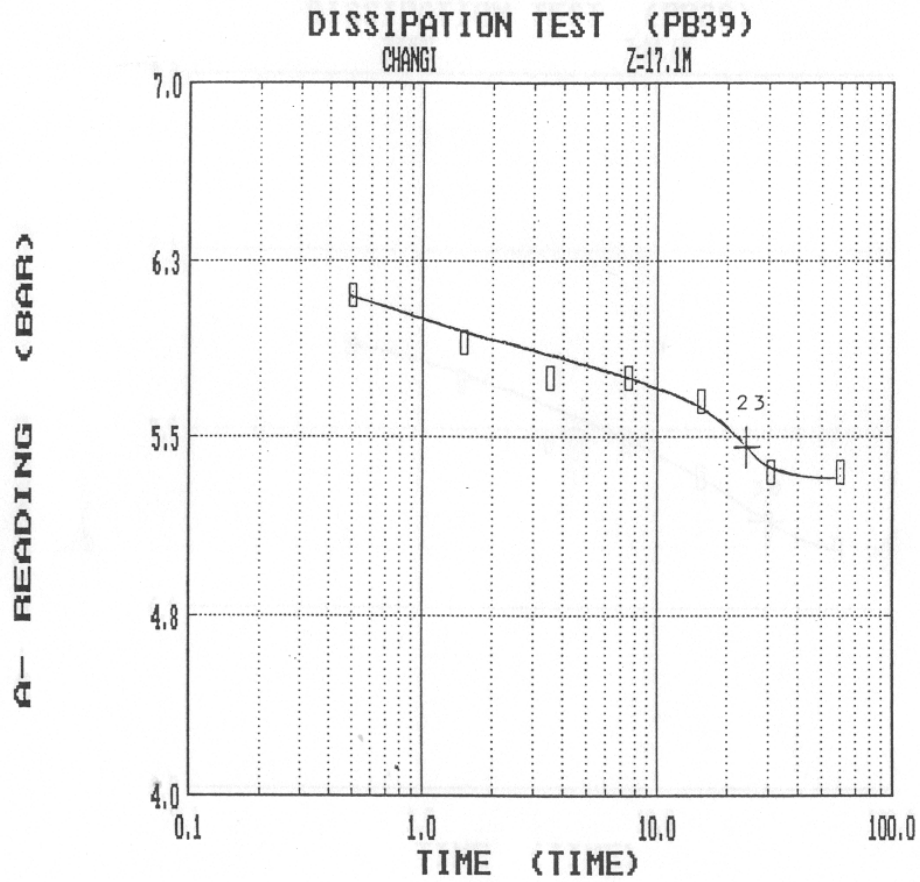


Figure 6.35 DMTC dissipation test prior to reclamation (Arulrajah et al., 2004o).



Calculations:

$$c_h(\text{DMTA}) * T_{\text{flex}} = 5 \text{ cm}^2$$

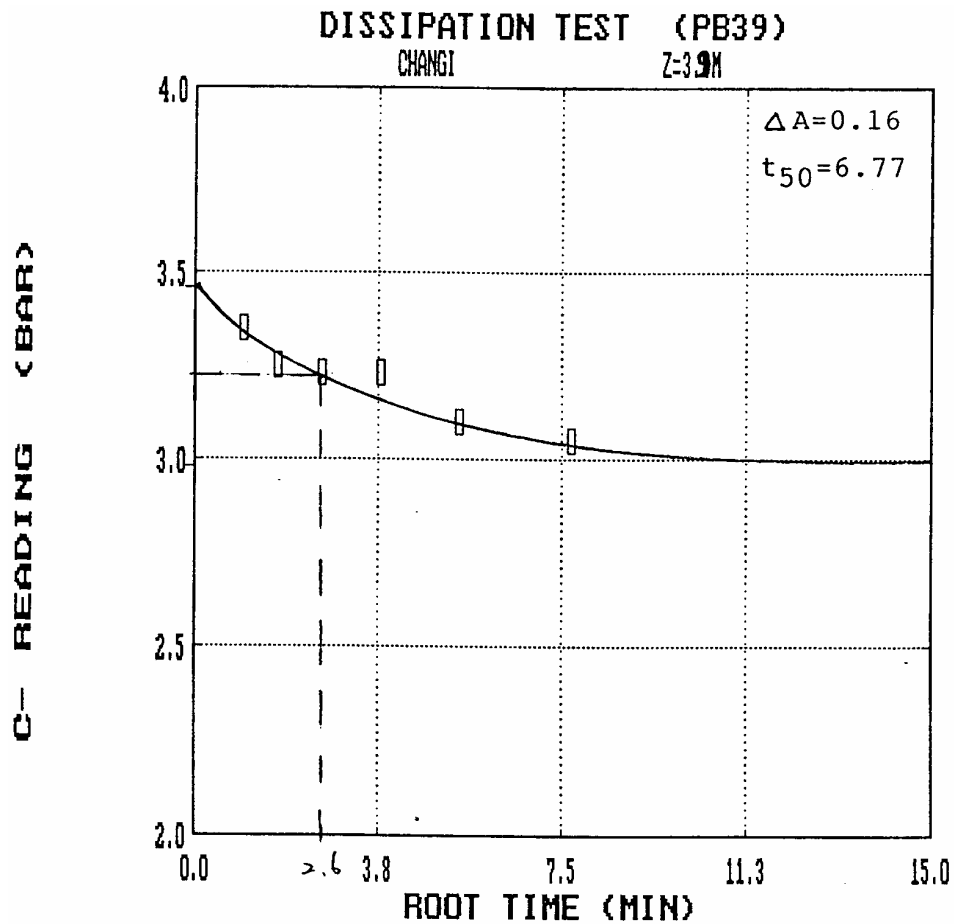
$$c_h(\text{DMTA}) = 5 / 23 = 0.217 \text{ cm}^2/\text{min} = 11.43 \text{ m}^2/\text{yr}$$

$$C_c / C_r = 5.8$$

$$c_h(\text{field}) = c_h(\text{DMTA}) * C_r/C_c = 11.43 * 1/5.8$$

$$c_h(\text{field}) = \underline{1.97 \text{ m}^2/\text{yr}}$$

Figure 6.36 Typical DMTA dissipation test and calculations prior to reclamation (elevation -20.39 mCD).



Calculations:

$$E_u / S_u = 150$$

$$A_r = 0.5 \text{ and therefore } \eta = T_{A_f=0.5} / T_{A_f=0.9} = 0.8$$

$$T_{50} = 1.2 * 0.8 = 0.96$$

$$c_h(\text{DMTC}) = 600 * T_{50} / t_{50} \text{ mm}^2/\text{min}$$

$$c_h(\text{DMTC}) = 600 * 0.96 / (2.6)^2 = 85.02 \text{ mm}^2/\text{min} = 44.71 \text{ m}^2/\text{yr}$$

$$C_c / C_r = 6.7$$

$$c_h(\text{field}) = c_h(\text{DMTA}) * C_r / C_c = 44.71 * 1 / 6.7$$

$$c_h(\text{field}) = \underline{6.68 \text{ m}^2/\text{yr}}$$

Figure 6.37 Typical DMTC dissipation test and calculations prior to reclamation (elevation -7.19 mCD).

6.7.4 Comparison of Flat Dilatometer Dissipation Tests

The comparison of the c_h results for the Vertical Drain Area and the Control Area is presented in Figure 6.38, while Figure 6.39 shows the k_h results.

c_h value is apparent to be higher in the Vertical Drain Area as compared to the Control Area. Despite the k_h being lower in the Vertical Drain Area, the c_h could be higher due to greater ratio of reduction in the coefficient of volume change, m_v . The in-situ results in the upper and lower marine clay layers indicate c_h values of 4-6 m^2/yr in the Vertical Drain Area and values of 4-6 m^2/yr in the Control Area.

The k_h values in the Vertical Drain Area is found to be lower than that in the Control Area. It is noted however that k_h values are indirectly obtained from c_h values. k_h values ranging from 10^{-9} to 10^{-10} m/s were obtained in the Vertical Drain Area while values of 10^{-9} m/s were obtained in the Control Area.

It is evident that the prior to reclamation DMT dissipation test has encountered the intermediate stiff layer strata at the lower elevations and hence the high initial c_h values. The DMT dissipation tests in the Vertical Drain Area and the Control Area also indicate higher c_h values in the intermediate stiff layer. Only DMTA readings method was carried out in both the Vertical Drain Area and the Control Area.

Figures 6.40 and 6.41 show the DMTA testing results for the Vertical Drain Area and Control Area after 23 months of surcharge loading. Figures 6.42 and 6.43 show the typical DMTA interpretation for the Vertical Drain Area and Control Area after 23 months of surcharge loading.

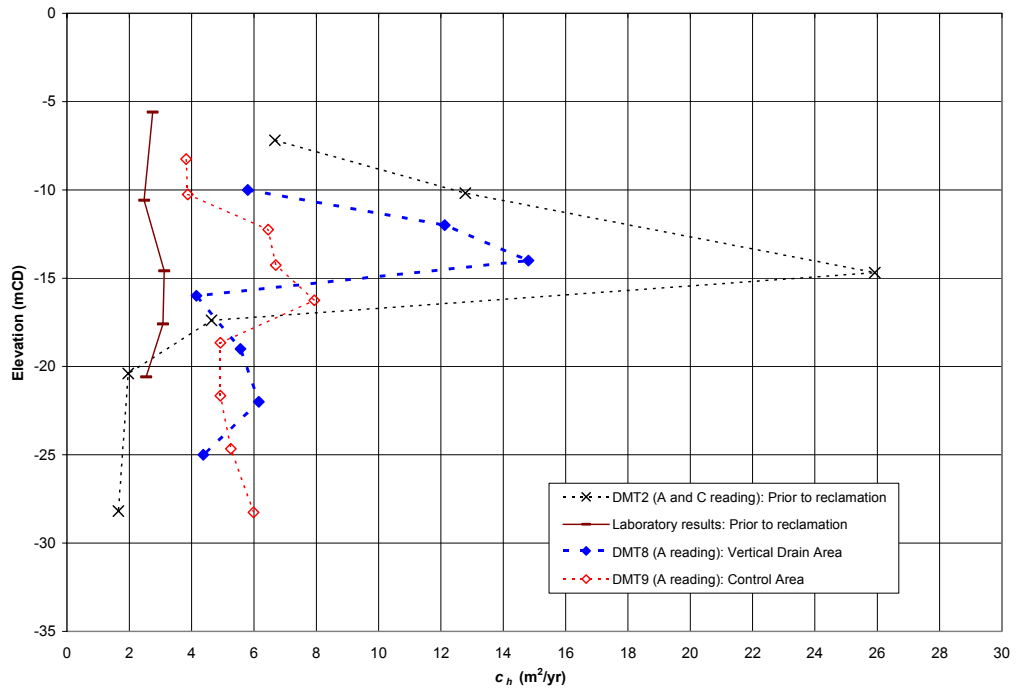


Figure 6.38 Comparison of coefficient of consolidation due to horizontal flow from DMTA dissipation test prior to reclamation and after 23 months of surcharge loading (Arulrajah et al., 2004i).

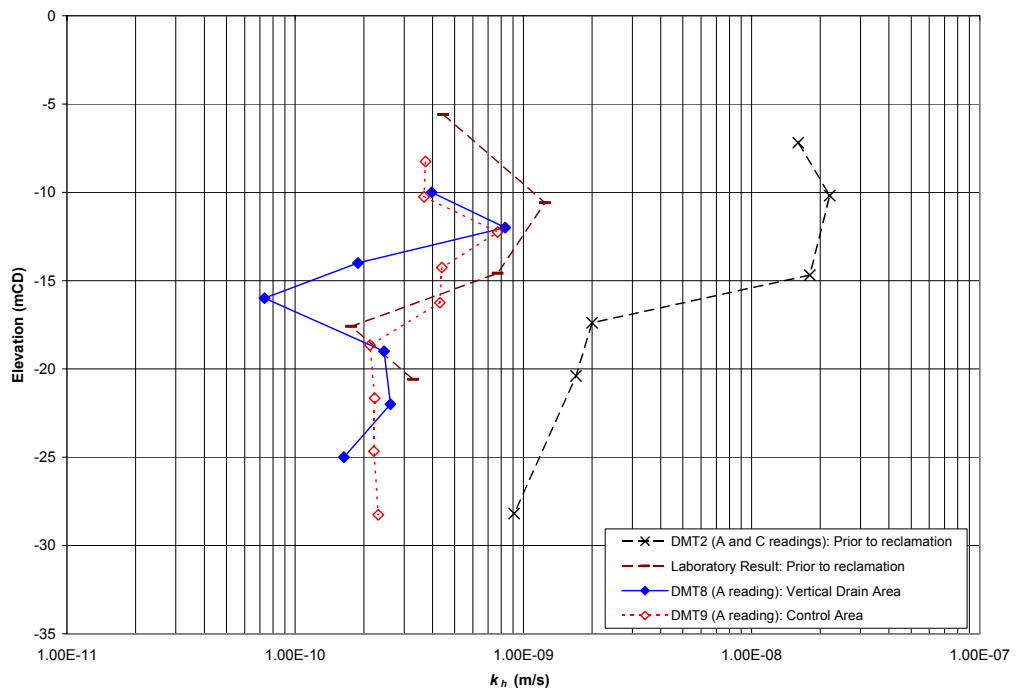


Figure 6.39 Comparison of horizontal hydraulic conductivity from DMTA dissipation test prior to reclamation and after 23 months of surcharge loading (Arulrajah et al., 2004i).

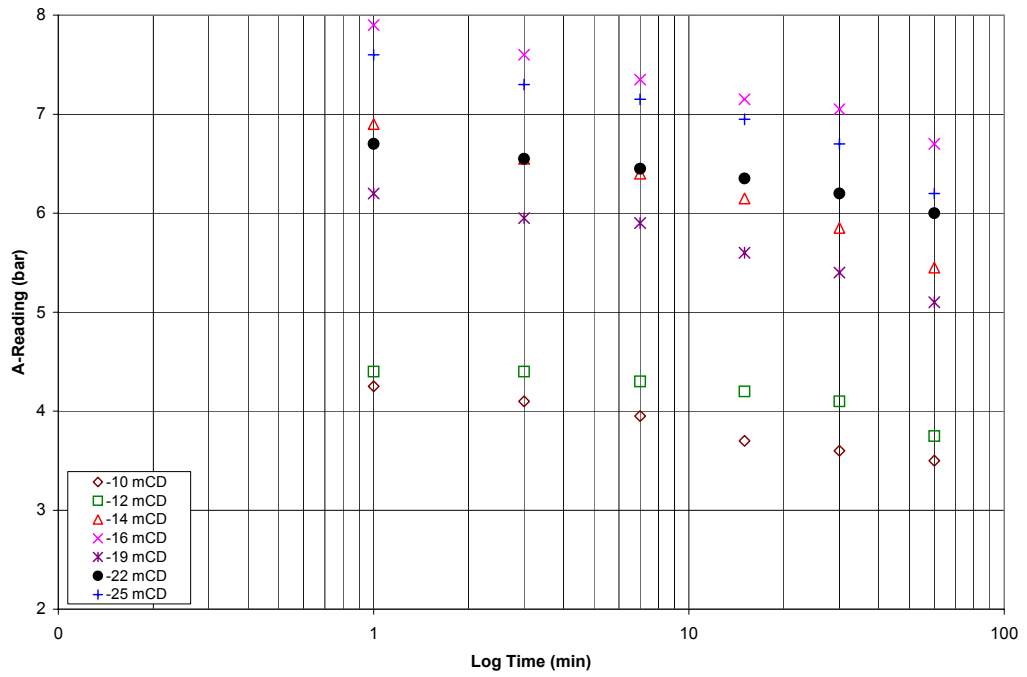


Figure 6.40 DMTA dissipation test at Vertical Drain Area (Arulrajah et al., 2004o).

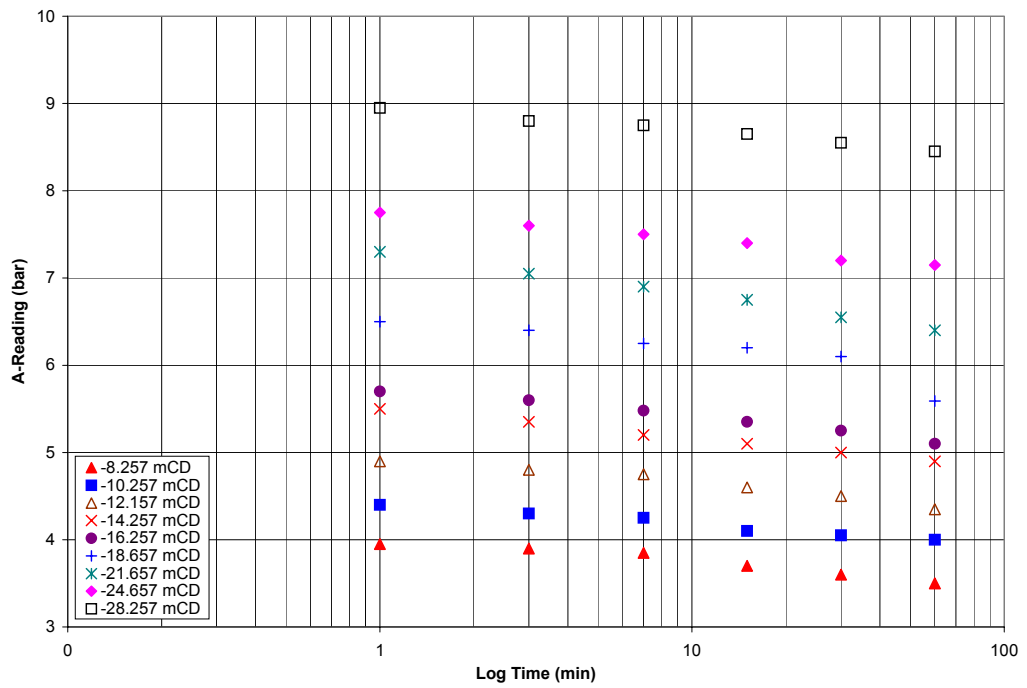
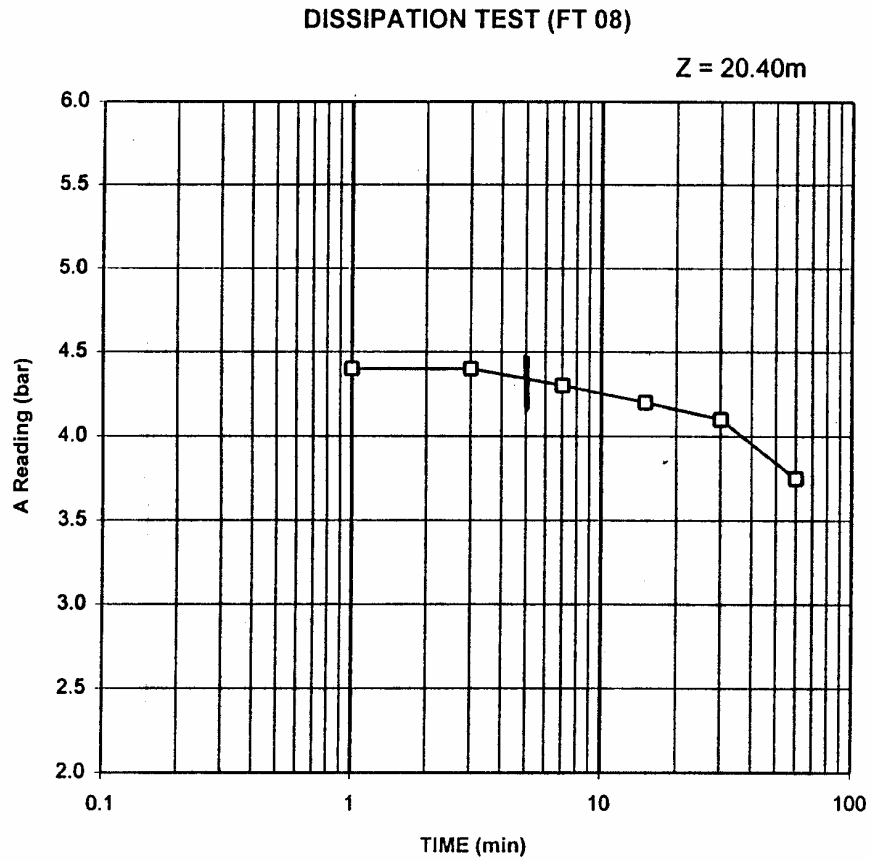


Figure 6.41 DMTA dissipation test at Control Area (Arulrajah et al., 2004o).



Calculations:

$$c_h(\text{DMTA}) \times T_{\text{flex}} = 5 \text{ cm}^2$$

$$c_h(\text{DMTA}) = 5 / 5 = 1 \text{ cm}^2/\text{min} = 52.56 \text{ m}^2/\text{yr}$$

$$C_c / C_r = 4.335$$

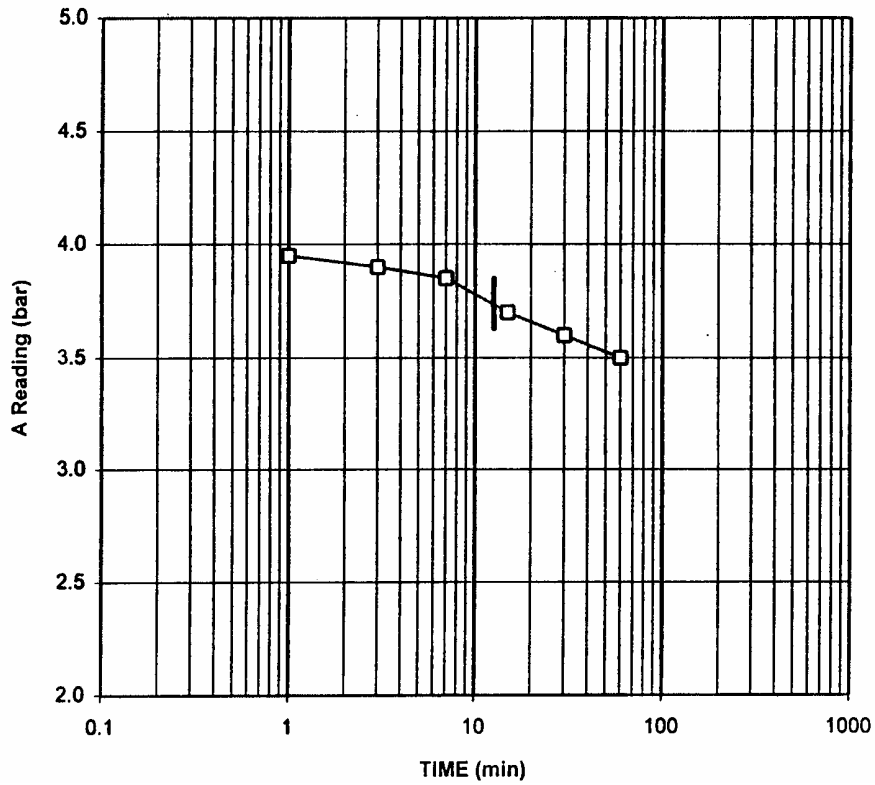
$$c_h(\text{field}) = c_h(\text{DMTA}) \times C_r / C_c = 52.56 \times 1 / 4.335$$

$$c_h(\text{field}) = \underline{12.12 \text{ m}^2/\text{yr}}$$

Figure 6.42 Typical DMTA dissipation test plot and calculations at Vertical Drain Area (elevation – 12 mCD) (Arulrajah et al., 2004o).

DISSIPATION TEST (FT 09)

Z = 18.00m



Calculations:

$$c_h(\text{DMTA}) \times T_{\text{flex}} = 5 \text{ cm}^2$$

$$c_h(\text{DMTA}) = 5 / 12 = 0.417 \text{ cm}^2/\text{min} = 21.9 \text{ m}^2/\text{yr}$$

$$C_c / C_r = 5.73$$

$$c_h(\text{field}) = c_h(\text{DMTA}) \times C_r / C_c = 21.9 \times 1 / 5.73$$

$$c_h(\text{field}) = \underline{3.82 \text{ m}^2/\text{yr}}$$

Figure 6.43 Typical DMTA dissipation test plot and calculations at Control Area (elevation – 8.257 mCD) (Arulrajah et al., 2004o).

6.8 Self-Boring Pressuremeter Test (SBPT)

The Cambridge-type self-boring pressuremeter with 6 strain measuring arms located at the mid-level (Cambridge In-Situ, 1993) was used for the testing purposes. The probe is about 83 mm in diameter and 1.4 meters in length and is made up of stainless steel and brass. Over the critical part of the instrument, the diameter is maintained to an accuracy of 0.1 mm. The instrument consists of strain gauge type transducers attached to the central core or pressuremeter body. The pressuremeter body is covered with a rubber membrane for direct recording of the radial displacement and the applied pressure. A rotary bit is present at the base of the equipment.

The in-situ testing of marine clay with the self-boring pressuremeter described in this chapter has been discussed in detail by the author (Arulrajah et al., 2004d, 2004h, 2004i, 2004p) during the course of this research study.

6.8.1 Self-Boring Pressuremeter Test Method

Mair and Wood (1987) have described the methods of testing of various pressuremeters including the self-boring pressuremeter. Windle and Wroth (1997) have described the determination of the undrained properties of clay by means of the self-boring pressuremeter. Whittle et al. (1993) has described the lift-off stress and analysis of the initial stress distribution of the six arm self-boring pressuremeter. Figure 6.44 shows the geometry and dimensions of the self-boring pressuremeter used in the research study. Figure 6.45 shows the self-boring pressuremeter and accessories.

Testing involves the advancement and insertion of the pressuremeter to the proposed depth by use of the self-boring technique. After the insertion of the pressuremeter, the rubber membrane was inflated by injection of gas pressure. Both the applied pressure and the corresponding displacement of the borehole (cavity) wall were measured during the test. Raw testing results are produced in plots of applied pressure versus radial cavity strain, which is interpreted by the cavity expansion theory.

Windle and Wroth (1997) suggested undrained shear strength can be estimated from the limit pressure from the self boring pressuremeter as follows:

$$c_u = (P_c - \sigma_{ho}) / [1 + \log_e (G / c_u)] \quad \text{Eq. (6.25)}$$

$$\text{or } c_u = (P_c - \sigma_{ho}) / N_p \quad \text{Eq. (6.26)}$$

$$N_p = 1 + \log_e (G / c_u)$$

Eq. (6.27)

where:

c_u is in units of kN/m^2

σ_{ho} is total horizontal stress (kN/m^2)

G is shear modulus (MPa)

N_p is the pressuremeter constant by Marsland and Randolph (1977).

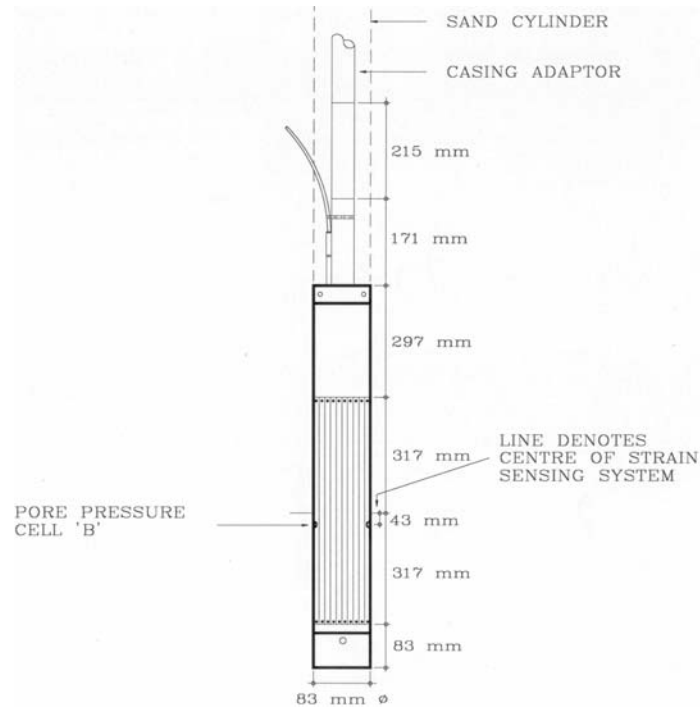


Figure 6.44 Geometry and dimension of self-boring pressuremeter (Cambridge In-Situ, 1993).



Figure 6.45 Self-boring pressuremeter and accessories.

For Singapore marine clays, N_p values of 6.6, 6.4 and 7.2 can be applied for the upper marine clay, intermediate clay and lower marine clay respectively (Bo, Arulrajah, Choa and Chang; 1998a). Estimation of shear modulus can be obtained from small unload-reload cycles. The undrained shear strength is obtained from the expansion tests.

The OCR for the pre-reclamation SBPT in the Vertical Drain Area was calculated from the SBPT shear strength values by using Eq. (6.5) which is also used for the FVT.

6.8.2 Comparison of Self-Boring Pressuremeter Tests

Since total stress can be measured from self-boring pressuremeter test, coefficient of earth pressure at rest, K_0 , can be calculated and OCR can then be estimated by this method for locations treated with vertical drains:

$$K_0 = \sigma_{ho}' / \sigma_{vo}' \quad \text{Eq. (6.28)}$$

where:

K_0 is coefficient of earth pressure at rest.

σ_{ho}' is effective lateral stress (kPa).

$$\text{OCR} = [(\sigma_{oc}) / (\sigma_{nc})]^{1/h} \quad \text{Eq. (6.29)}$$

where:

h is a constant of between 0.32 - 0.4 and is taken as 0.4 in this study.

The comparison of the SBPT results after 23 months of surcharge loading is shown in Figures 6.46 to 6.49. The SBPT test indicates that the degree of consolidation of the Vertical Drain Area had attained a degree of consolidation of about 80% while the Control Area had attained a degree of consolidation of about 20-30%.

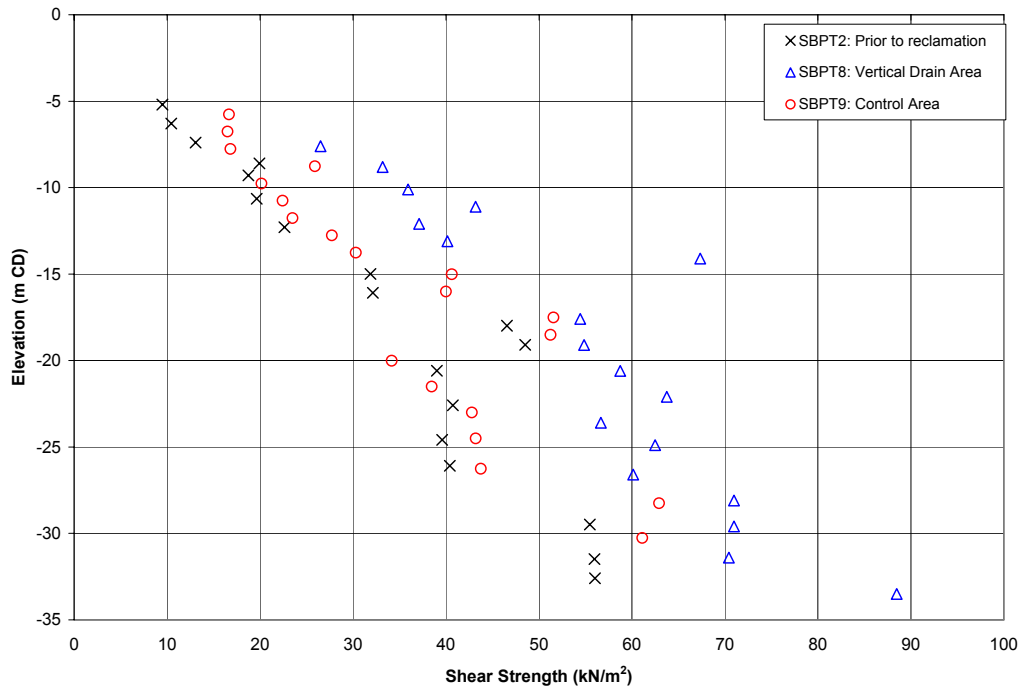


Figure 6.46 Variation of SBPT shear strength with elevation after 23 months of surcharge loading.

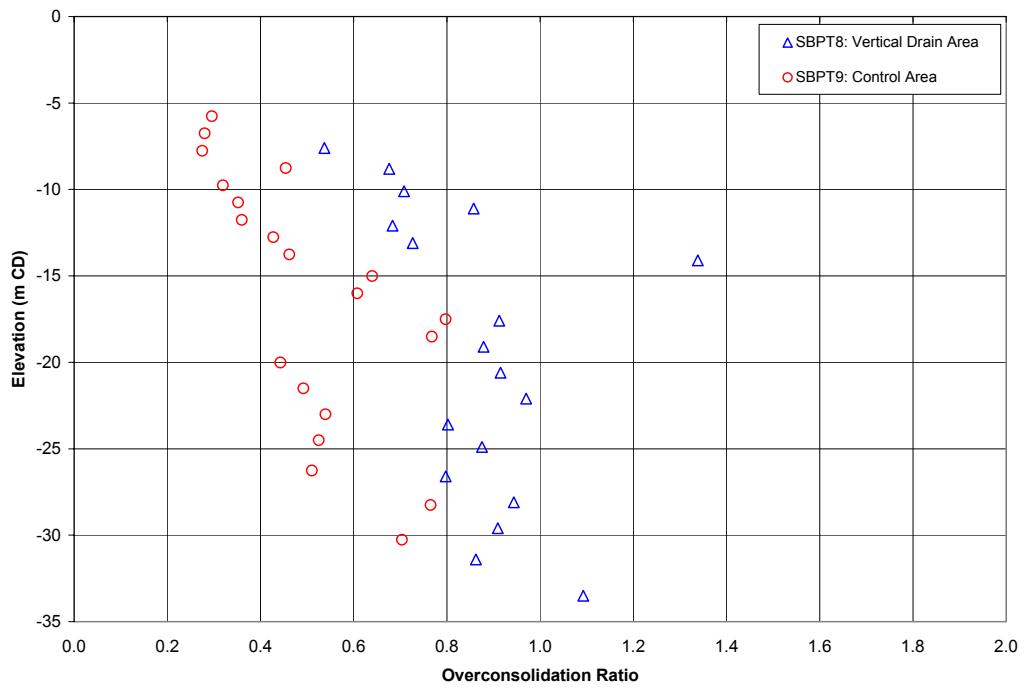


Figure 6.47 Variation of SBPT OCR with elevation after 23 months of surcharge loading.

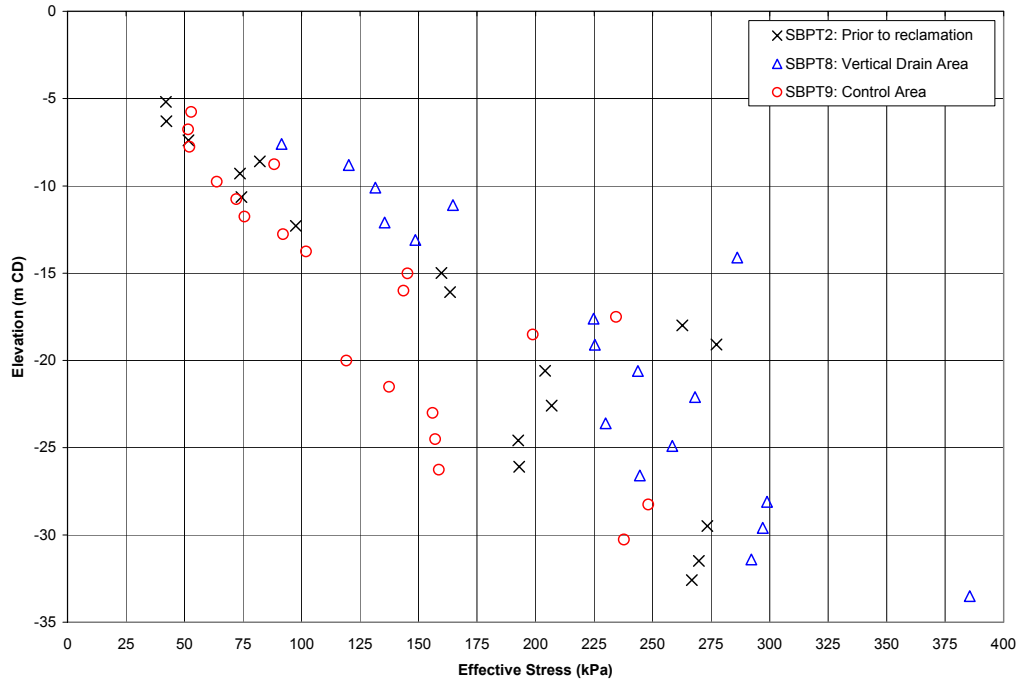


Figure 6.48 Variation of SBPT effective stress with elevation after 23 months of surcharge loading.

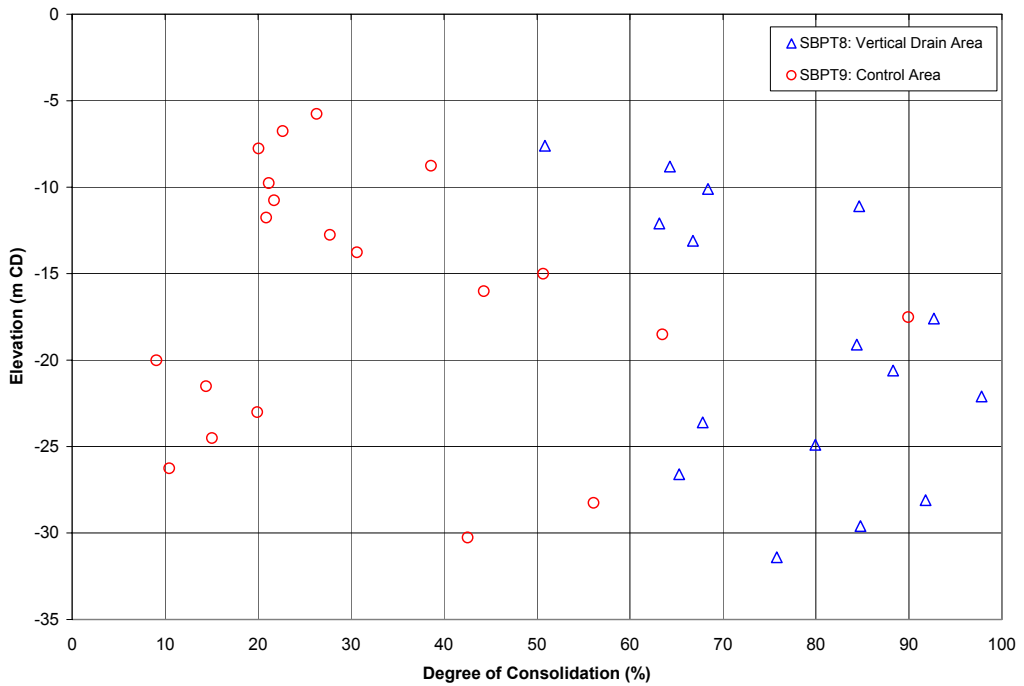


Figure 6.49 Variation of SBPT degree of consolidation with elevation after 23 months of surcharge loading.

6.8.3 Self-Boring Pressuremeter Dissipation Test

The pore pressure cells are located 43 mm below the centre of the pressuremeter probe. The holding test proceeds as a normal pressuremeter test until the point when the soil is to be unloaded. Instead of unloading at a constant rate of strain, the expanded cavity is held fixed at the current dimensions. The excess pore water pressure generated by the preceding expansion will begin to drain and the decay of pore pressure is recorded. When the level of excess pore pressure has fallen by slightly more than half, the test is terminated.

When the pore water pressures fall, the total pressure in the instrument will be greater than that required to maintain the cavity at a fixed size. Left alone, the cavity would continue to expand. An automatic strain control unit is used to monitor this tendency for the cavity to increase, and the unit vents a little of the pressure in the instrument to compensate. Hence, information about the decay of pore pressures is available directly from the pore water pressure transducers on the outside of the instrument and indirectly from the necessary decline in total pressure.

The analysis used was proposed by Clarke et al. (1979). The analysis assumes that the Gibson and Anderson model of soil deformation applies (Clarke et al., 1979) and hence that the pore water pressures generated by an undrained expansion can be calculated and converted to a time factor. Coefficient of consolidation due to horizontal flow can thus be worked out as follows:

$$c_h(\text{probe}) = T_{50} \gamma_0^2 / t_{50} \quad \text{Eq. (6.30)}$$

where:

c_h is in units of m^2/yr

γ_0 is the radius of cavity

T_{50} is theoretical time factor as estimated from the relationship given by Clarke et al. (1979)

t_{50} is time elapsed in years for 50% degree of consolidation to take place.

Similar to CPTU and DMT tests, the c_h values determined from SBPT corresponds to the unloading/reloading range and a correction based on Eq. (6.14) is required in order to obtain the c_h value for the NC range. The horizontal hydraulic conductivity can be calculated as follows in units of m/yr :

$$k_h = (c_h / G) \gamma_w [(1 - 2\mu) / \{2 - (1 - \mu)\}] \quad \text{Eq. (6.31)}$$

where:

k_h is in units of m/yr

G is shear modulus in MPa

μ is poisson ratio which was assumed to be 0.5 for the current test

γ_w is the unit weight of water

6.8.4 Comparison of Self-Boring Pressuremeter Dissipation Tests

The comparison of the c_h results for the Vertical Drain Area and the Control Area is presented in Figure 6.50, while Figure 6.51 shows the k_h results.

c_h value is seen to be higher in the Vertical Drain Area as compared to the Control Area. Despite the k_h being lower in the Vertical Drain Area, the c_h could be higher due to greater ratio of reduction in the coefficient of volume change, m_v . The in-situ results in the upper and lower marine clay layers indicate c_h values of 3-12 m²/yr in the Vertical Drain Area and values of 4-7 m²/yr in the Control Area. The SBPT dissipation tests in the Vertical Drain Area, Control Area and prior to reclamation also indicate higher c_h values in the intermediate stiff layer.

It also seems that k_h values in the Vertical Drain Area is higher than that in the Control Area which should not be the case and this is attributable to the indirect method of computing k_h from c_h values. k_h values ranging from 10^{-9} to 10^{-10} were obtained in the Vertical Drain Area while values of 10^{-9} to 10^{-10} were obtained in the Control Area.

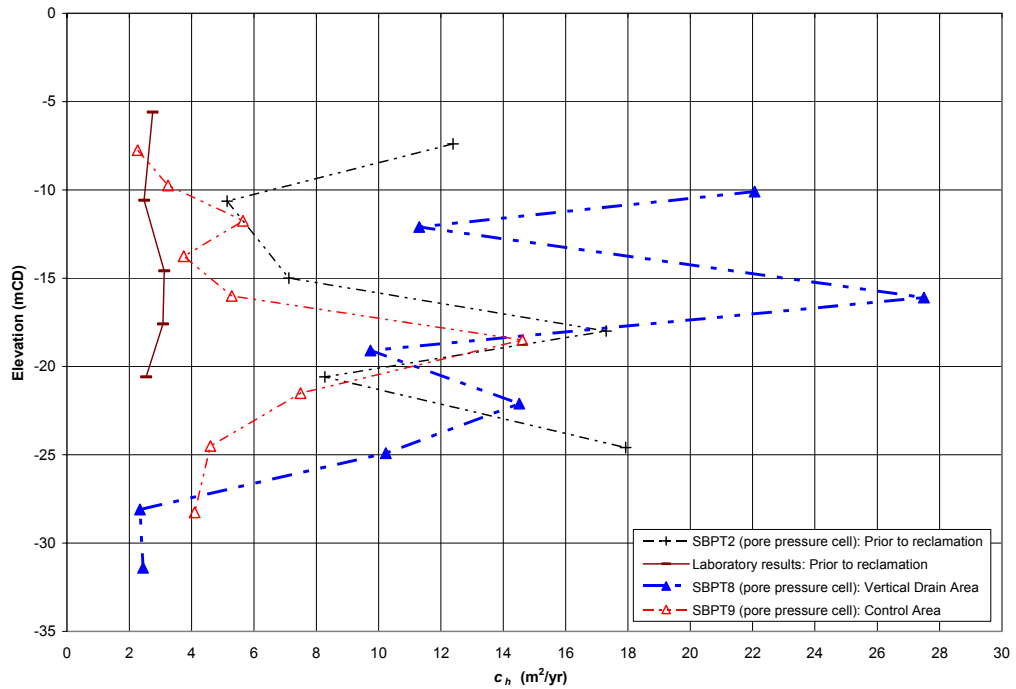


Figure 6.50 Comparison of coefficient of consolidation due to horizontal flow from SBPT dissipation test prior to reclamation and after 23 months of surcharge loading (Arulrajah et al., 2004i).

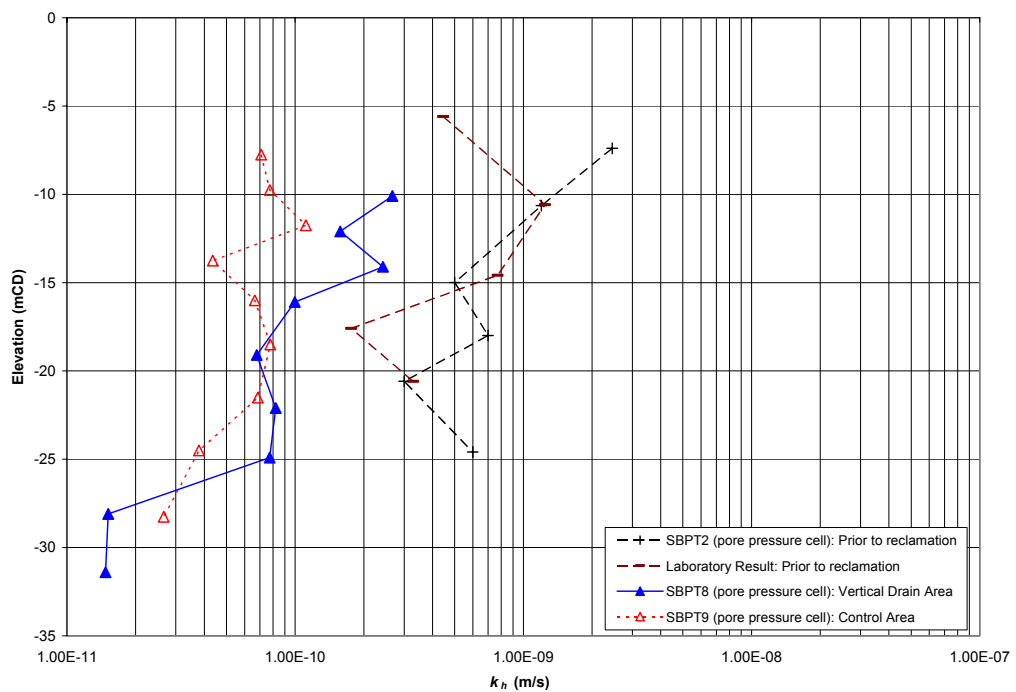


Figure 6.51 Comparison of horizontal hydraulic conductivity from SBPT (PPC) dissipation test prior to reclamation and after 23 months of surcharge loading (Arulrajah et al., 2004i).

6.9 BAT Permeameter Test (BAT)

The BAT permeameter developed by Torstensson (1983) was used in this study for the in-situ testing of horizontal hydraulic conductivity. This involves the functions of sampling of ground water and at the same time the measurement of pore water pressure in the sample container. Diameter of the BAT filter used is 30 mm and the length is 40 mm. Figure 6.52 shows the geometry and dimensions of the BAT permeameter used while Figure 6.53 shows the filter tip.

The key element in the BAT system is the filter tip. The different test adapters make a tight temporary connection to the filter tip with the aid of a hypodermic needle. When the test adapter is lowered down the extension pipe, it is coupled to the nozzle in the filter tip and gravity draws the hypodermic needle downward, penetrating the rubber disc mounted in the filter tip. The needle provides a hydraulic connection between the interior of the filter tip and the test adapter.

The in-situ testing of marine clay with the BAT permeameter described in this thesis has been discussed in detail by the author (Arulrajah et al., 2004d, 2004i) during the course of this research study.

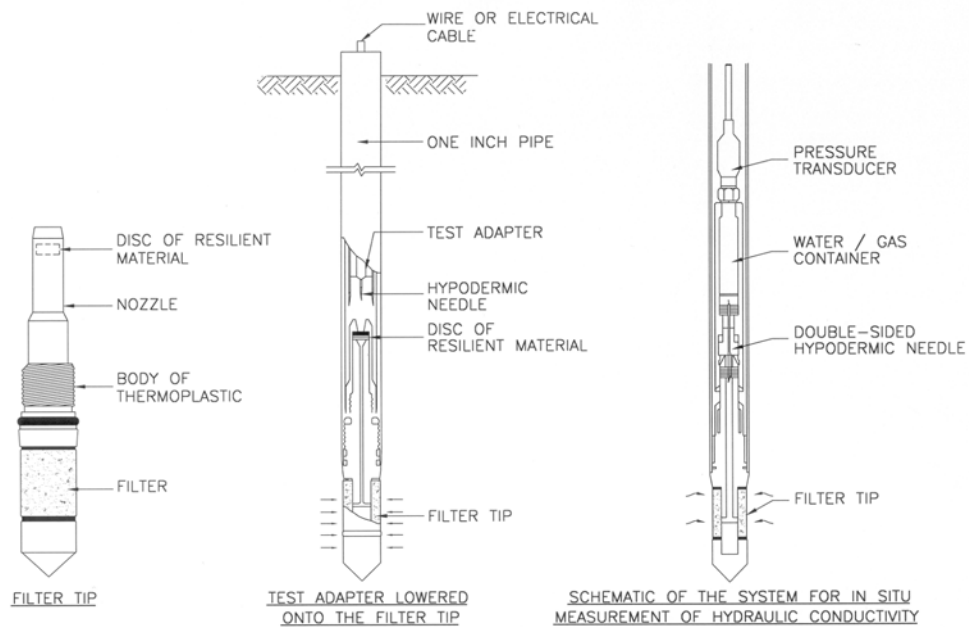


Figure 6.52 Geometry and dimension of BAT permeameter (Torstensson, 1983).



Figure 6.53 BAT permeameter filter tip.

6.9.1 *BAT Permeameter Dissipation Test*

The k_h results from the BAT tests can be used as the baseline results since the system measures horizontal hydraulic conductivity directly, whereas the other in-situ tests required the introduction of additional parameters to evaluate the hydraulic conductivity indirectly from c_h values.

The BAT permeameter test can be carried out either as an "inflow test" or as an "outflow test". In the former case the gas/water container is completely gas-filled at the start of the test. An inflow test can be conducted simultaneously with extraction of pore water sample. In an outflow test, the container is partially filled with compressed gas. The air in the chamber is evacuated (or pressurized) to any desired pressure. As water flows into (or out of) the probe, the air pressure in the chamber changes. A pressure transducer monitors the pressure change.

The test is based on measurement of flow into and out of a sample container. This rate is computed by measuring the pressure change in the container, which using Boyles's law can be translated into a volume change. Analysis of the time-pressure record thus yields the horizontal hydraulic conductivity. The quantity of flow and heads are computed from Boyle's Law and the measured change in the gas pressure in the chamber:

$$k_h = \frac{P_0 V_0}{Ft} \left[\frac{1}{P_0 U_0} - \frac{1}{P_t U_0} - \frac{1}{U_0^2} \ln \left(\frac{P_0 - U_0}{P_0} \times \frac{P_t}{P_t - U_0} \right) \right] \quad \text{Eq. (6.32)}$$

$$F = \frac{2 \pi L}{\ln \left[\frac{L}{d} + \sqrt{1 + \left(\frac{L}{d} \right)^2} \right]} \quad \text{Eq. (6.33)}$$

where:

k_h is the horizontal hydraulic conductivity in units of m/s

P_0 is absolute initial system pressure in kPa

V_0 is initial gas volume in m^3

F is shape factor and is calculated as 228.76 mm for the current test

U_0 is static pore water pressure in kPa

P_t is absolute pressure at time t in s

L is length of filter in m

d is diameter of filter in m

Figure 6.54 shows the typical permeability versus elapsed time plot for the BAT permeameter.

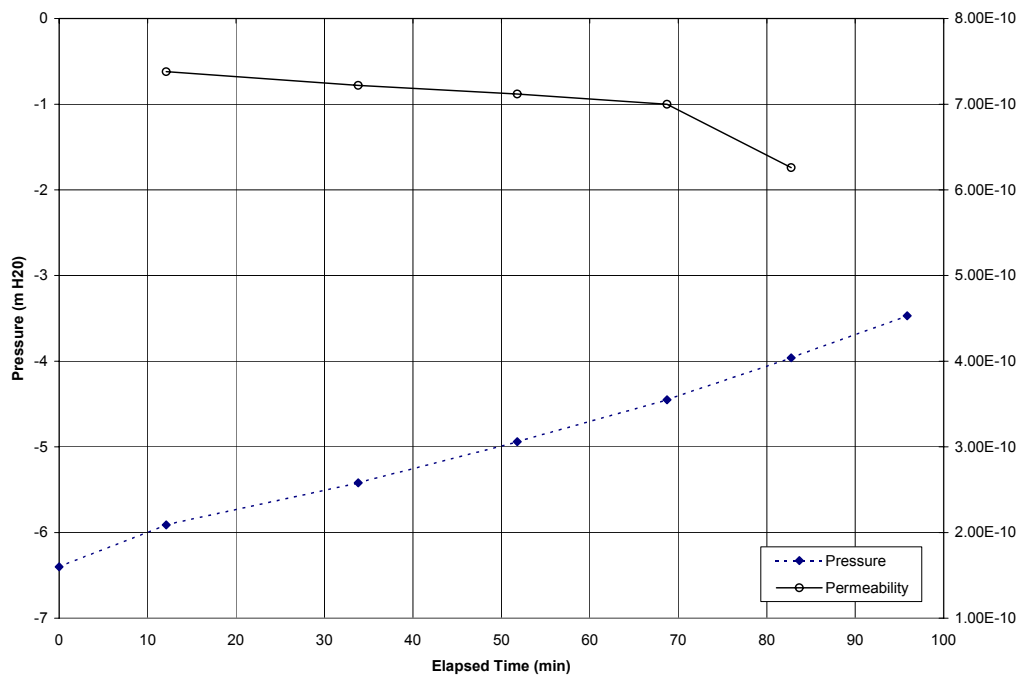


Figure 6.54 Typical BAT permeameter test prior to reclamation (elevation -7.19 mCD).

6.9.2 Comparison of BAT Permeameter Dissipation Tests

The comparison of k_h results from BAT for the Vertical Drain Area and the Control Area is presented in Figure 6.55. It is apparent that the horizontal hydraulic conductivity decreases in the Vertical Drain Area as compared to the prior to reclamation and the Control Area within the marine clay layer. This is as expected due to the smearing effect of the vertical drain treated area and confirms that there is a reduction of horizontal permeability from time to time during consolidation. Variations though are noted in the intermediate clay and alluvium layers.

As the BAT permeameter method of measurement is a direct method, as such the k_h values obtained here can be used as the benchmark values for this study. The coefficient of permeability prior to reclamation is in the order of 10^{-9} to 10^{-10} m/s. The coefficient of permeability is in the order of 10^{-9} to 10^{-10} m/s in the Vertical Drain Area and the Control Area after 23 months of surcharge loading.

Figure 6.56 indicates the variation of horizontal hydraulic conductivity with time. It is apparent that the horizontal hydraulic conductivity decreases in the Vertical Drain Area as compared to the prior to reclamation and the Control Area within the marine clay layer. This is as expected and confirms that there is a reduction of horizontal permeability from time to time during consolidation.

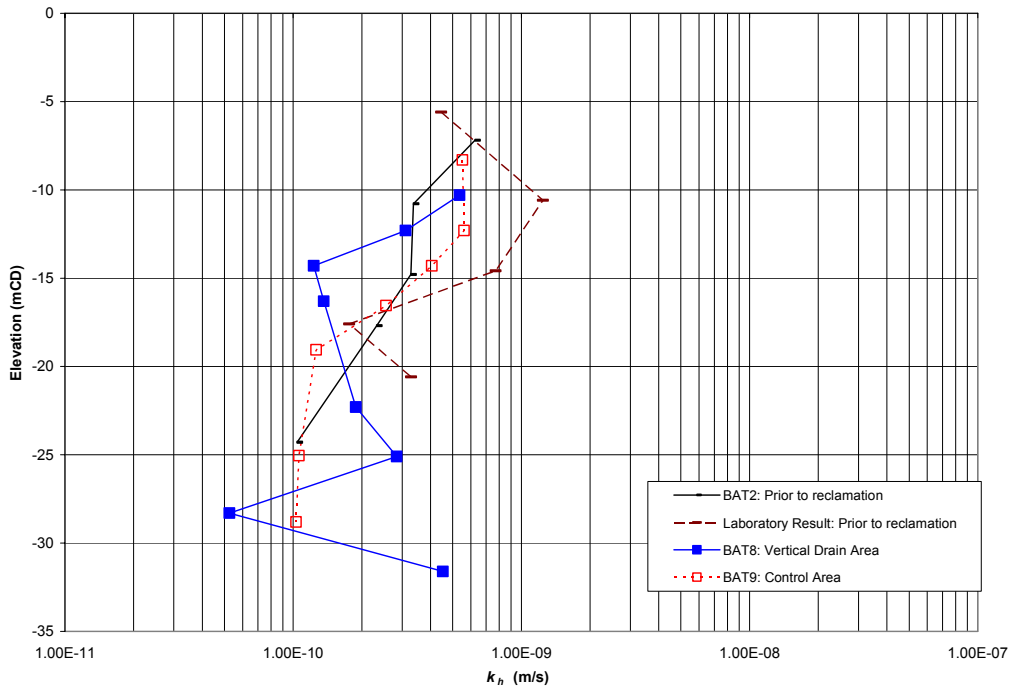


Figure 6.55 Comparison of horizontal hydraulic conductivity from BAT permeameter test prior to reclamation and after 23 months of surcharge loading (Arulrajah et al., 2004i).

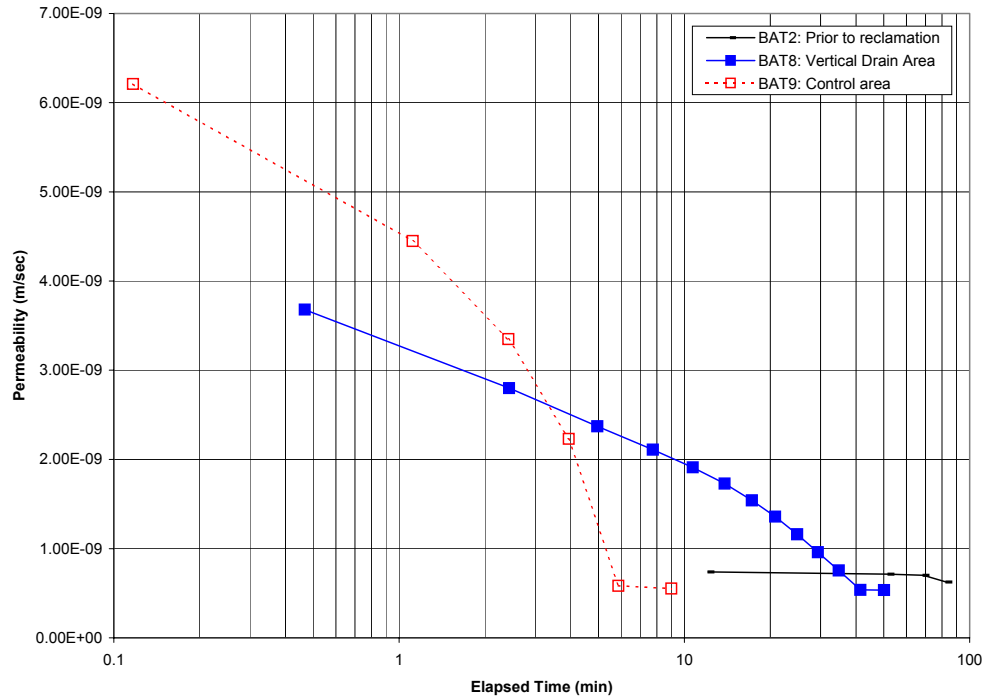


Figure 6.56 Comparison of horizontal hydraulic conductivity from BAT permeameter test versus elapsed time between Vertical Drain Area and Control Area.

6.10 Undrained Shear Strength, Overconsolidation Ratio and Degree of Consolidation of Marine Clay

The in-situ testing of undrained shear strength, overconsolidation ratio and degree of consolidation of marine clay described in this chapter has been discussed in detail by the author (Arulrajah et al., 2004d, 2004f, 2004h, 2004i, 2004o, 2004p) during the course of this research study.

6.10.1 Prior to Reclamation

Figures 6.57 to 6.59 shows comparisons between the shear strengths, OCR and effective stress for the various in-situ tests prior to reclamation.

The pre-reclamation in-situ test results by the various methods are in close agreement with each other. In the shear strength and OCR comparisons, the various tests indicate similar increasing trend profiles for increasing depths.

There is a clear distinction of higher shear strength and OCR values indicated by the various tests in the intermediate marine clay layer.

The values of undrained shear strength of the Singapore marine clay by the various methods are in good agreement with each other. The undrained shear strength obtained from the various test methods was analysed to obtain an empirical correlation of the undrained shear strength (c_u) of the marine clay at the In-Situ Test Site.

With respect to the comparison of shear strength values by the various testing methods, the CPT penetration test indicates slightly lower shear strength values for the lower marine clays. The shear strength values of the SBPT are slightly higher than that of the other test methods while the DMT and FVT results seem to have the closest agreement. The empirical correlation of shear strength increase with depth obtained from the in-situ tests at the In-Situ Test Site is as follows:

$$c_u = 7.06 + 1.7 z \text{ (where } z \text{ is depth below seabed in m)} \quad \text{Eq. (6.34)}$$

where:

c_u is in units of kN/m^2 .

The upper marine clay is overconsolidated with OCR of about 1.5 to 3. The lower marine clay is lightly overconsolidated with OCR of 1 to 2. The intermediate stiff clay is overconsolidated due to desiccation, with OCR of 1.5 to 3. The desiccated layer found close to the seabed is also found to register high OCR values. Higher OCR at seabed normally occurs due to hydrodynamic effect caused by wave and current action. It is apparent that the OCR from CPT is the lowest of the in-situ testing methods. This is possibly due to the value of the constant, K used in Eq. (6.9), for the OCR computations by the CPT.

With respect to the comparison of OCR and effective stress values by the various testing methods, the CPT test result are lower than that of the other test methods. This is especially more obvious for the lower marine clays. The FVT result is found to be the highest for the upper marine clay while the DMT results are found to be the highest for the lower marine clay. The results of the SBPT seem to be relatively close but slightly lower than the DMT.

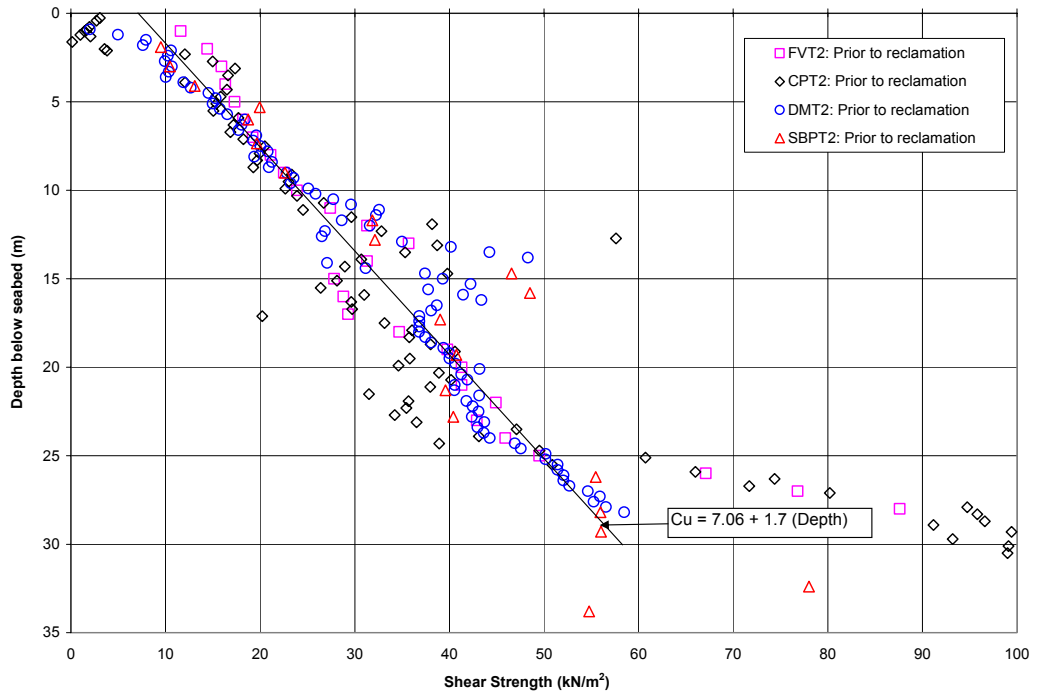


Figure 6.57 Variation of undrained shear strength with depth by various in-situ methods prior to reclamation (Arulrajah et al., 2004d).

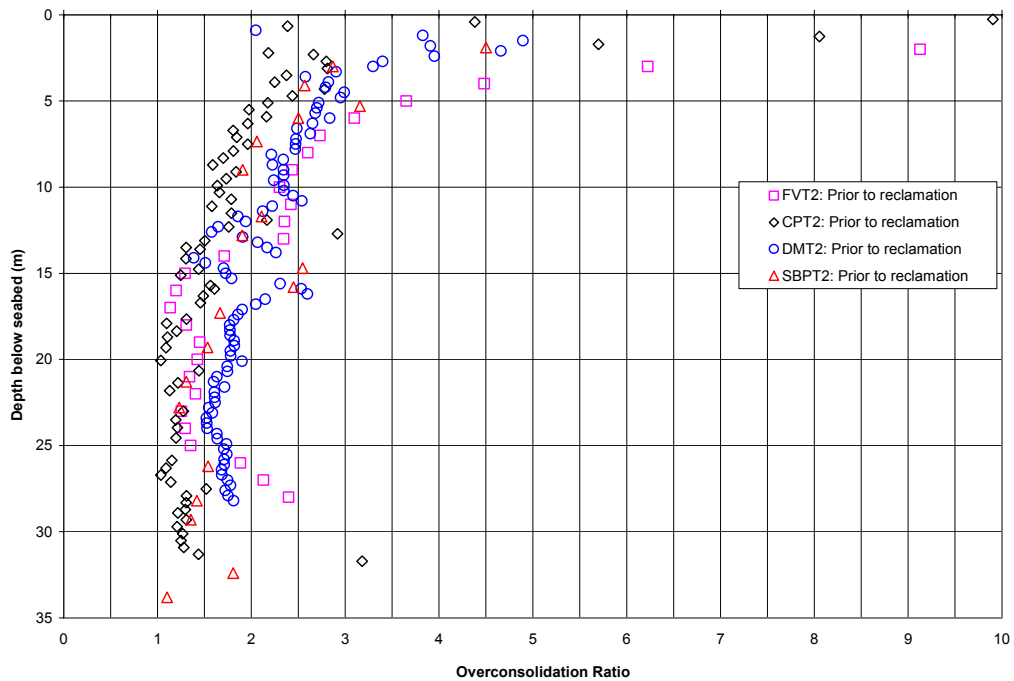


Figure 6.58 Variation of OCR with depth by various in-situ methods prior to reclamation (Arulrajah et al., 2004d).

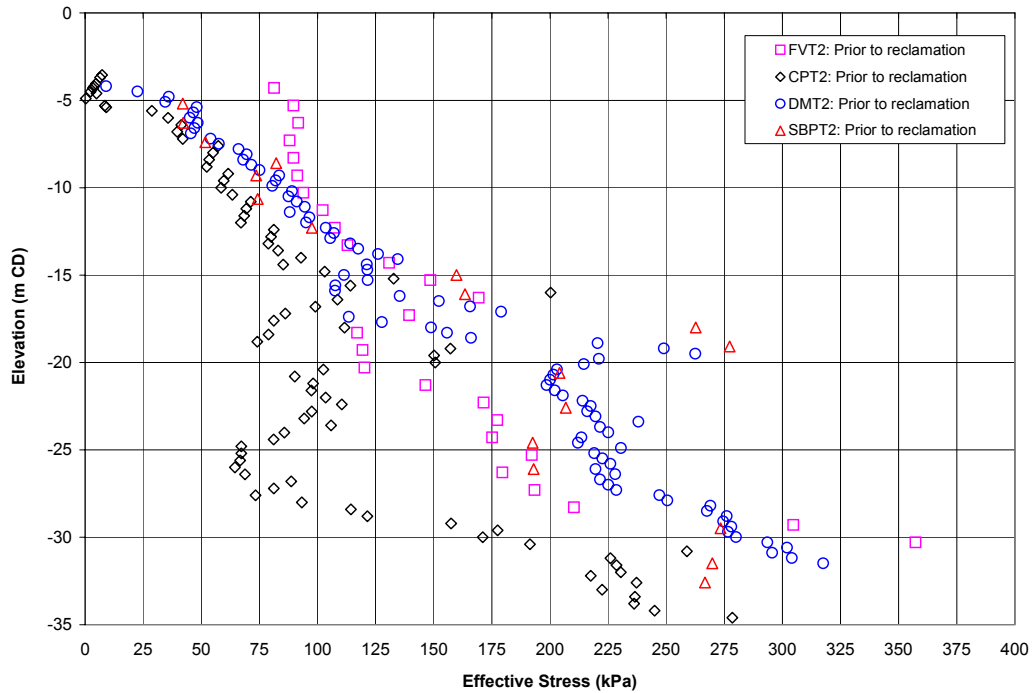


Figure 6.59 Variation of effective stress with elevation by various in-situ methods prior to reclamation.

6.10.2 Post-Improvement

The comparison of in-situ test results of the Vertical Drain Area and the Control Area by various testing methods is compared in Figures 6.60 to 6.63. In the shear strength, OCR, effective stress and degree of consolidation comparisons the post-improvement values obtained from various in-situ tests after a surcharge period of 23 months are found to be agreeable with each other. There is a clear distinction of higher values indicated by the various tests in the intermediate marine clay layer.

With respect to the shear strength results in the Vertical Drain Area the CPT and SBPT results are especially in close agreement while the DMT and FVT results are found to be lower than that of the other in-situ tests. In the Control Area the DMT shear strength results is found to be the highest while the CPT results are found to be lower than that of the other in-situ tests. In the Vertical Drain Area, the SBPT results indicate the highest OCR, effective stress and degree of consolidation values while the CPT results indicate the lowest. In the Control Area, the DMT results indicate the highest values while the FVT and SBPT tests indicate the lowest values. In the degree of consolidation comparison, the in-situ tests in the Vertical Drain Area indicate much higher degree of consolidation as compared to the Control Area.

The post improvement in-situ test results after 23 months of surcharge loading by the various test methods are in close agreement with each other. The improved areas indicate clear increases in the soil strength and consolidation properties due to the improvement works. The results also indicate the expected higher shear strengths, OCR, effective stress and degree of consolidation in the Vertical Drain Area as compared to the Control Area.

The post improvement in-situ test results in Figure 6.63 indicate that after 23 months of surcharge loading, the degree of consolidation of the Vertical Drain Area had attained a degree of consolidation generally in the range of about 70-80% while the Control Area had attained a degree of consolidation of about 30-40%.

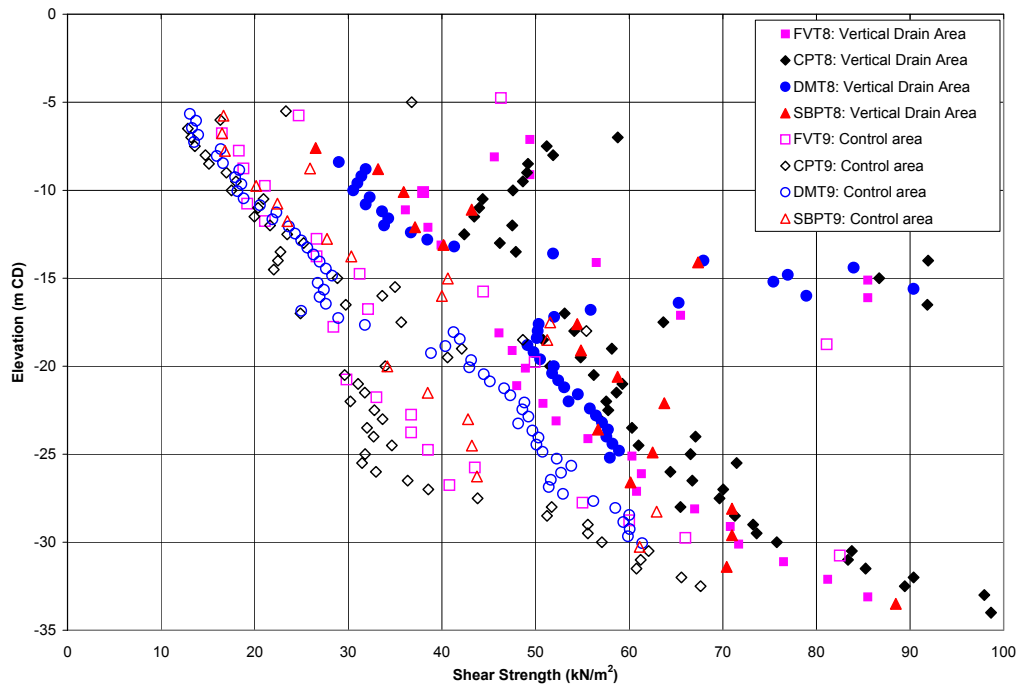


Figure 6.60 Comparison of shear strengths from in-situ testing between Vertical Drain Area and Control Area after 23 months of surcharge loading (Arulrajah et al., 2004h).

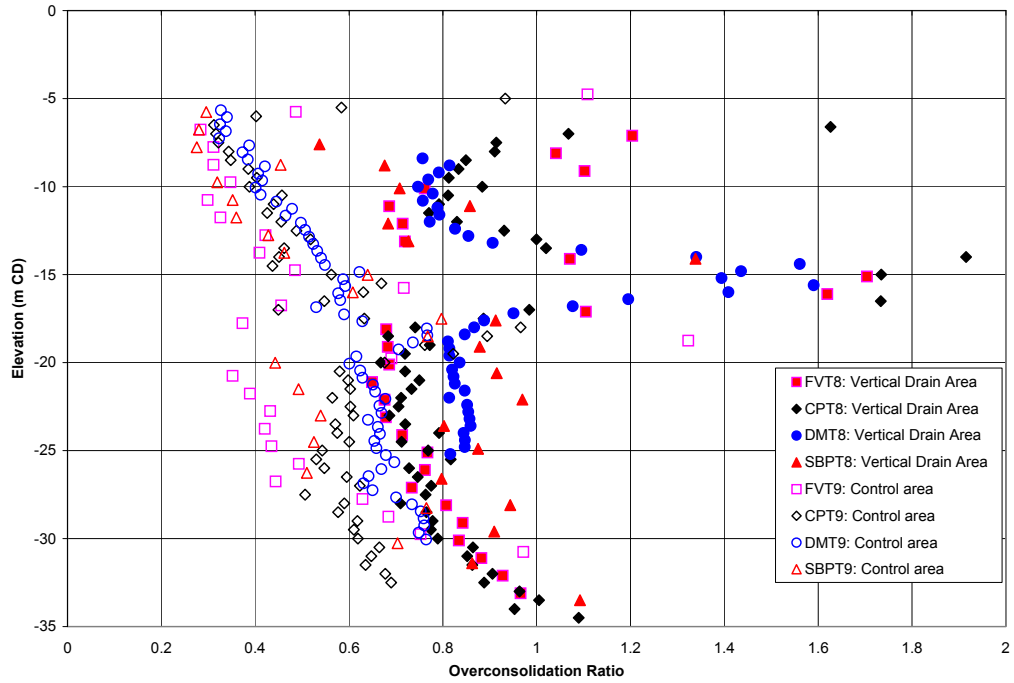


Figure 6.61 Comparison of overconsolidation ratio from in-situ testing between Vertical Drain Area and Control Area after 23 months of surcharge loading (Arulrajah et al., 2004h).

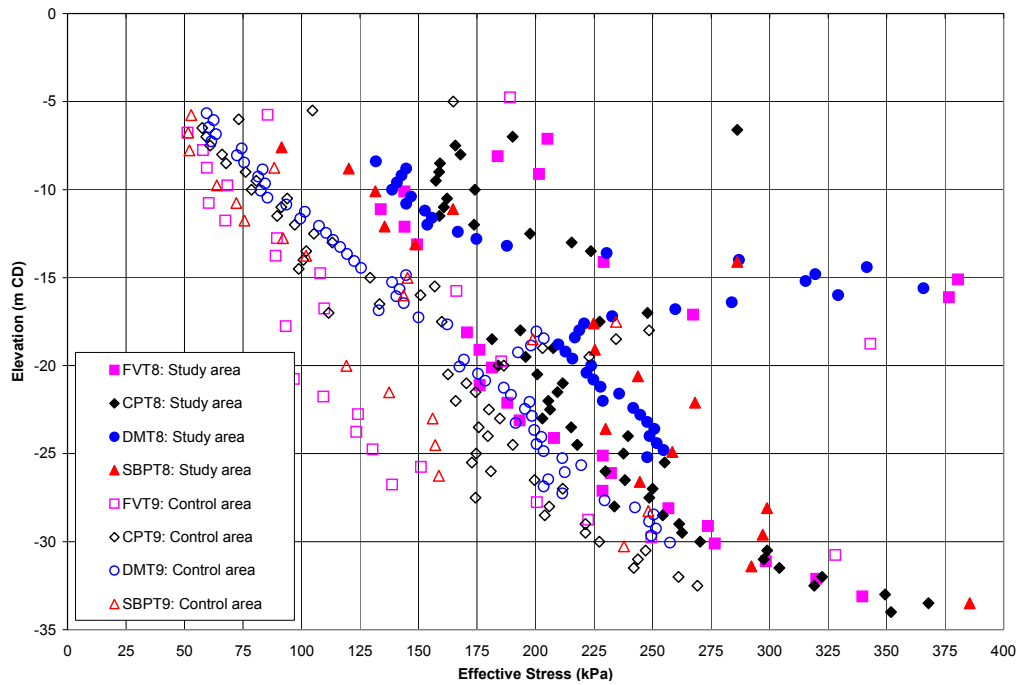


Figure 6.62 Comparison of effective stress from in-situ testing between Vertical Drain Area and Control Area after 23 months of surcharge loading (Arulrajah et al., 2004h).

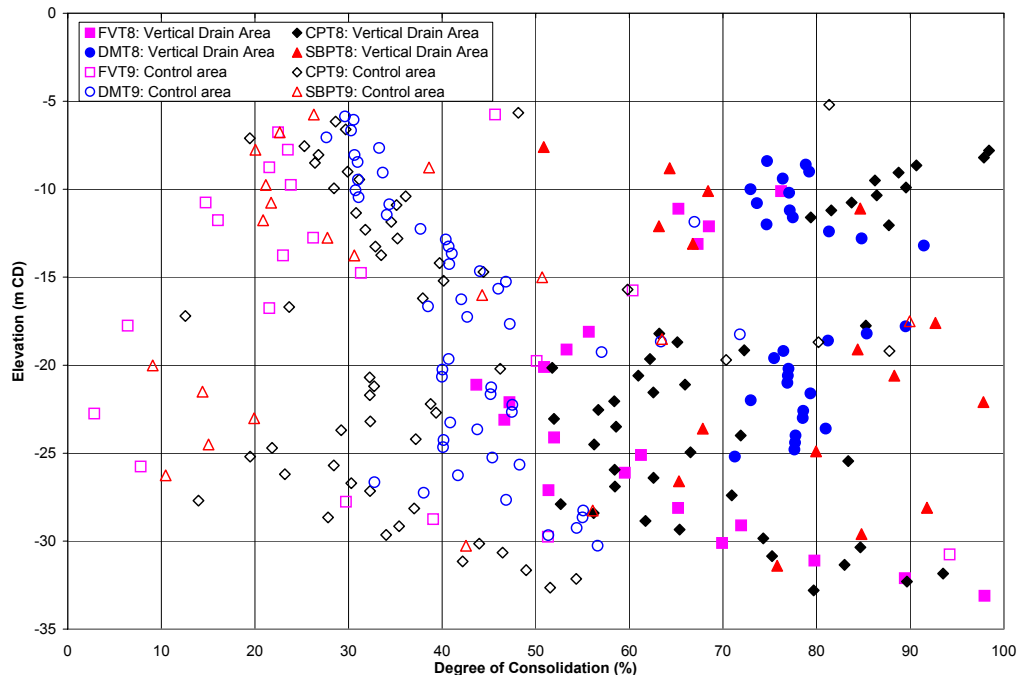


Figure 6.63 Comparison of degree of consolidation from in-situ testing between Vertical Drain Area and Control Area after 23 months of surcharge loading (Arulrajah et al., 2004h).

6.11 Coefficient of Consolidation due to Horizontal Flow of Marine Clay

In-situ dissipation tests by means of piezocone, dilatometer and self-boring pressuremeter have been used prior to reclamation and after a surcharge period of 23 months in the characterisation of the coefficient of consolidation due to horizontal flow of Singapore marine clay in this research study.

The in-situ dissipation testing of marine clay for determination of coefficient of consolidation due to horizontal flow described in this chapter has been discussed in detail by the author (Arulrajah et al., 2004d, 2004f, 2004i, 2004o) during the course of this research study. The findings are discussed in this section.

6.11.1 Prior to Reclamation

The pre-reclamation coefficient of consolidation due to horizontal flow (c_h) as obtained from various in-situ dissipation tests vary between 2 to 26 m^2/yr as shown in Figure 6.64. The CPTU results is found to be the closest to the laboratory testing results.

The c_h values for the laboratory tests were obtained from radial flow Rowe cell of 75 mm diameter and 30 mm thickness and also from horizontally cut 63.5 mm oedometer test samples. It is observed that all the methods indicate large c_h values in the intermediate stiff clay layer. The CPTU results is found to be the closest to the laboratory testing results.

The pre-reclamation CPTU dissipation test indicate that the c_h values of the upper and lower marine clay varies between 2 to 6 m^2/yr . c_h values of 4 to 7 m^2/yr were obtained in the intermediate stiff clay, separating the upper and lower marine clay layers. The pre-reclamation dissipation tests indicate large c_h values in the intermediate stiff clay layer.

Among the in-situ tests the c_h values in the marine clay layers from SBPT are the highest overall while that from the CPTU dissipation test indicate the least variations with depth. The DMT results are reasonable in the lower marine clay layer. The c_h determined by the DMT and SBPT is noted to be an order of magnitude greater than the laboratory data. It is observed that all the methods indicate large c_h values in the intermediate stiff clay layer. The actual depths of the intermediate clay layer may slightly vary from location to location due to slight variations in stratigraphy due to the formation history of the layer.

The smear effect also affects the CPTU and DMT measurements for c_h . In the CPTU and DMT dissipation test, a penetrometer has to be pushed into the clay and a smear effect similar to the insertion of a mandrel could have been introduced prior to the measurements. This as such could lead to the CPTU and DMT measurements being lower than that of the SBPT.

The c_h determined by the various in-situ testing methods are relatively higher overall as compared to the laboratory testing results. Horizontal laminations and micro lenses present in the marine clay profile, will lead to higher c_h values and subsequently higher k_h for the in-situ tests. The presence of laminations and lenses are difficult to be detected by the laboratory tests due to the sampling intervals and the sampling process. Furthermore, laboratory results are subject to various complexities such as borehole quality, sample quality, testing methods and method of interpretation which could lead to lower test values.

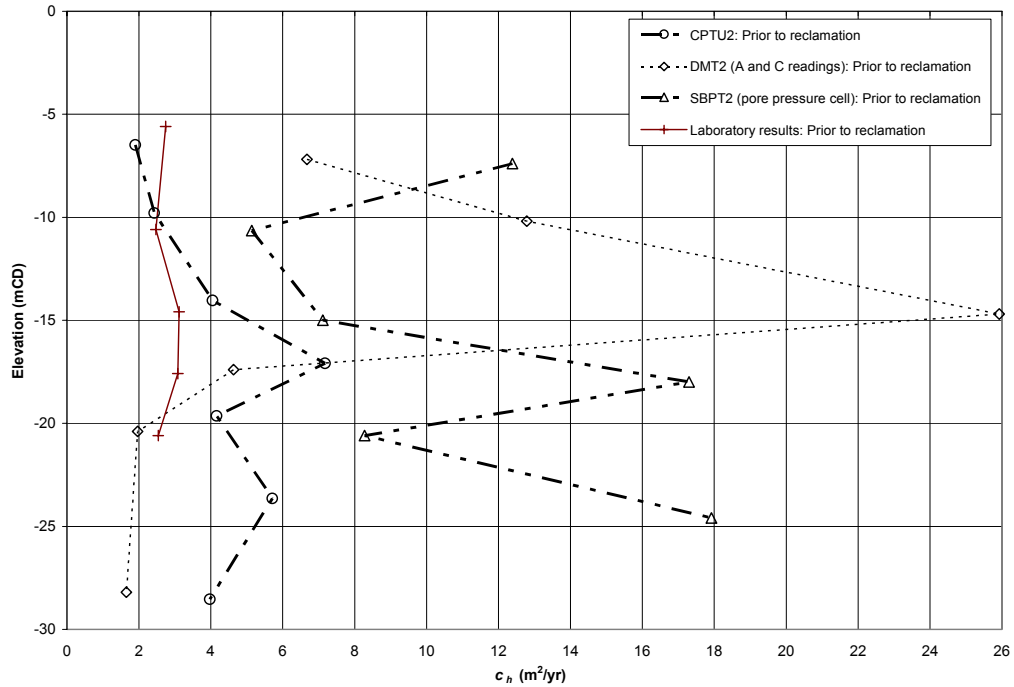


Figure 6.64 Prior to reclamation coefficient of consolidation due to horizontal flow from various in-situ dissipation tests (Arulrajah et al., 2004d).

6.11.2 Post-Improvement

The comparison between coefficient of horizontal consolidation between the Vertical Drain Area and Control Area from in-situ dissipation tests after 23 months of surcharge loading, is presented in Figure 6.65 and Figure 6.66. Figure 6.67 presents the coefficient of horizontal consolidation for the Vertical Drain Area. Figure 6.68 presents the coefficient of horizontal consolidation for the Control Area.

Increase in the c_h values is obtained in the intermediate marine clay layer in both the Vertical Drain and Control Area, due to the comparatively higher permeability of the intermediate stiff clay layer.

The c_h value are higher in the Vertical Drain Area at some elevations as compared to the Control Area. This is due to the greater reduction in the coefficient of volume change, m_v , after consolidation or it was simply affected by the correction factors used.

The CPTU results indicate that c_h varies between 3 and 6 m^2/yr in the Vertical Drain Area and between 3 and 5 m^2/yr in the Control Area, after 23 months of surcharge loading.

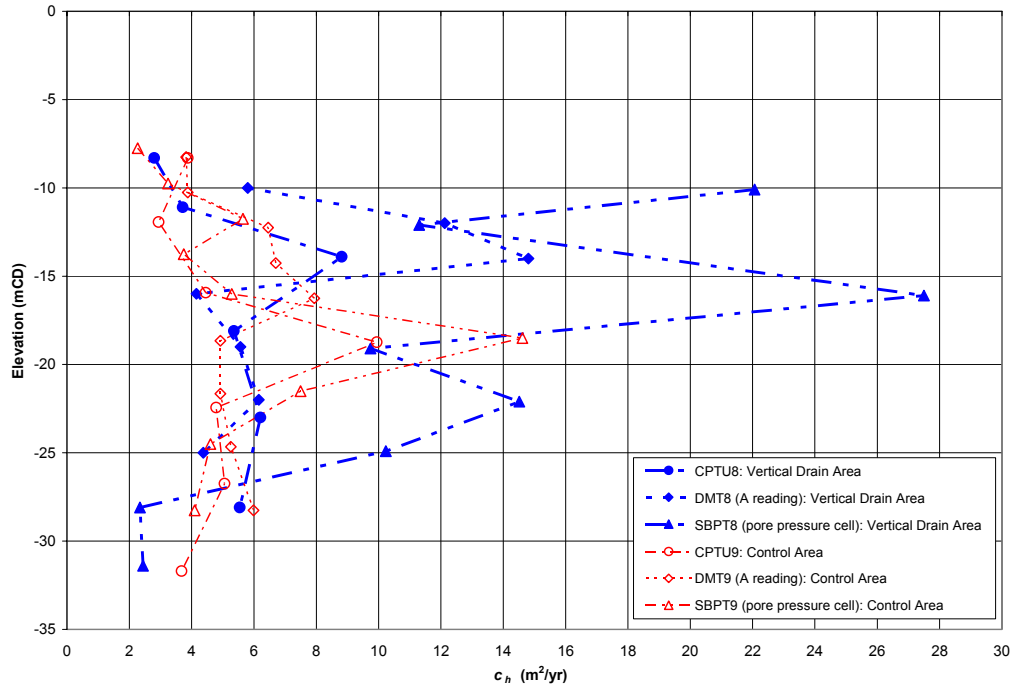


Figure 6.65 Comparison between coefficient of consolidation due to horizontal flow from in-situ dissipation tests between Vertical Drain Area and Control Area after 23 months of surcharge loading (Arulrajah et al., 2004i).

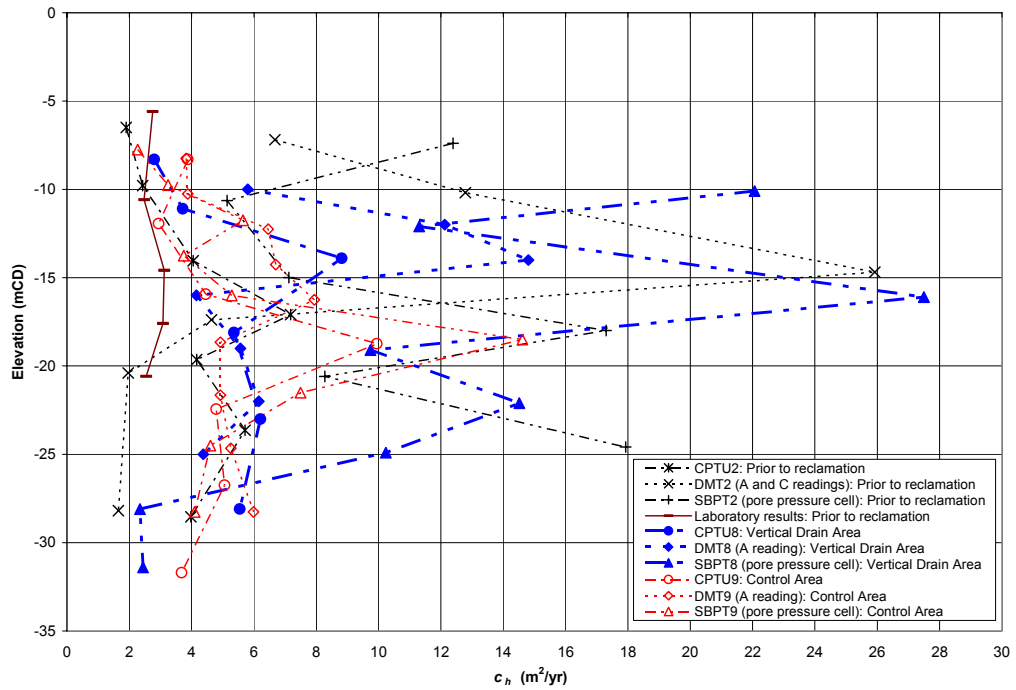


Figure 6.66 Comparison between coefficient of consolidation due to horizontal flow from in-situ dissipation tests between Vertical Drain Area and Control Area after 23 months of surcharge loading with prior to reclamation results.

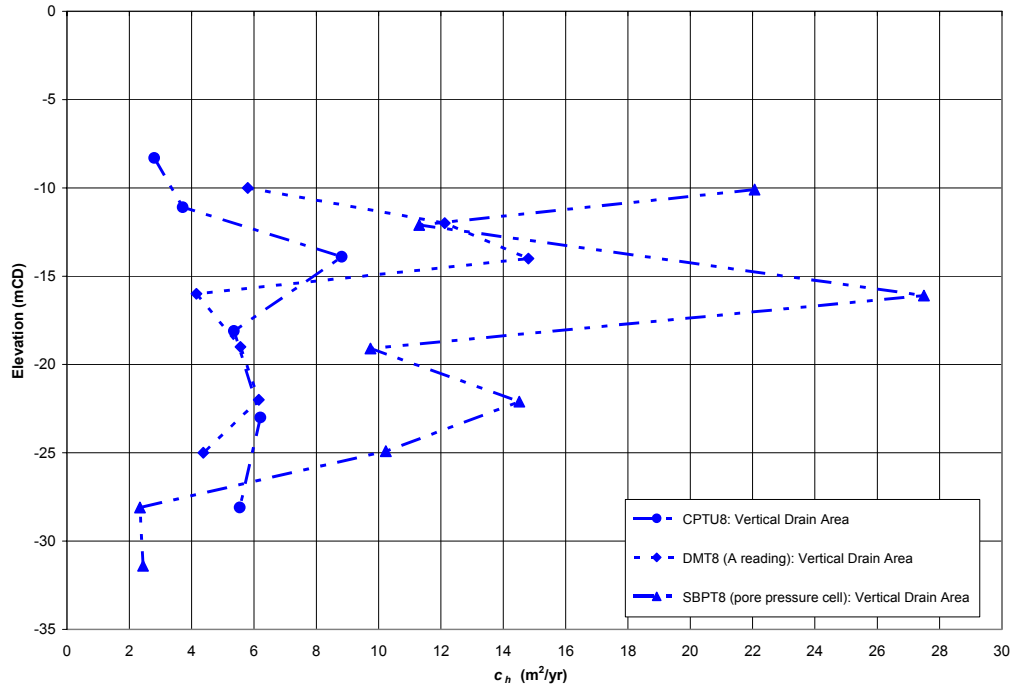


Figure 6.67 Comparison between coefficient of consolidation due to horizontal flow from in-situ dissipation tests for Vertical Drain Area after 23 months of surcharge loading.

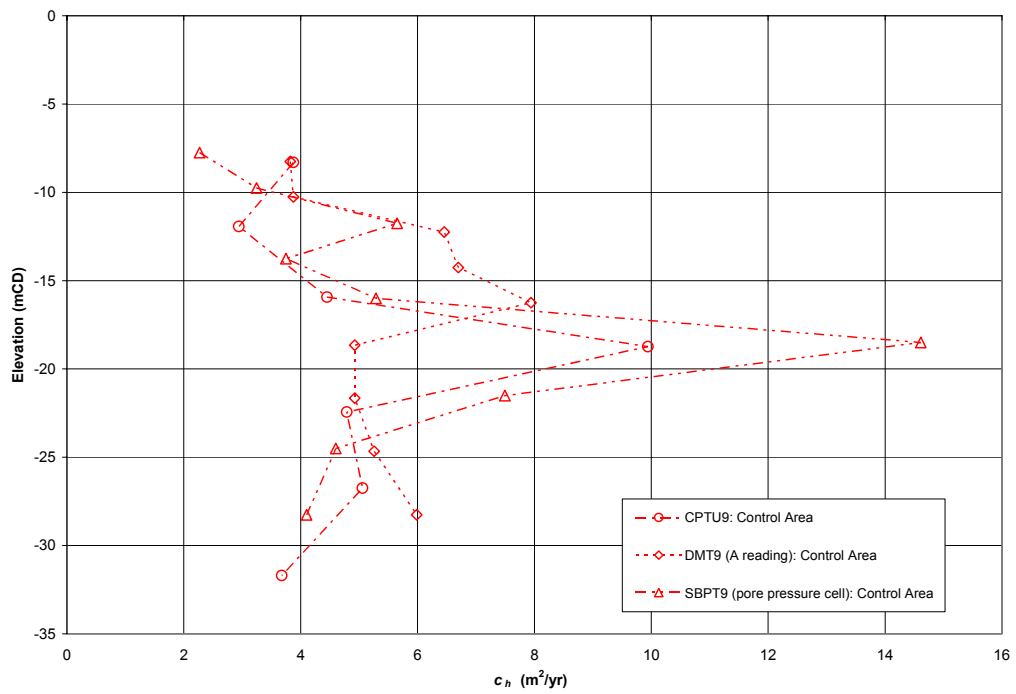


Figure 6.68 Comparison between coefficient of consolidation due to horizontal flow from in-situ dissipation tests for Control Area after 23 months of surcharge loading.

6.11.3 Discussion and Conclusions

The c_h determined by the various in-situ testing methods are relatively higher overall, with some exceptions, as compared to the laboratory testing results, as evident in the prior to reclamation test results. Horizontal laminations and micro lenses present in the marine clay profile, will lead to higher c_h values and subsequently higher k_h for the in-situ tests. The presence of laminations and lenses are difficult to be detected by the laboratory tests due to the sampling intervals and the sampling process. Furthermore, laboratory results are subject to various complexities such as borehole quality, sample quality, testing methods and method of interpretation which could lead to lower or variable test values.

It is apparent that c_h results vary between the various in-situ testing methods due to the differing assumption in cavity radius amongst other things in the various test methods. The varying c_h values will subsequently lead to differing k_h in the CPTU, DMT and SBPT results as k_h computations is worked out indirectly from c_h values.

The c_h value derived from the CPTU dissipation test is generally lower than those obtained from the other in-situ dissipation tests. The c_h value obtained from the DMT dissipation tests is usually smaller than that from the SBPT holding test. The c_h value obtained from the SBPT exhibits a larger variation in comparison with that of other tests. In general, the c_h value measured by the SBPT is much larger than those obtained from the other in-situ dissipation tests. The SBPT does not appear to be desirable for the measurement of c_h for soft marine clay at Changi, as the c_h values obtained from SBPT are normally too high to be directly used for the design. The c_h determined by the DMT and SBPT prior to reclamation is noted to be an order of magnitude greater than the laboratory data.

The smear effect affects the CPTU and DMT measurements for c_h . In the CPTU and DMT dissipation test, a penetrometer has to be pushed into the clay and a smear effect similar to the insertion of a mandrel could have been introduced prior to the measurements. This as such could lead to the CPTU and DMT measurements for c_h being lower than that of the SBPT. The c_h value seems to be higher in the Vertical Drain Area at some elevations as compared to the Control Area. This is attributed to the greater reduction in the coefficient of volume change, m_v , after consolidation or it could have been affected by the correction factors used.

In-situ dissipation tests using the CPTU is recommended by the author as the most suitable method for the determination of the c_h in soil improvement schemes involving vertical drains. However the c_h value directly measured by the CPTU holding test is normally too

high to be used directly in the design involving the use of vertical drains. A conversion would have to be made to convert the direct c_h value into the value in the normally consolidated state.

The pre-reclamation CPTU dissipation test indicate the c_h values in the marine clay varies between 2 to 6 m²/yr for the upper and lower marine clay layers. The CPTU results indicate that c_h varies between 3 and 6 m²/yr in the Vertical Drain Area and between 3 and 5 m²/yr in the Control Area, after 23 months of surcharge loading.

6.12 Horizontal Hydraulic Conductivity of Marine Clay

In-situ dissipation tests by means of piezocone, dilatometer, self-boring pressuremeter and BAT permeameter have been used after a surcharge period of 23 months in the characterisation of the horizontal hydraulic conductivity of Singapore marine clay in this research study. The in-situ dissipation testing of marine clay for determination of horizontal hydraulic conductivity described in this chapter has been discussed in detail by the author (Arulrajah et al., 2004d, 2004f, 2004i, 2004o) during the course of this research study.

6.12.1 Prior to Reclamation

The horizontal hydraulic conductivity, k_h as obtained from the various in-situ dissipation tests prior to reclamation are shown in Figure 6.69. Based on the results obtained, the BAT was found to give the lowest values whereas the dilatometer and CPTU gave the highest values. The same observation has been reported by Bo et al. (1998b) and Chu et al. (2002) in the reclamation site for tests carried out prior to land reclamation. The laboratory results are also close to that of the BAT results. Horizontal hydraulic conductivity of in-situ tests was found to range between 10^{-7} to 10^{-10} m/s for the marine clay.

The k_h results from the BAT tests can be used as the baseline results since the system measures horizontal hydraulic conductivity directly whereas the other in-situ tests required the introduction of additional parameters to evaluate the hydraulic conductivity indirectly from c_h values. The horizontal hydraulic conductivity prior to reclamation is in the order of 10^{-9} to 10^{-10} m/s based on the BAT results. Dilatometer and CPTU values range around 10^{-7} to 10^{-9} m/s while the SBPT are in the 10^{-8} to 10^{-9} m/s range. It can be observed that k_h values decrease with depth. The in-situ test results also show high k_h values in the intermediate dessicated zone.

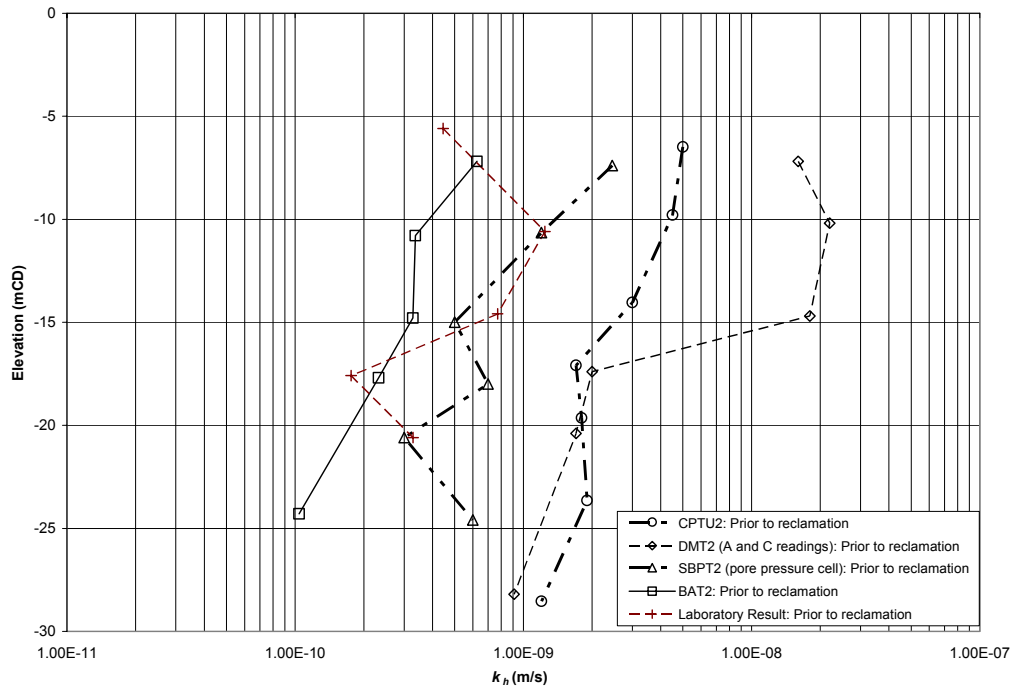


Figure 6.69 Prior to reclamation horizontal hydraulic conductivity from various in-situ dissipation tests (Arulrajah et al., 2004d).

6.12.2 Post-Improvement

The comparison between horizontal hydraulic conductivity between the Vertical Drain Area and Control Area from in-situ dissipation tests after 23 months of surcharge loading, is presented in Figure 6.70 and Figure 6.71. Figure 6.72 presents the horizontal hydraulic conductivity for the Vertical Drain Area. Figure 6.73 presents the horizontal hydraulic conductivity for the Control Area. Increase in the k_h values is obtained in the intermediate marine clay layer in both areas due to the higher permeability of the intermediate stiff clay layer.

The horizontal hydraulic conductivity is in the order of 10^{-9} to 10^{-10} m/s in the Vertical Drain Area and Control Area after 23 months of surcharge loading, based on the BAT results. The horizontal hydraulic conductivity decreases in the Vertical Drain Area as compared to the Control Area within the marine clay layer as evident in the BAT readings. This supports the theory that there is a reduction of vertical permeability from time to time during consolidation. The other in-situ testing methods however do not all accurately reflect this and it could be due to their indirect measurement of k_h readings from c_h values. As the Control Area has undergone only a small degree of consolidation, as such there is not much variation in the permeability of this area as compared to the prior to reclamation results.

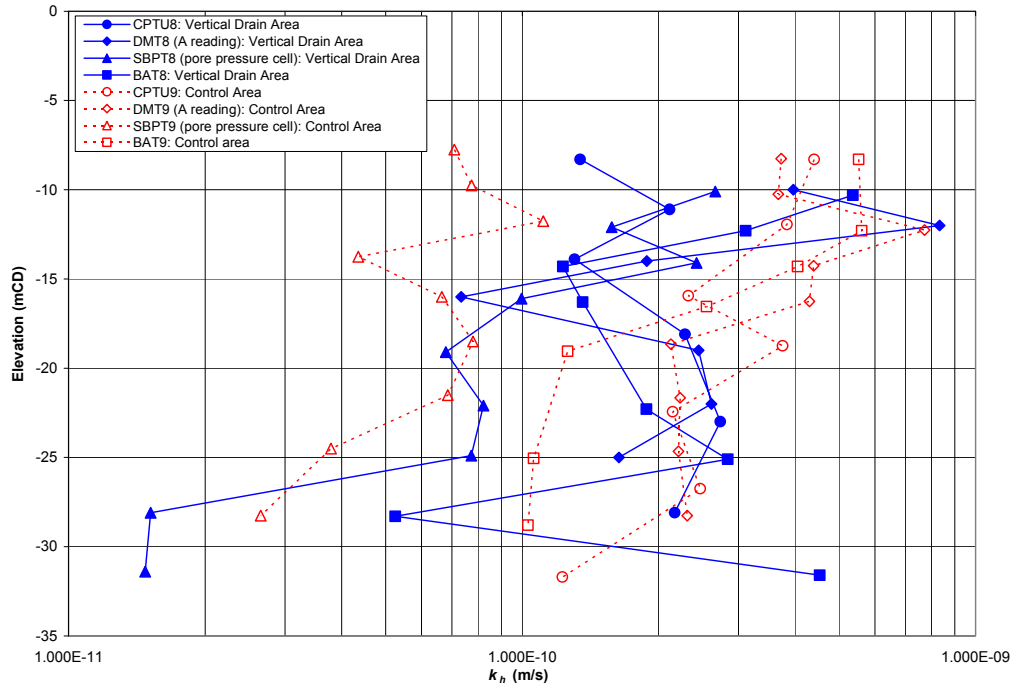


Figure 6.70 Comparison between horizontal hydraulic conductivity from in-situ dissipation tests between Vertical Drain Area and Control Area after 23 months of surcharge loading (Arulrajah et al., 2004i).

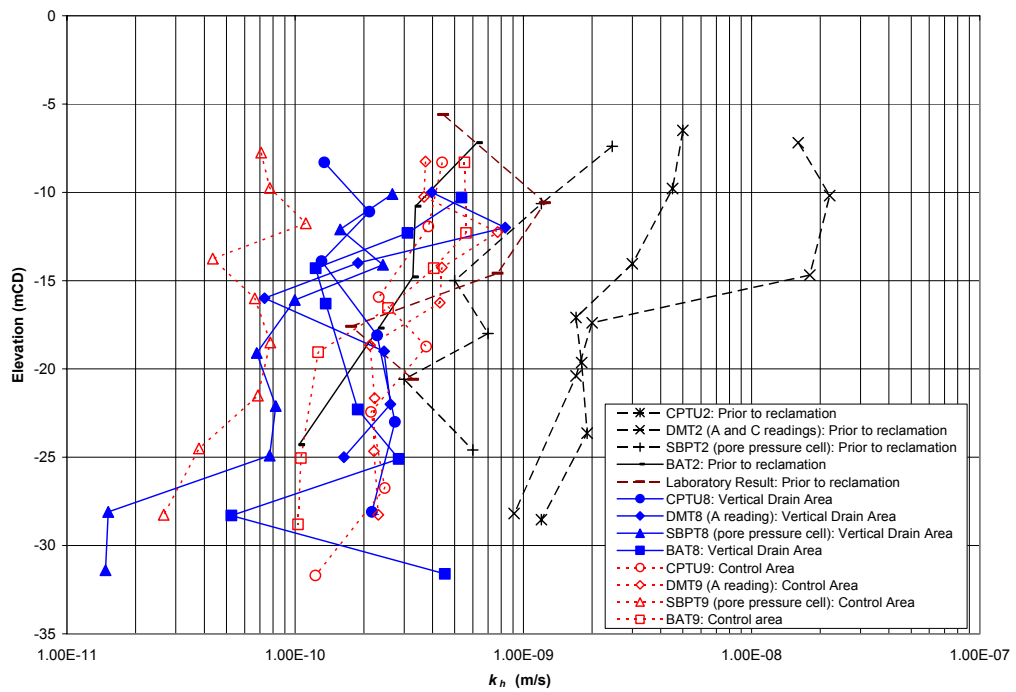


Figure 6.71 Comparison between horizontal hydraulic conductivity from in-situ dissipation tests between Vertical Drain Area and Control Area after 23 months of surcharge loading with prior to reclamation results.

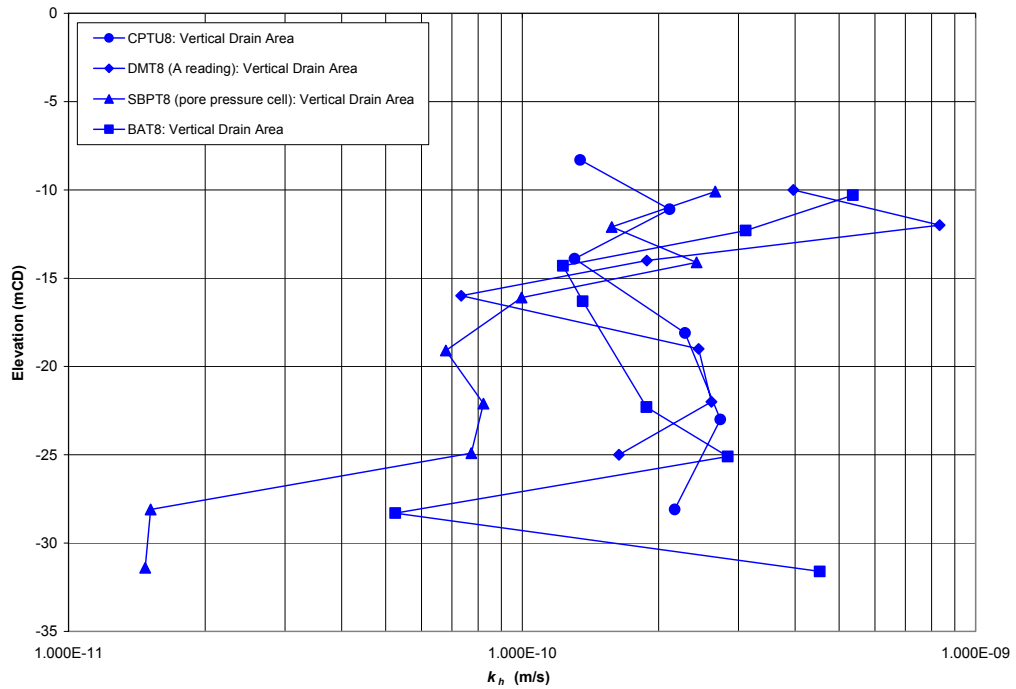


Figure 6.72 Comparison between horizontal hydraulic conductivity from in-situ dissipation tests for Vertical Drain Area after 23 months of surcharge loading.

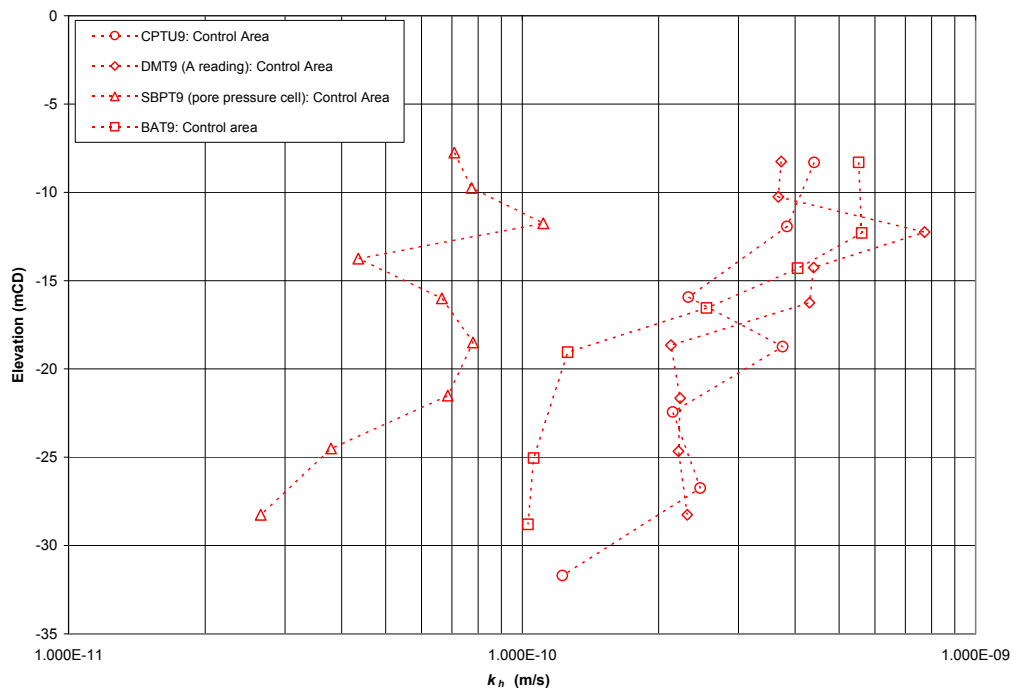


Figure 6.73 Comparison between horizontal hydraulic conductivity from in-situ dissipation tests for Control Area after 23 months of surcharge loading.

6.12.3 Discussion and Conclusions

In-situ dissipation tests using the BAT is recommended as the most suitable method for the determination of the k_h of marine clay, since the system measures horizontal hydraulic conductivity directly whereas the other in-situ tests required the introduction of additional parameters to evaluate the k_h indirectly from c_h values. The BAT results compared well with the CPTU and DMT results in the Control Area after 23 months of surcharge loading. The SBPT results was noted to be the most different from the BAT.

The horizontal hydraulic conductivity prior to reclamation is in the order of 10^{-9} to 10^{-10} m/s based on the BAT results. The horizontal hydraulic conductivity is in the order of 10^{-9} to 10^{-10} m/s in the Vertical Drain Area and Control Area after 23 months of surcharge loading.

The smear effect also affects the BAT, CPTU and DMT measurements for k_h . In the BAT, CPTU and DMT dissipation test, a penetrometer has to be pushed into the clay and a smear effect similar to the insertion of a mandrel could have been introduced prior to the measurements. This finding also indicates that when vertical drains are used in soft clay, the smear effect on the consolidation properties of soil has to be taken into consideration in the design (Chu et al. 2002). Smear effect also affects the k_h in the vertical drain treated area due to insertion of the vertical drain mandrel into the ground.

The smear effect for BAT permeameter could be greater than that for the CPTU, as the BAT permeameter had a filter with a larger surface area. This may explain why k_h measured by the BAT permeameter is normally lower than that by the CPTU, although the working mechanisms of the two tests are very similar. The SBPT should not be affected by the smear effect due to its self-boring mechanism.

It is apparent that the prior to reclamation k_h is higher than that of the Vertical Drain Area and Control Area after 23 months of surcharge loading. This is expected due to reduction in the void ratio after surcharge loading. It is also apparent that the k_h in the Vertical Drain Area is lower than that in the Control Area which is expected due to higher void ratio changes and smear effect and also supports the general belief that there is a reduction of vertical permeability from time to time during consolidation in the vertical drain treated area. Bo et al. (1998b) has reported that the permeability of soil in the smear zone could be reduced by 1 order of magnitude or to the k_h of the remoulded clay as a result of the smear zone. The smear zone was reported by Bo et al. (1998b) to be 4-5 times the equivalent diameter of the vertical drain. When drains are installed at close spacing, the back-calculated c_h values will generally be greatly influenced by this smear zone (Chu et al. 2002).

7.0 FIELD INSTRUMENTATION MONITORING OF LAND RECLAMATION PROJECTS ON MARINE CLAY FORMATIONS

7.1 Overview of Field Instrumentation Works

Land reclamation on soft compressible clays for vital facilities requires some form of soil improvement work. The prefabricated vertical drain with preloading method is a popular and well documented method of soil improvement of compressible soils. This method of ground improvement was used in the ongoing Changi East Reclamation Project in the Republic of Singapore. Prior to the removal of the surcharge load, the degree of improvement attained by the foundation soil must be ascertained to confirm whether the design criteria has been achieved. Field instrumentation monitoring is the only means available of providing continuous records of the ground behaviour from the point of instruments installation. Without a proper soil instrumentation method or program, it would be impossible to monitor the current degree of improvement of the soil at any point of time. By analyzing the field instrument monitoring results, it is possible to verify the degree of consolidation of the foundation soil before assessing whether the surcharge load can be removed in the field.

Prior to the installation of vertical drains in the Changi East Reclamation Project, an instrumentation programme was implemented which included the installation of settlement plates, deep settlement gauges, earth pressure cells, piezometers and water stand-pipes. During the process of consolidation, the settlement gauges monitoring data was analyzed by means of the Asaoka and Hyperbolic methods to determine the ultimate settlement and degree of consolidation of the underlying soft marine clay due to the fill and surcharge load. Piezometer monitoring data was used to determine the dissipation of excess pore water pressures and degree of consolidation of the marine clay.

In the reclamation project, various field instruments were installed in instrumentation clusters to enable the instruments functions to complement each other. All instruments found in the instrument clusters were extended and protected throughout the surcharge placement operations. The use of field instrumentation is essential for assessing the degree of consolidation of the marine clay under the reclaimed fill as this assessment is paramount to ascertain when the surcharge can be removed. Field instrumentation monitoring will provide a continuous record of the marine clay behaviour under the fill and surcharge load right from the point of the initial instrument installation. In land reclamation projects, instruments are installed either off-shore prior to reclamation or on-land after reclamation to the vertical

drain installation platform level. Field instruments suitable for the study of marine clay behaviour and monitoring of land reclamation works include the following:

- surface settlement plates
- deep settlement gauges
- multi-level settlement gauges
- liquid settlement gauges
- pneumatic piezometers
- electric piezometers
- open-type piezometers
- water standpipes
- inclinometers
- deep reference points
- earth pressure cells

The field instrumentation monitoring and assessment of marine clay in offshore land reclamation works described in this chapter has been discussed in detail by the author (Arulrajah et al., 2004b, 2004c) during the course of this research study. The assessment of field settlement plates by the Asaoka and Hyperbolic methods described in this thesis have been discussed in detail by the author (Arulrajah et al., 2003a, 2003b, 2004b, 2004c, 2004e, 2004g, 2004n) during the course of this research study. The assessment of piezometers described in this thesis have been discussed in detail by the author (Arulrajah et al., 2003b, 2004a, 2004b, 2004c, 2004e, 2004g, 2004i) during the course of this research study.

7.2 Field Instrumentation Monitoring

Prior to the removal of the surcharge load, the degree of improvement attained by the foundation soil must be ascertained to confirm whether the design criteria has been achieved. Field instrumentation monitoring is the only means available of providing continuous records of the ground behaviour from the point of instruments installation. Without a proper soil instrumentation method or program, it would be impossible to monitor the current degree of improvement of the soil at any point of time. By analyzing the field instrument monitoring results, it is possible to verify the degree of consolidation of the foundation soil before allowing the removal of the surcharge load. Back-analysis of the field settlement and

piezometer data will also enable the coefficient of consolidation due to horizontal flow to be closely estimated.

Field instrument monitoring was carried out at regular intervals so that the degree of improvement could be monitored and assessed throughout the period of the soil improvement works for the project. Instruments were monitored at close intervals of up to 3 times a week during sandfilling and surcharge placement operations. At other times the instrument was monitored usually at a frequency of once a week.

7.3 Off-shore Field Instrumentation

Off-shore field instrumentation was carried out prior to the commencement of the reclamation works. Off-shore platforms measuring 6 meters by 6 meters were installed at selected strategic locations at 30 meter offset from the proposed soil improvement areas. The purpose for offsetting the platforms from the proposed soil improvement areas is to ensure that the instruments and vertical drain rigs would not be damaged during the vertical drain installation works. The instrument platforms would act as a “Control Area” to enable comparisons to be made of this untreated area with the adjacent vertical drain treated areas.

The instrument platforms were installed by the driving of steel H-piles into the seabed. Following the driving of the H-piles, the platform and scaffoldings were installed. Instruments installed from the platform level include seabed settlement plates, deep settlement gauges, pneumatic piezometers, vibrating-wire electric piezometers, water stand-pipes and inclinometers. The instruments were installed at various elevations so as to study the deformation of the soil at the various elevations of each-sublayer. The instruments installed at the protection platform could therefore provide complete information of the soil behaviour throughout the entire reclamation fill and surcharge loading history of the marine clay. Total settlement of the seabed was measured with the seabed settlement plate while the settlement of the various layers were obtained from the deep settlement gauges. The continuous settlement data during the project including the initial sandfilling, surcharge placement and preloading periods of the location was therefore obtained. Excess pore water pressure build-ups and dissipation as a result of sand filling and surcharge placement operations and consolidation of the marine clay could also be studied at the various piezometer elevations. Figure 7.1 and 7.2 presents a schematic diagram and photo of an off-shore field

instrumentation platform. Figures 7.3 to 7.5 present photos of the various steps involved in the construction of a protection platform for off-shore field instrumentation works.

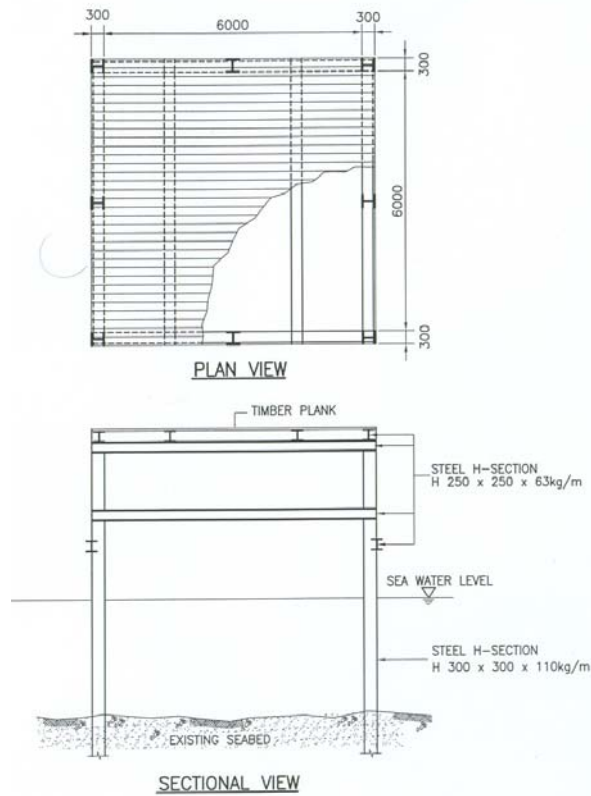


Figure 7.1 Schematic diagram of an off-shore field instrumentation platform (Arulrajah et al., 2004b).



Figure 7.2 Picture of an off-shore field instrumentation platform after initial reclamation (Arulrajah et al., 2004b).



Step 1: Installation of sheet-piles



Step 2: Protection Platform Construction



Step 3: Completion of Protection Platform

Figure 7.3 Construction steps 1,2,3 for off-shore field instrumentation works.



Step 4: Boring-rig for instrumentation



Step 5: Sand pumping towards instrument platform



Step 6: Reclamation proceeding towards protection platform

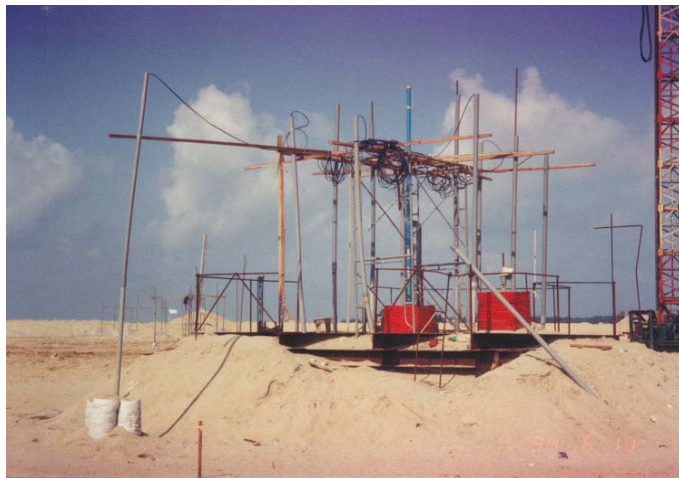
Figure 7.4 Construction steps 4,5,6 for off-shore field instrumentation works.



Step 7: Filling to platform level



Step 8: Preparation for final surcharge fill



Step 9: Top of surcharge level (+10 mCD)

Figure 7.5 Construction steps 7,8,9 for off-shore field instrumentation works.

7.4 On-Land Field Instrumentation

After the hydraulic sandfilling to an elevation of +4 mCD (where Mean Sea Level is at +1.6mCD) and just prior to the installation of the prefabricated vertical drains, instruments were installed in instrument clusters. The instrument clusters were installed throughout the reclamation site along the proposed runway, taxiway and linkways. Instrument clusters were installed at locations having typical soil profiles and at locations of variation of the soil profile and characteristics.

Types of instruments installed at the on-land instrument clusters are surface settlement plates, deep settlement gauges, multi-level settlement gauges, pneumatic piezometers, vibrating-wire electric piezometers, water stand-pipes, earth pressure cells and inclinometers.

The functions of the instruments are the same as those installed in the instrumented platforms but information from these instruments could only be obtained just prior to or soon after the installation of the prefabricated vertical drains. The information obtained however, is sufficient to assess the performance of the vertical drain since high magnitude of settlement and fast rate of dissipation of pore pressure occurred only after vertical drain installation. Figure 7.6 shows on-land field instrumentation clusters at the Project Site.



Figure 7.6 On-land field instrumentation clusters.

7.5 Long-Term Field Instrumentation

After the completion of soil improvement works comprising vertical drains and preloading, long-term monitoring instruments were installed in selected locations. The purpose of the instruments here was to monitor the long-term deformation behaviour of the treated marine clay. As the long-term instruments are relatively expensive to monitor using these capabilities, long-term monitoring instruments are recommended to be installed only after the completion of all ground improvement and sand densification works. Monitoring with these instruments can be carried out regularly till the handing over of these parcels of land.

Instruments used for the long-term field instrumentation works comprises of liquid settlement gauges and electric piezometers which are installed at various elevations of the marine clay. The long-term instruments are often extended to monitoring huts which are located at a safe location away from the movement of traffic and from the hands of potential vandals.

The long-term monitoring instruments are connected to an automatic data acquisition system powered by battery and solar panels. This multi-tasking operating system allows for continuous logging, control and storage of all measurements taken from the site under all weather conditions. Due to the auto-logging capabilities of the acquisition system, no manual recordings of the instrument readings was necessary. Figure 7.7 shows the typical arrangement of a long-term field instrumentation cluster.

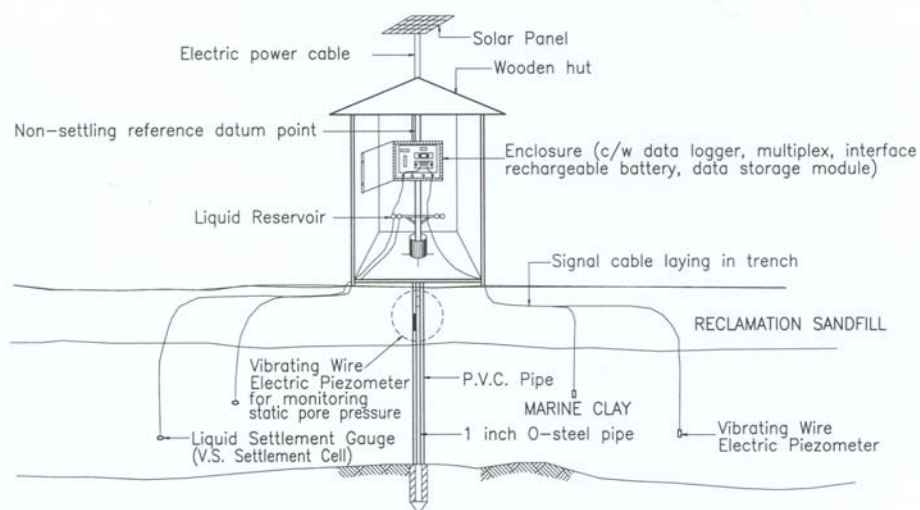


Figure 7.7 Typical details of long-term field instrumentation cluster (Arulrajah et al., 2004b).

7.6 Settlement Gauges

In the Project Site, several types of settlement monitoring instruments were installed to monitor the settlement of the marine clay under the reclaimed fill load. These are settlement plates, deep settlement gauges, multi-level settlement gauges and liquid settlement gauges, which will be described in detail in this section.

It was found that the settlement plates and the deep settlement gauges that were installed through the sandfill at the original seabed gave similar reading for the magnitude and rate of settlement. The multi-level settlement gauges was found to indicate far lower magnitudes of settlement as compared to the deep settlement gauges for the same sub-layers.

7.6.1 Settlement Plate

Settlement plates consist of seabed settlement plates and surface settlement plates. Seabed settlement plates consist of a concrete base plate while surface settlement plates consist of a steel base plate. Settlement plates, due to their relative low cost of production and monitoring are the most common instrument used in land reclamation and other ground improvement projects.

Seabed settlement plates were placed on the seabed at the off-shore field instrumentation platforms prior to the commencement of land reclamation works. Surface settlement plates were installed after reclamation to the vertical drain platform level of +4 mCD.

The surface settlement plates are installed just before or immediately after the installation of vertical drains in order to capture the ground deformations due to the rapid dissipation of excess pore water pressures as soon as vertical drains are installed. Surface settlement plates were installed approximately 0.5 meters beneath the vertical drain platform level of +4 mCD. The seabed and surface settlement plates are monitored from the time of installation till the point of surcharge removal works.

A PVC pipe extension is provided for the settlement plate to eliminate the effect of the settling sand fill gripping onto the rod of the settlement gauges. Measurements of field settlement is carried out by surveying the elevation of the top of the steel pipe. Figure 7.8 indicate the typical details of a seabed settlement plate while Figure 7.9 indicates the details of a surface settlement plate.

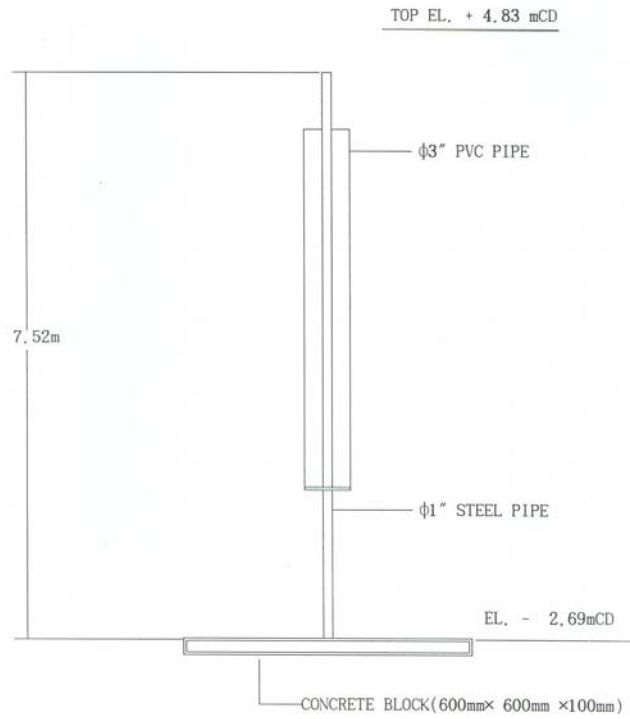


Figure 7.8 Typical details of a seabed settlement plate.

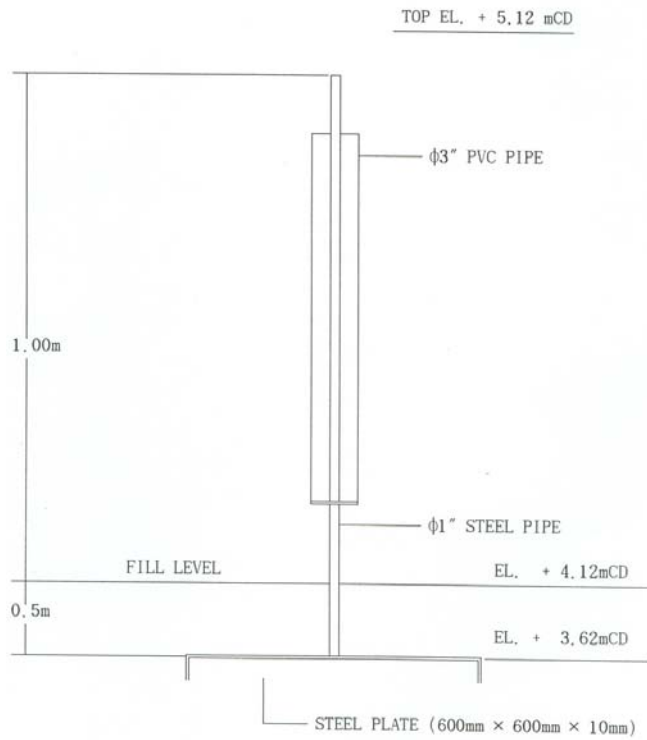


Figure 7.9 Typical details of a surface settlement plate.

7.6.2 Deep Settlement Gauge

The deep settlement gauges were installed prior to reclamation from the off-shore protection platforms. Deep settlement gauges were also installed in clusters on-land after reclamation to the vertical drain platform level either before or immediately after the installation of vertical drains. Deep settlement gauges used consisted of a screw plate at the end of the steel pipe.

Each deep settlement gauge is installed in a separate borehole at different elevations of the marine clay sub-layers. Installation at various elevations enables measurement of the magnitude of deformation of these sub-layers. The deep settlement gauge installed at the seabed level of the marine clay will provide the same magnitude and rate of settlement as that of the seabed or surface settlement plate installed at the same location. The deep settlement gauges that were installed in different sublayers indicated decreasing settlement with depth as would be expected. A PVC pipe extension is provided for the deep settlement gauges to eliminate the effect of the downdrag onto the rod of the settlement gauges. Measurements of field settlement is carried out by surveying the elevation of the top of the steel pipe. Figure 7.10 indicates the typical details of a deep settlement gauge.

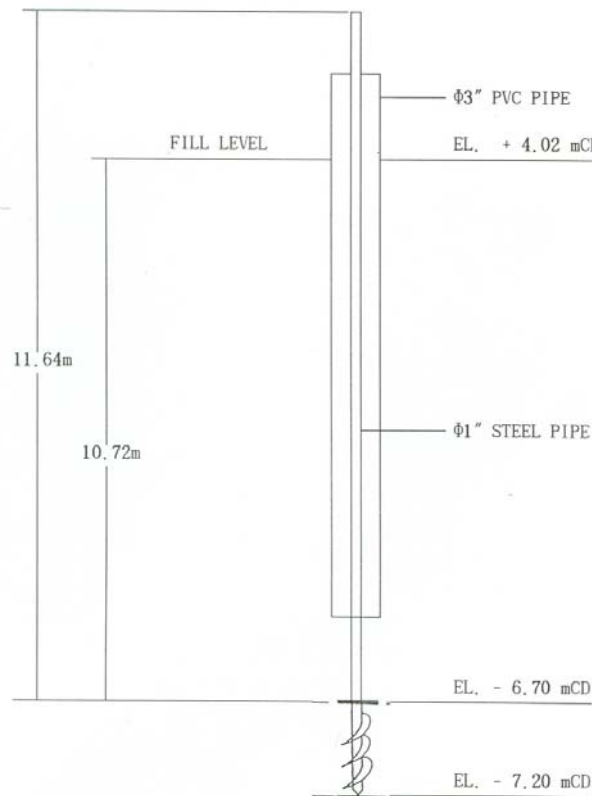


Figure 7.10 Typical details of a deep settlement gauge.

7.6.3 Multi-Level Settlement Gauge

The multi-level settlement gauges were installed prior to reclamation from the off-shore protection platforms. Multi-level settlement gauges were also installed on-land after reclamation to the vertical drain platform level either before or immediately after the installation of vertical drains.

The multi-level settlement gauge consists of a series of “spider” metal rings placed at various locations along an access tube with a magnetic datum at the base. The “spider” is a site jargon used to describe the several metal arms that project out of the metal ring. At the base of the access tube is a magnetic datum point. The multi-level settlement gauge access tube is installed into a borehole which is drilled to the hard formation of 3 consecutive Standard Penetration Test (SPT) of 50 blows. Installation in this manner will ensure that the spider metal rings will be at different designed elevation within the marine clay layer.

A magnetic beeping probe is used to monitor the settlement of the spiders at the various elevations. The magnetic probe will first be lowered to the datum point and from this reference point, the locations of the “spiders” are detected and recorded. The difference between the new recording locations of the spiders and their earlier locations will indicate the settlement of the sub-layer at which the spider is installed. In essence, the “spider” rings are supposed to settle together with the soil mass during consolidation settlement. The top of the access tube elevation is also recorded during each site monitoring to enable computation of the “spider” elevations.

The multi-level settlement gauges indicates far lower magnitudes of settlement as compared to the deep settlement gauges for the same sub-layers. There are several possibilities for this behaviour of the multi level settlement gauges (Bo, Arulrajah and Choa; 1998b) which are:

- although surrounding marine clay is settling, the magnetic “spiders” do not follow
- no deformation of grout together with marine clay
- jamming between “spider” metal ring and access tube
- the datum point is moving which results in the absolute movement not being recorded since the instrument measures relative movement.
- lateral deflection could overestimate the vertical distance between magnetic datum and “spiders” thus causing underestimation of settlement of sub-layers.

Figure 7.11 indicates the typical details of a multi-level settlement gauge. Figure 7.12 indicates the typical accessories required for a multi-level settlement gauge. Figure 7.13 indicates a comparison of settlement measured by deep settlement gauges and multi-level settlement gauges.

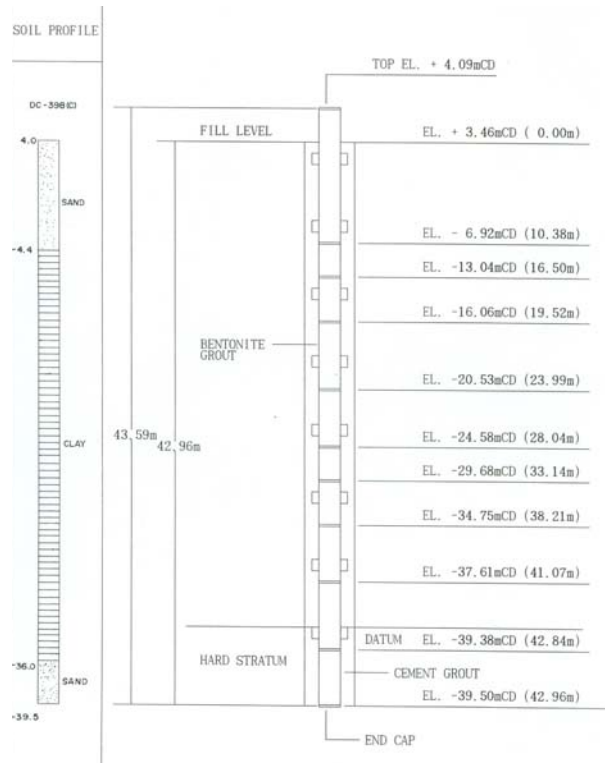


Figure 7.11 Typical details of a multi-level settlement gauge.



Figure 7.12 Accessories of a multi-level settlement gauge.

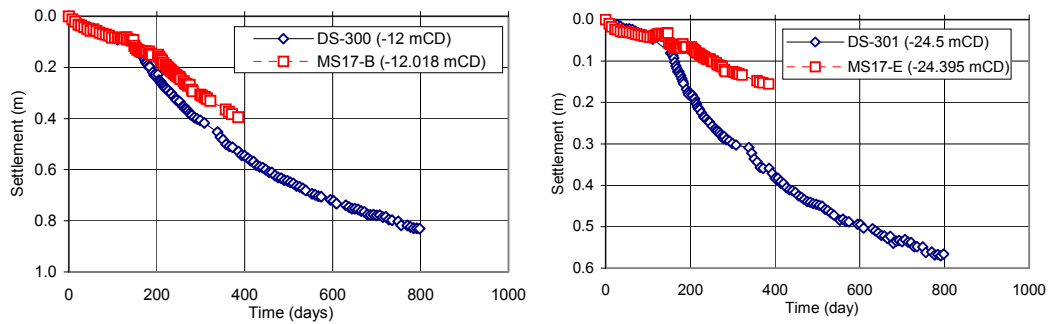


Figure 7.13 Comparison of settlement measured by deep settlement gauges and multi-level settlement gauges.

7.6.4 Liquid Settlement Gauge

The liquid settlement gauge can be monitored automatically and as such was used for long-term instrumentation monitoring. The liquid settlement gauge consists of two liquid-filled tubes attached to a pressure transducer. The liquid-filled tubes serve as a column of water. The pressure transducer measures the pressure exerted by the column of water. The top of tubing serves as a reference datum and is terminated to a reference elevation reservoir typically mounted on a post on stable ground away from the measured area. The bottom of the tubing is connected to a pressure transducer and is placed on the ground for which the settlement is to be monitored. The tube and transducer settle together with the surrounding ground, effectively increasing the height of the column of water and the pressure of the transducer. Settlement is obtained by computing the change in differential elevation between the pressure transducer and the reference reservoir.

The transducer in the liquid settlement gauge converts the pressure of the liquid column to a tensional load on a steel strip that is fixed at both ends. When excited by a magnetic coil, the steel strip vibrates at its natural frequency generating voltage pulses that are transmitted to the readout device. The readout device counts a set number of pulses and computes a natural period, the inverse of the frequency. The square of the natural frequency is proportional to the tension in the steel strip and hence the pressure exerting the load on the strip.

Figure 7.14 indicates the typical details of a liquid settlement gauge while Figure 7.15 shows a liquid settlement gauge.

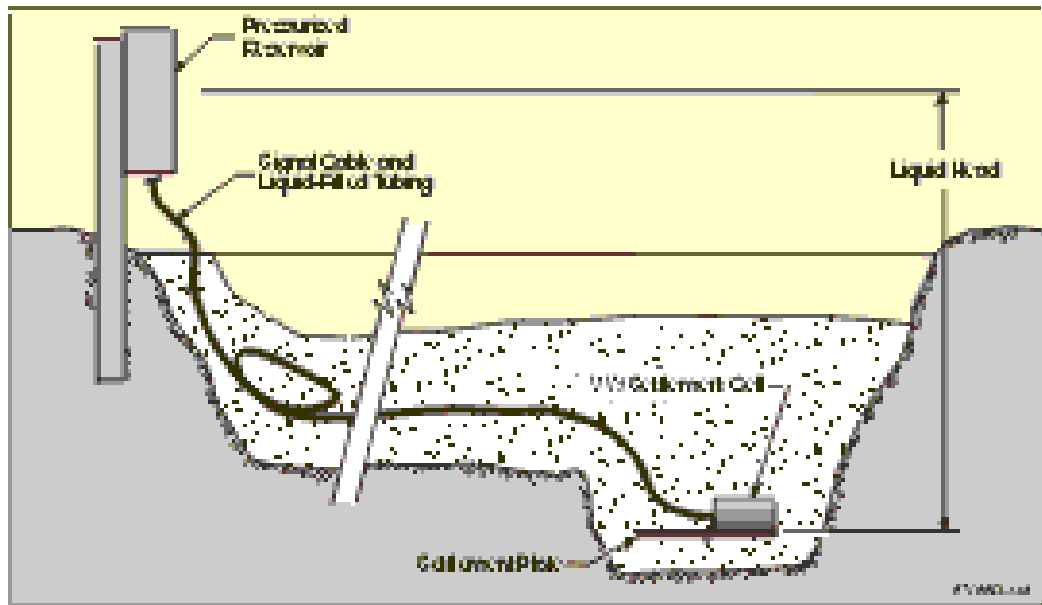


Figure 7.14 Schematic details of a liquid settlement gauge (Courtesy of Sinco).



Figure 7.15 Liquid settlement gauge (Courtesy of Sinco).

7.7 Assessment of Settlement Data

More realistic assessment of average degree of consolidation as well as degree of consolidation for sub-layers can be carried out by using ultimate primary consolidation settlement predicted from settlement monitoring data. This can be worked out by the Asaoka (Asaoka 1978) and Hyperbolic (Tan 1993) methods. Ultimate settlement can be well predicted after getting sufficient field settlement monitoring data. The assessment of field settlement plates by the Asaoka and Hyperbolic methods described in this thesis have been discussed in detail by the author (Arulrajah et al., 2003a, 2003b, 2004b, 2004c, 2004e, 2004g, 2004n) during the course of this research study.

7.7.1 Asaoka Method

Asaoka (1978) has suggested a procedure modified for application to consolidation problems with vertical drains using Barron (1948) solution for pure radial drainage. The Asaoka procedure generates a straight-line only if the soil behaviour fulfils the assumptions of Terzaghi's theory of one-dimensional consolidation. The use of the Asaoka method for the assessment of the degree of consolidation of marine clays with vertical drains in land reclamation projects has been previously described by Bo, Arulrajah and Choa (1997a, 1997b) and Choa et al. (1981).

In the Asaoka analysis procedure, the time settlement curve of the settlement gauge is first plotted. Following this, a series of settlement values $s_1, s_2 \dots s_i$ is selected, such that s_i is the settlement at time i and that the selected time interval in the analysis, $\Delta t = (t_i - t_{i-1})$ is constant. The next step is to plot the points (s_{i-1}, s_i) . These points should lie on a straight line defined as follows:

$$s_i = s_0 + \beta s_{i-1} \quad \text{Eq. (7.1)}$$

where:

s_0 and β are two constants which depend on the selected time interval Δt .

The ultimate settlement (S_{ult}) can then be predicted at the intercept of this line and a 45 degree line (illustrated in Chapter 9). In the case of placement of additional fill, the straight line will be deviated after the point the additional fill is placed. When the settlement is relatively small compared to the thickness of the clay layer, the shifted line becomes almost parallel to the initial line (Asaoka, 1978).

The constant β , represents the slope of the constructed straight line. The coefficient of consolidation due to horizontal flow can be back analysed from settlement data (Asaoka 1978):

$$c_h = d_e^2 F(n) \log_e \beta / 8\Delta t \quad \text{Eq. (7.2)}$$

where:

d_e is the diameter of equivalent soil cylinder = 1.13 x Drain Spacing (square pattern).

$F(n)$ is the drain spacing factor.

7.7.2 *Hyperbolic Method*

The use of the Hyperbolic method for the assessment of the degree of consolidation of marine clays with vertical drains in land reclamation projects has been described by Bo, Arulrajah and Choa (1997a, 1998b) and Choa et al. (1981).

The Hyperbolic method is also useful in tracing the loading history of ground improvement works. Changes in the loading sequence will appear as deviations from the Hyperbolic line, which can be easily detected (Tan, 1993). In the Hyperbolic method, the relationship between consolidation settlement and time is postulated to approach a Hyperbolic curve given by the following equation:

$$t/s = c + m t \quad \text{Eq. (7.3)}$$

This is a straight line in a t/s versus t plot. The equation shows that the ultimate settlement is given by $1/m$, which is the inverse of the slope Tan et al. (1993, 1995, 1996).

The ultimate settlement can be easily predicted once sufficient data are available to show that the behaviour approaches the Hyperbolic line and that c and m can be estimated (illustrated in Chapter 9). A degree of consolidation of at least 60% (Tan, 1995) should be attained by the foundation soil in order for the c and m constants to be estimated for cases of combined vertical and radial drainage. This can be estimated based on analysing the field settlement by using Equation (7.5). Tan (1995) stated that good estimates of the total primary settlement can be estimated by the inverse slope ($1/m$) multiplied by the theoretical slope factor (α) for cases of combined vertical and radial drainage:

$$\text{Ultimate Settlement} = \alpha (1 / m)$$

$$\text{Eq. (7.4)}$$

The α factor used in the assessment is based on the relationship chart proposed by Tan (1995) shown in Figure 7.16:

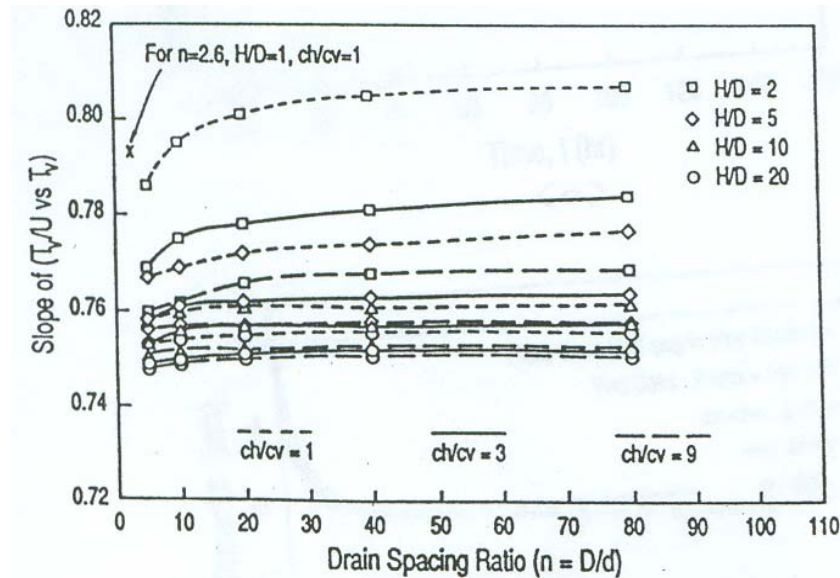


Figure 7.16 Relationship of slopes (α) of initial linear segments (between U_{60} and U_{90}) of theoretical hyperbolic plots (Tan, 1995).

7.7.3 Degree of Consolidation of Settlement Gauges

From measured settlement and predicted ultimate settlement, degree of consolidation can be computed by using the following equation:

$$U\% = S_t / S_{ult} \quad \text{Eq. (7.5)}$$

where:

S_t is settlement at time t

S_{ult} is ultimate primary settlement

$U\%$ is the degree of consolidation

If deep settlement gauges are installed in the sub-layers, degree of consolidation of sub-layers can also be estimated by applying Equation (7.5) and hence the degree of consolidation of sub-layers can also be estimated. However, this relationship will not be applicable for the overconsolidated layers which do not follow Terzaghi's theory.

7.8 Piezometers

In the Project Site, three types of piezometers were installed to monitor the dissipation of excess pore pressures of the marine clay under the reclaimed fill load. These are pneumatic piezometers, vibrating-wire electric piezometers and open-type piezometers. The piezometers were installed in individual boreholes at various predetermined elevations in the marine clay. The piezometers were installed in the same instrument clusters as the water stand-pipes and settlement gauges. The pneumatic piezometer and electric piezometer indicate similar measurements for piezometric elevation and excess pore water pressures. Installation of piezometers at the same elevations as the deep settlement gauges enabled for the correction of the piezometer tip due to large strain settlements of the marine clay under the reclaimed fill.

Prior to the piezometer installation, a site calibration was conducted in a large diameter water well to check on the manufacturer's calibration. As such, a site calibration chart is produced for each piezometer prior to their installation plotting measured pressure against pressure of water on the piezometer. Piezometer tips are packed in a sand bag and saturated in the water at least twenty-four hours before installation. After installation in a borehole, sand was placed again to a certain limit and a bentonite seal suitable for marine conditions was placed on top of the sand column. The borehole was backfilled to the original seabed level with original soil. Alternatively, the borehole could be backfilled with a good mixture of bentonite cement permeability of which is equal to or lower than the natural soil. This is because backfilling with sand will lead to a lower measurement of the excess pore pressure at the location due to the rapid dissipation of pore pressure along the sand fill column above the piezometer (Bo et al., 2003).

7.8.1 *Pneumatic Piezometer*

Pneumatic piezometers were installed in the off-shore protection platforms as well as in the on-land field instrumentation clusters. The pneumatic piezometer consists of a pneumatic transducer which has been permanently installed in a borehole. Tubing runs from the transducer to a terminal on the surface. Readings for pneumatic piezometers are obtained with a pneumatic indicator. To obtain a pressure reading, the operator connects the transducer tubing to the indicator and directs a flow of compressed nitrogen gas to the transducer. When the transducer tubing brings a flow of gas back to the surface, the operator knows the transducer has been activated and shuts off the flow of gas. Gas pressure inside the transducer now balances water pressure outside and the reading is recorded.

In the initial stages, the pneumatic piezometers were subject to a high damage rate attributable to the pinching of the tubing due to the large strain settlements which led to the loss of valuable data until they were replaced. This was however corrected by installing a protective casing throughout the length of the cables and by housing the piezometer in a guard shell. As such, gripping and pinching of the cable due to lateral stress and settlement was overcome. Figure 7.17 indicates the typical details and photo of a specially modified pneumatic piezometer with protected guard cell.

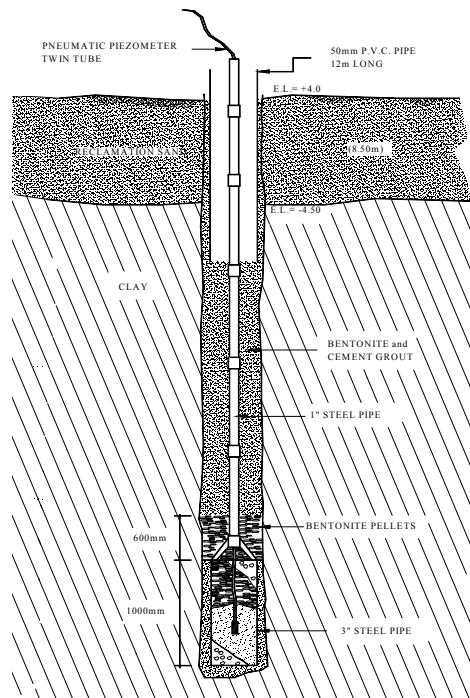


Figure 7.17 Typical details and photo of pneumatic piezometer with protected guard cell. (photo courtesy of Dr M.W.Bo).

7.8.2 Electric Piezometer

The vibrating-wire electric piezometers were installed in the on-land field instrumentation clusters as well as the long-term field instrumentation clusters. The electric piezometer consists of a transducer which converts water pressure to tensional load on a steel strip that is fixed at both ends. When excited by a magnetic coil, the steel strip vibrates at its natural frequency, generating voltage pulses that are transmitted to the readout device. The readout device counts a set number of pulses and computes a natural period, the inverse of the natural frequency. The square of the natural frequency is proportional to the tension in the steel strip and hence, the pressure exerting the load on the strip. Figure 7.18 indicates the typical details of an electric piezometer while Figure 7.19 shows an electric piezometer.

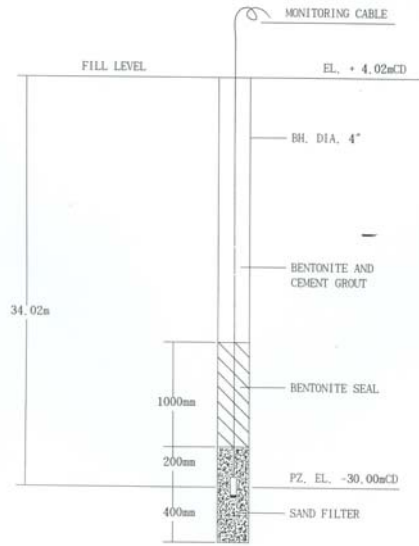


Figure 7.18 Typical details of an electric piezometer.



Figure 7.19 Electric piezometer (Courtesy of Sinco).

7.8.3 Open-Type Piezometer

Open-type piezometers are installed in sub-layers with permeable sand formations. The purpose of the installation was to determine the drainage condition of the sub-layer at which the piezometer was installed. Installation of the open-type piezometer at the vertical drain anchoring formation level in vertical drain areas could confirm whether the vertical drains were double draining to the top sand fill layer and the anchoring layer as often assumed in the design of vertical drains for the Changi area of Singapore. A water-level indicator which emits a buzzing sound on contact with water is used to determine the water level. Figure 7.20 indicates the typical details of an open type piezometer. Figure 7.21 indicates the typical details of a water level indicator.

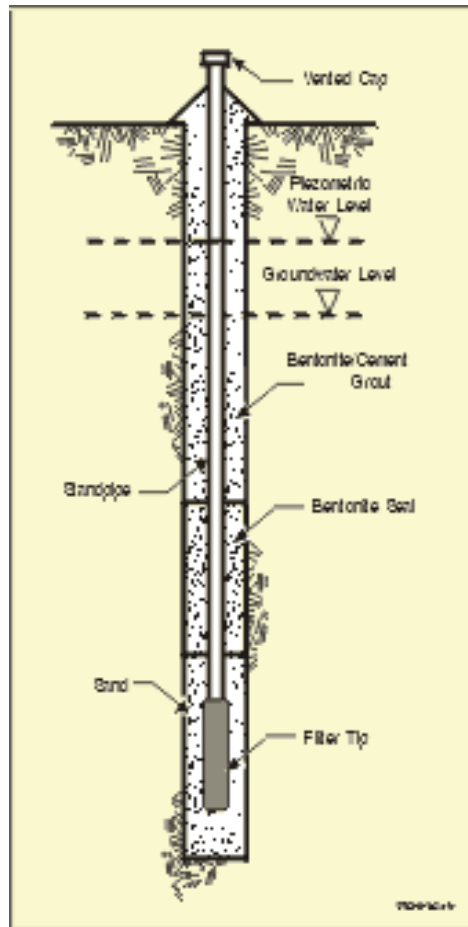


Figure 7.20 Typical details of an open-type piezometer.



Figure 7.21 Typical details of water level indicator .

7.8.4 Water Stand-Pipe

Water stand-pipes were installed at the sand formation within piezometer clusters so as to measure the hydrostatic water level at these locations. This enabled the evaluation of the excess pore water pressures for the piezometers by determining the piezometric elevation and subsequently the excess pore water pressures. The water stand-pipe consists of water intake opening slots that are small enough to prevent the ingress of the surrounding soil into the stand-pipe. A geofabric is often wrapped around the slotted portion of the water stand-pipe. Figure 7.22 indicates the typical details of a water standpipe. A water-level indicator which emits a buzzing sound on contact with water is used to determine the water level.

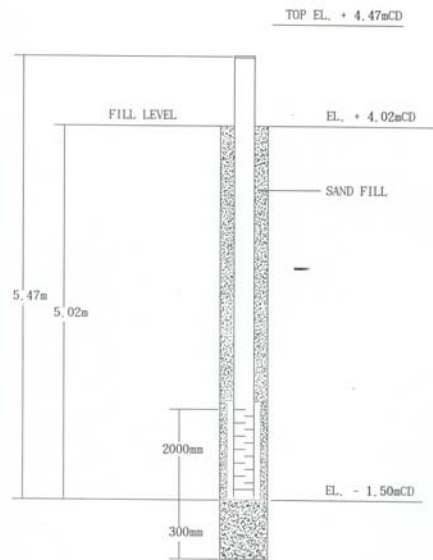


Figure 7.22 Typical details of a water stand-pipe.

7.9 Assessment of Piezometer Monitoring Data

The method of assessment of piezometers described in this thesis have been discussed in detail by the author (Arulrajah et al., 2003b, 2004a, 2004b, 2004c, 2004e, 2004g, 2004n) during the course of this research study.

7.9.1 Degree of Consolidation

Pneumatic piezometers were installed in the same clusters as the settlement gauges, close to the same elevation as the settlement gauges to enable for correction of the piezometer tip due to large strain settlement. Water stand-pipes were installed in the clusters so as to measure the static water level at these locations and hence to ascertain the excess pore water pressures of the piezometers.

The piezometers indicates measurements for piezometric head. Piezometers are utilized to measure the pore pressure in the soil. If regular monitoring is carried out to measure the piezometric head together with the static water level, changes of excess pore pressure due to additional load and thus degree of consolidation can be computed.

Average degree of dissipation is defined as ratio of excess pore pressure at time “t” upon initial excess pore pressure. The method of computation of degree of consolidation is the same used as that used earlier in the CPTU dissipation tests:

$$U(\%) = 1 - (U_t / U_i) \quad \text{Eq. (7.6)}$$

where:

U_t = excess pore pressure at time “t” in kPa

U_i = initial excess pore pressure = additional load ($\Delta\sigma'$) in kPa

Piezometers were installed at different elevations and as such, the average degree of consolidation for the whole compressible unit as well as the average degree of consolidation of the sub-layers were determined.

Due to the large strain settlements at site, all raw piezometer readings taken were corrected to account for the new elevation of the piezometer at each monitoring due to the settlement of the piezometer tip. The settlement of the adjacent deep settlement gauges in the field instrumentation cluster at about the same respective elevation was used to adjust the settlement of the piezometer tips. Correction is essential and if not made will lead to an underestimation of the degree of dissipation of the excess pore water pressure.

7.9.2 Back-Analysis of Coefficient of Consolidation due to Horizontal Flow

From field pore pressure measurements, the coefficient of consolidation due to horizontal flow can be back-analysed. The first step is the determination of the degree of consolidation at the particular time using Eq (7.6). Subsequently, the nondimensional time factor, T_h has to be determined with the following equation:

$$U_r = 1 - \exp \frac{-8T_h}{F(n)} \quad \text{Eq. (7.7)}$$

where:

U_r = Average degree of consolidation with respect to radial flow

T_h = Non-dimensional time factor for consolidation by horizontal drainage

$F(n)$ = Vertical drain factor

$$F(n) = \frac{n^2}{(n^2 - 1)} \log_e(n) - \frac{3n^2 - 1}{4n^2} \quad \text{Eq. (7.8)}$$

where:

n = drain spacing ratio = d_e / d_w

d_e = 1.13 x drain spacing (square pattern) or 1.05 x drain spacing (triangular pattern)

d_w = $[2(a + b)] / \pi$, where a is the drain width and b is the drain thickness

Coefficient of consolidation due to horizontal flow, c_h can be calculated by either using the total time method or the incremental time method (Bromwell and Lambe, 1968) :

Total time method:

$$c_h = \frac{T_h d_e^2}{t} \quad \text{Eq. (7.9)}$$

Incremental time method:

$$c_h = \frac{T_{h2} - T_{h1}}{t_2 - t_1} d_e^2 \quad \text{Eq. (7.10)}$$

where:

t is time

7.10 INCLINOMETER

Inclinometers consist of a grooved plastic or aluminium casing installed vertically in a borehole socketed to the firm/dense stratum. For installation in marine and nearshore conditions, the use of the plastic casing is advisable as it is not subject to corrosion. Four longitudinal, equally spaced inner grooves control the directional orientation of the sensor. The sensor is lowered to the base of the casing and is then gently withdrawn upwards at frequent depths of intervals. The sensor readings are recorded and displayed on a portable digital indicator at the ground surface. In this manner, the inclinometer readings are taken in

the four orientation directions and subsequently converted to lateral displacements. Consecutive readings at the same depths, taken at periodic monitoring intervals are used to determine the depths, magnitudes and rates of movement of the marine clay due to the reclaimed fill.

Inclinometers at site are normally installed along the slopes of the sandfilling and surcharge placement works. Inclinometers are monitored continuously during the sandfilling and surcharge placement operations to determine and control the rate and magnitude of lateral displacement. Should the rate and magnitude of lateral displacement be too high as determined by the Engineer, the sandfilling and surcharge operations will be slowed down or stopped and necessary remedial action will be taken. Inclinometers are installed in boreholes which are terminated at SPT N-values of 3 consecutive 100 blow counts. Since the inclinometer is measuring relative movement rather than absolute movement, its toe has to be anchored in the dense/hard stratum to ensure that there is no settlement at this non-lateral displacement formation. Any lateral displacement at the toe will lead to an underestimation of absolute lateral movement of soil along the inclinometer. Figure 7.23 indicates the typical details of an inclinometer. Figure 7.24 illustrates the comparison of lateral deflection monitored in inclinometers anchored at SPT of 50 blows with that anchored at SPT of 100 blows formation. As evident, the inclinometer anchored in the lower SPT formation indicates lower lateral displacement than the actual absolute displacement due to movement at the toe.

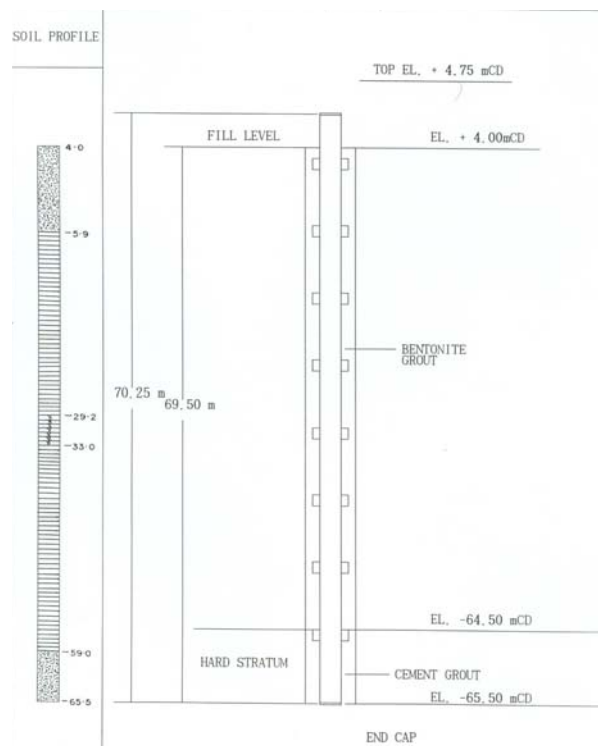


Figure 7.23 Typical details of an inclinometer.

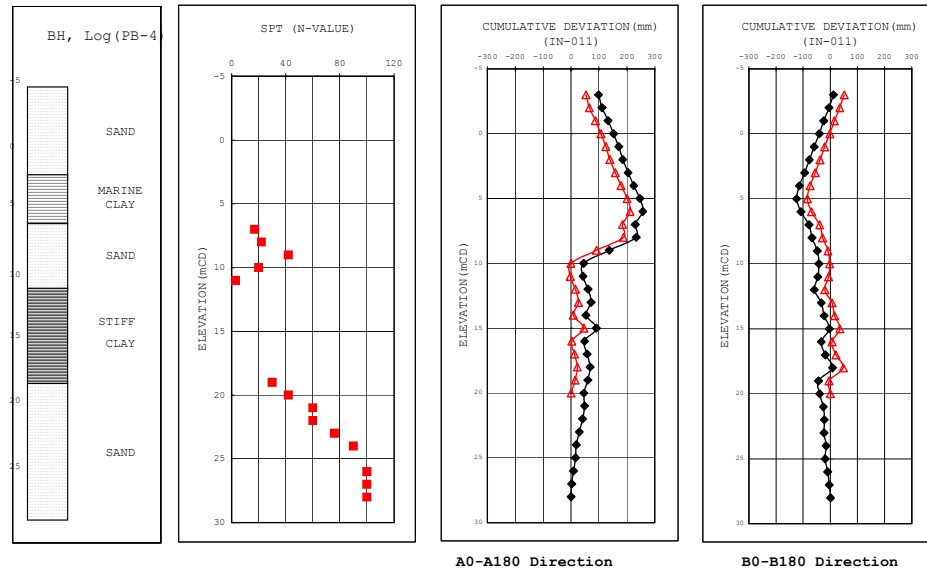


Figure 7.24 Comparison of lateral displacement between inclinometers anchored at SPT 50 blows and SPT 100 blows (Arulrajah et al., 2004b; Bo, Arulrajah and Choa 1998b).

7.11 DEEP REFERENCE POINT

The deep reference point is essentially the survey datum reference point to which all elevation measurements of instruments are tied in too. It is essential as such that the deep reference point is installed in a very dense/hard formation to ensure that it is not subject to any settlements. The deep reference point is positioned at locations at the site which are far from other permanent survey benchmarks.

7.12 EARTH PRESSURE CELL

Earth pressure cells measure the combined pressure of effective stress and pore-water pressure. With the installation of water stand-pipes close by, the vertical effective stress of the surcharge load can be computed. The total pressure cell is formed from two circular plates of stainless steel which are welded together to form a sealed cavity which is filled with fluid. A pressure transducer is connected to this cell which is installed with its sensitive surface in direct contact with the soil. The total pressure acting on the sensitive surface is transmitted to the fluid inside the cell and measured by the pressure transducer. Earth pressure cells are installed in a trench 0.5 to 0.6 meters deep, at the vertical drain platform level (elevation of +4 mCD) just prior to the placement of the surcharge load. The total

pressure cell is backfilled with sand prior to the placement of surcharge. Figure 7.25 indicates the typical details of a total pressure cell.

Earth pressure cells should be installed with their sensitive side facing upward in order to measure correctly the surcharge load. Figure 7.26 highlights the comparative plot of earth pressure between earth pressure cells installed with sensitive side facing up and down for a 6 meter height of surcharge (surcharge elevation +10 mCD). As evident, the cells placed with the sensitive side facing upwards provides an accurate reading of the imposed surcharge load.

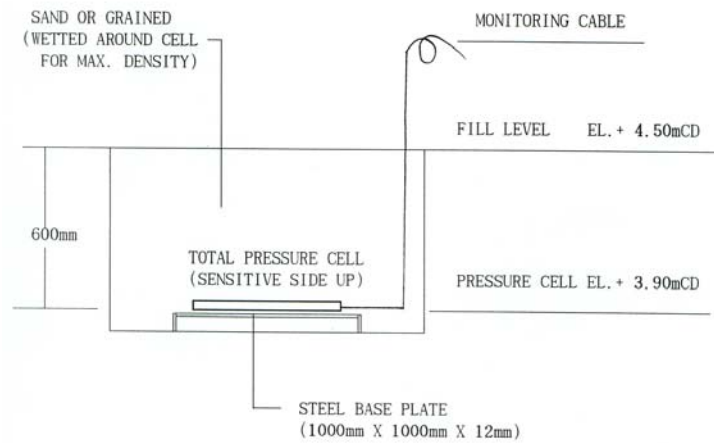


Figure 7.25 Typical details of a total pressure cell.

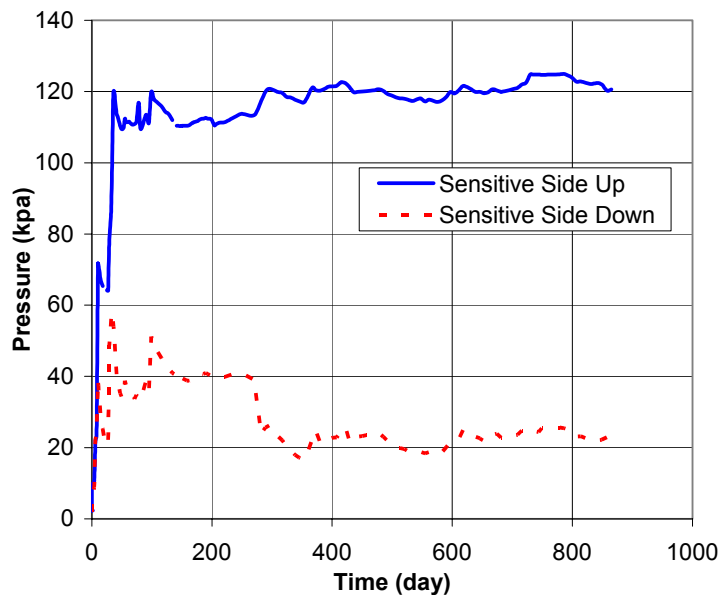


Figure 7.26 Comparison between the results of earth pressure between cells placed with sensitive side up and down (Arulrajah et al., 2004b; Bo, Arulrajah and Choa; 1998b).

8.0 FIELD INSTRUMENTATION OF MARINE CLAY CASE STUDIES

Field instrumentation case studies of the behaviour of marine clay under reclamation fills was carried out at two locations in the project site. In the field instrumentation case studies, the behaviour of the marine clay was monitored for sub-areas with and without vertical drains. Long duration field instrumentation monitoring was carried out at regular intervals at the case study locations.

The first field instrumentation case study location was located beyond the northern tip of the runway and is referred to as the Pilot Test Site. The field instrumentation case study at the Pilot Test Site described in this chapter has been discussed in detail by the author (Arulrajah et al., 2003a, 2004g, 2004e, 2004l, 2004n) during the course of this research study.

The second field instrumentation case study location was situated at the same location as the in-situ testing site and is referred to as the In-Situ Test Site. The field instrumentation case study at the In-Situ Test Site described in this chapter has been discussed in detail by the author (Arulrajah et al., 2004c, 2004b, 2003b) during the course of this research study. The location of the field instrumentation case study sites within the Changi East Reclamation Project site is shown in Figure 8.1.

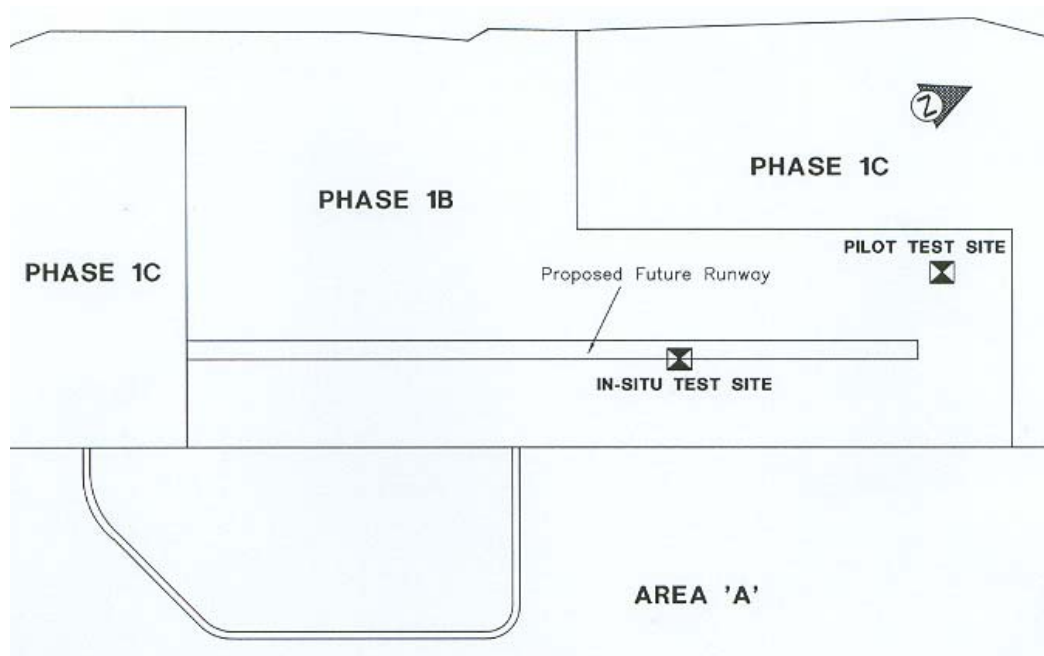


Figure 8.1 Location of field instrumentation case study sites (Arulrajah et al., 2004d).

8.1 FIELD INSTRUMENTATION OF MARINE CLAY CASE STUDY: PILOT TEST SITE

The location of the Pilot Test Site is in the northern area of the project just beyond the runway tip. The field instruments at these locations were installed on-land at the vertical drain platform level of +4 mCD just before or soon after vertical drain installation. The Pilot Test Site consisted of 4 sub-areas, three of which were installed with vertical drains at various spacings. Long duration field settlement monitoring was carried out at regular intervals at these sub-areas.

The seabed elevation is about -6 mCD (Admiralty Chart Datum, where mean sea level is +1.6 mCD) while the thickness of the soft marine clay in the location was up to 40 meters thick. Land reclamation was first carried out to the vertical drain platform elevation of +4 mCD. Field instruments comprising of surface settlement plates, deep settlement gauges, pneumatic piezometers, vibrating-wire electric piezometers and water stand-pipes were installed from the platform level where vertical drains were installed. The field instruments were installed prior to vertical drain installation. Prefabricated vertical drains were installed to depths of up to 45 meters in the various sub-areas. Following the installation of vertical drains, surcharge was next placed by hydraulic filling to an elevation of +7 mCD simultaneously for all the sub-areas. As such, an assessment could be carried out and compared between the sub-areas treated with vertical drains at various spacings when subjected to the same surcharge preload. The analysis of the field instrumentation results for the various sub-areas was carried out 32 months after surcharge placement which equates to a total monitoring duration of about 42 months.

The field instrumentation case study at the Pilot Test Site described in this chapter has been discussed in detail by the author (Arulrajah et al., 2003a, 2004a, 2004e, 2004g, 2004j, 2004l, 2004n) during the course of this research study. The summary of the vertical drain spacing in the various sub-areas based on the design requirements is indicated in Table 8.1.

Table 8.1. Summary of Pilot Test Site sub-area vertical drain spacings (Arulrajah et al., 2003a).

Pilot Test Site Sub-Areas	Vertical Drain Square Spacing
A2S-71	2.0 meter x 2.0 meter
A2S-72	2.5 meter x 2.5 meter
A2S-73	3.0 meter x 3.0 meter
A2S-74	No Drain

Figure 8.2 shows the layout plan of the Pilot Test Site. The profile of field instrumentation at the Pilot Test Site is shown in Figure 8.3. Figures 8.4 to 8.7 indicate the instrument elevations.

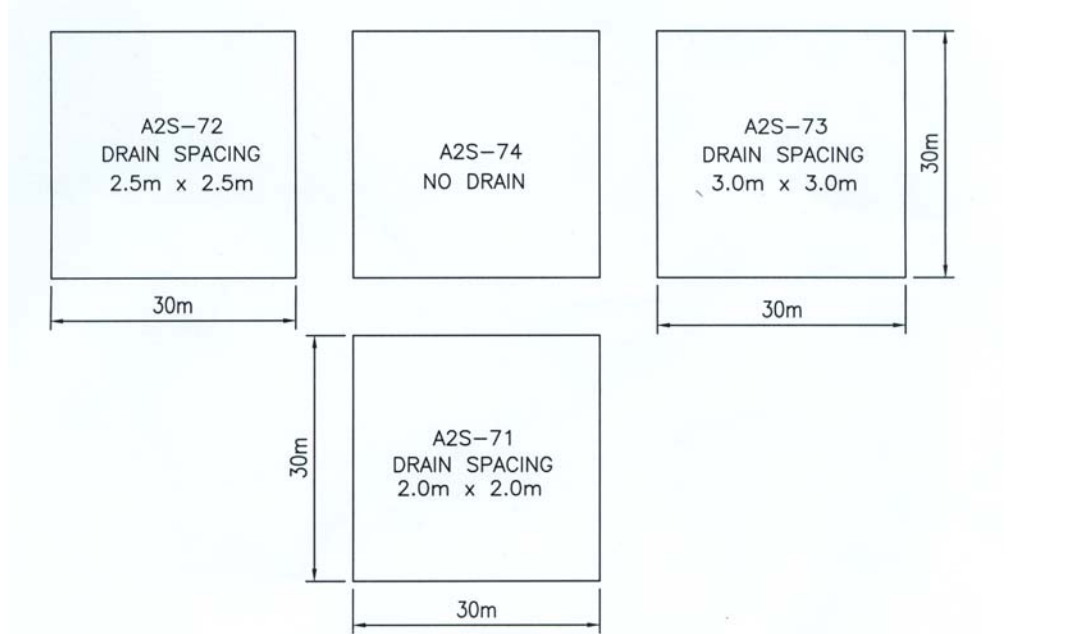


Figure 8.2 Layout plan and vertical drain spacing of sub-areas at the Pilot Test Site (Arulrajah et al., 2003a).

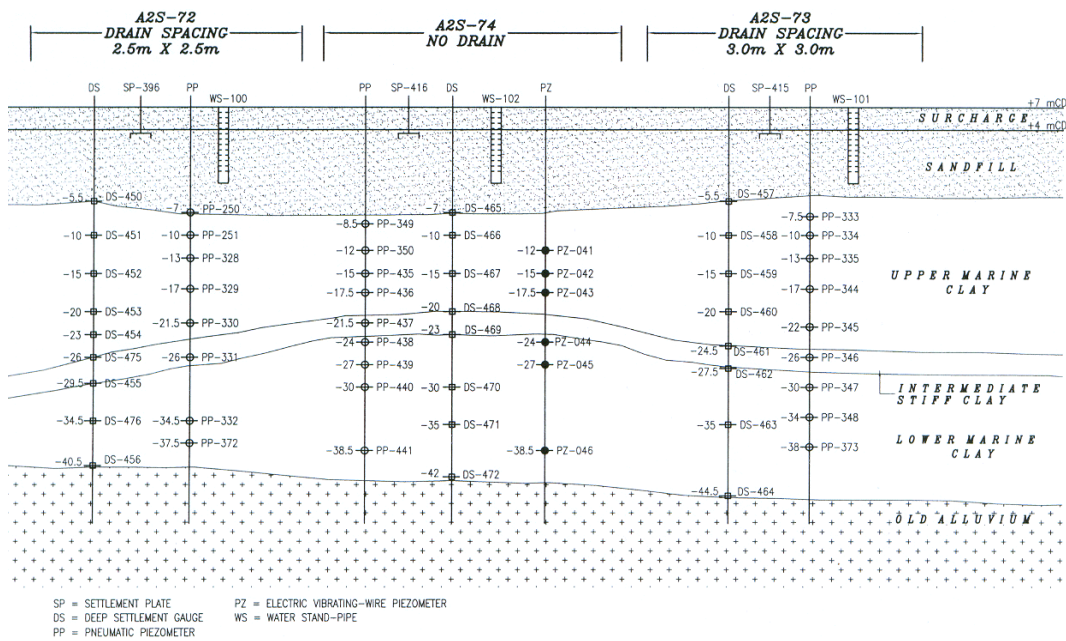


Figure 8.3 Cross sectional profile showing instrument elevations at the Pilot Test Site (Arulrajah et al., 2004e).

REFERENCE CPT:DC-470		SETTLEMENT GAUGES	PNEUMATIC PIEZOMETERS	ELECTRIC PIEZOMETERS
ELEVATION (m CD)	SOIL TYPE	E.L. (m CD)	E.L. (m CD)	E.L. (m CD)
		+4	RECLAMATION SAND FILL	SP-346 3.5
-7.1	UPPER MARINE CLAY	DS-444 -6	PP 245 -8	PZ 35 -8
		DS-445 -12	PP 246 -12	PZ 36 -12
		DS-473 -16	PP 247 -16	PZ 37 -16
		DS-446 -20	PP 248 -20	PZ 38 -20
		DS-447 -26	PP 249 -27	PZ 39 -27
-28.7	LOWER MARINE CLAY	DS-448 -28.5		
		DS-474 -33	PP 369 -33	PZ 40 -33
-35.1	SAND	DS-449 -37.5		
-37.7				

Figure 8.4 Instrument elevations in A2S-71 (2.0m x 2.0m).

REFERENCE CPT:DC-586		SETTLEMENT GAUGES	PNEUMATIC PIEZOMETERS
ELEVATION (m CD)	SOIL TYPE	E.L. (m CD)	E.L. (m CD)
		+4	RECLAMATION SAND FILL
-5.7	UPPER MARINE CLAY	DS-450 -5.5	PP-250 -7
		DS-451 -10	PP-251 -10
		DS-452 -15	PP-328 -13
		DS-453 -20	PP-329 -17
		DS-454 -23	PP-330 -21.5
		DS-475 -26	PP-331 -26
		DS-455 -29.5	
-29.8	LOWER MARINE CLAY	DS-476 -34.5	PP-332 -34.5
		DS-456 -40.5	PP-372 -37.5
-40.7	SAND		
-41.85			

Figure 8.5 Instrument elevations in A2S-72 (2.5m x 2.5m).

REFERENCE CPT:DC-588		SETTLEMENT GAUGES	PNEUMATIC PIEZOMETERS
ELEVATION (m CD)	SOIL TYPE	E.L. (m CD)	E.L. (m CD)
+4	RECLAMATION SAND FILL	SP-415 3.5	
-5.4	UPPER MARINE CLAY	DS-457 -5.5	PP-333 -7.5
		DS-458 -10	PP-334 -10
		DS-459 -15	PP-335 -13
		DS-460 -20	PP-344 -17
		DS-461 -24.5	PP-345 -22
-24.4	INTERMEDIATE STIFF CLAY	DS-462 -24.5	PP-346 -26
-27.3	LOWER MARINE CLAY	DS-463 -27.5	PP-347 -30
		DS-463 -35	PP-348 -34
		DS-464 -44.5	PP-373 -38
-44.75			

Figure 8.6 Instrument elevations in A2S-73 (3.0m x 3.0m).

REFERENCE CPT:DC-587		SETTLEMENT GAUGES	PNEUMATIC PIEZOMETERS	ELECTRIC PIEZOMETERS
ELEVATION (m CD)	SOIL TYPE	E.L. (m CD)	E.L. (m CD)	E.L. (m CD)
+4	RECLAMATION SAND FILL	SP-416 3.5		
-7.1	UPPER MARINE CLAY	DS-465 -7	PP-349 -8.5	
		DS-466 -10	PP-350 -12	PZ-041 -12
		DS-467 -15	PP-435 -15	PZ-042 -15
		DS-468 -20	PP-436 -17.5	PZ-043 -17.5
-20.4	INTERMEDIATE STIFF CLAY	DS-469 -20	PP-437 -21.5	
-22.5	LOWER MARINE CLAY	DS-470 -23	PP-438 -24	PZ-044 -24
		DS-470 -30	PP-439 -27	PZ-045 -27
		DS-471 -35	PP-440 -30	
		DS-472 -42	PP-441 -38.5	PZ-046 -38.5
-42.5				

Figure 8.7 Instrument elevations in A2S-74 (No Drain).

8.1.1 Analyses of Settlement Gauges

The surface settlement plates which was installed 0.5 meters beneath the vertical drain platform level in the reclamation sand and the deep settlement gauges which was installed at the top surface of the compressible marine clay gave similar readings for magnitude and time rate of settlement. This indicates that the settlement contribution of the sandfill layer is minimal as would be expected. The deep settlement gauges that were installed in the different sub-layers indicate decreasing settlement with depth as would be expected.

Figure 8.8 compares the surface settlement plate results between the various sub-areas in the Pilot Test Site. The A2S-71 (2.0m x 2.0m) sub-area records the highest magnitude and rate of settlement as compared to the other sub-areas due to its closer drain spacing. The A2S-74 (no drain) sub-area on the other hand records the least magnitude and rate of settlement. Normally, for the same surcharge and the same thickness of clay, the same amount of ultimate settlement is obtained after a long time. However, in the Pilot Test Site, variations in settlements is due to slight variation of soil profile at the various sub-areas. Furthermore, settlement of the sub-areas prior to the installation of prefabricated vertical drains will also result in variations in the magnitude of surcharge load and hence the ultimate settlement. This is because the sub-areas were surcharged to the same elevation rather than same load. The significant improvement of the vertical drain treated areas compared to the A2S-74 (no drain) sub-area is clearly evident in the figure. It can be observed that the closer the vertical drain spacing, the higher the corresponding magnitude of settlement. Sub-area A2S-71 (2.0m x 2.0m) with the closest drain spacing indicates the highest settlement readings while the untreated sub-area A2S-74 (no drain) indicates the least. This indicates that the vertical drain is functioning as expected.

Figure 8.9 compares the field settlement isochrones between the various sub-areas of the Pilot Test Site at various durations after surcharge. The settlement gauges indicate increasing settlement in the marine clay with the increase in the surcharge duration. The marine clay is observed to be softer and with higher compression parameters at the upper layer. The gauges installed in the very deep underlying dense sand layer indicates minimal settlement with the increasing surcharge duration which is expected. The settlement gauges indicate increasing settlement in the marine clay with the increase in the surcharge duration. The marine clay is observed to be softer and with higher compression parameters in the upper marine clay layer. The settlement gauges installed in the very deep underlying dense sand layer indicates minimal settlement with the increasing surcharge duration which is expected. The settlement isochrones confirm that the sub-area with the closer drain spacing registers the higher settlements. The settlement isochrones indicate the trend of decreasing settlement for the

deeper deep settlement gauges which is due to the marine clay increasing with density, stiffness, strength and compression parameters decreasing with depth. Minimal settlement is recorded in the hard old alluvium layer. Plotting settlement isochrones is a useful means of checking whether the settlement gauges for the clusters are functioning properly.

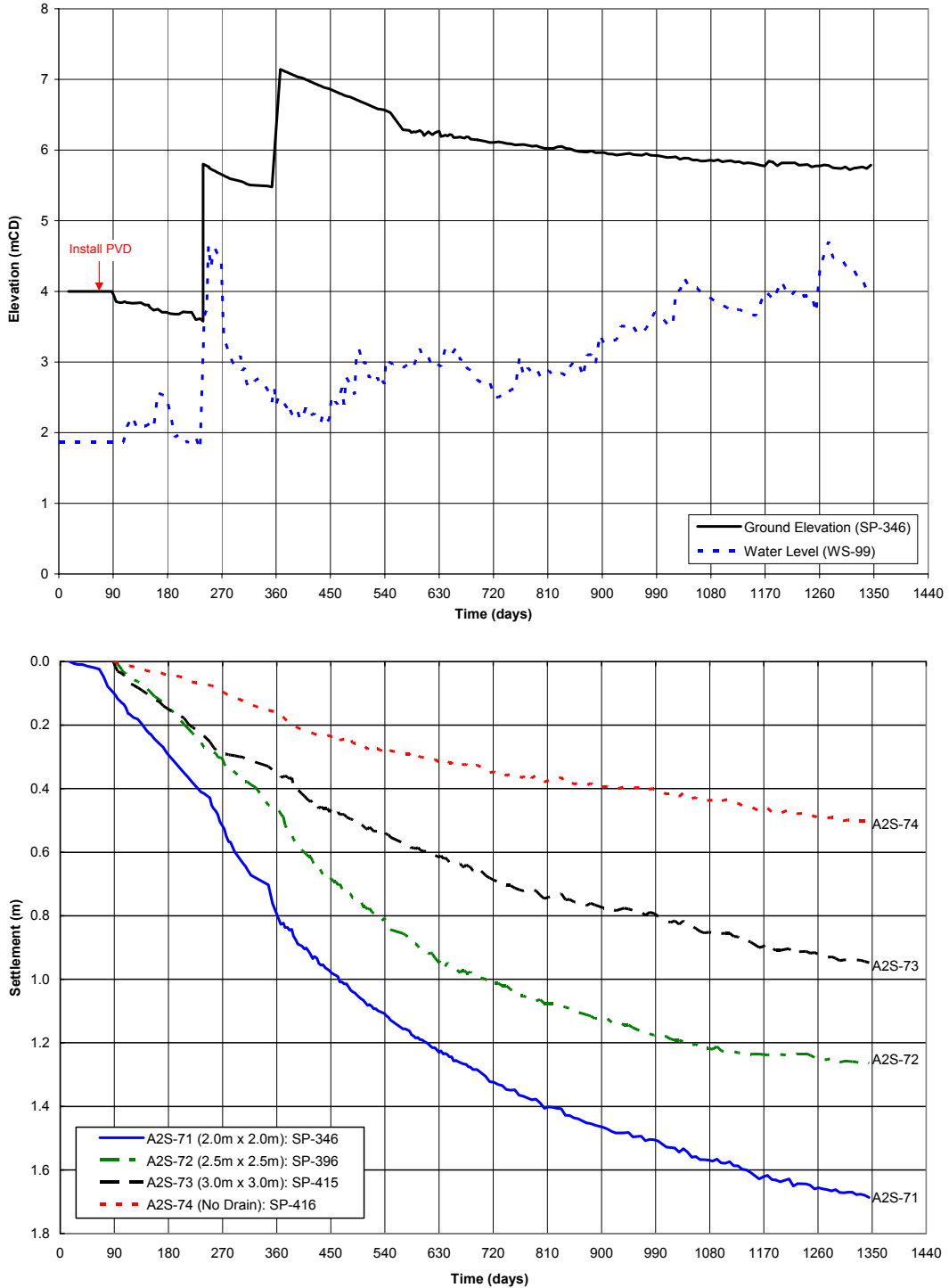


Figure 8.8 Comparison of field settlement between sub-areas at the Pilot Test Site (Arulrajah et al., 2003a).

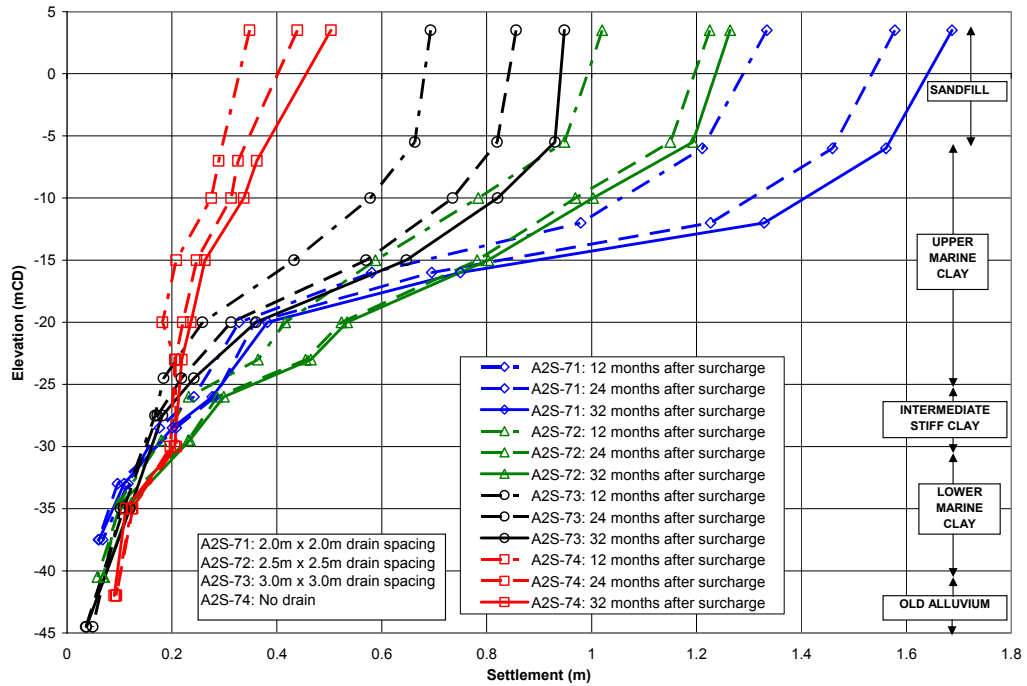


Figure 8.9 Comparison of field settlement isochrones between sub-areas at the Pilot Test Site (Arulrajah et al., 2004g).

Figures 8.10 indicates the magnitudes of settlements of the A2S-71(2.0m x 2.0m) sub-area in the Pilot Test Site. Figures 8.11 indicates the magnitudes of settlements of the A2S-72 (2.5m x 2.5m) sub-area in the Pilot Test Site. Figures 8.12 indicates the magnitudes of settlements of the A2S-73 (3.0m x 3.0m) sub-area in the Pilot Test Site. Figures 8.13 indicates the magnitudes of settlements of the A2S-74 (No Drain) sub-area in the Pilot Test Site.

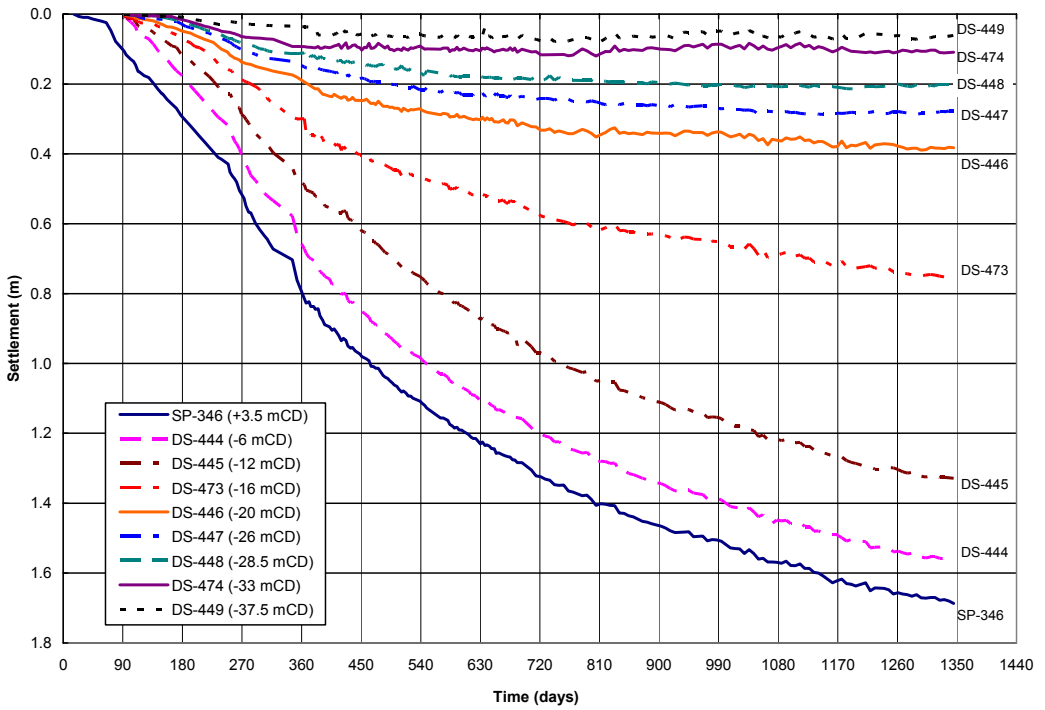
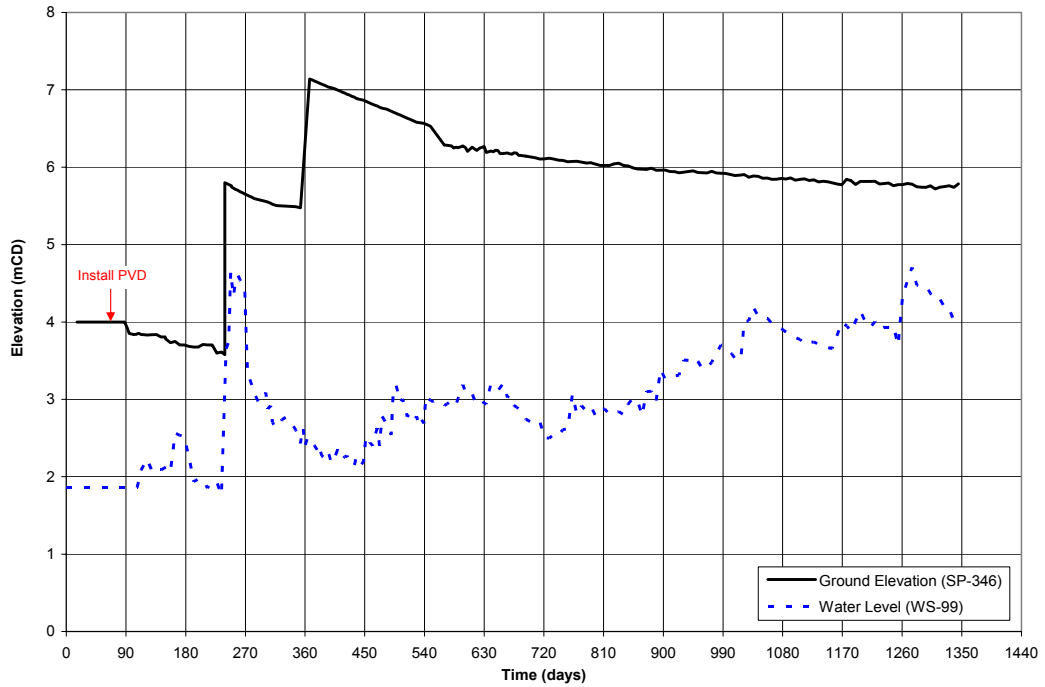


Figure 8.10 Field settlement results of settlement plate and deep settlement gauges at A2S-71 (2.0m x 2.0m) (Arulrajah et al., 2004g).

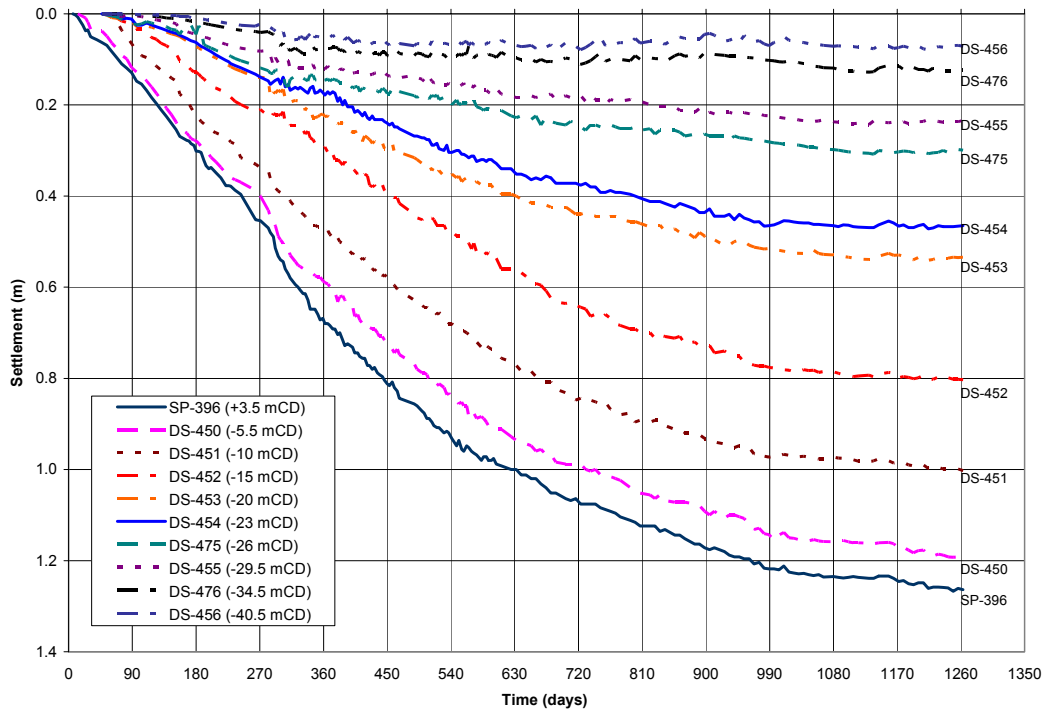
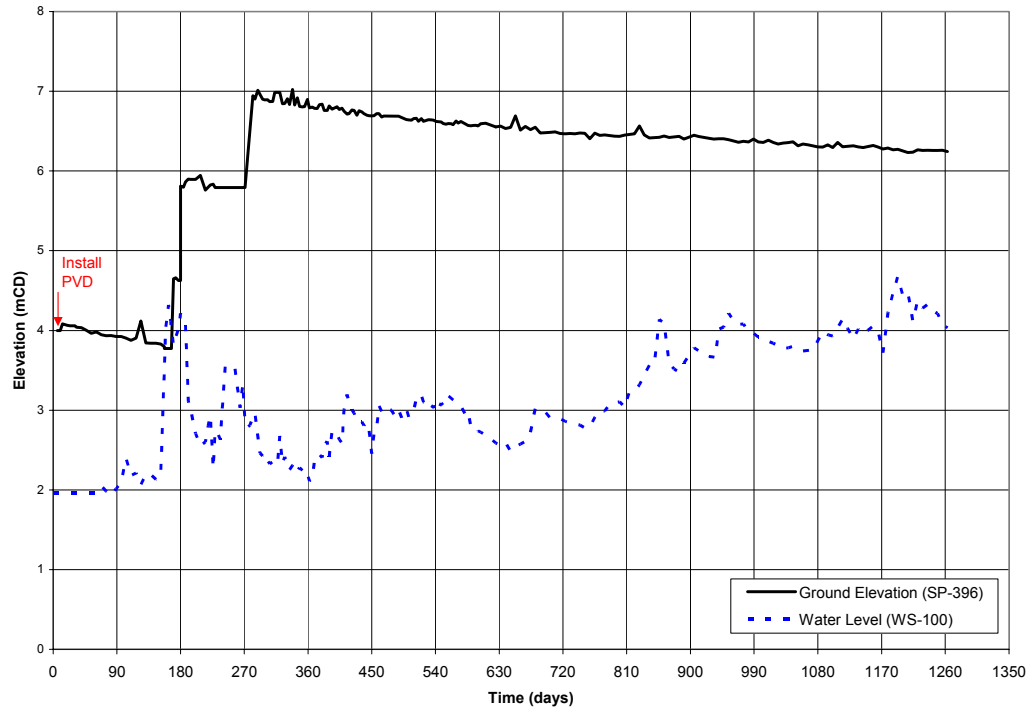


Figure 8.11 Field settlement results of settlement plate and deep settlement gauges at A2S-72 (2.5m x 2.5m) (Arulrajah et al., 2004g).

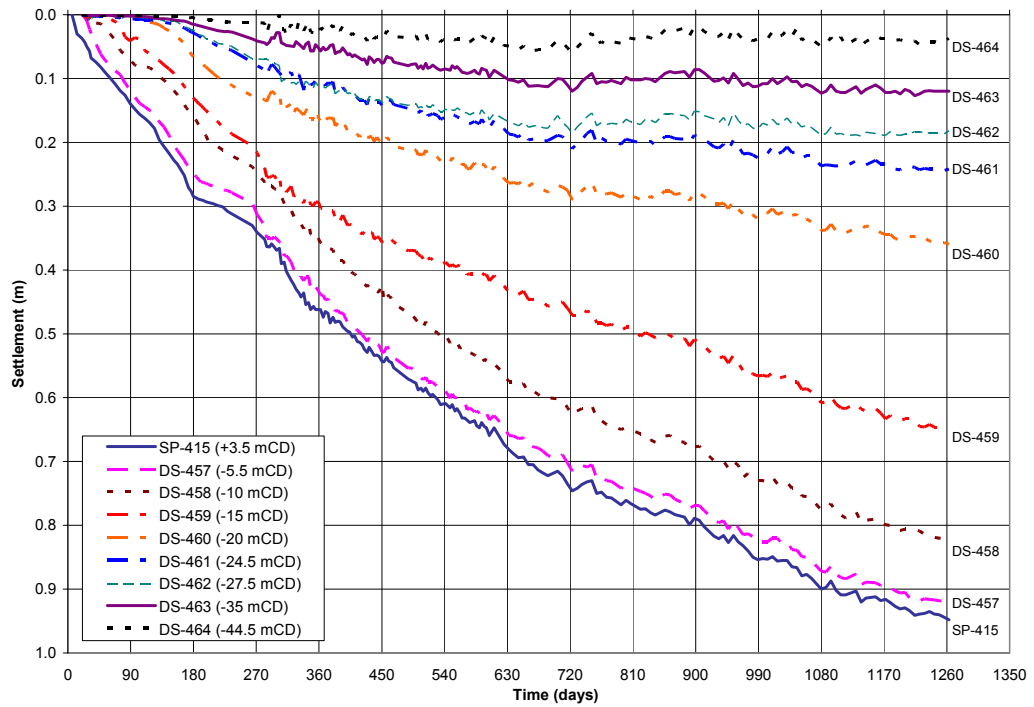
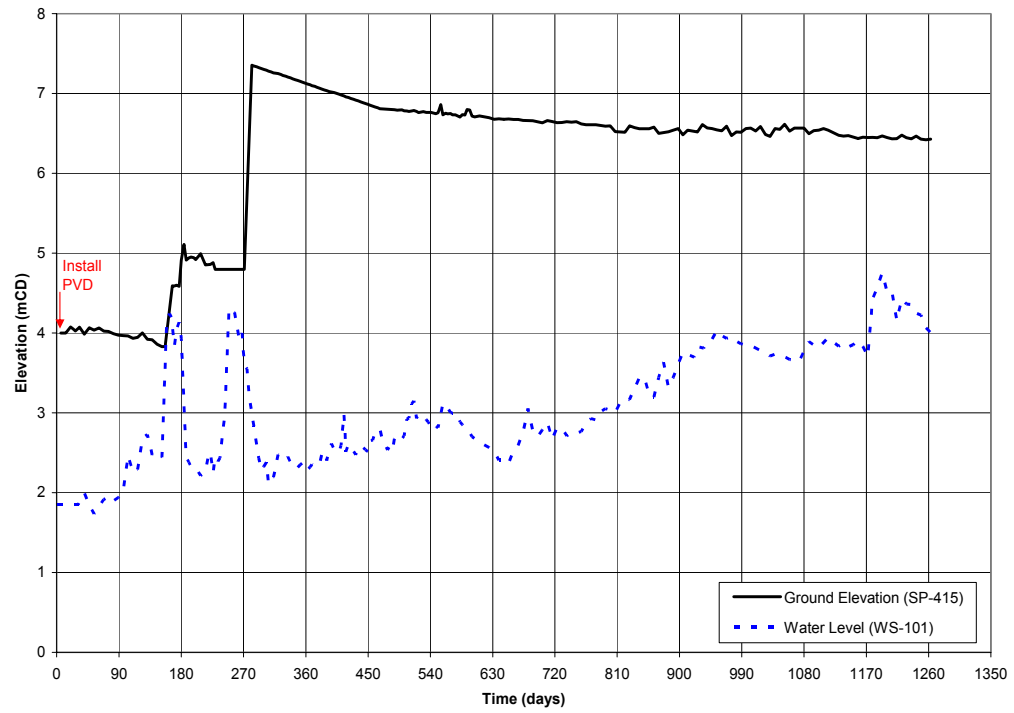


Figure 8.12 Field settlement results of settlement plate and deep settlement gauges at A2S-73 (3.0m x 3.0m) (Arulrajah et al., 2004g).

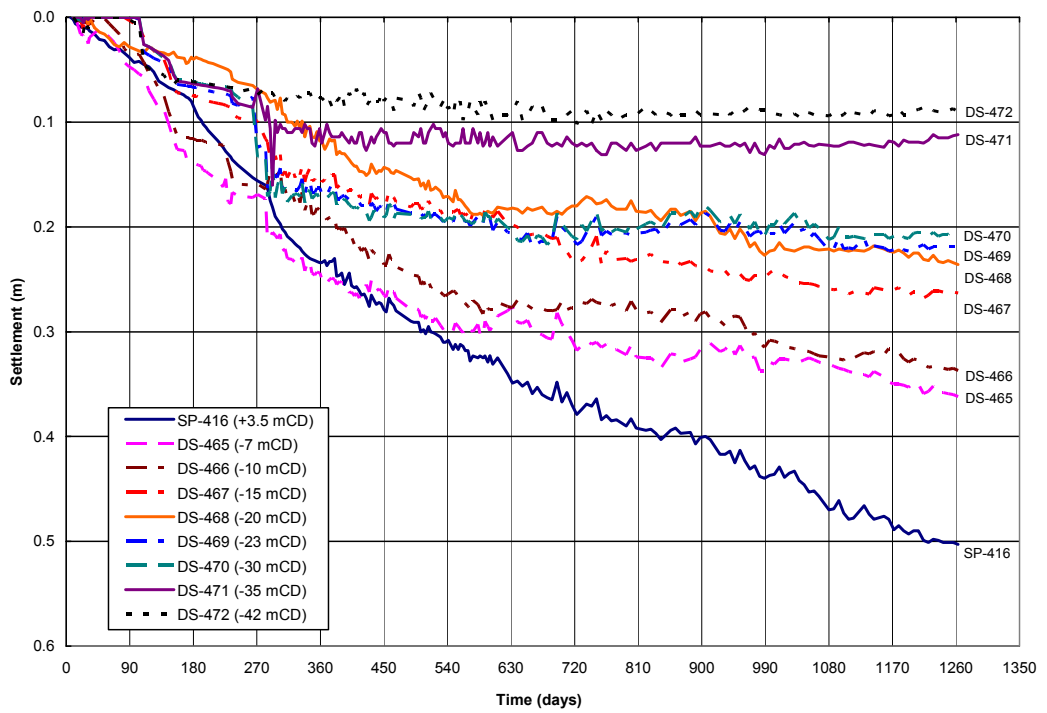
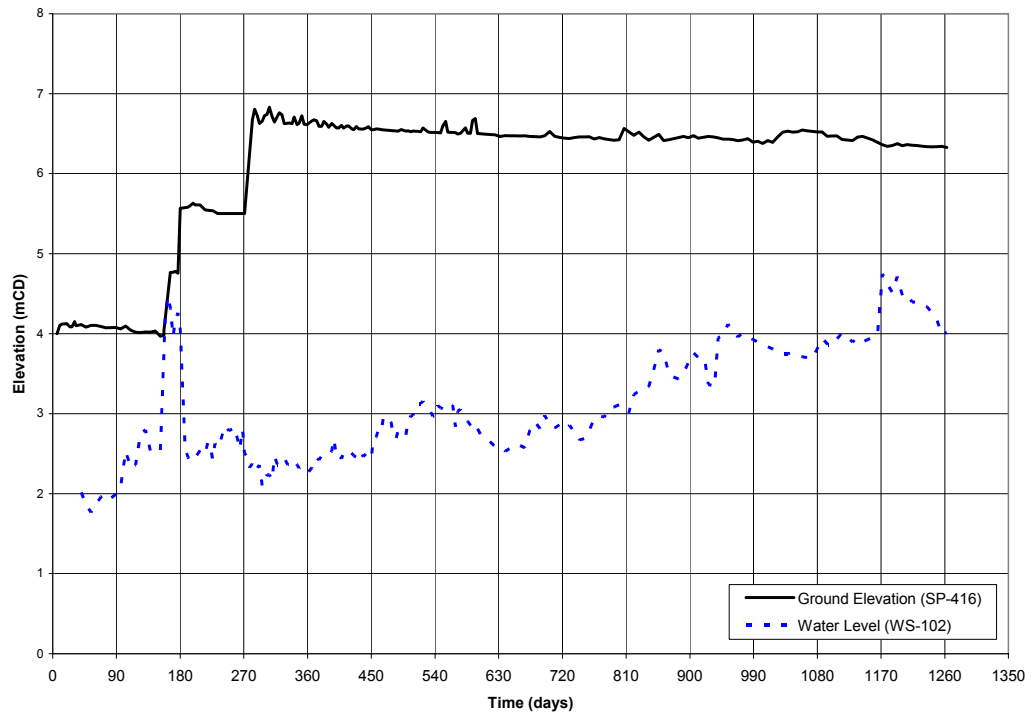


Figure 8.13 Field settlement results of settlement plate and deep settlement gauges at A2S-74 (No Drain) (Arulrajah et al., 2004g).

Figure 8.14 to Figure 8.16 shows the typical Asaoka plot predictions for the settlement plates at the A2S-71, A2S-72 and A2S-73 sub-areas of the Pilot Test Site 32 months after surcharge at time intervals of 28 and 56 days.

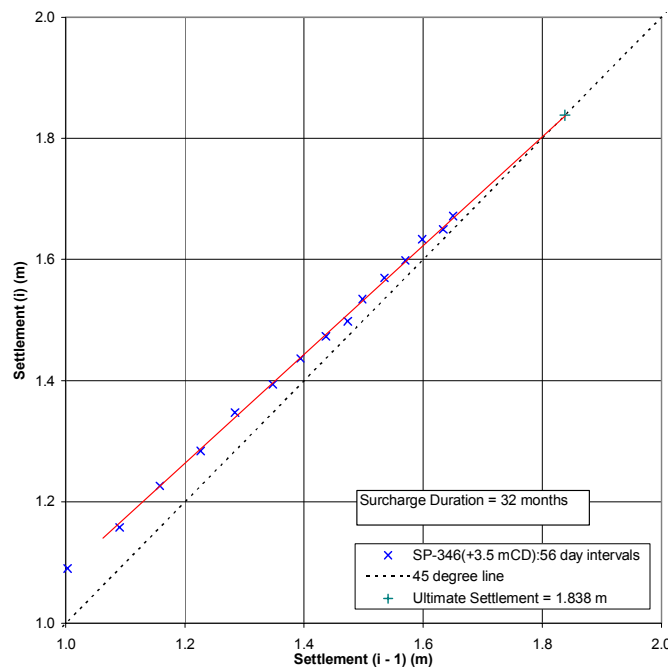
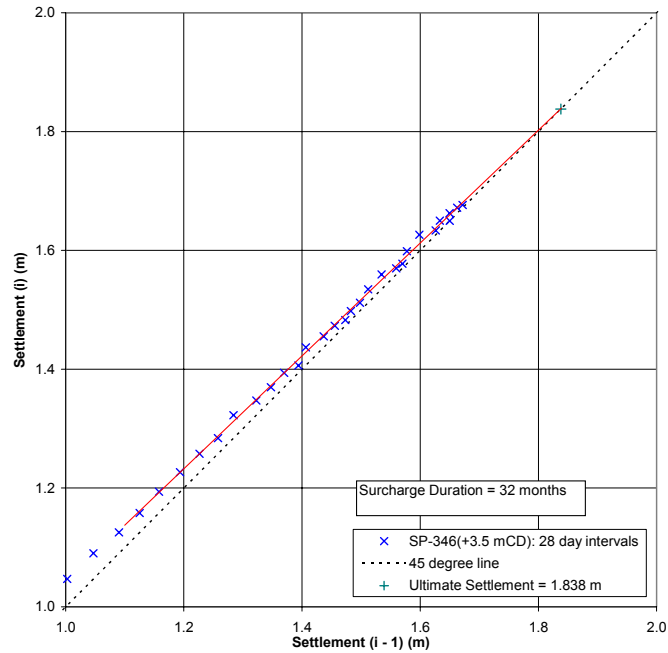


Figure 8.14 Asaoka plot for A2S-71 (2.0m x 2.0m) at time interval of 28 and 56 days (Arulrajah et al., 2004g).

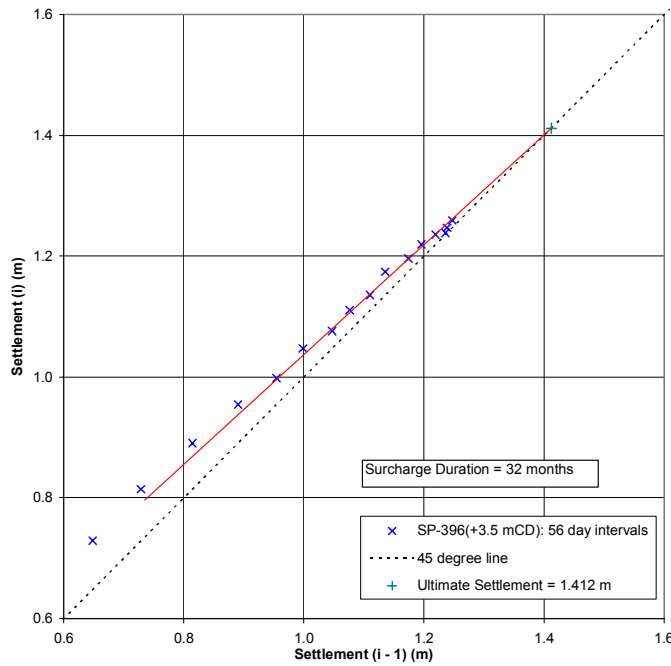
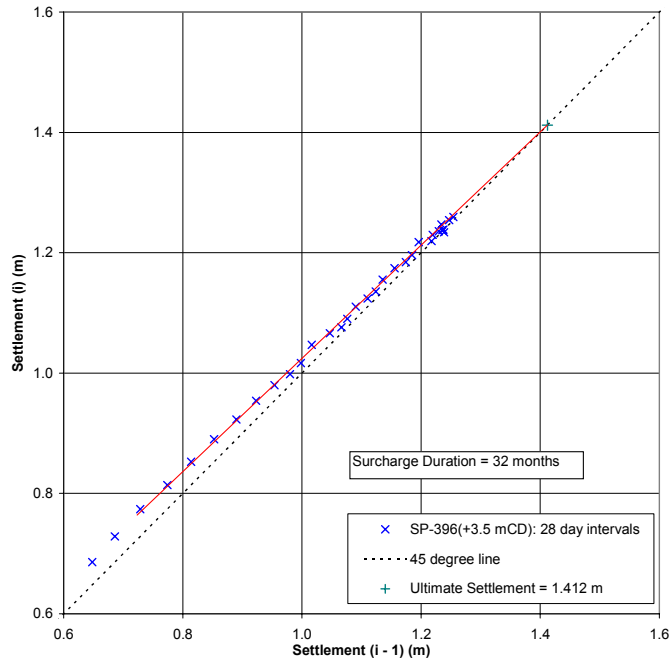


Figure 8.15 Asaoka plot for A2S-72 (2.5m x 2.5m) at time interval of 28 and 56 days (Arulrajah et al., 2004g).

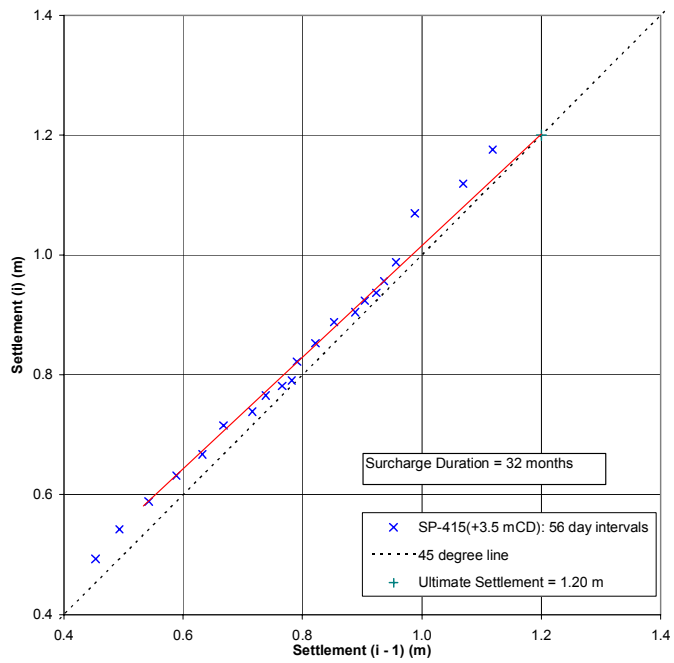
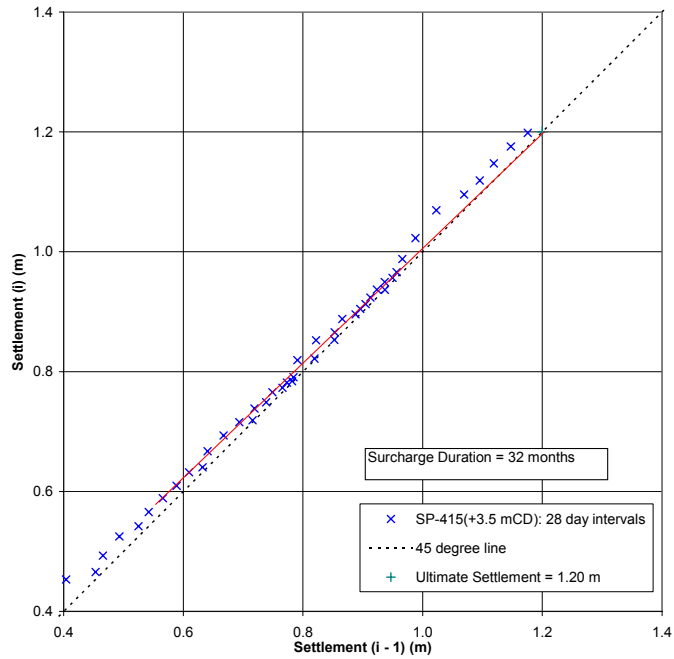


Figure 8.16 Asaoka plot for A2S-73 (3.0m x 3.0m) at time interval of 28 and 56 days (Arulrajah et al., 2004g).

Figure 8.17 and 8.22 shows the combined settlement gauges and settlement plate Hyperbolic plot predictions at the A2S-71, A2S-72 and A2S-73 sub-areas of the Pilot Test Site 32 months after surcharge placement.

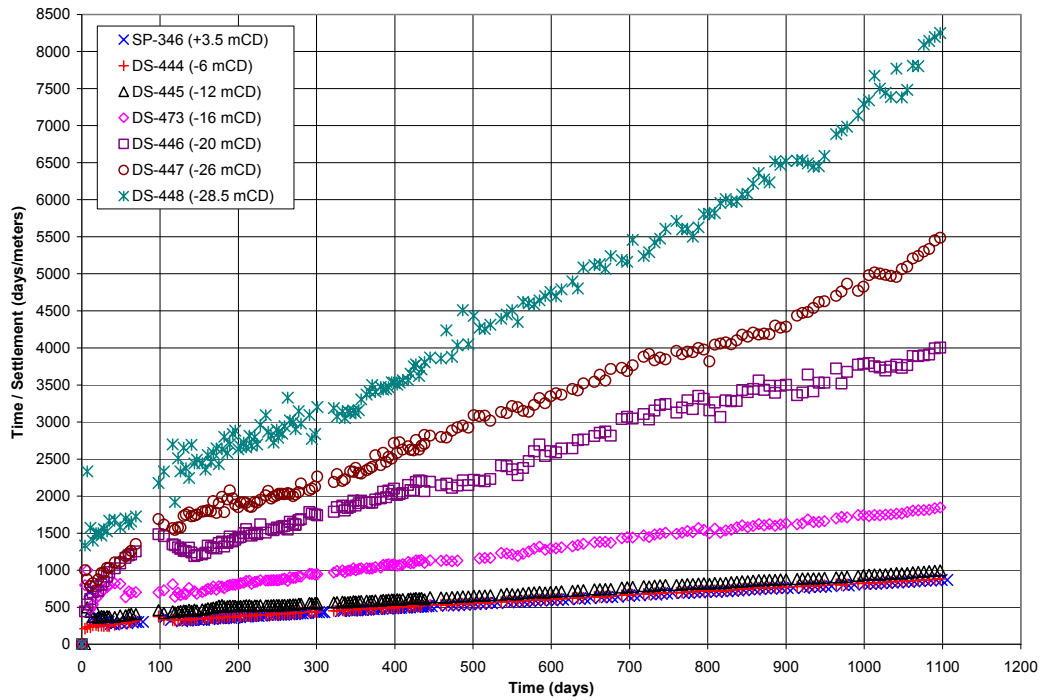


Figure 8.17 Combined Hyperbolic plot of settlement gauges at A2S-71 (2.0m x 2.0m) (Arulrajah et al., 2004g).

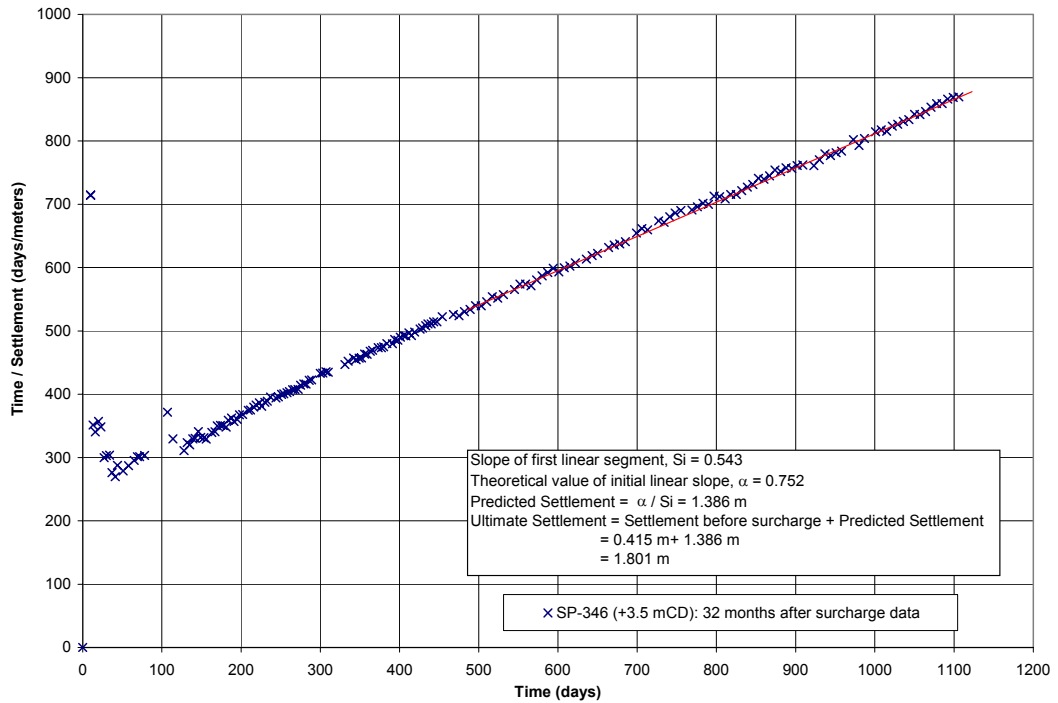


Figure 8.18 Hyperbolic plot at A2S-71 (2.0m x 2.0m) after surcharge duration of 32 months (Arulrajah et al., 2004g).

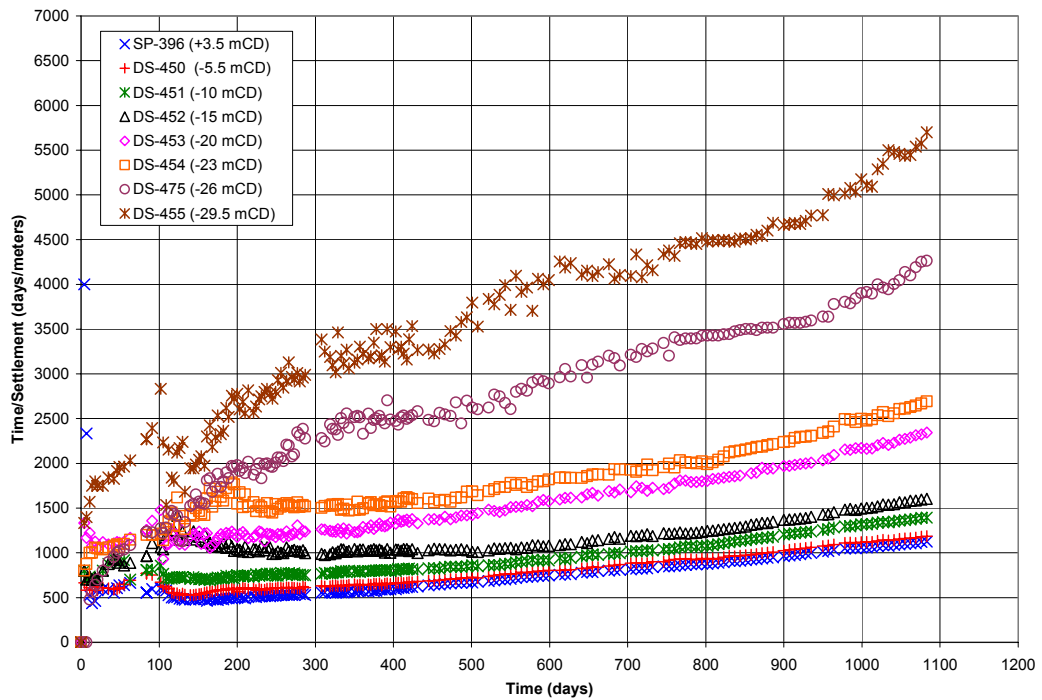


Figure 8.19 Combined Hyperbolic plot of settlement gauges at A2S-72 (2.5m x 2.5m) (Arulrajah et al., 2004g).

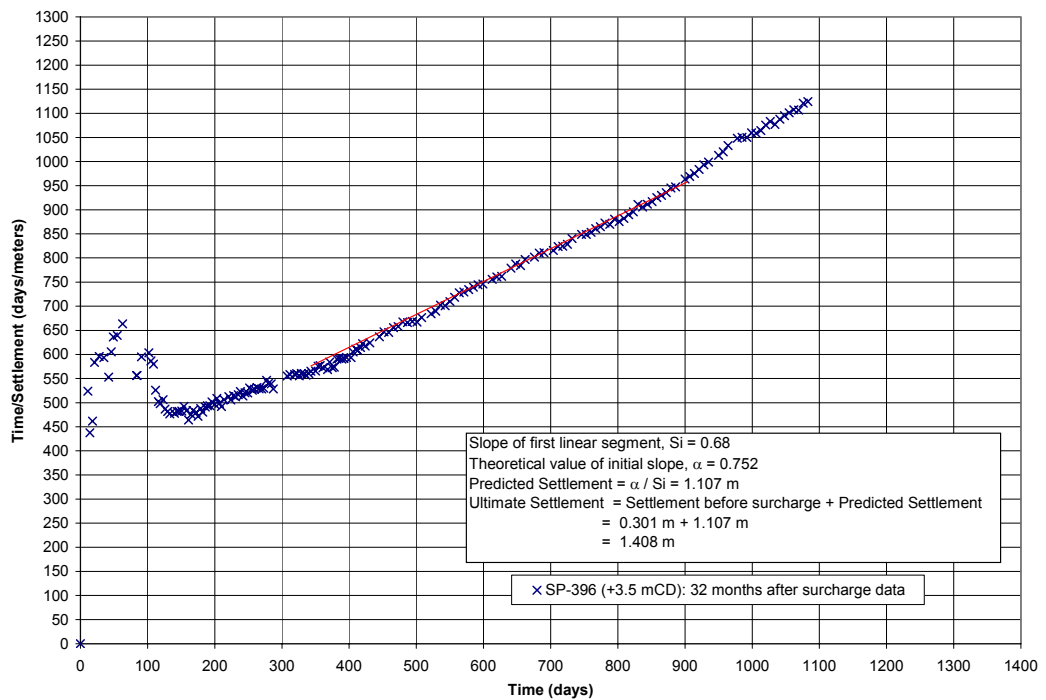


Figure 8.20 Hyperbolic plot at A2S-72 (2.5m x 2.5m) after surcharge duration of 32 months (Arulrajah et al., 2004g).

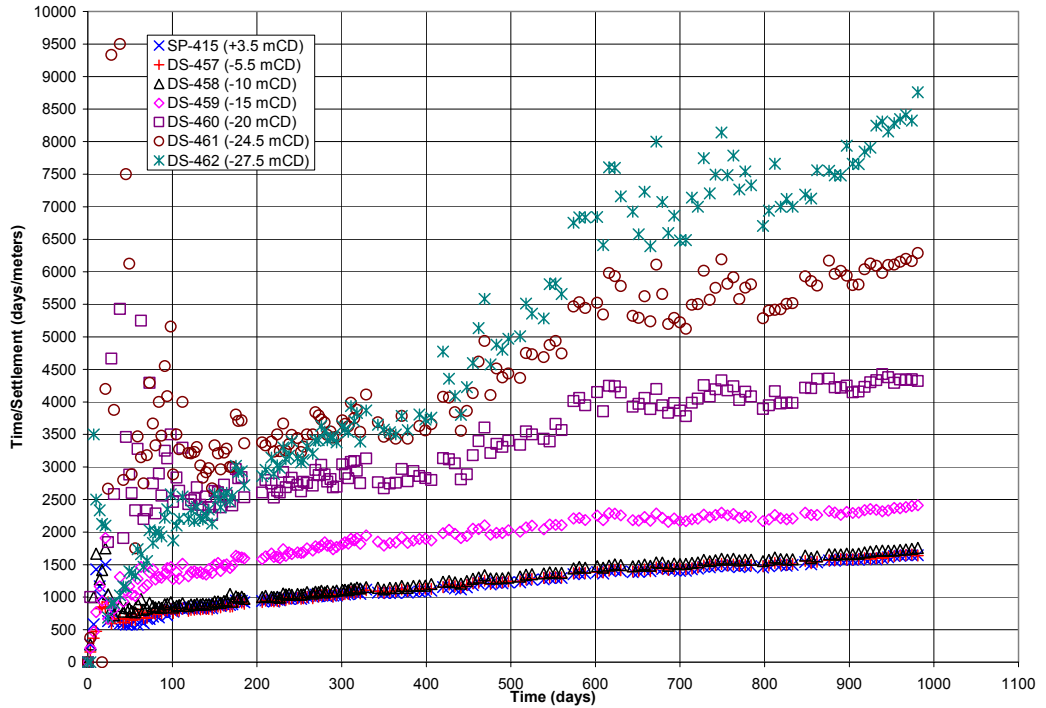


Figure 8.21 Combined Hyperbolic plot of settlement gauges at A2S-73 (3.0m x 3.0m) (Arulrajah et al., 2004g).

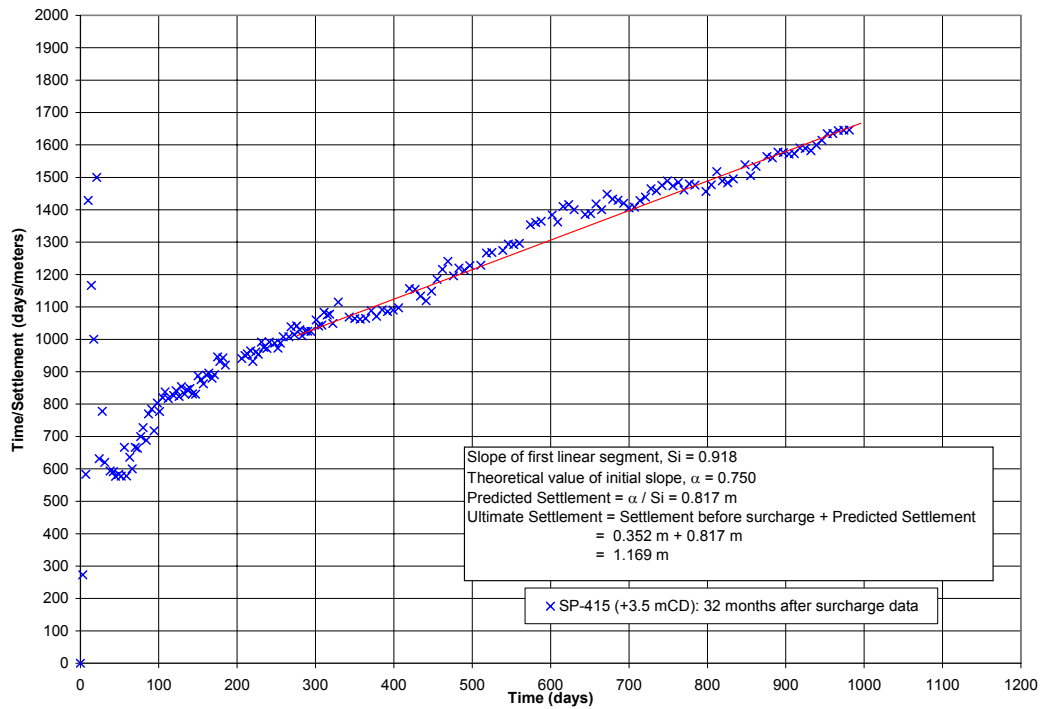


Figure 8.22 Hyperbolic plot at A2S-73 (3.0m x 3.0m) after surcharge duration of 32 months (Arulrajah et al., 2004g).

8.1.2 Analyses of Piezometers

All the piezometers indicate a marked increase in piezometric elevations and excess pore water pressures during the surcharge placement which is indicated at around the 120 to 150 day mark. This is followed by a gradual dissipation of the excess pore water pressures during the surcharge period in the sub-areas with vertical drains which indicates gaining degree of consolidation of the marine clay over time. The excess pore water pressure is derived from the difference of the total pore water pressure and the hydrostatic pore water pressure. The A2S-74 (No Drain) sub-area also indicates this trend but to a far smaller magnitude to the vertical drain treated areas.

At approximately the 1170 day mark, some piezometers pick up a slight rise in piezometric elevation and excess pore water pressures which is attributable to the surcharge placement at site of areas adjacent and close to these sub-areas. As such the piezometers are noted to be sensitive to the surcharge placement operations and the loading pressure bulbs of these adjacent areas.

Damage to piezometers is indicated by the extreme shooting-up in the piezometric elevation and excess pore water pressures readings of certain piezometers. Damage can also be indicated by a sudden loss of signal which could be attributable to damage from moving machinery.

The piezometer monitoring data for all the sub-areas have been corrected to account for the settlement of the piezometer tip.

The piezometer elevations and excess pore water pressures for the A2S-71 (2.0m x 2.0m) sub-area is shown in Figure 8.23 and Figure 8.24. The piezometer elevations and excess pore water pressures for the A2S-72 (2.5m x 2.5m) sub-area is shown in Figure 8.25 and Figure 8.26. The piezometer elevations and excess pore water pressures for the A2S-73 (3.0m x 3.0m) sub-area is shown in Figure 8.27 and Figure 8.28. The piezometer elevations and excess pore water pressures for the A2S-74 (No Drain) sub-area is shown in Figure 8.29 and Figure 8.30. In the said figures, the electric piezometers are denoted as PZ while the pneumatic piezometers are denoted as PP.

Higher excess pore pressures were recorded in the A2S-71 (2.0m x 2.0 m) and A2S-74 (no drain) sub-areas which indicates comparatively lower effective stress than the other sub-areas.

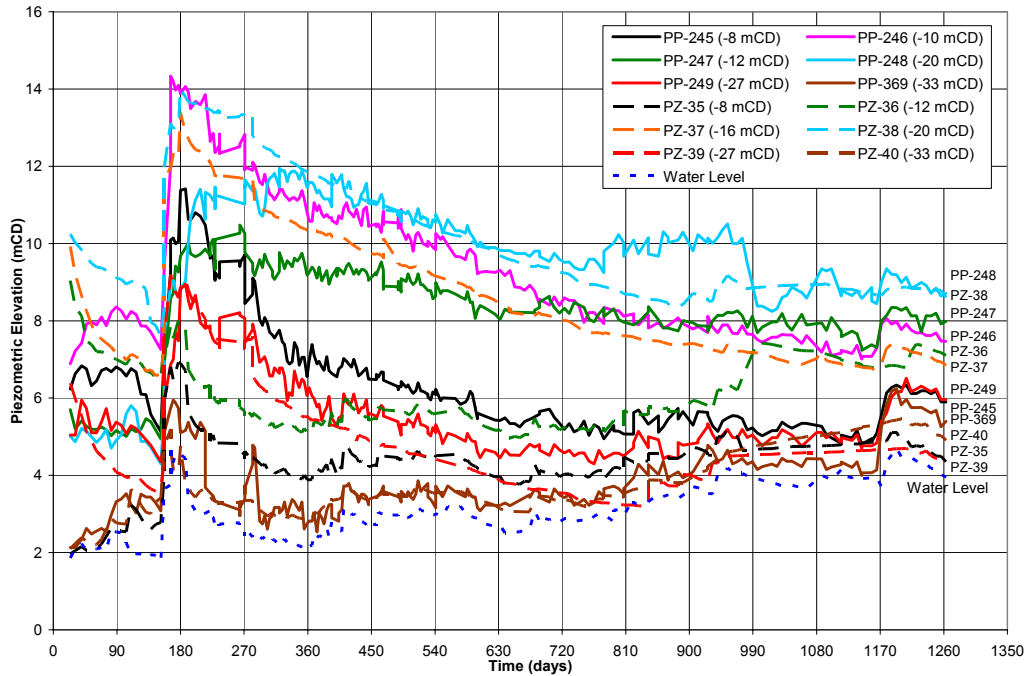


Figure 8.23 Piezometric elevations at A2S-71 (2.0m x 2.0m) (Arulrajah et al., 2004g).

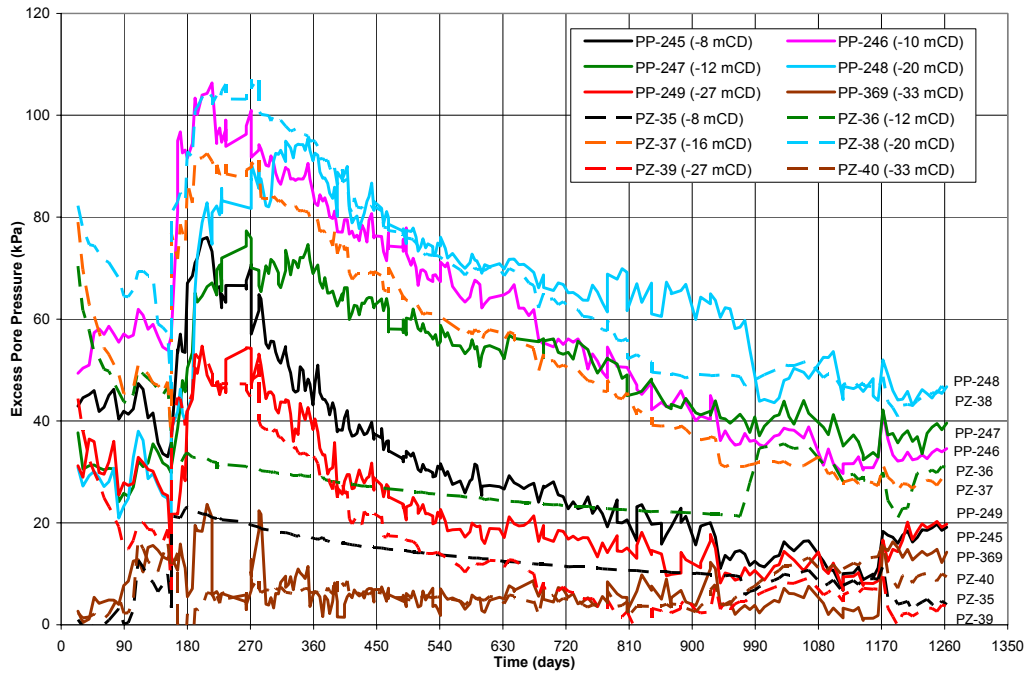


Figure 8.24 Excess pore water pressures at A2S-71 (2.0m x 2.0m) (Arulrajah et al., 2004g).

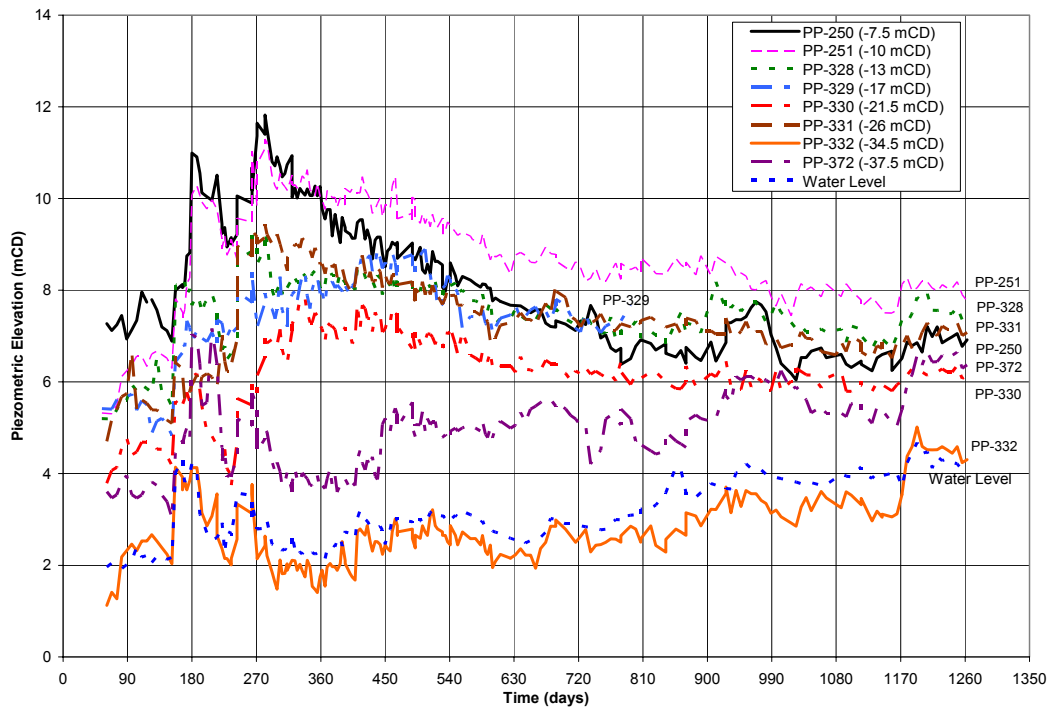


Figure 8.25 Piezometric elevations at A2S-72 (2.5m x 2.5m) (Arulrajah et al., 2004g).

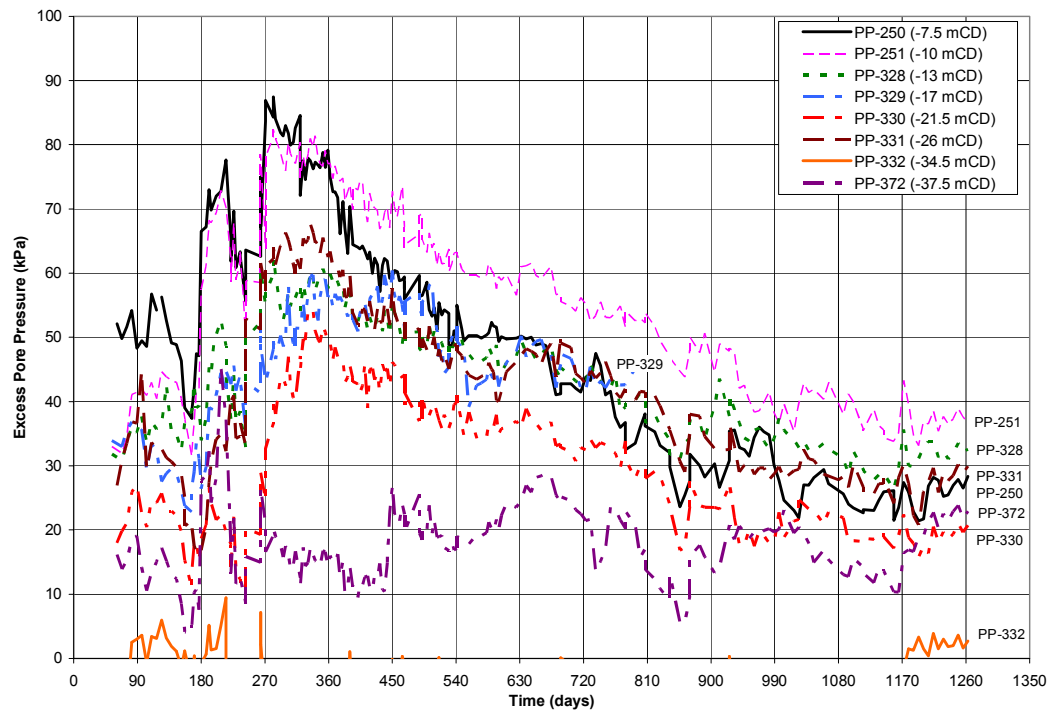


Figure 8.26 Excess pore water pressures at A2S-72 (2.5m x 2.5m) (Arulrajah et al., 2004g).

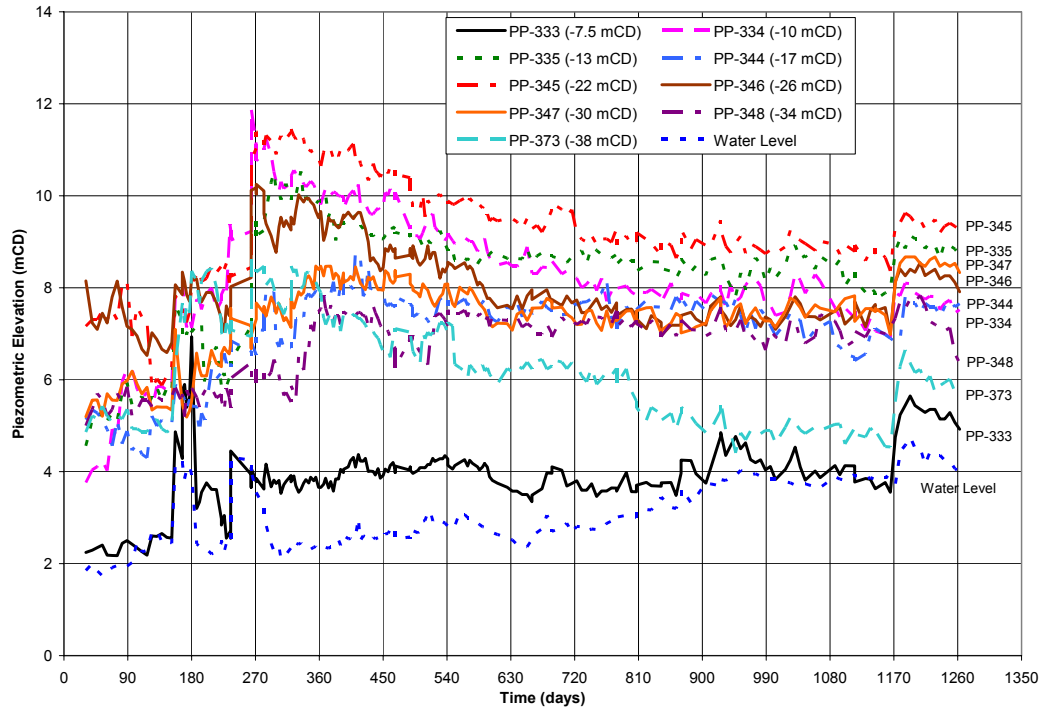


Figure 8.27 Piezometric elevations at A2S-73 (3.0m x 3.0m) (Arulrajah et al., 2004g).

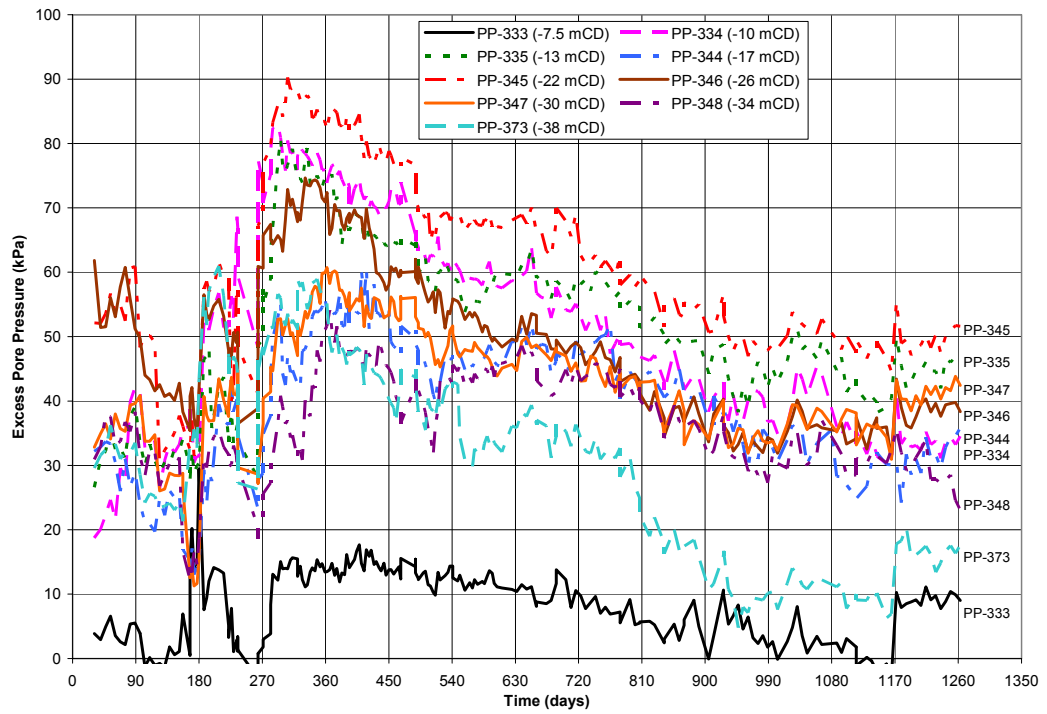


Figure 8.28 Excess pore water pressures at A2S-73 (3.0m x 3.0m) (Arulrajah et al., 2004g).

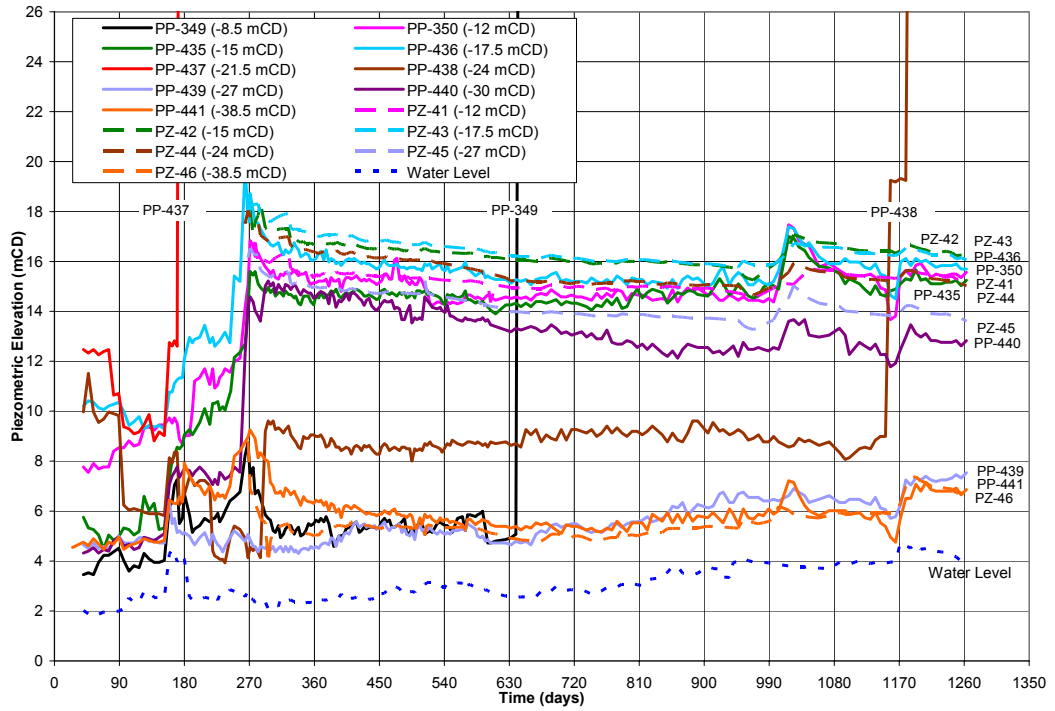


Figure 8.29 Piezometric elevations at A2S-74 (No Drain) (Arulrajah et al., 2004g).

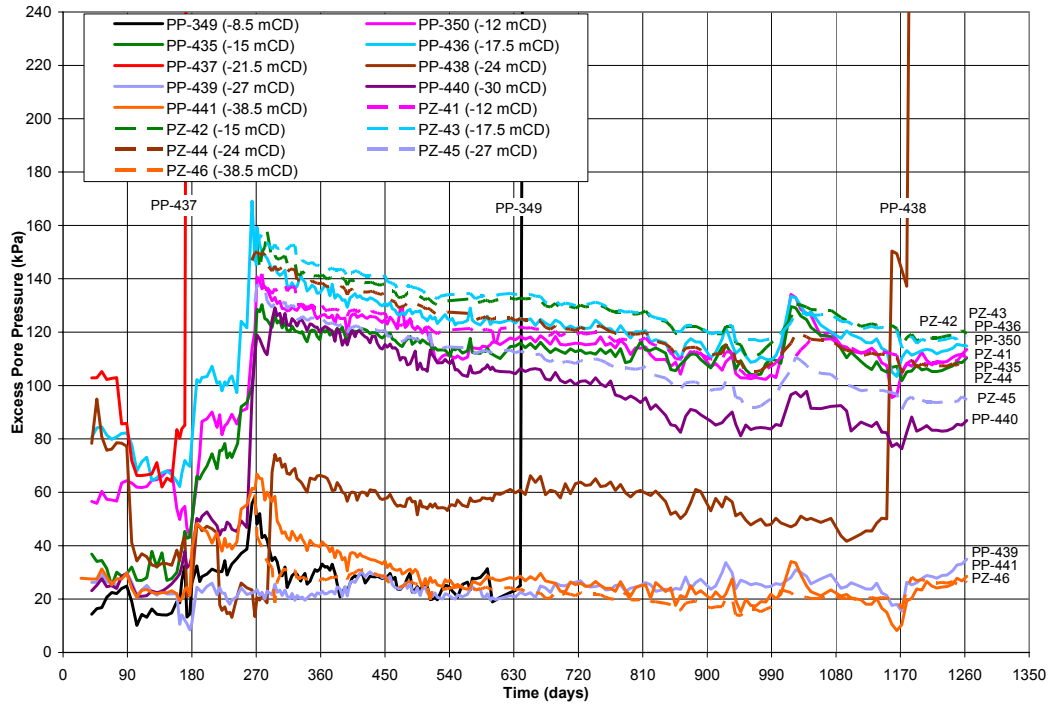


Figure 8.30 Excess pore water pressures at A2S-74 (No Drain) (Arulrajah et al., 2004g).

Figure 8.31 to 8.33 indicates the comparison of excess pore pressure isochrones between the sub-areas 12, 24 and 32 months after surcharge. Non-uniform variation of the excess pore pressure regarding elevation is due to slight difference in the installed location of the piezometer from the vertical drains as well as the presence of thin sand lenses (so-called microlayers).

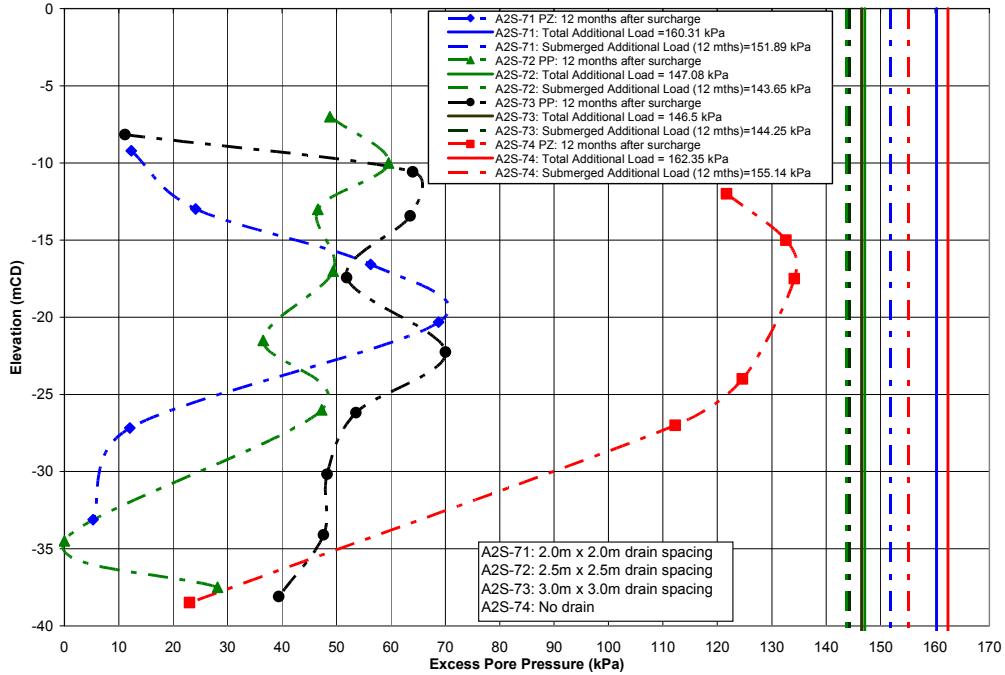


Figure 8.31 Comparison of piezometer excess pore pressure isochrones between sub-areas 12 months after surcharge.

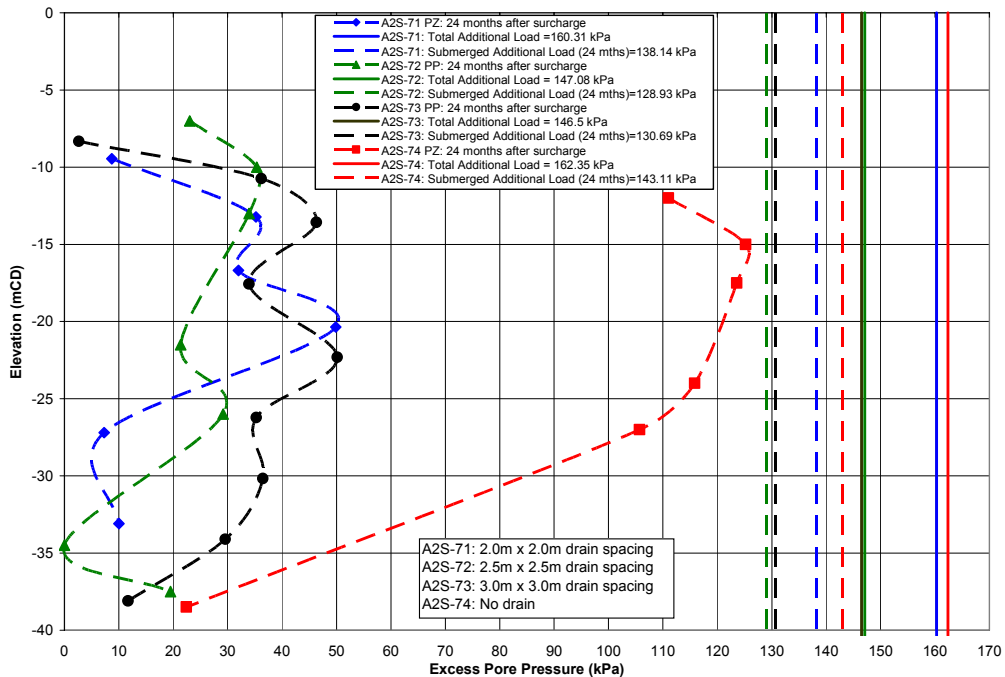


Figure 8.32 Comparison of piezometer excess pore pressure isochrones between sub-areas 24 months after surcharge

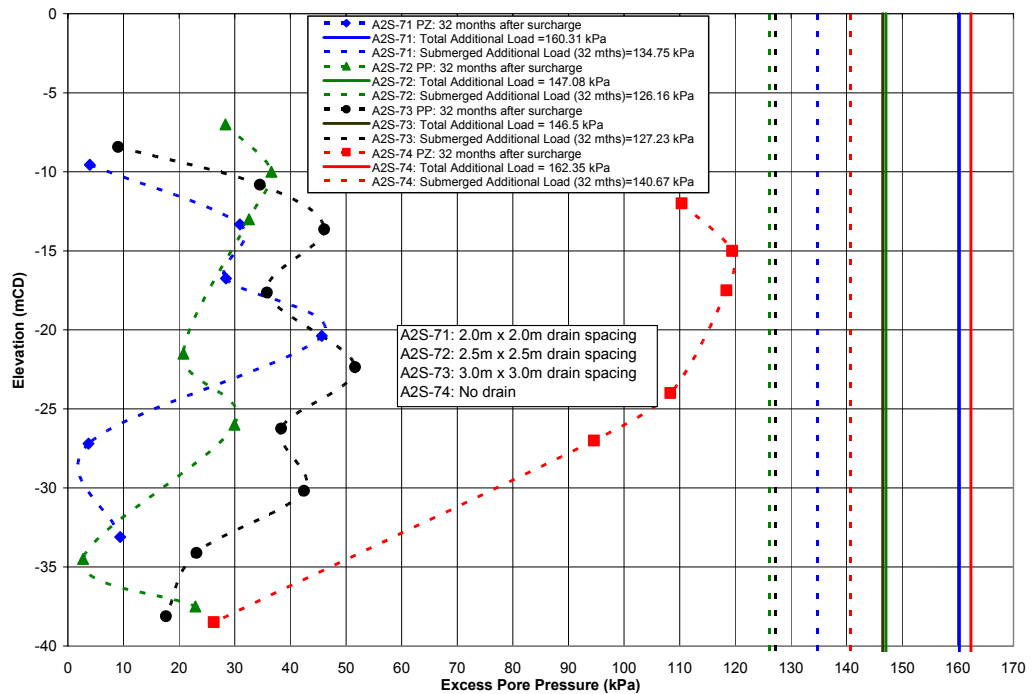


Figure 8.33 Comparison of piezometer excess pore pressure isochrones between sub-areas 32 months after surcharge (Arulrajah et al., 2004g).

Figure 8.34 indicates the comparison of excess pore pressure isochrones between the sub-areas various periods after surcharge. Figure 8.35 indicates the comparison of degree of consolidation between the sub-areas 32 months after surcharge. Relatively rapid dissipation of excess pore water pressure with time is clearly evident in the vertical drain treated sub-areas as compared to the No Drain sub-area. The sub-area with the closer vertical drain spacing is found to generally register the higher degree of consolidation at a particular elevation. Some exceptions to this is found at certain elevation which could be due to the slightly varying soil profiles that exist between the various sub-areas. Furthermore, the presence of sand seams in the marine clay will increase the permeability of the marine clay and enable the excess pore water pressure in it to drain relatively rapidly.

The piezometers installed close to the reclamation sand boundary close to the top of the marine clay are found to register increasingly lower excess pore water pressure with time and thus higher degree of consolidation, which is due to it being installed close to the drainage boundary. Piezometers installed close to the dense sand layer at the bottom of the marine clay is also found to register increasingly lower excess pore water pressure with time and thus higher degree of consolidation, confirming that there is bottom drainage of excess pore water pressure into the permeable sand layer. Evidently from the findings of the figures, the degree of consolidation is highest at the sub-area with the closest vertical drain spacing and lowest for the No Drain sub-area. The summary of the degree of consolidations for the

various sub-areas will be reported later in the section 8.1.4 when the piezometer readings are compared with the settlement plate readings.

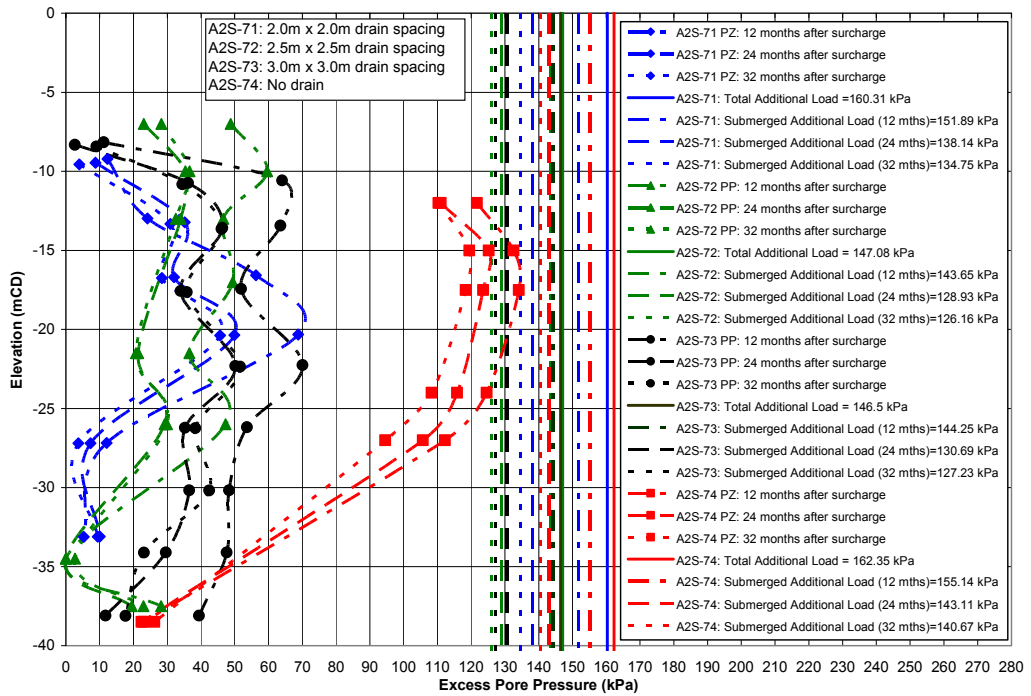


Figure 8.34 Comparison of piezometer excess pore pressure isochrones between sub-areas various periods after surcharge.

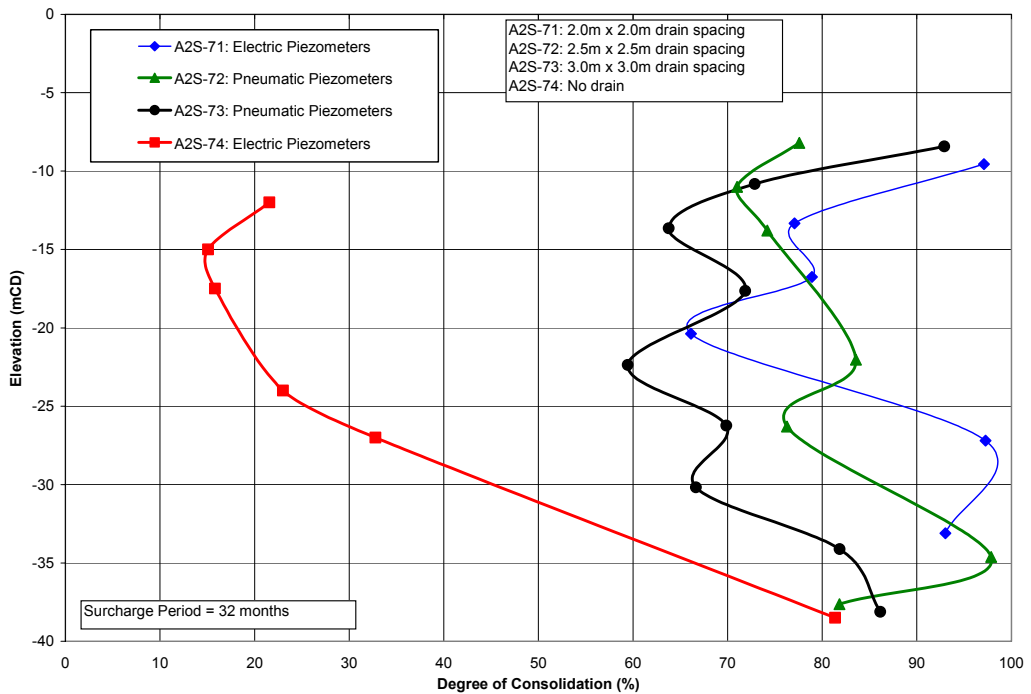


Figure 8.35 Comparison of degree of consolidation between sub-areas 32 months after surcharge (Arulrajah et al., 2004g).

8.1.3 Comparison between Electric and Pneumatic Piezometers

The performance of the electric (PZ) and pneumatic (PP) piezometers installed in marine clay in the Pilot Test Site was studied and has been reported by the author during the course of this research (Arulrajah et al., 2004). The results obtained from the two types of piezometers were compared to ascertain the performance of the piezometers installed in the marine clay and subject to the reclaimed fill load and surcharge load. The piezometers were compared for the A2S-71 (2.0 m x 2.0 m) and A2S-74 (No Drain) sub-areas where the two types of piezometers were both installed at the same elevations in the marine clay for comparison purposes. The excess pore pressure isochrones obtained from the piezometers monitoring data were compared at various periods of time after the placement of surcharge. Both the electric and pneumatic piezometer readings were corrected for the settlement of the piezometer tip.

Figure 8.36 indicates the cross-sectional profile showing piezometer locations at the A2S-71 (2.0 m x 2.0 m) and A2S-74 (No Drain) sub-areas. Figure 8.37 indicates the comparison of the excess pore pressure isochrones from electric and pneumatic piezometers monitoring data among the sub-areas at 12, 24 and 32 months after surcharge. Figure 8.38 shows the comparison of the excess pore pressure isochrones at the various time intervals after surcharge placement. Figure 8.39 indicates the comparison of degree of consolidation between pneumatic and electric piezometers for the various piezometer elevations 32 months after surcharge.

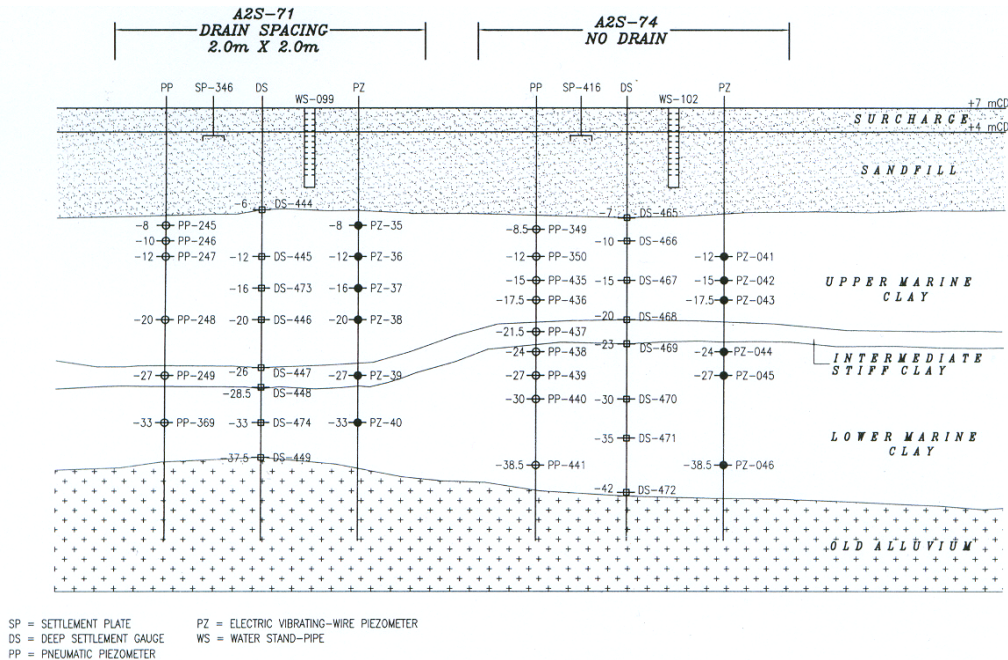


Figure 8.36 Cross-sectional profile showing piezometer locations at the A2S-71 (2.0 m x 2.0 m) and A2S-74 (No Drain) sub-areas (Arulrajah et al., 2004).

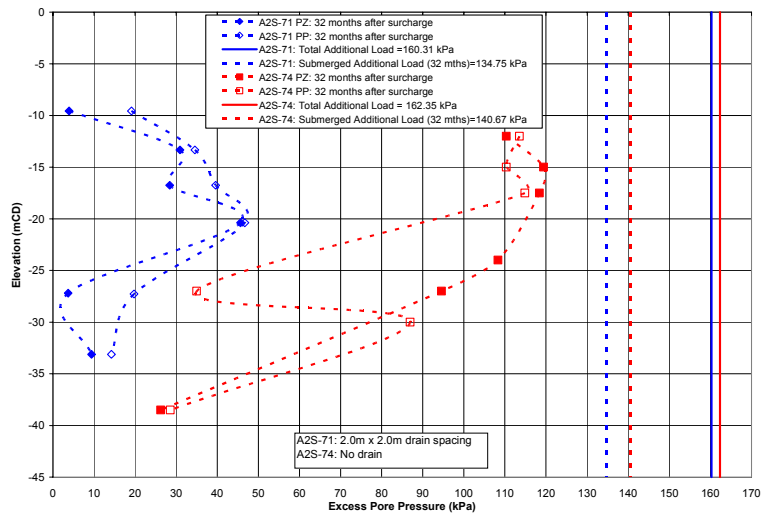
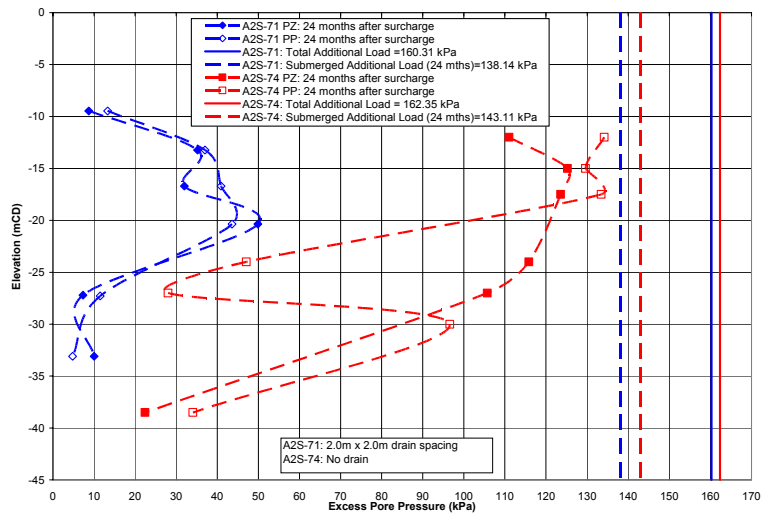
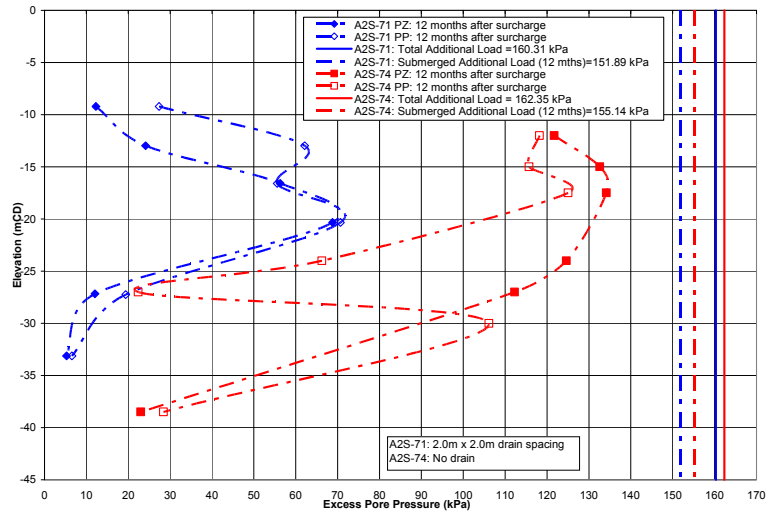


Figure 8.37 Comparison between electric (PZ) and pneumatic (PP) piezometer excess pore pressure isochrones at 12, 24 and 32 months after surcharge (Arulrajah et al., 2004).

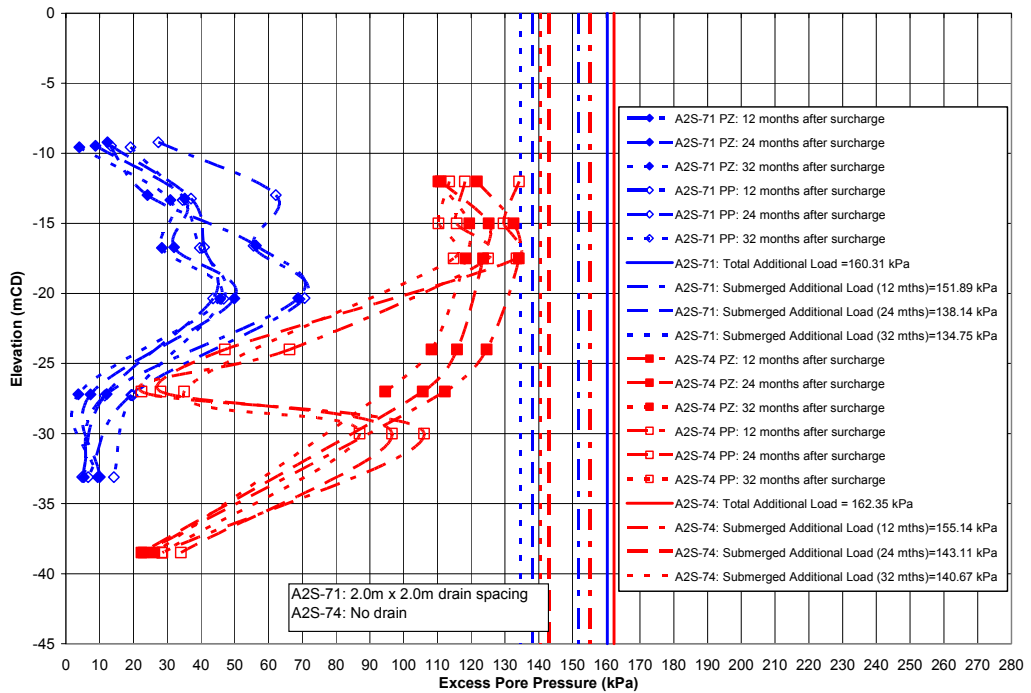


Figure 8.38 Comparison between electric (PZ) and pneumatic (PP) piezometer excess pore pressure isochrones at various periods after surcharge (Arulrajah et al., 2004).

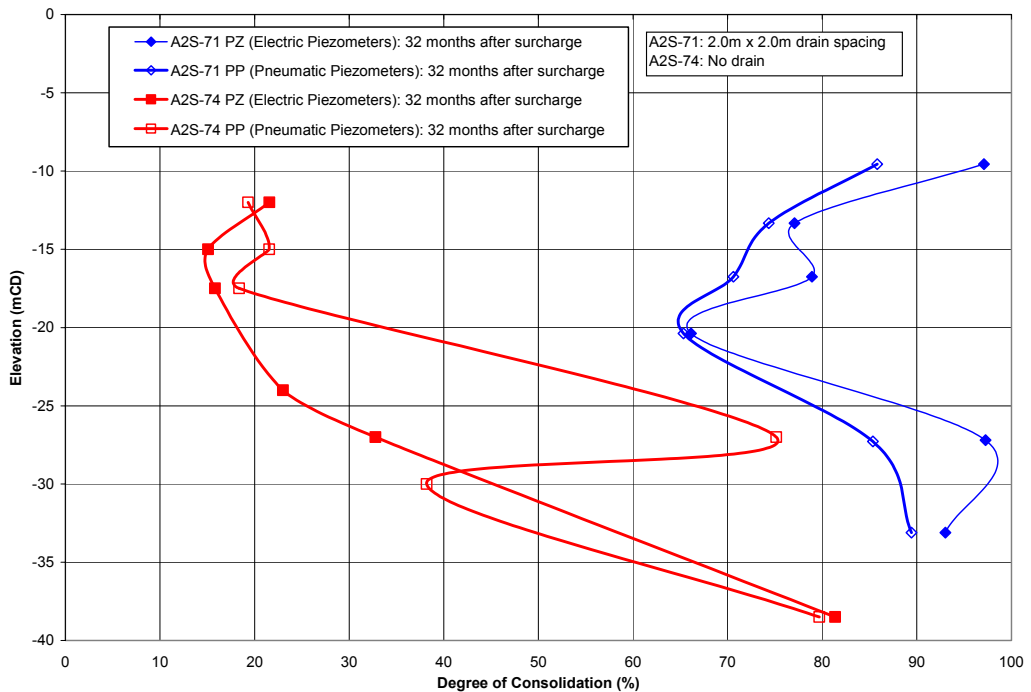


Figure 8.39 Comparison of degree of consolidation between electric (PZ) and pneumatic (PP) piezometer 32 months after surcharge (Arulrajah et al., 2004).

The comparison of the excess pore pressure isochrones indicate that in the vertical drain treated sub-area A2S-71(2.0 m x 2.0 m), electric piezometers consistently provide a lower excess pore pressure than the pneumatic piezometers installed at the same corresponding elevation. The shape of the excess pore pressure isochrones of the two types of piezometers are of the same trend in the various sub-layers thus indicating that the measurement of the excess pore pressures by the piezometers are consistent for both types of piezometers at the same corresponding elevation.

In the untreated sub-area A2S-74 (No Drain), the lower elevation pneumatic piezometer provides lower excess pore pressure than the electric piezometers installed at the same corresponding elevation. However, at deeper elevations, the electric piezometer is found to provide lower excess pore pressures. In this location, the shape of the excess pore pressure isochrones of the two types of piezometers are generally of the same trend in the various sub-layers. This indicates that the measurement of the excess pore pressures by the piezometers are consistent for both types of piezometers at the same corresponding elevation. It is to be noted that the pneumatic piezometer at the elevation of -27 mCD has been installed in a layer with sand seams or a sandy layer due to the very low excess pore water pressure at that elevation.

The comparisons of the degree of consolidation indicate that in the vertical drain treated sub-area A2S-71(2.0m x 2.0m), electric piezometers generally provides a higher degree of consolidation than the pneumatic piezometers installed at the same corresponding elevation. The shape of the degree of consolidation isochrones of the two types of piezometers are of the same trend in the various sub-layers, thus indicating that the measurement of the degree of consolidation are consistent for both types of piezometers at the same corresponding elevation.

In the untreated sub-area A2S-74 (No Drain), the shallower elevation pneumatic piezometer generally registers higher degree of consolidation than the electric piezometers installed at the same corresponding elevation. However at deeper elevations, the electric piezometer is found to register higher degree of consolidation. The shape of the degree of consolidation isochrones of the two types of piezometers are generally of the same trend in the various sub-layers indicating that the measurement of the degree of consolidation are consistent for both types of piezometers at the same corresponding elevation.

Table 8.2 below summarises the degree of consolidation of the sub-areas based on the isochrones of the electric piezometers at various periods after surcharge placement. The electric piezometer indicates that at the end of the surcharging period of 32 months, the sub-area with the vertical drains (A2S-71: 2.0 x 2.0) has achieved a degree of consolidation of 86.2 % while the untreated sub-area (A2S-74) has achieved a degree of consolidation of only 37.0 %. Dissipation of excess pore water pressure readings is faster in the vertical drain treated sub-area. This indicates that the vertical drains installed in the project are performing to improve the soil drainage system.

Table 8.2 Comparison of average degree of consolidation using electric piezometers at various periods after surcharge placement.

Sub-Area	Electric Piezometers	12 mths.	24 mths.	32 mths.
A2S-71 (2.0m x 2.0m)	Degree of Consolidation, U (%)	79.7	83.0	86.2
A2S-74 (No Drain)	Degree of Consolidation, U (%)	35.3	35.5	37.0

The findings of the comparison between pneumatic and electric piezometers indicate that there is reasonable agreement in readings between the two types of piezometers. As such, either type of piezometer can be used for the monitoring of the marine clay behaviour under reclaimed fills. The slight variations could be due to differences in the soil stratification or the sensitivity of the piezometer.

8.1.4 Comparison of Degree of Consolidation and c_h between Sub-Areas

Table 8.3 summarises the comparison of degree of consolidation between the settlement plates and piezometers at the various sub-areas 32 months after surcharge. The degree of consolidation of the vertical drain treated sub-areas is far greater than that of the No Drain sub-area.

The Asaoka method indicates that the sub-area with the closest vertical drain spacing has attained the highest degree of consolidation for the various surcharging durations. At the end of the surcharging period of 32 months, the sub-area with the closest vertical drain spacing (A2S-71: 2.0 x 2.0) has achieved a degree of consolidation of 91.8 % while that with the furthest vertical drain spacing (A2S-73: 3.0 x 3.0) has achieved a degree of consolidation of 79.0 %. The study reveals that the c_h value of the marine clay, as defined in chapter 7, is lowest at the sub-area with the closest vertical drains spacing (A2S-71: 2.0 x 2.0) and highest at the sub-area with the furthest vertical drain spacing (A2S-73: 3.0 x 3.0). This can be

attributed to the higher degree of smear effect at locations with closer drain spacing. However reduction of c_h with time is due to reduction of void ratio as consolidation progress.

Table 8.3 Comparison of Asaoka, Hyperbolic and piezometer methods at Pilot Test Site 32 months after surcharge - 41.9 months of monitoring (Arulrajah et al., 2004g).

Sub-Area	Comparison	Asaoka	Hyperbolic	Piezometer
A2S-71 2.0 x 2.0 m	Ultimate Settlement (m)	1.838	1.801	-
	Settlement to date (m)	1.687	1.687	-
	Degree of Consolidation, U (%)	91.8	93.7	86.2
	Back-Analysed c_h (m ² /year)	1.08	-	1.30
A2S-72 2.5 x 2.5 m	Ultimate Settlement (m)	1.412	1.408	-
	Settlement to date (m)	1.264	1.264	-
	Degree of Consolidation, U (%)	89.5	89.8	82.5
	Back-Analysed c_h (m ² /year)	1.22	-	1.94
A2S-73 3.0 x 3.0 m	Ultimate Settlement (m)	1.200	1.169	-
	Settlement to date (m)	0.948	0.948	-
	Degree of Consolidation, U (%)	79.0	81.1	73.1
	Back-Analysed c_h (m ² /year)	2.20	-	2.23
A2S-74 No Drain	Degree of Consolidation, U (%)	-	-	37.0

The Hyperbolic method indicates that at the end of the surcharging period of 32 months, the sub-area with the closest vertical drain spacing (A2S-71: 2.0 x 2.0) has achieved a degree of consolidation of 93.7 % while that with the furthest vertical drain spacing (A2S-73: 3.0 x 3.0) has achieved a degree of consolidation of 81.1 %.

Normally, for the same surcharge and the same thickness of clay, the same amount of ultimate settlement is obtained after a long time. However, in the Pilot Test Site, variations in the final predicted settlements is due to variation of soil profile at the various sub-areas. In addition higher excess pore pressure was recorded in the A2S-71 (2.0m x 2.0 m) and A2S-74 (no drain) sub-areas which indicates comparatively lower effective stress than the other sub-areas. Furthermore, settlement of the sub-areas prior to the installation of instruments will also result in variations in the settlement measured after installation of instruments.

The piezometer indicates that at the end of the surcharging period of 32 months, the sub-area with the closest vertical drain spacing (A2S-71: 2.0 x 2.0) has achieved a degree of consolidation of 86.2 % while the untreated sub-area (A2S-74) has achieved a degree of consolidation of only 37.0 %.

The piezometer monitoring data indicates that the c_h value of the marine clay is lowest at the sub-area with the closest vertical drains spacing (A2S-71: 2.0 x 2.0) and highest at the sub-area with the furthest vertical drain spacing (A2S-73: 3.0 x 3.0). This is in similar agreement with the c_h values back-calculated by the Asaoka method and confirms the higher degree of smear effect at locations with closer drain spacing. However reduction of c_h with time is due to reduction of void ratio as consolidation progress.

8.1.5 Findings for Field Instrumentation of Pilot Test Site

The magnitude of settlement and thereby degree of consolidation is highest in sub-area A2S-71 (2.0 x 2.0 m) which has the closest vertical drain spacing and lowest in A2S-74 (No Drain). Similarly, dissipation of excess pore water pressure readings is evidently faster in the closer spacing vertical drain treated sub-area. This indicates that the vertical drains installed in the project are performing to improve the soil drainage system.

The ultimate settlement and degree of consolidation obtained by the Asaoka and Hyperbolic methods is found to converge to be in excellent agreement with each other after the surcharge period of 32 months. The degree of consolidation predicted by the Hyperbolic method is found to be slightly higher than that of the Asaoka method, as illustrated in Table 8.3.

The piezometer indicates lower degree of consolidation as compared to field settlement predictions. Similar findings for lower piezometer readings compared to field settlement predictions have been reported by Bo et al. (1999). This can be attributable to the possible pinching of the piezometer cables due to the large strain settlements of the reclaimed fill.

The degree of consolidation of the Pilot Test Site, as obtained by the Asaoka, Hyperbolic and Piezometer methods is summarised as follows:

Sub-area A2S-71 (2.0 x 2.0 m) had attained a degree of consolidation of about 93 %.

Sub-area A2S-72 (2.5 x 2.5 m) had attained a degree of consolidation of about 90 %.

Sub-Area A2S-73 (3.0 x 3.0 m) had attained a degree of consolidation of about 80%.

Sub-Area A2S-74 (No Drain) had attained a degree of consolidation of about 37.0 %.

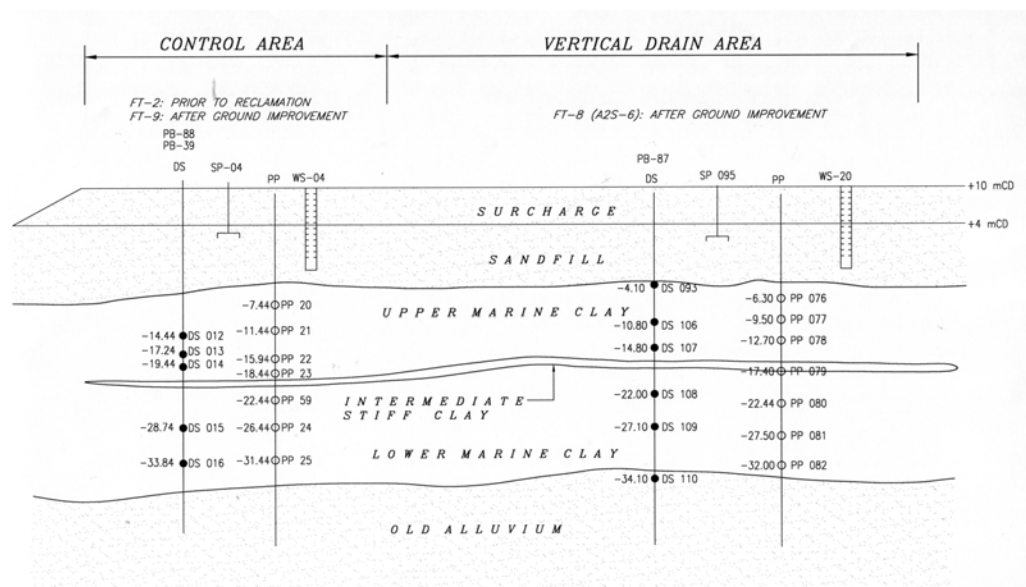
The c_h values back-calculated by the Asaoka and piezometer methods 32 months after surcharge placement is found to be in good agreement. The Asaoka and piezometer methods indicate that the back-analysed c_h value of the marine clay is lowest at the sub-area with the closest vertical drains spacing (A2S-71: 2.0 x 2.0) and highest at the sub-area with the furthest vertical drain spacing (A2S-73: 3.0 x 3.0). This can be attributed to the higher degree of smearing effect at locations with closer drain spacing. However reduction of c_h with time is interpreted to be due to reduction of void ratio as consolidation progress.

For soft marine clay, the smear effect can be quite significant at locations installed with vertical drains (Chu et al., 2002). Bo et al. (1998b) has reported that the permeability of soil in the smear zone could be reduced by 1 order of magnitude or to the horizontal hydraulic conductivity of the remoulded clay as a result of the smearing. When drains are installed at close spacing, the back-calculated c_h values will generally be greatly influenced by this smear zone (Chu et al., 2002).

At the Pilot Test Site, the findings of the comparison between pneumatic and electric piezometers indicate that there is reasonable agreement in readings between the two types of piezometers. As such either type of piezometer can be used for the monitoring of the marine clay behaviour under reclaimed fills. A proper protective guard cell is required for the pneumatic piezometer to counter for the effect of possible pinching of the piezometer cable due to the large strain settlements of the reclaimed fill.

8.2 FIELD INSTRUMENTATION OF MARINE CLAY CASE STUDY: IN-SITU TEST SITE

The location of the second instrumentation case study is the same location as that of the In-Situ Test Site described earlier in Chapter 6. Field instruments comprising of surface settlement plates, deep settlement gauges, pneumatic piezometers and water stand-pipes were installed and monitored at both the Vertical Drain Area and the untreated Control Area. The instruments in the Control Area were installed prior to reclamation in an off-shore instrument platform. The Control Area was not treated with vertical drains. These instruments were protected as the reclamation filling works commenced in the area. Instruments in the Vertical Drain Area were installed on-land at the vertical drain platform level of +4 mCD just before or soon after vertical drain installation at 1.5 meter square spacing. Surcharge was placed at this case study area to the elevation of +10 mCD for both the Vertical Drain Area as well as the Control Area. The construction sequence for both these areas are identical as sand pumping operations were carried out for the entire case study area. The analysis of the instrumentation results was carried out for both the Vertical Drain Area and Control Area after a monitoring period of about 26 months which equates to a surcharging period of 20 months. The profile of the instrument elevations at the In-Situ Test Site is shown in Figure 8.40 while Figures 8.41 and 8.42 indicate the instrument elevations. The field instrumentation case study at the In-Situ Test Site described in this chapter has been discussed in detail by the author (Arulrajah et al., 2003b, 2004b, 2004c) during the course of this research study.



SP = Settlement Plate, DS = Deep Settlement Gauge, PP = Pneumatic Piezometer, WS = Water Stand-Pipe

Figure 8.40 Cross Sectional soil profile showing field instrumentation elevations at the In-Situ Test Site (Arulrajah et al., 2004b).

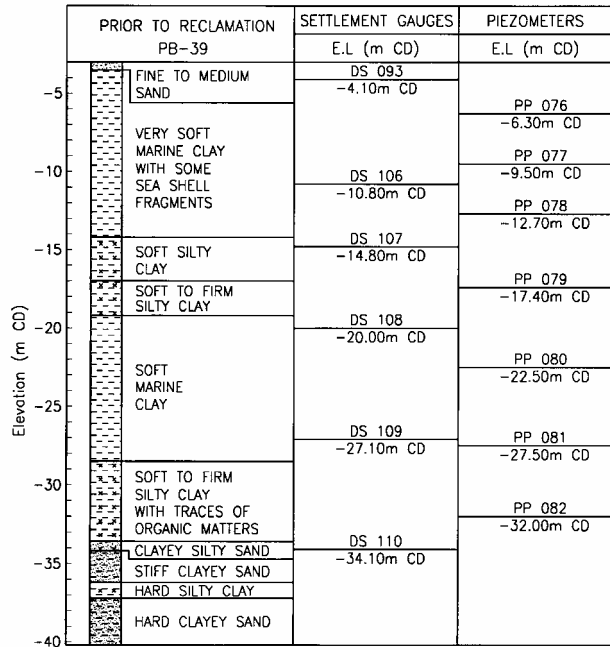


Figure 8.41 Instrument elevations in Vertical Drain Area.

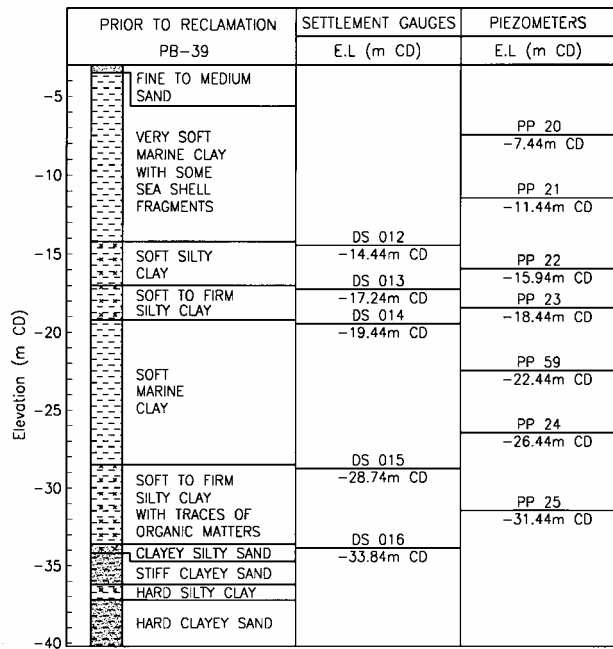


Figure 8.42 Instrument elevations in Control Area.

8.2.1 Analyses of Settlement Gauges

The surface settlement plate which was installed at the vertical drain platform level for the Vertical Drain Area and the deep settlement gauge which was installed at the top surface of the compressible marine clay gave similar readings for magnitude and time rate of settlement. This indicates that the settlement contribution of the sandfill layer is minimal as also indicated in the Pilot Test Site. The deep settlement gauges that were installed in the different sub-layers indicate decreasing settlement with depth as would be expected.

Figure 8.43 compares the settlement plate results between the Vertical Drain Area and Control Area. The vast improvement of the Vertical Drain Area as compared to the untreated Control Area is clearly evident in Figure 8.43. This indicates that the vertical drains are functioning as per their requirements at the In-Situ Test Site.

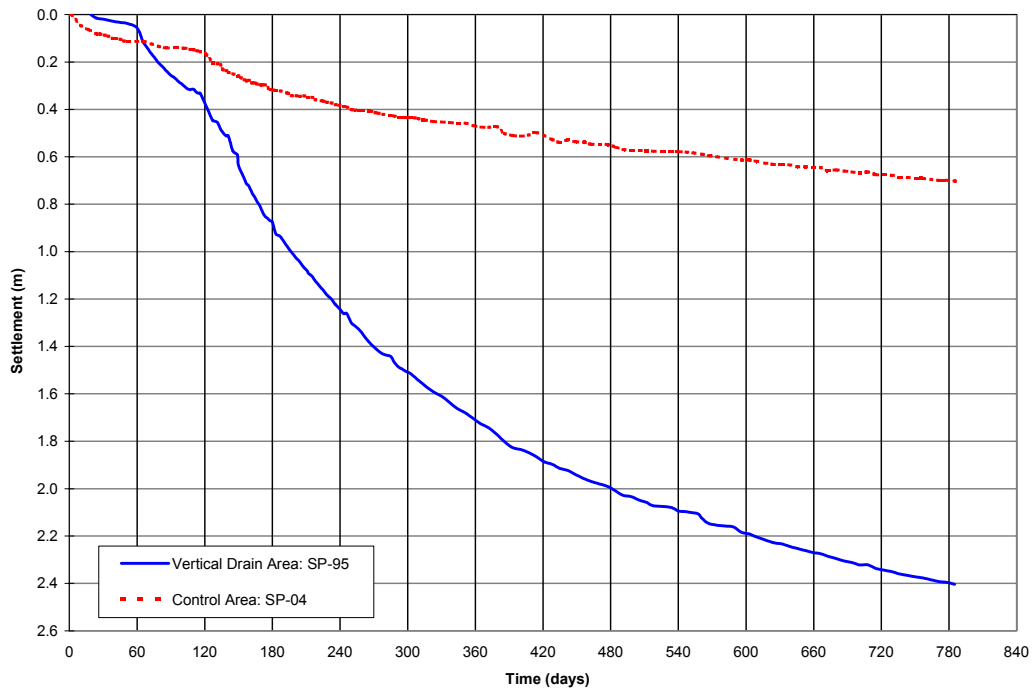


Figure 8.43 Comparison of field settlement between Vertical Drain Area and Control Area (Arulrajah et al., 2004b).

Figure 8.44 compares the field settlement isochrones between the Vertical Drain Area and Control Area. The settlement isochrones confirm that the Vertical Drain Area registers higher settlements than the Control Area. The settlement isochrones indicate the trend of decreasing settlement for the deeper settlement gauges which is due to the marine clay increasing with density, stiffness, compression parameters and strength with depth.

It was found that the settlement plates (SP-95) and the deep settlement gauge (DS-93) that were installed at the original seabed level gave similar reading for the magnitude and rate of settlement. The deep settlement gauges that were installed in the different sub-layers indicate decreasing settlement with depth as would be expected.

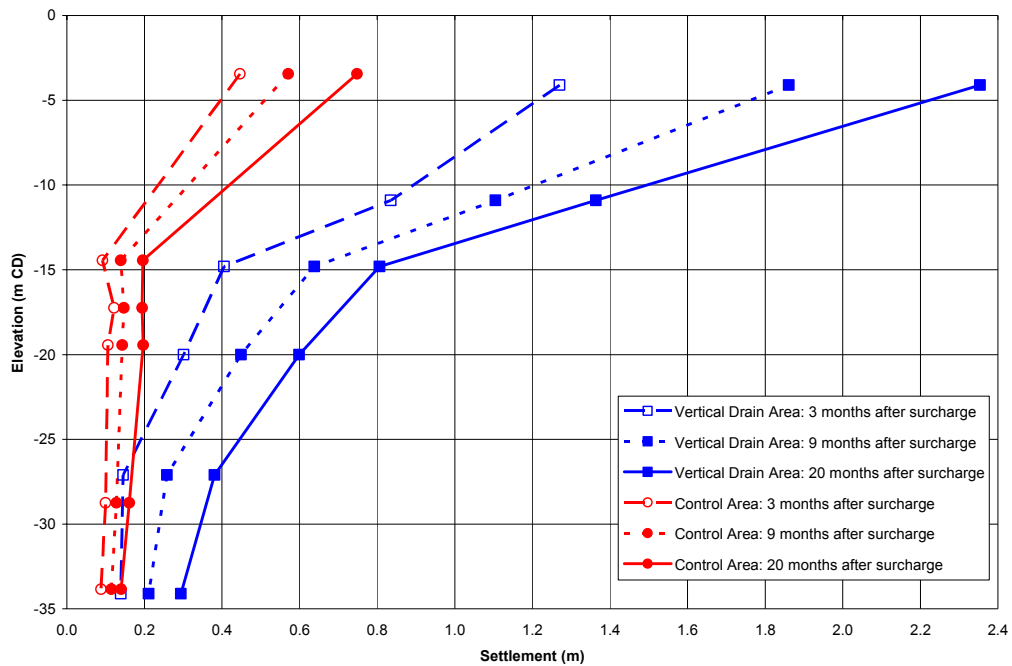


Figure 8.44 Comparison of field settlement isochrones between Vertical Drain Area and Control Area (Arulrajah et al., 2004c).

Figures 8.45 and 8.46 indicate the magnitudes of settlements in the Vertical Drain Area and the Control Area. As expected, the Vertical Drain Area indicated much higher settlement readings as compared to the Control Area due to the soil improvement works. This indicates that the vertical drains are functioning as per their requirements.

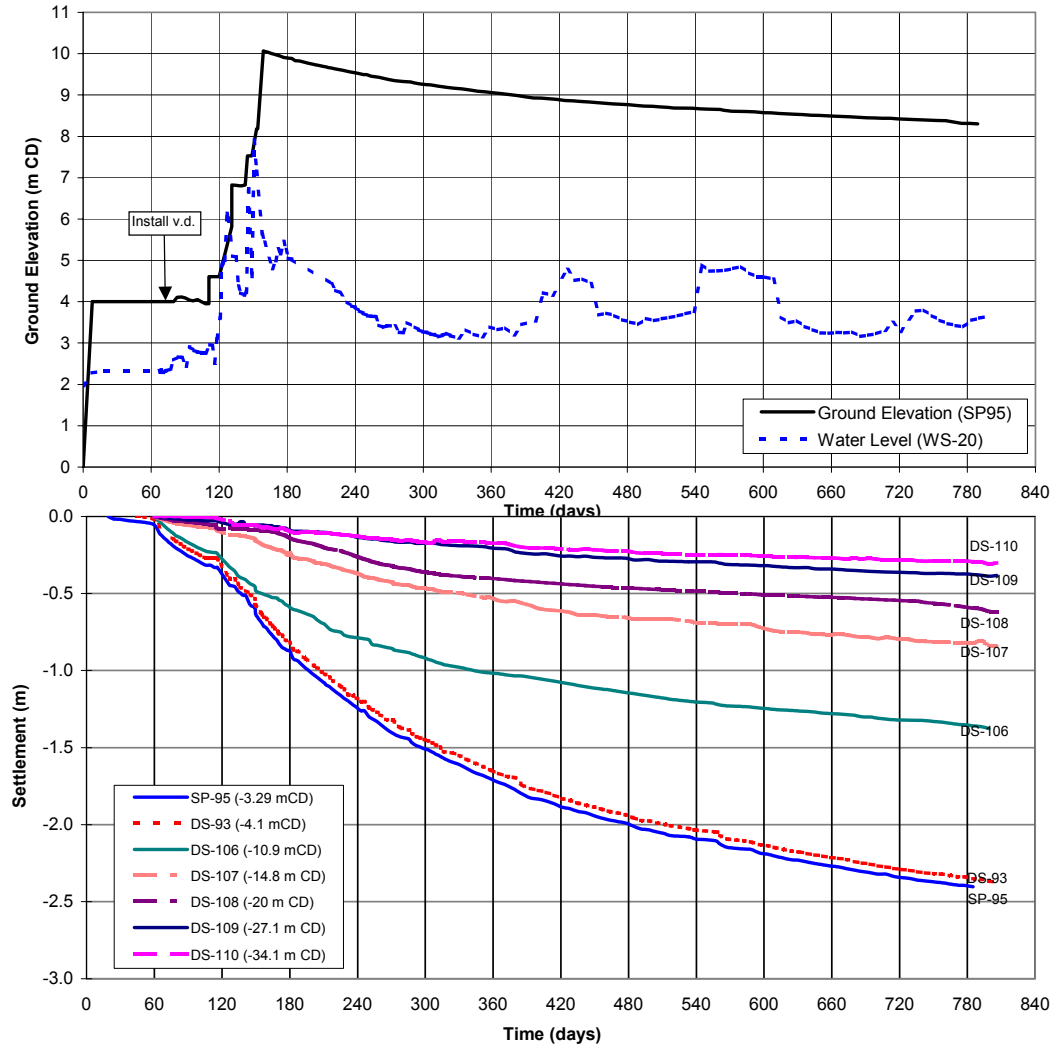


Figure 8.45 Field settlement results of settlement gauges at Vertical Drain Area (1.5m x 1.5 m) (Arulrajah et al., 2004b).

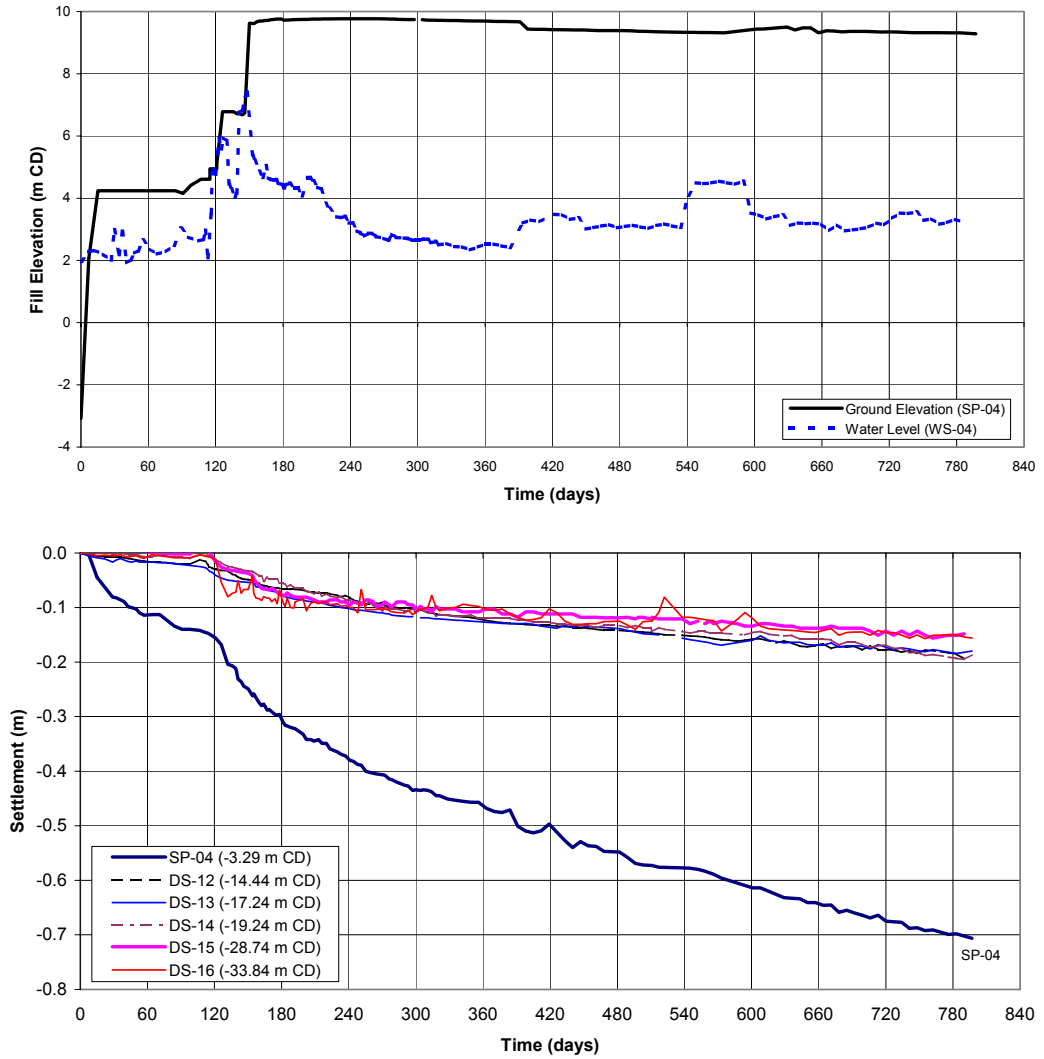


Figure 8.46 Field settlement results of settlement gauges at Control Area (No Drain) (Arulrajah et al., 2004b).

Figure 8.47 shows the typical Asaoka plot and interpretations for the settlement plate in the Vertical Drain Area.

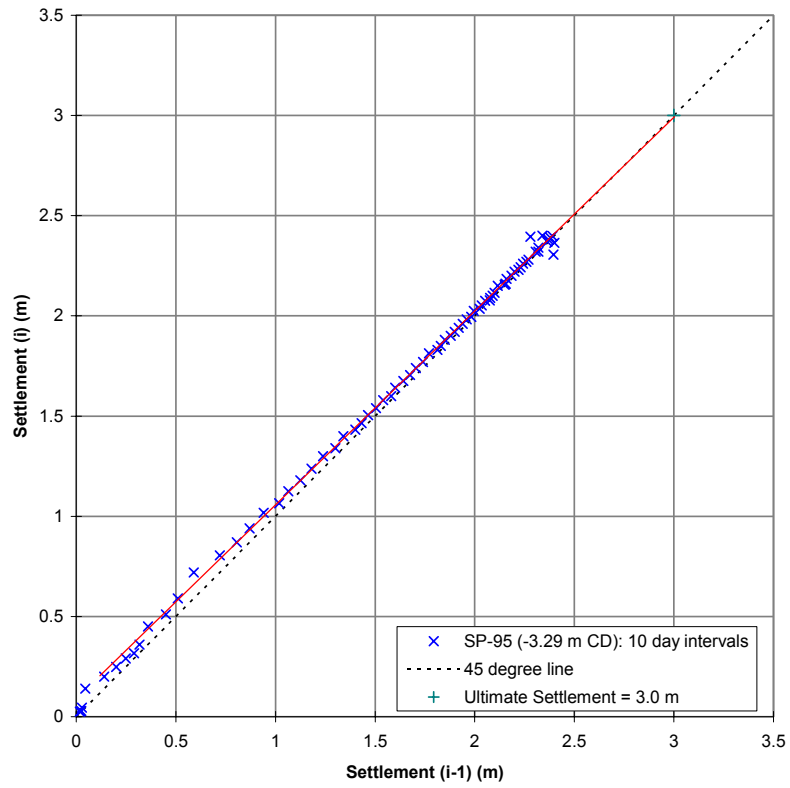


Figure 8.47 Asaoka plot of settlement plate at Vertical Drain Area (Arulrajah et al., 2004b).

Figures 8.48 and 8.49 shows the typical Hyperbolic plots and interpretations for the settlement gauge at a particular elevation in the Vertical Drain Area.

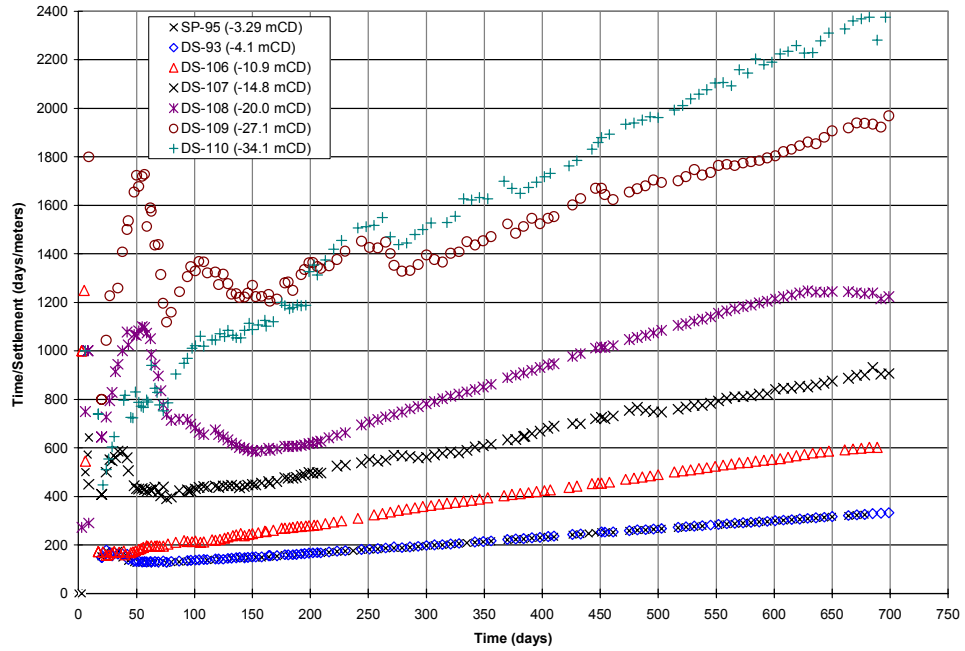


Figure 8.48 Combined Hyperbolic plot of settlement gauges at Vertical Drain Area (Arulrajah et al., 2003b).

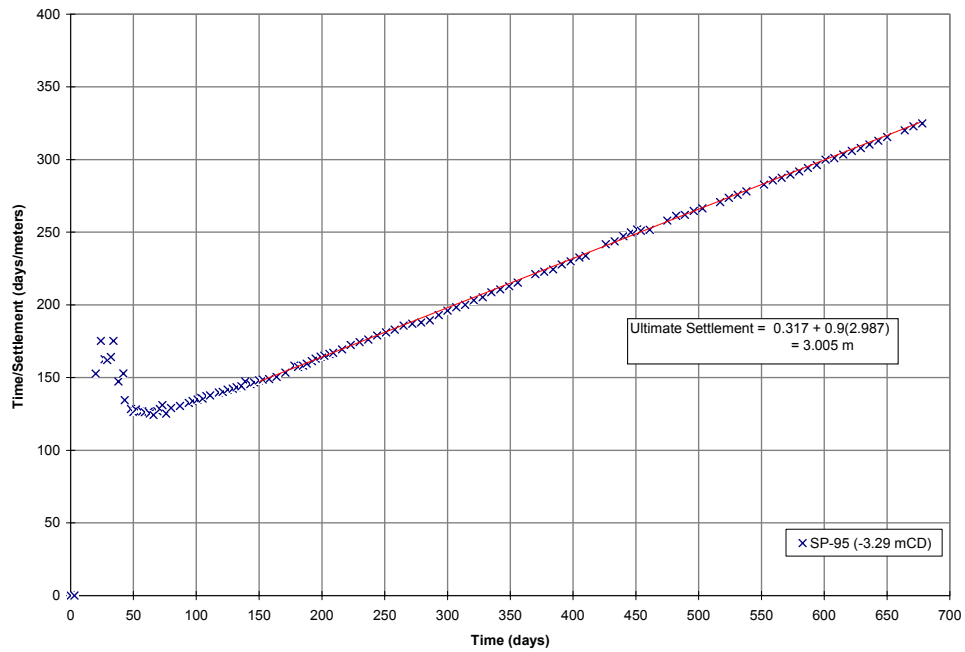


Figure 8.49 Hyperbolic plot of settlement plate at Vertical Drain Area (Arulrajah et al., 2004b).

8.2.2 Analyses of Piezometers

The piezometer monitoring data in the Vertical Drain Area inclusive of correction of the piezometer tip is shown in Figure 8.50. The piezometer monitoring data in the Control Area is shown in Figure 8.51.

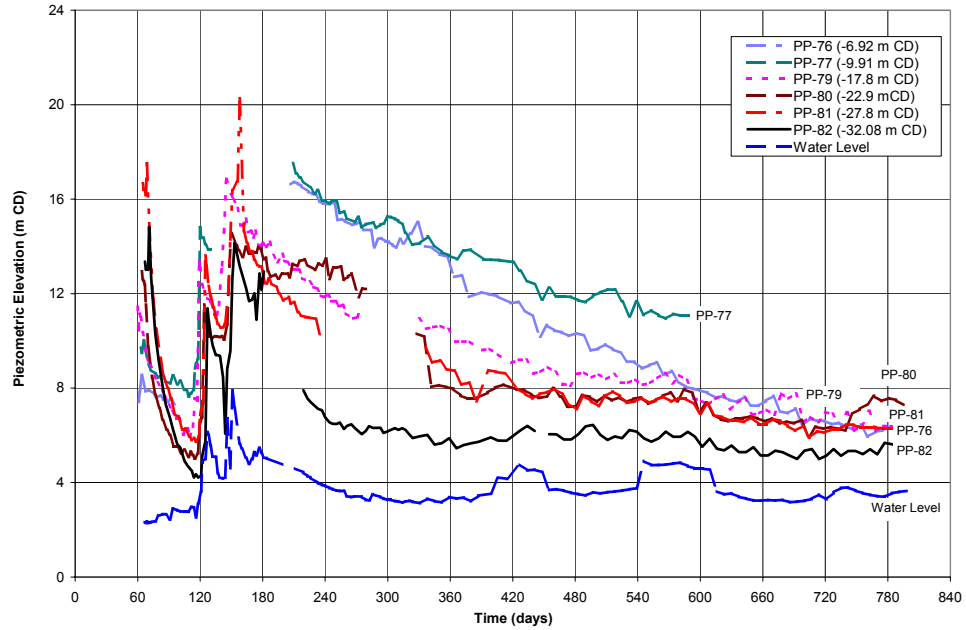


Figure 8.50 Piezometric Elevations at Vertical Drain Area (1.5m x 1.5m).

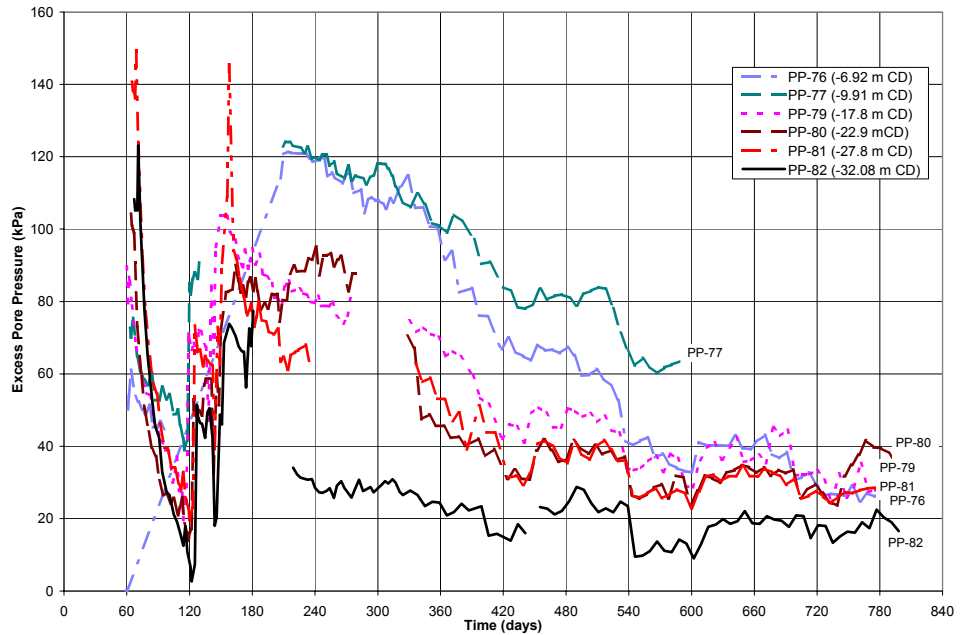


Figure 8.51 Excess pore water pressures at Vertical Drain Area (1.5m x 1.5m) (Arulrajah et al., 2004c).

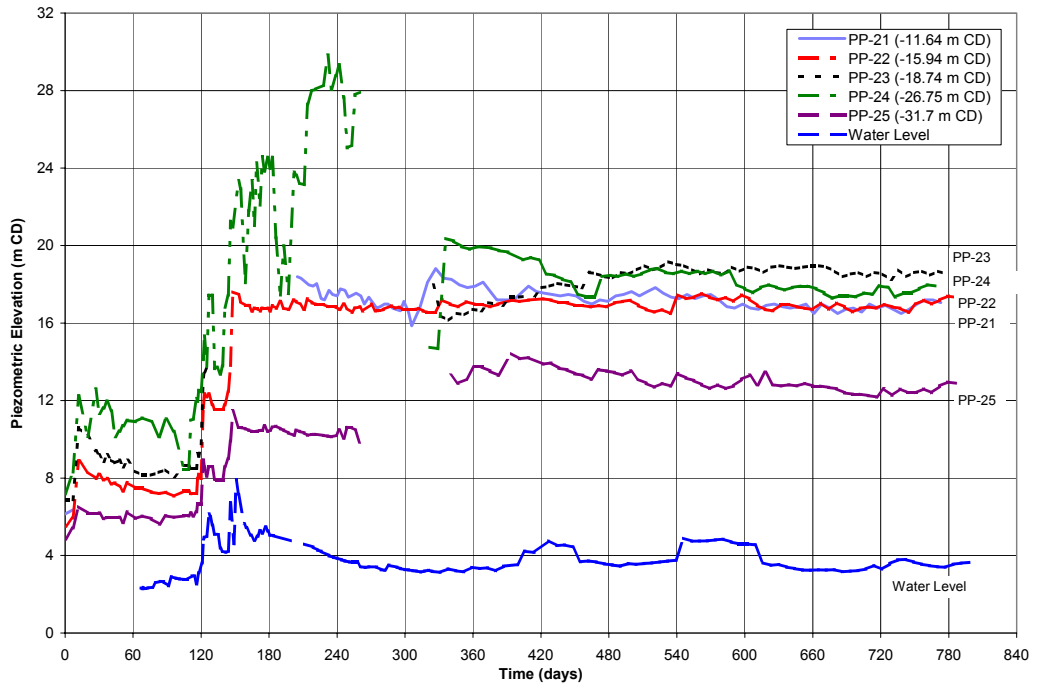


Figure 8.52 Piezometric elevations at Control Area (No Drain).

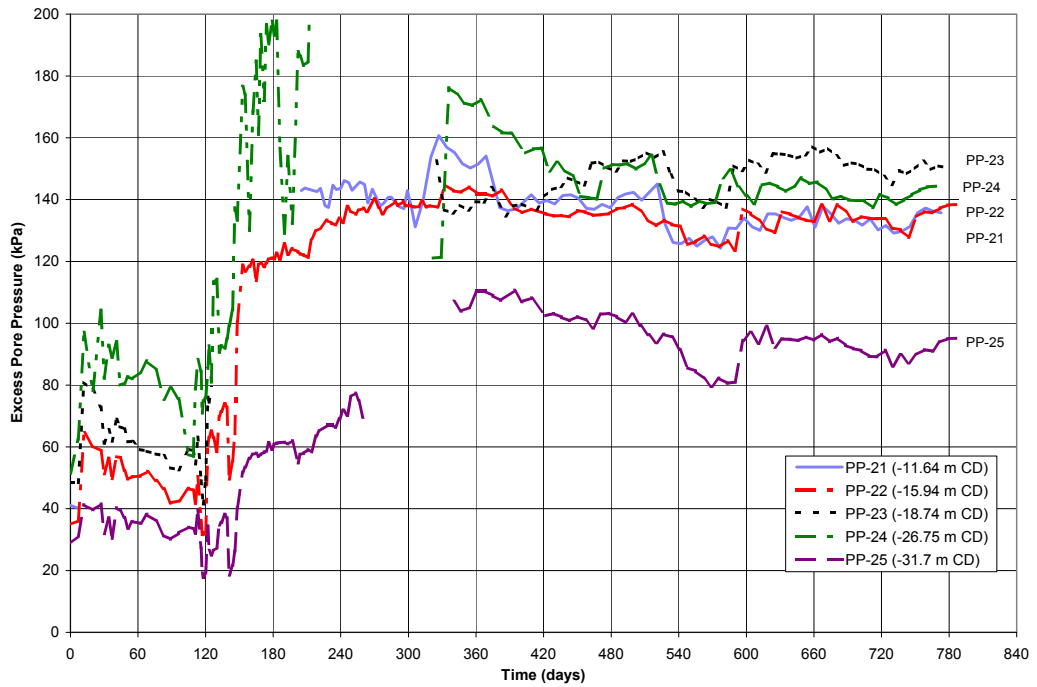


Figure 8.53 Excess pore water pressures at Control Area (No Drain) (Arulrajah et al., 2003b).

Figure 8.54 indicates the comparison of excess pore pressure isochrones between the Vertical Drain Area and Control Area. The rapid dissipation of excess pore water pressure with time is clearly evident in the Vertical Drain Area. The slow rate of dissipation of excess pore water pressure with time is also noted at the Control Area. It is evident that the degree of consolidation of the Vertical Drain Area is far greater than that of the Control Area as would be expected. The Vertical Drain Area is found to register the higher degree of consolidation at each particular elevation. Piezometers installed close to the dense sand layer at the bottom of the marine clay is also found to register a high degree of consolidation thus confirming that there is bottom drainage of excess pore water pressure into the permeable sand layer.

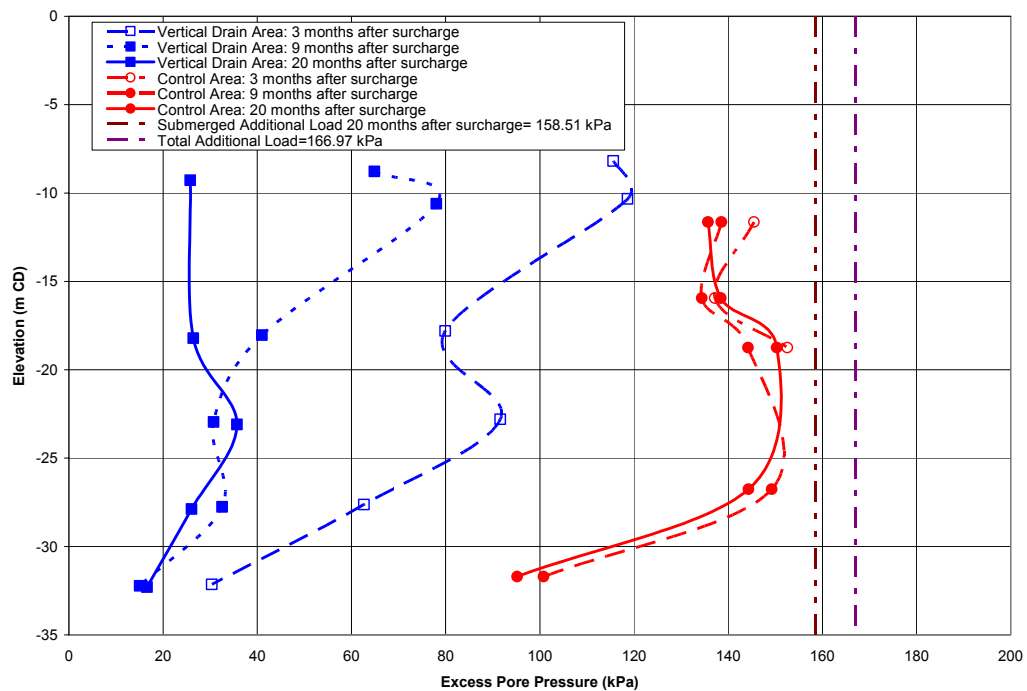


Figure 8.54 Comparison of piezometer excess pore pressure isochrones between Vertical Drain Area and Control Area 20 months after surcharge (Arulrajah et al., 2004b).

8.2.3 Comparison of Degree of Consolidation

Table 8.4 compares the degree of consolidation of the Vertical Drain Area by the various assessment methods. The degree of consolidation of the piezometers is found to tie in well with that of the settlement gauges at the Vertical Drain Area which is about 80%. The degree of consolidation of the piezometers in the Control Area is about 20%. Figure 8.55 compares the degree of consolidation as obtained from the settlement gauge and piezometer results at the Vertical Drain Area and Control Area. The greater rate of dissipation of excess pore water pressure with time is evident in the Vertical Drain Area.

Table 8.4 Comparison of Asaoka, Hyperbolic and piezometer methods at In-Situ Test Site 20 months after surcharge (Arulrajah et al., 2004b).

Sub-Area	Comparison	Asaoka	Hyperbolic	Piezometer
Vertical Drain 1.5 x 1.5 m	Ultimate Settlement(m)	3.000	3.005	-
	Settlement to date (m)	2.404	2.404	-
	Degree of Consolidation,U%	80.1	80.0	80.0
Control No Drain	Degree of Consolidation, U%	-	-	20.0

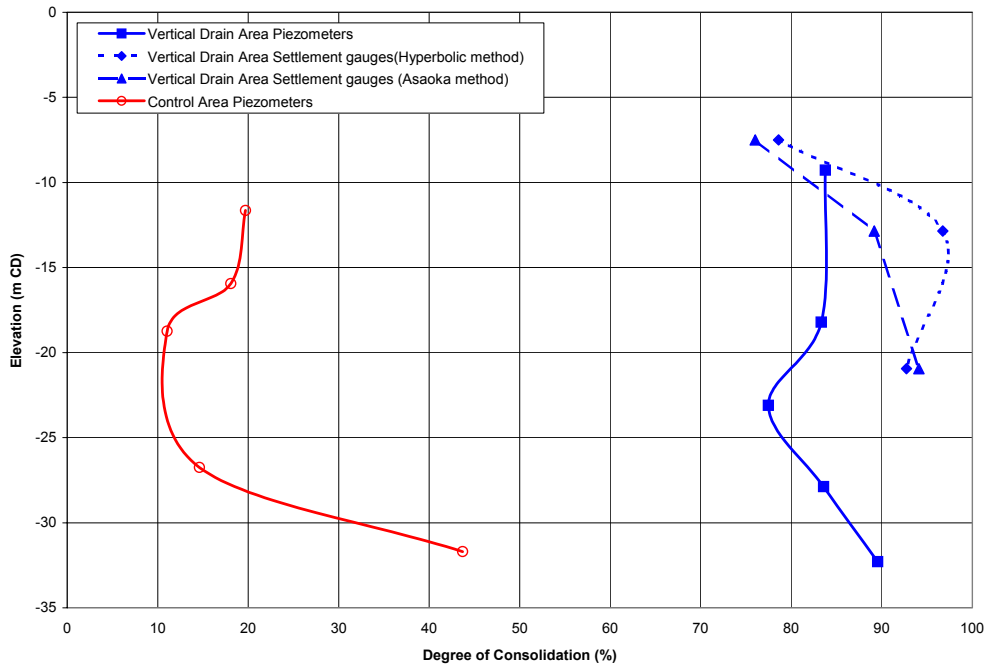


Figure 8.55 Comparison of degree of consolidation at Vertical Drain Area and Control Area 20 months after surcharge (Arulrajah et al., 2004b).

8.2.4 Back-Analysis of Field Consolidation Compression Parameters

The field magnitude of settlement is very similar to the predicted settlement based on laboratory parameters found in Table 8.5.

Back-analyses were carried out to determine the void ratio changes against effective stress based on piezometer and settlement data at the Vertical Drain Area. The void ratio versus effective stress curve for each sub-soil layer was then generated. From these actual field parameters of compression index, recompression index and yield stress values were

compared with the laboratory parameters used in the design prediction. Field void ratio versus effective stress curve for sub-layers is shown in Figure 8.56.

It can be seen in Table 8.5 that the compression parameters used in design stage are quite similar to field parameters back-analysed from field performance. This is the reason that actual field settlement is very close to the predicted settlement.

Table 8.5 Comparison of laboratory prediction and back-analysed field soil parameters (Bo, Arulrajah and Choa, 1997b).

Elevation (mCD)	C_c		C_r		P_c	
	Laboratory	Field	Laboratory	Field	Laboratory	Field
-7.50	1.00	0.875	0.13	-	41.3	< 40
-12.85	1.00	1.133	0.13	0.590	93.9	90
-17.40	0.25	0.343	0.10	0.030	272.9	133.7
-23.55	0.80	0.551	0.17	0.018	235.5	181.6

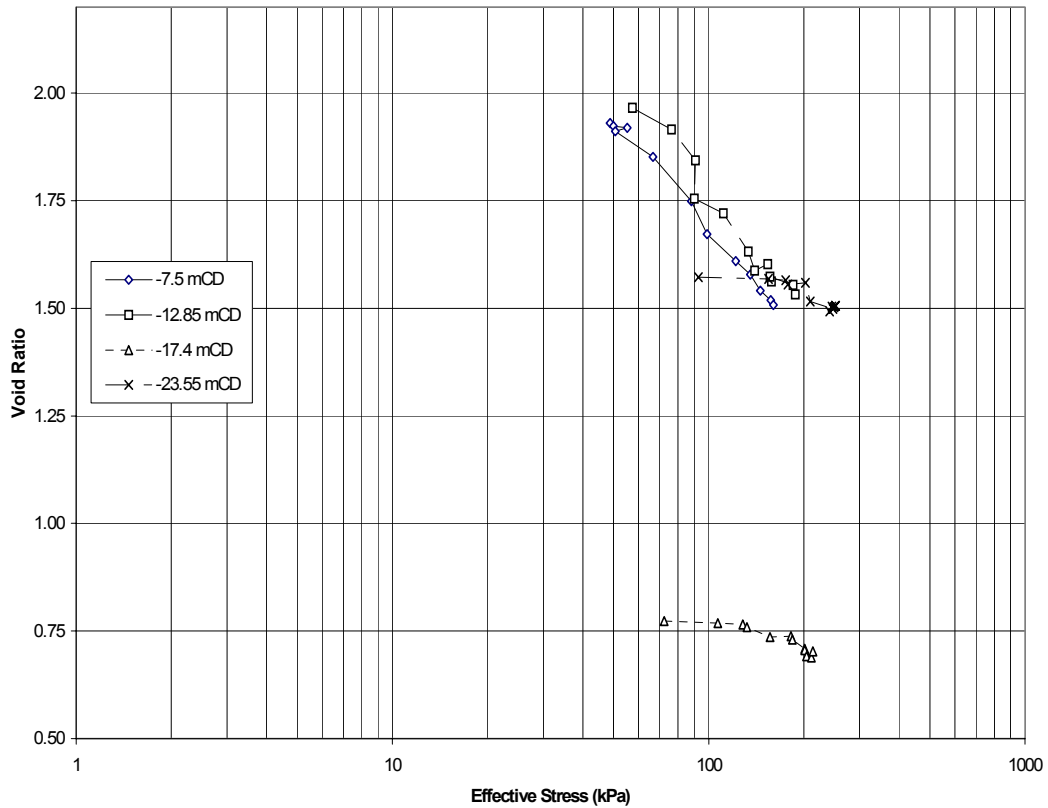


Figure 8.56 Field void ratio versus effective stress for sub-layers.

8.2.5 Back-Analyses of Coefficient of Consolidation due to Horizontal Flow

It was found from the back-analyses of the settlement monitoring results by Asaoka (1978) method that the actual field coefficient of consolidation due to horizontal flow is only 0.78 m²/year. This is lower than the corresponding value of c_h obtained from the in-situ holding test results as discussed in section 6.11 and that used in the design as discussed in section 5.9.

However, field measurement of coefficient of consolidation due to horizontal flow measured prior to reclamation by the various in-situ testing methods is much higher than the back analysed and design c_h values.

This is further confirmation that the permeability anisotropy of Singapore marine clay at Changi is not significant thus confirming the findings of Tavenas (1983) and Larsson (1981).

The summary of the back analysed c_h results of settlement gauges is given in Table 8.6.

Table 8.6 Back analysed c_h results of settlement gauges (Asaoka method).

Settlement Gauge	Elevation	Back analysed c_h (m ² /yr)
SP-95	- 3.29	0.78
DS-93	- 4.1	0.69
DS-106	- 10.9	1.11
DS-107	-14.8	0.85
DS-108	-20.0	1.18
DS-109	-27.1	0.82

Despite the in-situ testing measured coefficient of consolidation due to horizontal flow being much higher than the assumed values used in the design stage, actual field time rate of consolidation is slower than the predicted time rate. Back-analysed c_h values are also much lower than the in-situ. As such, there are only three possibilities which are: a) reduction of horizontal and vertical permeability from time to time during consolidation b) well resistance and smear effects and c) clogging of vertical drains after some time.

8.2.6 Findings for Field Instrumentation of In-Situ Test Site

The ultimate settlement predicted from the settlement gauges by the Hyperbolic and Asaoka prediction methods was found to be about 3 meters. The assessment of degree of consolidation is found to be in good agreement for the Asaoka, Hyperbolic and piezometer methods. The settlement gauges and piezometers indicate that the degree of consolidation of the Vertical Drain Area had attained a degree of consolidation of about 80%. This is in good agreement with the in-situ testing results.

The piezometers indicate that the Control Area had only attained a degree of consolidation of about 20%. The field instrumentation results in the Vertical Drain Area indicates much higher degree of improvements as compared to the Control Area which indicates that the vertical drains are performing to improve the soil drainage system.

Compression parameters obtained from the laboratory which were used for prediction is very similar to the actual back-analysed parameter. Back-analysed c_h values are also much lower than the in-situ which is due to: a) reduction of horizontal and vertical permeability from time to time during consolidation b) well resistance and smear effects and c) clogging of vertical drains after some time.

9.0 EVALUATION OF OBSERVATIONAL METHODS OF ASSESSING IMPROVEMENT OF MARINE CLAY UNDER RECLAMATION FILLS

Thick deposits of soft marine clay are commonly present in the coastal regions of the tropics. The use of prefabricated vertical drains with preloading option is the most widely-used ground improvement method for the improvement of soft clays in land reclamation projects. Surcharge of equivalent working load after taking into account submergence effect and settlement of the reclaimed land is placed until the required degree of consolidation of the soft clay is obtained. The assessment of the degree of consolidation of the marine clay is of paramount importance before the removal of preload. This analysis can be carried out by means of observational methods.

Field settlement monitoring data can be used to ascertain the settlement of the reclaimed fill from the time of initial installation. The field settlement data can be analysed by the Asaoka and Hyperbolic methods to predict the ultimate settlement of the reclaimed land under the surcharge fill. Back-analysis of the field settlement data will also enable the coefficient of consolidation due to horizontal flow to be closely estimated. Factors that affect prediction by the Asaoka method are the period of assessment after surcharge placement as well as the time interval used for the analysis. Factors that affect prediction by the Hyperbolic method are the period of assessment after surcharge placement.

Piezometer monitoring data can be analysed to obtain the degree of consolidation of the improved marine clay. Piezometers were analysed to investigate the various factors that affect their analysis. Factors that affect the analysis of piezometers include period of assessment, hydrogeologic boundary condition, settlement of piezometer tip and reduction of initial imposed load due to submergence effect.

It is to be noted that the Asaoka and Hyperbolic assessment methods was not reported for the A2S-74 (No Drains) sub-area in this chapter, as the degree of consolidation did not reach a high enough value to enable an interpretation.

The aim of this chapter is to highlight the significance and impact of these factors in the field settlement assessment and back-analysis of coefficient of consolidation due to horizontal flow of soft clays and with special regard to coastal marine clays. The study was carried out using the data obtained from the Pilot Test Site sub-areas. Factors affecting field instrumentation assessment of marine clay treated with prefabricated vertical drains

described in this chapter have been discussed in detail by the author (Arulrajah et al., 2003a, 2004a , 2004e) during the course of this research study.

9.1 Factors Affecting Assessment by the Asaoka Method

The magnitude of ultimate settlement, degree of consolidation and coefficient of consolidation due to horizontal flow can be predicted by the Asaoka method as described in section 7.7.1. The prediction of ultimate settlement by the Asaoka method is affected by the period of assessment after surcharge placement as well as by the time interval used for the assessment.

Factors affecting assessment by the Asaoka method have been discussed in detail by the author (Arulrajah et al., 2003a, 2004e) during the course of this research study. The assessment by the Asaoka method was carried out for the sub-areas for assessment periods of 12, 24 and 32 months after surcharge placement with the use of various time intervals.

Tables 9.1, 9.2 and 9.3 compare the magnitude of ultimate settlement (S_{ult}), degree of consolidation ($U\%$) (as defined in section 7.7.3) and coefficient of consolidation due to horizontal flow (c_h) predicted by the Asaoka method. The predictions were carried out using various selected time intervals as tabulated in Tables 9.1, 9.2 and 9.3. The predictions were carried out with assessment periods of 12, 24 and 32 months after surcharge for the various vertical drain treated sub-areas of the Pilot Test Site.

Table 9.1 Asaoka method with various time intervals 12 months after surcharge - 21.6 months of monitoring (Arulrajah et al., 2004e).

Sub-Area	Asaoka	7 days	14 days	21 days	28 days	42 days	56 days
A2S-71 2.0 x 2.0m	S _{ult} (m)	1.895	1.893	1.890	1.872	1.872	1.872
	S _t (m)	1.334	1.334	1.334	1.334	1.334	1.334
	U%	70.4	70.5	70.6	71.3	71.3	71.3
	c _h (m ² /yr)	1.78	1.35	1.40	1.29	1.27	1.06
A2S-72 2.5 x 2.5m	S _{ult} (m)	1.520	1.517	1.515	1.500	1.500	1.500
	S _t (m)	1.020	1.020	1.020	1.020	1.020	1.020
	U%	67.1	67.2	67.3	68.0	68.0	68.0
	c _h (m ² /yr)	2.62	1.42	1.55	1.30	1.33	1.27
A2S-73 3.0 x 3.0m	S _{ult} (m)	1.280	1.270	1.260	1.250	1.250	1.250
	S _t (m)	0.693	0.693	0.693	0.693	0.693	0.693
	U%	54.1	54.6	55.0	55.4	55.4	55.4
	c _h (m ² /yr)	3.87	3.00	1.96	2.07	2.03	1.99

Table 9.2 Asaoka method with various time intervals 24 months after surcharge - 33.7 months of monitoring (Arulrajah et al., 2004e).

Sub-Area	Asaoka	7 days	14 days	21 days	28 days	42 days	56 days
A2S-71 2.0 x 2.0m	S _{ult} (m)	1.875	1.873	1.870	1.850	1.850	1.850
	S _t (m)	1.578	1.578	1.578	1.578	1.578	1.578
	U%	84.2	84.2	84.4	85.3	85.3	85.3
	c _h (m ² /yr)	1.93	1.24	1.22	1.17	1.16	1.14
A2S-72 2.5 x 2.5m	S _{ult} (m)	1.450	1.445	1.440	1.420	1.420	1.420
	S _t (m)	1.225	1.225	1.225	1.225	1.225	1.225
	U%	84.5	84.8	85.1	86.3	86.3	86.3
	c _h (m ² /yr)	2.87	1.86	1.78	1.46	1.25	1.20
A2S-73 3.0 x 3.0m	S _{ult} (m)	1.248	1.243	1.242	1.240	1.240	1.240
	S _t (m)	0.856	0.856	0.856	0.856	0.856	0.856
	U%	68.6	68.9	68.9	69.0	69.0	69.0
	c _h (m ² /yr)	4.94	3.43	2.81	2.09	2.06	1.75

Table 9.3 Asaoka method with various time intervals 32 months after surcharge - 41.9 months of monitoring (Arulrajah et al., 2004e).

Sub-Area	Asaoka	7 days	14 days	21 days	28 days	42 days	56 days
A2S-71 2.0 x 2.0m	$S_{ult}(m)$	1.857	1.855	1.850	1.838	1.838	1.838
	$S_t(m)$	1.687	1.687	1.687	1.687	1.687	1.687
	U%	90.8	90.9	91.2	91.8	91.8	91.8
	$c_h(m^2/yr)$	2.20	1.56	1.44	1.19	1.08	1.08
A2S-72 2.5 x 2.5m	$S_{ult}(m)$	1.438	1.435	1.430	1.412	1.412	1.412
	$S_t(m)$	1.264	1.264	1.264	1.264	1.264	1.264
	U%	87.9	88.1	88.4	89.5	89.5	89.5
	$c_h(m^2/yr)$	1.95	1.59	1.53	1.48	1.35	1.22
A2S-73 3.0 x 3.0m	$S_{ult}(m)$	1.220	1.215	1.210	1.200	1.200	1.200
	$S_t(m)$	0.948	0.948	0.948	0.948	0.948	0.948
	U%	77.7	78.0	78.3	79.0	79.0	79.0
	$c_h(m^2/yr)$	5.62	4.79	3.31	2.25	2.09	2.20

9.1.1 Period of assessment after surcharge placement and selection of time interval

The study revealed that a longer period of assessment (32 months) after initial placement of surcharge will provide a decrease in the predicted ultimate settlement and a subsequent increase in the assessment of the degree of consolidation. Furthermore, the study reveals that at any particular period of assessment the longer the time interval used, the lower is the predicted ultimate settlement and subsequently the higher the corresponding degree of consolidation. This is illustrated in Figures 9.1 and 9.2. Similar findings have been reported previously by Bo et al. (1999). It is apparent that the degree of consolidation of the marine clay converges to the actual value as a longer time of assessment and increasing time intervals is used in the back-analysis.

At small time intervals, the data points are cluttered together which make it difficult to accurately assess the best-fit line through the data points. Using a larger time interval on the other hand will require a long term field instrumentation monitoring programme in order to enable sufficient data points to be obtained in order to assess the best-fit line through the data points.

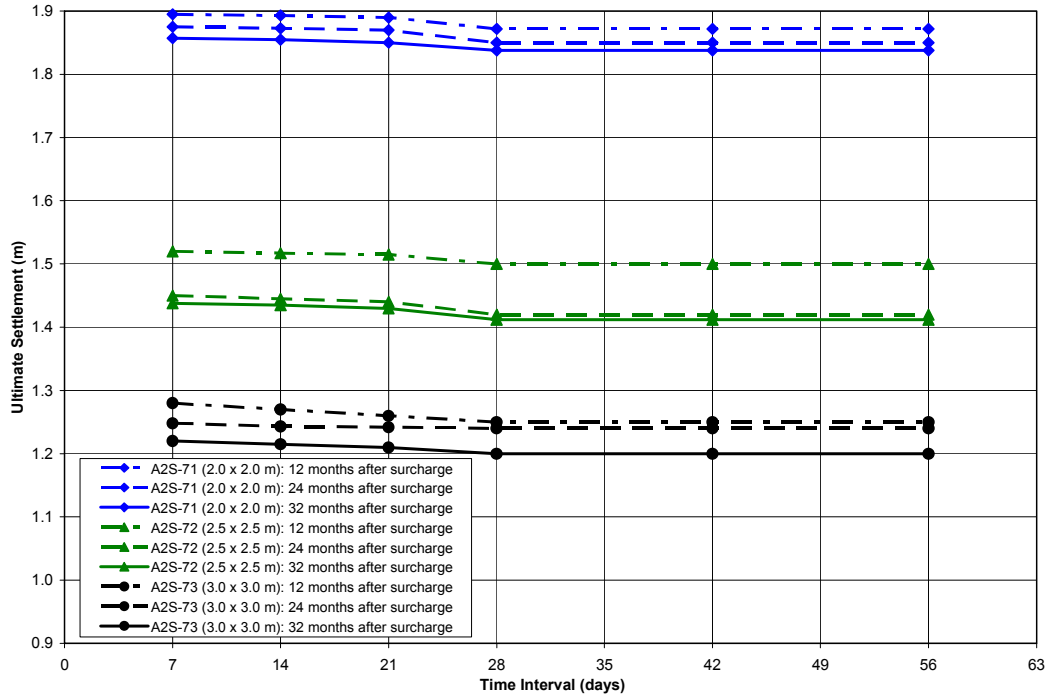


Figure 9.1 Comparison of variation in ultimate settlement for various time intervals by the Asaoka method.

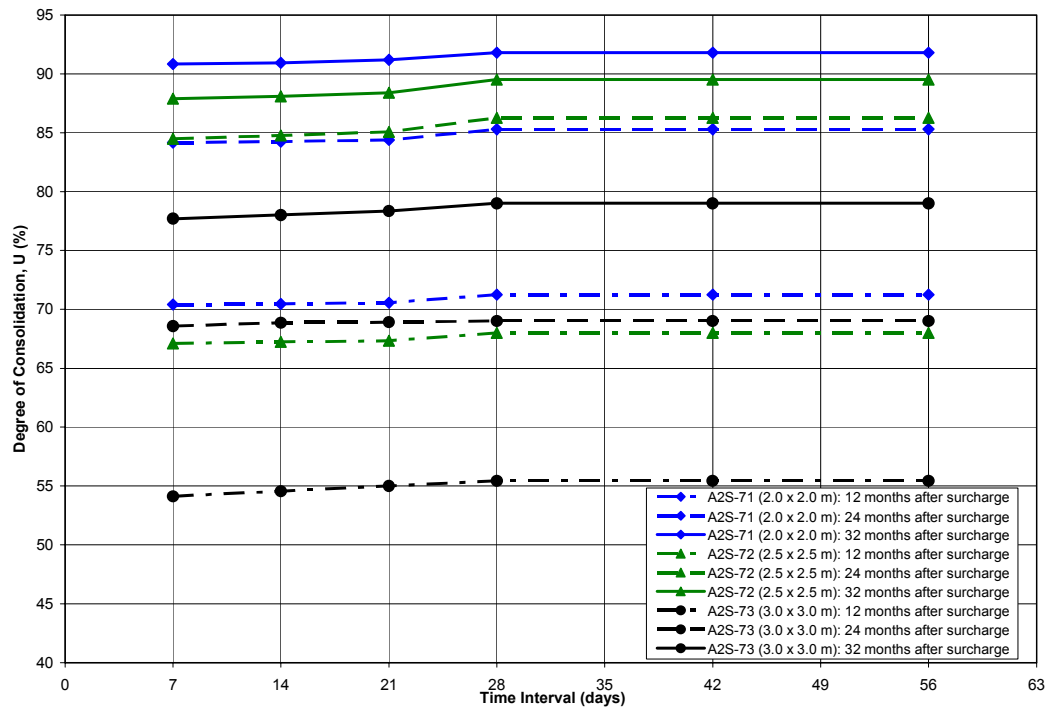


Figure 9.2 Comparison of variation in degree of consolidation for various time intervals by the Asaoka method.

It is apparent in Figure 9.1, that as the time interval increases, a cut-off time interval is obtained after which increasing time intervals would converge to the same magnitude of ultimate settlement. This cut-off time interval in this study is after 28 days as the ultimate settlement is predicted to be the same from 28 day to 56 day time intervals. However, the use of increasing time intervals would be restricted by the number of data points available to assess the best-fit line. As such, the use of increasing time intervals was curbed to 56 days.

As expected, the sub-area with the closest vertical drain spacing has attained the highest degree of consolidation for the various surcharging durations. At the end of the surcharging period of 32 months, the sub-area with the closest vertical drain spacing (A2S-71: 2.0 x 2.0) has achieved a degree of consolidation of 91.8 % while that with the furthest vertical drain spacing (A2S-73: 3.0 x 3.0) has achieved a degree of consolidation of 79.0 %. It is to be noted that the Asaoka method assessment was not reported for the A2S-74 (No Drains) sub-area as the degree of consolidation did not reach a high enough value to enable an interpretation.

9.1.2 Back-Analysed Coefficient of Consolidation due to Horizontal Flow

c_h value was previously thought to be theoretically independent of the chosen time interval (Holtz et al., 1991). However the author's study on the effect of the period of assessment and time interval used reveals that there is a trend of the c_h value generally increasing at longer periods of assessment after surcharge placement. Furthermore, it was found that the c_h value decreases with increasing time intervals. This is illustrated in Figure 9.3. It is apparent that the coefficient of consolidation due to horizontal flow, c_h value of the clay converges to the final value as longer time of assessment and increasing time intervals are used in the back-analysis.

The study reveals that the c_h value of the marine clay is lowest at the sub-area with the closest vertical drains spacing (A2S-71: 2.0 x 2.0) and highest at the sub-area with the furthest vertical drain spacing (A2S-73: 3.0 x 3.0). This may be attributed to the higher degree of smear effect at locations with closer drain spacing.

For soft marine clay, the smear effect can be quite significant at locations installed with vertical drains (Chu et al., 2002). Bo et al. (2000b) has reported that the permeability of soil in the smear zone could be reduced by 1 order of magnitude or to the horizontal hydraulic conductivity of the remoulded clay as a result of the smearing. When vertical drains are installed at close spacing, the back-calculated c_h values will generally be greatly influenced by this smear zone (Chu et al., 2002).

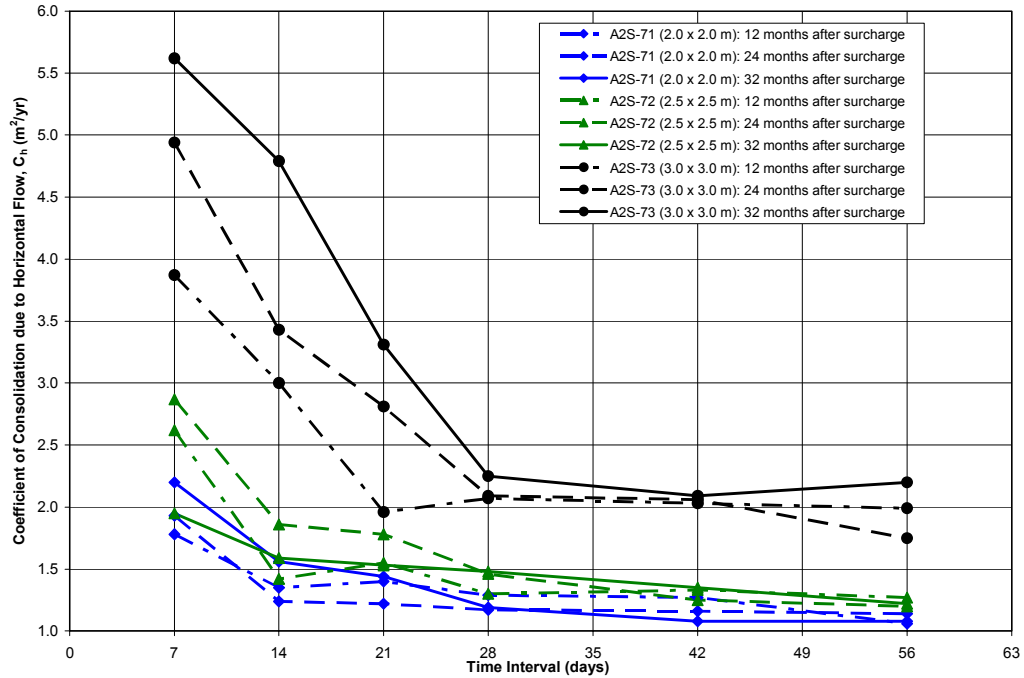


Figure 9.3 Comparison of variation in coefficient of consolidation due to horizontal flow for various time intervals by the Asaoka method.

Figure 9.4, 9.5 and 9.6 show the Asaoka plots at A2S-71 sub-area (2.0m x 2.0m) 12, 24 and 32 months after surcharge.

Figure 9.7, 9.8 and 9.9 show the Asaoka plots at A2S-72 sub-area (2.5m x 2.5m) 12, 24 and 32 months after surcharge.

Figure 9.10, 9.11 and 9.12 show the Asaoka plots at A2S-73 sub-area (3.0m x 3.0m) 12, 24 and 32 months after surcharge.

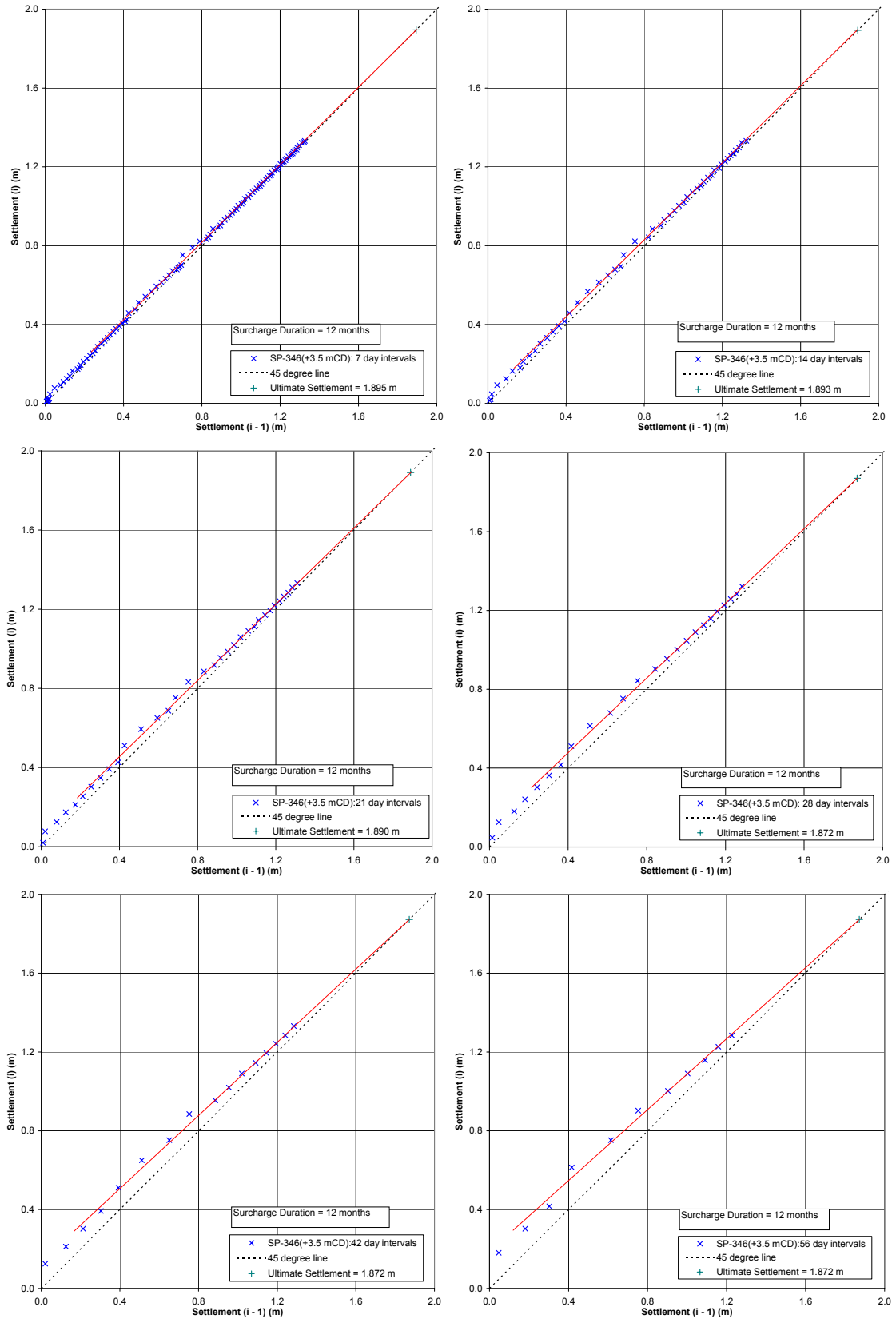


Figure 9.4 Asaoka plots at A2S-71 sub-area (2.0m x 2.0m) 12 months after surcharge. (Arulrajah et al., 2004e).

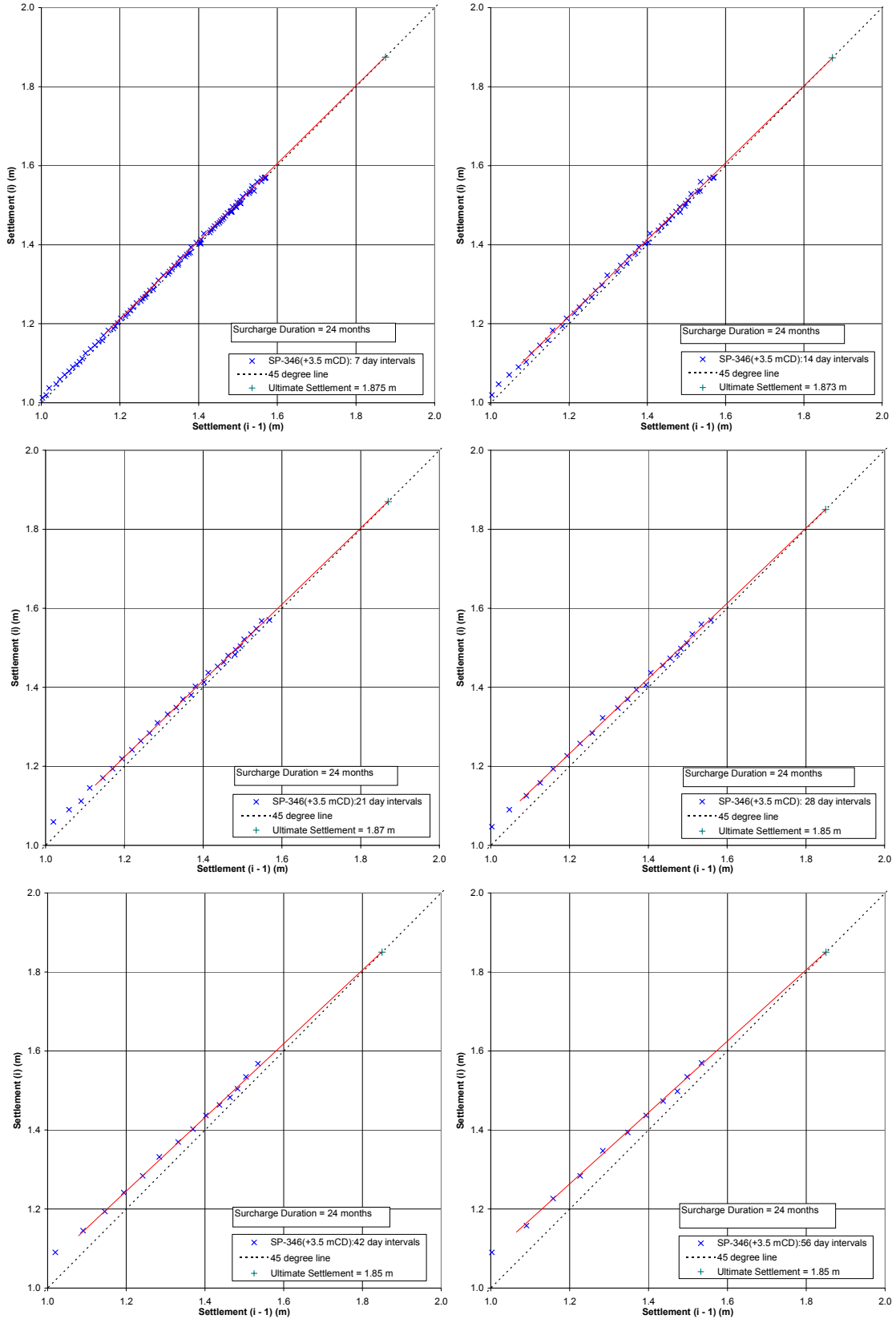


Figure 9.5 Asaoka plots at A2S-71 sub-area (2.0m x 2.0m) 24 months after surcharge.

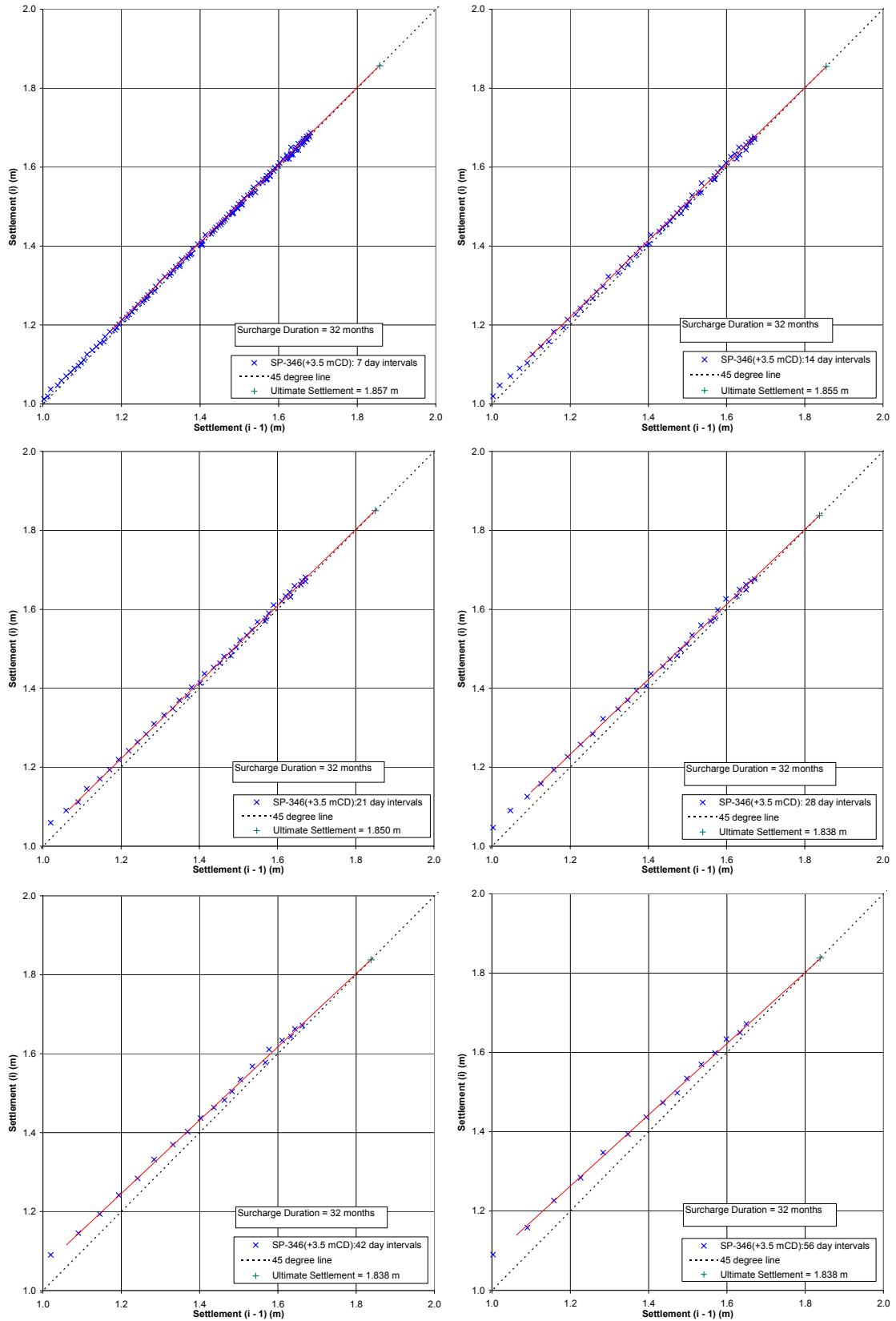


Figure 9.6 Asaoka plots at A2S-71 sub-area (2.0m x 2.0m) 32 months after surcharge. (Arulrajah et al., 2003a).

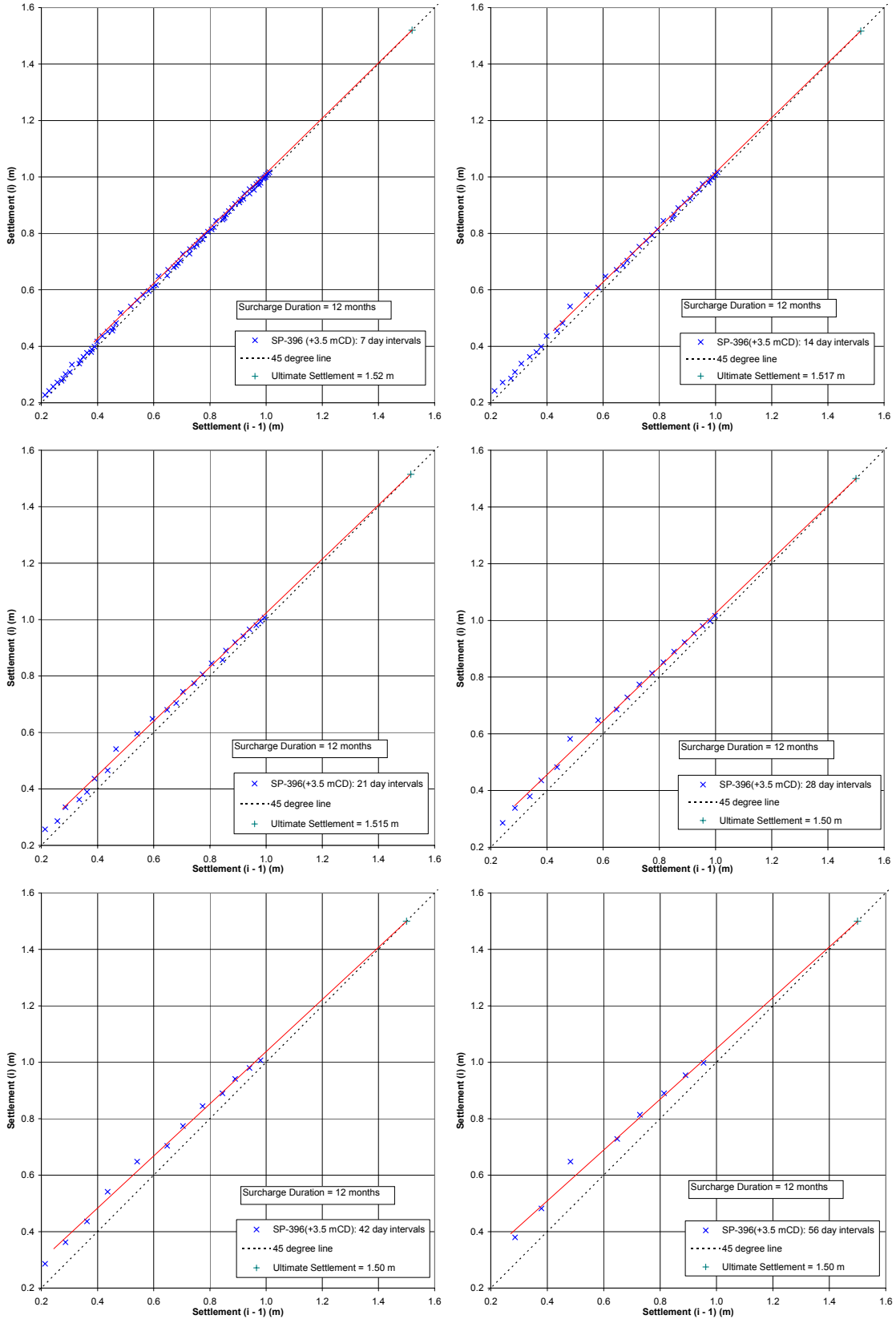


Figure 9.7 Asaoka plots at A2S-72 sub-area (2.5m x 2.5m) 12 months after surcharge.

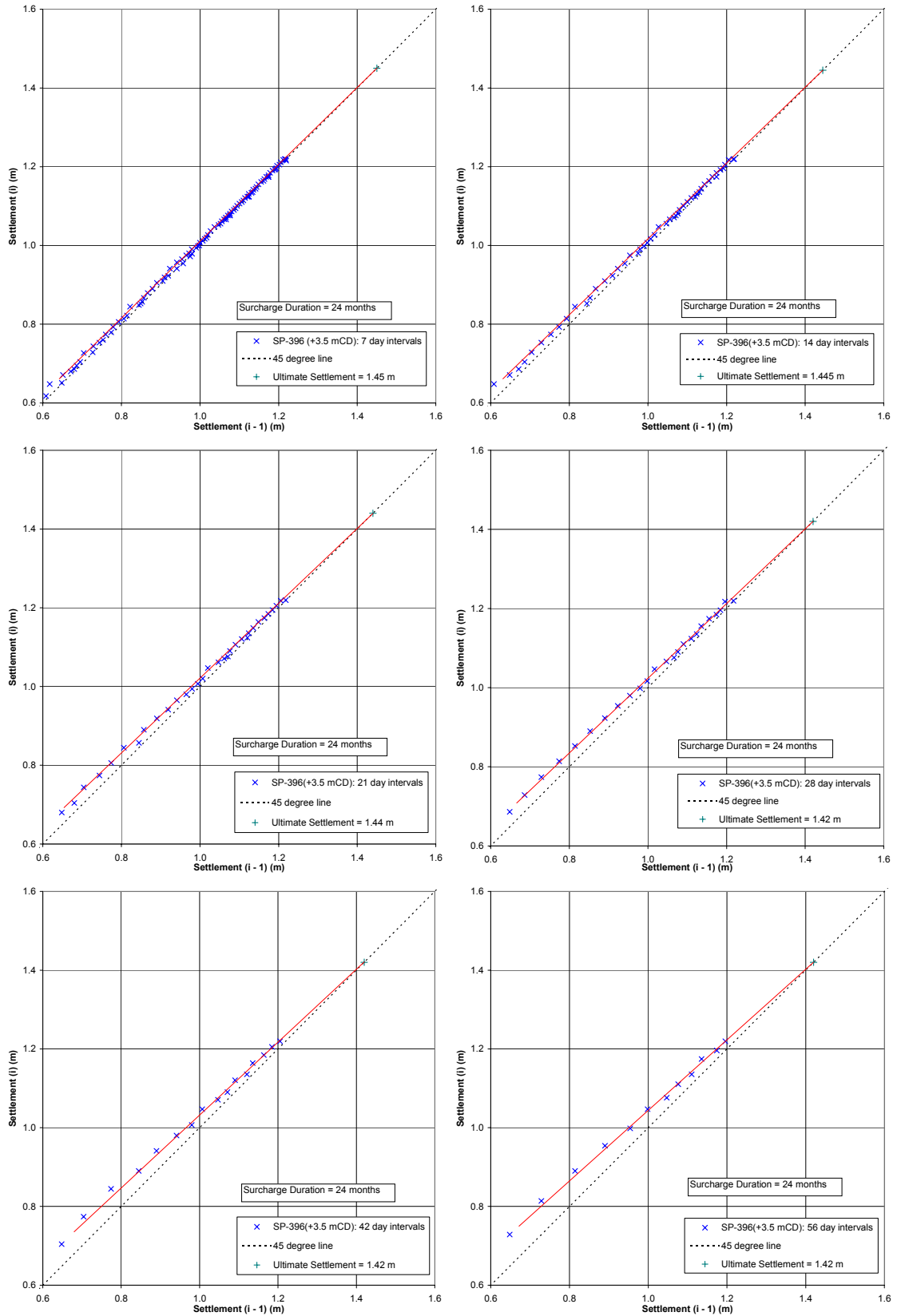


Figure 9.8 Asaoka plots at A2S-72 sub-area (2.5m x 2.5m) 24 months after surcharge.

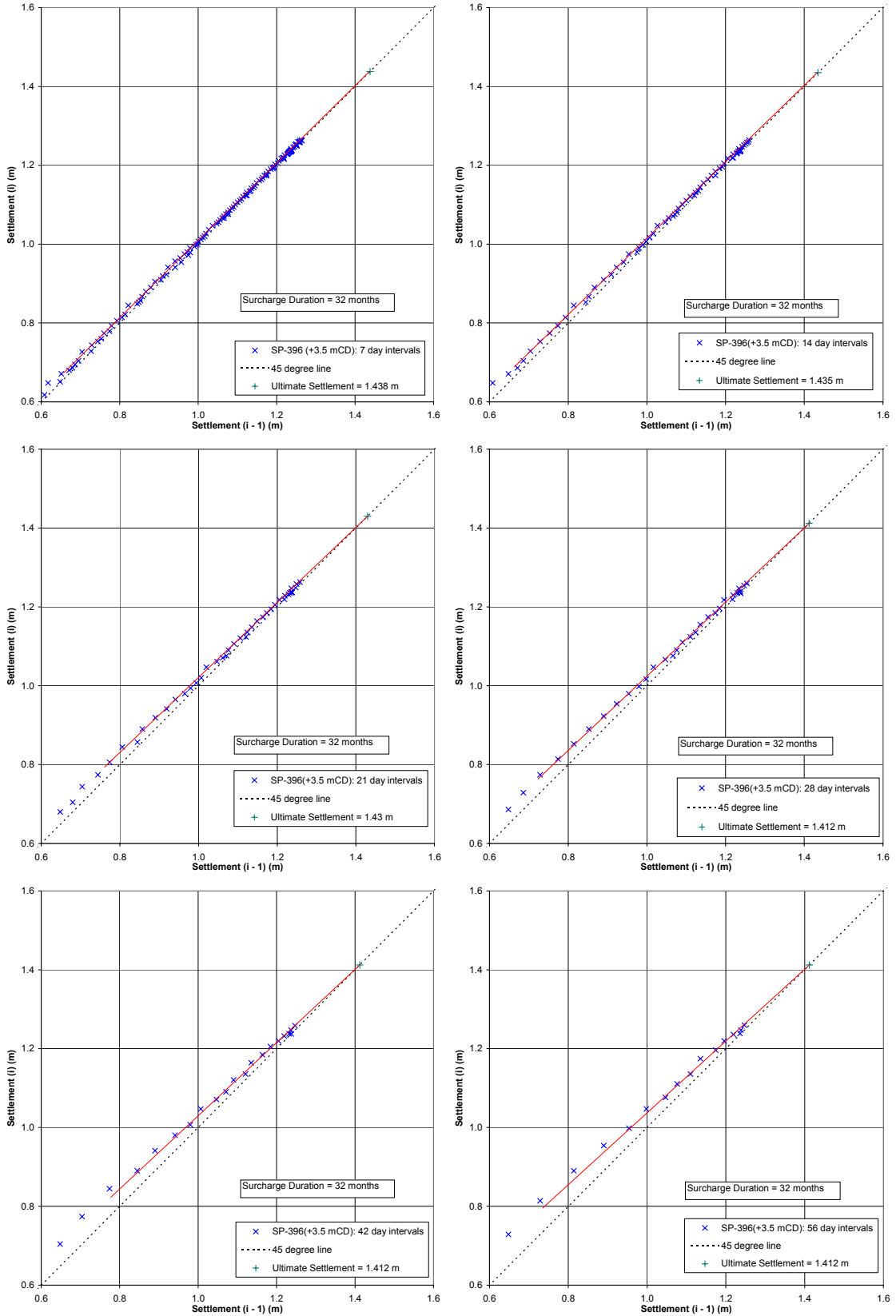


Figure 9.9 Asaoka plots at A2S-72 sub-area (2.5m x 2.5m) 32 months after surcharge.

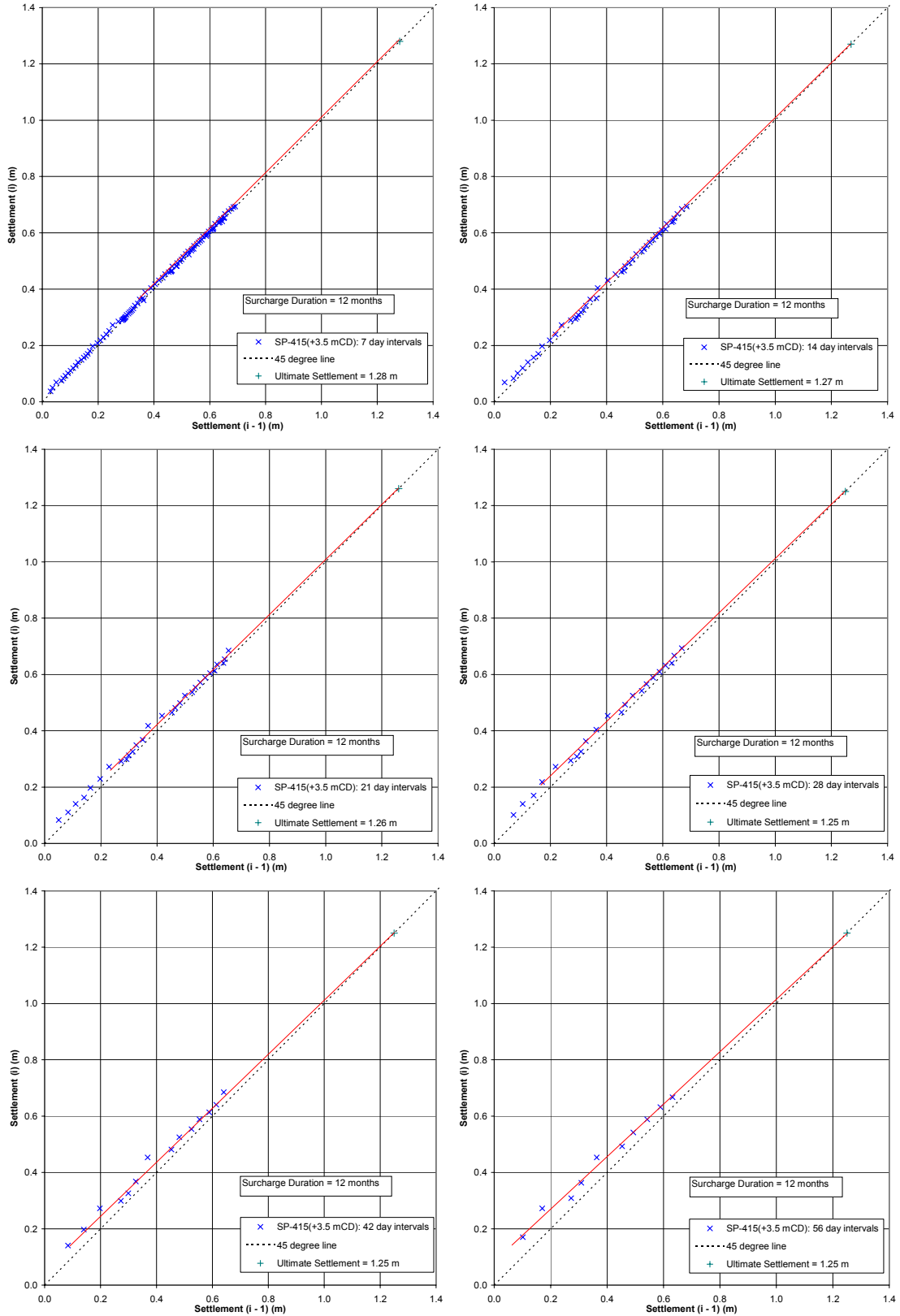


Figure 9.10 Asaoka plots at A2S-73 sub-area (3.0m x 3.0m) 12 months after surcharge.

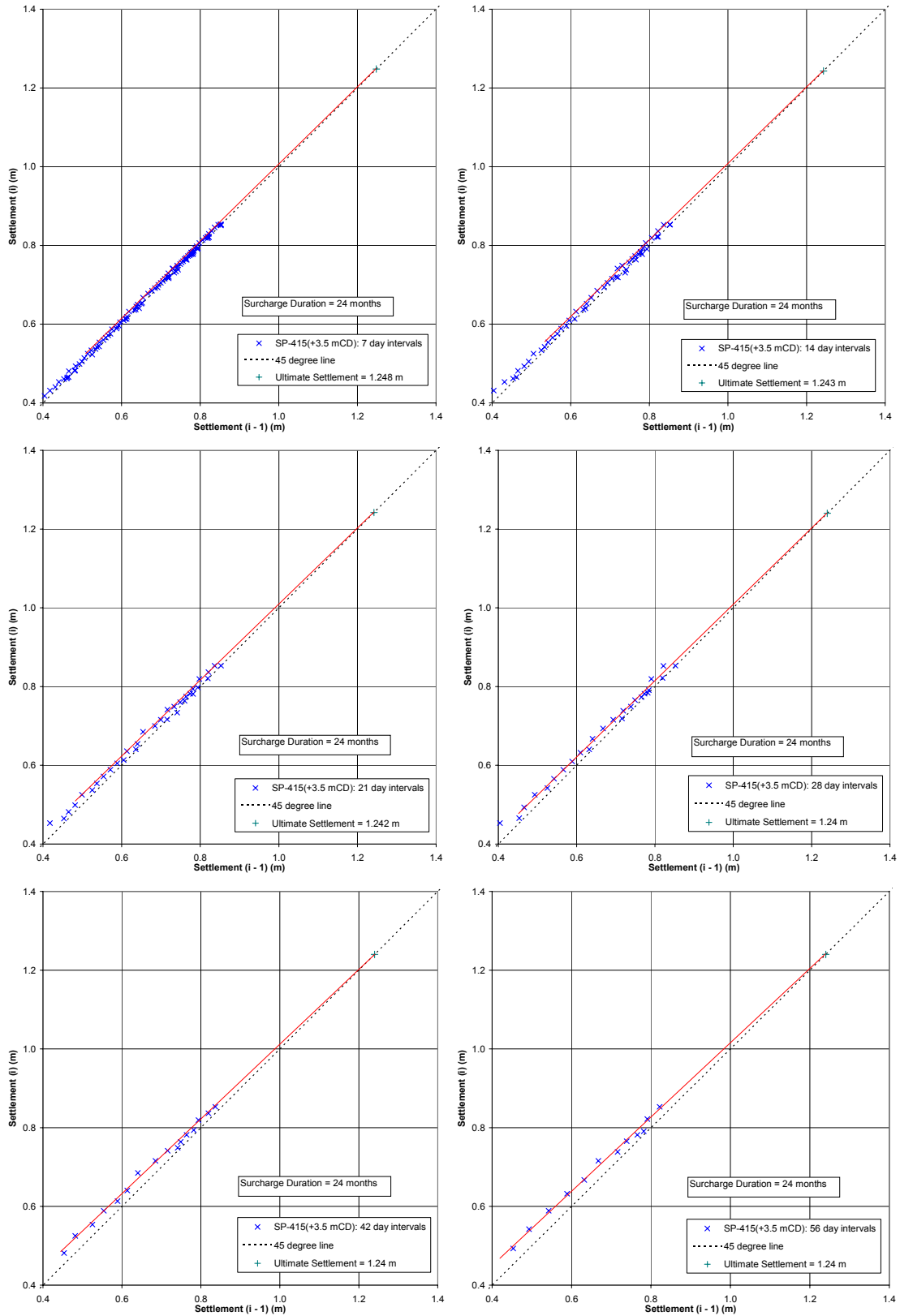


Figure 9.11 Asaoka plots at A2S-73 sub-area (3.0m x 3.0m) 24 months after surcharge.

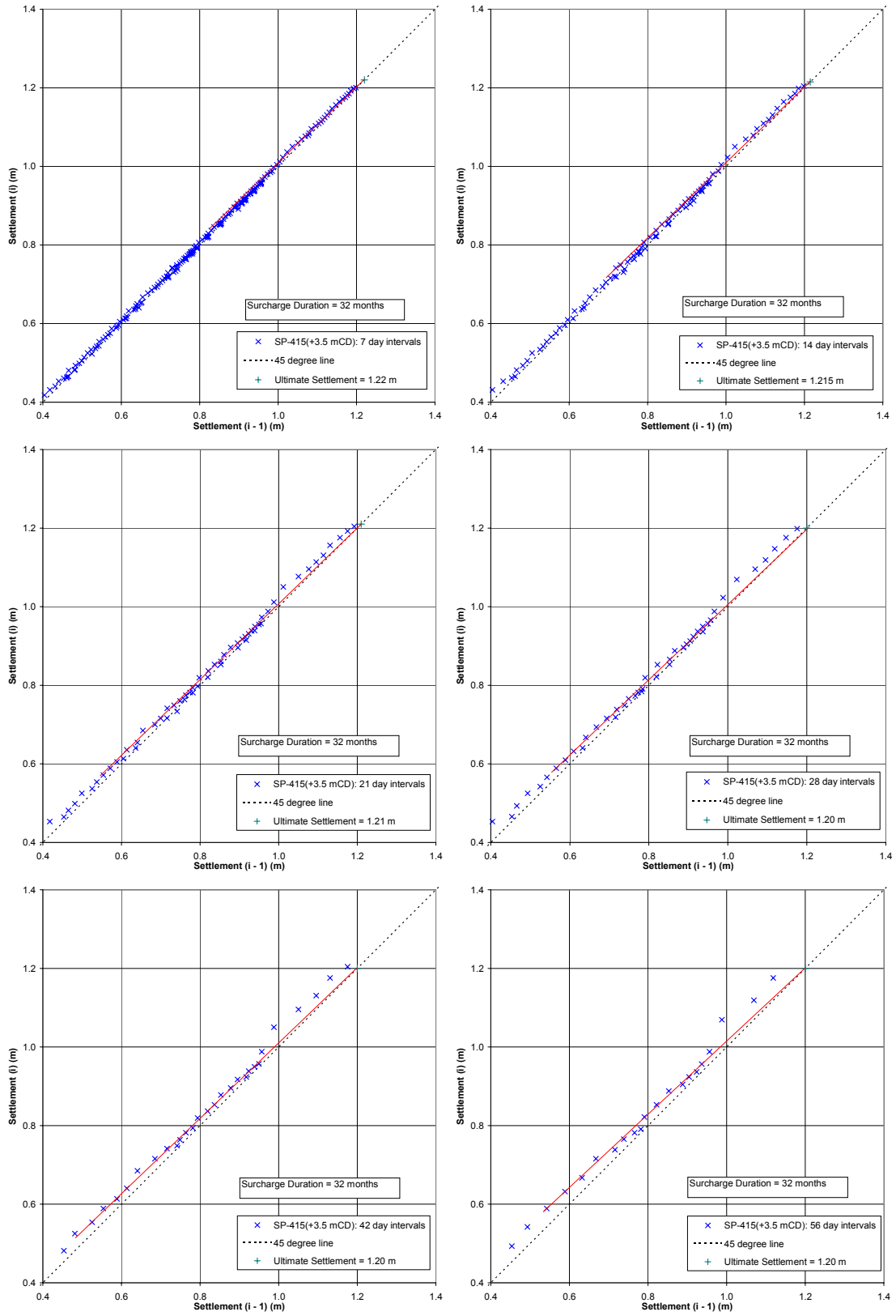


Figure 9.12 Asaoka plots at A2S-73 sub-area (3.0m x 3.0m) 32 months after surcharge.

9.2 Factors Affecting Assessment by the Hyperbolic Method

The magnitude of ultimate settlement and degree of consolidation can be predicted by the Hyperbolic method as described in section 7.7.2. Factors affecting assessment by the Hyperbolic method have been discussed in detail by the author (Arulrajah et al., 2003a, 2004e) during the course of this research study. The assessment by the Hyperbolic method was carried out for the sub-areas for assessment periods of 12, 24 and 32 months after surcharge placement. Table 9.4 compares the magnitude of ultimate settlement and degree of consolidation predicted by the Hyperbolic method using various periods of assessment after surcharge placement.

Table 9.4 Hyperbolic method at 12, 24 and 32 months after surcharge placement - 21.6, 33.7 and 41.9 months of monitoring (Arulrajah et al., 2004e).

Sub-Area	Hyperbolic	12 months	24 months	32 months
A2S-71 2.0 x 2.0 m	Ultimate Settlement(m)	1.749	1.758	1.801
	Settlement to date (m)	1.334	1.578	1.687
	Degree of Consolidation, U (%)	76.3	89.7	93.7
A2S-72 2.5 x 2.5 m	Ultimate Settlement(m)	1.380	1.405	1.408
	Settlement to date (m)	1.020	1.225	1.264
	Degree of Consolidation, U (%)	73.9	87.2	89.8
A2S-73 3.0 x 3.0 m	Ultimate Settlement(m)	1.096	1.126	1.169
	Settlement to date (m)	0.693	0.856	0.948
	Degree of Consolidation, U (%)	63.2	76.0	81.1

The slope of Hyperbolic plot is changing with time and varies with the period of assessment as described in section 7.7.2. The ultimate settlement predicted is found to increase with increasing period of assessment as evident in Table 9.4. Correspondingly, the degree of consolidation will decrease with the increasing period of assessment. Similar behaviour has been reported by Bo et al. (2003a). If an assessment is made too early after surcharge placement, this will lead to an overestimation of the degree of consolidation of the marine clay. Table 9.4 indicates that the sub-area with the closest vertical drain spacing has attained the highest degree of consolidation for the various surcharging durations. At the end of the surcharging period of 32 months, the sub-area with the closest vertical drain spacing (A2S-71: 2.0 x 2.0) has achieved a degree of consolidation of 93.7 % while that with the furthest vertical drain spacing (A2S-73: 3.0 x 3.0) has achieved a degree of consolidation of 81.1 %. It is to be noted that the Hyperbolic method assessment was not reported for the A2S-74 (No Drains) sub-area as the degree of consolidation did not reach a high enough value to enable

an interpretation. Figure 9.13 shows the Hyperbolic plots at assessment periods of 12, 24 and 32 months after surcharge placement for the A2S-71 sub-area.

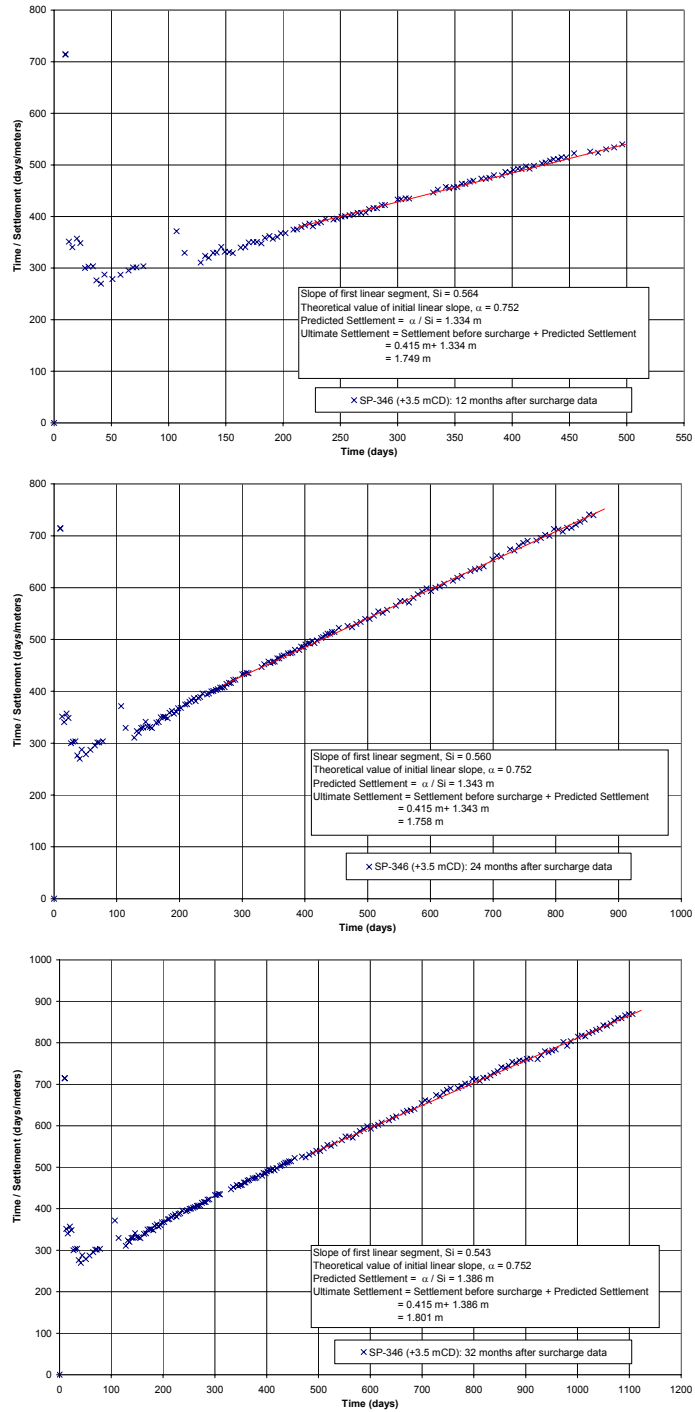


Figure 9.13 Hyperbolic plots at A2S-71 for various periods of assessments after surcharge (Arulrajah et al., 2003a).

Figure 9.14 shows the Hyperbolic plots at assessment periods of 12, 24 and 32 months after surcharge placement for the A2S-72 sub-area.

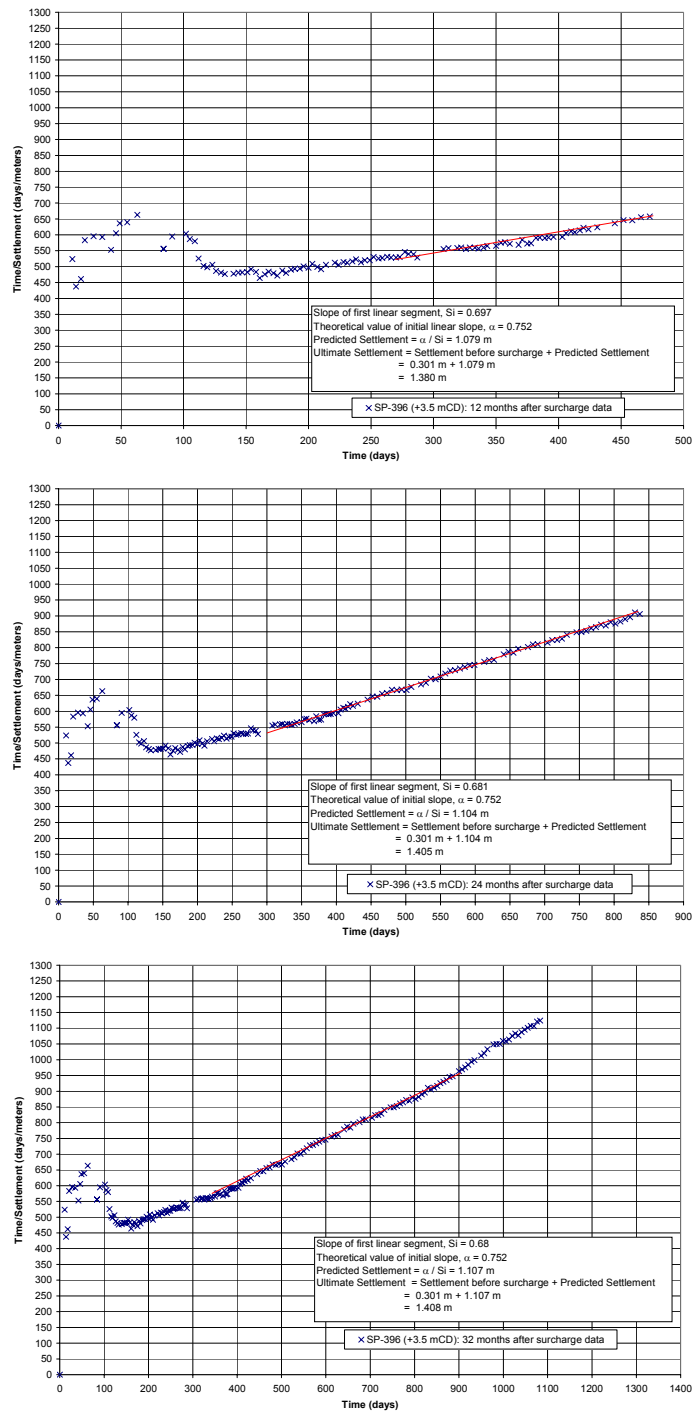


Figure 9.14 Hyperbolic plots at A2S-72 for various periods of assessments after surcharge.

Figure 9.15 shows the Hyperbolic plots at assessment periods of 12, 24 and 32 months after surcharge placement for the A2S-73 sub-area.

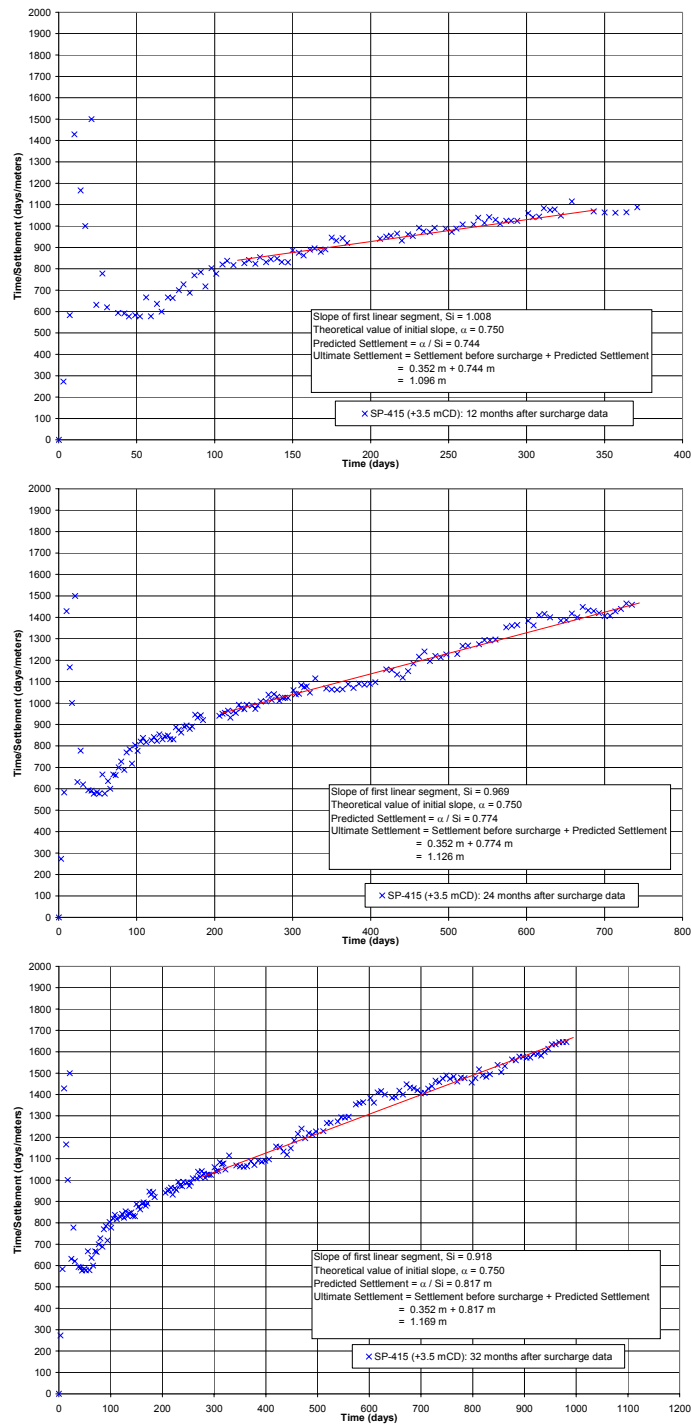


Figure 9.15 Hyperbolic plots at A2S-73 for various periods of assessments after surcharge.

9.3 Factors Affecting Assessment by Piezometers

Based on the ratio of the excess pore water pressure reading of the piezometer and the initial excess pore water pressure, the degree of consolidation of the piezometer can be ascertained. Factors that affect piezometer analyses include period of assessment after surcharge placement, hydrogeologic boundary phenomenon, correction for settlement of the piezometer tip and reduction of initial imposed load. Factors affecting assessment by the piezometer method have been discussed in detail by the author (Arulrajah et al., 2004a 2004e) during the course of this research study. The predictions were carried out with assessment periods of 12, 24 and 32 months after surcharge for the various vertical drain treated sub-areas of the Pilot Test Site. Table 9.5 compares the degree of consolidation ($U\%$) and coefficient of consolidation due to horizontal flow (c_h) predicted by the piezometer method.

9.3.1 Period of assessment after surcharge placement

Pore water pressure is dissipating with increasing periods of assessment and as such there is a lower remaining excess pore water pressure with increasing periods of assessment. Correspondingly, the degree of consolidation will increase with increasing period of assessment. The isochrones of the excess pore water pressures is interpreted to obtain the average degree of consolidation of the various sub-areas. Figures 9.16 to 9.19. shows the excess pore water pressure isochrones of the various sub-areas for various periods of assessment. Table 9.5 indicates that the sub-area with the closest vertical drain spacing has attained the highest degree of consolidation for the various surcharging durations. At the end of the surcharging period of 32 months, the sub-area with the closest vertical drain spacing (A2S-71: 2.0 x 2.0) has achieved a degree of consolidation of 86.2 % while A2S-74(No Drain) has achieved a degree of consolidation of 37.0%. This is a small increase compared to the degree of consolidation after surcharging period of 24 months.

9.3.2 Back-Analysed Coefficient of Consolidation due to Horizontal Flow

At the Pilot Test Site, c_h prediction from piezometers (section 7.9.2) was carried out by the total time method. It is apparent that the coefficient of consolidation due to horizontal flow, c_h value of the clay is reducing with time and as longer time of assessment is used in the back-analysis by piezometer method. The piezometer monitoring data indicates that the c_h value of the marine clay is lowest at the sub-area with the closest vertical drains spacing (A2S-71: 2.0 x 2.0) and highest at the sub-area with the largest vertical drain spacing (A2S-73: 3.0 x 3.0). This is in similar agreement with the c_h values back-calculated by the Asaoka

method and confirms the higher degree of smear effect at locations with closer drain spacing. However reduction of c_h with time is due to reduction of void ratio as consolidation progress.

Table 9.5 Comparison of average degree of consolidation using piezometers for 12, 24 and 32 months after surcharge placement - 21.6, 33.7 and 41.9 months of monitoring (Arulrajah et al., 2004e).

Sub-Area	Piezometers	12 mths.	24 mths.	32 mths.
A2S-71 2.0 x 2.0 m	Degree of Consolidation, U (%)	79.7	83.0	86.2
	Back-Analysed c_h (m ² /year)	2.80	1.56	1.30
A2S-72 2.5 x 2.5 m	Degree of Consolidation, U (%)	73.9	81.9	82.5
	Back-Analysed c_h (m ² /year)	3.99	2.54	1.94
A2S-73 3.0 x 3.0 m	Degree of Consolidation, U (%)	63.0	72.2	73.1
	Back-Analysed c_h (m ² /year)	4.51	2.90	2.23
A2S-74 (No Drain)	Degree of Consolidation, U (%)	35.3	35.5	37.0

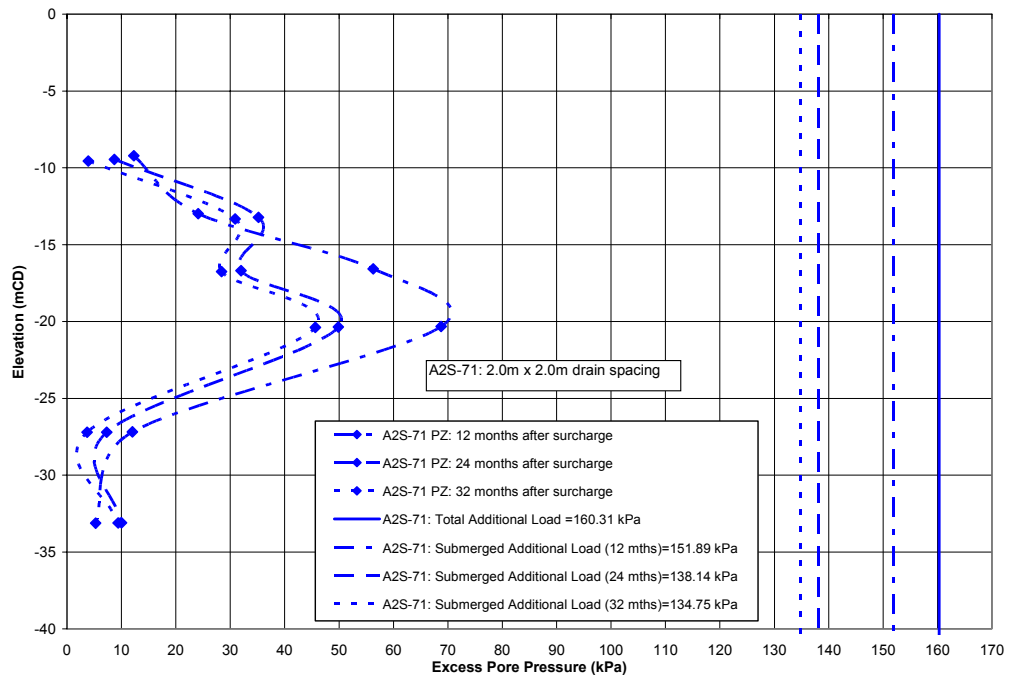


Figure 9.16 Comparison of A2S-71 (2.0 x 2.0 m) piezometer excess pore pressure isochrones 12, 24 and 32 months after surcharge (Arulrajah et al., 2004e).

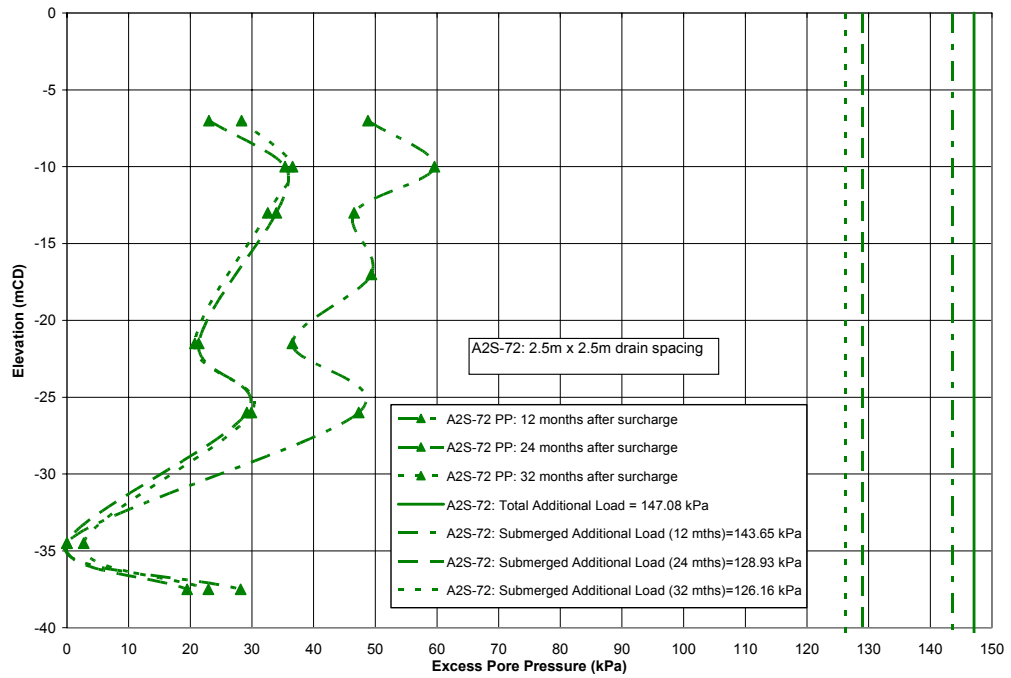


Figure 9.17 Comparison of A2S-72 (2.5 x 2.5 m) piezometer excess pore pressure isochrones 12, 24 and 32 months after surcharge (Arulrajah et al., 2004a).

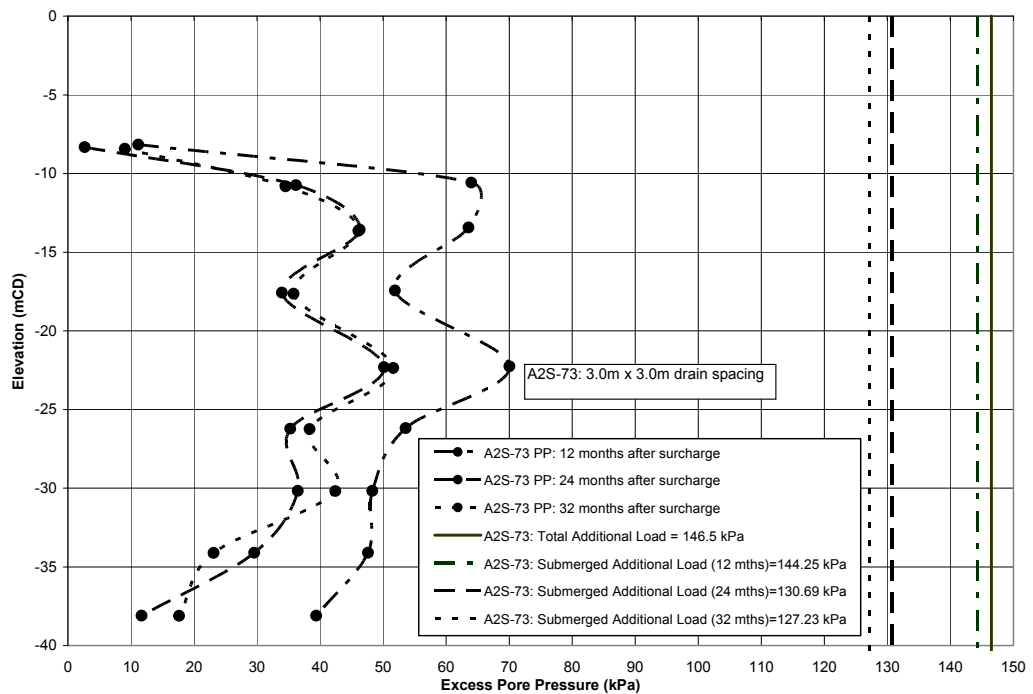


Figure 9.18 Comparison of A2S-73 (3.0 x 3.0 m) piezometer excess pore pressure isochrones 12, 24 and 32 months after surcharge (Arulrajah et al., 2004a).

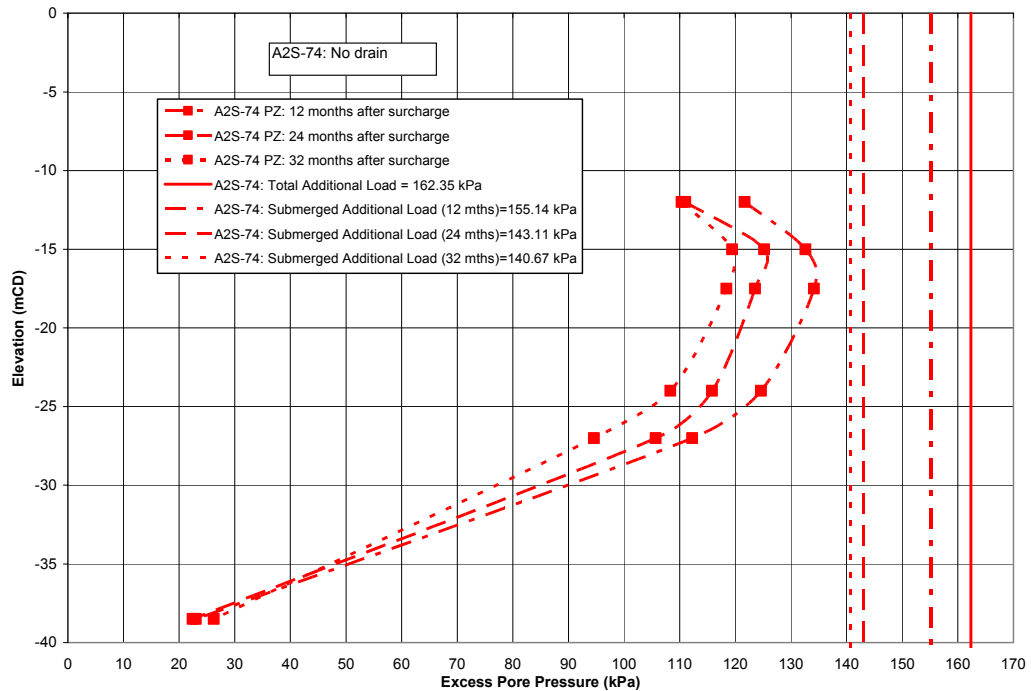


Figure 9.19 Comparison of A2S-74 (No Drain) piezometer excess pore pressure isochrones 12, 24 and 32 months after surcharge (Arulrajah et al., 2004e).

9.3.3 Hydrogeologic Boundary Phenomenon

If the piezometer is installed in offshore condition prior to reclamation, the initial excess pore water pressure can be obtained during the monitoring as the initial static pore pressure is known. Otherwise, the initial excess pore pressure has to be calculated from the assumed bulk density of the fill material (Bo et al., 1999). For the case of land reclamation projects, it is common to assume a bulk density of 17 to 19 kN/m³ for the sand fill material. Bo et al. (1999) has measured the density of sand in the same reclamation project as varying from 15 kN/m³ to 19 kN/m³. As such, the calculated excess pore pressure based on assumed bulk density of the fill material could lead to an over-estimation of excess pore pressure for land fill cases and an underestimation for hydraulic filling.

Initial excess pore pressure is usually assumed to be equal to the applied additional load. However, it could vary from the in-situ measured pore pressure after loading for some cases where clay layer is underlain by the hydrogeologic boundary. Figure This phenomenon has been explained by Schiffman et al. (1994). In such cases, the profile of pore pressure after additional load could be lower than that calculated. 9.20 illustrates this phenomenon. Overestimation of degree of consolidation would occur if the initial lower pore pressure is not taken into consideration. Situations like this will arise when the clay layer is underlain by a water aquifer which is being extracted for water supply. However, the hydrogeologic boundary phenomenon does not arise in the Pilot Test Site.

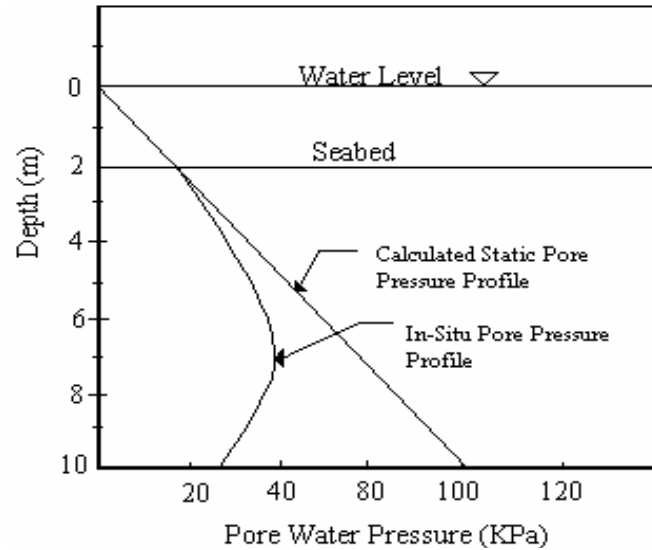


Figure 9.20 In-situ pore pressure which is lower than static pore pressure due to hydrogeologic boundary (after Schiffman et al., 1994).

9.3.4 Correction for Settlement of Piezometer Tip

Due to the large strain settlements at site, all piezometer raw readings taken have to be corrected to account for the new elevation of the piezometer due to the settlement of the piezometer tip. Without correction, the calculated piezometric elevation would be higher than the actual and this will subsequently lead to the underestimation of the degree of consolidation. This behaviour has been reported by Bo, Arulrajah and Choa (1998b).

Figure 9.21, 9.22 and 9.23 shows the comparison of corrected and uncorrected piezometric elevation, excess pore pressures and isochrones respectively for the Pilot Test Site.

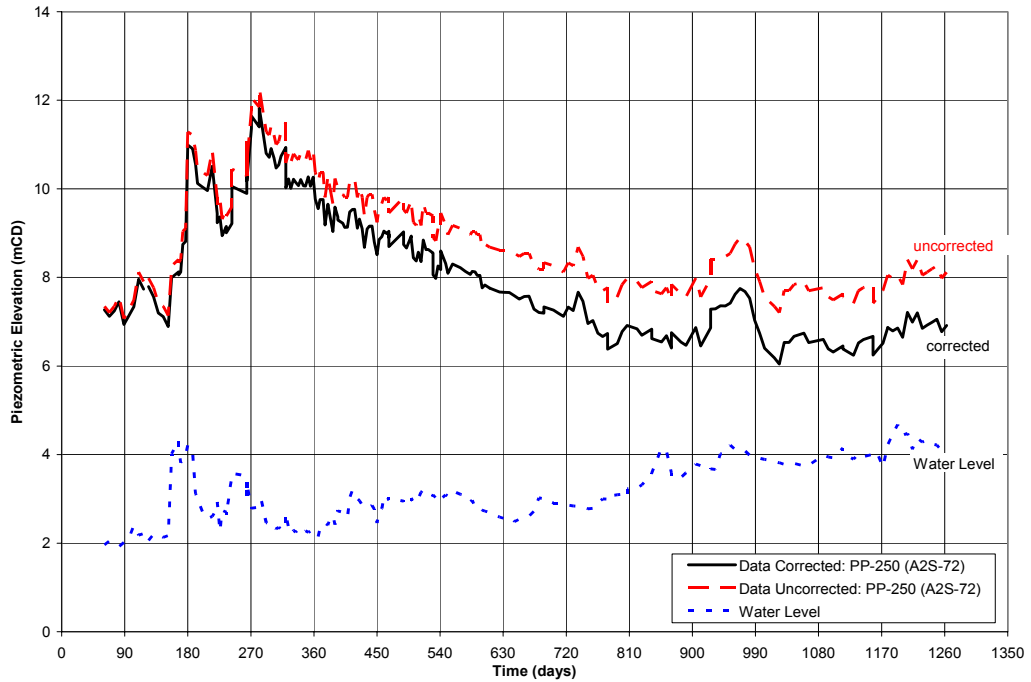


Figure 9.21 Comparison between corrected and uncorrected piezometric elevation (A2S-72: PP-250) (Arulrajah et al., 2004e).

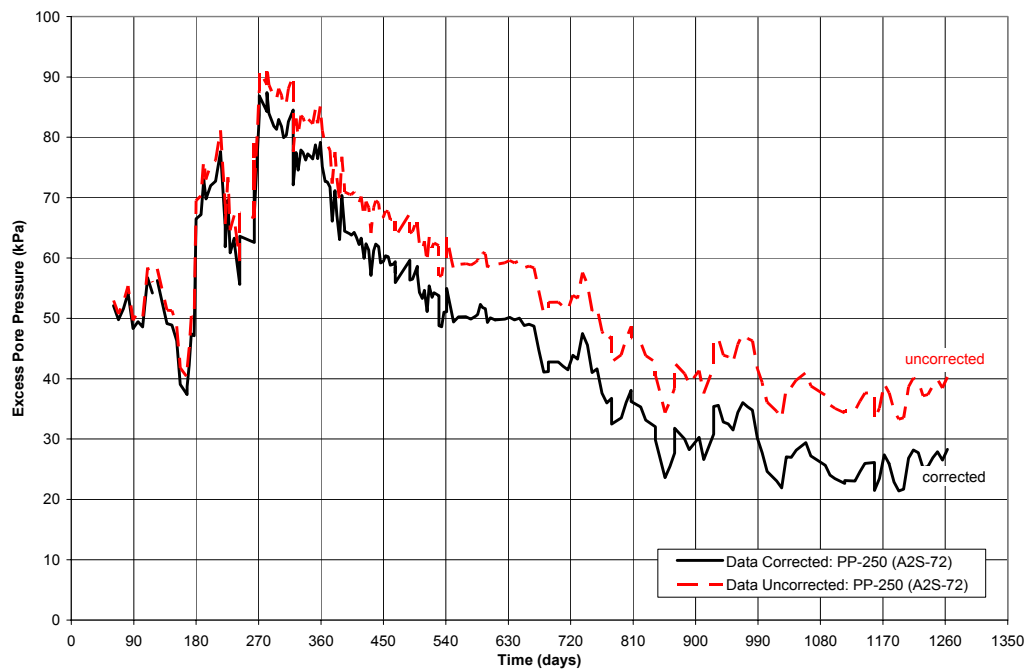


Figure 9.22 Comparison between corrected and uncorrected excess pore pressure (A2S-72: PP-250) (Arulrajah et al., 2004a).

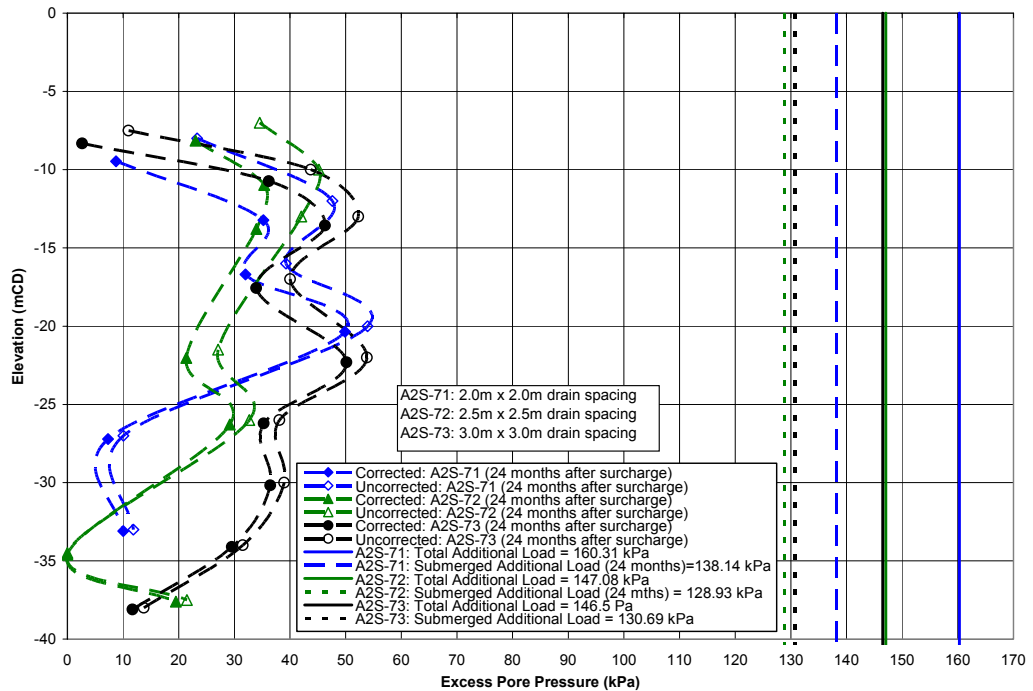


Figure 9.23 Comparison between corrected and uncorrected piezometer excess pore pressure isochrones 24 months after surcharge at Pilot Test Site (Arulrajah et al., 2004e).

9.3.5 Reduction of Initial Imposed Load

For marine clay when reclamation fill is imposed, the marine clay can seldom gain the effective stress equivalent to the initial imposed load due to the following reasons:

- Reduction of load due to sinking of fill below groundwater level
- Rise in groundwater level due to seasonal recharge

This behaviour was first reported by Mesri and Choi (1985). As such, degree of consolidation based on the initial imposed load is likely to be underestimated since the available effective additional load at assessed time is smaller than the initial load (Bo et al., 1999).

9.4 Comparison between Asaoka, Hyperbolic and Piezometer Methods

The comparison of degree of consolidation and back-analysed c_h between the Asaoka (28 day interval), Hyperbolic and piezometers is summarised in Tables 9.6, 9.7 and 9.8 using periods of assessment of 12, 24 and 32 months after surcharge placement.

Table 9.6 Comparison between Asaoka, Hyperbolic and piezometer methods 12 months after surcharge - 21.6 months of monitoring (Arulrajah et al., 2004e).

Sub-Area	Comparison	Asaoka	Hyperbolic	Piezometer
A2S-71 2.0 x 2.0 m	Ultimate Settlement(m)	1.872	1.749	-
	Settlement to date (m)	1.334	1.334	-
	Degree of Consolidation, U (%)	71.3	76.3	79.7
	Back-Analysed c_h (m ² /year)	1.06	-	2.80
A2S-72 2.5 x 2.5 m	Ultimate Settlement(m)	1.500	1.380	-
	Settlement to date (m)	1.020	1.020	-
	Degree of Consolidation, U (%)	68.0	73.9	73.9
	Back-Analysed c_h (m ² /year)	1.27	-	3.99
A2S-73 3.0 x 3.0 m	Ultimate Settlement(m)	1.250	1.096	-
	Settlement to date (m)	0.693	0.693	-
	Degree of Consolidation, U (%)	55.4	63.2	63.0
	Back-Analysed c_h (m ² /year)	1.99	-	4.51

Table 9.7 Comparison between Asaoka, Hyperbolic and piezometer methods 24 months after surcharge - 33.7 months of monitoring (Arulrajah et al., 2004e).

Sub-Area	Comparison	Asaoka	Hyperbolic	Piezometer
A2S-71 2.0 x 2.0 m	Ultimate Settlement (m)	1.850	1.758	-
	Settlement to date (m)	1.578	1.578	-
	Degree of Consolidation, U (%)	85.3	89.7	83.0
	Back-Analysed c_h (m ² /year)	1.14	-	1.56
A2S-72 2.5 x 2.5 m	Ultimate Settlement (m)	1.420	1.405	-
	Settlement to date (m)	1.225	1.225	-
	Degree of Consolidation, U (%)	86.3	87.2	81.9
	Back-Analysed c_h (m ² /year)	1.20	-	2.54
A2S-73 3.0 x 3.0 m	Ultimate Settlement (m)	1.240	1.126	-
	Settlement to date (m)	0.856	0.856	-
	Degree of Consolidation, U (%)	69.0	76.0	72.2
	Back-Analysed c_h (m ² /year)	1.75	-	2.90

Table 9.8 Comparison between Asaoka, Hyperbolic and piezometer methods 32 months after surcharge - 41.9 months of monitoring (Arulrajah et al., 2004e).

Sub-Area	Comparison	Asaoka	Hyperbolic	Piezometer
A2S-71 2.0 x 2.0 m	Ultimate Settlement (m)	1.838	1.801	-
	Settlement to date (m)	1.687	1.687	-
	Degree of Consolidation, U (%)	91.8	93.7	86.2
	Back-Analysed c_h (m ² /year)	1.08	-	1.30
A2S-72 2.5 x 2.5 m	Ultimate Settlement (m)	1.412	1.408	-
	Settlement to date (m)	1.264	1.264	-
	Degree of Consolidation, U (%)	89.5	89.8	82.5
	Back-Analysed c_h (m ² /year)	1.22	-	1.94
A2S-73 3.0 x 3.0 m	Ultimate Settlement (m)	1.200	1.169	-
	Settlement to date (m)	0.948	0.948	-
	Degree of Consolidation, U (%)	79.0	81.1	73.1
	Back-Analysed c_h (m ² /year)	2.20	-	2.23

The ultimate settlement predicted by the Asaoka method is slightly decreasing with increasing periods of assessment, as illustrated in Figure 9.24. Subsequently, the degree of consolidation predicted by the Asaoka method is increasing with increasing periods of assessment, as illustrated in Figure 9.25. The ultimate settlement predicted by the Hyperbolic method on the other hand is increasing with increasing periods of assessment, as illustrated in Figure 9.24. Subsequently, the degree of consolidation predicted by the Hyperbolic method is decreasing with the increasing periods after surcharge placement, as illustrated in Figure 9.25. The ultimate settlement and degree of consolidation obtained by the two methods is found to converge to an excellent agreement with each other as the surcharge period increases. The degree of consolidation predicted by the Hyperbolic method is found to be slightly higher than that of the Asaoka method.

The degree of consolidation predicted by the piezometers is found to be in good agreement with the Asaoka and Hyperbolic methods for the early period of assessment as shown in Figure 9.24. However as the assessment period increases, the piezometer indicates lower degree of consolidation as compared to field settlement predictions, as illustrated in Figure 9.25. Similar findings for lower piezometer readings compared to field settlement predictions have been reported by Bo et al. (1999). This can be attributed to the non-linearity of the stress-strain behaviour of soil (Mikasa, 1995). In the non-linearity theory, the effective stress gain is slower in initial stage whereas settlement rate is faster in this stage (Bo et. al, 2003a). Therefore the degree of consolidation worked out from settlement ratio is much greater than that worked out from pore pressure.

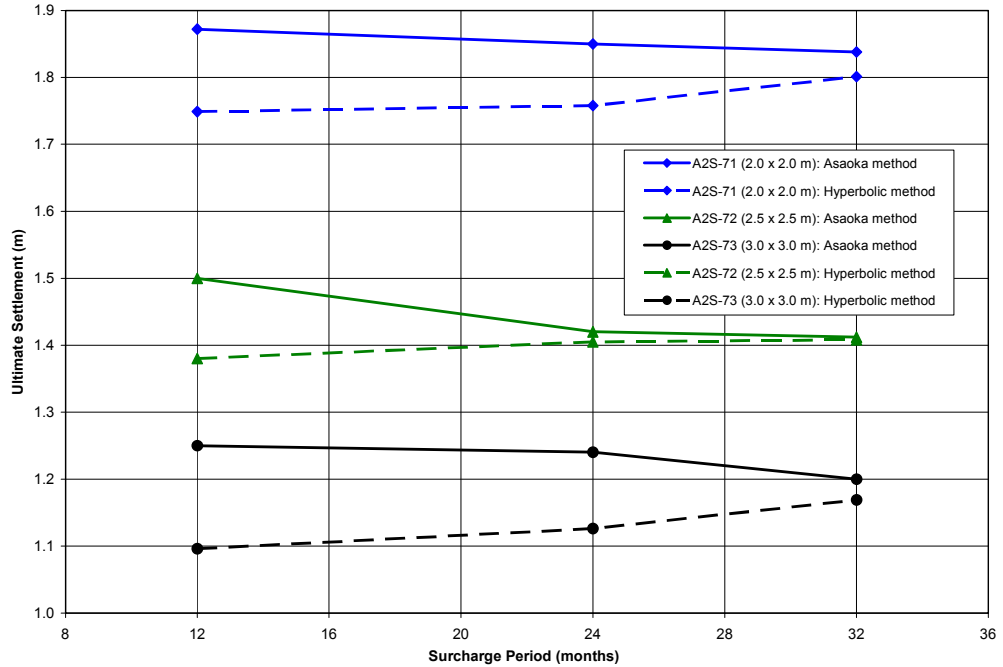


Figure 9.24 Comparison between variation in ultimate settlement at various surcharge periods by the Asaoka and Hyperbolic methods (Arulrajah et al., 2004e).

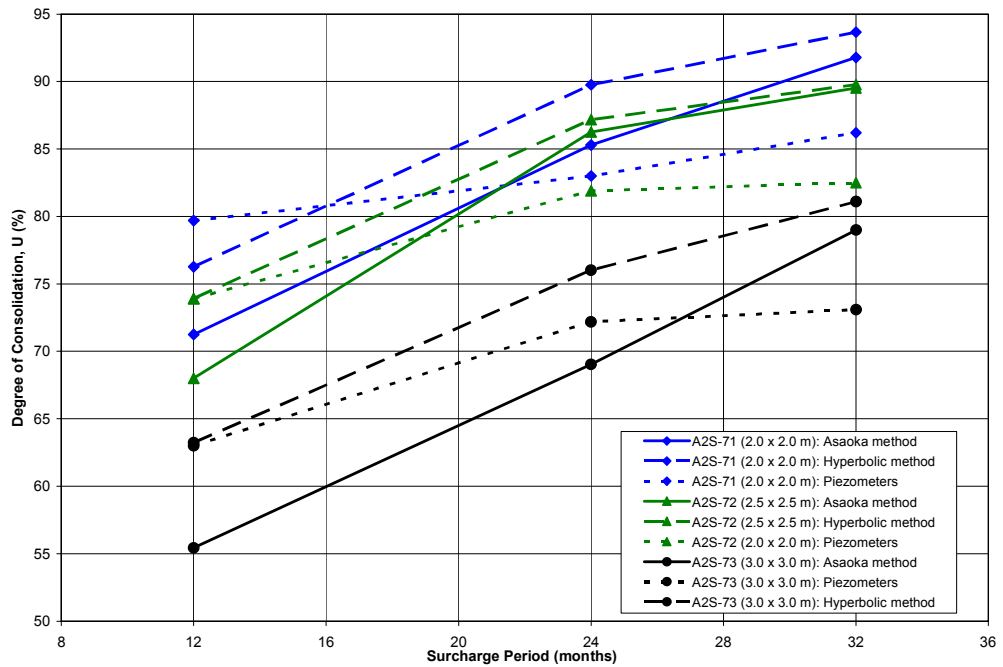


Figure 9.25 Comparison between variation in degree of consolidation at various surcharge periods by the Asaoka, Hyperbolic and piezometer methods (Arulrajah et al., 2004e).

The back-analysed c_h by the Asaoka method indicates that there is a trend of the c_h value generally increasing at longer periods of assessment after surcharge placement. This is illustrated in Figure 9.26. The coefficient of consolidation due to horizontal flow, c_h value of the clay converges to the final value as longer time of assessment is used in the back-analysis by the Asaoka method. The study reveals that the c_h value of the marine clay is lowest at the sub-area with the closest vertical drains spacing (A2S-71: 2.0 x 2.0) and highest at the sub-area with the furthest vertical drain spacing (A2S-73: 3.0 x 3.0). This can be attributed, amongst other reasons, to the higher degree of smear effect at locations with closer drain spacing. However reduction of c_h with time is due to reduction of void ratio as consolidation progress.

The back-analysed c_h by the piezometer method indicates that there is a trend of the c_h value generally decreasing at longer periods of assessment after surcharge placement. This is illustrated in Figure 9.26. It is apparent that the coefficient of consolidation due to horizontal flow, c_h value of the clay is reducing with time and as longer time of assessment is used in the back-analysis by piezometer method.

The c_h values back-calculated by the Asaoka and piezometer method after 32 months of surcharge placement is found to be in good agreement. The piezometer monitoring data indicates that the back-analysed c_h value of the marine clay is lowest at the sub-area with the closest vertical drains spacing (A2S-71: 2.0 x 2.0) and highest at the sub-area with the furthest vertical drain spacing (A2S-73: 3.0 x 3.0). This is in agreement with the c_h values back-calculated by the Asaoka method and supports that the higher degree of smear effect at locations with closer drain spacing. However reduction of c_h with time is due to a reduction of void ratio as consolidation progresses.

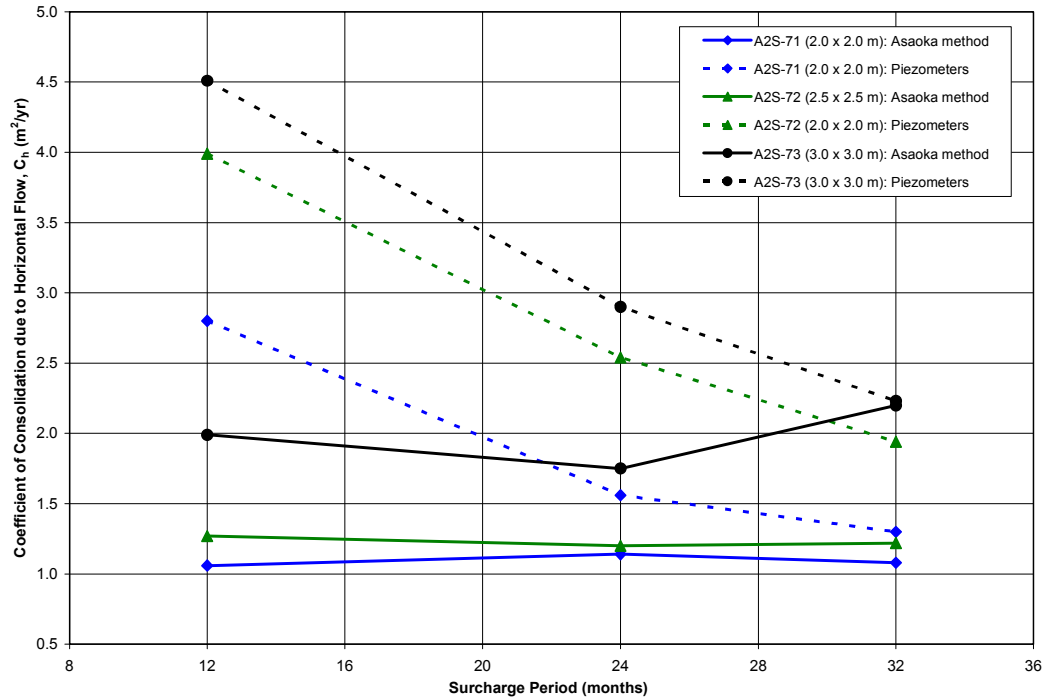


Figure 9.26 Comparison between variation in c_h at various surcharge periods by the Asaoka and piezometer methods (Arulrajah et al., 2004e).

9.5 Findings and Recommendations

The author's findings of the Asaoka method reveal that the magnitude of ultimate settlement decreases and the degree of consolidation subsequently increases as a longer period of assessment is used in the prediction. It is apparent that as the time interval increases, a cut-off time interval is obtained after which increasing time intervals would converge to the same magnitude of ultimate settlement. In the study of the vertical drain areas in the Pilot Test Site, the cut-off time interval was determined to be 28 days.

The author's findings reveal that the c_h value back-analysed by the Asaoka method is dependant on the time interval used for the prediction. The c_h value predicted by the Asaoka method decreases and converges to the final value as a longer time of assessment and increasing time intervals is used in the back-analysis. The study reveals that the c_h value of the marine clay is lowest at the sub-area with the closest vertical drains spacing and highest at the sub-area with the largest vertical drain spacing which is attributed to the larger smear effect at locations with closer drain spacing. The author recommends that for the Asaoka method a longer time interval has to be used for the ultimate settlement and c_h predictions. The author's findings of the Hyperbolic method reveal that the magnitude of ultimate settlement increases and subsequently the degree of consolidation decreases as a longer

period of assessment is used in the prediction. The prediction of ultimate settlement and degree of consolidation is found to be in excellent agreement for the two methods especially when the period of assessment increases.

The degree of consolidation predicted by the piezometers is found to be in good agreement with the Asaoka and Hyperbolic methods for the early period of assessment. However as the assessment period increases, the piezometer indicates lower degree of consolidation as compared to field settlement predictions. This can be attributed to the non-linearity of the stress-strain behaviour of soil (Mikasa, 1995).

The back-analysed c_h by the piezometer method indicates that there is a trend of the c_h value generally decreasing at longer periods of assessment after surcharge placement. It is apparent that the coefficient of consolidation due to horizontal flow, c_h value of the clay is reducing with time as longer time of assessment is used in the back-analysis by piezometer method. The c_h values back-calculated by the Asaoka and piezometer method after 32 months of surcharge placement is found to be in good agreement. This is in similar agreement with the c_h values back-calculated by the Asaoka method and confirms the higher degree of smear effect at locations with closer drain spacing.

10.0 FINITE ELEMENT MODELING OF MARINE CLAY DEFORMATION UNDER RECLAMATION FILLS

Modeling of the consolidation behaviour of marine clay and prefabricated vertical drains (PVD) under reclamation fills and surcharge was carried out by the finite element modeling (FEM) method with the Plaxis Version 8 (2002) numerical modeling software. The analyses included the modeling of the consolidation behaviour of marine clay under reclamation fills with and without prefabricated vertical drains.

Modeling of the sub-areas treated with vertical drains was carried out by both the axis-symmetric unit cell and full-scale analysis methods using a 2D model. Modeling of control areas which was not treated with prefabricated vertical drains was carried out by means of full-scale analysis. The numerical analysis of marine clay deformation with and without vertical drain was carried out for the Pilot Test Site and In-Situ Test Site described earlier. Each of the test sites comprise of vertical drain treated sub-areas and untreated sub-areas which were both reclaimed and preloaded under the same conditions. The results of the finite element modeling analysis were compared with that obtained by means of observational methods. The finite element analysis was carried out by the author using the Plaxis Version 8 (2002) numerical modeling software.

The finite element modeling of marine clay deformation under reclamation fills described in this chapter have been discussed in detail by the author (Arulrajah et al., 2004j) during the course of this research study.

10.1 Theory of Finite Element Modeling of Prefabricated Vertical Drains

In the modeling of the vertical drains in Bangkok clay by Lin et al. (2000), the interface element was used with the same soil property as the adjacent soil except for its permeability. Furthermore, the conversion scheme for well resistance was achieved by using interface elements. The well resistance was automatically considered in interface element for axis-symmetric and plane strain unit cells by the equivalent discharge capacity of interface elements to that of vertical drain.

For the axis-symmetric unit cell analysis of vertical drains in this study, the author has applied the methodology first proposed by Lin et al. (2000) in the consideration of the smear effect by using the equivalent horizontal permeability of soil surrounding the vertical drains. The

modeling of the Singapore marine clay treated with vertical drains was however modified to incorporate the marine clay multi-layers present in Singapore marine clay at Changi.

The conversion schemes from axi-symmetric to plane strain condition as proposed by Lin et al. (2000) was used for the full scale analysis method. For the modeling of prefabricated vertical drains in the full scale analysis method in this study, the author has used the drain element of the Plaxis Version 8 (2002) numerical modeling software.

It is necessary to consider the smear effect for the consolidation rate of vertical drain treated ground with finite permeability. Smear effect comes about due to the installation of vertical drains into the originally undisturbed soil. The installation of the vertical drains will result in disturbance of the adjacent soil surrounding the mandrel. The resulting smear zone will depend on the shape of the mandrel, the anchor rod and the method of installation. Bergado et al. (1992) has verified the diameter of the smear effect radius to be twice the equivalent cross-sectional area of the mandrel for soft Bangkok clay.

Since prefabricated vertical drain has a limited discharge capacity, the effect of well resistance varies with the permeability of the surrounding soils, the discharge capacity and the length of the vertical drain drainage path. Consequently the well resistance may affect the distribution of excess pore water pressure with depth and distance from the vertical drain during the consolidation. The contribution of well resistance is minimal for such long lengths of vertical drains and as such can be ignored in the numerical modeling analyses. Lin et al. (2000) states that previous analysis of field performance of vertical drains in soft clay deposits indicated that well resistance is negligible when the well resistance factor, R is greater than 5 as defined in the following equation:

$$R = q_w / (k_h l_m^2) \quad \text{Eq. (10.1)}$$

where:

q_w is the discharge capacity of the vertical drain in m^3/s

k_h is the horizontal permeability of the undisturbed soil in m/s

l_m is the length of the vertical drain in m

10.2 Axi-Symmetric Unit Cell Analysis of Prefabricated Vertical Drain

The vertical drains installed in the test sites were modeled in an axi-symmetric unit cell analysis by the author with the Plaxis Version 8 (2002) software. Figure 10.1 depicts the prefabricated vertical drain in axi-symmetric radial flow.

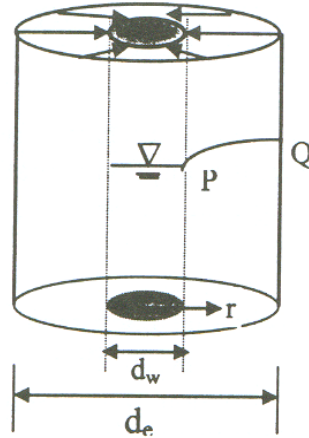


Figure 10.1 Axi-symmetric radial flow (Lin et al., 2000).

The method used for the consideration of the smear effect in the unit cell analysis is by using the equivalent horizontal permeability of surrounding soils, k_e (Lin et al., 2000) which is defined as:

$$k_e = \frac{k_h \ln(r_e/r_w)}{\ln(r_e/r_s) + (k_h/k_s)\ln(r_s/r_w)} \quad \text{Eq. (10.2)}$$

where:

r_e is the radius of influence zone in units of m

r_w is the equivalent radius of vertical drain in units of m

r_s is the radius of smear zone in units of m

k_h is the horizontal permeability of the undisturbed soil in units of m/day

k_s is the horizontal permeability of soil within the smear zone in units of m/day

In the axi-symmetric unit cell analysis of the vertical drain, the equivalent horizontal permeability of the surrounding soil was taken as twice that of the equivalent vertical permeability. Figure 10.2 shows the schematic depiction of the conversion of the axi-symmetric unit cell from undisturbed marine clay with smear zone to that of equivalent horizontal permeability of surrounding soils.

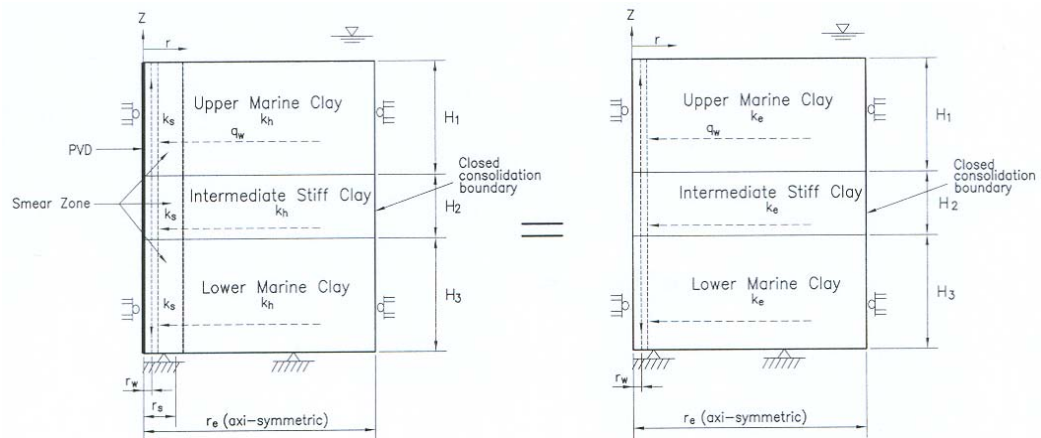


Figure 10.2 Conversion of the axi-symmetric unit cell from undisturbed marine clay with smear zone to that of equivalent horizontal permeability of surrounding soils (Arulrajah et al.,2004j).

Table 10.1 indicates the soil parameters used for the finite element modeling of vertical drain by the axi-symmetric unit cell analysis. The parameters were obtained from laboratory testing results.

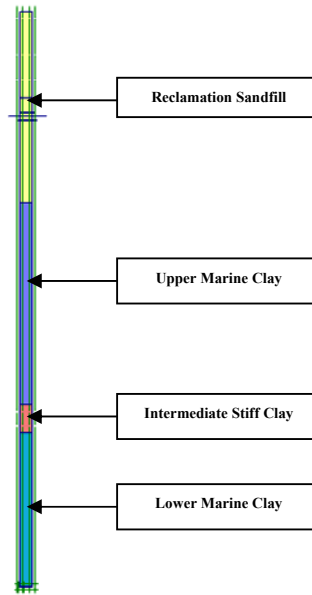
Figure 10.3 shows the deformed mesh while Figure 10.4 shows the vertical displacement by the axi-symmetric unit cell analysis of the Vertical Drain Area at the In-Situ Test Site, 20 months after surcharge placement.

Figure 10.5 shows the deformed mesh while Figure 10.6 shows the vertical displacement by the axi-symmetric unit cell analysis of the A2S-71 sub-area (2.0m x 2.0m) at the Pilot Test Site, 32 months after surcharge placement.

Figure 10.7 shows the deformed mesh while Figure 10.8 shows the vertical displacement by the axi-symmetric unit cell analysis of the A2S-72 sub-area (2.5m x 2.5m) at the Pilot Test Site, 32 months after surcharge placement.

Figure 10.9 shows the deformed mesh while Figure 10.10 shows the vertical displacement by the axi-symmetric unit cell analysis of the A2S-73 sub-area (3.0m x 3.0m) at the Pilot Test Site, 32 months after surcharge placement.

Table 10.1 Soil parameters for axi-symmetric unit cell analysis of PVD
(Arulrajah et al., 2004j)



<i>Mohr-Coulomb</i>		Reclamation Sandfill
Type		Drained
γ_{unsat}	[kN/m ³]	17.00
γ_{sat}	[kN/m ³]	20.00
k_h	[m/day]	1.000
k_v	[m/day]	1.000
E_{ref}	[kN/m ²]	13000.000
ν	[-]	0.300
G_{ref}	[kN/m ²]	5000.000
E_{oed}	[kN/m ²]	17500.000
c_{ref}	[kN/m ²]	1.00
ϕ	[°]	31.00
ψ	[°]	0.00

Notations:
 γ = soil unit weight
 k = permeability
 E_{ref} = Young's modulus
 ν = poisson's ratio
 G_{ref} = Shear modulus
 E_{oed} = Oedometer modulus
 c_{ref} = Cohesion
 ϕ = friction angle
 ψ = dilatancy angle
 λ^* = modified compression index
 κ^* = modified swelling index

<i>Soft-Soil</i>	Upper Marine Clay	Intermediate Stiff Clay	Lower Marine Clay
Type	Undrained	Undrained	Undrained
γ_{unsat}	[kN/m ³] 15.00	15.00	15.00
γ_{sat}	[kN/m ³] 15.50	15.50	16.00
k_e	[m/day] 2.66E-5	6.25E-5	2.81E-5
k_v	[m/day] 1.33E-5	3.13E-5	1.41E-5
λ^*	[-] 0.150	0.060	0.170
κ^*	[-] 0.018	0.011	0.025
c	[kN/m ²] 1.00	1.00	1.00
ϕ	[°] 27.00	32.00	27.00
ψ	[°] 0.00	0.00	0.00
ν_{ur}	[-] 0.150	0.150	0.150
K_0^{nc}	[-] 0.55	0.47	0.55

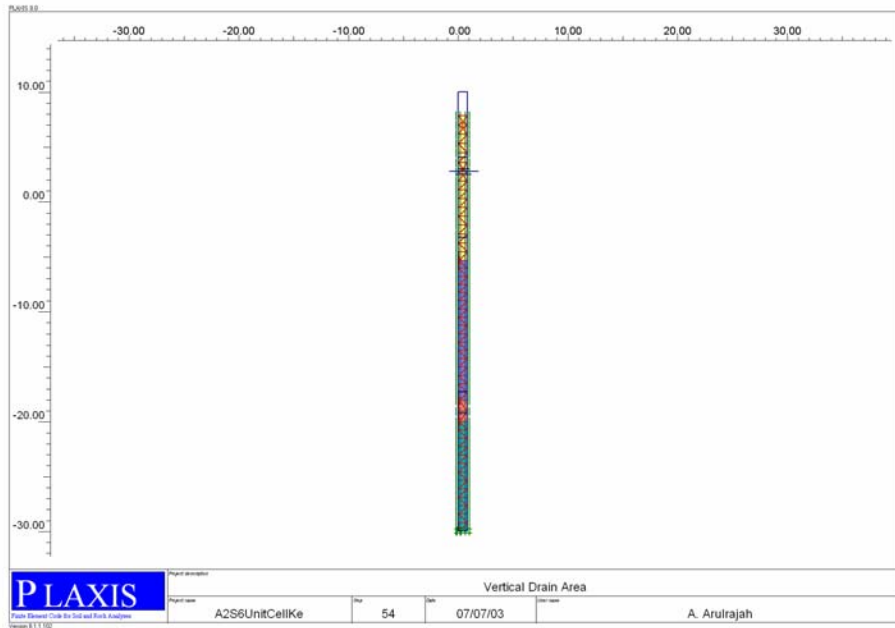


Figure 10.3 Deformed mesh by axi-symmetric unit cell analysis of Vertical Drain Area (1.5m x 1.5m) at the In-Situ Test Site, 20 months after surcharge placement.

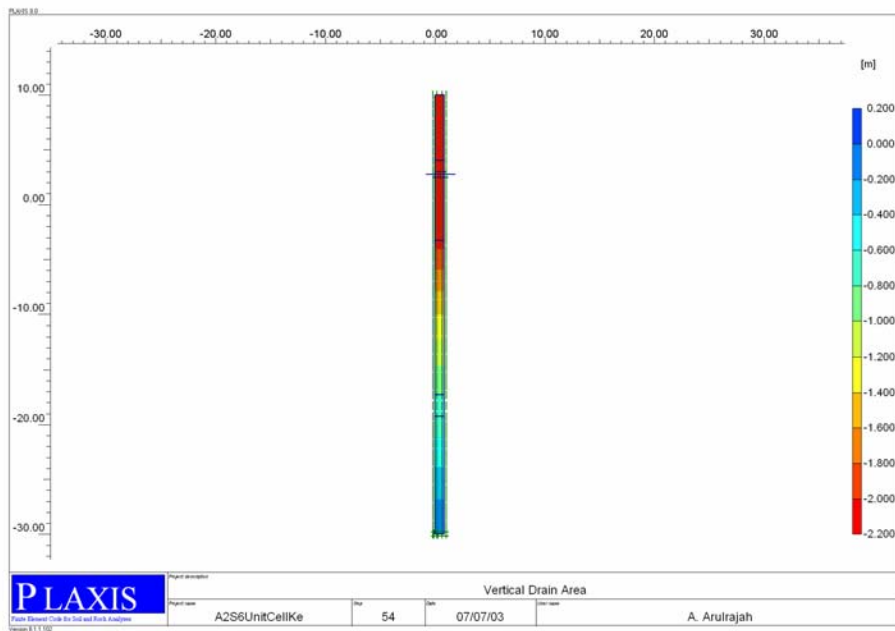


Figure 10.4 Vertical displacement by axi-symmetric unit cell analysis of Vertical Drain Area (1.5m x 1.5m) at the In-Situ Test Site, 20 months after surcharge placement.

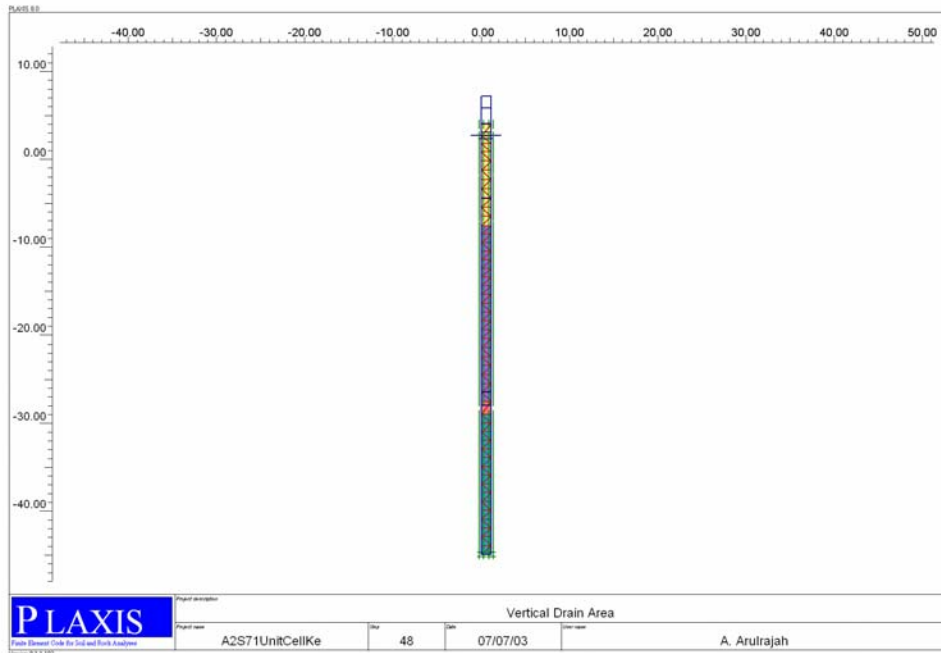


Figure 10.5 Deformed mesh by axi-symmetric unit cell analysis of A2S-71 sub-area (2.0m x 2.0m) at the Pilot Test Site, 32 months after surcharge placement.

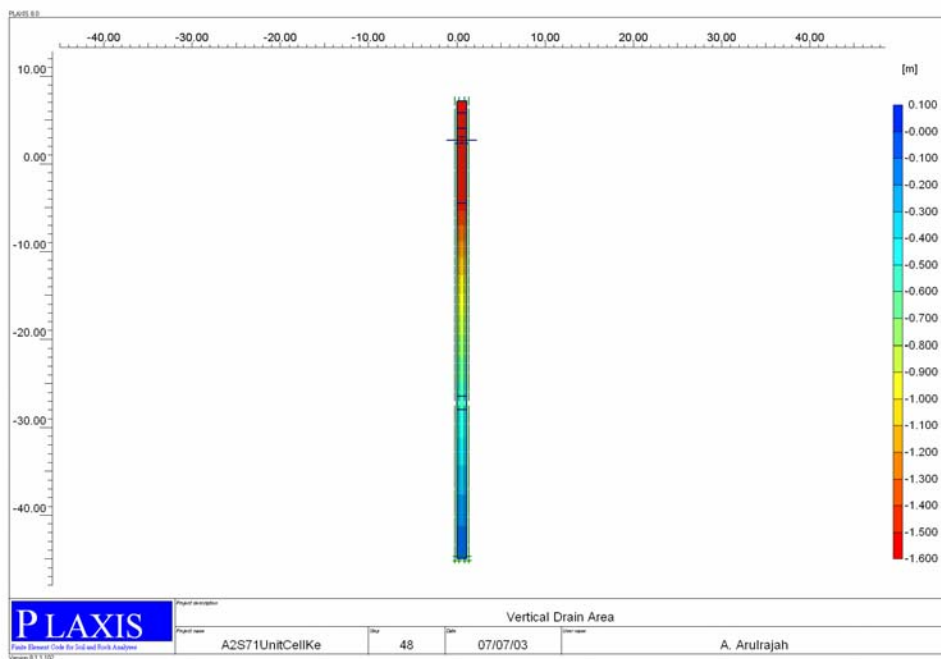


Figure 10.6 Vertical displacement by axi-symmetric unit cell analysis of A2S-71 sub-area (2.0m x 2.0m) at the Pilot Test Site, 32 months after surcharge placement.

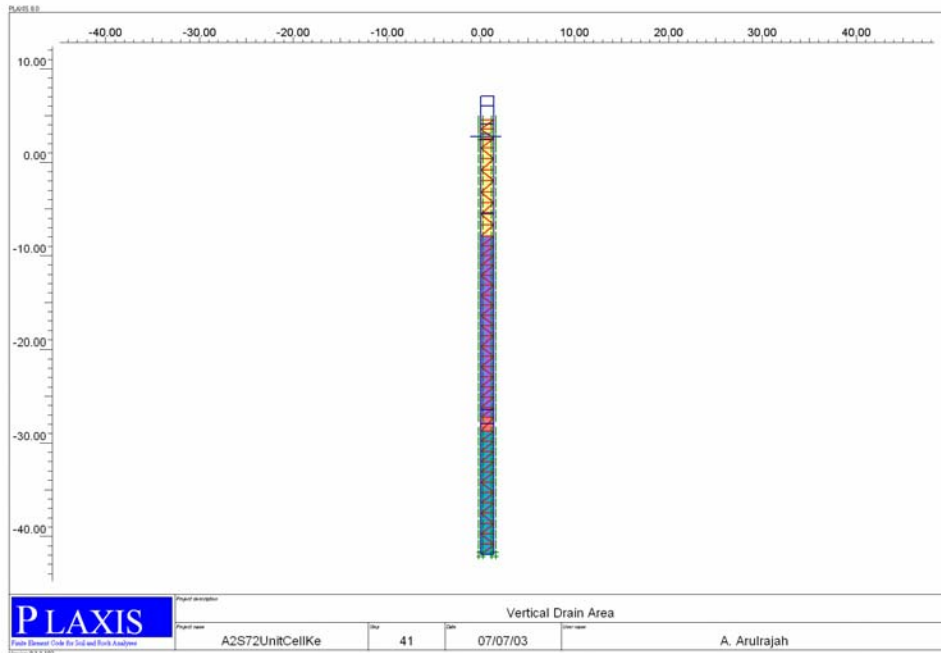


Figure 10.7 Deformed mesh by axi-symmetric unit cell analysis of A2S-72 sub-area (2.5m x 2.5m) at the Pilot Test Site, 32 months after surcharge placement.

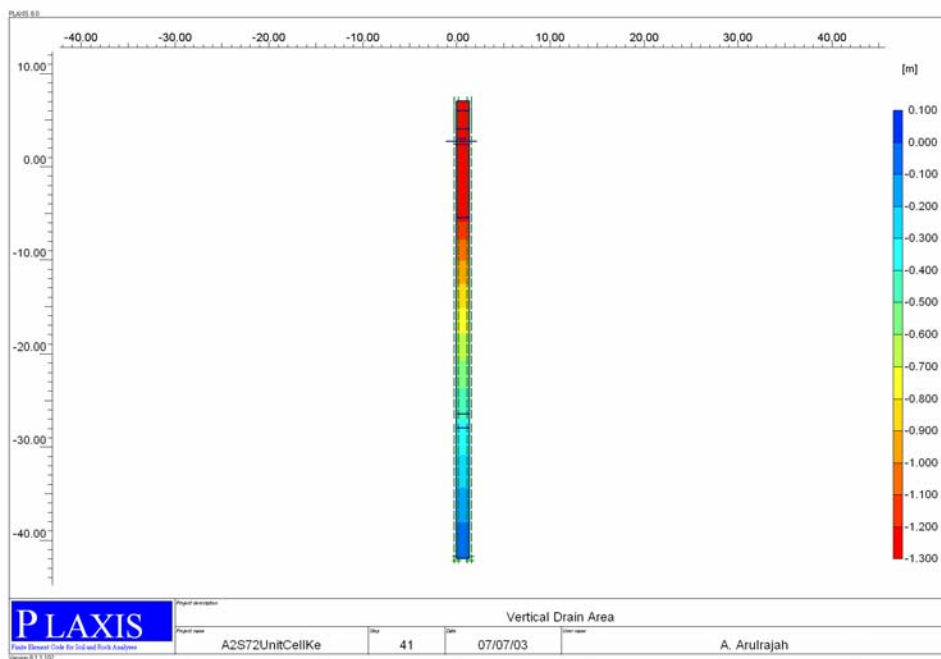


Figure 10.8 Vertical displacement by axi-symmetric unit cell analysis of A2S-72 sub-area (2.5m x 2.5m) at the Pilot Test Site, 32 months after surcharge placement.

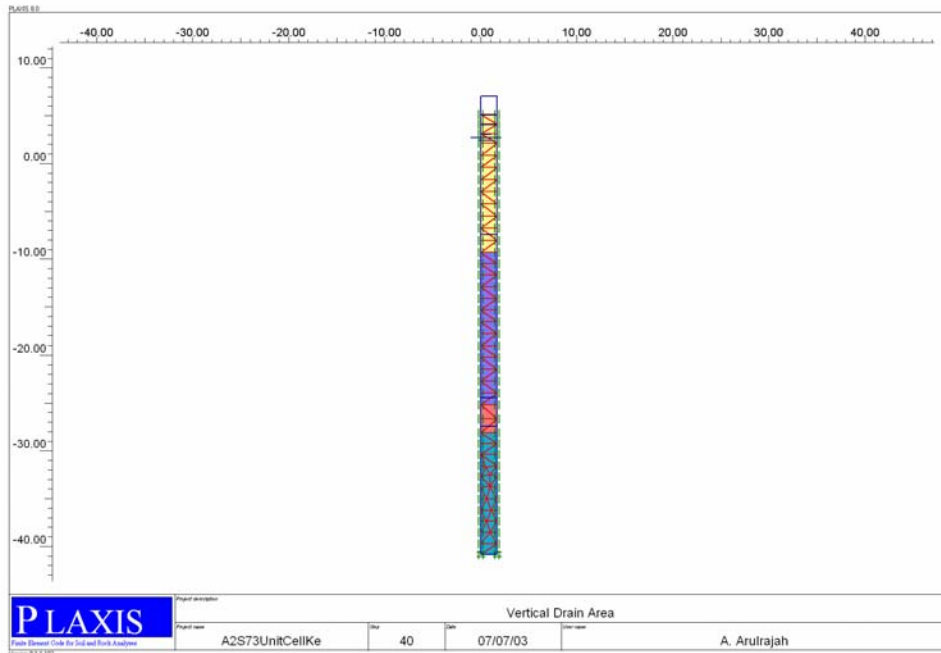


Figure 10.9 Deformed mesh by axi-symmetric unit cell analysis of A2S-73 sub-area (3.0m x 3.0m) at the Pilot Test Site, 32 months after surcharge placement.

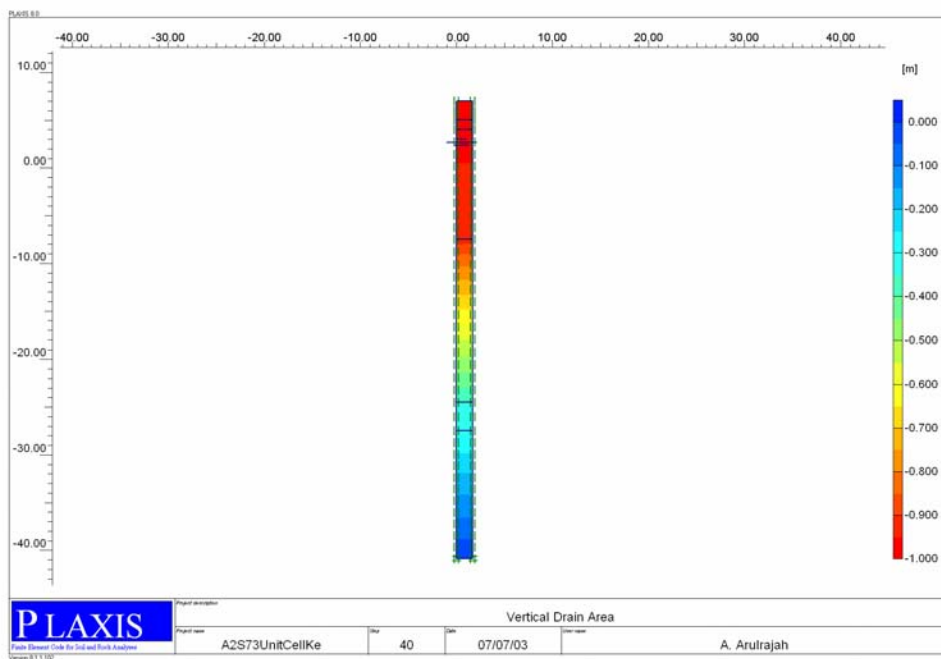


Figure 10.10 Vertical displacement by axi-symmetric unit cell analysis of A2S-73 sub-area (3.0m x 3.0m) at the Pilot Test Site, 32 months after surcharge placement.

10.3 Full Scale Analysis of Prefabricated Prefabricated Vertical Drains

The drain element available in the Plaxis Version 8 (2002) finite element program was used by the author to model the vertical drains for the Vertical Drain Area at the In-Situ Test Site by the full-scale analysis method. This method uses the open consolidation boundary condition at which, the excess pore water pressure is set to zero during the consolidation process in all nodes that belong to a drain.

The 6-node triangular element was adopted in the analysis. The element provides second order interpolation functions for displacement and its stiffness matrix is evaluated by numerical integration using 3 integration points.

In the modeling of the ground improvement, the following conditions were considered :-

- Consolidation analysis was performed under 2-D plane strain condition.
- Marine clay layers were simulated by using the Soft Soil Model
- Sandfill layer was simulated by using the Mohr-Coulomb Model.

In the full scale analyses finite element model, the conversion of permeability for an axis-symmetric radial flow to that of a plain strain flow with smear effect was carried out. In the finite element method analysis, pore water flow in the plain strain unit cell is considered as 2-D plane strain flow.

The conversion from radial flow of an axis-symmetric unit cell to 2-D plane flow of continuous drainage wall systems of plane strain unit cell can be carried out by the method of Lin et al. (2000). Figure 10.11 depicts the prefabricated vertical drain in 2-D plain strain flow.

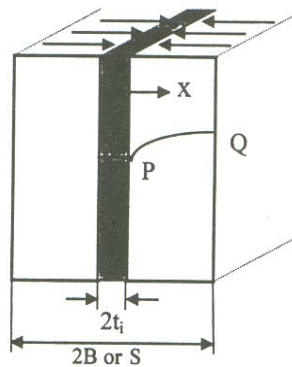


Figure 10.11 PVD in 2-D plane strain flow (Lin et al., 2000).

The equivalent permeability of the marine clay with consideration for smear effect can be calculated by the conversion of the axi-symmetric unit cell to that of a plain strain unit cell (Lin et al., 2000):

$$k_{\text{hpl}} = \frac{k_{\text{hax}} \pi}{6 [\ln(n_i/s) + (k_{\text{hax}}/k_{\text{sax}})\ln(s) - 0.75]} \quad \text{Eq. (10.3)}$$

where:

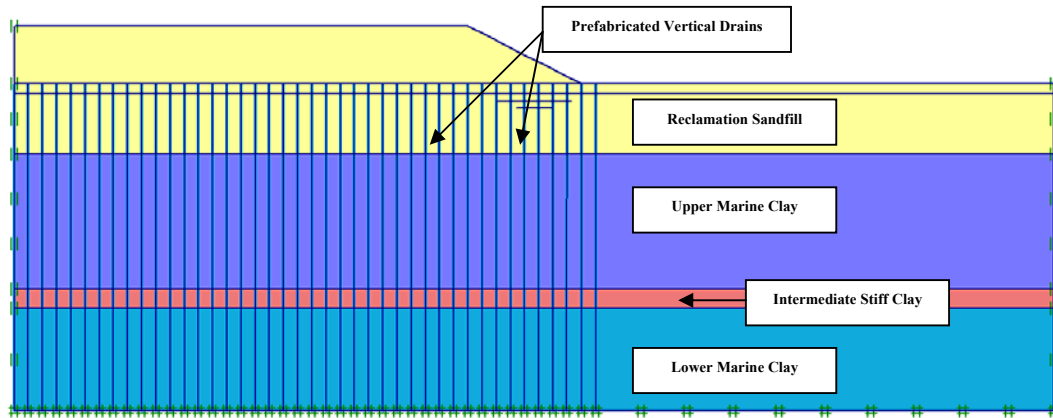
- k_{hpl} is the horizontal permeability of undisturbed zone in plane strain unit cell
- k_{hax} is the horizontal permeability of undisturbed zone in axi-symmetric unit cell
- k_{sax} is the horizontal permeability of the smear zone in axi-symmetric unit cell
- n_i is the influence ratio given by r_c/r_w
- s is the smear ratio given by r_s/r_w

The equivalent horizontal permeability of the marine clay after applying the conversion from axi-symmetric flow to plane strain flow with smear effect consideration was used in the finite element analysis of the vertical drains for the full scale analysis.

Table 10.2 indicates the soil parameters used for the finite element modeling of vertical drains by the full scale analysis.

Figure 10.12 shows the deformed mesh while Figure 10.13 shows the extreme vertical displacements by the full scale analysis for the Vertical Drain Area at the In-Situ Test Site, 20 months after surcharge placement.

Table 10.2 Soil parameters for full scale analysis of PVD (Arulrajah et al., 2004j).



<i>Mohr-Coulomb</i>		Reclamation Sandfill
Type		Drained
γ_{unsat}	[kN/m ³]	17.00
γ_{sat}	[kN/m ³]	20.00
k_h	[m/day]	1.000
k_v	[m/day]	1.000
E_{ref}	[kN/m ²]	13000.000
ν	[-]	0.300
G_{ref}	[kN/m ²]	5000.000
E_{oed}	[kN/m ²]	17500.000
c_{ref}	[kN/m ²]	1.00
ϕ	[°]	31.00
ψ	[°]	0.00

Notations:
 γ = soil unit weight
 k = permeability
 E_{ref} = Young's modulus
 ν = poisson's ratio
 G_{ref} = Shear modulus
 E_{oed} = Oedometer modulus
 c_{ref} = Cohesion
 ϕ = friction angle
 ψ = dilatancy angle
 λ^* = modified compression index
 κ^* = modified swelling index

<i>Soft-Soil</i>	Upper Marine Clay	Intermediate Stiff Clay	Lower Marine Clay
Type	Undrained	Undrained	Undrained
γ_{unsat}	[kN/m ³]	15.00	15.00
γ_{sat}	[kN/m ³]	15.50	15.50
k_{hpl}	[m/day]	4.67E-6	1.10E-5
k_v	[m/day]	2.34E-6	5.50E-6
λ^*	[-]	0.150	0.060
κ^*	[-]	0.018	0.011
c	[kN/m ²]	1.00	1.00
ϕ	[°]	27.00	32.00
ψ	[°]	0.00	0.00
ν_{ur}	[-]	0.150	0.150
K_0^{nc}	[-]	0.55	0.47

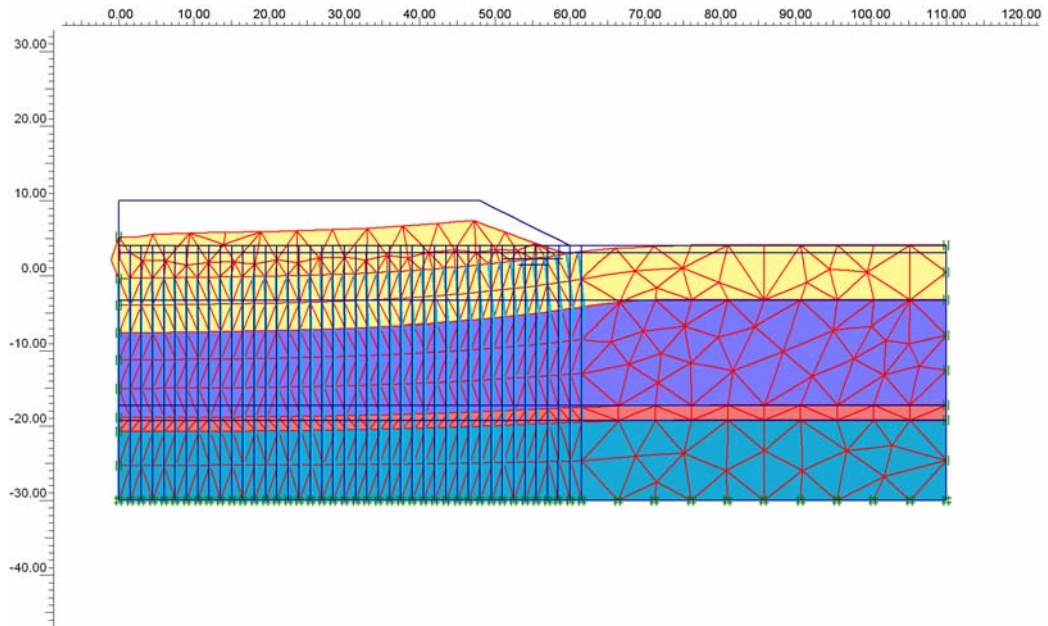


Figure 10.12 Deformed mesh by full scale analysis of Vertical Drain Area (1.5m x 1.5m) at In-Situ Test Site, 20 months after surcharge placement (Arulrajah et al., 2004j).

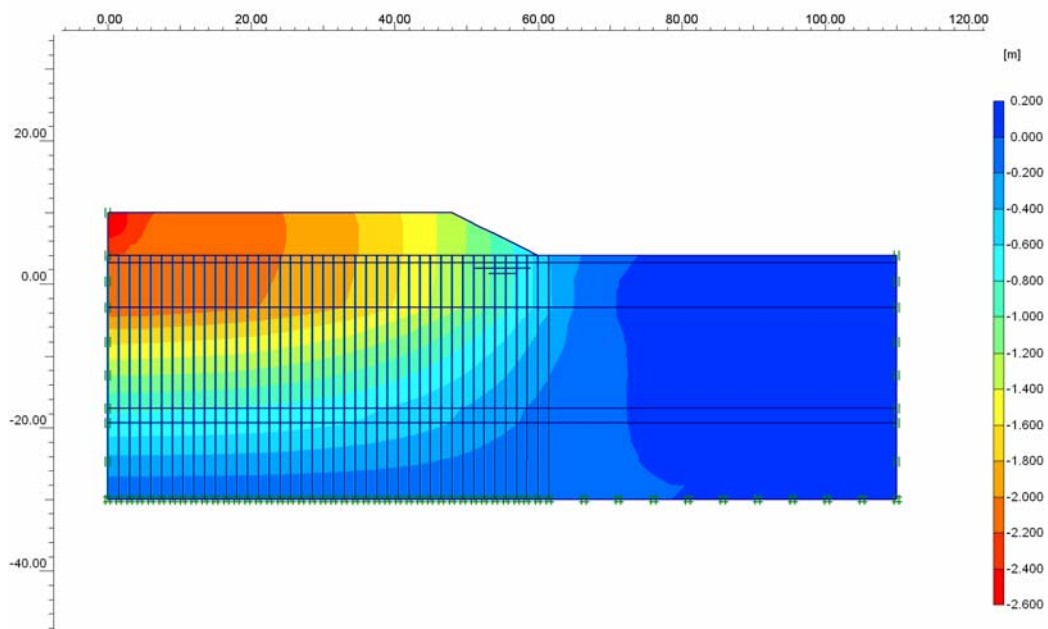


Figure 10.13 Vertical displacement by full scale analysis of Vertical Drain Area (1.5m x 1.5m) at In-Situ Test Site, 20 months after surcharge placement (Arulrajah et al., 2004j).

10.4 Full Scale Analysis of Untreated Control Embankments

In the full scale numerical modeling of the untreated control embankments of the Pilot Test Site and In-Situ Test Site where no vertical drains were installed but where surcharge of the same height was placed, the 6-node triangular element was adopted in the analysis.

The horizontal permeability of the undisturbed soil was taken as twice the vertical permeability of the undisturbed soil based on the properties of Singapore marine clay:

$$k_h = 2 k_v \quad \text{Eq. (10.4)}$$

where:

k_h is the horizontal permeability of the undisturbed soil

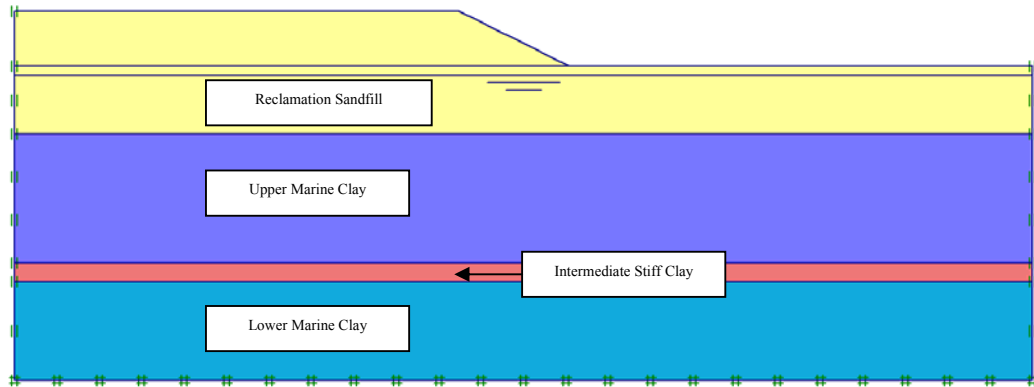
k_v is the vertical permeability of the undisturbed soil

Table 10.3 indicates the soil data parameters used for the finite element modeling of untreated control embankment by the full scale analysis.

Figure 10.14 shows the deformed mesh while Figure 10.15 shows the extreme vertical displacements by the full scale analysis for the untreated Control Area at the In-Situ Test Site, 20 months after surcharge placement.

Figure 10.16 shows the deformed mesh while Figure 10.17 shows the magnitude of the extreme vertical displacements by the full scale analysis for the No Drain Area at the Pilot Test Site, 32 months after surcharge placement.

Table 10.3 Soil parameters for full scale analysis of untreated control embankment (Arulrajah et al., 2004j)



<i>Mohr-Coulomb</i>		Reclamation Sandfill
Type		Drained
γ_{unsat}	[kN/m ³]	17.00
γ_{sat}	[kN/m ³]	20.00
k_h	[m/day]	1.000
k_v	[m/day]	1.000
E_{ref}	[kN/m ²]	13000.000
ν	[-]	0.300
G_{ref}	[kN/m ²]	5000.000
E_{oed}	[kN/m ²]	17500.000
c_{ref}	[kN/m ²]	1.00
ϕ	[°]	31.00
ψ	[°]	0.00

Notations:
γ = soil unit weight
k = permeability
E_{ref} = Young's modulus
ν = poisson's ratio
G_{ref} = Shear modulus
E_{oed} = Oedometer modulus
c_{ref} = Cohesion
ϕ = friction angle
ψ = dilatancy angle
λ^* = modified compression index
κ^* = modified swelling index

<i>Soft-Soil</i>	Upper Marine Clay	Intermediate Stiff Clay	Lower Marine Clay	
Type	Undrained	Undrained	Undrained	
γ_{unsat}	[kN/m ³]	15.00	15.00	15.00
γ_{sat}	[kN/m ³]	15.50	15.50	16.00
k_h	[m/day]	3.67E-5	8.64E-5	3.89E-5
k_v	[m/day]	1.84E-5	4.32E-5	1.95E-5
λ^*	[-]	0.150	0.060	0.170
κ^*	[-]	0.018	0.011	0.025
c	[kN/m ²]	1.00	1.00	1.00
ϕ	[°]	27.00	32.00	27.00
ψ	[°]	0.00	0.00	0.00
ν_{ur}	[-]	0.150	0.150	0.150
K_0^{nc}	[-]	0.55	0.47	0.55

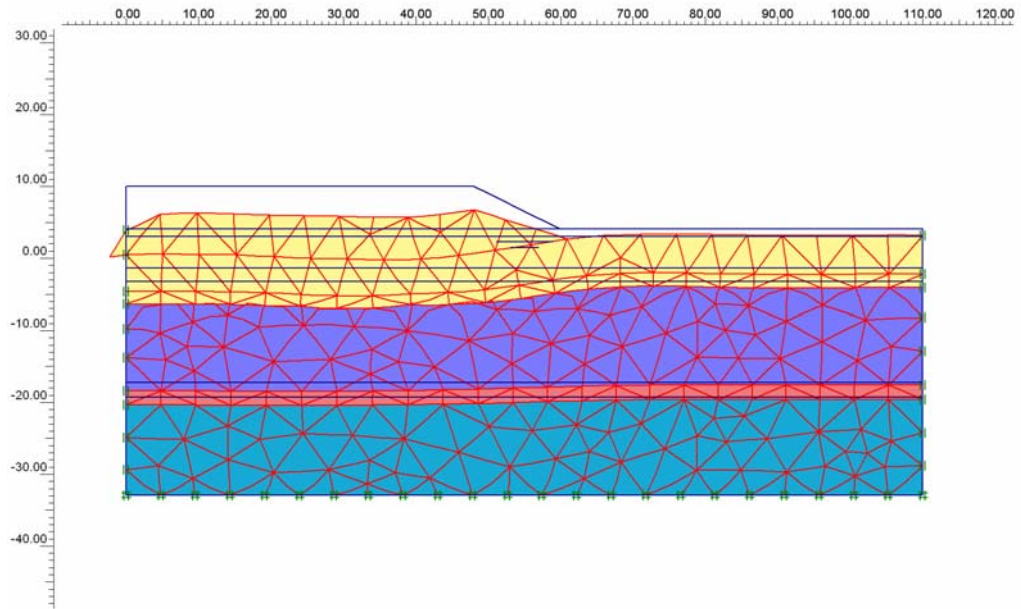


Figure 10.14 Deformed mesh by full scale analysis of Control Area (No Drain) at In-Situ Test Site, 20 months after surcharge placement (Arulrajah et al., 2004j).

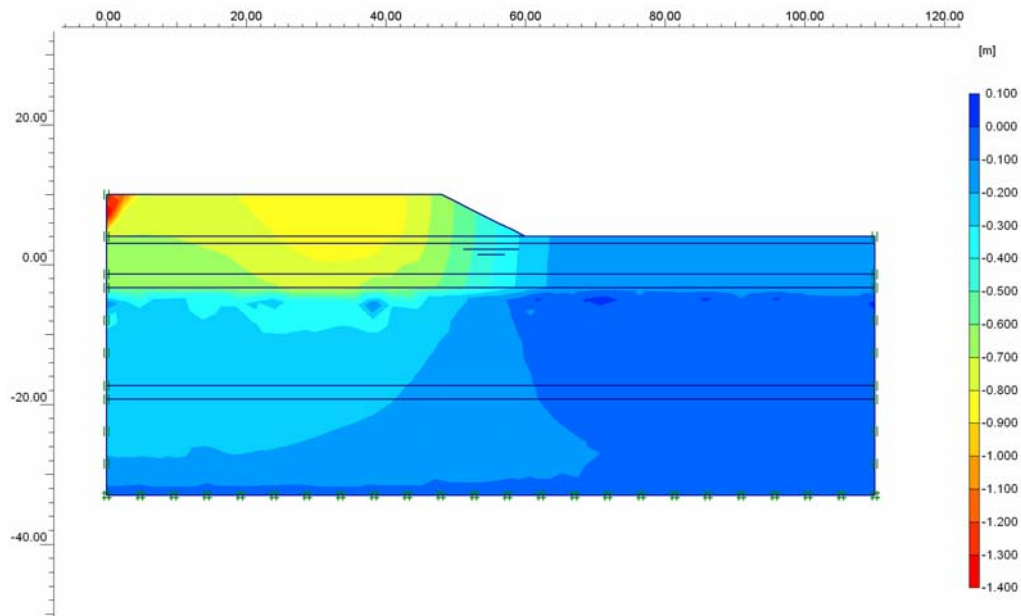


Figure 10.15 Vertical displacement by full scale analysis of Control Area (No Drain) at In-Situ Test Site, 20 months after surcharge placement (Arulrajah et al., 2004j).

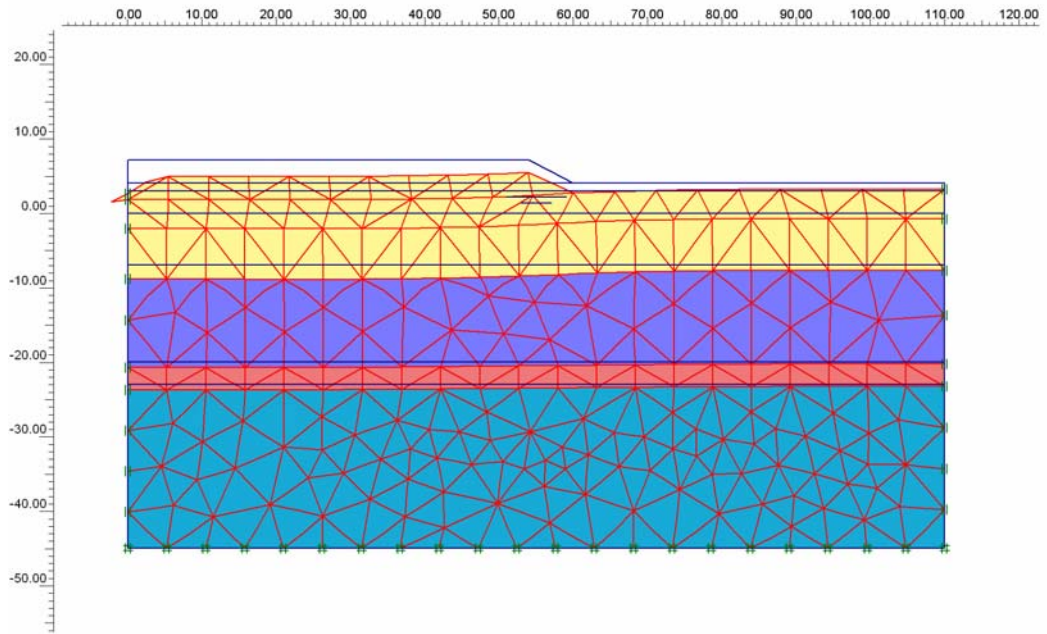


Figure 10.16 Deformed mesh by full scale analysis of A2S-74 sub-area (No Drain) at Pilot Test Site, 32 months after surcharge placement.

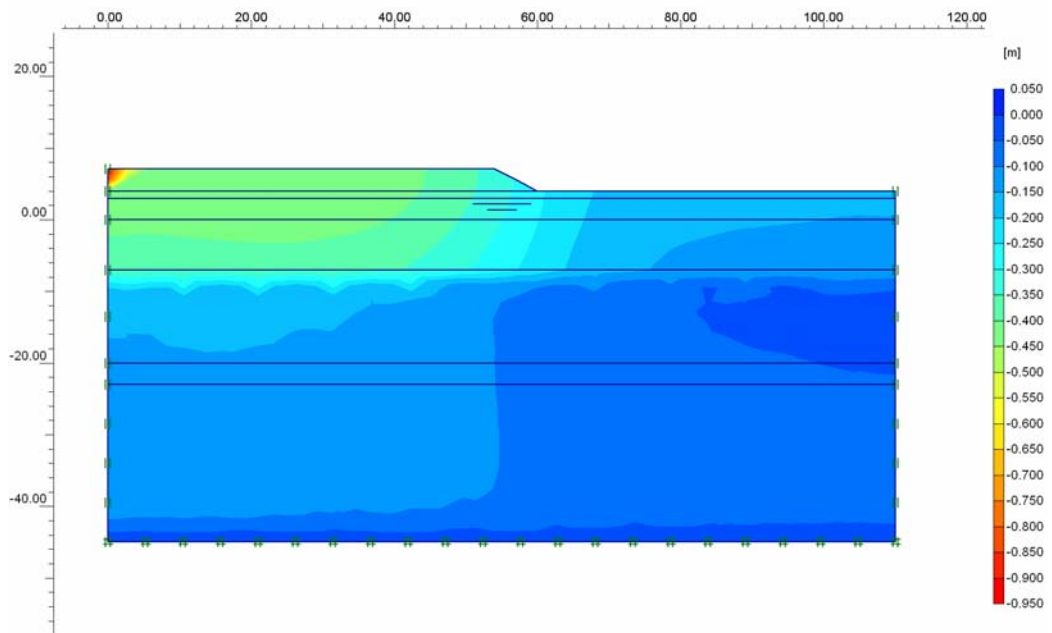


Figure 10.17 Vertical displacement by full scale analysis of A2S-74 sub-area (No Drain) at Pilot Test Site, 32 months after surcharge placement.

10.5 Comparison of Finite Element Modeling Results

10.5.1 In-Situ Test Site

Table 10.4 and Figure 10.18 illustrate the comparison of the finite element modeling results between the actual field settlement and the Plaxis Version 8 (2002) numerical modeling method for the In-Situ Test Site, 20 months after surcharge placement. Figure 10.19 illustrates the comparison between ultimate settlement by finite element modeling with actual field settlement ,after 20 months of surcharge loading, at the In-Situ Test Site. Excellent agreements were obtained from the finite element modeling analysis as compared to the actual field settlements for both the embankment with vertical drains as well as the control embankment. The matching techniques used in the finite element analysis of the vertical drains were based on that used previously in the modeling of Bangkok clays with PVD. The modeling of the Singapore marine clay treated with vertical drains was however modified to incorporate the marine clay multi-layers present at the project site in Changi. The modeling technique used by the author is found to provide similar excellent agreements in their use for the modeling of Singapore marine clay with vertical drains. The axis-symmetric unit cell and the full scale analysis of vertical drains were both found to be in excellent agreement with each other and with the actual field settlement results at the Pilot Test Site.

The axis-symmetric unit cell analysis result is found to be settling at a slightly slower rate than the full scale analysis and the actual field settlement after 360 days. As evident for the Vertical Drain Area in Table 10.4 and Figure 10.18 there is a difference of only 0.144 meters of settlement between the actual field settlement (2.404 meters) and the axis-symmetric unit cell FEM analysis (2.260 meters) after a surcharge period of 20 months. The axis-symmetric unit cell analysis is noted to provide a slightly lower settlement than that of the full scale analysis.

The full scale analysis with the use of the newly introduced drain element on the other hand is found to match very well with the actual field settlement until the 630 day period. As evident for the Vertical Drain Area in Table 10.4 and Figure 10.18, there is a difference of only 0.084 meters of settlement between the actual field settlement (2.404 meters) and the full scale FEM analysis (2.320 meters) after a surcharge period of 20 months. In the author's analysis of the full scale embankment with vertical drains for the In-Situ Test Site, the newly introduced drain element was successfully utilised instead of the interface element previously used for the modeling of Bangkok clay.

The full scale analysis of the untreated Control Area is also found to be in excellent agreement with the actual field settlement. The settlements are found to be in very close agreement after the final monitoring period of 785 days. As evident for the Control Area in Table 10.4 and Figure 10.18, there is a difference of only 0.019 meters of settlement between the actual field settlement (0.706 meters) and the full scale FEM analysis (0.687 meters) for the untreated Control Area after a surcharge period of 20 months.

Table 10.5 indicates the comparison of Asaoka, Hyperbolic, piezometer and finite element modeling methods at the In-Situ Test Site. As evident in Table 10.5, the ultimate settlement obtained by the finite element modeling method is found to be lower than that predicted by the Asaoka and Hyperbolic prediction methods for the Vertical Drain Area (1.5m x 1.5m). The degree of consolidation obtained by the finite element modeling method for the Vertical Drain Area (1.5m x 1.5m) is subsequently slightly higher than that obtained by the Asaoka, Hyperbolic and piezometer methods. For the Vertical Drain Area, a degree of consolidation of 87.8% was obtained from the FEM method as compared to 80.1% from the Asaoka method, 80.0% from the Hyperbolic method and 80.0% from the piezometer method. The degree of consolidation obtained by the finite element modeling method for the untreated Control Area is also found to be slightly higher than that obtained by the piezometer method. For the Control Area, a degree of consolidation of 27.9% was obtained from the FEM method as compared to 20.0% from the piezometer method.

Table 10.4 Comparison between finite element modeling results with actual field settlement at In-Situ Test Site, 20 months after surcharge placement (Arulrajah et al., 2004j).

Sub-Area	Field Settlement to Date (m)	Full Scale FEM Analysis (m)	Axi-symmetric Unit Cell FEM Analysis (m)
Vertical Drain 1.5m x 1.5m	2.404	2.320	2.260
Control No Drain	0.706	0.687	-

Table 10.5 Comparison of settlement assessed by Asaoka, Hyperbolic, piezometer and finite element modeling methods at In-Situ Test Site, 20 months after surcharge placement (Arulrajah et al., 2004j).

Sub-Area	Comparison	Asaoka	Hyperbolic	Piezometer	FEM
Vertical Drain 1.5m x 1.5m	Ultimate Settlement (m)	3.000	3.005	-	2.640
	Settlement to date (m)	2.404	2.404	-	2.320
	Degree of Consolidation (%)	80.1	80.0	80.0	87.8
Control No Drain	Ultimate Settlement (m)	-	-	-	2.465
	Settlement to date (m)	0.706	0.706	-	0.687
	Degree of Consolidation (%)	-	-	20.0	27.9

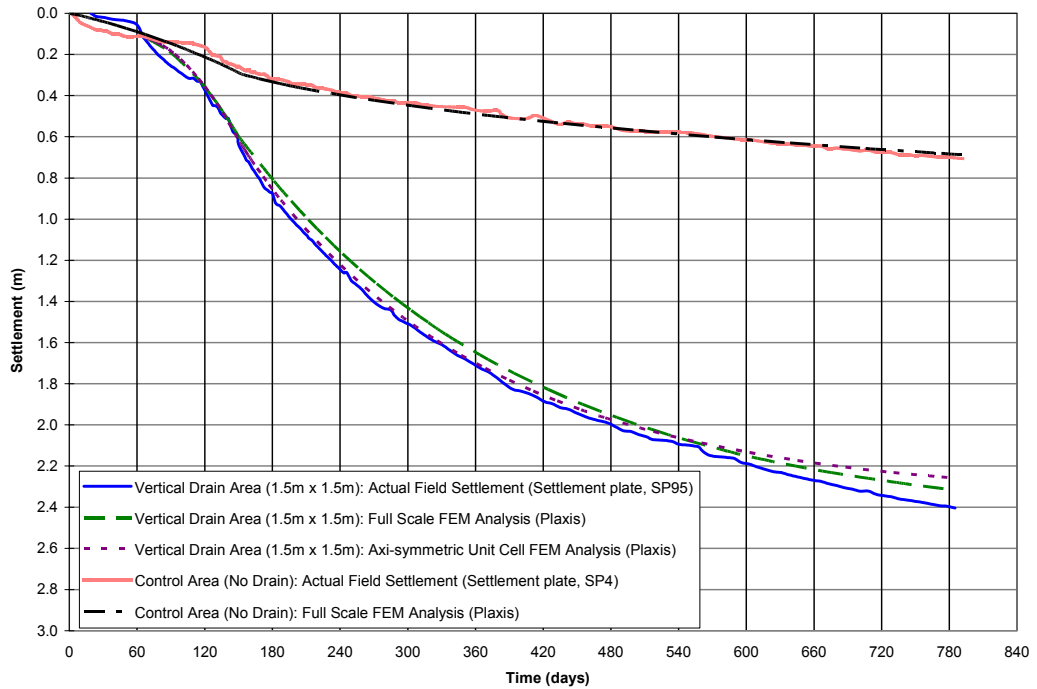


Figure 10.18 Comparison between finite element modeling results with actual field settlement at In-Situ Test Site 20 months after surcharge placement (Arulrajah et al., 2004j).

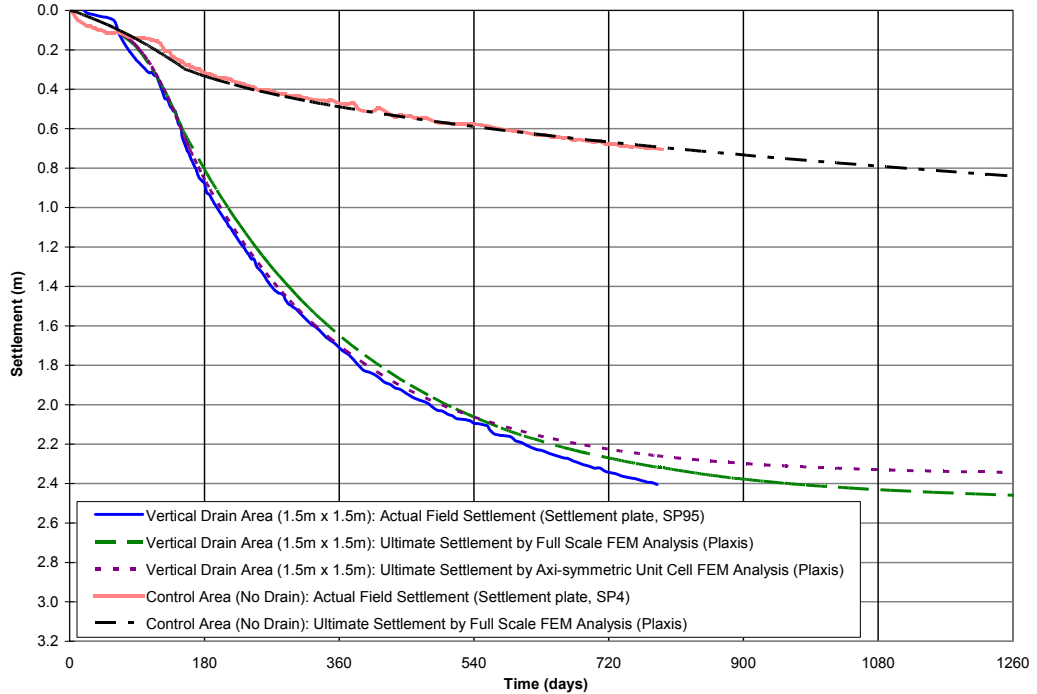


Figure 10.19 Comparison between ultimate settlement by finite element modeling with actual field settlement at In-Situ Test Site (Arulrajah et al., 2004j).

10.5.2 Pilot Test Site

Table 10.6 and Figure 10.20 illustrate the comparison of the finite element modeling results between the actual field settlement and the Plaxis Version 8 (2002) numerical modeling method for the Pilot Test Site, 32 months after surcharge placement. Figure 10.21 illustrates the comparison between ultimate settlement by finite element modeling with actual field settlement at Pilot Test Site. Excellent agreements were obtained from the finite element modeling analysis as compared to the actual field settlements for both the embankment with vertical drains as well as the control embankment.

The matching techniques used in the finite element analysis of the vertical drains were based on that used previously in the modeling of Bangkok clays with PVD by the axi-symmetric unit cell analysis method. The modeling of the Singapore marine clay treated with vertical drains was however modified to incorporate the marine clay multi-layers present in Singapore marine clay at Changi. The modeling technique used by the author is found to provide excellent agreement in their use for the modeling of Singapore marine clay with vertical drains. The axi-symmetric unit cell analysis of vertical drains was found to be in excellent agreement with the actual field settlement results at the Pilot Test Site.

The axi-symmetric unit cell analysis result is found to be in good agreement with the actual field settlement for sub-areas A2S-71 (2.0m x 2.0m) and A2S-73 (3.0m x 3.0m). The axi-symmetric unit cell analysis result is found to be settling at a slightly slower rate than the actual field settlement for sub-area A2S-72 (2.5m x 2.5m).

As evident in Table 10.6 and Figure 10.20 there is a difference of only 0.021 meters of settlement between the actual field settlement (1.687 meters) and the axi-symmetric unit cell finite element modeling analysis (1.666 meters) for sub-area A2S-71 (2.0m x 2.0m) after a surcharge period of 32 months. There is a difference of only 0.002 meters of settlement between the actual field settlement (1.264 meters) and the axi-symmetric unit cell finite element modeling analysis (1.262 meters) for sub-area A2S-72 (2.5m x 2.5m). There is a difference of only 0.012 meters of settlement between the actual field settlement (0.948 meters) and the axi-symmetric unit cell finite element modeling analysis (0.960 meters) for sub-area A2S-73 (3.0m x 3.0m).

The full scale analysis of the untreated control embankment of the A2S-74 (No Drain) sub-area is also found to be in excellent agreement with the actual field settlement. The settlements are found to be in very close agreement after the surcharge period of 32 months (monitoring period of 41.9 months). As evident for sub-area A2S-74 (No Drain) in Table

10.6 and Figure 10.20, there is a difference of only 0.068 meters of settlement between the actual field settlement (0.503 meters) and the full scale finite element modeling analysis (0.435 meters) for the untreated A2S-74 sub-area after a surcharge period of 32 months (monitoring period of 41.9 months).

Table 10.7 indicates the comparison of ultimate settlement and degree of consolidation assessed by using Asaoka, Hyperbolic, piezometer and finite element modeling methods at the Pilot Test Site. As evident in Table 10.7, the ultimate settlement obtained by the finite element modeling method is found to be slightly lower than that predicted by the Asaoka and Hyperbolic prediction methods for the A2S-71 (2.0m x 2.0m) sub-area. The degree of consolidation obtained by the finite element modeling method for the A2S-71 sub-area is subsequently slightly higher than that obtained by the Asaoka, Hyperbolic and piezometer methods. For the A2S-71 sub-area, a degree of consolidation of 95.6% was obtained from the FEM method as compared to 91.8% from the Asaoka method, 93.7% from the Hyperbolic method and 86.2% from the piezometer method.

The ultimate settlement obtained by the finite element modeling method is found to be slightly higher than that predicted by the Asaoka and Hyperbolic prediction methods for the A2S-72 (2.5m x 2.5m) and A2S-73 (3.0m x 3.0m) sub-areas. The degree of consolidation obtained by the finite element modeling method for the A2S-72 and A2S-73 sub-areas is subsequently slightly lower than that obtained by the Asaoka, Hyperbolic and piezometer methods. For the A2S-72 sub-area, a degree of consolidation of 87.9% was obtained from the FEM method as compared to 89.5% from the Asaoka method, 89.8% from the Hyperbolic method and 82.5% from the piezometer method. For the A2S-73 sub-area, a degree of consolidation of 78.9% was obtained from the FEM method as compared to 79.0% from the Asaoka method, 81.1% from the Hyperbolic method and 73.1% from the piezometer method.

The degree of consolidation obtained by the finite element modeling method for the untreated A2S-74 (No Drain) sub-area is also found to be slightly lower than that obtained by the piezometer method. For the untreated A2S-74 sub-area, a degree of consolidation of 33.9% was obtained from the FEM method as compared to 37.0% from the piezometer method.

In conclusion, it can be said that reasonable agreements were obtained from the finite element modeling analysis as compared to the actual field settlements for both the vertical drain treated embankments as well as the untreated control embankments at both the In-Situ

Test Site and Pilot Test Site. The axi-symmetric unit cell and the full scale analysis of vertical drains were found to be in reasonable agreement with each other and with the actual field settlement results.

Table 10.6 Comparison of settlement between finite element modeling results with actual field settlement at Pilot Test Site 32 months after surcharge (Arulrajah et al., 2004j).

Sub-Area	Field Settlement to Date (m)	Full Scale FEM Analysis (m)	Axi-symmetric Unit Cell FEM Analysis (m)
A2S-71 2.0 x 2.0 m	1.687	-	1.666
A2S-72 2.5 x 2.5 m	1.264	-	1.262
A2S-73 3.0 x 3.0 m	0.948	-	0.960
A2S-74 No Drain	0.503	0.435	-

Table 10.7 Comparison of settlement and degree of consolidation assessed by Asaoka, Hyperbolic, piezometer and finite element modeling methods at Pilot Test Site 32 months after surcharge (Arulrajah et al., 2004j).

Sub-Area	Comparison	Asaoka	Hyperbolic	Piezometer	FEM
A2S-71 2.0 x 2.0 m	Ultimate Settlement (m)	1.838	1.801	-	1.743
	Settlement to date (m)	1.687	1.687	-	1.666
	Degree of Consolidation (%)	91.8	93.7	86.2	95.6
A2S-72 2.5 x 2.5 m	Ultimate Settlement (m)	1.412	1.408	-	1.436
	Settlement to date (m)	1.264	1.264	-	1.262
	Degree of Consolidation (%)	89.5	89.8	82.5	87.9
A2S-73 3.0 x 3.0 m	Ultimate Settlement (m)	1.200	1.169	-	1.217
	Settlement to date (m)	0.948	0.948	-	0.960
	Degree of Consolidation (%)	79.0	81.1	73.1	78.9
A2S-74 No Drain	Ultimate Settlement (m)	-	-	-	1.281
	Settlement to date (m)	0.503	0.503	-	0.435
	Degree of Consolidation (%)	-	-	37.0	33.9

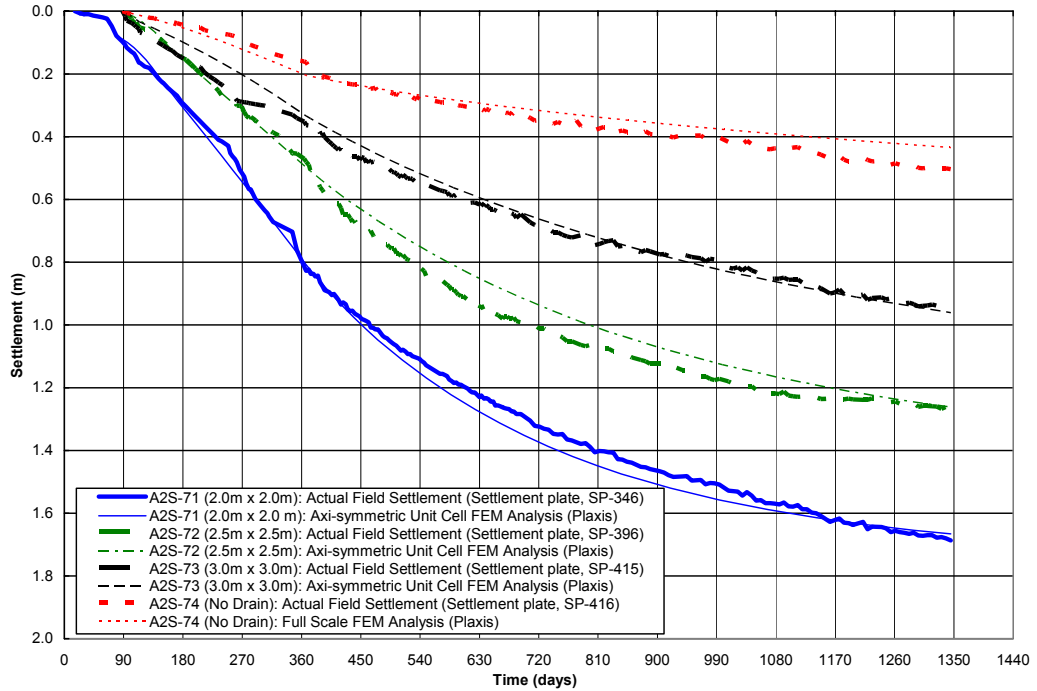


Figure 10.20 Comparison between finite element modeling results with actual field settlement at Pilot Test Site, 32 months after surcharge placement (Arulrajah et al., 2004j).

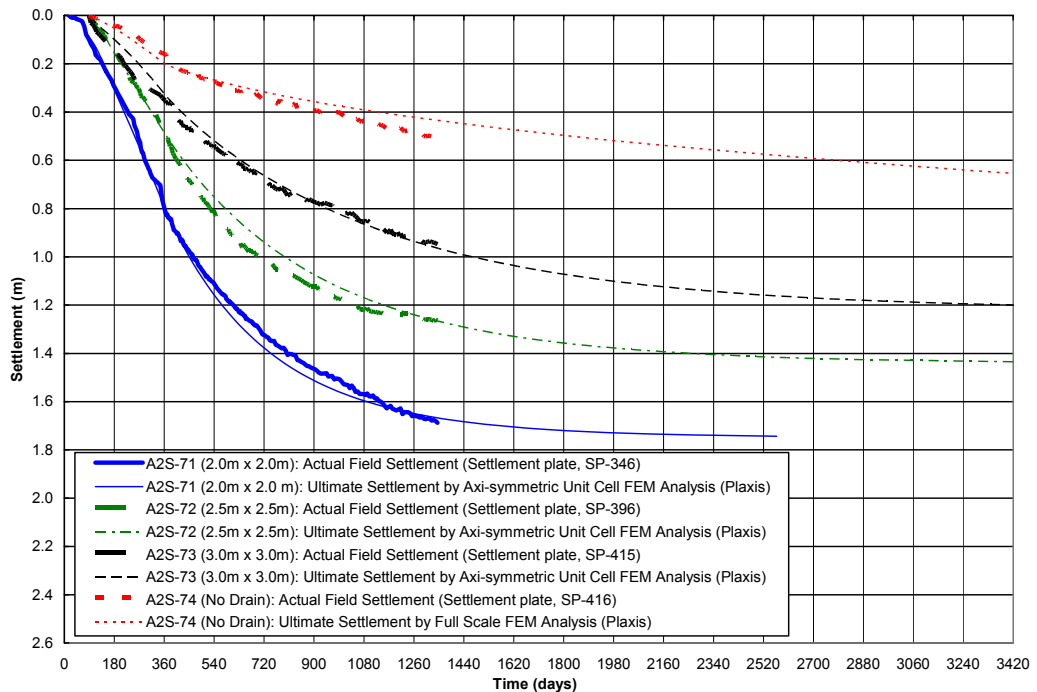


Figure 10.21 Comparison between ultimate settlement by finite element modeling with actual field settlement at Pilot Test Site (Arulrajah et al., 2004j).

11.0 PERFORMANCE VERIFICATION OF MARINE CLAY TREATED WITH PREFABRICATED VERTICAL DRAINS

The vertical drain performance was verified for the In-Situ Test Site by using the c_h obtained from back-analysis by the Asaoka Method and by finite element modeling with the Plaxis Version 8 (2002) numerical modeling software.

11.1 Back-Analysis Using c_h from Asaoka Method

Conventional calculations by applying Barron (1948), Hansbo (1979) and Yoshikuni and Nakanodo (1974) theories with well resistance and smear effect were compared with the actual field performance. The conventional vertical drain design with a c_h of 0.78 m²/year obtained from back-analysis by applying the Asaoka method was generated (section 8.2.5).

The c_h of 0.78 m²/year which was obtained from back-analysis by the Asaoka method was compared to the actual field performance. It was found that the calculated time rate of settlement curve with a c_h of 0.78 m²/year is similar to the field curve as shown in Figure 11.1. This is apparent especially up to the surcharge period of 12 months, after which the field settlement curve slows down.

Based on the settlement plate monitoring results (SP-095), a settlement of 0.691 meters was recorded during filling operations from the vertical drain platform level (+4 mCD) to the surcharge level (+10 mCD). This settlement was incorporated in the comparison of degree of consolidation between field and the back-analysis for the Vertical Drain Area.

11.2 Proposed Modified Asaoka Equation

Settlement at any point of time, S_t can be calculated as a fraction of the final settlement S_{ult} from the following Asaoka equation (Hausmann, 1990):

$$\frac{S_t}{S_{ult}} = 1 - \frac{8}{\pi^2} \exp \left(- \left(\frac{8 c_h' + \pi^2 c_v}{d_c^2 \alpha} \right) \frac{t}{4 H_o^2} \right) \quad \text{Eq.(11.1)}$$

where:

d_e = equivalent diameter of cylinder of soil around drain (=1.128s for square) (m)

c_v = coefficient of consolidation for vertical flow (m²/yr)

c_h' = effective value of coefficient of consolidation due to horizontal flow (m²/yr)

H_o = thickness of layer (m)

t = time elapsed since application of surcharge (yr)

$\alpha = [(n^2 \ln n) / (n^2 - 1)] - [(3n^2 - 1)/4n^2]$

$n = d_e / d$

d = equivalent drain diameter (m)

However, the above equation is suitable for a single layer of clay only. The author proposes that the equation be modified to allow for the analysis of multiple layers of marine clay (in this case being upper marine clay, intermediate clay and lower marine clay) by means of consideration for the equivalent thickness of the marine clay.

Equivalent Thickness

As the marine clay consists of several layers (in this case being three), the author proposes that the equivalent thickness of the marine clay has to be calculated to enable the input values of the equivalent thickness, equivalent drainage and coefficient of vertical consolidation values into the proposed modified Asaoka equation. The equations used for computation of equivalent thickness of marine clay is defined as follows:

Equivalent Thickness of layer 1, $H1'$:

$$H1' = H1(c_{vi} / c_{v1})^{0.5} \quad \text{Eq.(11.2)}$$

where:

c_{vi} is an initial assumed value

Total Equivalent thickness of all layers, H_{T1}' :

$$H_{T1}' = H1' + H2' + H3' \dots Hn' \quad \text{Eq.(11.3)}$$

Equivalent drainage thickness, H_{dri} :

$$H_{dri} = H1' / 2 \quad \text{Eq.(11.4)}$$

The author suggests the incorporation of the equivalent coefficient of consolidation for vertical flow, c_{vi} and equivalent thickness of the layers, H_{Ti}' into the equation. The modified Asaoka equation proposed by the author for multiple layers of marine clay is defined as follows :

$$\frac{S_t}{S_{ult}} = 1 - \frac{8}{\pi^2} \exp \left(- \left(\frac{8 c_h'}{d_e^2 \alpha} + \frac{\pi^2 c_{vi}}{4 H_{Ti}'^2} \right) t \right) \quad \text{Eq.(11.6)}$$

where:

H_{Ti}' = equivalent total thickness of the marine clay layers

c_{vi} = equivalent coefficient of consolidation for vertical flow

The c_h of 0.78 m²/year which was obtained from back-analysis by the Asaoka method (section 8.2.5) was used in the equation. It was found that the calculated time rate of settlement curve with a c_h of 0.78 m²/year is also similar to the field curve as shown in Figure 11.1. This is apparent especially up to the surcharge period of 12 months, after which the field settlement curve slows down. The proposed modified Asaoka equation ties in very well with the back-analysis results by conventional method and as such can be used in future instead of back-analysing using the conventional calculations.

11.3 Conventional Design of PVD with Back-Calculated c_h

The conventional design method for vertical drains was carried out with consideration for well resistance and smear effect and with using a c_h to c_v ratio of 2. The predicted rate of settlement is found to be much faster than that of the actual field settlement as shown in Table 11.1 and Figure 11.1. Similar findings have been reported by Bo, Arulrajah and Choa (1997b) and Chun et al. (1997).

The conventional design method for vertical drains was also carried out with consideration for well resistance and smear effect but this time by using the back-calculated c_h of 0.78 m²/yr. It is observed in Figure 11.1 that the calculated time rate of settlement by the conventional design method using the back-calculated c_h of 0.78 m²/yr is similar with the field curve especially up to the surcharge period of 12 months, after which the field settlement curve slows down.

11.4 Finite Element Modeling of PVD

Finite element modeling of the vertical drains was carried out with the Plaxis Version 8 (2002) numerical modeling software by both the axi-symmetric unit cell analysis and full scale embankment analysis methods by means of the conventional modeling method using $k_h = 2k_v$ for Singapore marine clay as described in the previous chapter. It is evident in Figure 11.1, that the rate of consolidation for the axi-symmetric unit cell analysis and full scale embankment finite element modeling methods is faster than that of the actual field settlement.

Finite element modeling was also carried out using the back-calculated $c_h = 0.78 \text{ m}^2/\text{yr}$ by the axi-symmetric unit cell analysis method. The calculated time rate of settlement is found to be similar to that of the field curve if the back-calculated $c_h = 0.78 \text{ m}^2/\text{yr}$ is used in the finite element modeling analysis as illustrated in Figure 11.1. Similar findings have been reported previously by Bo, Arulrajah and Choa (1997b) and Balasubramaniam et al. (1995) with the use of the Sage Crisp Finite element modeling program.

Table 11.1 indicates the vertical drain performance verification comparison of settlement and degree of consolidation by various methods.

Figure 11.1 illustrates the vertical drain performance verification comparison of degree of consolidation by various methods.

Table 11.1 Comparison of vertical drain performance verification by settlement and degree of consolidation by various methods 20 months after surcharge placement (Arulrajah et al., 2004j).

Methods Employed (PVD Spacing of 1.5 m square)	Ultimate Settlement (m)	Settlement to date (m)	Degree of Consolidation U (%)
Actual Field Settlement: Hyperbolic method	3.005	2.404	80.0
Actual Field Settlement: Asaoka method	3.000	2.404	80.1
Conventional Method: Well resistance and smear effect	3.005	2.923	97.3
Full Scale FEM Analysis (Plaxis): $k_h = 2k_v$	2.640	2.320	87.8
Unit Cell FEM Analysis (Plaxis) $k_h = 2k_v$	2.480	2.260	91.1
Conventional Method: Back-calculated $c_h = 0.78 \text{ m}^2/\text{yr}$	3.000	2.553	85.1
Proposed Modified Asaoka Eqn: Back-calculated $c_h = 0.78 \text{ m}^2/\text{yr}$	3.000	2.530	84.3
Unit Cell FEM Analysis (Plaxis): Back-calculated $c_h = 0.78 \text{ m}^2/\text{yr}$	2.454	1.987	80.9
FEM Analysis (Sage Crisp): Back-calculated $c_h = 0.78 \text{ m}^2/\text{yr}$	2.963	2.489	84.0

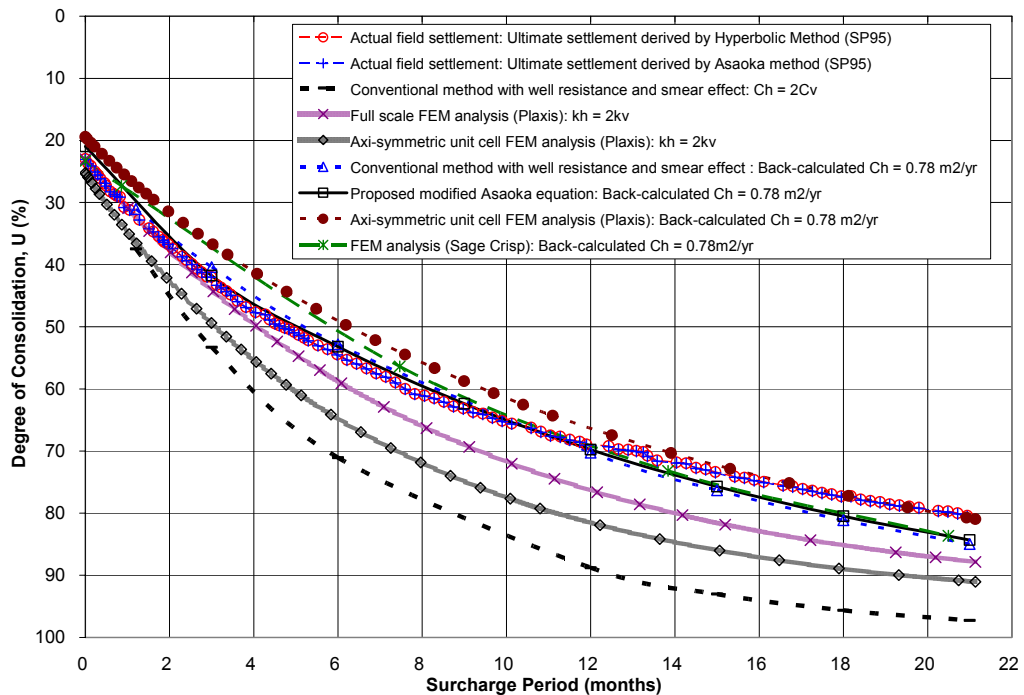


Figure 11.1 Vertical drain performance verification comparison of degree of consolidation by various methods at 20 months after surcharge (Arulrajah et al., 2004j).

11.5 Findings and Discussion

Findings

Table 11.1 and Figure 11.1 indicate that field time rate of consolidations is in good agreement with the newly proposed modified Asaoka method and the conventional method using the back-calculated $c_h = 0.78$ m²/yr (section 8.2.5). The actual field settlement measurement is slightly slower than the proposed modified Asaoka and the conventional method using the back-calculated $c_h = 0.78$ m²/yr by only about 5% as indicated in Table 11.1. The newly proposed modified Asaoka equation is found to be in good agreement with the conventional method using the back-calculated c_h . As such, it is proposed that the proposed modified equation can be used in similar multi-layer schemes of marine clay and can be used in future instead of using the conventional method with back-calculated c_h .

Field measurement of coefficient of consolidation due to horizontal flow measured prior to reclamation by the various in-situ testing equipments is much higher than the back-analysed and designs (c_h) values (section 6.11). As such, it is recommended based on these findings that the assumed coefficient of consolidation due to horizontal flow in the design stage should not be more than 1.5 times that of the coefficient of consolidation for vertical flow when thick layers of homogeneous clay are in existence. The field settlement curve is noted to be slowing down after one year of surcharging period.

Discussion

The major factor that accounts for the lower c_h values back-calculated from field settlement measurements is the smear effect incurred from the insertion of the mandrel during the installation of vertical drains. For soft marine clay, the smear effect can be quite significant as the spacing of the drains is normally 1.5 meters. Bo et al. (1998f) has reported that the permeability of soil in the smear zone could be reduced by 1 order of magnitude or to the k_h of the remoulded clay as a result of the smear zone. The smear zone was found to be 4-5 times the equivalent diameter of the vertical drain Bo et al. (1998f). When drains are installed at close spacing, the back-calculated c_h values will generally be greatly influenced by this smear zone. It is also to be noted that prior to reclamation in-situ measured c_h values, are c_h with existing overburden pressure and its value would be reduced to a certain degree after increasing the additional load. This can be seen in the reduction of c_h values in the laboratory with each load increment.

In addition to this, the reduction of the rate of settlement after some time could be due to reduction of permeability of the vertical drain filter due to clogging and reduction of permeability in surrounding soil due to void ratio changes. Therefore the usage of c_h values from in-situ test prior to reclamation may not be so conservative since this c_h value accounts for the existing overburden pressure and would be reduced with the increments in fill load.

Furthermore, the boundary condition for in-situ tests and for field conditions with vertical drains is different. As such, average c_h values surrounding the effective area of vertical drain could be different from in-situ tests, which have a smaller effective flow area.

Vertical drains installed in the project are performing to improve the soil drainage system, however their conventional design performance is slightly slower than that predicted by field measurements. An exact superimposed time rate of settlement curves between field and prediction is extremely difficult to obtain since there are various natural variations, which cannot be modelled.

12.0 CONCLUSIONS

The conclusion of this research is sub-divided into various sub-sections.

12.1 Characteristics and Mineralogy of Singapore Marine Clay at Changi

The findings of the characteristics and mineralogy of Singapore Marine Clay is listed below:

- (1) The upper marine clay has a liquid limit of between 80-95%, plastic limit of between 20-28% and water content of 70-88%. The upper marine clay is generally overconsolidated with OCR of about 1.5-2.5. The upper marine clay has a compression index (C_c) of 0.6-1.5 and secondary compression index (C_α) of 0.012-0.025. The laboratory testing results indicate that the coefficient of consolidation for vertical flow (c_v) of the upper marine clay is between 0.47-0.6 m²/year while the coefficient of consolidation due to horizontal flow (c_h) is between 2-3 m²/year.
- (2) The lower marine clay has a liquid limit of 65-90%, plastic limit of 20-30% and water content of 40-60%. The lower marine clay is lightly overconsolidated with OCR of 2. The lower marine clay has a compression index (C_c) of 0.6-1.0 and secondary compression index (C_α) of 0.012-0.023. The laboratory testing results indicate that the coefficient of consolidation for vertical flow (c_v) of the lower marine clay is between 0.8-1.5 m²/year while the coefficient of consolidation due to horizontal flow (c_h) is between 3-5 m²/year.
- (3) The intermediate stiff clay is sandwiched between the upper marine clay and lower marine clay. The intermediate stiff clay has a liquid limit of about 50%, plastic limit of 18-20% and water content of 10-35%. The intermediate stiff clay is moderately overconsolidated due to desiccation, with OCR of 3-4. The intermediate stiff clay has a compression index (C_c) of 0.2-0.3 and secondary compression index (C_α) of 0.0043-0.023. The laboratory testing results indicate that the coefficient of consolidation for vertical flow (c_v) of the intermediate marine clay is between 1-4.5 m²/year while the coefficient of consolidation due to horizontal flow (c_h) is between 5-10 m²/year.

- (4) Vertical hydraulic conductivity values, k_v from laboratory tests was found to range between 2×10^{-10} to 1.5×10^{-8} m/s for the Singapore marine clay.

The relationship between in-situ initial void ratio and vertical hydraulic conductivity change index, c_{kv} is found to be only $c_{kv} = 0.3e_0$ for Singapore marine clay at Changi.

Horizontal hydraulic conductivity values from laboratory testing was found to range between 3×10^{-9} to 8×10^{-8} m/s. It was found that the hydraulic conductivity anisotropy is negligible for the Singapore marine clay at Changi.

- (5) An empirical correlation was obtained for the pre-reclamation field vane shear strength variation with depth. The c_u/σ_{vo}' ratio of the marine clay was found to be 0.37. This indicates that the clay is overconsolidated as c_u/σ_{vo}' ratio is greater than 0.25. The sensitivity of the marine clay at Changi varies from 3 to 8 which can be described as highly sensitive.
- (6) Under the Scanning Electron Microscope, the clays appear poorly consolidated. The fabric of the marine clay appears to be generally open with porosities optically estimated at up to 30%. The X-Ray Diffraction analysis indicates the major content of minerals to be kaolinite and smectite with 'mica' and chlorite being the minor minerals.
- (7) Photographic identification of Singapore marine clay shows the brownish-blue upper and lower marine clay layer consists of organic deposits and fine sand particles. The intermediate stiff clay layer is reddish due to oxidation of the layer as a result of exposure of the seabed to the atmosphere during the rise and fall of the sea levels in the geological past.

12.2 In-Situ Testing of Marine Clay under Reclamation Fills

The findings of the In-Situ Test Site are listed below:

- (1) In the prior to reclamation series of in-situ tests, similar profiles were obtained for the shear strength and OCR. The undrained shear strength of the Singapore marine clay by the various methods is in good agreement with each other. The undrained shear strength obtained from the various in-situ test methods was analysed to obtain an empirical correlation of the undrained shear strength of the marine clay at the In-Situ Test Site.

- (2) The upper marine clay is generally overconsolidated with OCR of about 1.5 to 3. The lower marine clay is lightly overconsolidated with OCR of 1 to 2. The intermediate stiff clay is overconsolidated due to desiccation, with OCR of 1.5 to 3.

The dessicated layer found close to the seabed is also found to register high OCR values. Higher OCR at seabed normally occurs due to hydrodynamic effect caused by wave and current action.

It is apparent that the OCR from CPT is the lowest of the in-situ testing methods. This is possibly due to the value of the constant used in the OCR computations by the CPT.

- (3) In the post improvement series of in-situ tests after a surcharge period of 23 months, the shear strength, OCR, effective stress and degree of consolidation obtained from various in-situ tests are found to be agreeable with each other

- (4) The post improvement in-situ tests indicated clear increases in the soil strength and degree of improvement which is as expected. The results also indicate the expected higher increases in strength, overconsolidation ratio, effective stress and degree of consolidation between the Vertical Drain Area as compared to the untreated Control Area.

The post improvement in-situ tests indicate that the degree of consolidation of the Vertical Drain Area had attained a degree of consolidation of about 70-80% while the Control Area had attained a degree of consolidation of about 30-40%.

- (5) Piezocone dissipation tests have been utilised as a tool to obtain the piezometric heads of marine clays after ground improvement as well as to assess the degree of consolidation of the improved marine clay. The results indicated that pore pressure measured from the CPTU holding tests are in agreement with those measured by the piezometers tests in both the Vertical Drain Area and adjacent untreated Control Area.

The CPTU test results were also successfully used for the determination of the equilibrium pore pressure and degree of consolidation of the improved areas as confirmed by the field instrumentation results. This suggests that the quasi-static piezometric pressures from the piezocone dissipation tests may be used as an alternative to piezometer instrumentation in measuring piezometric pressure in consolidation stage.

The Vertical Drain Area was found to have attained a degree of consolidation of 80-85% based on the CPTU results. The Control Area without vertical drains on the other hand has attained a degree of consolidation of 10-22% based on the CPTU results.

- (6) In-situ dissipation test using the piezocone is recommended as the most suitable method for the determination of the c_h of marine clay. The prior to reclamation CPTU results is found to be the closest to the laboratory testing results.

The pre-reclamation CPTU dissipation test indicate that the c_h values of the upper and lower marine clay varies between 2 to 6 m^2/yr . c_h values of 4 to 7 m^2/yr were obtained in the intermediate stiff clay, separating the upper and lower marine clay layers. The pre-reclamation CPTU results is found to be the closest among the in-situ dissipation tests to the laboratory testing results.

The post-improvement CPTU results in the upper and lower marine clay layers indicate c_h varies between 3 and 6 m²/yr in the Vertical Drain Area and between 3 and 5 m²/yr in the Control Area, after 23 months of surcharge loading.

- (7) The c_h determined by the various in-situ testing methods are relatively higher overall as compared to the laboratory testing results, as evident in the prior to reclamation test results. Horizontal laminations and micro lenses present in the marine clay profile, will lead to higher c_h values and subsequently higher k_h for the in-situ tests. The presence of laminations and lenses are difficult to be detected by the laboratory tests due to the sampling intervals and the sampling process. Furthermore, laboratory results are subject to various complexities such as borehole quality, sample quality, testing methods and method of interpretation which could lead to lower test values.
- (8) It is apparent that c_h results vary between the various in-situ testing methods due to the differing assumption in cavity radius in the various test methods. The varying c_h values will subsequently lead to differing k_h in the CPTU, DMT and SBPT results as k_h computations is worked out indirectly from c_h values.
- (9) The c_h value derived from the CPTU dissipation test is generally lower than those obtained from the other in-situ dissipation tests. In general, the c_h value measured by the SBPT is much larger than those obtained from the other in-situ dissipation tests. The c_h determined by the DMT and SBPT prior to reclamation is noted to be an order of magnitude greater than the laboratory data.

The smear effect affects the CPTU and DMT measurements for c_h . In the CPTU and DMT dissipation test, a penetrometer has to be pushed into the clay and a smear effect similar to the insertion of a mandrel could have been introduced prior to the measurements. This as such could lead to the CPTU and DMT measurements for c_h being lower than that of the SBPT.

- (10) The c_h value seems to be higher in the Vertical Drain Area at some elevations as compared to the Control Area. This is due to the greater reduction in the coefficient

of volume change, m_v , after consolidation or it was simply affected by the correction factors used.

- (11) In-situ dissipation tests using the BAT is recommended as the most suitable method for the determination of the k_h of marine clay, since the system measures horizontal hydraulic conductivity directly whereas the other in-situ tests required the introduction of additional parameters to evaluate the k_h indirectly from c_h values. The horizontal hydraulic conductivity prior to reclamation is in the order of 10^{-9} to 10^{-10} m/s based on the BAT results.

The horizontal hydraulic conductivity is in the order of 10^{-9} to 10^{-10} m/s in the Vertical Drain Area and the Control Area after 23 months of surcharge loading.

It is apparent that the prior to reclamation k_h is higher than that of the Vertical Drain Area and Control Area after 23 months of surcharge loading. This is expected due to reduction in the void ratio after surcharge loading.

It is also apparent that the k_h in the Vertical Drain Area is lower than that in the Control Area which is expected due to higher void ratio changes and smear effect.

The results from the BAT permeameter tests confirm that there is a reduction of vertical permeability from time to time during consolidation in the vertical drain treated area.

- (12) The smear effect also affects the BAT, CPTU and DMT measurements for k_h . In the BAT, CPTU and DMT dissipation test, a penetrometer has to be pushed into the clay and a smear effect similar to the insertion of a mandrel could have been introduced prior to the measurements. Smear effect also affects the k_h in the vertical drain treated area due to insertion of the vertical drain mandrel into the ground.

The smear effect for BAT permeameter could be greater than that for the CPTU, as the BAT permeameter had a filter with a larger surface area. This may explain why k_h measured by the BAT permeameter is normally lower than that by the CPTU, although the working mechanisms of the two tests are very similar. The SBPT should not be affected by the smear effect due to its self-boring mechanism.

12.3 Field Instrumentation of Marine Clay Case Studies

The findings of the Pilot Test Site and In-Situ Test Site are listed as follows:

- (1) Instrumentation monitoring by means of settlement gauges and piezometers is found in the research to be a reliable method to continually assess the degree of consolidation of vertical drains in land reclamation projects.

- (2) At the Pilot Test Site, the magnitude of settlement is highest in sub-area A2S-71 (2.0 x 2.0 m) which has the closest vertical drain spacing and lowest in A2S-74 (No Drain). Higher magnitudes of settlement and higher degree of consolidation are obtained as closer vertical drain spacing is used. Similarly, dissipation of excess pore water pressure readings is evidently faster in the closer spacing vertical drain treated sub-area. The ultimate settlement and degree of consolidation obtained by the Asaoka and Hyperbolic methods is found to converge to be in excellent agreement with each other after the surcharge period of 32 months. The degree of consolidation predicted by the Hyperbolic method is found to be slightly higher than that of the Asaoka method. The piezometer indicates lower degree of consolidation as compared to field settlement predictions. The degree of consolidation of the Pilot Test Site is as follows:

Sub-area A2S-71 (2.0 x 2.0 m) had attained a degree of consolidation of about 93 %.
Sub-area A2S-72 (2.5 x 2.5 m) had attained a degree of consolidation of about 90 %.
Sub-Area A2S-73 (3.0 x 3.0 m) had attained a degree of consolidation of about 80%.
Sub-Area A2S-74 (No Drain) had attained a degree of consolidation of 37.0 %.

- (3) At the Pilot Test Site, the findings of the comparison between pneumatic and electric piezometers indicate that there is reasonable agreement in readings between the two types of piezometers. As such either type of piezometer can be used for the monitoring of the marine clay behaviour under reclaimed fills. Proper protective guard cell is required for the pneumatic piezometer to counter for the effect of possible pinching of the piezometer cable due to the large strain settlements of the reclaimed fill.

- (4) At the In-Situ Test Site the settlement gauges and piezometers indicate that the degree of consolidation of the vertical drain treated Vertical Drain Area had attained a degree of consolidation of more than 80% while the Control Area had attained a degree of consolidation of less than 20%. This is in good agreement with the in-situ testing results.

The results of the design predictions are found to be in good agreement with that of the field instrumentation results. The degree of consolidation obtained by the design predictions is found to be only slightly higher than that of the field instrumentation results. For the Vertical Drain Area, a degree of consolidation of 83.3% was obtained from the design predictions as compared to 80.1% from the Asaoka method, 80.0% from the Hyperbolic method and 80.0% from the piezometer method.

- (5) Compression parameters obtained from the laboratory which were used for prediction is very similar to the actual back-analysed parameters. Back-analysed c_h values are also much lower than the in-situ which is due to reduction of horizontal and vertical permeability from time to time during consolidation, well resistance and smear effect and clogging of vertical drains after some time.

12.4 Evaluation of Observational Methods of Assessing Improvement of Marine Clay under Reclamation Fills

- (1) The author's findings of the Asaoka method reveal that the magnitude of ultimate settlement decreases and the degree of consolidation subsequently increases as a longer period of assessment is used in the prediction. It is apparent that as the time interval increases, a cut-off time interval is obtained after which increasing time intervals would converge to the same magnitude of ultimate settlement. In the study of the vertical drain areas in the Pilot Test Site, the cut-off time interval was determined to be 28 days.
- (2) The author's findings reveal that the c_h value back-analysed by the Asaoka method is dependant on the time interval used for the prediction. The c_h value predicted by the

Asaoka method decreases and converges to the final value as a longer time of assessment and increasing time intervals is used in the back-analysis.

- (3) The study reveals that the c_h value of the marine clay is lowest at the sub-area with the closest vertical drains spacing (A2S-71: 2.0 x 2.0) and highest at the sub-area with the furthest vertical drain spacing (A2S-73: 3.0 x 3.0). This may be attributed to the higher degree of smear effect at locations with closer drain spacing. This is confirmed by similar trends obtained by the Asaoka and piezometer back-analysis. However reduction of c_h with time is due to reduction of void ratio as consolidation progress.
- (4) The author recommends that for the Asaoka method a longer time interval has to be used for the ultimate settlement and c_h predictions. The use of a longer time interval will require a long term field instrumentation monitoring programme in order to enable sufficient data points to be obtained in order to assess the best-fit line through the data points.
- (5) The author's findings of the Hyperbolic method reveal that the magnitude of ultimate settlement increases and subsequently the degree of consolidation decreases as a longer period of assessment is used in the prediction.
- (6) The prediction of ultimate settlement and degree of consolidation is found to be in excellent agreement for the Asaoka and Hyperbolic methods especially when the period of assessment increases.
- (7) The degree of consolidation predicted by the piezometers is found to be in good agreement with the Asaoka and Hyperbolic methods for the early period of assessment. However as the assessment period increases, the piezometer indicates lower degree of consolidation as compared to field settlement predictions. This can be attributed to the non-linearity of the stress-strain behaviour of soil (Mikasa, 1995).

- (8) The back-analysed c_h by the piezometer method indicates that there is a trend of the c_h value generally decreasing at longer periods of assessment after surcharge placement. It is apparent that the coefficient of consolidation due to horizontal flow, c_h value of the clay is reducing with time and as longer time of assessment is used in the back-analysis by piezometer method.
- (9) The study of the piezometer method reveals that the c_h value of the marine clay is lowest at the sub-area with the closest vertical drains spacing and highest at the sub-area with the largest vertical drain spacing which is attributed to the larger smear effect at locations with closer drain spacing. This is in similar agreement with the c_h values back-calculated by the Asaoka method and confirms the higher degree of smear effect at locations with closer drain spacing. However, reduction of c_h with time is due to reduction of void ratio as consolidation progress.
- (10) The c_h values back-calculated by the Asaoka and piezometer method after 32 months of surcharge placement in the Pilot Test Site is found to be in good agreement and confirm the higher degree of smear effect at locations with closer drain spacing.

12.5 Finite Element Modeling of Marine Clay and Vertical Drains

The findings of the finite element modeling of the In-Situ Test Site and Pilot Test Site are listed below:

- (1) Reasonable agreements were obtained from the finite element modeling analysis as compared to the actual field settlements for both the vertical drain treated embankments as well as the untreated control embankments at both the In-Situ Test Site and Pilot Test Site. The axi-symmetric unit cell and the full scale analysis of vertical drains were found to be in excellent agreement with each other and with the actual field settlement results.
- (2) The techniques used in the finite element analysis of the vertical drains were based on that used previously in the modeling of Bangkok clays with PVD. The modeling of the Singapore marine clay treated with vertical drains was however modified to incorporate the marine clay multi-layers present in Singapore marine clay at Changi.

The modeling technique used by the author is found to provide similar reasonable agreements in their use for the modeling of Singapore marine clay with vertical drains.

(3) In-Situ Test Site Finite Element Modeling Findings:

The ultimate settlement obtained by the finite element modeling method is found to be lower than that predicted by the Asaoka and Hyperbolic prediction methods for the Vertical Drain Area (1.5m x 1.5m). The degree of consolidation obtained by the finite element modeling method for the Vertical Drain Area (1.5m x 1.5m) is subsequently slightly higher than that obtained by the Asaoka, Hyperbolic and piezometer methods. For the Vertical Drain Area, a degree of consolidation of 87.8% was obtained from the FEM method as compared to 80.1% from the Asaoka method, 80.0% from the Hyperbolic method and 80.0% from the piezometer method.

The degree of consolidation obtained by the finite element modeling method for the untreated Control Area is also found to be slightly higher than that obtained by the piezometer method. For the Control Area, a degree of consolidation of 27.9% was obtained from the FEM method as compared to 20.0% from the piezometer method.

(4) Pilot Test Site Finite Element Modeling Findings:

The ultimate settlement obtained by the finite element modeling method is found to be slightly lower than that predicted by the Asaoka and Hyperbolic prediction methods for the A2S-71 (2.0m x 2.0m) sub-area. For the A2S-71 sub-area, a degree of consolidation of 95.6% was obtained from the FEM method as compared to 91.8% from the Asaoka method, 93.7% from the Hyperbolic method and 86.2% from the piezometer method.

The ultimate settlement obtained by the finite element modeling method is found to be higher than that predicted by the Asaoka and Hyperbolic prediction methods for the A2S-72 (2.5m x 2.5m) and A2S-73 (3.0m x 3.0m) sub-areas. For the A2S-72 sub-area, a degree of consolidation of 87.9% was obtained from the FEM method as compared to 89.5% from the Asaoka method, 89.8% from the Hyperbolic method and 82.5% from the piezometer method. For the A2S-73 sub-area, a degree of consolidation of 78.9% was obtained from the FEM method as compared to 79.0%

from the Asaoka method, 81.1% from the Hyperbolic method and 73.1% from the piezometer method.

The degree of consolidation obtained by the finite element modeling method for the untreated control A2S-74 (No Drain) sub-area is also found to be slightly lower than that obtained by the piezometer method. For the untreated A2S-74 sub-area, a degree of consolidation of 33.9% was obtained from the FEM method as compared to 37.0% from the piezometer method.

12.6 Performance Verification of Marine Clay Treated with Prefabricated Vertical Drains

The performance verification of prefabricated vertical drains was studied at the In-Situ Test Site and findings are as follows:

- (1) The field time rate of consolidations is found to be in good agreement with the newly proposed modified Asaoka method and the conventional method using the back-calculated $c_h = 0.78 \text{ m}^2/\text{year}$. The actual field measurement is slightly slower than the proposed modified Asaoka and the conventional method using the back-calculated $c_h = 0.78 \text{ m}^2/\text{year}$ by only about 5%. The newly proposed modified Asaoka equation is found to be in good agreement with the conventional method using the back-calculated c_h . As such, it is proposed that the proposed modified equation can be used in similar multi-layer schemes of marine clay and can be used in future instead of using the conventional method with back-calculated c_h assumed as a ratio of c_v .

- (2) It was found from the back-analyses of the field instrumentation monitoring results that the actual field coefficient of consolidation due to horizontal flow is only $0.78 \text{ m}^2/\text{year}$. However, field measurement of coefficient of consolidation due to horizontal flow measured prior to reclamation by the various in-situ testing equipments is much higher than the back-analysed and design (c_h) values. As such, it is recommended based on these findings that the assumed coefficient of consolidation due to horizontal flow in the design stage should not be more than 1.5 times that of the coefficient of consolidation for vertical flow when thick layers of homogeneous clay are in existence. The adoption of too high an assumed c_h to c_v

ratio, will predict a design rate of settlement that is faster than that of the actual field settlement.

- (3) The field curve is noted to be slowing down after one year of surcharging period. This may be an indication of a reduction in permeability of the vertical drain filter due to clogging. This may also be due to the reduction of permeability in the surrounding soil due to void ratio changes in the later stage of the consolidation.
- (4) Vertical drains installed in the project are performing to improve the soil drainage system, however their performance is slightly slower than that predicted. An exact superimposed time rate of settlement curves between field and prediction is extremely difficult to obtain since there are various natural variations, which cannot be modelled. As such, it would be more effective to design the vertical drain especially where thick layers of homogeneous clay exist with a lower specified degree of consolidation but with a higher surcharge load (higher additional load) in order to gain the equivalent stress gain within a shorter duration when vertical drains are fully performing.

REFERENCES

Aas, G. (1967). "A Study of the Effect of Vane-Shape and Rate of Strain on the Measured Values of In-Situ Shear Strength of Clays", International Conference on Soil Mechanics and Foundation Engineering, Montreal, Canada, pp. .

Arulrajah, A., Nikraz, H. and Bo, M.W. (2003a). "Factors Affecting Field Settlement Assessment and Back-Analysis by the Asaoka and Hyperbolic Methods", *Australian Geomechanics*, Journal of the Australian Geomechanics Society, Vol. 38, No. 2, June, pp. 29-37.

Arulrajah, A. and Nikraz, H. (2003b). "Comparison of Degree of Improvement Assessed by Observational Methods Using Field Instrumentation", *Field Measurements in Geomechanics: 6th International Symposium on Field Measurements in GeoMechanics*, Swets & Zeitlinger, The Netherlands, September, pp. 3-10.

Arulrajah, A., Nikraz, H. and Bo, M.W. (2004a). "Factors Affecting Assessment and Back-Analysis by Piezometer Monitoring", *Australian Geomechanics*, Journal of the Australian Geomechanics Society, Vol. 39, No. 1, March, pp. 49-60.

Arulrajah, A., Bo, M.W. and Nikraz, H. (2004b). "Field Instrumentation Monitoring of Land Reclamation projects on Marine Clay Foundations", *Australian Geomechanics*, Journal of the Australian Geomechanics Society, Vol. 39, No. 1, March, pp. 69-78.

Arulrajah, A. and Nikraz, H. (2004c). "Field Instrumentation Assessment of Offshore Land Reclamation Works", *Journal of the International Society of Offshore and Polar Engineering*, Vol. 14, No. 4, December, pp. 315-320.

Arulrajah, A., Nikraz, H. and Bo, M.W. (2004d). "In-Situ Testing of Singapore Marine Clay at Changi", *Geotechnical and Geological Engineering*, An International Journal, Kluwer Academic Publishers, Vol. 23, No. 2, April 2005, pp. 111-130.

Arulrajah, A., Nikraz, H. and Bo, M.W. (2004e). "Factors Affecting Field Instrumentation Assessment of Marine Clay Treated With Prefabricated Vertical Drains", *Geotextiles and Geomembranes*, Journal of the International Geosynthetics Society, Vol. 22, No. 5, October, pp. 415-437.

Arulrajah, A., Bo, M.W., Nikraz, H. and Hashim, R. (2004f). "Piezocone Dissipation Testing of Singapore Marine Clay at Changi", *Geotechnical Engineering*, Journal of the Southeast Asian Geotechnical Society (accepted October 2003; in print).

Arulrajah, A., Nikraz, H. and Bo, M.W. (2004g). "Observational Method of Assessing Improvement of Marine Clay", *Ground Improvement*, Journal of the International Society of Soil Mechanics and Geotechnical Engineering, Vol. 8, No. 4, October, pp. 151-169.

Arulrajah, A., Nikraz, H. and Bo, M.W. (2004h). "Assessment of Marine Clay Improvement under Reclamation Fills by In-Situ Testing Methods", *Geotechnical and Geological Engineering*, An International Journal, Kluwer Academic Publishers (accepted October 2004; in print)

Arulrajah, A., Nikraz, H., Bo, M.W. and Hashim, R. (2004i). "In-situ Pore Water Pressure Dissipation Testing of Marine Clay under Reclamation Fills", *Geotechnical and Geological Engineering*, An International Journal, Kluwer Academic Publishers (accepted August 2004; in print)

Arulrajah, A., Nikraz, H. and Bo, M.W. (2004j). "Finite Element Modeling of Marine Clay Deformation under Reclamation Fills", *Ground Improvement*, Journal of the International Society of Soil Mechanics and Geotechnical Engineering (accepted August 2004; in print).

Arulrajah, A., Nikraz, H. and Bo, M.W. (2004l). "Comparison Between the Performance Of Pneumatic and Electric Piezometers in a Land Reclamation Project", *International Conference on Geotechnical Engineering*, Beirut, Lebanon, May, pp. 899-904.

Arulrajah, A., Nikraz, H. and Bo, M.W. (2004m). "Preloading and Prefabricated Vertical Drains Design for Offshore Land Reclamation Projects", *International Conference on Geotechnical Engineering*, Beirut, Lebanon, May, pp. 351-356.

Arulrajah, A., Nikraz, H. and Bo, M.W. (2004n). "Assessment of Marine Clay Improvement by Observational Methods", *International Symposium on Engineering Practice and Performance of Soft Deposits*, Osaka, Japan, June, pp. 269-274.

Arulrajah, A., Bo, M.W. and Nikraz, H. (2004o). "Characterization of Soft Marine Clay using the Flat Dilatometer", *2nd International Conference on International Site Characterisation*, Porto, Portugal, September, pp. 287-292.

Arulrajah, A., Bo, M.W. and Nikraz, H. (2004p). "Pre-Reclamation Characteristics of Marine Clay using In-Situ Testing Methods", *2nd International Conference on International Site Characterisation, Porto*, Portugal, September, pp. 1041-1046.

Arulrajah, A. and Bo Myint Win (1995). *Reclamation at Changi East-Phase 1C Geotechnical Design Report*, Singapore, April (unpublished).

Asaoka, A. (1978). "Observational procedure of settlement prediction" *Soil and Foundations, Japanese Society of Soil Mechanics and Foundation Engineering*, Vol. 18, No. 4, pp. 87-101.

Baligh, M. M., Levadoux J. N. (1986). Consolidation after Undrained Piezocone Penetration. II: Interpretation, *Journal of Geotechnical Engineering, ASCE*, Vol. 112, No. 7, pp. 727-745.

Balasubramaniam, A.S., Bergado, D.I., Long, P.V. and Thayalan (1995). "Experiences with Sand Drains and Prefabricated Vertical Drains in Ground Improvement of Soft Clays", *Seminar on Engineering for Coastal Development*, Singapore.

Balasubramaniam, A.S., Gurung, S.B., Kusakabe, O. and Kim, S.R. (1993). "On the Plastic Volumetric Strain of Bangkok Clay", 11th Southeast Asian Geotechnical Conference, May, Singapore, pp. 73-78.

Barron, P. (1948). "Consolidation of Fine Grained Soils by Drain Wells", *Trans ASCE* Vol. 113, pp. 718-754.

Bergado, D.T., Chai, J.C., Alfaro, M.C. and Balasubramaniam, A.S. (1992). *Improvement Techniques of Soft Ground in Subsiding and Lowland Environment*.

Bergado, D.T., Alfaro, M.C. and Balasubramaniam, A.S. (1996). "Improvement of Soft Bangkok Clay using Vertical Drains", *Geotextiles and Geomembranes*, Vol. 12, No. 7, 615-663.

Bjerrum, L. (1967). "Geotechnical Properties of Norwegian Marine Clays", *Norwegian Geotechnical Institute*.

Bo Myint Win, Arulrajah, A. and Choa, V. (1997a). "Assessment of Degree of Consolidation in Soil Improvement Project", *International Conference on Ground Improvement Techniques*, May, Macau, pp. 71-80.

Bo Myint Win, Arulrajah, A. and Choa, V. (1997b). "Performance Verification of Soil Improvement Work with Vertical Drains", *30th Anniversary Symposium of the Southeast Asian Geotechnical Society*, November, Bangkok, Thailand.

Bo Myint Win, Choa, V. and Arulrajah, A. (1997c). "Large Deformation Due to Additional Load on Slurry-like Foundation Soil", *International Conference on Foundation Failure*, May, Singapore.

Bo Myint Win, Arulrajah, A. and Choa, V. (1997d). "Large Deformation of Slurry-like Soil", *International Symposium on Deformation and Progressive Failure in Geomechanics*, October, Nagoya, Japan.

Bo Myint Win, Arulrajah, A., Choa, V. and Chang, M.F. (1998a). "Site Characterization for a Land Reclamation Project at Changi in Singapore", *Geotechnical Site Characterisation*, Robertson and Mayne (editors), Balkema, Rotterdam, Vol. 1, pp. 333-338.

Bo Myint Win, Arulrajah, A. and Choa, V. (1998b). "Instrumentation and Monitoring of Soil Improvement Work in Land Reclamation Projects", *8th International Congress of the International Association for Engineering Geology and the Environment*, Balkema, Rotterdam, pp. 385-392.

Bo Myint Win, Arulrajah, A. and Choa, V. (1998c). "Hydraulic Conductivity of Singapore Marine Clay", *The Quarterly Journal of Engineering Geology*, Vol. 31, Part 4, November, pp. 291-299.

Bo Myint Win, Arulrajah, A., Choa, V. and Na, Y.M. (1998d). "Land Reclamation on Slurry-like Soil Foundation", *Problematic Soils*, Yonagisawa, Morota and Mitachi (eds.) Balkema, Rotterdam, pp. 763-766.

Bo Myint Win, Bawajee, R. and Choa, V. (1998f). "Smear Effect due to Mandrel Penetration", *2nd International Conference on Ground Improvement Techniques*, Singapore.

Bo Myint Win, Bawajee, R. and Rahardjo, P.P. (1998g). “Physical Characteristics of Jakarta Bay Silt”, 13th Southeast Asian Geotechnical Conference, November, Taipei, Taiwan.

Bo Myint Win, J. Chu and Choa, V. (1999). “Factors Affecting the Assessment of Degree of Consolidation”, *Field Measurements in Geomechanics*, Balkema, Rotterdam, pp. 481-486.

Bo Myint Win, Chang, M.F., Arulrajah, A. and Choa, V. (2000a). “Undrained Shear Strength of the Singapore Marine Clay at Changi from In-Situ Tests”, *Geotechnical Engineering Journal of the Southeast Asian Geotechnical Society*, Vol. 31, No. 2, August, pp. 91-107.

Bo Myint Win, Bawajee, R., Chu, J. and Choa, V. (2000b). “Investigation of Smear Zone around Vertical Drain”, *3rd International Conference on Ground Improvement Techniques*, Singapore, pp. 109-114.

Bo Myint Win, Choa, V. and Zeng, X.Q. (2000c). “Electro-Osmosis Properties of Singapore Marine Clay”, *International Symposium on Coastal Geotechnical Engineering*, Yokohama, Japan.

Bo Myint Win, Chu, J. and Choa, V. (2000d). “Discharge Capacity of Prefabricated Vertical Drains”, *2nd Asian Geosynthetics Conference*, Kuala Lumpur, Malaysia.

Bo Myint Win (2002). “Deformation of Ultra-Soft Soil”, *Doctor of Philosophy Thesis*, Nanyang Technological University, Singapore

Bo M. W., Chu, J, Low, B. K. and Choa, V. (2003a). *Soil Improvement – Prefabricated Vertical Drain Techniques*, Thomson Learning, Singapore.

Bo, M.W., Choa, V. and Hong, K.H. (2003b). “Material Characteristic of Singapore Marine Clay at Changi”, *The Quarterly Journal of Engineering Geology and Hydrogeology*, Vol 36, Part 4. pp. 305-321.

Bo M. W. and Choa, V. (2004). *Reclamation and Ground Improvement*, Thomson Learning, Singapore.

Brand, E.W. and Premchitt, J. (1989). "Moderator's Report for the Predicted Performance of the Muar Test Embankment", *International Symposium on Trial Embankments on Malaysian Marine Clays*, November, Kuala Lumpur, Malaysia.

Broms, B. B. (1987). "Stability of Soft Clay in South East Asia", *Proceedings of the Fifth International Seminar, Case Histories in Soft Clay*, December 1987, Singapore.

Broms, B. B., Chu, J. and Choa, V. (1994). "Measuring the Discharge Capacity of Band Drains by a New Drain Tester", *Proceedings of the 5th International Conference on Geotextiles, Geomembranes and Related Products*, Vol. 3, Singapore, pp. 803-806.

British Standard BS6349. (1991). "Maritime Structures, Part 5. Code of Practice for Dredging and Land Reclamation".

Broms, B.B., Chu, J. and Choa, V. (1994). "Measuring the Discharge Capacity of Band Drains by a New Drain Tester", *Proceedings of the 5th International Conference on Geotextiles, Geomembranes and Related Products*, Vol. 3, 803-806, Singapore.

Bromwell, L.G. and Lambe, W.T. (1968). "A Comparison of Laboratory and Field values of c_v for Boston Blue Clay" Soils publication 205 Massachusetts Institute of Technology, Cambridge, Massachusetts.

Bujang, B.K. Huat (1996). "Observational Method of Predicting the Settlement", *12th Southeast Asian Geotechnical Conference*, Kuala Lumpur.

Bujang, B.K. Huat (2002). "Hyperbolic Method for Predicting Embankment Settlement", *2nd World Engineering Congress*, Kuching.

Butterfield, R. (1979). "A Natural Compression Law for Soil (an advance on e-log p)", *Geotechnique* 29, No. 4, pp. 469-480.

Cadling, L. and Odenstad, (1950). "The Vane Borer, An Apparatus for Determining the Shear Strength of Clay Soils Directly in the Ground", *Swedish Geotechnical Institute*, Stockholm.

Cambridge In-Situ (1993). Pre-reclamation Self-Bored Pressuremeter Tests, *Reclamation at Changi East Phase 1B Report*, Singapore.

Campanella, R.G and Robertson, P.K. (1988). "Current Status of the Piezometer Test", *Penetration Testing, I* Sopt-1 De Ruiter(ed) Balkema, Rotterdam, pp. 93-116.

Cao, L.F. (1998). "Analysis of Cone Pressuremeter Test in Clay", *13th Southeast Asian Geotechnical Conference*, Taipei, Taiwan.

Carrillo, N. (1942). "Simple Two and Three Dimensional Cases in the Theory of Consolidation of Soils", *J. Math. and Phys.*, 21, 1-5.

Carroll, R.G. (1983). "Geotextile Filter Criteria", *Transportation Research Record*, 916, 46-53.

Casagrande, A. (1936), "The Determination of the Pre-Consolidation Load and its Practical Significance", *Proceedings of the First International Conference on Soil Mechanics*, Cambridge, Mass., Vol. 3, 60-64.

Chang, M.F. (1986). "The Flat Dilatometer and Its Application to Singapore Clays" *Proceedings of the 4th International Seminar Field Instrumentation and In-situ Measurements*, Nanyang Technological Institute, Singapore.

Chang, M.F. (1991). "The stress history of Singapore marine clay", *Geotechnical Engineering*, Vol. 22, No. 1: pp. 5-21.

Chang, M.F. (1991). "Interpretation of overconsolidation ratio from in-situ tests in recent deposits in Singapore and Malaysia", *Canadian Geotechnical Journal*, Vol. 28, No. 2.

Chang, M.F. (1994). *Short Course on In-Situ Testing of Foundation Soils for Earthworks*, Nanyang Technological University, Singapore.

Chang, M.F., Choa, V., Bo Myint Win and Cao, L.F. (1997). "Overconsolidation ratio of a seabed clay from in-situ Tests" *14th International Conference on Soil Mechanics and Foundation Engineering*, Hamburg.

Chang, M.F., Choa, V., Cao, L.F. and Arulrajah, A. (1998). "Evaluating the State of Consolidation of Clay at a Reclaimed Site" *1st International Conference on Site Characterization, Atlanta, USA*.

Choa, V., Karunaratne, G., Ramaswamy, S.D., Vijjaratnam, A. and Lee, S.L. (1979). "Consolidation of Changi Marine Clays of Singapore Using Flexible Drains", *7th European Regional Conference on Soil Mechanics and Foundation Engineering*, England, Vol. 3, pp. 29-36.

Choa, V., Karunaratne, G. P., Ramaswamy, S. D., Vijjaratnam, A. and Lee, S. L. (1979b). "Pilot Test for Soil Stabilization at Changi Airport", *6th Asian Regional Conference on Soil Mechanics and Foundation Engineering*, Singapore, Vol. 1, pp. 141-144.

Choa, V., Vijjaratnam, A. Karunaratne, G. P., Ramaswamy, S. D., and Lee, S. L. (1979c). "Pilot Test for Soil Stabilization at Changi Airport", *7th European Regional Conference on Soil Mechanics and Foundation Engineering*, Brighton, Vol. 3, pp. 29-36.

Choa, V., Karunaratne, G., Ramaswamy, S.D., Vijjaratnam, A. and Lee, S.L. (1981). "Drain Performance in Changi Marine Clay", *10th International Conference on Soil Mechanics and Foundation Engineering, Volume 3*, pp. 623-626, Stockholm, Sweden.

Choa, V. (1984). "Consolidation of Marine Clay under Reclamation Fills", *Doctor of Philosophy Thesis*, National University of Singapore, Singapore.

Choa, V. (1985). "Preloading and vertical drains", *3rd International Geotechnical Seminar*, Singapore.

Choa, V. (1991). "Reclamation on Soft Ground for Port and Airport Development", Keynote Lecture. *Proceedings of the Seminar on Reclamation – Important Current Issues*. Geotechnical Division of the Hong Kong Institution of Engineers, pp. 1-32.

Choa, V. and Wong, K.S. (1992). *Reclamation at Changi East Phase 1B–Geotechnical Investigation Report*, Singapore, November 1992.

Choa, V. (1994). "Application of the Observational Method to Hydraulic Fill Reclamation Projects", *Geotechnique*, 44, No. 4, pp. 735-745.

Choa, V., Chu, J., Bawajee, R., Bo, M.W., Arulrajah, A. (1996). "The Strength and Consolidation Behaviour of Singapore Marine Clay at Changi", *12th Southeast Asian Geotechnical Conference*, May, Kuala Lumpur, Malaysia, pp.81-85.

Choa, V., Bo, M.W. and Chu, J. (2001). "Soil Improvement Works for the Changi East Reclamation Project", *Ground Improvement*, Vol. 5, No. 4, 141-153.

Choa, V. (1995). "Changi East Reclamation Project", *Proceedings of the International Symposium on Compression and Consolidation of Clayey Soils*, IS-Hiroshima, Japan. Yoshikuni and Kusakabe (eds.), Balkema, Rotterdam, Vol. 2.

Chu, J. and Choa, V. (1995). "Quality Control Tests of Vertical Drains for a Land Reclamation Project", *Compression and Consolidation of Clayey Soils*, Yoshikuni and Kusakabe (eds), 43-48.

Chu J., Bo Myint Win, Chang M. F., and Choa V. (2002). "Consolidation and permeability properties of Singapore marine clay", *Journal of Geotechnical and Geoenvironmental Engineering*, ASCE, Vol. 128, No. 9, pp. 724-732.

Chun, B.S., Kim, Y.N., Lee, K.I., Chae, Y.S., Cho, C.H., Bang, E.S. (1997). "A Comparative Study on the Consolidation Theory of Vertical Drains", *International Conference on Ground Improvement Techniques*, May, Macau.

Clarke, B.G., Carter, J.P. and Wroth, C.P. (1979). "In-Situ Determination of the Consolidation Characteristics of Saturated Clays", *Proceedings of the 7th European Conference on Soil Mechanics and Foundation Engineering*, Vol. 2, 207-213.

De Beer, E.E., Goelen, E., Heynew, W.J. and Joustra, K. (1988). Cone Penetration Test (CPT): International Reference Test Procedure, *Proceedings of the 1st International Symposium on Penetration Testing*, Orlando, U.S.A, Vol. 2, pp. 737-744.

Duncan, J. M. (1993). "Limitation of Conventional Analysis of Consolidation Settlement", *Journal of Geotechnical Engineering*, Vol. 119, No. 9, pp. 1333-1359.

Dunnicliff, J. (1988). *Geotechnical Instrumentation for Monitoring Field Performances*, John Wiley and Sons.

Feng, T.W. (1993). "Consolidation Properties of a Lacustrine Clay in Taipei", 11th Southeast Asian Geotechnical Conference, May, Singapore, pp. 117-120.

Flaate, K. (1966). "Factors Influencing the Results of Vane Tests", *Canadian Geotechnical Journal*, Vol. 3, No. 1, pp. 18-31.

Gupta, R.C. (1983). "Determination of the In-Situ Coefficient of Consolidation and Permeability of Submerged Soils Using Electrical Piezoprobe Sounding" ,*PhD Thesis*, University of Florida.

Gupta, R.C. and Davidson, J.L. (1986). "Piezoprobe Determined Coefficient of Consolidation", *Soils and Foundations*, Vol. 26, No. 3, pp. 12-22.

Hanna, T.H. (1985). *Field Instrumentation in Geotechnical Engineering*, Trans Tech Publications, 1st Edition.

Hansbo, S. (1979). "Consolidation of Clay by Band-Shaped Prefabricated Drains" *Ground Engineering*, 12, 5, pp. 16-25.

Hansbo, S., Jamiolkowski, M. and Kok, L. (1981). "Consolidation by Vertical Drains", *Geotechnique*, Vol. 31, pp. 45-66.

Hansbo, S. (1983). "How to Evaluate the Properties of Prefabricated Vertical Drains", Proceedings 8th European Conference on Soil Mechanics and Foundation Engineering, Volume 3, Helsinki, pp.1238-1239.

Hausmann, M. R. (1990). *Engineering Principles of Ground Modification*, International Edition, McGraw-Hill, Singapore, pp. 251-265.

Holtz, R.D. and Kovacs, W.D. (1981). *An Introduction to Geotechnical Engineering*, Prentice-Hall, Inc., Englewood Cliffs, N.J. 07632.

Holtz, R.D. and Christopher, B.R. (1987). "Characteristics of Prefabricated Drains for Accelerating Consolidation", Proceedings 9th European Conference on Soil Mechanics and Foundation Engineering, Vol. 2, Dublin, pp..903-906.

Holtz, R.D., Jamiolkowski, M.B., Lancellotta, R., Pedroni, R. (1991). *Prefabricated Vertical Drains–Design and Performance*, CIRIA Ground Engineering Report: Ground Improvement, Butterworth-Heinemann Ltd., London.

Hussein, A.N., McGown, A. and Nik Hassan, N.R. (1996). "Geotechnical Characteristics of the Coastal Soft Soil Deposits at Kuala Perlis, Malaysia", 12th Southeast Asian Geotechnical Conference, May, Kuala Lumpur, Malaysia, pp. 113-118.

Imai, G. (1995). "Analytical examination of the foundation to formulate consolidation phenomena with inherent time-dependence" *Compression and Consolidation of Clayey Soils*, Balkema, Rotterdam.

Indraratna, B. and Redana I. W. (1998). "Laboratory Determination of Smear Zone due to Vertical Drain Installation", *Journal of Geotechnical Engineering*, Feb., Vol. 124, No. 2, pp. 180-184.

Indraratna, B. and Bamunawita. C. (2002). "Soft Clay Stabilization by Mandrel Driven Geosynthetic Vertical Drains", *Australian Geomechanics: Journal of the Australian Geomechanics Society*, Vol. 37, No. 5, December 2002.

Jan De Nul (2003). "Dredging Activities", Company Information.

Janbu, N. (1969). "The Resistance Concept Applied to Deformation of Soils", 7th International Conference on Soil Mechanics, Mexico.

Karunaratne, G. P., Tan, S. A., Lee, S. L. and Choa, V. (1989). "Analysis of Flexible Drains in Changi Reclamation", *Canadian Geotechnical Journal*, Vol. 26, pp. 401-417.

Kim, S. S., Kang, M.S. and Jung, S.Y. (1999). "The Geotechnical Characteristics of Marine Deposit Soil and Its Distribution", *Characterization of Soft Marine Clays*, Tsuchida and Makase (eds), Balkema, Rotterdam.

Kremer, R.R.H.J., Oostven, J.P., Van Weele, A.F. Dejager, W.F.J. and Meyvogel, I.J. (1983). "The Quality of Vertical Drainage", *Proceedings of the 8th European Conference on Soil Mechanics and Foundation Engineering*, Vol. 2, 721-726, Helsinki.

Larsson, R. (1981). "Drained Behaviour of Swedish Clays", Swedish Geotechnical Institute, Report No. 12, Sweden.

Lee, H.J., Chang, C.T., Lee, C.C. and Fang, J.S. (1993). "Geotechnical Characteristics of the Keelung River in the Taipei Basin", 11th Southeast Asian Geotechnical Conference, May, Singapore, pp. 153-158.

Leroueil, S., Lerat, P., Hight, D.W. and Powell, J.J.M. (1992). "Hydraulic Conductivity of a Recent Estuarine Silty Clay at Bothkennar", *Geotechnique*, 42, 275-288.

Leroueil, S. (1999). "Geotechnical Characteristics of Eastern Canada Clays", *Characterization of Soft Marine Clays*, Tsuchida and Makase (eds), Balkema, Rotterdam.

Lin, D.G., Kim, H.K. and Balasubramaniam A.S. (2000). "Numerical Modeling of Prefabricated Vertical Drain", *Geotechnical Engineering Journal of the Southeast Asian Geotechnical Society*, Vol. 31, Number 2, August 2000.

Lunne, T. and Lacasse, S. (1999). "Geotechnical Characteristics of Low Plasticity Drammen Clay", *Characterization of Soft Marine Clays*, Tsuchida and Makase (eds), Balkema, Rotterdam.

Mair, R.V and Wood, D.M. (1987). *Pressuremeter Testing Methods and Interpretation*, CIRIA Ground Engineering Report : Insitu Testing.

Malaysian Highway Authority (1987). *Lay-By in the Sungai Muar Plain Assessment of the Ground Improvement Methods: Factual Report on Geotechnical Investigation*, Vol. 1, June.

Marchetti, S. (1980). "Insitu Tests by Flat Dilatometer", *Journal of the Geotechnical Engineering Division, ASCE*, Vol. 106, No. GT3, Proc Paper 15290, pp. 299-321.

Marchetti, S. and Crapps, D.K. Flat Dilatometer Manual (1981). Schmertmann and Crapps Inc., Gainesville, Florida, USA.

Marchetti, S. and Totani, G. (1989). "C_h Evaluation from DMTA Dissipation Curves, Proceedings of 12th International Conference on Soil Mechanics and Testing Engineering, Vol. 1, pp. 281-286.

Marsland, A. and Randolph, M.F. (1977). "Comparison of the Results from Pressuremeter Tests and Large In-situ Plate Tests in London Clay", *Geotechnique*, Vol. 27, No. 2, pp. 985-992.

- Mayne, P.W. and Mitchell, J.K. (1988). "Profiling of Overconsolidation Ratio in Clays by Field Vane", *Canadian Geotechnical Journal*, Vol. 25, No. 1, pp. 150-157.
- Mesri, G. and Rokhsar, A. (1974). "Theory of Consolidation for Clays", *ASCE Journal of Geotechnical Engineering Division*, 100 (C. T8), pp. 889-904.
- Mesri, G. and Choi, Y. K. (1985). "Settlement Analysis of Embankment on Soft Clays", *Journal of Geotechnical Engineering*, Vol. III, No. 4, pp. 441-463.
- Mesri, G. and Lo, D.O.K. (1991). "Field Performance of Prefabricated Vertical Drains", *Proceedings of the International Conference on Geotechnical Engineering for Coastal Development*, Yokohama, Vol. 1, pp. 231-236.
- Mikasa, M. (1995). "Two Basic Questions on Consolidation", *Compression and Consolidation of Clayey Soils*, Yoshikuni and Kusakabe (eds), Balkema, Rotterdam, pp. 1097-1098.
- Mimura, M. and Jang, W. (2003). "Long-Term Settlement of Reclaimed Marine Structural Pleistocene Clay Deposits", *Proceedings of the 2nd Conference on Advances in Soft Soil Engineering and Technology*, Putrajaya, Malaysia, pp. 335-351.
- Na, Y. M., Choa, V., Bo Myint Win and Arulrajah, A. (1998). "Use of Geosynthetics for Reclamation on Slurry-Like Soil Foundation", *Problematic Soils*, Yanagisawa, Moroto and Mitachi (eds), Balkema, Rotterdam, pp.767-771.
- Norwegian Geotechnical Society (1979). *Recommended Procedures for Vane Borings*, August.
- Onoue, A. (1988). "Consolidation by Vertical Drains Taking Well Resistance and Smear into Consideration", *Soil and Foundations*, Vol. 28, No 4, pp. 165-174.
- Plaxis (2002). "Finite Element Code for Soil and Rock Analyses", 2D-Version 8, *Plaxis b.v.*, Netherlands.
- Pitts, J. (1983). "The origin, Nature and Extent of Recent Deposits in Singapore", *Proceedings, 1st Int'l Seminar on Construction Problems in Soft Soils*, Nanyang Technological Institute, Singapore, pp. JP1-18.

Poulos, H.G., Lee, C.Y. and Small, J.C. (1989). "Prediction of Embankment Performance on Malaysian Marine Clays", *International Symposium on Trial Embankments on Malaysian Marine Clays*, November, Kuala Lumpur, Malaysia.

Public Works Department – Singapore (1976), *The Geology of Singapore*, Publication by the Public Works Department, Singapore.

Raharjo, P.P. (1998). "Site Characterization for reclamation project in North Jakarta", 13th Southeast Asian Geotechnical Conference, November, Taipei, Taiwan, pp. 275-280.

Rendulic, L. (1936). "Porenziffer und Porenwasserdruck in Tonen", *Bauingenieur*, 17,559.

Rowe, R.W. and Barden, L. (1966). "A New Consolidation Cell", *Geotechnique*, Vol. 26, No. 2, 162-170.

Rowe, R.W. (1968). "The Influence of Geological Features of Clay Deposits on the Design and Performance of Sand Drains", *Proc. Inst. Civil Engrs*, Paper 7058-S, 1-72.

Saaidin Abu Bakar (1992). "Settlement Prediction at Muar Flat Using Asaoka's Method", *Proceedings of the Symposium Prediction versus Performance in Geotechnical Engineering*, pp. 387-394.

Skempton, A. W. (1954). "The Pore Pressure Coefficients A and B", *Geotechnique*, 4, pp. 143-147.

Schaefer, V.R. Ground Improvement, Ground Reinforcement and Ground Treatment Development 1987-1997, Geotechnical Special Publication No. 69, American Society of Civil Engineers, pp.45-62

Schiffman, R. L., McArthur, J. M. and Gibson, R. E. (1994). "Consolidation of Clay Layer: Hydrogeologic Boundary Condition". *Journal of Geotechnical Engineering*, Vol. 120, No. 6, pp. 1089-1095.

Schmertmann, J.H. (1988). "The Coefficient of Consolidation Obtained from p_2 Dissipation in the DMT", *Proc. Geotechnical Conference*, Pennsylvania Dept. of Transportation.

Shibuya, S. and Tamrakar, S.B. (1999). "In-Situ and Laboratory Investigations Into Engineering Properties of Bangkok Clay", *Characterization of Soft Marine Clays*, Tsuchida and Makase (eds), Balkema, Rotterdam.

Sinco, (1998). "Slope Indicator-Geotechnical and Structural Instrumentation", Manual.

Skempton (1969). The Consolidation of Clays by Gravitational Compaction, *Quarterly Journal of the Geological Society of London*, Vol. 125, pp 373-411.

Sridharan, A., and Sreepada, R.A. (1981). "Rectangular hyperbola fitting method for one-dimensional consolidation" *Geotech Testing J.* C4(4), pp. 161-168.

Sridharan, A., Abraham, B.M and Jose, B.T. (1991). "Improved technique for estimation of preconsolidation pressure" *Geotechnique*, 41(2), pp. 1-6.

Sugawara, N. (1988). "On the Possibility of Estimating In-situ OCR using Piezocone (CPTU)", *Penetration Testing*, Vol. 2, pp. 985-992.

Tan, Siew-Ann (1993). "Ultimate Settlement by Hyperbolic Plot for Clays with Vertical Drains" *Journal of Geotechnical Engineering, ASCE*, Vol. 119, No. 5, pp. 950-956.

Tan, Siew-Ann (1995). "Validation of Hyperbolic Method for Settlement in Clays with Vertical Drains" *Soil and Foundations, Japanese Society of Soil Mechanics and Foundation Engineering* Vol. 35, No. 1, March, pp. 101-113.

Tan, Siew-Ann (1996). "Comparison of the Hyperbolic and Asaoka Observational Method of Monitoring Consolidation with Vertical Drains" *Soil and Foundations, Japanese Society of Soil Mechanics and Foundation Engineering* Vol. 36, No. 3, June, pp. 31-41.

Tavenas, F., Leblond, P., Jean, P. and Leroueil, S. (1983). "The Permeability of Natural Clays." Part 1: Methods of Laboratory Measurement. *Canadian Geotechnical Journal*, 20, 629-644.

Taylor, D.W. (1948). *Fundamentals of Soil Mechanics*, Wiley, New York.

Terzaghi, K. (1925). "Erdbaumechnik auf bodenphysikalischer" *Grundlage*. Vienna, Deuticke.

- Terzaghi, K. (1943). "Theoretical Soil Mechanics", John Wiley, New York.
- Torstensson, B.A. (1983). *BAT Monitoring System*, BAT AB, Stockholm,.
- Torstensson, B.A., Petsonk, A.M. (1986). "A Device for In-Situ Measurement of Hydraulic Conductivity", *Proceedings of the 4th International Seminar Field Instrumentation and In-situ Measurements*, Nanyang Technological Institute, Singapore.
- Urban Housing Development of Singapore (2000). "21st Century Singapore – Land Reclamation in Singapore", Print Article, Singapore.
- Van Impe, W.F. (1989). *Soil Improvement Techniques and Their Evolution*, A.A. Balkema, Rotterdam, pp. 77-88.
- Wang, T.R. and Chen, W.H (1996). "Development in Application of Prefabricated Drains in Treatment of Soft Soils", General Report. *Proceedings of the 3rd Symposium on Weak Ground Improvement using PVDs*, Oct., 13-40 (in Chinese), Lianyuangang, China.
- Whittle, R.W., Dalton, J.C.P. and Hawkins, P.G. (1993). "Shear Modulus and Strain Excursion in the Pressuremeter Test", *Predictive Soil Mechanics*, Thomas Telford, London.
- Windle, D and Wroth, C.P. (1997). "The use of a Self boring Pressuremeter to determine the Undrained Properties of Clays", *Ground Engineering*, Vol. 10, No. 6, pp. 37-46.
- Xie, K.H. (1987). "Consolidation Theories and Optimisation Design for Vertical Drains", *Doctor of Philosophy Thesis*, Hewing University, China.
- Yashima, A., Shigematsu, H. and Oka, F. "Microstructure and Geotechnical Property of Osaka Pleistocene Clay", *Characterization of Soft Marine Clays*, Tsuchida and Makase (eds), Balkema, Rotterdam.
- Yong, K.Y., Karunaratne, G.P. and Lee, S.L. (1990). "Recent Developments in Soft Clay Engineering in Singapore", *Kansai International Geotech Forum '90*, Osaka, Japan.
- Yoshikuni, H. and Nakanodo, H. (1974). "Consolidation of Fine-Grained Soils by Drain Well with Filter Permeability", *Soils and Foundations*, 14, 2, pp. 35-46.

Note: For copyright reasons the appendices to this thesis have not been reproduced.

APPENDIX 1: Published refereed journal papers resulting from this study

APPENDIX 2: Published refereed conference papers resulting from this study

References to papers listed on p. ii-iv of this thesis

(ADT Co-ordinator, Curtin University of Technology, 29/7/05)